ANALYTICAL APPLICATIONS OF ULTRASOUND

M.D. LUQUE DE CASTRO
AND F. PRIEGO CAPOTE

ANALYTICAL APPLICATIONS OF ULTRASOUND

TECHNIQUES AND INSTRUMENTATION IN ANALYTICAL CHEMISTRY

ANALYTICAL APPLICATIONS OF ULTRASOUND

M.D. Luque de Castro and F. Priego Capote

*Department of Analytical Chemistry, Marie Curie Building
Campus of Rabanales, University of Córdoba, 14071
Córdoba, Spain*

ELSEVIER

Working together to grow
libraries in developing countries

www.elsevier.com | www.bookaid.org | www.sabre.org

ELSEVIER   BOOK AID
International   Sabre Foundation

FOREWORD

Ultrasound is an energy source that has potential for enhancing many steps in an analysis, yet analytical chemists generally have limited knowledge of this. Over forty years ago, I remember using an ultrasonic probe to disrupt cells in biological samples, not realizing this type of energy has many other useful applications. In fact, I was pleasantly surprised when the ultrasonic toothbrush (another type of probe) appeared on the market (invented by a University of Washington dentist) and thought, why didn't I think of that! This book lays the foundation for practicing analytical chemists to think similarly of ways to exploit ultrasound energy.

Professor Luque de Castro and Dr. Priego Capote have assembled a vast amount of information about ultrasound, and this unique book is timely, given advances in ultrasound equipment and demonstrations of how this energy has been used to enhance various steps of analyses, which suggest that more can be done.

What can ultrasound be used for? It depends in part on the imagination of the analyst. But just some examples are:

- cleaning of apparatus;
- assisting sample dissolution;
- facilitating filtration;
- degassing;
- assisting derivatization reactions;
- detection systems; and
- non-destructive testing.

Given the limited literature on analytical applications of ultrasound, the authors provide information from other sources that suggest ways in which we can use it in the analytical laboratory. They discuss the principles of ultrasound and the variables we must consider in adapting ultrasound to different problems.

The book is divided into two parts. Part I deals with the use of ultrasound in sample preparation, including general aspects of sample preparation of solids, liquids and heterogeneous samples (Chapter 2), and ultrasound to assist digestion (Chapter 3), leaching (Chapter 4), handling of heterogeneous systems – slurry formation, aggregation, filtration, nebulization, defoaming, degassing (Chapter 5), liquid–liquid extraction, homogenization, emulsification (Chapter 6), and chemical reactions (Chapter 7). Chapter 8 discusses topics such as ultrasound-assisted levitation and its applications, and ultrasound-assisted electroanalytical techniques. Part II deals with the use of ultrasound in detection. Chapter 9 describes types of ultrasound-based detection techniques, based on sample–ultrasound interactions, including transmission, pulse echo, interferometric, resonance, back-scatter Rayleigh surface wave and diffraction measurements, among others. Chapter 10 presents examples on applications of ultrasound-based detection techniques.

This book provides a wealth of information for those interested in exploiting ultrasound to enhance different steps in an analysis and is a recommended reading.

Gary D. Christian
Department of Chemistry
University of Washington
Seattle, WA 98195-1700 USA

This page intentionally left blank

PREFACE

Ultrasound is a ubiquitous form of energy known and used, albeit to a rather disparate extent, in many areas of chemistry. Thus, in organic chemistry, ultrasound is used so widely – particularly to facilitate synthetic reactions – that it has been the subject matter of a number of books. By contrast, no dedicated book on the use of this type of energy in analytical chemistry had previously been published. This is quite surprising as ultrasound can be of help virtually throughout the analytical process; however, it can be easily understood if one considers that few analytical chemists are aware of its enormous potential and even fewer have used it for analytical purposes.

In fact, as shown in this book, ultrasound can facilitate to a greater or lesser extent almost every step of the analytical process or even preliminary operations such as cleaning labware or degassing solvents. Thus, in relation to solid samples, ultrasound can dramatically expedite dissolution, digestion, leaching and slurry formation; and facilitate the formation of a solid phase by crystallization or agglomeration, or its separation by filtration, for example. As regards liquid samples, ultrasound can facilitate or accelerate emulsification; the extraction, formation or separation of a gas; and a variety of derivatization (complex formation, hydrolysis, redox) reactions. In addition, ultrasound is the underlying principle of some detection techniques widely used in medicine but very scarcely known by analytical chemists.

The authors' primary aim in writing this book was to provide an overview of appropriate length to help analytical chemists assess the potential uses of ultrasound in a variety of chemical fields. Another aim was to discuss ultrasound-based detection techniques in a systematic manner in order to clear the enormous confusion around some concepts. The authors would like to apologize in advance for any significant omissions resulting from the vast scope of the topic and the absence of analytical chemists with whom to discuss some specially elusive aspects of ultrasound. As long as readers believe the book provides them with an up-to-date, balanced description of the potential of ultrasound in analytical chemistry, the authors' will feel rewarded for the effort.

Finally, the authors would like to express their gratitude to Antonio Losada, MSc, for his linguistic revision of the manuscript.

The Authors
Córdoba, May 2006

This page intentionally left blank

CONTENTS

CHAPTER 1

Introduction: Fundamentals of Ultrasound and Basis of its Analytical Uses

1.1. INTRODUCTION

Ultrasound (US) is simply sound pitched above human hearing that is used at present for a growing variety of purposes in diverse areas. At home, ultrasound is typically used for communication with animals (dog whistles), as well as in burglar alarms, anemometers and jewellery cleaners. In hospitals, doctors use ultrasound to remove kidney stones without surgery, treat cartilage injuries and image fetal development during pregnancy. Ultrasonic scalpels are used by surgeons to cut precisely where they want without exerting any pressure. In industry, ultrasound provides an effective tool for synthesizing fine chemicals, emulsifying cosmetics and foods, welding plastics, cutting alloys, large-scale cleaning and identifying flaws in concrete buildings. Figure 1.1 shows the sound ranges and the principal fields of use of ultrasound. Humans can hear frequencies from about 16 Hz to 18 kHz. The broad range of ultrasound in the figure, which spans frequencies from 20 kHz to the GHz range (*i.e.* usually lower for gases than for liquids and solids) can be split into two distinct regions, namely: a power region and a diagnostic region. The former, on the low-frequency end, allows enough acoustic energy for cavitation to be produced. Cavitation is the origin of sono-chemical effects. Practical sonochemical frequencies usually range from 20 to 40 kHz simply because this is the range typically afforded by laboratory equipments. However, because acoustic cavitation in liquids can be generated well above the previous frequencies, recent sonochemical research and equipment development activities have involved a much broader range (see Fig. 1.1). High-frequency US — which possesses a low amplitude and power — from around 5 MHz and above produces no cavitation, so it is used for medical scanning, chemical analysis and the study of relaxation phenomena, among other applications.

Specialists in ultrasound such as Mason [1] have identified three main "strands" in ultrasonics research, namely:

(1) Sonochemistry with its origin in chemistry and physics. This includes traditional applications such as synthesis, catalysis and fundamental studies of cavitation involving mainly academia, and also more recent uses such as environmental protection (both biological and chemical), material science (new catalytic materials, improved extraction, crystallization, new methods in polymer technology), electrochemistry (providing improved plating electrosynthesis and electroanalysis) and biotechnology (modification of enzyme and whole-cell activities).
(2) Power ultrasound with its origin in engineering and processing, which includes cleaning, welding and materials processing at the industrial level.
(3) Diagnostic ultrasound for non-destructive testing and medical scanning, which has aroused much interest in both academia and industry.

According to Mason, mutual connections between the three strands can help strengthen and expand research. He has identified three areas where such connections exist, namely:
 (i) the use of focused ultrasound in cancer therapy, where the development of transducer arrays is linked to the physical effect of power ultrasound and the sonochemically improved performance of chemotherapeutic agents;

 (ii) the design and production of nanoparticles, which links sonochemistry to ultrasonic precipitation and the surface effects of cavitation; and

(iii) chemical engineering, where designing a sonochemical reactor entails conducting a sonoluminescence study. Analytical chemistry is one case in point that is concerned with the three strands, namely:

(1) sonochemistry, which is widely used in sample preparation procedures (*e.g.* digestion, leaching, liquid–liquid extraction, derivatization, etc.);

(2) power ultrasound, which facilitates cleaning, degassing, filtration, etc. on the analytical laboratory scale; and

(3) diagnostic ultrasound for deriving analytical information from the behaviour of US towards a particular system.

Traditionally, the community of scientists engaged in US work has been divided into those who use ultrasound for measuring without altering the medium (as with high-frequency, low-power ultrasound for non-destructive testing) and those who exploit it to produce physical or chemical effects on the medium (high-power, low-frequency ultrasound in sonochemistry). Analytical chemists mainly belong to the latter group, but are increasingly joining the former.

According to sonochemists, sonochemistry has reached a time for change [2]. The members of the European Society of Sonochemistry (ESS) are beginning to ask what the best role for ESS in the future would be. The aim should be to expand the horizons of sonochemistry while maintaining chemistry as one of the core interests [3,4]. In past years, a number of processes involving US have deemed unfit for inclusion under the umbrella of sonochemistry, even though they are still of interest to the chemical community.

In the meantime, analytical chemists have identified further uses of US; thus, an increasing number of analytical processes have been facilitated or improved by the use of ultrasound and new, more interesting modes of ultrasound-based and ultrasound-assisted detection have been developed. However, only part of the analytical community has been directly involved in these developments. Possibly, the analytical uses of US have not yet come of age; however, it may be an appropriate time to discuss in a structured manner the areas where analytical chemists may find this form of energy, which has so far been virtually ignored by most, a useful tool.

Although, as the name implies, the frequency region in all US applications is always beyond the sound frequency, the prefix "sono" and the adjective "acoustic" are commonly
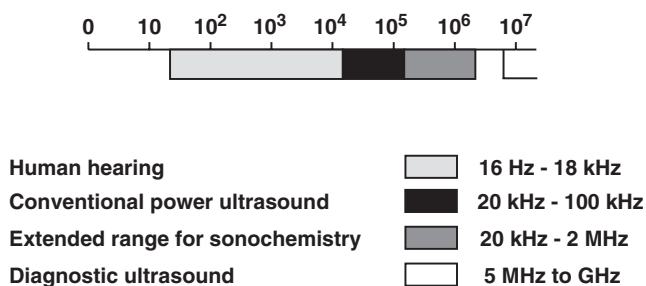
FIGURE 1.1. *Frequency ranges of sound and ultrasound. (Reproduced with permission of Wiley-VCH — modified — Ref. [8].)*

used in this area (*e.g.* sonochemistry). The authors recommend that, when operating at frequencies higher than 18 kHz, the prefix "ultrasono" be used instead of "sono". The change, however, would be rather difficult to introduce; in fact, the latter prefix has been used in most US-related publications, so it is retained in this book.

As the most commonly used analytical effects of US are produced at the kilohertz frequency and the devices for producing these effects are either baths or probes, these are the subjects of Chapters 1–8, the specific diagnostic or detection range and the devices used in it being the subject of Chapters 9 and 10.

Table 1.1 shows the most general applications of US in alphabetical order.

TABLE 1.1. *Main general applications of ultrasound.*

Abatement	Fluidization
Acceleration	Foaming
Agglomeration	Food dehydration
Agitation	Fractionation
Atomization	Grinding
Biological cell disruption	Homogenization
Bleaching	Insertion
Blending	Joining
Bonding	Levitation
Catalysis	Liquids processing
Cavitation	Machining
Cell disruption (biological)	Mixing
Cleaning	Nebulization
Compaction	Particle size reduction
Curing	Pollution abatement
Cutting	Processing
Deagglomeration	Reflowing (hot melt adhesive)
Deflocculation	Scission
Degassing	Separation
Degreasing	Size reduction
Dehydration	Soldering
Disaggregation	Solids processing
Disintegration	Solubilization
Dispersion	Sonocatalysis
Disruption	Sonochemistry
Dissociation	Sonolysis
Dissolution	Sonoluminescence
Drying	Staking
Emulsification	Streaming
Erosion	Surface processing (as in cleaning)
Extraction	Surgical
Fatigue testing	Suspension
Filtration enhancement	Tissue disruption
Fine particle dispersion	Welding (metals)

1.2.   PHYSICAL PRINCIPLES OF ULTRASOUND

Being a sound wave, ultrasound is transmitted through any substance, solid, liquid or gas possessing elastic properties. The movement of a vibrating body (the sound source) is communicated to the molecules of the medium, each of which transmits the motion to an adjoining molecule before returning to approximately its original position. In liquids and gases, particle oscillation takes place in the direction of the wave and produces longitudinal waves. Because they additionally possess shear elasticity, solids can also withstand tangential stress and produce transverse waves, where particles move normal to the direction of the wave. One example of transverse wave is that obtained when a stone is dropped into a pool of water. On the other hand, a longitudinal wave is produced, for example, when a coiled spring anchored at one end is given a sharp push from the other end. The action causes a disturbance in the spring which "runs" through the whole length by expansion and compression. If the disturbance in the pool or spring is periodically repeated, expansion and compression cycles travelling through a medium will occur. Compression cycles push molecules together, whereas expansion cycles pull them apart.

In a liquid, the expansion cycle produces negative pressure that pulls molecules away from one another. If the US intensity is high enough, the expansion cycle can create bubbles or cavities in the liquid. Such is the case when the negative pressure exerted exceeds the local tensile strength of the liquid, which varies depending on its nature and purity. The process by which bubbles form, grow and undergo implosive collapse is known as "cavitation". The steps involved in the process are depicted in Fig. 1.2.
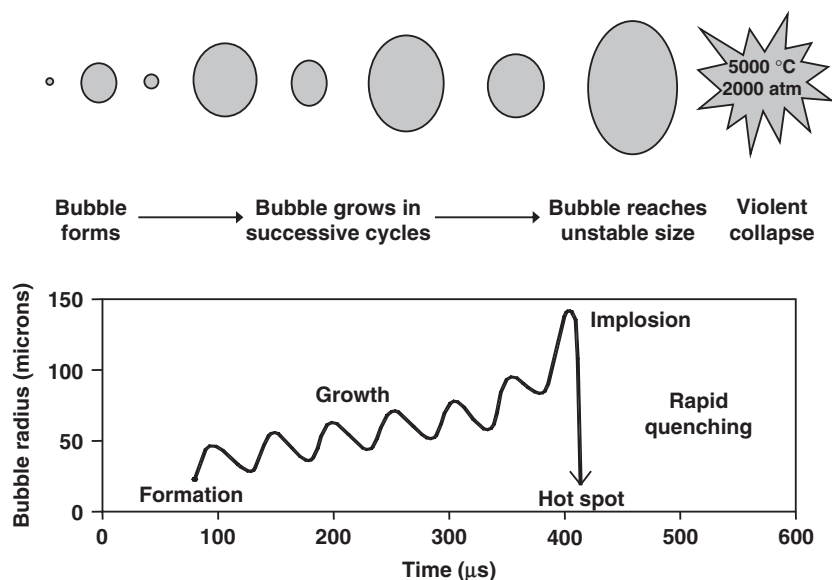
FIGURE 1.2. *Two manners of representing the development and collapse of cavitation bubbles. (Reproduced with permission of Wiley-VCH and Elsevier — modified — Refs. [8,39], respectively.)*

The significance of cavitation to sonochemistry is not so much on how the bubbles form, but rather what happens when they collapse. At some point, a bubble can no longer absorb the energy efficiently from the ultrasound so it implodes. Rapid adiabatic compression of gases and vapours within the bubbles or cavities produces extremely high temperatures and pressures. Suslick [5] estimated the temperature of these hotspots to be about 5000 °C, which is equivalent to that on the surface of the sun. The pressure is roughly 2000 atm, which is higher than that at the Marianas Trench — the deepest point in the ocean. The size of the bubbles is very small relative to the total liquid volume, so the heat they produce is rapidly dissipated with no appreciable change in the environmental conditions — this is why cavitation is also known as "cold boiling". The cooling following collapse of a cavitational bubble has been estimated to be in the region of 10 billion °C/s — a million times faster than that of a red-hot iron rod plunged into water. Acoustic cavitation thus provides a unique interaction between energy and matter, which has been characterized by using electrochemical, luminescent and photographic techniques [6].

When cavitation occurs in a liquid close to a solid surface, the dynamics of cavity collapse change dramatically. In pure liquids, the cavity retains its spherical shape during collapse as its surroundings are uniform. Close to a solid boundary, however, cavity collapse is rather asymmetric and produces high-speed jets of liquid. Liquid jets driving into the surface at speeds close to 400 km/h have been observed. The impact of the jets on the solid surface is very strong. This can result in serious damage to impact zones and produce newly exposed, highly reactive surfaces. Distortions of bubble collapse depend on the surface several times larger than the resonant size of the bubble.

1.2.1. Factors influencing cavitation

This section examines variables influencing the cavitation phenomenon in a manner that can be adjusted to fulfil specific purposes.

Gas and particulate matter

The acoustic pressure needed to cause cavitation in water has been estimated to be approximately 1500 atm. In practice, cavitation occurs at considerably lower values (<20 atm) as a result of the presence of weak spots in the liquid that reduce its tensile strength. There is now sufficient experimental evidence to suggest that one cause of weak spots is the presence of gas molecules in the liquid. Thus, degassing a liquid has been found to raise the cavitation threshold (*i.e.* the applied acoustic pressure required for cavitation bubbles to form). Increasing the gas content of a liquid lowers the cavitational threshold and reduces the intensity of the shock wave released as the bubble collapses. Thus, when the primary source of sonochemical effects is cavitational collapse, a bubbled gas should be used to produce a large number of nucleation sites. Monoatomic gases are preferable to diatomic and polyatomic gases for this purpose. Thus, He, Ar and Ne are used in preference to diatomics such as N_2, air or O_2; on the other hand, gases such as CO_2 are the most unsuitable.

The presence of particulate matter — especially that of trapped vapour gas nuclei in their crevices and recesses — has also been found to lower the cavitation threshold. This is required under these conditions are of paramount importance in the clinical field, where ultrasound is widely used in applications such as high-intensity focused ultrasound (HIFU),

extracorporeal shock wave lithotripsy (ESWL) and sonodynamic therapy. Also, research on bubble and bubble cloud dynamics in the clinical range of ultrasound frequency and intensity is an ongoing task [7].

External (applied) pressure

Increasing the external pressure raises the rarefaction pressure required to initiate cavitation. The application of external pressures which would cause any suspended gas molecules to dissolve, thereby effectively removing the gas nuclei, has also been found to raise the cavitation threshold. More importantly, increasing the external pressure increases the cavitation collapse intensity and as a result enhances sonochemical effects. Qualitatively, there should no longer be a resultant negative pressure phase of the sound wave, so no cavitation bubbles should form.

Solvent viscosity

Because the negative pressure in the expansion or rarefaction cycle must overcome the natural cohesive forces acting in the liquid, any increase in such forces will raise the cavitation threshold. One way of increasing these forces is by increasing the viscosity of the liquid. Table 1.2 illustrates the influence of viscosity on the pressure amplitude (P_A) at which cavitation starts in various liquids at 25 °C, at a hydrostatic pressure of 1 atm. The effect, though not insignificant, is hardly dramatic.

Solvent surface tension

Cavitation requires the formation of a liquid–gas interface. Thus, one might expect the use of a solvent of low surface energy per unit area to lower the cavitation threshold. Although the phenomenon is not as simple as it may seem, the addition of a surfactant to an aqueous solution certainly facilitates cavitation.

Solvent vapour pressure

Cavitation bubbles do not enclose a void. During the expansion phase of cavitation bubble generation, vapour from the surrounding liquid will permeate the interface. This produces

TABLE 1.2. *Sound pressure (P_A) producing cavitation in various liquids under a hydrostatic pressure of 1 atm.*

Liquid	η (poise)	p (g/cm^3)	c (km/s)	P_A (atm)
Castor oil	6.30	0.969	1.477	3.90
Olive oil	0.84	0.912	1.431	3.61
Corn oil	0.63	0.914	1.463	3.05
Linseed oil	0.38	0.921	1.468	2.36
CCl$_4$	0.01	1.60	0.926	1.75

Reproduced with permission of Wiley-VCH, Ref. [8].

a small pressure within the bubble, thereby reducing the pressure difference between cavity and bulk. It is difficult to induce cavitation in a solvent of low vapour pressure because less vapour will enter the bubble. A more volatile solvent will support cavitation at lower acoustic energy and produce vapour-filled bubbles. Unfortunately, however, sonochemical effects are based on the energy produced by cavitation bubble collapse, which is cushioned by vapour in the bubbles. Hence, solvents with high vapour pressures easily generate vapour-filled bubbles, but their collapse is cushioned and therefore less energetic.

Applied frequency

As the frequency of irradiation is increased, the rarefaction phase shortens and the amplitude (power) of irradiation has to be increased to maintain an equivalent amount of cavitational energy in the system. In other words, more power is required at a higher frequency if the same cavitational effects are to be maintained. This is due to the fact that completely rupturing a liquid to obtain voids that may be subsequently filled with gas or vapour requires a finite time. With high-frequency sound waves, the time required to create a bubble may exceed that available during the rarefaction cycle. At 20 kHz, for example, the rarefaction cycle lasts 25 μs and reaches its peak negative pressure in 12.5 μs; at 20 MHz, however, the rarefaction cycle lasts only 0.025 μs. One might thus anticipate that, as the frequency increases, producing cavitation bubbles during the available time will be increasingly difficult and increased sound intensities (*i.e.* greater amplitudes) will have to be employed over the shorter periods to ensure that cohesive forces in the liquid are efficiently overcome. This effect is illustrated in Fig. 1.3, which shows the variation of the threshold intensity with the frequency for both aerated and gas-free water. As expected, the threshold for aerated water is lower than that for gas-free water, and the threshold intensity increases with increase in frequency. In fact, ten times more power is required to make water cavitate at 400 kHz than at 10 kHz. For this reason, frequencies in the range 20–50 kHz have
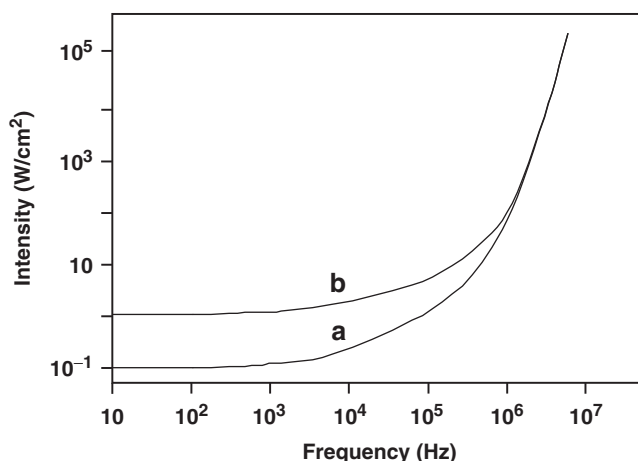
FIGURE 1.3. *Variation of the threshold intensity with frequency in aerated (a) and air-free water (b). (Reproduced with permission of Ellis Horwood, Ref. [25].)*

traditionally been used for cleaning purposes and subsequently been found useful in sonochemistry. As can be seen in Fig. 1.3, little additional energy is required to cause water to cavitate at 50 kHz relative to 10 kHz. Below 18 kHz, however, there may be some noise discomfort to the user since this frequency is within the audible range. This is why sonochemical applications normally involve frequencies above 20 kHz.

Temperature

In general, the cavitation threshold has been found to increase with decreasing temperature. This may in part be due to an increase in either the surface tension or viscosity of the liquid as the temperature decreases, or to a decrease in the liquid vapour pressure. Increasing the temperature facilitates cavitation at a lower acoustic intensity. This is a direct consequence of the rise in vapour pressure associated with heating the liquid — at higher temperatures near the solvent boiling point, a large number of cavitation bubbles are generated concurrently. The higher is the vapour pressure the lower will be the applied acoustic amplitude required to ensure that the "apparent" hydrostatic pressure is exceeded. Unfortunately, the effects of cavitational collapse are also reduced as the bubbles will act as a barrier to sound transmission and dampen the effective ultrasonic energy from the source entering the liquid medium. Therefore, in order to maximize sonochemical effects any experiment should be conducted at as low a temperature as possible or by using a solvent of low vapour pressure. The mathematical equations that relate these variables and their effects on the bubbles are beyond the scope of this book and can be found elsewhere [8].

Intensity

The sonication intensity is directly proportional to the square of the vibration amplitude of the ultrasonic source. As a rule, increasing the intensity increases the sonochemical effects; however, the ultrasonic energy a system can take is limited. Thus, cavitation bubbles, which are initially difficult to create at the higher frequencies as a result of the shorter duration of rarefaction cycles, are now possible by virtue of the collapse time, temperature and pressure on collapse being mutually dependent. However, the sonication intensity cannot be increased indefinitely as the maximum possible bubble size is also dependent on the pressure amplitude. As the pressure amplitude is increased, bubbles may grow so large on rarefaction that the time available for collapse will be inadequate. In fact, it has been unequivocally established that:

(1) A minimum sonication intensity level is required to reach the cavitation threshold.
(2) When a large amount of ultrasonic power enters a system, the solution produces a large number of cavitation bubbles many of which coalesce into even larger, longer-lived bubbles that will hinder the transport of acoustic energy through the liquid.
(3) At high vibrational amplitudes, the US source will be unable to maintain contact with the liquid throughout the cycle. This is technically known as *decoupling* and considerably reduces the efficiency with which power can be transferred from the source to the medium. Decoupling is especially strong when large numbers of cavitation bubbles build up at or near the emitting surface of the transducer.
(4) The transducer material used in the sonicator will eventually break down as the size changes in the transducer grow large enough to fracture the material.

Field type

Acoustic cavitation is empirically known to be induced much more efficiently and reproducibly in a standing wave field than in a progressive one; also suspended particles exposed to an ultrasound standing wave are known to be driven by an axial force to concentrate in nodal or antinodal planes. This phenomenon has received substantial attention in recent years.

The magnitude of Rayleigh microstreaming convective drag on microparticles in water in a 3.2 MHz ultrasonic standing wave has been shown to be comparable to the lateral direct radiation force in the nodal plane and to significantly influence microparticle aggregation [9]. Using single half-wavelength chamber the transducer was excited in order to obtain a single particle aggregate with an estimated sound pressure amplitude of 0.5 MPa; the microstreaming velocity in the nodal plane was calculated from the particle image velocity and found to be comparable to the value obtained in the light of Rayleigh's theory. Further evidence of the significance of microstreaming was provided by the fact that the velocities for particles 1 and 25 μm in size were similar in magnitude, but opposite in direction.

Recently, this phenomenon was found to be induced at a relatively low ultrasonic intensity, even with progressive waves by the second harmonic overlapping the fundamental one [10]. This finding is of paramount importance as regards the clinical applicability of US, and also in sonochemical uses involving systems sensitive to high ultrasound intensities.

Attenuation

For a variety of reasons, the intensity of US is attenuated (*i.e.* decreased) as it progresses through the medium. Part of the energy is dissipated in the form of heat, which is hardly appreciable in the bulk medium during sonication. The extent of attenuation is inversely proportional to the sonication frequency. This can be illustrated with the case of sound attenuation through pure water. Thus, US at 118 kHz is reduced to half its original intensity after passing through 1 km of water. At 20 kHz, the distance required to achieve the same reduction in intensity is much greater (30 km). Therefore, obtaining identical intensities in a medium at a given distance from an ultrasonic source at variable frequencies entails using a higher initial power in the sources with the higher sound frequencies.

Types of ultrasound cavitation

Depending on the particular type of bubbles, ultrasound cavitation can be transient or stable. In the *transient* type, also known as *inertial cavitation*, bubbles are either voids or vapour bubbles, which are believed to be produced by intensities above 10 W/cm^2. They exist for one, or at most a few acoustic cycles, and expand to a radius of at least twice their initial size before collapsing abruptly on compression and often disintegrating into small bubbles. The smaller bubbles formed can act as nuclei for further bubbles or, if their radius is sufficiently small, they can simply dissolve into the bulk solution under the action of the very large surface tension forces present. The lifetime of transient bubbles is believed to be too short to allow any mass flow by diffusion of gas into or out of the bubbles; by contrast, evaporation and condensation of liquid are believed to occur freely. In the absence of gas to cushion the implosion, the bubbles will collapse highly abruptly.

Theoretical considerations by Noltingk and Neppiras [11], subsequently expanded by Flynn [12] and Neppiras [13], that assume adiabatic collapse of the bubbles, allow the temperature and pressure within the bubble at the time of total collapse to be calculated.

Stable or *non-inertial cavitation* was at one time thought to be of little significance in terms of chemical effects. Thus, stable bubbles are believed to contain mainly gas and some vapour, and to be produced at fairly low intensities (1–3 W/cm^2); also, they are assumed to oscillate, often in a non-linear manner, about some equilibrium size over many acoustic cycles. Their timescale is sufficiently long for mass diffusion of gas and thermal diffusion to occur, and hence for evaporation and condensation of vapour, which are bound to have significant long-term effects. Differences in mass transfer rate across the gas–liquid interface may result in bubble growth. The mechanism by which small micro-bubbles in the liquid — which normally dissolve instantly under surface tension — grow is termed as "rectified diffusion". In the expansion phase of the acoustic cycle, gas diffuses from the liquid into the bubble; in the compression phase, gas diffuses out of the bubble into the liquid. Because the interfacial area is greater in the expanded phase, inward diffusion is greater than outward diffusion and results in overall growth of the bubble. As the bubble grows, the acoustic and environmental conditions of the medium will change and the bubble may become a transient bubble and collapse — less abruptly than a vapour-filled transient bubble, however, as the implosion will be cushioned by the gas.

Tests involving new, more sophisticated measurement tools have provided new inter-pretations and equations for the cavitation phenomenon [14,15]. The thermal and non-thermal effects of non-inertial cavitation, and the chemical and mechanical effects of inertial cavitation in relation to their impact on ultrasound safety have recently been investigated [16].

Cavitation is not exclusive of ultrasound. Thus, hydrodynamic cavitation can simply arise from passage of the liquid through a constrictor such as a throttling valve, orifice plate, Venturi tube, etc. On passage through the constrictor, the kinetic energy — velocity — of the liquid increases at the expense of the pressure. Various types of hydrodynamic cavitation reactors have been reported and their most salient features reviewed [17]. Also, the effects of ultrasound and hydrodynamic cavitation on oxidation processes have recently been compared [18].

1.3.   CHEMICAL ASPECTS OF ULTRASOUND

The high temperature and pressure created within a collapsing cavitation bubble pro-duced by US radiation cause the formation of free radicals and various other species; thus, sonication of pure water causes its thermal dissociation into H and OH radicals, the latter forming hydrogen peroxide by recombination [19–21]. These radicals constitute one of the essential pieces of evidence for the phenomena classified as sonochemistry. Table 1.3 shows the main reactions occurring in water irradiated with US. Some of the radical species generated, which have been detected in a number of ways including spin trapping, have been cited as potential pollutant destruction agents on the grounds of their extremely high redox potentials (*e.g. $E° = +2.8$* V for OH radicals [22]. There is less evidence for the behaviour and detection of H·, even though, in principle, it is produced in amounts equivalent to those of OH· in the primary solvent degradation step (see Table 1.3). The two radicals are rather different in chemical nature, however. Thus, the OH radical is known to initiate a number of reactions in solution; by contrast, the H radical can be rapidly captured by molecular oxygen. If the water contains some salt such as potassium iodide [23] or copper sulphate [24], then other free radicals in addition to the species in Table 1.3 can be expected to be released.

TABLE 1.3. *Principal free radicals produced during ultrasonic irradiation of water and their reactions.*

$H_2O \rightarrow OH\cdot + H\cdot$
$OH\cdot + H\cdot \rightarrow H_2O$
$2\ OH\cdot \rightarrow H_2O_2$
$OH\cdot + OH\cdot \rightarrow H_2 + O_2$
$2\ H\cdot \rightarrow H_2$
$2\ OH\cdot \rightleftarrows O\cdot + H_2O$
$2\ O\cdot \rightleftarrows O_2$
$H_2O\cdot + 2H\cdot \rightarrow H_2O + H_2$
$H_2O\cdot + H_2O\cdot + O_2 \rightarrow 2H_2O_2$
$HO\cdot + H_2O \rightarrow H_2O_2 + H\cdot$
Additional reactions in the presence of oxygen
$O_2 \rightarrow 2\ O\cdot$
$O_2 + O\cdot \rightarrow O_3$
$O_2 + H\cdot \rightarrow OOH\cdot$ (or $OH\cdot + O$)
$O\cdot + OOH\cdot \rightleftarrows OH\cdot + O_2$
$O\cdot + H_2O \rightarrow 2\ OH\cdot$

Another major chemical phenomenon related to ultrasonic cavitation is sonoluminescence, by which a tiny light is formed in a cool liquid. This form of light emission results from the high-temperature formation of reactive chemical species in excited electronic states. Emitted light from such states provides a spectroscopic probe for the cavitation effect. Some electrical and thermal theories on this phenomenon have been reported [25].

1.3.1. Some rules of sonochemistry

Based on the existing sonochemical literature, ultrasonic irradiation seems to have been developed on a practical rather than on a theoretical basis. Justification for enhanced reactivity and process acceleration in general were largely rationalized by using the intuitively straightforward "hot spot" approach. Critics of ultrasound regarded it merely as a super-agitation tool. Careful examination and classification of published material on sonochemistry have allowed an empirical classification to be established [26,27]. While the classification focuses on the chemical effects of sonochemistry, it should also be recognized that, in some cases, US does act in a mechanical sense and provides outstanding results through super agitation. Occasionally, the mechanical and chemical effects occur simultaneously. The three rules derived from published material on sonochemistry are as follows [8]:

– Rule 1 applies to homogeneous processes, and states that the reactions which are sensitive to the sonochemical effect are those that proceed *via* radical or radical–ion intermediates. This means that sonication can effect reactions proceeding through radicals and that ionic reactions are not likely to be modified by such irradiation.

– Rule 2 applies to heterogeneous systems, which are more complex and where reactions proceeding *via* ionic intermediates can be stimulated by the mechanical effects of cavitational agitation. This has been termed "false sonochemistry", even though many industrialists may argue that the word "false" is incorrect here because if ultrasonic irradiation assists a reaction, the reaction is indeed assisted by sonication and thus "sonochemical". In fact, the true test for "false sonochemistry" is that similar results should, in principle, be obtained by using an efficient mixing system in place of sonication. Such a comparison is not always possible, however.

– Rule 3 applies to heterogeneous reactions with mixed mechanisms (*i.e.* radical and ionic). These will have their radical component enhanced by sonication, even though the general mechanical effect from Rule 2 may still apply. There are two possible situations for heterogeneous systems involving two different mechanism paths. If the two mechanisms lead to the same product(s) (*i.e.* the process is "convergent"), the sole effect will be an increase in the overall rate. On the other hand, if the radical and ionic mechanisms lead to different products, then sonochemical switching will be possible through a favoured radical pathway. In such "divergent" processes, sonication actually changes the nature of the reaction products.

Note that a very high-speed stirrer can have effects similar to those of sonication on heterogeneous systems. This may well be a case with the processes induced by hydrodynamic cavitation rather than acoustic cavitation [28,29].

The physical effects of ultrasound in relation to analytical chemistry have not yet been rationalized.

1.4. TYPES OF ANALYTICALLY USEFUL ULTRASOUND DEVICES: ADVANTAGES AND DISADVANTAGES

The source of high-energy vibrations in ultrasonic equipment is a transducer designed to convert either mechanical or electrical energy into ultrasound. There are three main types of US sources, namely: gas driven, liquid driven and electromechanical. The first type of source is used mainly in whistles and sirens. On the other hand, liquid-driven transducers are useful in applications where homogenization and efficient mixing are important. Finally, electromechanical transducers are the type used in analytical devices, even when homogenization and efficient mixing are required.

The two major types of electromechanical transducers are based on the piezoelectric and magnetostrictive effects; the former is most commonly used to power bath- and probe-type sonicators. Although more expensive than mechanical transducers, electromechanical transducers are by far the most flexible and widely used. Laser-induced ultrasound is a more recent type of transducer.

1.4.1. The piezoelectric transducer

The most common way of producing and detecting ultrasound utilizes the piezoelectric properties of certain crystalline materials, such as quartz. Figure 1.4 shows a simplified depiction of a quartz crystal. If a thin section of the crystal is cut in such a way that the large surfaces are normal to the *x* axis the resulting section will exhibit two complementary properties, namely: (1) the direct effect (*viz.* when pressure is applied across the large surfaces of the section, a charge of identical size with opposite signs will be produced on
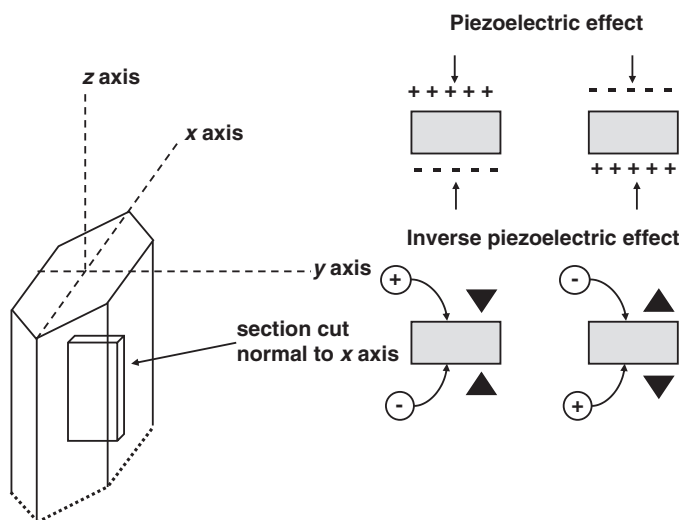
FIGURE 1.4. *The piezoelectic effect as produced by an x-cut quartz. (Reproduced with permission of Wiley-VCH, Ref. [8].)*

each face, the polarity being reversed if tension is applied across the surface); and (2) the inverse effect (*viz*. if a charge is applied to one face of the section, then the whole section will either expand or contract depending on the polarity of the applied charge).

Thus, applying rapidly reversing charges to piezoelectric material causes fluctuations in its dimensions. This effect can be harnessed with a view to transmitting ultrasonic vibrations from the crystal section through whatever medium it might be in. However, it cannot drive a given piece of piezoelectric crystal efficiently at every frequency. Optimum performance will only be obtained at the natural resonance frequency of the particular sample, which depends upon its dimensions. For an *x*-cut quartz crystal, a transducer 2.88-mm thick will have a natural frequency of 1 MHz, and one with 0.288-mm thick a frequency of 10 MHz. This is why most conventional sonochemistry equipment, whether baths or probes, uses a fixed frequency and why no comparative studies at widely differing frequencies have so far been performed using the same piece of equipment. Commercially available modulated, multimode, multifrequency US generators have opened the door for this type of test [30].

There are many piezoelectric materials besides quartz. Three of the more commonly used are barium titanate ($BaTiO_3$), lead metaniobate ($PbNb_2O_6$) and the mixed crystal lead zirconate–titanate. They are ferroelectric compounds (*i.e*. they are spontaneously polarized and the polarity altered by mechanical deformation). These materials cannot be obtained as large single crystals; rather, they are ground with binders and sintered under pressure at a temperature above 1000 °C to obtain a ceramic material. Usually, two elements are combined in order to increase the overall mechanical motion. The use of such different types of materials has allowed ultrasonic generators of variable power and frequency to be developed for a wide range of applications.

Piezoelectric devices based on using the so-called "1–3 composites", which consist of an array of piezoelectric pillars embedded in a pliable material providing a transducer in

the form of a flexible sheet, have opened up new avenues for development. The fact that the emitting face is a combination of ceramic and plastic substantially facilitates acoustic transmission into aqueous systems.

1.4.2. Commercial ultrasound apparatus for analytical applications

Of the four types of laboratory ultrasonic apparatus commercially available for practising chemists in general (namely, whistle reactors, ultrasonic cleaning baths, probes and cup-horn devices) analytical chemists, except for a few specialists working in (or with) ultrasound detectors, use mainly cleaning baths and probes both of which are usually operated at a fixed frequency dependent on the particular type of transducer, that is usually 20 kHz for common probe systems and 40 kHz for baths. Both types of devices are described below.

The ultrasonic cleaning bath

This is probably the most affordable and inexpensive piece of ultrasonic equipment available, which is why so many analytical chemists first use cleaning baths. A cleaning bath generally consists of a stainless steel tank with transducers clamped to its base, as shown in Fig. 1.5. One of the basic parameters in ultrasonic engineering is power density, which is defined as the electrical power delivered to the transducer divided by the transducer radiating surface area. An ultrasonic bath, which is a low-intensity device, uses a power intensity at the transducer face of about 1–5 W/cm^2 in modern piezoelectric transducers and operates at a frequency of 40 kHz. For the typical small size ultrasonic cleaning bath (1.5-l capacity), a single transducer is sufficient to drive it with a power rating of around 50 W. For larger devices (up to 50000 l), an array of transducers is required to introduce a high power density into the liquid. The frequency and power of an ultrasonic bath depend on the type and number of transducers it contains. The laboratory bath design has a few variants: some devices operate at different, albeit fixed, frequencies. Also, some cleaning baths use a "frequency sweep" of a few kilohertz about a central
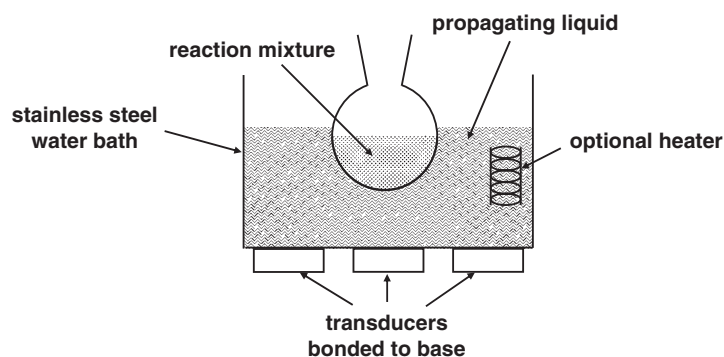
FIGURE 1.5. *A typical ultrasonic cleaning bath. (Reproduced with permission of Wiley-VCH, Ref. [8].)*

frequency in order to avoid standing waves in the tank. In this way, every part of the cleaning device is subjected to cavitation as wave nodes alternate in height from the base. Most recent commercially available designs include thermostatic control, time digital control, and integrated thermometer and data memory. Interestingly, some drawbacks of bath sonicators relating to power control and wave sonication have been neatly overcome. Thus, Bandelin [31], a firm specializing in ultrasonic equipment, manufactures the SONOREX DIGITAL 10P series, with power control over the range 10–100%, and also two-part ultrasonic cleaning units with additional lateral ultrasound, *i.e.* multifrequency devices (*e.g.* 25 and 40 kHz in the same bath). Unfortunately, these devices are only available in high volumes (from 115 to 239 l for industrial cleaning), but will foreseeably be scaled down for analytical use. On the other hand, the firm Raypa makes equipment that affords full-wave and half-wave operation (so-called "UCI" models) [32].

Choosing an appropriate ultrasonic bath. The usual way of subjecting an analytical system in a discrete manner to US by using a bath is simply by dipping the vessel containing the target analytical system in the sonicated bath. The energy supplied by the transducer must be strong enough to penetrate the walls of the vessel and cause cavitation in the chemical system. Not all laboratory cleaning baths are powerful enough for this purpose, so it is important to check any bath for power before using it to sonicate an analytical system, whether discrete or continuous. The easiest test to apply in all cases involves dipping a piece of ordinary household aluminium foil into the sonicated bath water, containing a detergent, for about 30 s. A bath which is suitable for sonochemistry will perforate the foil extensively within this period.

Advantages and disadvantages of ultrasonic baths. Although the cleaning bath is the piece of ultrasonic equipment most widely used by chemists, it is not necessarily the most effective. The advantages of using an ultrasonic bath are as follows:

(1) The US bath is the most widely available laboratory source of ultrasonic radiation.
(2) Small cleaning baths are inexpensive.
(3) The acoustic field is fairly evenly distributed throughout the bath liquid.
(4) No special adaptation of chemical apparatus is required. This allows conventional glassware to be used and facilitates the addition of chemicals, the use of high or low pressures or even an inert atmosphere.
(5) Using the cleaning bath itself as the reaction vessel affords more extensive bath treatment at an increased irradiation power. The use of this type of energy input, however, is subject to some restrictions.

On the other hand, the disadvantages of using an ultrasonic bath can be summarized as follows:

(1) The amount of power dissipated from the bath into the analytical system is usually not very large — less than 5 W/cm^2.
(2) The energy input must be assessed on an individual basis for each system as the amount of power actually delivered will depend on the bath size, the vessel type in batch steps or manifold type in continuous steps, wall thickness and bath position.
(3) Maintaining the temperature in the bath is difficult unless the US device is furnished with some automatic thermal control. Most cleaning baths warm up during operation, especially after prolonged use. This is not a problem if a heater is used to establish thermal equilibrium, but can lead to inconsistent results when working at or below room temperature.

There are two possible solutions to this problem, namely: (a) operating over very short periods during which the temperature can be assumed to remain essentially constant, or (b) circulating cold water or adding ice to the bath. If using ice, one should bear in mind that solids alter the characteristics of sonic wave transmission. Whichever method is chosen, it is the temperature inside the vessel that should be monitored as this is often a few degrees above that of the bath liquid.

(4) Not all cleaning baths operate at the same frequency. This may have some impact on the results, particularly when attempting to reproduce previously reported tests. Most manufacturers use frequencies around 40 kHz, but 20-kHz baths are available and some dedicated baths use higher frequencies.

(5) Although a few manufacturers make cleaning baths with adjustable power, most baths have no such control. One can always place a rheostat between the mains and the bath to accomplish some power control.

(6) The decline in power with time and the lack of uniformity in the transmission of US typical of inexpensive cleaning baths are two sources of high irreproducibility. For the above reasons, the use of laboratory cleaning baths should be restricted to cleaning operations or the removal of dissolved gases, which are indeed their principal intended uses.

Ultrasonic probes

Many of the disadvantages in using a simple cleaning bath in sonochemistry can be avoided by using an ultrasonic probe (also called a "sonotrode") instead. A sonotrode delivers its energy on a specific zone, cavitation in which is thus dramatically boosted. Also, probes are not subjected to any exhaustion restrictions, so they are much more suitable for use in analytical chemistry than are ultrasonic baths.

In addition, ultrasonic probes are more flexible as regards construction, so they can be easily designed for specific purposes. Some variables with a strong influence on US characteristics including the direction, amplitude and frequency of the vibrations at the point of application or the way the workpiece is clamped can be adjusted with a view to maximizing the effects on the process within the constraints of the ultrasonic system.

A US probe comprises the following components:

– A *power supply* to convert mains electrical power to the frequency, voltage and current required by the ultrasound system. All three must be continually monitored and automatically adjusted to keep the system operating properly.
– A *transducer* (or *converter*) to convert electrical power into mechanical vibrations. This is a tuned system resonating at the operating frequency.
– A *transducer cover* to protect the user from high voltages and the transducer from accidental damage. A cover is normally fitted around the ceramic discs, electrodes and electrical connections.
– *Piezoelectric ceramic discs*, which are the heart of the transducer. As a voltage is applied, the discs expand and contract along the transducer axis. Several discs (usually 2 or 4) are used to increase the movement produced. Using an even greater number of discs ensures that high voltage will be applied within transducer only.
– *Electrodes*, which are located on both sides of each ceramic disc and are used to apply the voltage that causes it to expand and contract.
– A *machine screw* (normally high-tensile steel) running through the centre of the transducer that clamps the ceramic discs together. The screw should be kept under

compressive stress, even when the transducer is stretched to its maximum, in order to prevent the discs from cracking.

– The *front-end* of the transducer (titanium or high-strength aluminium alloy), which is used to transmit its motion to the rest of the system.

– A *back-block* (usually steel or titanium) that provides a mass behind the ceramic discs to balance the motion of the transducer.

– An optional *booster* or interstage (titanium or high-strength aluminium alloy) fitted between the transducer and the ultrasonic tool. This is also resonant at the operating frequency. It alters — usually increases — the vibration amplitude and may also be used to mount all the mechanical parts of the ultrasonic system.

– The *extender*, which is not an essential part of the device as it is only required in order to reach into narrow vessels, through vessel necks or into process streams. These "extenders tips" are usually made in half-wave and full-wave length increments. They consist of simple cylinders, solid or tapped for a tip. Solid extenders are actually more than a wavelength increment and have to be fitted to tapped horns, so they are made longer than the wavelength increment by the length of the regular replaceable tip in order to maintain resonance.

– The *sonotrode*, which is the sole part of the system that can be exchanged as a function of the particular application. Sonotrodes come in all shapes and sizes, depending on the intended use; like other components, however, it should be resonant at the operating frequency. The material from which it is constructed (steel, stainless steel, titanium alloy, ceramics) should be a compromise between the needs of ultrasound and those of the application. This is an amplifying element also known as *horn* (or *probe*, which is also the name given to the whole device) and includes, or is fitted with, a *tip*. The latter is the radiating surface of the horn, which irradiates acoustic energy outwards to do work. Tips may be either removable or integrated with the final output element.

Originally, ultrasound probes were simply adaptations of biological cell disrupters. These involve direct immersion of a metal probe into the system under study.

Horn design. The probe, sonic horn or velocity transformer, is driven by the transducer and ultrasound enters the analytical system *via* the probe tip. The intensity of sonication (*i.e.* the vibrational amplitude of the tip) can be controlled by altering the power input to the transducer. There are alternative ways to control the power input to a system depending on the probe design, which is very important in US engineering. The variables to be considered in designing a horn include length, shape and gain. The vibrational amplitude of the piezoelectric crystal itself is normally so small that the intensity of sonication attainable by directly coupling the transducer to the analytical system is not large enough to cause cavitation. The horn acts as an amplifier for the transducer vibration, so its precise shape will determine the magnitude of the gain or mechanical amplification of the vibration. Accordingly, the horn is occasionally referred to as the "velocity transformer".

The *length* of the horn is a key variable. The wavelength of ultrasound in a material is dictated by both the nature of the material and the frequency of the sound wave. With titanium alloy horns, the wavelength for 20-kHz sound is about 26 cm, which constitutes the absolute limit of length for titanium horns. The horns can be as short as half a wavelength; however, should the distance between the transducer and the sample being processed need to be increased, they can be designed in multiples of half wavelengths. This can be accomplished by screwing one horn into another to build up the overall length.

The *shape* of the horn greatly affects its performance. Figure 1.6 shows a selection of different horn shapes. Uniform horns are horns fashioned in the shape of a uniform
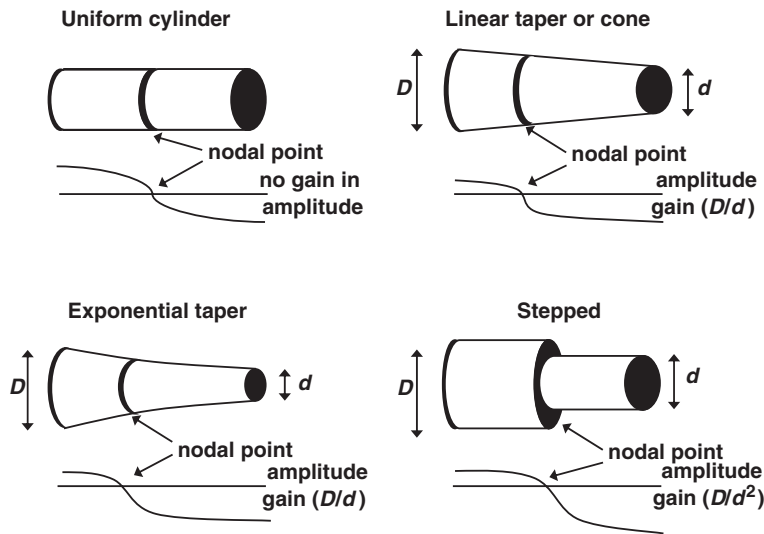
F<small>IGURE</small> 1.6. *Shapes of acoustic horns and magnification factors. (Reproduced with permission of Wiley-VCH, Ref. [8].)*

cylinder (*e.g.* 13 cm in length) subjected to an ultrasonic vibration (*e.g.* 20 kHz) at one end that produces an exactly identical vibration at the other end. However, there will be no vibration at the midpoint of the cylinder because this is the nodal point of the wave. If the cylinder needs to be reduced in diameter at its midpoint to 0.5 of the original cross-sectional area, then when the vibrational energy is applied to the larger end, the smaller end will automatically undergo a doubling of its energy density (the energy applied at the larger end will now emerge through half the area at the smaller end). In order to deliver this increased intensity, the tip, the vibrational frequency of which is fixed at 20 kHz, must vibrate at an increased amplitude. The horn will be acting as a velocity amplifier. For a simple "stepped" design, the amplification factor will always be the ratio of the cross-sectional area and this type of horn can easily accommodate variable gains, as shown in Fig. 1.7. The significance of the position where the "step" is placed should be appreciated. It is always at the nodal point of the horn because vibration is zero at this point (*i.e.* no stress is present). If the size reduction does not occur precisely at this null point, stress will develop (Fig. 1.6). Step horns provide maximum amplification (high gain) with high stress at the step; linear and exponential horns avoid stress with amplification factors given by the ratio of the end diameters rather than cross-sectional areas as with stepped horns. The linear taper is the easier design to manufacture, but its potential magnification is normally restricted to approximately 4-fold. On the other hand, the exponential taper provides higher magnification factors; its shape, however, makes it more difficult to manufacture, but the small diameter of the working end and its length make it particularly well suited to micro applications.

Because the amplification factor of the horn is dictated by its shape, measurements can be made on any surface normal to the longitudinal centreline. This affords measuring outside a sealed pressure vessel, even by direct contact, without breaching the vessel.

central electrode

case

double amplitude (peak-to-peak)

back driver

convertor

stack

25.4 μm

transducer crystals

front driver

gain factor = 1.25

31.75 μm

gain factor = 4

disruptor horn

127 μm

gain factor = 4

probe microtip

508 μm theoretical
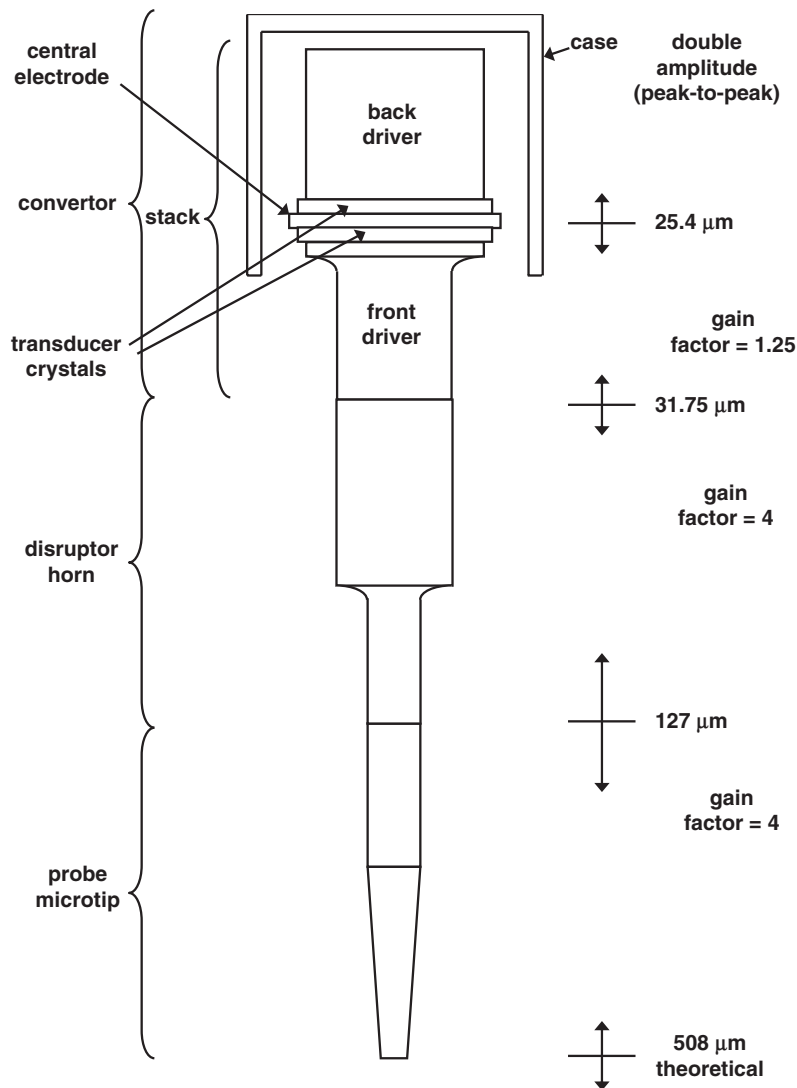
FIGURE 1.7. *Gain of an ultrasonic probe as a function of the diameter ratio.*

Choosing an appropriate ultrasonic probe. As noted earlier, a large maximum power density can be obtained at the radiating tip depending on the particular horn design used. The density achieved can be as high as several hundred watt per square centimetre. Until recently, the choice of probe sonicators was somewhat limited. At present, however, they normally have the following facilities: (a) variable power that can usually be adjusted by using a dial from zero to a maximum output of about 150 W/cm^2 through a probe tip 2.5 cm in diameter; (b) a pulse generator to allow intermittent sonication; (c) a range of

interchangeable horns and replaceable tips; and (d) a variety of extenders, flow-cells and other units.

Advantages and disadvantages of ultrasonic probes

Probe devices undoubtedly provide the most efficient method for transmitting ultrasonic energy into an analytical process or step.
   The advantages of using an ultrasound probe for this purpose are as follows:

(1) The ultrasonic power delivered by a horn is directly related to the magnitude of vibration of the tip. This can be readily controlled *via* the power input to the transducer, which allows precise regulation of the power supplied to the system. Maximum powers of several hundred watt per square centimetre can thus be easily achieved.
(2) Ultrasonic streaming from the tip of the probe operated at moderate power is often sufficient to provide bulk mixing when dipped in the target system since energy losses during the transfer of ultrasound through the bath media and reaction vessel walls are eliminated.
(3) Most modern units have a pulse facility allowing the operator to sonicate repeatedly for fractions of a second. This gives adequate time for "cooling" between pulses.
(4) The probe can be tuned to give optimum performance (tuning here is the process whereby the entire probe assembly is brought into resonance with the transducer). Modern equipment is normally fitted with an automatic frequency regulator.
(5) The ultrasonic intensity and size of sample to be irradiated can be matched fairly accurately for optimum effect.
(6) Modern commercial devices are designed to operate with a variety of frequencies, power ranges, detachable metal probes of different horn and tip diameters and other accessories from a number of manufacturers.

   On the other hand, disadvantages of ultrasound probes in this context include the following:

(1) As with all systems which operate using piezoelectric transducers, optimum performance is obtained at a fixed frequency. For most commercial probe systems such a frequency is 20 kHz and, although it is possible to drive them at their overtones (*i.e.* 40 or 80 kHz), the power dissipation at overtones is very much reduced. In order to operate successfully at different frequencies, it is best to purchase individual amplifier–horn systems tailored to one's individual requirements.
(2) As with baths, there is a problem over accurate temperature control unless some precautions are taken. The use of specially designed vessels alleviates much of this difficulty.
(3) The high intensity of irradiation in the zone close to the tip may produce radical species potentially interfering with the normal course of the experiment.
(4) Cavitation, which is the source of the main effects of ultrasound, is also the origin of a common problem with probe systems: tip erosion, which occurs despite the fact that most probes are made of a titanium alloy. There are two unwanted side effects associated with erosion, namely: (a) metal particles eroded from the tip will contaminate the system; and (b) physical shortening of the horn reduces efficiency — eventually, the horn will be too short to be efficiently tuned. The latter problem is avoided by

fitting the probe with screw-on tips in the form of studs. This avoids the need for a costly replacement of the whole horn.

(5) Special seals will be required if the horn is to be used in refluxing systems, inert atmospheres or at pressures above (or below) ambient level.

(6) Laboratory probe systems are generally only suitable for small systems, although multiple probes will cope with larger volumes.

An example of commercial US probe and additional units. One salient example is the Branson Sonifier II, which is a flexible laboratory unit available in two power levels usually required for disintegration and homogenization. This probe is widely used in analytical laboratories for assistance to any type of reaction and process, as discussed at length in Chapters 2–8. The power supply converts conventional 50-Hz line voltage to high-frequency electrical energy at 20 kHz. Figure 1.8 depicts some of the accessories available for this model, which range from cup horns with a water jacket to a continuous-flow attachment and are described below.

The following types of cells are available in addition to the standard horn (C in Fig. 1.8), standard microtip (H) and special microtip with proper coupling section (F) and extender (I).

Cup horn (B in Fig. 1.8), which constitutes a special type of ultrasonic bath where the energy is supplied by an inverted horn sealed into the bottom of a water jacket or cup. This allows better temperature control of the sonicated system and of power, at the expense of a limited cell volume and reduced power relative to a standard.

Accessory system
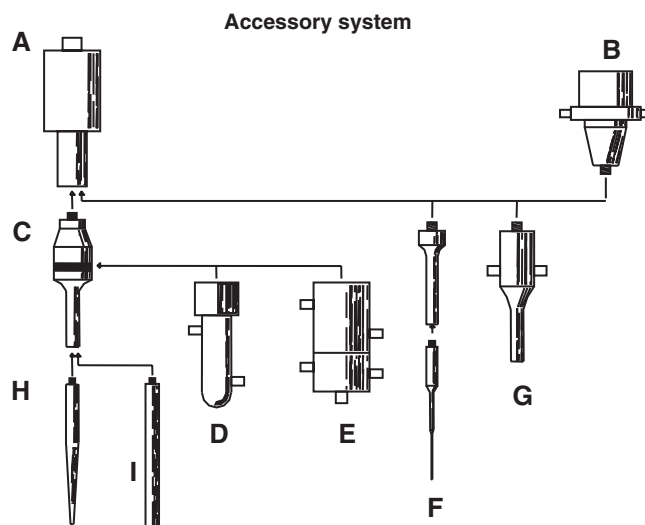
FIGURE 1.8. *The Branson Sonifier^R II and accessories. A — converter, B — cup horn, C — standard horn, D — sealed atmosphere chamber with water jacket, E — continuous flow-cell attachment, F — special microtip with coupling section, G — flow-through horn, H — standard microtip and I — extender. (Reproduced with permission of Branson Ultrasonics Corporation.)*

Sealed atmosphere chambers (D), which are particularly useful when special working atmospheric conditions are required.

Continuous flow-cells (E), through which the fluid under study is circulated while subjected to ultrasonication. A double chamber is used for cooling by circulating cold water through a closed circuit or an ice–salt mixture is employed to maintain low temperatures. One or more liquids are pumped into the cell, mixed and processed in the annulus, which is controlled *via* an adjustable orifice that can be moved in and out axially and is furnished with interchangeable orifice plates that afford full control over the process parameters.

Flow-through horns, or *tubular horns* (G), which possess a hollow core tip and two inlets or orifices at the non-vibrating, nodal point of the horn. This type of horn radiates radially outwards at right angles to the longitudinal axis, which allows it to process material placed in a pipe around it, a beaker or other vessel. This design ensures uniform mixing of two components by passing one fluid through the horn into the centre of the cavitational field, where it meets the other fluid coming radially inward from the body of the cell in which the flow-through horn is dipped. Because the latter fluid travels radially inward, all aliquots pass along a radius of equal length, thus ensuring uniform sonication and mixing with the former fluid directly in the cavitation field at the end of the horn.

The operator can control the way US is applied to the sample by specifying the required parameters for the test.

One can optionally use a temperature probe to measure the temperature of the liquid surrounding the vessel or chamber during the ultrasound-assisted process if the temperature especially influences the process concerned. One can set a maximum allowable temperature in the surrounding liquid, so that ultrasonication will be automatically stopped if the specified temperature is reached. There are four possible operational modes, namely:

– The continuous mode, where US is applied to the sample for a preset time.
– The pulse mode, where US is repeatedly switched on and off during the experiment, the operator setting the length of the on–off intervals.
– The temperature mode, in which US is applied until the sample reaches a given temperature; and
– The pulse–pause mode, which is used to maintain the temperature within a specific range. Ultrasound is applied to the sample while keeping the sample temperature between the limits of this range. This mode allows the sample temperature to be kept within the range while continuing the ultrasonic treatment during the process time.

Ultrasonication variables. Relationships

Intensity and power in probe sonication are two closely related but different concepts. Thus, *power*, which is measured in watts, is the energy required to move the mechanical masses used to create cavitation in a liquid or, in other words the energy required to drive the radiating surface of a given horn, at a specified amplitude of vibration (the excursion or stroke), against a specified load at the fixed resonant frequency of the device. On the other hand, *intensity* is a measure of the energy available per unit volume of liquid and is directly related to amplitude. It is the intensity of cavitation rather than the total power applied that determines the effectiveness of sonication. Intensity is directly related to the amplitude of the radiating face of the tip or horn. It is therefore such *amplitude* that must be delivered, maintained and monitored. For an ultrasonic liquid processor to be truly effective, it must provide controlled amplitude under variable load conditions within the specifications. This is accomplished by regulating the power output in order to maintain

the frequency against any imposed load, usually by adjusting the voltage applied on piezoelectric crystals or the magnetic coil in a magnetorestrictive device. The horn or probe tip can be assimilated to a piston travelling through a liquid cylinder. At the usual frequencies involved (generally 20 kHz or higher), the liquid molecules do not have time to restore fully after each stroke, so the extreme pressures and vacuum typical of this process are produced. The energetics are thus virtually identical to a simple hydraulics problem: the larger the piston (radiating face) diameter is, the longer will be the stroke (amplitude), the faster the stroke rate (frequency), the higher the static head (pressure), the more resistant and cold the liquid (viscosity), and the higher the power required to move the radiating face. Similarly, the faster and the further the tip is moved, the higher will be the energy imparted to the cavitation bubble and the greater the intensity of the energy released in the bubble implosion. As a result, the amount of power drawn depends on the geometry of the radiator–liquid arrangement and the intensity is only related to the amplitude (excursion) of the radiating face. The amount of power required to provide and maintain such an intensity is thus a multi-variable parameter.

In addition, the efficiency of cavitation is influenced by a number of variables and so, as a result, is the power drawn. As the load on the generator increases, the vibrating body reacts by decelerating, slowing in frequency. A well-designed generator will respond with more voltage to accelerate the motion of the radiating masses, thereby increasing the frequency. Once the system reaches its voltage limit, the amplitude cannot be increased further. In addition, and similar to "cleaning", once cavitation bubbles "blanket" the radiating face, an increase in amplitude will produce no more cavitation. Therefore, *blanketing* is a limiting phenomenon in the cavitation field: the density of the bubble cloud becomes so high that no further cavitation is possible by supplying additional energy — similar to the thermal boiling temperature, above which no further change of state occurs. The blanketing threshold is the intensity of cavitation where blanketing occurs. For practical purposes, such a threshold may be considered a relative term based on the efficiency of conversion from increased radiated energy to increased cavitation.

Ultrasonic devices operating in the air are subject to minimal pressure, so they require minimal power to maintain the amplitude.

Ultrasound power measurement. Although any report on the results obtained by using an ultrasound-assisted system should state the make and model of the irradiation source used, this is generally not so. Unfortunately, the power input to the chemical system is occasionally reported only as a quoted maximum rating for the equipment. A 500-W does not necessarily deliver 500 W of ultrasonic power into the target when operated at its highest setting. Some standard method of measurement is thus required in order to record the actual power input to the chemical system. Measurement methods for this purpose can be physical (*e.g.* those involving measurement of the vibration amplitude of a probe system, the real electrical power to the transducer or calorimetric measurements of the ultrasonic power entering a chemical system) and chemical (*e.g.* those used by the iodine, Fricke, terephthalate and nitrophenol dosimeters). The two types of methods are described in detail elsewhere [33,34].

Comparing bath and probes

As noted earlier, the power supplied by baths (particularly cleaning baths) decreases with time; as a result, the energy of baths is not supplied in a constant way, which can have significant consequences over long preparation times. This requires applying the energy

for an additional time in order to offset its decline with time. Also, the local ultrasound intensity delivered by baths is strongly affected by many external parameters including the water level for ultrasound transmission, the ultrasound intensity, the shape of the vessel and its position, etc. As a consequence of the formation of standing waves, the local intensity in a flask placed in a US cleaner is markedly influenced by changes in the experimental conditions, which has a strong impact on precision. Therefore, the optimal sonication conditions for each ultrasound bath must be established on an individual basis. This restricts the use of baths in processes that are strongly influenced by the ultrasound intensity. Concerning the water level, if this is significantly lower than half the wavelength of the ultrasound in water (λ = 2.3 cm), then the ultrasound intensity decreases with increasing distance from the sound source. When the water level is equal to or greater than $\lambda/2$, intensity profiles of standing waves are observed. Finally, when the water level is approximately a multiple of $\lambda/2$, resonating standing waves appear that result in extreme local ultrasound intensities. The problem is that the shape of the profiles changes when variables such as the ultrasound intensity, solvent level or shape, or position of the leaching vessel are modified. Also, in the absence of temperature control by recirculation of the water contained in the bath, the precision is even more seriously affected. Another serious problem arising when trying to reproduce previously reported tests is that ultrasonic baths operate at frequencies and powers dependent on the transducers they use, the geometries of which are specific to the particular manufacturer. This often precludes direct comparison of data obtained with different ultrasonic baths.

By contrast, ultrasonic probes have the advantage over ultrasonic baths in that they deliver their energy on a localized sample zone, thereby providing more efficient cavitation in the liquid. Also, they are not subjected to any exhaustion restrictions, so they are much more suitable for use in analytical chemistry than are ultrasonic baths. However, probes tend to uncouple; as a consequence, cavitation occurs only at the radiating surface and only marginal ultrasound intensity can be detected elsewhere in the surrounding liquid.

Traditionally, one of the principal advantages of baths over probes has been the ability to handle several samples simultaneously. Conventional probes process samples one by one. Currently available high-sample throughput probe devices allow the simultaneous sonication of up to 12 samples.

Earliest commercial uses and subsequent non-analytical uses of ultrasound

The *echo-sounder*, which was invented and developed by Paul Langévin in 1917, was the first commercial application of US. Subsequently, it became the underwater SONAR (SOund Navigation And Ranging) system for submarine detection during World War II. The early echo-sounder simply sent a pulse of ultrasound from the keel of a boat to the bottom of the sea, from which it was reflected back to a detector also on the keel. For sound waves, because the distance travelled through a medium was one-half the product of the time by the velocity (and the velocity of sound in seawater is accurately known), the distance to the bottom was gauged from the time taken for the signal to return to the boat. If some foreign objects (*e.g.* a submarine) were to come between the boat and the bottom of the seabed, an echo was produced from this in advance of the bottom echo.

Essentially, all imaging from medical ultrasound to non-destructive testing relies on the same pulse-echo type of approach, but with considerably refined electronic hardware.

The refinements enable the equipment not only to detect reflections of the sound wave from the hard, metallic surface of a submarine in water, but also much more subtle changes in the media through which sound passes (*e.g.* those between different tissue structures in a body). This type of application uses high-frequency ultrasound (in the range 2–10 MHz) primarily because the short wavelengths involved facilitate detection of small areas of phase change (*i.e.* they provide increased "definition"). The analytical uses of high-frequency ultrasound for detection purposes are essentially concerned with measurement of either the velocity of sound through a medium or the degree to which sound is absorbed (attenuated) as it passes through it. These applications are diagnostic in nature and have no effect on the chemistry of the target. These analytical uses and the particular tools they involve are discussed in Chapters 9 and 10.

Commercial ultrasound devices for high-throughput analysis

Developments in areas where a large number of samples must be analysed in as short a time as possible rely on automating existing analytical methods. Sonication had until recently never been used in automated methods for high-throughput pharmaceutical, biochemical, clinical and screening analysis primarily because sonicators could not accommodate such numbers of samples. However, some companies such as MatriCal Inc. or Hielscher Ultrasound Technology have recently made commercially available devices that allow all steps of the analytical process involving the use of ultrasound as an auxiliary form of energy to be implemented in an automated manner. Thus, the SonicMan™ is a high-throughput sonication system equipped with disposable 96-, 384- or 1536-well plates and capable of delivering sound energy at 20 kHz from 0 to 1150 W and pulses that can be adjusted in 0.1-s intervals up to 20 s. The transmitted energy is estimated to be 12 W/pin for a 96-well plate and 3 W/pin for a 384-well plate at full power; also, the energy is supplied evenly across all pins.

The tips are disposable parts, so, should they become contaminated or fail after prolonged sonication, they are easy and relatively inexpensive to replace. A "pin tip" has a useful life of approximately 200–300 s of sonication at 100% power. The tip is an injection-moulded part coated on both sides with silicone rubber layers and through which "pins" are inserted. The 40-durometer silicone rubber on the upper surface provides a compliant layer such that when the sonic horn is applied to the surface of the tip, any pins that are slightly higher will be depressed until all pins are in uniform contact with the sonic horn. This ensures that each pin in any format will be fully coupled to the sonic horn. The soft 20-durometer silicone rubber layer on the bottom of the tip is used to seal each well from other wells surrounding it such that there will be no cross-contamination between wells during sonication. The pins are made of brass with a nickel coating that in turn is electroplated with a 10-μm-thick gold coat as early tests on plain brass pins revealed that some chemicals (particularly those with very low pH or containing reactive sulphur groups) can react with the pins. Such was not the case with electroplated-gold-coated pins.

Scale up ultrasonic devices

Large-scale processing using power US is not a new concept. The industrial uses of power US were recognized in the 1960s, as reflected in many specialized articles [35]. Progress has been faster over the last few years for two main reasons, namely the

broader awareness of the potential for ultrasonic processing, and an ever-widening span of uses that have attracted attention and investments from an increasing number of firms.

There are essentially two different types of large-scale US-assisted chemical plants: batch and flow type. Sometimes, the flow system is an integral part of the batch processing equipment, where it acts as a loop attached to the main vat.

Small-scale experiments are occasionally adapted to large-scale work; this requires an accurate knowledge of the type of sonochemistry involved in the process.

The first question to be answered in scaling up a sonochemical reaction is whether the reaction is in fact truly sonochemical or simply the result of an ultrasonically induced mechanical effect. Thus, in a solid–liquid heterogeneous reaction, power ultrasound may only serve as an efficient mixing method system — for particle fragmentation, deagglomeration and (or) dispersion. In this situation, ultrasonic pretreatment of a slurry may well be all that is required before the reaction is allowed to take place in the conventional manner. However, if ultrasound has a real effect on the chemistry of the system, then arrangements must be made to provide sonication during the reaction itself. Scaling up a true sonochemical process requires answering the following major questions:

(1) What is the most suitable sonolysis system for the reaction mixture to be processed?
(2) What are the best reaction conditions?
(3) What will be the energy implications of using ultrasound rather than traditional methodology?

These questions are not easily answered because of the large number of factors to be considered. Thus, optimizing the sonication conditions entails carefully examining the variables influencing cavitation, namely:

(1) The reaction medium (particularly its viscosity, vapour pressure, the nature and concentration of any dissolved gases and the presence of any solid particles before, during, or after reaction).
(2) The reaction conditions, including the temperatures and pressures involved, which may well vary during a conventional process.
(3) The type of sonic system used (particularly its power and frequency) and the chemical reactor (its size and geometry).

Although most scaled up US-assisted systems have traditionally been chemical systems, there is a growing trend to exploit US energy for assisting physical processes in the biochemical field; such is the case with a large-scale acoustic filter for perfusion of cell cultures [36] or a novel h-shaped ultrasonic resonator for the separation of biomaterials [37].

Ultrasound devices for industrial use

Industry uses special devices similar to ultrasonic baths and probes but appropriately scaled up in size and ultrasound irradiation power. The UIP16000 model from Hielscher Ultrasound Technology is by far the most powerful ultrasonic processor available worldwide; the apparatus is capable of delivering a continuous power of 16 000 W at efficiency above 80%. Such powerful systems have been developed in response to the demand for the ultrasonic treatment of liquids on a large scale; in fact, the ultrasound power required usually increases in proportion to the amount of liquid to be treated within a certain time.

It is therefore more cost effective to use a large ultrasonic system supplying 80 kW to process liquids at a flow-rate of 10 m^3/h than to use 5 ultrasonic processors with a power of 16 kW each or 40 processors with a power of 2 kW each. The robustness of the transducer enables its use under heavy-duty industrial conditions. Also, the processor can be designed to be explosion-proof. Like the transducer and the flow cell, the generator is housed in two connected compact stainless steel cabinets. This makes the device self-contained, robust and easy to install. The standard footprint of a 16-kW system is just 600 mm × 1200 mm.

Recently [38], Prosonix has been launched as a new American company with the aim of exploiting academic technology to apply ultrasonics to crystallization control and process intensification on a commercial scale.

Immersible transducers

An immersible transducer is a radiating device accommodated in a housing which can be submerged in a liquid bath to energize the liquid and produce cavitation. An immersible transducer placed in a still tank therefore turns that tank into an ultrasonic cleaner. The immersible transducer is, in effect, a standard tank (turned inside out) with the radiating surface on the outside and the transducers on the inside.

1.4.3. Maintenance and troubleshooting of ultrasound devices

Failure modes in horns

Horns — transducers, extenders and (or) boosters — can fail for various reasons. Thus, horns behave as longitudinal bells that are carefully crafted to resonate "primarily" in the axial mode. Like any elastic body, when a horn shrinks in one or two dimensions, it must expand in the other(s). By analogy with a differential piston, a small excursion of the larger diameter will result in an increased excursion of the smaller diameter. Because mass must be conserved, the centre of mass — hopefully the nodal point, where the molecules are being alternately forced together and apart, both radially and axially in opposite cycles — has the greatest stress. Thus, the fatter the horn (*i.e.* the lower its aspect ratio), the more likely it will be to heat and fail at the nodal point. The horn ends (especially that exhibiting the higher amplitude of excursion, where the molecules are primarily in alternating longitudinal tension and compression) have the highest strain (see Fig. 1.9). Thus, the strain is worst where the connections are made to the convertor–front driver–transducer and at the tip — if removable. Any imperfection in material or construction at either the node or the antinodes, then, will become a stress raiser (a point of likely failure).

At the node centres, the most critical place is the step, where (*viz.* the transition from one diameter to another) any notch from damage or from poor design or machining is almost guaranteed to cause failure, especially at high amplitudes. Similarly, at antinodes (ends), any flaw in the connecting stud, grit in the joint, non-planar mating of the opposing faces or skewed alignment, for example, will almost certainly cause heating and eventual failure. In cases of extreme extension (as in ultra-high amplitude microtips), operating near or at the tensile limit of the material, the slightest discrepancy can cause virtually instantaneous failure. Such failure is not catastrophic, except financially: the horn, tip or stud merely fractures and falls apart, sometimes almost instantaneously. Quite often, however, the immediate precursor and warning is a screech of tortured metal.

	Amplitude	Strain	Stress
stud			
antinode	low	low	zero
horn			
node	zero	zero	high
antinode	high	high	zero
tip			
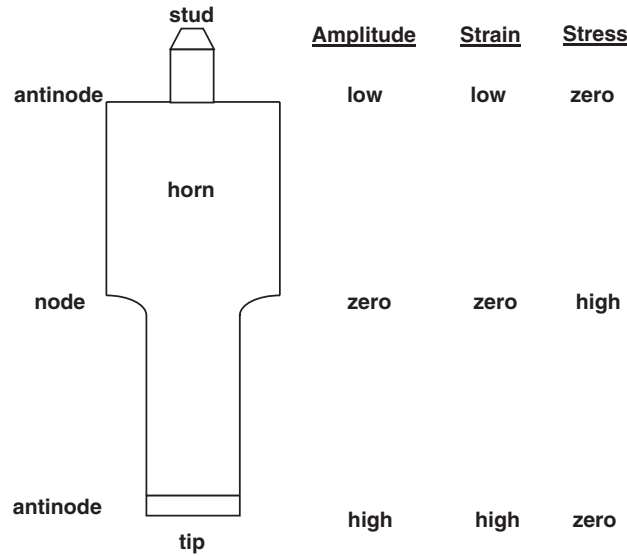
FIGURE 1.9. *Performance of the different zones in a horn.*

Like the bath, the probe does suffer from the same difficulty regarding temperature control. This problem has been alleviated or circumvented in modern devices by using the pulse-mode or temperature-mode operation. The pulse facility was originally designed for biological cell disruption, where temperature control is crucial and allows ultrasound power to be delivered intermittently, thereby allowing for periods of cooling. The time (*i.e.* the pulse length) for which the sound energy is delivered to the system is controlled by an instrument setting and may be varied from 0%, where no energy is supplied, to 100%, which is continuous application of the energy. For sonochemical applications, however, there is a minimum time period (pulse) which must be exceeded if any cavitational effects are to be observed. This is a consequence of the time delay between the application of the acoustic excitation (*i.e.* the sound wave) and the onset of cavitation; as a result, the pulse of acoustic energy may not be present long enough for the cavitation bubble to be produced. By way of example, let us consider the growth of a bubble of radius 8×10^{-5} cm in water at ambient temperature at 1 atm under an applied field of frequency 5 MHz and pressure amplitude (P_A) of 4 atm. For the first 1/8 of the acoustic cycle (*i.e.* 25 ns), the bubble size will increase only slightly (ca. 5%). Even after 1/4 of a cycle (*i.e.* 50 ns), it will have grown by only about 30%. During the next 1/4 of a cycle, it will grow to a size large enough (approximately twice its initial radius) to collapse totally (*i.e.* for cavitation to occur under the action of the applied acoustic field). Thus, if the pulse is present for less than 1/4 of a cycle (50 ns) at this frequency, the bubble will not have sufficient time to grow to a size causing it to collapse. In general, the threshold intensity decreases as the pulse length increases and an upper limit for pulse length is usually reached after which the threshold remains independent of the pulse length. At 20 kHz, such an upper limit is approximately 20 ms.

Pulsed operation should not be confused with the *duty cycle* as used in medical ultrasound applications or adopted for pulsed operation in users' manuals for commercial

equipment. In medical parlance, the duty cycle refers to the on–off ratio for scanning which involves the emission of pulse of extremely short duration (*e.g.* 10^{-5} s) spanning only a few cycles of ultrasound in the megahertz range. It is in the longer, off period that the echoes are detected. By way of contrast, a chemical sonicator pulse of 0.5 s spans 10 000 cycles at 20 kHz.

Maintenance of tips

The vast bulk of tips and horns are made of titanium alloy, monel, nickel, "bell metal" alloys, glass, ceramic or single-crystal radiating faces. The very action of cavitation erodes — and, to a smaller degree, accelerates corrosion of — the radiating surface of the replaceable tip or solid horn. Performance degrades in proportion to the degree of roughness of the surface until a point is reached, if the tip does not disintegrate or stop resonating first, where no significant energy passes into the liquid sample. Tips which are so heavily eroded that the dendritic peaks and valleys are obvious to the unaided eye can trap air or gas bubbles in the concavities and ultimately stop radiation. Most manufacturers supply tips with a smooth finish, but it is a waste of time and money to mirror-polish tips as the finish will matte almost instantly on use. The wear pattern is generally symmetrical on a round or rectangular face, with a small rim of uneroded material remaining around the edge and the balance of the face becoming gradually darker as material is eroded and the surface roughened. The exception to this is when wear occurs in an abrasive particulate suspension, in which case the impact of the particles polishes the surface even as it erodes it. Serious erosion usually occurs in concentric rings and really severe erosion can eat into the dendritic structure of the tip, even perforating through the back end (the tip–horn joint), in which case the horn itself becomes eroded and useless. Moreover, when erosion progresses so far that pitting extends into the smooth, erosion-free circumferential ring at the edge of the tip face, the tip (or solid horn) is irreparable and must be replaced.

   Tip life can be best extended by polishing the tip — its radiation surface only — with abrasive paper or cloth. The face should never be lathed as too much material will be removed and, taking into account that the tip is a part of a finely tuned resonant body, the removal of material will shorten the tip length and thus raise the natural resonant frequency.

   In order to properly dress a worn tip — when the erosion has progressed beyond simply matting of the finish — the tip or horn should be held absolutely normal to a piece of fine carbide grit paper or emery cloth — never sandpaper — placed on a hard, flat work surface, and worked lightly across the grit in a circular pattern. The tip must never be rocked or scored by bearing down heavily as anything that detracts from a smooth, flat finish will cause accelerated erosion.

Minimization of ultrasound side effects

Some side effects of ultrasound may be detrimental in specific situations and reduce the efficiency of ultrasonic power.

Foaming and aerosoling. When foam forms in a lab sample, it interposes bubbles between the radiating surface and the body of the liquid to be treated or in which treatment is to occur. This is somewhat akin to "blanketing", but is the result of gas bubbles, not cavitation bubbles, interfering with free radiation of acoustic energy into the bath.

The process is self-limiting. Once foam is formed, especially in viscous liquids, sonication must be stopped and the liquid degassed. In some cases (*e.g.* at a low viscosity), bubbles may rise against gravity and escape through the liquid surface. If, however, they persist, short bursts of energy (pulsing) with long rest times in between may suffice to break the foam. A fine mist of the parent liquid can be sprayed against the foam to break it; ultrasonic nozzles excel at this. In extreme cases, centrifuging and (or) vacuum must be applied or the sample may even have to be discarded. Foaming can be detected by a change in the sound level and a fluctuating reading on the power bar graph.

Similarly, on the reverse stroke, molecules of liquid adhering to the surface of a vibrating object may be dragged above the interface (liquid surface) and released, or even ultrasonically nebulized and driven off balistically, into the atmosphere (*i.e.* "aerosoled"). This can obviously increase significant risks if the liquid is toxic or contains biohazards. Various techniques, the description of which is beyond the scope of this book, are available for minimizing aerosoling or preventing aerosol escape. When aerosoling occurs, little or no energy couples reliably to the solution, and excessive top-layer heating results. This problem can be remedied by placing the probe as deep as possible and setting the amplitude control to a low level (10–20%) for a few seconds, followed by a gradual increase of the amplitude to the required level.

In order to avoid foaming or aerosoling, the horn can always be dipped enough below the surface of the liquid to prevent violent motion or agitation on the surface. This problem is more critical when processing small volumes (*e.g.* 0.3–5 ml). Use of a conical-shaped tube or vial such as a cut-down Eppendorf tube is recommended in this situation to raise the liquid level without increasing the volume, thereby permitting the horn to be inserted more deeply below the liquid surface level.

Bubbles formed in the bulk liquid sample during sonication may also represent sonochemical degradation products or high volatiles driven out by cavitation. If any such phenomena are to be expected, then appropriate chemical analyses should be performed before undertaking a critical process.

Flammable or explosive volatiles may be driven out by cavitation and ignition. Virtually no sonication devices are explosion-proof and only extreme measures can render them explosion resistant.

Discolouration. This phenomenon can occur in the processed sample if the tip touches the side of a glass tube or beaker and small glass particles are released, the sample acquiring a greyish colour as a result. Excessive tip corrosion can also cause a greying or darkening condition.

Sterilization. This operation, intended to prevent cross-contamination, can be easily carried out by removing either the horns or tips from the converter and autoclaving them. It is faster, easier and equally effective, however, to sterilize these units by immersing them in a beaker containing alcohol or other disinfectant and then, turning the power on for a few seconds. This operation also removes unwanted residues from the horn or tip.

1.5.   ULTRASONICS, HEARING AND HEALTH

Questions are sometimes raised about the potential harmful effects of ultrasound produced by laboratory-scale devices. Available data indicates that airborne ultrasonic fields do not appear to be hazardous to humans. There are, in fact, no known physiological effects from airborne ultrasound. Ultrasonic "sickness" appears to be largely psychosomatic,

engendered by apprehension or fear of the unknown. Most "awareness" of these processes is due to hearing the "high-audible" components of the noise, not ultrasound. The frequencies used range from 20 kHz and above. The upper threshold of normal human hearing is around 16 kHz. Individuals capable of hearing 20 kHz and above report only a "sensation", rather than discomfort. It should be stressed to concerned individuals that the creation of sound waves involves no electromagnetic radiation. The acoustic energy passing through the air is at intensities far lower than those emitted by high-fidelity equipment; there is therefore no reason to fear harm, for example, to a fetus *in utero*.

The sound emanating from an open vessel in which an ultrasonic processing horn is being operated is radiated primarily through the air–water interface and secondarily through the walls and bottom of the vessel. Ordinary industrial ear muffs or stopples will block the greater part of this noise, which is primarily in the 5–8 kHz range. Processing often takes place in a fume hood or fume enclosure which will effectively dissipate the sound energy. Special sound reduction cabinets are available to enclose the processor and vessel, however. The sound emanating from ultrasonic cleaners is also primarily radiated through the air–water interface. Any minor change in temperature, depth, or surfactancy of the cleaning solution, or in the bulk of material or number of objects immersed in the tank (or the depth of immersion), will dramatically reduce such noise. The degree to which the cleaning solution has been degassed will also have a significant effect on noise output. Use of a tank cover, preferably with an elastomeric gasket between it and the tank rim, is also helpful.

It is important to isolate the processor, vessel, or cleaning tank from tables, walls, ducts, or other furnishings which could act as, or transmit vibrations to, resonant surfaces. Tanks and generators should be mounted on elastomeric feet. Processing convertors and cells should be held in elastomeric clamps. Tubing connections to processing cells should always be flexible, both to minimize sound transmission and to avoid interference with the resonant horn. Proper attention to such details will prevent potential annoyance to personnel and complaints about mysterious maladies. In mechanical operations such as welding, tip contact against a hard object can generate formidable levels of sound; effective protection should therefore be provided in these situations.

One major source of internal sound (as opposed to that from the process) is that emanating from a loose or damaged horn or tip, or from a failing stack; it can be incredibly loud and piercing — and, also, harmful. Similarly, many manufacturers and users of ultrasonic equipment routinely test it in open spaces without acoustic radiation protection; in so doing, they place their workers at risk and are liable for the consequences. Thus, again similarly, anyone working under such conditions must either do something about it or quit — or suffer attendant hearing loss. Unexplained inaudible sound at very high frequencies can cause a reaction of anxiety, of unease, while that at very low frequency can cause depression; understandably, none of these reactions occur when the subject is aware of the situation.

1.6.   USING ULTRASOUND TO ASSIST VARIOUS STEPS OF THE ANALYTICAL PROCESS

Although the use of ultrasound to assist sample preparation has so far been limited in relation to its potential [39,40], few analytical chemists are unaware that US can help, improve, accelerate or automate the preliminary steps of the analytical process — particularly those preceding sampling (*e.g.* cleaning the lab material or degassing solvents). Ultrasound has also found a variety of uses in the detection step ranging from

improving the way that the sample reaches the detector or detection itself to the development of little-known special detection techniques [41].

Therefore, analytical chemists can exploit ultrasound as soon as they start developing a method for purposes such as expediting and (or) improving the performance of the different steps to be carried out. This book therefore focuses on the ways the analytical chemists can use US energy in order to facilitate an educated choice relying on an appropriate knowledge of the potential impact of US on each step of the analytical process.

With this aim in view, the chapters that follow this exposition of principles of US, the ways they are implemented in the various types of devices available, and their advantages and restrictions, are structured as follows: Part I (Chapters 2–8) is devoted to US and sample preparation; and Part II (Chapters 9 and 10) deals with US and detection.

Specifically, Chapter 2 discusses the concept of sample preparation and its implications. Ways of minimizing or avoiding the main problems posed by solid and liquid samples with the aid of US applied in the typical scenarios for two analytical chemical works (*viz.* discrete and continuous systems) are proposed. Also, the use of US prior to sample preparation is discussed before dealing with specific sample preparation methods suited to the physical state of the sample and the treatment it required for presentation to continuous separation equipment (whether a chromatograph or a capillary electrophoresis module) or directly to the detector for monitoring, detection, characterization and (or) quantification.

Chapters 3 and 4 deal with US-assisted treatment of solid samples involving variable degrees of dissolution. Thus, Chapter 3 is devoted to processes involving total dissolution of a solid, usually by the use of a drastic treatment like digestion; and Chapter 4 deals with partial dissolution of the target components in order to enable the use of a less drastic solution than digestion (*e.g.* leaching). The processing of fine solid particles suspended in a liquid (slurry) with the help of US, which causes some dissolution before the suspension reaches an atomic detector, in addition to other heterogeneous systems such as agglomeration, filtration, crystallization, defoaming, nebulization and sonophoresis, are the subject matters of Chapter 5.

Chapter 6 is concerned with analytical steps involving liquid samples (or liquids resulting from the steps discussed in Chapters 3 and 4). Thus, liquid–liquid extraction, emulsification and homogenization, among others, can be assisted by US under appropriate conditions.

Chapter 7 deals with other types of US assistance to enhance reactions of analytical interest including derivatization and reagent generation, or ultrasound-assisted oxidation or hydrolysis reactions.

Finally, Chapter 8 discusses some well-established detection techniques such as electroanalysis, which has been greatly improved by US assistance and led to the development of sonoelectroanalysis, and others in which ultrasound has provided a more efficient way of placing or transporting the sample — or the solution resulting from a given treatment — to the detection point (*e.g.* ultrasound-assisted levitation or nebulization).

Part II of the book deals with lesser known aspects of US for the analytical chemists such as its use as an energy source for detection purposes. Thus, ultrasound-based detection techniques (*viz.* US spectrometry in its various modes including ultrasound attenuation, ultrasonic velocity, resonant ultrasound, laser-generated, ultrasound reflection and acoustic wave impedance spectroscopies) are dealt with in Chapter 9. Finally, Chapter 10 is devoted to selected applications of US spectrometry — mostly non-analytical applications from which, however, analytical chemists can derive new, interesting analytical uses for ultrasound-based detection techniques.

References

1. T.J. Mason, *Ultrason. Sonochem.*, 10 (2003) 175.
2. M. Chanon and J.L. Luche, Sonochemistry: Quo Vadis, in J.L. Luche (Ed.), *Synthetic Organic Chemistry*, Plenum Press, New York, 1998.
3. K.S. Suslick and G.J. Price, *Annu. Rev. Mater. Sci.*, 29 (1999) 295.
4. M. Ashokkumar and F. Grieser, *Rev. Chem. Eng.*, 15 (1999) 41.
5. K.S. Suslick, *The Year Book of Science and Future, Encyclopedia Britannica*, Chicago, 1994, p. 138.
6. P.R. Birkin, J.F. Power, M.E. Abdelsalam and T.G. Leighton, *Ultrason. Sonochem.*, 10 (2003) 203.
7. Y. Matsumoto, J.S.Allen, S. Yoshizawa, T. Ikeda and Y. Kaneko, *Exper. Thermal Fluid Sci.*, 29 (2005) 255.
8. T.J. Mason and J.P. Lorimer, *Applied Sonochemistry*, Wiley-VCH, Weinheim, 2002.
9. J.F. Spengler, W.T. Coakley and K.T. Christensen, *AIChE J.*, 49 (2003) 2773.
10. S. Umemura, K. Kawabata, N. Nugita, K. Sasaki and N. Yumita, *Intern. Congress Series*, 1274 (2004) 164.
11. B.E. Noltingk and E.A. Neppiras, *Proc. Phys. Soc. B (London)*, 63B (1950)674, 64B (1951) 1032.
12. H.G. Flynn, in W.P. Mason (Ed.), *Physical Acoustics* vol. 1B, Academic Press, New York, 1964.
13. E.A. Neppiras, *Phys. Rep.*, 61 (1980) 160.
14. C. Campos-Pozuelo, C. Granger, C. Vanhille, A. Mossatov and B. Dubus, *Ultrason. Sonochem.*, 12 (2005) 79.
15. V. Sáez, A. Frías-Ferrer, J. Iniesta, J. González-García, A. Aldaz and E. Riera, *Ultrason. Sonochem.*, 12 (2005) 67.
16. N. Kudo and K. Yamamoto, *Intern. Congress Series*, 1274 (2004) 129.
17. P.R. Gogate and A.B. Pandit, *Ultrason. Sonochem.*, 12 (2005) 21.
18. G.V. Ambulgekar, S.D. Samant and A.B. Pandit, *Ultrason. Sonochem.*, 12 (2005) 85.
19. K.S. Suslick, *Scient. Amer.*, Feb. (1989) 80.
20. L.R.F. Carvalho, S.R. Souza, B.S. Martins and M. Korn, *Anal. Chim. Acta*, 317 (1995) 171.
21. C.A. Wakeford, R. Blackburn and P.D. Lickiss, *Ultrason. Sonochem.*, 6 (1999) 141.
22. H.N. McMurray and B.P. Wilson, *J. Phys. Chem.*, 103 (1999) 3955.
23. G. Wibetoe, D.T.Takuwa, W. Lund and G. Sawula, *Fresenius J. Anal. Chem.*, 363 (1999) 46.
24. P.R. Birkin, J.F. Power and T.G. Leighton, *Chem. Commun.*, 21 (2001) 2230.
25. T.J. Mason and J.P. Lorimer, *Sonochemistry: Theory, Applications and Uses of Ultrasound in Chemistry*, Ellis Horwood, Chichester, 1989.
26. J.L. Luche, Sonochemistry: From Experiment to Theoretical Considerations, in T.J. Mason (Ed.), *Advances in Sonochemistry*, JAI Press, London, 1993.
27. J.L. Luche, C. Einhorn and J.V. Sinisterra-Gago, *Tetrahedron Lett.*, 31 (1990) 4125.
28. V.S. Moholkar, P.S. Kumar and A.B. Pandit, *Ultrason. Sonochem.*, 6 (1999) 53.
29. J. Reisse, C. Caulier, Y. Dekerckheer Kegelaers, N. Segebarth and K. Martik, *Sonochemistry and Sonoluminescence*, NATO ASI Series, Kluwer Academic Publishers, 1999, p. 205.
30. http://activeultrasonics.com
31. Bandelin Electronics, GmbH & Co KG Heinrichstraβe 3-4, D-12207, Berlin, Germany: http://www.bandelin.com
32. R. Espinar, S.L. Avda. del Vallés, 322 Pol. Ind. "Els Bellots", 08227 Terrassa, Barcelona, Spain: http://www.raypa.com
33. T.J. Mason, *Practical Sonochemistry. User's Guide to Applications in Chemistry and Chemical Engineering*, Ellis Horwood, Chichester, 1991.
34. T.J. Mason, *Sonochemistry*, Oxford University Press, Oxford, 1999.
35. T.J. Mason, *Ultrason. Sonochem.*, 7 (2000) 145.

36. V.M. Gorenflo, L. Smith, B. Dedinsky, B. Persson and J.M. Piret, *Biotechnol. Bioeng.*, 80 (2002) 438.
37. H. Böhm, L.G. Briarty, K.C. Lowe, E. Benes and M.R. Davey, *Biotechnol. Bioeng.*, 82 (2003) 74.
38. Business Concentrates, *C&EN*, April 10, 2006.
39. M.D. Luque de Castro and J.L. Luque-García, *Acceleration and Automation of Solid Sample Treatment*, Elsevier, Amsterdam, 2002.
40. F. Priego-Capote and M.D. Luque de Castro, *Trends Anal. Chem.*, 23 (2004) 644.
41. F. Priego-Capote and M.D. Luque de Castro, *Trends Anal. Chem.*, 23 (2004) 829.

CHAPTER 2

Generalities on Ultrasound-Assisted Sample Preparation

2.1. GENERALITIES ON SAMPLE PREPARATION: THE CONCEPT
OF "SAMPLE PREPARATION"

The analytical process involves preliminary operations, measurement of the analytical signal, and acquisition and processing of the information it provides. The first step in the process varies and includes operations such as sampling, dissolution or leaching (of solid samples), filtration, clean-up, preconcentration and derivatization.

Sampling is a complex process by virtue of the large number of factors which can influence it; such factors include sample homogeneity, the type of sampling model (*e.g.* randomized, stratified) used, the physical state of the system (solid, liquid, gas) and its stability, and the analyst's expertise. Consequently, the complexity of the sampling operation depends on the particular application, which makes generalization impossible. In addition, some analytical methods exclude sampling in the analytical process as the sample would be unchanged before and after the process. Therefore, sampling can be dealt with separately.

A sample can be named differently at different stages of the sampling process (see Fig. 2.1). Although the definitions of sample at the different stages are beyond the scope of this book and can be found elsewhere [1], the last two in Fig. 2.1 require some clarification for easier understanding here. Thus, "test sample" is the name given to "the sample taken or formed from the laboratory sample by a process involving homogenization using physical or mechanical treatments such as grinding, drilling, milling or sieving"; therefore, the sample only requires physical changes to reach this stage. On the other hand, the "analytical sample" is "the final product of sampling, which serves for the determination of at least one quality characteristic" and "is obtained by subsampling the test sample directly or by chemically or physically treating the test sample or a subsample of it, to provide a form suitable for analysis". From the latter definition it follows that the solution obtained after solid–liquid extraction (the extract), dialysis (the dialysate) or elution from a sorbent (the eluate) is an "analytical sample". This generic name is shortened by most analytical chemists, who name any solution from any process — after which only a minimum part of the sample is contained in the solution — "sample". In order to avoid potential misunderstanding, the authors have chosen to use the unequivocal name of the solution resulting for each specific treatment (*viz.* extract, dialysate, eluate) throughout the book.

The other preliminary operations following sampling can be dealt with as a whole in relation to the concept "sample preparation" (SP). This term is widely used at present, but is occasionally confused with sample pretreatment as the boundary between the two (*i.e.* where sample pretreatment ends or what precedes and follows sample preparation), if any, is rather ill-defined. To the authors' minds, sample preparation includes every step required to make the sample — or, rather, the target analytes contained in the original sample — ready for insertion into the measuring instrument and may involve more than one step; this is consistent with IUPAC's statement that "sample preparation is intended to transfer or transform the analytes into measurable forms" [2]. On the other hand, sample pretreatment can be envisaged as the first step in sample preparation or as a step
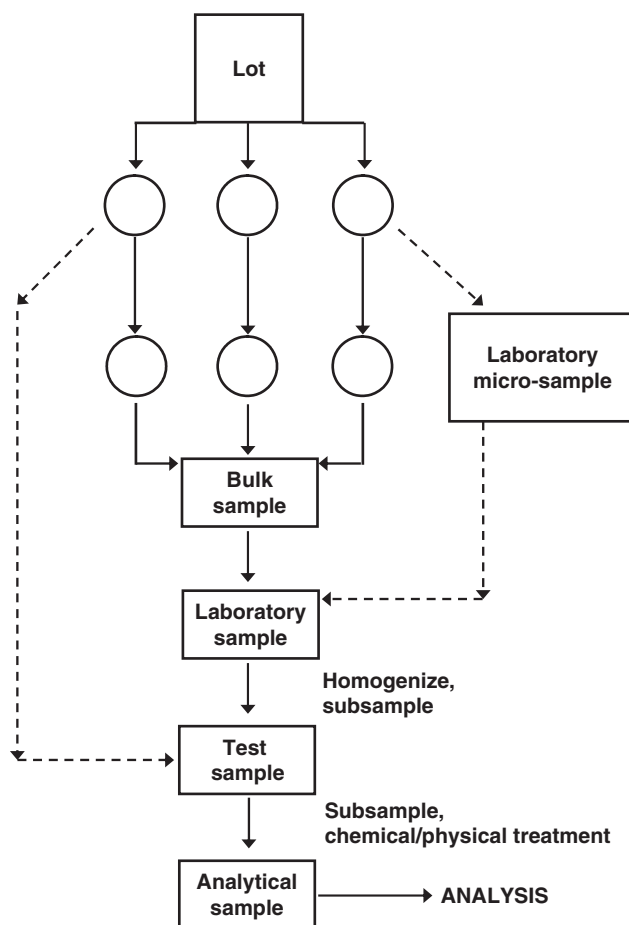
FIGURE 2.1. *Schematic diagram of the sampling stages and associated terminology.*

preceding one other specific action (*e.g.* a pretreatment for either subsequent liquid–liquid extraction or insertion of a solution into a chromatograph). From this point of view, it is unclear when such a step finishes and detection starts in some cases (*e.g.* ionization in methods using MS detection or vapourization and atomization treatments in atomic detectors).

Sample preparation is most often a necessity as even the simplest samples are frequently unsuitable for direct analysis. The need in most cases arises from excessive dilution or concentration of the target analytes in the sample or from incompatibility with standard instrument operation procedures. A large number of SP approaches have been devised to enable the detection of analytes that range from classical operations, many of which (*e.g.* calcination, wet digestion or Soxhlet leaching) have been used for centuries, to modern operations reported less than two decades ago (*e.g.* supercritical fluid leaching). In any case, both classical and modern operations are being continuously improved.

Sample preparation is the most crucial step and also the bottleneck of most analytical methodologies; also, it constitutes the principal source of error in the analytical process and remains one of the most time-consuming steps. In fact, in modern uncertainty evaluation methods, the uncertainty associated with chemical preparation of the sample will be a part of the uncertainty budget of the final result [3]. Therefore, an improvement in SP can greatly help the analytical process. The foregoing has led to the increasing recognition of SP as a legitimate area of specialization in analytical chemistry in response to the growing advances and reliance on instrumental analysis. In fact, SP equipment is evolving like chromatography and spectroscopy in the past. However, SP is still consolidating, albeit incredibly rapidly.

Efforts at introducing novel sample preparation modes are frequently not accompanied by implementation for the development of analytical methods. By way of example, most methods of analysis adopted by official bodies rely on traditional SP techniques. This can be ascribed to the fact that traditional methods are used in routine analytical laboratories and analysts know their functioning quite well. However, the traditional SP methods also have well-known shortcomings such as those derived from the use of toxic organics and multi-step procedures that often result in the loss of analytes and preclude integration with the other steps of the analytical process. Recycling pure solvents causes more problems than it solves and is generally unfeasible in spite of the increasing availability of integrated solvent management programmes.

This situation is changing for many reasons and new sample preparation techniques are being introduced at a steady pace. Automation and miniaturization in sample preparation are two widespread current trends that meet the needs of analytical chemistry and are implicitly included among the research priorities of the twenty-first century. This is a consequence of the development of miniaturized analytical separation systems, which has been recognized as one of the most important endeavours in this context as it fulfils many requirements and enables rapid analyses at low operational costs and causes no environmental pollution problems. Typical examples of miniaturized separation systems include the equipment for analytical separations involving hyphenated techniques such as LC-MS or CE-MS, which have been developed over the last few decades. After learning about the success of micro-scale separation techniques, many scientists are trying to find ways to miniaturize sample preparation processes especially suited to these micro-scale separation systems. The most recent trend in SP is therefore miniaturization and the focus is on how to miniaturize the process and which medium to use for the extraction and preconcentration of sample components. The benefits are obvious: shorter analysis time, reduced solvent and sample consumption, and the ability to process large numbers of samples simultaneously.

Concerning solvent consumption, the costs associated with the use, transport and disposal of solvents in general these days provide an economic incentive to minimize it. In addition, this is consistent with existing policies aimed at reducing environmental contamination in view of the renewed awareness about the pollution and hazards of the organic solvents and inorganic acids on which many current sample preparation methods rely, which has promoted international initiatives to suppress their use. This phasing out of solvents is poised to induce a major change in analytical methodologies and also provides an opportunity to formulate practical alternatives to existing sample preparation methods. This is the case with the recent SP methods based on the use of water as the only solvent [4,5].

The attention given to SP technology is increasing to a much greater extent than it has in the past, such that it has become an acceptable area of academic interest for knowing traditional methods and innovating new methods, but rarely for receiving

appropriate funding. Users at present know much more about traditional sample preparation procedures than they did in the past, and they are realizing the influence of sample matrix characteristics on, for example, analyte extractability in terms of a fundamental knowledge on extraction kinetics and thermodynamic analyte–matrix interactions.

Concerning new SP approaches, however, the present trend is to develop new methods or improving existing ones in order to overcome the shortcomings of classical SP. Examples of the latter include the use of auxiliary energies to assist sample preparation steps, or the development of new materials for solid-phase extraction. The ideal sample preparation technique should be solvent-free — or, at least, use as little solvent as possible — applicable to a wide range of matrices and hence to a variety of situations; also, it should allow simultaneous separation and concentration of the target analytes, and be amenable to on-site use.

New sample preparation technologies have been slow to develop despite their proved advantages over some of the older technologies. Modern SP methods include in-tube solid-phase microextraction [6] and liquid-phase microextraction [7], and have been largely devoted to bioanalytical applications — mainly to ensure biospecificity or a high selectivity — and membrane technologies [8]. The greatest hurdle that keeps practitioners from adopting new analytical methods is the expenses, in terms of both capital cost and training requirements, involved. Thus, in spite of many strong driving forces such as increased sample loads, decreasing skilled labour force, increased worker safety and less exposure to chemical hazards, the need for enhanced productivity, better quality data with increasing regulatory constraints, and the greater need for information management, automation of SP and integration of information management into the analytical process have been accepted with some reluctance.

2.2.   PREPARATION OF SOLID SAMPLES

As noted earlier, some of the steps that precede the insertion of the treated sample into the instrument for measurement (*e.g.* dissolution, clean-up, preconcentration, individual separation, derivatization) can have a critical influence on accuracy and precision depending on the particular step. All analytical processes include a sample preparation step which is a function of a number of factors such as the physical state of the sample, the nature of the sample matrix and analytes or the type of detector, for example. The first distinction therefore refers to the nature of the sample: solid, liquid or gas. Solid samples are the most difficult to process as most analytical instruments cannot handle them. Therefore, the first operation in solid sample preparation involves transferring the target analytes to a liquid phase. This can be carried out in various ways including total dissolution of the test sample or partial dissolution or separation of a portion thereof. The different choices, which can be assisted by ultrasound, are depicted in Fig. 2.2, and discussed in the following sections.

2.2.1. Definitions

As defined by IUPAC, "dissolution is the process of mixing two phases with the formation of a new homogeneous phase (*i.e.* the solution)". No distinction is made regarding nature of the phases.

There are various ways of dissolving a solid, of which suspension in a solvent with agitation is the simplest, but also unfeasible in most cases. On the other hand, digestion
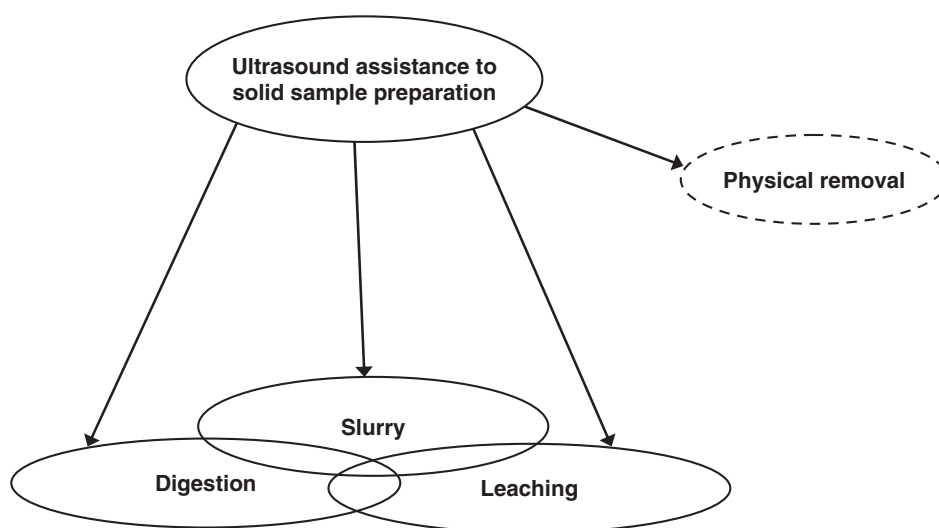
FIGURE 2.2. *Classification of US-assisted solid sample preparation procedures.*

is the choice requiring the strongest conditions. The word *digestion* has several, rather different meanings. Thus, the Oxford English Dictionary (OED) defines it as "the operation of dissolving a substance by the action of heat and moisture", whereas Webster's Third New International Dictionary (WTNID) provides the definitions "the process by which a material is softened or decomposed by heat or moisture or a chemical, often under pressure" and "the process by which soluble ingredients are extracted from plant or animal materials by warming a liquid". The last definition is fairly close to that for a solid–liquid extraction and therefore departs from the former WTNID definition and OED's. IUPAC defines digestion as "a chemical process for softening or solubilizing a material with heat, chemical reagents, and moisture". Accordingly, the digestion process must be performed with the assistance of heat, chemical reagents and pressure. Also, calorific energy can be substituted or aided by other auxiliary energies in order to accelerate sample digestion. There are various ways of dissolving a sample by digestion depending on the particular conditions. Thus, if the sample is mixed with an appropriate flux material, heated until melting and then allowed to cool before the fusion cake is dissolved in a suitable solvent, the process is called *fusion*; if the digestion is carried out with pure or mixed concentrated acids or bases, we are referring to *wet digestion*, and to *dry ashing* when the sample is heated at 400–500°C in a muffle furnace for several hours and the target elements are either converted into gaseous species and collected into an appropriate absorber for determination or kept as a residue and dissolved into a suitable acid for analysis. Dry ashing is especially commonplace as a pretreatment step in the analysis of organic samples for metallic and non-metallic elements. The three previous classical treatments have been used for a long time, and frequently officially recognized as digestion methods. Enzymatic digestion is a more recent process with a high potential [9]. Digestion involves dissolving

the whole sample produced by a chemical reaction — mainly oxidation or reduction — which destroys the initial structure of the matrix. However, digestion occasionally fails to ensure complete dissolution owing to the presence of compounds insoluble under the digestion conditions used or formed during digestion by interaction with some reagents (*e.g. aqua regia*). This is known as "partial digestion" or "selective digestion" as only a portion of sample and (or) some analytes are dissolved. This may be preferred to total decomposition if the relative concentrations of the analytes in the test sample can provide rich enough information. A filtration or centrifugation step is mandatory in this case in order to remove suspended matter.

Another way of passing the target analytes to a liquid phase is *solid–liquid extraction*, which is also known as *leaching* or *lixiviation*. The term extraction is defined as "the act of separating or otherwise obtaining (as constituent elements or juices) from a substance by treating it with a solvent, distilling, evaporating, subjecting to pressure or centrifugal force, or by some other chemical or mechanical process" by WTNID and as "the action of obtaining (elements, juices, etc.) from a thing or substance by any chemical operation". To IUPAC, extraction is "a separation method in which a liquid solvent causes the transfer of one or more analytes into it from contact with a second liquid or solid phase mixture". The word "extraction" is generic because it states nothing about the nature of the phases involved in the extraction process or how it is performed. Also, IUPAC's definition does not distinguish between the solid or liquid nature of the initial phase of the analyte. Therefore, it can be confusing, so "leaching" is more appropriate to refer to solid–liquid extraction. The WTNID definition of leaching is "the process or an instance of separating the soluble components from some material by percolation", and the OED definition "subjecting to the action of percolating water with a view to removing the soluble constituents". Although the OED definition is restricted to water, the term is also applicable to solvents other than water. IUPAC's definition is similar to the WTNID definition, so leaching is the specific concept for solid–liquid extraction by solubilization of the analytes, which also coincides with lixiviation. Usually, other sample components that behave like the analytes are also removed. As passage of analytes to a liquid phase is accomplished by more or less selective solubilization, the sample matrix rarely loses its initial appearance. The difference between digestion and leaching is clear even in visual terms.

Based on the most widely accepted meanings of leaching and digestion, the former process is more desirable whenever possible. Leaching the sample with complete removal of the target analytes provides a less complex liquid and the possibility of avoiding interferences. However, leaching is not a specific step, but only more selective than digestion because it maintains most matrix interferences in the solid. It is therefore common to use clean-up steps after leaching in order to remove any species that behave like the target analytes in the leaching step. However, complete dissolution of the analytes must be ensured if they are to be quantified precisely. Special care must be exercised in applying to natural samples a method that has been developed with spiked matrices.

Another choice for solid sample preparation is the use of slurries (see Fig. 2.2). This choice has been used mainly for the determination of metallic elements with atomic detectors and has the advantage that this is the only sample preparation step required (in addition to grinding, sieving, etc.). Slurries for insertion into electrothermal atomizers are prepared by adding a liquid to the solid material, which is previously ground, sieved — if necessary — weighed and placed in a container for analysis. One requirement is that the slurry should remain stable during the time required up to analysis. Slurries are therefore an alternative to digestion that dispenses with the need to decompose

the sample and also to leaching in those cases where obtaining a high efficiency in a short time is difficult. The introduction of slurries into atomic detectors combines some of the principal advantages of direct solid and liquid analysis. The advantages of the former include: (a) expeditious sample preparation times; (b) decreased analyte losses through volatilization or other phenomena prior to analysis; (c) reduced analyte losses through retention by an insoluble matrix in the case of leaching; (d) decreased likelihood of contamination by reagents, containers, etc.; (e) increased sensitivity resulting from the need for no sample dilution; (f) avoidance of hazardous acid, toxic or environmentally unfriendly solvents; and (g) the ability to selectively analyse microamounts of solids. On the other hand, the advantages of direct liquid analysis include: (a) the ability to introduce microamounts of samples into atomic detectors without the need to alter the instrument (conventional liquid sample handling apparatus such as autosamplers can be used for this purpose); (b) that to use simple liquid standards for quantitative calibration; and (c) that to add chemical modifiers. Also, the principal advantages of incorporating slurry preparation into the analytical process are as follows: (a) the ability to use an autosampler for unattended operation, thereby avoiding potential errors in transfers between containers; (b) that to process several replicates with a single aliquot and hence obtain a more accurate measure of precision; (c) that to manipulate large amounts of sample to improve representativeness; and (d) that to easily alter the slurry concentration by changing the solid–liquid ratio in order to fit the analytical signal within the best interval of the calibration curve.

Although digestion, leaching and slurry preparation refer to three different operations, the distinction is purely theoretical. Thus, the three terms are used interchangeably by many authors, either because they pay little attention to the specific mechanism by which analytes are made ready for determination or because a confluence of processes conceals the precise underlying mechanism. Thus, the following overlapped processes are possible:

(a) Overlapped digestion and leaching. The conditions used in some leaching methods are so strong that they destroy the sample structure. Therefore, one cannot speak of complete digestion since a suspended residue that is crumbly in appearance most times is obtained as a result. This sample treatment is made more similar to digestion by the presence of a number of matrix interferences that are dissolved together with the target analytes, so the process is far from selective.

(b) Overlapped digestion and slurry preparation. When the conditions used to obtain the slurry are so drastic that they cause complete dissolution of the sample, the process is actually a digestion. Most often, slurry preparation involves the use of low acid concentrations (about 5% v/v) and some other reagents (*e.g.* detergents such as Triton X–100) to increase the stability of the slurry [10]. However, the use of drastic conditions occasionally results in complete sample dissolution rather than suspension. The use of auxiliary energies (*e.g.* microwaves, ultrasound) also favours total dissolution.

(c) Overlapped leaching and slurry preparation. Partial dissolution of suspended particles always occurs during slurry formation and transfer to the detector, so more or less selective partial leaching occurs depending on the particular characteristics of the liquid phase. Partial and total leaching of the slurry can be distinguished by centrifugation in order to remove suspended matter. The difference in concentration between the slurry and solution upon centrifugation will be a measure of the leaching process.

2.2.2. Misused terms

Suspension in a solvent with agitation, which constitutes the simplest and most time consuming — and, also often, the most unfeasible choice — is regarded as a direct dissolution method. When assisted by US, this operation is also termed dissolution, which is in fact the general name designating the phenomenon as such; more precisely, however, if total dissolution of the sample is accomplished, then one should speak about digestion as auxiliary energy — and also reagents many times to facilitate dissolution — was used. In some other cases, only partial, selective dissolution is pursued, but the general term is also used. Some examples can help one match the appropriate term to each type of process.

Misused terms in relation to ultrasound-assisted solid sample pretreatment

Digestion. The influence of ultrasound on the dissolution kinetics of phosphate rock in HNO_3 solutions [11] and variables affecting it (*viz.* particle size, reaction temperature, acid concentration, amplitude of US power) were studied by Tekin [12]. The term dissolution in the presence of auxiliary energy and an acid seems inappropriate in this case as the process is more like a true digestion. Another case in point is the dissolution of pyrite ores in acid and $Fe_2(SO_4)_3$ solutions, which is improved by 30% with respect to the absence of US energy [13].

Chemat *et al*. [14] found the joint use of US and microwaves for the treatment of edible oils for the determination of copper to shorten the time taken by this step to about a half that was required in the classical procedure (heating in a Büchi digestor) or with microwave assistance, nitric acid and hydrogen peroxide. However, they did not state the specific medium where the microwave–US-assisted method was implemented and assumed US to have mechanical effects only, even though they mentioned a cavitational effect. This is a very common mistake in working with US that is clarified in an extensive discussion by Chanon and Luche [15] of the division of sonochemistry applications into reactions which were the result of "true" and "false" effects. Essentially, these terms refer to real chemical effects induced by cavitation and those effects that can be ascribed to the mechanical impact of bubble collapse. The presence of one of these phenomena only has not been demonstrated in the work of Chemat *et al*. [14] — despite the illustrative figure in their article — so their ascribing the results to purely mechanical effects of US was unwarranted.

Ultrasound is widely used as a pretreatment with a view to accelerating the subsequent anaerobic digestion of waste-activated sludge or stabilized sludge. There is some debate over what type of phenomenon does the US produce. Wang *et al*. [16] believe that US dissolves organic substances; Tiehm *et al*. [17] state that both sludge hydrolysis and raw sludge disintegration occurs. Also, Chiu *et al*. [18] claim that the joint effect of an alkaline medium and US produces hydrolysis, which they assessed from the amounts of soluble COD, organic nitrogen, and total volatile fatty acids produced, and also from biochemical acid potential-enhanced tests. Enhancements amounted to 84%, which clearly reflects the favourable effect of US. On the other hand, Onyeche *et al*. [19] state that US pretreatment of stabilized sludge causes cell disruption. On the other hand, Chu *et al*. [20] call this step a "weak" ultrasonic pretreatment and state that the total ultrasonic energy input to biosolids is inadequate to fully disrupt the floc structure of the cell walls as reported earlier. The discrepancy may have arisen either from the differences in the thorough study of the sonolytic effect or in US power and energy.

Whichever name is given to the US effect of improving sludge for subsequent anaerobic digestion, one important outcome is that sonication does not affect the bacteria that affect digestion [21].

Leaching. The general term "dissolution" is also widely used when only a portion of the solid is brought to a liquid phase. Such is the case with dissolution of crystallized salts in building materials [22], where only the target salts are put into solution. This is also a clear case of selective leaching that reflects the efficiency of US: the time required when the sample is subject to shaking at 60°C, 72 h, is reduced to only 45 min under 50-kHz US.

"Isolation" is also occasionally used instead of leaching or lixiviation. Such is the case with the procedure conducted under the influence of neutral protease and high-intensity US to dissolve starch in rice [23]. Inspection of the starch structure by high-performance size-exclusion chromatography and scanning microscopy revealed no damage to the molecular network or the starch granule surface; however, sonication increased the peak viscosities of rice starch.

"Extraction" is also widely used in connection with solids; in fact, the names of some techniques such as supercritical fluid extraction include this word even though leaching is the actual underlying phenomenon in most instances. In the presence of US, some authors add the qualifier "cold" to clarify that no bulk heating is produced by this energy. This jargon is frequently used in relation to the leaching of metals from a variety of solids, especially soil and sludge [24].

"Dissolution" was also used instead of leaching by Trofimov *et al.* [25] in studying the US enhancement of the leaching kinetics — approximately 100% — of uranium oxides in supercritical carbon dioxide. Readers cannot be aware of the actual phenomenon involved until the authors state that after "adding hydrogen peroxide to the supercritical system, other uranium oxides different from UO_3 can be extracted". Also, readily dissolved solids have been subjected to US for faster dissolution (*e.g.* milk powder for the determination of iron [26]). Strictly speaking, the use of auxiliary energy made the operation of digestion proper, even though the authors referred it as dissolution.

Slurry preparation. The isolated phenomenon of fine particles remaining in suspension during their transfer to a nebulizer — the most frequent use of slurries in analytical chemistry — is unusual. Partial dissolution of the solid to an extent dependent on the solubility of the sample components always occurs and is significantly or drastically enhanced by the presence of US. Such is the case with the determination of arsenic in sediments, coal and fly ash slurries, where, following suspension of the sample powder in *aqua regia* and hydrofluoric acid, US was applied for 30 min. Then, the slurry was diluted with hydrochloric acid and allowed to stand for 48 h before hydride generation and transportation to an AA spectrometer [27]. The process was more akin to partial digestion than to slurry formation, but the authors failed to compare it with total digestion.

Some contradictory results are obtained in the comparison of results in the determination of arsenic after ultrasonic slurry sampling — the use of "sampling" is not most appropriate in this case as the sampling step is before the slurry formation — ultrasound-assisted extraction — "leaching" has been the correct word in this case — and microwave-assisted digestion [28], which will be treated in detail in Chapter 5.

Also incorrect was the use of "slurry" to refer to the treatment of biological samples in a 3% nitric acid solution that were subject to US in autosampler cups prior to transferring the supernatant to an ETAA spectrometer [29]. This was clearly a US-assisted leaching step that took place in autosampler cups.

Physical removal. The physical removal of target analytes, which involves separating volatile species from a solid by heating or magnetically separating metals in most cases, has never to date been assisted by US energy. This void is shown by dashed lines in Fig. 2.2. Scientists working in these fields are encouraged to study the effect of applying ultrasound to their target systems.

2.3.   PREPARATION OF LIQUID SAMPLES

Although liquid samples are seemingly less prone to requiring energy assistance for proper development, acceleration or automation of a given step, a number of sample preparation steps are indeed improved by ultrasound. Figure 2.3 shows the most salient examples including and excluding a chemical reaction assisted by US.

2.3.1. Ultrasound-assisted liquid sample preparation involving chemical reactions

Any system involving a homogeneous liquid in which bubbles are produced is strictly not homogeneous; in sonochemistry, however, it is not unusual to deem systems under ultrasound homogeneous. Sonochemical effects generally occur inside the collapsing bubble, where extreme conditions are produced, or at the interface between the cavity and the bulk liquid, where the conditions are far less extreme, or in the bulk liquid immediately surrounding the bubble, where the dominant effects are mechanical in nature.

Derivatization has been assisted by US in some cases, both in continuous [30] and in batch approaches [31] and provides substantially improved product formation in all cases. Because the US was intended to improve a reaction, the origin of the effect was generally not studied and the effect was occasionally ascribed to degassing by US [31].
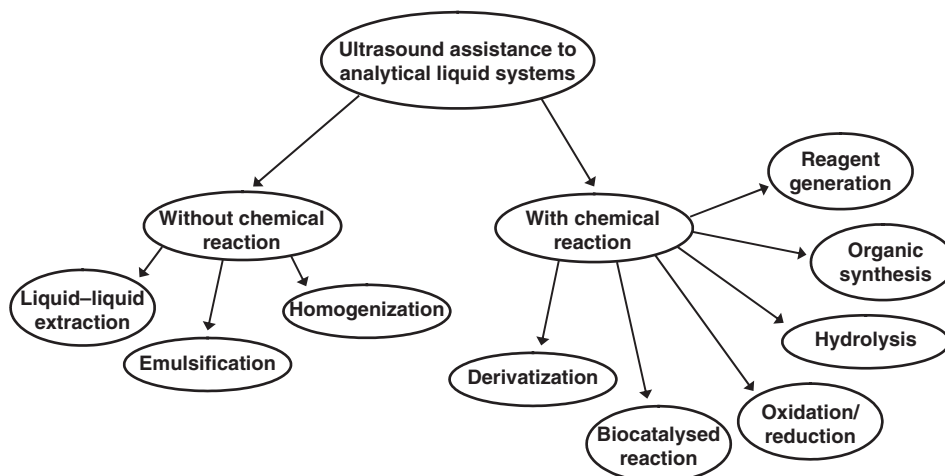
FIGURE 2.3. *Classification of US-assisted liquid systems.*

The accelerating effect of US on the determination of phosphate by the Molybdenum Blue method was ascribed to depolymerization of molybdate, which was thought to speed up its reaction with phosphate and increase the sensitivity [32].

Biocatalysed reactions assisted by US have mainly to do with *enzymatic digestion* [9]. These processes, which can involve solid, liquid and heterogeneous samples, are far from real digestions as only the target analytes are removed, the remaining sample components preserving their appearance, in most cases. This is a relatively novel use of the US–enzyme couple, particularly in hydrolysis reactions [33]. By contrast, US assistance to the joint use of enzymatic catalysis and supercritical fluids, which has aroused much analytical interest [34], continues to be unexplored as yet.

Oxidation reactions are dramatically enhanced by US energy, as discussed in detail in Chapter 7. Analytically, US-assisted oxidation reactions are of enormous interest. Two cases in point are the determination of the oxidative stability of edible oils [35], where the analysis time is reduced from 129 h to only 50.5 min, and the degradation of highly contaminated organic compounds, which is typically 10 000 times faster than natural aerobic degradation [36].

Organic syntheses, which are usually activated by heat or light, for example, have found an excellent energy source for the acceleration and (or) activation in ultrasound. This application of US has been the subject of specialist books [37,38] or chapters thereof [39]. One case in point is the mediated electrosynthesis of carbon–carbon bonds in totally "green" surfactant-free emulsion media generated by the application of power ultrasound to a two-phase water–organic medium [40]. The authors called these immiscible media erroneously as "mixtures".

Hydrolysis. Ultrasound assistance to hydrolysis reactions largely involves organic systems — both liquids and solid–liquid systems, which are dealt with here simply to reduce the number of subheadings — but also in inorganic systems — mostly heterogeneous. One example of the latter is the improved photocatalytic activity of titania-only materials fabricated by an ultrasound-assisted hydrolysis process, on which US has an elusive effect [41]. In any case, organic hydrolysis is by far a much common application of US. These reactions almost invariably require high-intensity ultrasound [42,43]. When two immiscible phases are involved — which is most often — the authors consider the liquid–liquid interphase as interface [44].

Reagent generation. US has scarcely been used to generate reagents, even though it has proved highly effective for this purpose (*e.g.* with oxidant species [45,46]). The effect of US on these reactions has not been properly explained or exploited so far, however.

2.3.2. Ultrasound-assisted liquid sample preparation without chemical reaction

The way ultrasound accelerates physical operations in liquid sample preparation is poorly known and difficult to generalize because of the different nature of the target phenomena. In some, whether any chemical reaction occurs is unclear even though the outcome suggests the absence of chemical changes.

Liquid–liquid extraction from an aqueous layer to an organic phase or *vice versa* is strongly affected by the presence of US, albeit not always in a favourable manner. Thus, some systems are helped by this energy [47], others experience undesirable emulsification. Those systems where a chemical reaction is coupled to the liquid–liquid extraction step benefit the most as a consequence of the influence of US on both. Such is the case

with the continuous liquid–liquid extraction without phase separation and subsequent hydrolysis of paracetamol in suppositories [48].

Emulsion is greatly promoted by US. This is the phenomenon occurring between two liquid immiscible phases by which one (dispersed) phase distributes in the other (continuous) phase in the form of small droplets with diameters in general exceeding 0.1 µm. Generally speaking, emulsions are thermodynamically unstable; however, their stability can be improved by using additives (*e.g.* a surface-active agent or a finely divided solid). The effect of US is based on droplet disruption in sonicated liquid–liquid systems as a result of cavitation. These systems are hardly used in analytical chemistry but widely employed by the pharmaceutical industry.

Homogenization is effectively assisted by US without any alteration of the chemical characteristics of the system. This may be required one or several times during sample preparation in order to facilitate contact between solutions, or can be used prior to sampling in order to ensure representativeness in the studied system. Thus, US-assisted homogenization is widely used in the analytical laboratory, but has been scarcely studied or optimized during the development of specific analytical methods. Because the time required for US-assisted homogenization of liquids is usually very short, analytical chemists tend to use it for longer times and refer to these procedures with such vague sentences as "after adding the reagent, dip the container into an ultrasonic bath for *x* min".

2.4. PREPARATION OF HETEROGENEOUS SAMPLES

The main purpose of US in handling heterogeneous media is for separating a solid from a liquid phase, dissolving it, or enhancing or accelerating the formation of a solid phase. The solid phase can exist in the sample as such or be formed as a result of, mainly, a chemical reaction (*e.g.* precipitation), but also a physical phenomenon (*e.g.* crystallization or aggregation).

2.4.1. Ultrasound-assisted filtration and aggregation

Filtration is one of the usual ways to separate phases, which is dramatically facilitated by US. Although the primary uses of this effect are in the industrial field — where retention of suspended solids within a porous medium subjected to US has been widely studied [49] — its analytical applications warrant some comment. Thus:

(a) Filtration has been used to separate a solid phase formed in a chemical reaction involved in a SP process — where US has scarcely been used to facilitate filtration. One of the few examples of this use is the development of an automated on-line system for bioprocess control based on flow injection, ultrasound filtration and coupled charge detection [50]. A more frequent use of US associated to filtration is as an *in situ* measuring technique for the non-invasive study of fouling and cleaning during filtration [51].

(b) Filtration is also used as a preliminary operation in the preparation of samples containing undesirable particles, where analytical chemists have taken advantage of the experience gathered in the industrial field. This step is poorly discussed in the analytical literature, but has been widely studied in connection with the performance of filtration membranes in the presence and absence of US under different conditions

and US frequencies. As discussed in detail in Chapter 5, the US frequencies used range from 0.66 MHz and its 15th harmonic — which provide a unique way of facilitating separation of concentrated microparticles [52] — to the kilohertz range (20 kHz), which is used to ultrafilter suspended solutions [53].

Sonophoresis is another special type of US-assisted filtration in which the skin acts as a filter.

Aggregation is another use of US radiation forces to handle suspended particles. The main difference with precipitation is that this involves the formation of a solid phase in a homogeneous liquid phase under US radiation; on the other hand, aggregation (or agglomeration), which should be called "sonoaggregation" (or sonoagglomeration) under the action of US, involves the formation of larger particles from existing small ones upon fast, efficient agglomeration facilitated by US. Aggregation is a phenomenon that analytical chemists hardly look for; on the contrary, it is undesirable in dealing with samples containing suspended particles. Once again, this phenomenon is dealt with in this section simply to illustrate another application of US in analytical chemistry: the aim is to obtain large particles in a heterogeneous system with a view to facilitate the separation of the solid phase if the phases are to be isolated. This can be used prior to or after sampling, and also during sample preparation if a finely divided solid forms during SP.

2.4.2. Ultrasound-assisted dissolution of the solid phase in heterogeneous samples

Analytically, solids in a heterogeneous sample are dissolved in order to determine some component of the solid phase or one randomly distributed between both phases. The specific US-assisted process that occurs is rarely identified or given an inappropriate name, in most cases. Thus, in preparing milk samples for the determination of mercury by AFS, the name "slurry sampling" was used in connection with the liquid phase resulting from sonication of the samples in the presence of 8% (v/v) *aqua regia*, 2% antifoam and 1% hydroxylamine hydrochloride for 10 min, followed by treatment with 8 mM KBr and 1.6 mM $KBrO_3$ in a hydrochloric acid medium [54]. The treatment was not called digestion, because it was compared with a similar treatment for the subsequent determination by ICP-MS of 45 elements in milk using microwave-assisted digestion [55].

Another frequent mistake in this context is to use "face" and "phase" indifferently. A case in point is the description of a method for the quantitative mechanistic study of ultrasonically enhanced reactions which occur at the solid–liquid interphase [56].

Dissolution of solid phases in clinical samples is possibly one of the areas of greatest success for US [57–59], as is biochemical field cell lysis [60].

Beyond the scope of this book, but also worth mentioning, is the use of US to assist heterogeneous organic reactions involving a metal as a reagent or catalyst, which is discussed in some detail in Chapter 5 [37–39].

2.4.3. Ultrasound-assisted formation of a solid phase: sonocrystallization and sonoprecipitation

Sonocrystallization is the currently accepted name for the use of power ultrasound to control and accelerate the course of a crystallization process. This effect had previously been used in the salting-out process for years, and has been found to have a favourable

effect on the initial nucleation stage of crystallization (*viz.* for reducing both the induction period and the metastable zone before nucleation starts at a lower level of supersaturation). Ultrasound hence influences the crystallization process [61]. The effect of bubbles on the sonocrystallization of water [62], that of US parameters on the crystal structure of palm oil [63], and the wide use of this energy on food technology [64], illustrate the usefulness of US in this area.

Like crystallization, US also successfully assists the formation of extremely finely divided and uniform particles, which can be termed *sonoprecipitation*. This effect, which has not yet been used in analytical chemistry and might facilitate sample preparation in nephelometric or turbidimetric methods, has been widely exploited by the pharmaceutical industry to prepare liquid dispersions of drugs for oral or subcutaneous administration where extremely small particle sizes ensure stable suspensions of the drug and faster assimilation into the body. On a laboratory scale, US-assisted precipitation of magnesium carbonate in a model system has been studied [65].

2.4.4. Ultrasound-assisted gas–liquid systems

There are three major uses of US in analytical systems involving gas–liquid systems, which can exist as such or be created during sample preparation, namely: nebulization, defoaming and degassing.

Nebulization is a physical process widely used in analytical chemistry for introducing samples into atomic spectrometers [66]. Ultrasonic nebulizers are the most effective devices for this operation. Rather than a step preceding sample preparation, nebulization is a sample preparation operation and so close to detection that the nebulizer is a component of flame and plasma spectrometers that influences their efficiency. This warrants separate discussion on ultrasonic nebulizers in Chapter 8.

Non-analytical uses of US-assisted nebulization span the medical and pharmaceutical fields, where *aerosoling* or *aerolization* is more frequently used than nebulization [67,68]. The use of ultrasound to assist the formation of micro-to-nano drops as the first step of spray-drying (atomization) also falls in this group, albeit in the industrial area.

Defoaming is the operation by which foam is removed. Foam is the dispersion of a gas in a liquid where the distances between individual bubbles are very small. In a foam system, the volume ratio of gas to liquid is very high and the bulk density approaches that of a gas. Foam can cause problems in analytical operations such as chromatographic separation and molecular spectrometric detection.

Acoustic transducers operating at 10 and (or) 20 kHz can be effectively used to defoam liquids by placing the acoustic source above the liquid surface upon which the foam is being produced. There is some controversy concerning the frequency of US capable of causing defoaming; this is discussed in some detail in Chapter 5 [69,70]. No dedicated acoustic defoamers have to date been reported in the analytical literature even though foaming is a frequent problem in analytical laboratories, particularly when working with surfactants.

Degassing is an analytical operation usually preceding sample preparation that involves removing dissolved gases from a liquid (particularly in liquid chromatography). Like all other preliminary operations, degassing is discussed in detail in Section 2.6, where the effect of US on its efficiency is clarified. In any case, degassing may also be necessary when a gas is formed during SP. No specific uses of US for degassing during SP have to date been reported, however, despite their potential.

2.5. DISCRETE *VERSUS* CONTINUOUS APPROACHES TO ULTRASOUND-ASSISTED SAMPLE PREPARATION

The steps involved in SP can be performed (a) in a discrete or batch manner or (b) in a continuous fashion. The most salient differences between the two are as follows:

In a discrete approach, the analytical system is confined in a vessel or container through the walls of which US energy is transmitted if an ultrasonic bath is used. The use of a US probe in this case can involve either to dip it into the vessel or into the transmitting liquid where the vessel is located. The complexity of the analytical system determines the type of vessel or container to be used, namely: an open or closed, atmospheric pressure or pressurized device, a jacket-tailored device for maintaining the optimum temperature, etc.

In a continuous approach, the analytical system rarely comes into contact with the US source, which is accommodated in the transmitting liquid surrounding the dynamic system. Whether or not the sample is placed in a fixed position of the dynamic system depends on its particular state. Thus, if the sample is a solid, it is held in a chamber furnished with filters at its ends through which a leaching or digesting solution is circulated. Obviously, the chamber is the zone subjected to US. When the sample is a liquid, it can either be circulated through the dynamic system or stopped for a preset time to be subjected to ultrasonic radiation in order to facilitate a chemical reaction, a liquid–liquid extraction, emulsification, homogenization, crystallization, precipitation, etc. The design of the dynamic system depends on the particular process and the working conditions under which it is developed.

2.5.1. Commercial and custom equipments for ultrasound-assisted sample preparation

The absence of commercial equipment for US-assisted sample preparation clearly reflects that the analytical chemists give little importance to this way of accelerating the operations. For this reason, most applications in this area have been developed by using standard laboratory materials such as round-bottomed flasks or even beaker or precipitation vessels. Some authors have implemented US-assisted sample preparation in commercially available cells specially designed for organic synthesis or have designed and constructed their own custom devices.

Commercial and laboratory-made equipments for batch ultrasound-assisted sample preparation

Chemical reactions often require vapour-tight apparatus, the slow addition of reagents or the use of an inert or pressurized atmosphere. These requirements are met by commercially available sonochemical equipments some of the simplest types are shown in Fig. 2.4 and described below.

The so-called "Rosett cell" can be fitted with a flanged lid as shown in Fig. 2.4A. The design of this cell allows an irradiated reaction mixture to be sonically propelled from the end of a probe around the loops of the vessel and thus provides both cooling (when the vessel is immersed in a thermostated bath) and efficient mixing. A polytetrafluoroethylene (PTFE) sleeve ensures a vapour-tight fitting between the probe and the glass joint. Alternatively, an ordinary reaction vessel can be adapted for sonic mixing by providing an
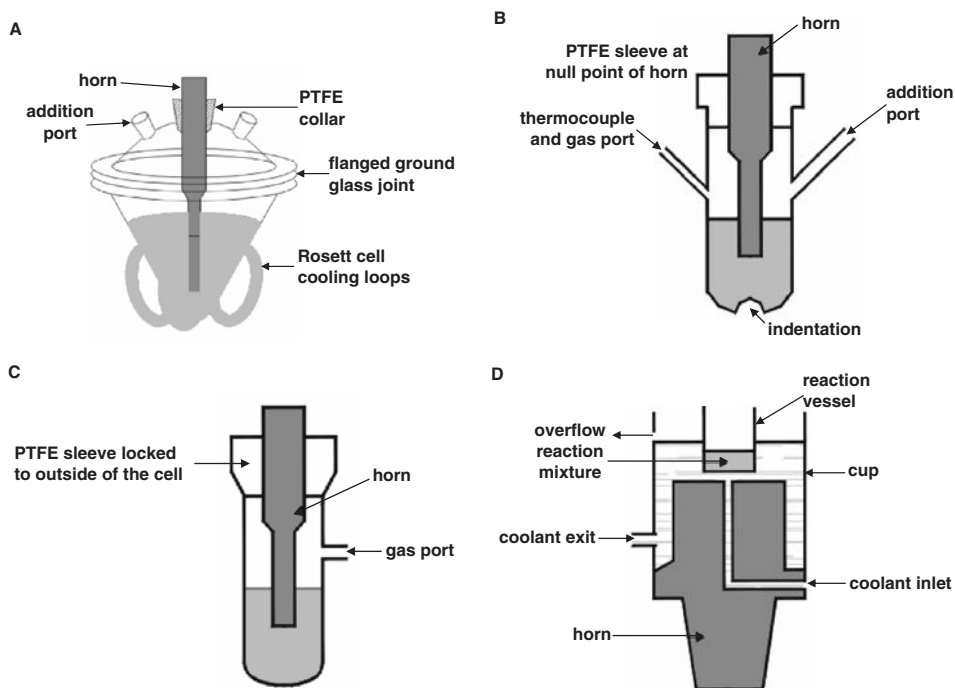
FIGURE 2.4. *Commercial discrete devices for chemical reactions assisted by ultrasound probes. (A) Rosett cell, (B) indented cell, (C) Suslick cell and (D) cup horn.*

indentation on its base in order to disperse the sonic waves, as they are reflected from the base (Fig. 2.4B). In situations where high pressures are used, the reactor proposed by Suslick (Fig. 2.4C) is especially useful. Another commercially available cell type is the cup horn, which is a form of ultrasonic bath in which energy is imparted by an inverted horn sealed into the bottom of a water jacket or cup that enables temperature control of the sonicated system in addition to power control (Fig. 2.4D).

Although most US-assisted analytical operations performed in a discrete manner (*e.g.* digestion, lixiviation and derivatization) can be implemented with conventional laboratory materials, some authors have designed special batch approaches for specific purposes, as illustrated in Figs. 2.5 and 2.6. The devices in Fig. 2.5 are very simple, their minimal complexity responding to the need for thermostation (Fig. 2.5A) or thermostation plus agitation and oxygen bubbling (Fig. 2.5B). In both cases, conventional US probes are directly dipped in the target analytical system. The experimental set-up shown in Fig. 2.5A was designed for the US-assisted leaching of heavy metals from sewage sludge prior to ICP-AES analysis. The sample cell was a simple glass container perfectly fitted to the thermostated water jacket, in which the sample and the optimum amount of acid solution were placed and sonicated at different amplitudes and times, with or without air bubbling during the leaching step. An all-glass sonotrode was used to avoid deterioration in the highly acidic medium used [71]. Figure 2.5B illustrates the US-assisted leaching of silver
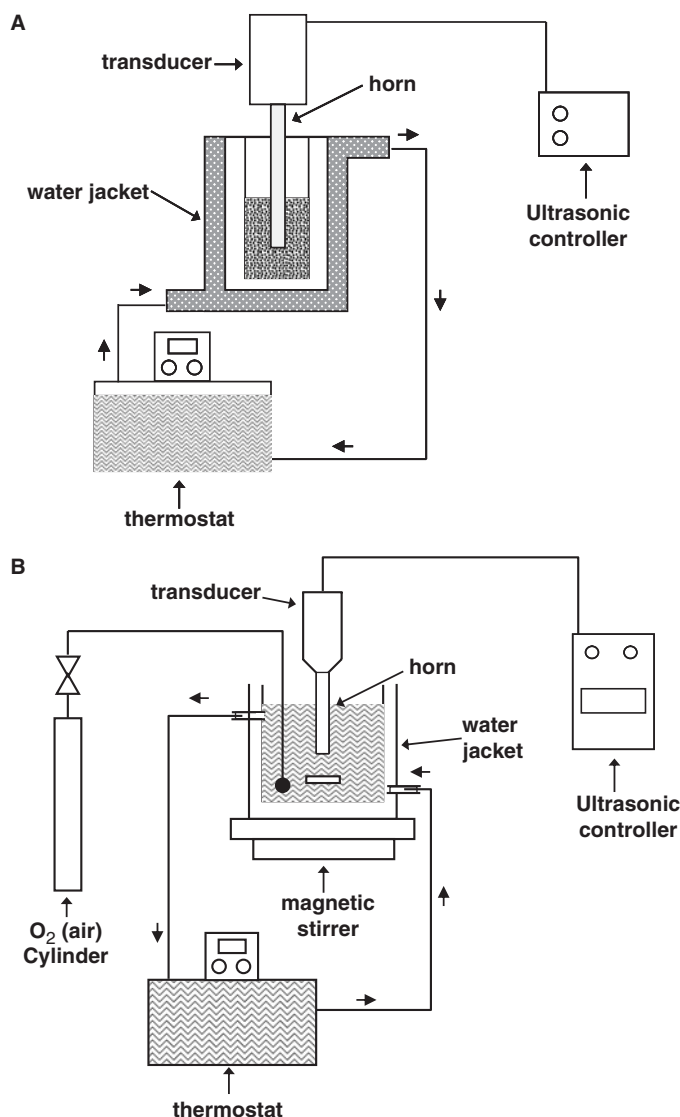
FIGURE 2.5. *Simple laboratory designs of batch cells for US-assisted chemical systems. (A) Thermostated cell and (B) cell provided with thermostation, agitation and oxygen bubbling. (Reproduced with permission of Elsevier, Refs. [71,72].)*

from ores helped by the reaction of the analyte with thiourea. The set-up consists of a cylindrical jacketed-glass reactor subjected to continuous agitation and oxygen bubbling in order to favour silver oxidation. Because the probe was made of titanium, a medium US power had to be used in order to prevent the tip from premature pitting and erosion; in any case, the probe tip was replaced after 40 h of use [72].
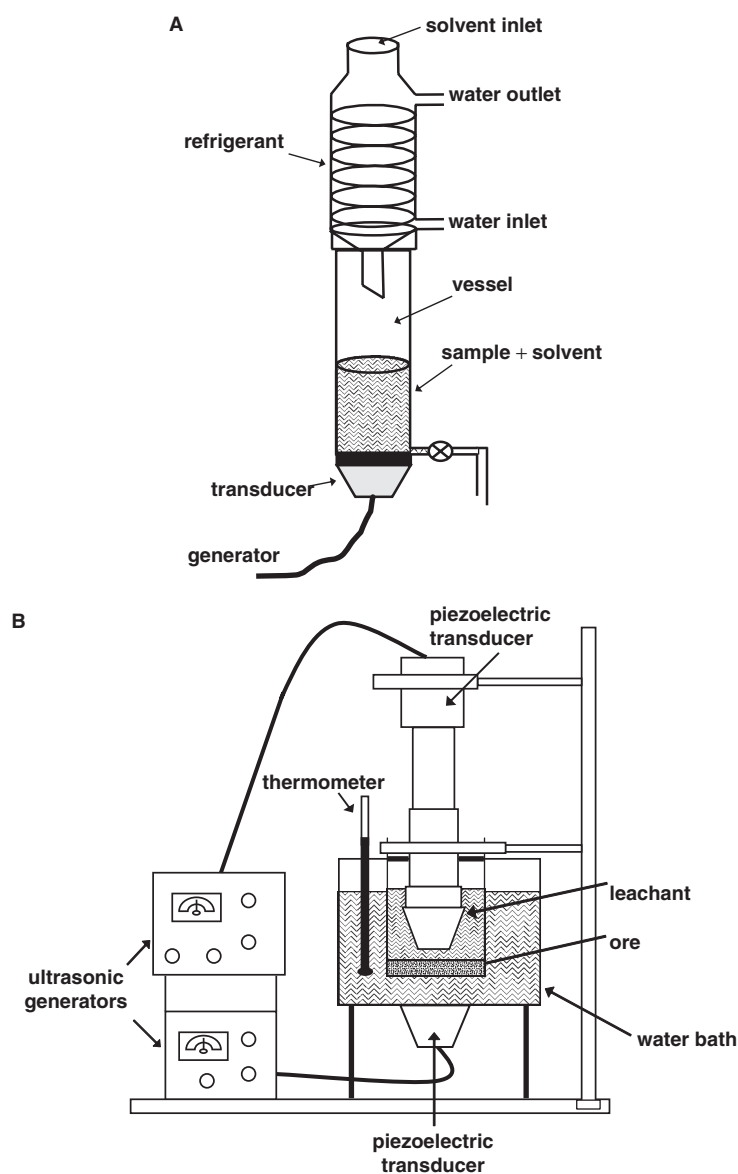
Figure 2.6. *Laboratory designs of batch cells for US-assisted chemical systems. (A) Cell with closely locked transducer and (B) special cell provided with two transducers of different frequency. (Reproduced with permission of Springer-Verlag, Ref. [73] and Elsevier, Ref. [74].)*

The designs in Fig. 2.6 are a little more complex than the previous ones. That in Fig. 2.6A was designed for leaching particulate organic matter from airborne particles. As can be seen, the transducer was closely locked to the glass sample vessel and a condenser was connected to prevent evaporation losses. After leaching, the organic extract was delivered through the valve at the bottom of the vessel [73]. The design of Fig. 2.6B was used to examine the influence of dual-frequency US on leaching and constructed from a cup horn of 20 kHz frequency and 375 W power co-axially located exactly above and face-to-face with a transducer of higher frequency (transducers of 40 kHz, 80 W; 43 kHz, 250 W and 720 kHz, 21 W were assayed) to increase the leaching efficiency [74].

Filtration is mandatory in batch work when a solid phase remains as such at the end of the process.

Commercial and laboratory-made equipments for continuous ultrasound-assisted sample preparation

One of the greatest advantages of continuous US-assisted operations is their ease of on-line connection to other operations in order to facilitate automation of the overall analytical process. In this way, the solutions obtained after each step need not be handled by the operator or come in contact with the atmosphere — which can be of enormous interest for some analytical systems.

Figure 2.7 shows selected commercial devices for assisting dynamic systems by US. A continuous flow-cell such as that of Fig. 2.7A allows the fluid concerned to circulate under ultrasonication. A double chamber facilitates cooling or heating of the dynamic system during ultrasonication. One or two (or even more) liquids can be pumped into the cell, mixed and processed in the annulus, controlled by an adjustable orifice that can be moved in and out axially and with interchangeable orifice plates, thus providing full control over the process parameters. A flow-through or tubular horn furnished with a hollow core tip and two inlets or orifices at the non-vibrating, nodal point of the horn such as that of Fig. 2.7B is also commercially available. This design ensures uniform mixing of two components by passing one fluid through the horn in the centre of the cavitational field, where it meets the other fluid coming radially inward from the body of the cell into which the flow-through horn is dipped. These cells require an additional device for propelling the fluids through them. Commercial continuous nebulizers can also be assisted by US, as shown in Chapter 8.

The development of laboratory-made continuous systems for US-assisted sample preparation requires more complex material and skilled designers than do batch systems. Thus, a propulsion (or aspiration) device — usually a peristaltic pump — is mandatory for propelling the fluids through the dynamic system. In addition, switching and (or) injection valves may be required for proper functioning of the system. The flexibility of these systems is discussed at length in Chapters 3–8, so only a few, general examples, are depicted in Fig. 2.8 and dealt with here.

Depending on the particular application, a continuous US-assisted system must propel the fluids (a) in a single direction (mainly for derivatization, filtration, degassing) or (b) alternately back and forth in order to bring the two phases involved (two immiscible liquids in liquid–liquid extraction, and a solid and a liquid phase in leaching or digestion) into contact many times. In this way, less diluted extracts, leaching or digestion solutions are obtained. In the former case, the design of the continuous approach must be suited to the characteristics of the chemical system. Thus, proper mixing of the sample

A

opening at top is
internally threaded

inlets/
outlets

inlets/
outlets

flow-through
attachment

B

stud

flow-through
horn

inlet/
outlet

hollow core
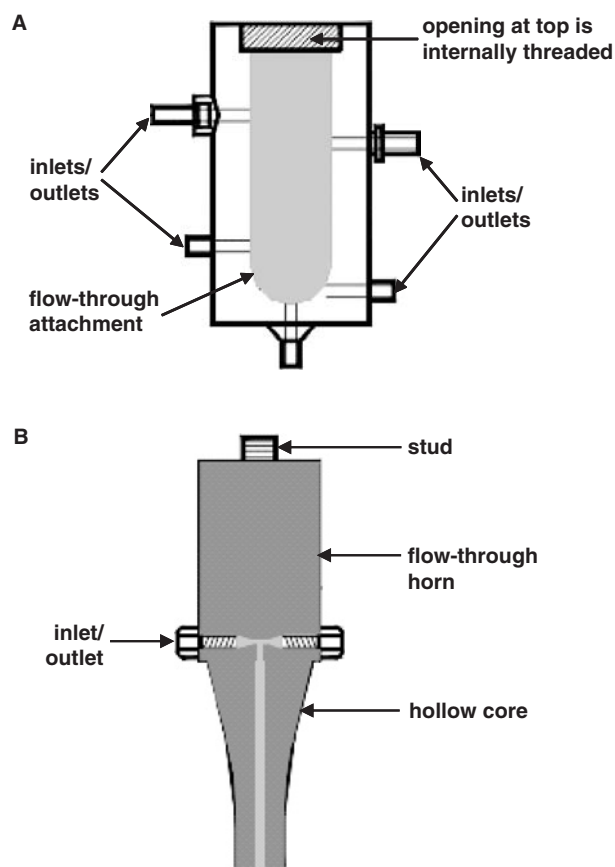
FIGURE 2.7. *Flow-through cells for US-assisted chemical systems. (A) Jacketed cell for thermostation and (B) flow-through horn.*

(or the liquid resulting from a previous step) with a buffer or derivatizing reagent will require using a number of channels and merging points. Figure 2.8A shows a selected example of this type of system.

Figures 2.8B and C illustrate the two choices available when the direction of the flow in the dynamic approach is changed at preset intervals by programming. The former figure shows an open system in which the fluid passes alternately through the chamber in the two directions until the desired development level is reached. Then, the programmed propelling unit works only in one direction in order to drive the fluid to a reservoir, the detector or other dynamic unit for development of another step. Figure 2.8C shows a closed circuit including switching valves for keeping a given volume of fluid circulating through the chamber (usually containing a solid). After the preset time for proper development of the step has elapsed, valve SV is switched and the solution delivered as required. A more detailed description of these systems can be found in subsequent chapters.
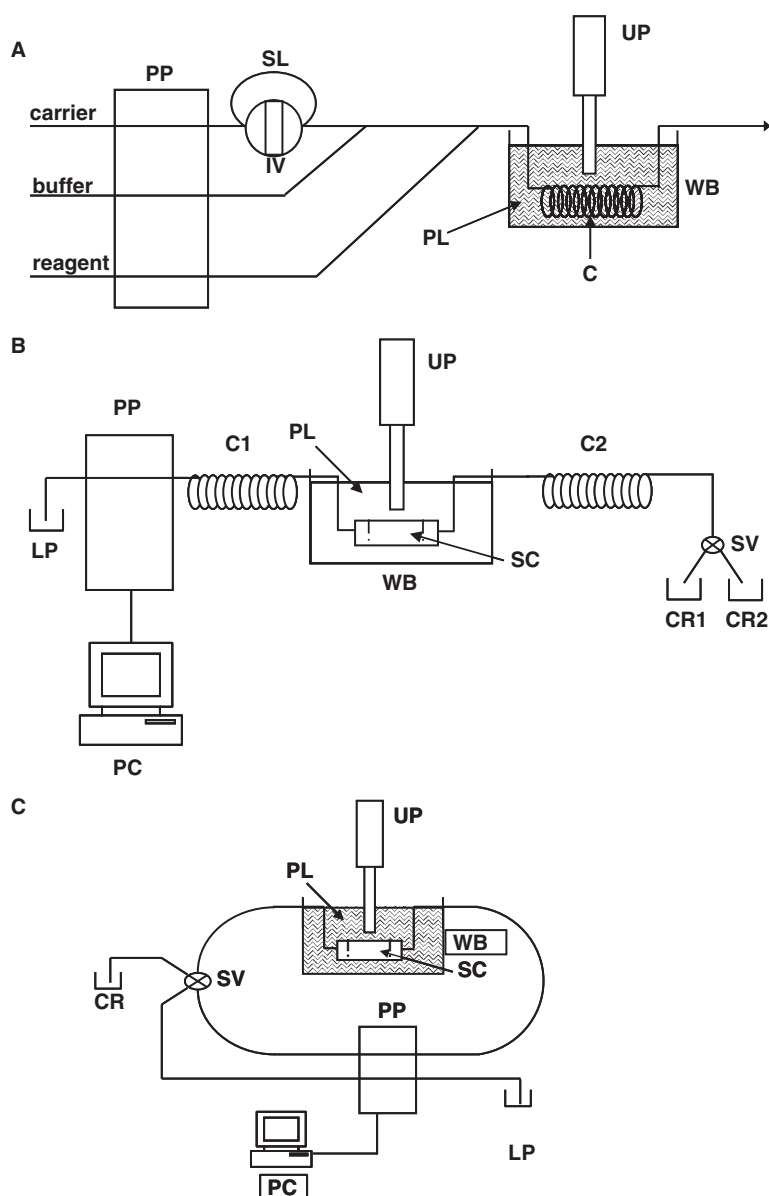
FIGURE 2.8. *Continuous-flow laboratory manifolds for US-assisted processes. (A) One-way system for liquid-liquid extraction, (B) Open, one- or two-way leaching system and (C) Closed, one- or two-way leaching system. C — coil, CR — collection reservoir, IV — injection valve, LP — liquid phase, PC — personal computer, PL — propagating liquid, PP — peristaltic pump, SC — sample cell, SL — sample loop, SV — switching value, UP — ultrasound probe and WB — water bath.*

All continuous laboratory-made systems share two common features, namely: (a) the chamber or portion of the dynamic system subjected to US action is dipped in the transmitting liquid; and (b) after the US-assisted step is completed, the liquid phase is delivered for subjection to the next continuous or discrete step, which, in the simplest case, is detection.

2.6. ANALYTICAL USES OF ULTRASOUND PRIOR TO SAMPLE PREPARATION

The steps discussed in this section are invariably close to sample preparation. While cleaning is clearly outside the scope of sample preparation, degassing may or may not be used as a preliminary operation in analytical chemistry; however, it is most frequently employed prior to the analytical process. Its use within the process is discussed in Chapter 5. A physical process such as atomization when understood as the formation of finely divided droplets is rarely used in analytical chemistry, even though it could be employed for sample conservation instead of lyophilization. The potential ways in which US can be used to improve it are discussed in Section 2.6.3, which is devoted to US-assisted atomization.

2.6.1. Ultrasound-assisted cleaning

Ultrasonic cleaning is a major application of power US. Few laboratories currently do not have any access to an ultrasonic cleaning bath. The cleaning of surfaces and porous materials with the aid of US involves stripping away oxides and other films, emulsifying oil coatings, suspending particulates, enhancing detergency or degreasing without using a hydrocarbon solvent.

Although cleaning is a mandatory operation prior to starting an analytical process, it is hardly described in analytical publications. The wide use of US to assist the cleaning of analytical material — from glassware to columns through the widely varied devices and units suffering from clogging or bad functioning caused by dirt — is clearly reflected in the presence of ultrasonic cleaning baths in not only analytical, but also virtually any type of laboratory. The variety of ultrasonic cleaning baths commercially available is another clear reflection of their widespread use.

With some contaminants, ultrasonic cleaning is best carried out in aqueous solutions of alkaline, acid and (or) surface-active substances. This is appropriate for water-soluble impurities or for impurities that react chemically with the alkaline or acidic substances contained in the bath to give water-soluble products. Aqueous ultrasonic cleaning is also used when the impurities are hard, sparingly soluble and loosely bound to the substrate (*e.g.* graphite, soot, silica). However, many impurities do not respond to economical cleaning in water solutions and require an effective organic solvent instead. The solvent to be used should easily dissolve the impurities, not damage the cleaned substrate, be safe (*i.e.* non-toxic, non-explosive, non-flammable and environmentally friendly) and exhibit a high sensitivity to the factors that intensify cleaning. The last requirement is often ignored and an inappropriate solvent is chosen frequently as a result. Table 2.1 summarizes the properties of available solvents for ultrasonic cleaning as compiled by Niemczewski [75].

The efficiency and limitations of US-assisted cleaning have been classified into two different categories [76]. One involves enhancing mass transport *via* acoustic streaming and microstreaming, which accelerates the dissolution of soluble contaminants. The other

TABLE 2.1. *Solvents Available for Ultrasonic Cleaning.*

	Solvent	Chemical name and empirical formula	Producer	Boiling point (°C)	Flash point (°C)	Hazard class (German vbf)
1	NPM	*N*-methylpyrrolidone (C_5H_9NO)	BASF	204.3	91	B III
2	Dowanol DPM	Dipropylene glycol monomethyl ether ($C_7H_{16}O_3$)	DOW	189	75	B III
3	Dowanol TPM	Tripropylene glycol monomethyl ether ($C_{10}H_{22}O_4$)	DOW	243	121	—
4	Dowanol PnB	Propylene glycol mono *n*-butyl ether ($C_7H_{16}O_2$)	DOW	171	63	A III
5	Dowanol DPnB	Dipropylene glycol mono *n*-butyl ether ($C_{10}H_{22}O_3$)	DOW	229	111	–
6	Dowanol TPnB	Tripropylene glycol mono *n*-butyl ether ($C_{13}H_{28}O_4$)	DOW	274	133	–
7	Dowanol DPnP	Dipropylene glycol monopropyl ether ($C_9H_{20}O_3$)	DOW	213	88	A III
8	Dowanol TPnB-H	Propylene glycol buthyl ether ($C_7H_{16}O_2$)	DOW	>274	>124	–
9	Dowanol PGDA	Propylene glycol diacetate ($C_7H_{12}O_4$)	DOW	191	86	A III
10	Proglyde DMM	Dipropylene glycol dimethyl ether ($C_8H_{18}O_3$)	DOW	175	65	A III
11	Clenvex AS58	Mixture of aliphatic hydrocarbons (isoparaffins)	Castrol	180–200	56–58	A III
12	Clenvex AS105	Mixture of paraffins and naphthenes	Castrol	230–260	105	–
13	Cleaner IC-1	Mixture of aliphatic hydrocarbons (cyclo. n. iso). Monohydric alcohol and polyhydric alcohol	Shell	174–199	65	A III
14	Topklean EC-16	Mixture of aliphatic hydrocarbons (cyclo. n. iso) and emulsifier	Shell	184–198	64	A III
15	Topklean EC-20	Mixture of aliphatic hydrocarbons (cyclo. n. iso). Alcohols and oxygenated solvents	Shell	174–199	65	A III
16	Cleaner C-153	Mixture of aliphatic hydrocarbons (cyclo. N. iso) with a chain length of C_{10}–C_{12} and inhibitor	Shell	184–198	64	A III
17	Cleaner A-151	Mixture of aliphatic hydrocarbons (cyclo. N. iso) with a chain length of C_{10}–C_{12}. Oil penetration improving agent and inhibitor	Shell	184–305	64	A III

Continued

TABLE 2.1. *cont'd.*

18	Cleaner D-7	Mixture of aliphatic hydrocarbons (cyclo. N. iso) with a chain length of C_{10}–C_{12}. Oil penetration improving agent and inhibitor	Shell	225–305	99	A III
19	Fluid 105	Mixture of aliphatic hydrocarbons (isoparaffins) with a chain length of mainly C_{12} and special dewatering additive	Shell	187–212	60	A III
20	Degreaser 107	Mixture of aliphatic carbons (isoparaffins) with a chain length of C_{10}–C_{12} and inhibitor	Shell	187–212	60	A III
21	Hydrofluoroether	Methoxynonafluorobutane (C_4F_9O CH_3)	3M	54	None	–
	HFE-7100					
22	Hydrofluoroether azeotrope HFE-	50% Methoxynonafluorobutane + 50% *trans*-1,2-dichlorethylene	3M	41	None	–
	71DE					
23	Vertrel XF (HFC 43-10 mee)	2.3-Dihydrodecafluoropentane ($C_5H_2F_{10}$)	Du Pont	55	None	–
24	Vertrel XM. XE.	Azeotropes of Vertrel XF with methanol, ethanol,	Du Pont	37–54	None	–
	MCA. SMT. X-P10	*trans*-1,2-dichloroethylene and isopropanol				

Reproduced with permission of Elsevier, Ref. [75].

involves mechanical effects arising when cavitation occurs close to the boundary. The stresses involved can lead to pitting and are also used to disrupt cells in biological applications. The use of shock waves, collision of the bubble's wall on the surface upon collapse and microjetting has also been considered. Unlike laser-induced bubbles, the size and position of which above the surface can be very precisely controlled, ultrasonic bubbles appear randomly where "cavitation nuclei" are present. Such nuclei can be surface inhomogeneities, bubbles remaining from previous cavitation events or impurities. Also, because multiple cavitational events occur at once, the local sound field and acoustic pressures vary with time and are then impossible to control. The accelerating action of US in dissolving particles in a cleaning process is therefore very complex. Scanning electron microscopy (SEM) studies have shown that the surface particles become both smoothed and pitted as a result of sonication. Therefore, it seems that multiple mechanisms are occurring simultaneously: microstreaming acts to smooth particle surfaces and dissolve particles, while shock waves and microjets imploding on the particle surfaces both shear and pit the surface of the particles. The presence of organic matter such as humic acids in the particles further increases the complexity of the system [77].

The study of vibroacoustic characteristics of ultrasonic cleaners as a function of their operational low- or high-frequency (kilohertz and megahertz ranges, respectively) has shown that the cleaning mechanism of the former relies mostly on cavitation in the cleaning liquid, and that of the latter on the high-frequency acceleration in the liquid [78].

Well-established cleaning approaches such as that based on the effect of high-speed water jets can be improved by subjecting the jet to ultrasonic forced modulation [79].

Commercial and custom-made ultrasonic cleaning systems

Most manufacturers of ultrasonic cleaning equipment offer a wide variety of apparatus from table top devices of less than a gallon capacity to 250–300 gallons in some cases. Thus, American firms such as Miraclean Cleaning Systems, Ashville, NY; Alexy Associates Inc., Bethel, NY; Blue Wave Ultrasonics, Davenport, IO; Bowden Industries Inc., Huntsville, AL; Branson Ultrasonics Corp., Jamestown, NY; CAE Ultrasonics, Danbury, CN; Greco Brothers, Providence, RI; Jensen Fabricating Engineers Inc., Berlin, CN; L&R Mfg. Co., Kearny, NJ; Lewis Cleaning Systems, Oxford, CN; Misonix Inc., Farmingdale, NY; PowerSonics LLC, Elsersburg, MD; Ramco Equipment Corp., Hillside, NJ; Sonicor Instrument Corpo, Copiague, NY; Telsonic Ultrasonics, Bridgeport, NJ; Ultra Clean Equipment, Clinton, CN; Ultrasonics Power Corp., Freeport, IL; and Zenith Ultrasonics, Norwood, NJ provide such devices with characteristics that differ greatly in some cases.

An ultrasonic cleaning apparatus where the cleaning fluid and the dirty object minutely vibrate in two different directions [80], and an ultrasonic cleaning method in which ultrasonic energy of different frequencies is simultaneously applied [81] are two typical examples that have gained two representative patents in this field. Specially designed US cleaners for the simultaneous treatment of 96–384 microplates have been marketed by Biotek.

Clinical and food ultrasonic cleaning

For over 40 years, much has been done on the purported ability of high frequency or high intensity ultrasound application to disinfect and sterilize. Sterilization is defined as the

absolute killing of all disease organisms — fungus spores included. Disinfection is not as rigorously defined and does not necessarily include inactivation of spores. The strongest advocates of US admit that ultrasound do not sterilize, by themselves, under normal use in an ultrasonic cleaning tank such as those used by dentists. Also, no reputable manufacturer has ever claimed any such property. The existing ultrasonic equipment can, and routinely does, disrupt all bacteria, virii and fungi under controlled laboratory conditions, but it is a totally different type of device than an ultrasonic cleaner. Such equipment, termed high-intensity probes or disruptors, under such trade names as SONICATOR, SONIFIER, or VIBRA-CELL, applies sound on a very small area to disrupt organisms and produces energy densities many orders of magnitude higher than that available in even the best ultrasonic cleaning tank.

In addition to direct disinfection and sterilization, several surprisingly successful experiments about a decade ago led to the development of a number of highly proprietary processes in which ozone and other purifiers are introduced into chemical and wastewater flows in the presence of a cavitational field. The outcome has been greatly improved efficiency of the chemical action and the obtainment of purified or even potable water at economical costs.

Ultrasonic technologies span a wide range of hospital and dental applications including cleaning and disinfection of surgical and dental instruments. The germicidal efficiency of sonication in the presence and absence of a chemical disinfectant in an ultrasonic bath delivering a frequency of 35 kHz and an intensity of 0.66 W/cm^2 was tested in cultures of *Staphylococcus aureus*, *Pseudomonas aeruginosa* and *Candida albicans* that were exposed to ultrasound and to an amine-based disinfectant at non-bactericidal concentrations. Ultrasonication for 60 min alone caused no significant killing of the bacteria or yeast; however, it boosted the efficacy of the disinfectant against *S. aureus* and *P. aeruginosa*. *Candida albicans* was more resistant to this combined effect, which was not reduced inside rubber tubes [82]. According to the authors of the study, the influence of the sonication intensity and frequency and the effects of cavitation should be clarified before this form of energy is accepted as an integral part of the cleaning and disinfection process of medical instruments. The effectiveness of ultrasound for the removal of metallic particles from the surface of stainless steel and Ni–Ti endodontic instruments has also been demonstrated [83].

The ultrasound-assisted decontamination of minimally processed fruits and vegetables was studied on a small scale (2 l) and large scale (40 l). The reductions in *Salmonella typhimurium* attached to iceberg lettuce obtained by cleaning with water, chlorinated water, US with water and US with chlorinated water were 0.7, 1.7, 1.5, 2.7 logs, respectively. The cleaning action of cavitation appears to remove cells attached to the surface of fresh produce, thereby rendering the pathogens more susceptible to the sanitizer. The frequency of US (25, 32–40, 62–70 kHz) had no significant effect on the decontamination efficiency. Despite the results, the authors believe that, because of the high capital investment required and the expenses incurred in the optimization and water treatment processes, it is unlikely that the fresh produce industry would be willing to take up this technology. Furthermore, the additional one log reduction achieved by applying US to a chlorinated water bath does not completely eliminate the risk of pathogens on fresh produce [84].

Possibly, the high value added to the processed food will facilitate the implementation of non-invasive ultrasonic apparatus for the removal of fouling in food processing equipments. With this aim, an ultrasonic apparatus operating at a frequency of 40 kHz was developed for dislodging biofilms from food processing equipments in order to assess the effectiveness of cleaning protocols. The optimum sonication conditions for the removal

of biofilms and quantification by ATP-bioluminescence was established and a laboratory-scale industrial meat process was developed to test the approach. The results showed biofilm removal by sonication for 10 min to be reproducible and four times greater than with the swabbing method (83% removal of fouling *versus* 20% with the latter). Unlike the swabbing method, the ultrasonic apparatus — which is easy to use and can be operated by an unskilled operator — permits the immediate demonstration (within 1 min) of inefficiency in an industrial meat cleaning protocol [85].

Ultrasonic cleaning of membranes

Filtration membrane fouling is characterized by an "irreversible" decline in flux. Most of the dedicated literature published over the past two decades has focused on fouling rather than cleaning, even though what appears to be a fouling problem may in fact be a cleaning problem, which is more important in ultrafiltration (UF) systems. A variety of chemical and physical cleaning methods currently exists for cleaning a fouled membrane and it has been suggested that the cleaning frequency and the severity of such cleaning procedures govern the membrane's lifetime. Considerable progress has been made in understanding fouling formation, the interaction between foulants, the membrane and the operating conditions with a view to designing new, better cleaning methods [86].

Ultrasound assistance has proved effective for cleaning membranes of widely different materials with substantial advantages over traditional cleaning procedures as shown by flux measurements, SEM and ultrasound echo measurements [51]. A comparison of the efficiency of three types of cleaning methods (*viz.* forward-flushing, ultrasonic cleaning and ultrasound with forward-flushing) revealed that US combined with forward-flushing provided a new effective method for the recovery of permeate flux through nylon microfiltration (MF) membranes. A high forward-flushing velocity and a low cleaning solution (water) temperature under fixed US conditions were found to result in a higher cleaning efficiency. In addition, on-line US can reduce membrane fouling and enhance permeate flux [87]. The factors affecting US efficiency in cleaning particle-fouled ceramic membranes and possible underlying mechanisms have been investigated. Based on flux measurements, an increased US power intensity and low frequency improve particle removal. These results, together with SEM images, suggest that cavitational mechanisms (*e.g.* microstreaming and microstreamers) are important in detaching particles from the membrane surface, while turbulence associated with US (*i.e.* acoustic streaming) plays a role in the transport of particles away from the surface following detachment. Micro-jets seemingly produced no significant removal relative to microstreamers, although evidence of micro-jet pitting was visible in SEM images of the fouled surface. In addition, SEM images did not expose any apparent damage to the membrane surface, even after long periods of US at a high power intensity and a low frequency (20 W/cm^2, 20 kHz) [88]. In any case, membrane deterioration depends strongly on the nature of the membrane as revealed by a study on the effect of 47-kHz US on polyethersulphone, polyvinylidenefluoride and polyacrylonitrile. Major changes in some membranes were observed upon irradiation by monitoring the variations of pore density, porosity and pore size distribution in homogeneous areas of the membranes by using image analysis before and after irradiation [89].

Ultrasound cleaning has also been used to remove fouling from UF polysulphone and MF cellulose membranes used to treat peptone and milk aqueous solutions, respectively. The US employed had 28, 45 and 100 kHz frequency with 23 W/cm^2 output power. With 28-kHz US, water was found to be effective for recovery from a deteriorating condition due to fouling; US-enhanced permeability of membranes was also observed. It is worth noting

that US decreased the fouling condition in both types of membrane when irradiated before fouling [90].

Ultrafiltration of whey is a major membrane-based process in the dairy industry; however, the commercial availability of this application has been limited by membrane fouling, which has a concomitant influence on the permeation rate. Ultrasound cleaning of these fouled membranes has revealed that the effect of US energy is more significant in the absence of a surfactant, but is less markedly influenced by temperature and trans-membrane pressure. The results suggest that US acts primarily by increasing turbulence within the cleaning solution [91].

Ultrasonic cleaning of fine mineral suspensions

Some of the main reasons for cleaning mineral surfaces include the need to remove: (1) contaminants attached as surface coatings, which is often required with glass-making sands; (2) surface coatings masking a surface property of a mineral which would normally allow it to be separated from others (*e.g.* in the electrostatic separation of mineral sands); and (3) surface compounds such as the oxidation products of a mineral, which may prevent or delay the attachment of dissolved chemicals intended to alter surface properties in order to enable separation by techniques such as froth flotation. The study of the factors influencing the surface cleaning of silica and heavy metal sands has led to the knowledge of the relationship between US power input and the particle size of the surface coatings removed [92], and facilitated the reduction of iron oxide in a silica sand from 0.025% to less than 0.012% Fe_2O_3 — the difference between material suitable for clear glass containerware and that suitable for tableware [93].

Ultrasonic cleaning of metal surfaces

The type of solvent to be used and synergistic effects on the US-assisted cleaning of metal surfaces depend greatly on the target surface and the subsequent treatment to which the clean surface is to be subjected.

Surface preparation of steels and other metals and alloys is essential prior to most finishing processes (particularly coating and vacuum coating). Otherwise, yields will suffer. Aqueous and organic solvent ultrasonic cleaning have been assayed for achieving the highest possible quality surfaces without inflicting any damage to the components. Aqueous ultrasonic cleaning provides excellent results for surface cleaning of steel prior to finishing. The method is preferred over organic solvent-based methods for obvious environmental reasons [94]. On the other hand, the sequential treatment of the substrate surface with a cotton gauze soaked with an organic solvent and ultrasonic cleaning with an organic solvent provides an adhesive surface of Ti–Ni alloy for sputter deposition of pure titanium film [95].

The jewellery industry also uses ultrasonic cleaning, which buys a sizable fraction of the existing commercial apparatus for cleaning purposes.

2.6.2. Ultrasound-assisted degassing

Ultrasound-based degassing involves removing gases from solutions without the need for heat or vacuum. The cavitational effects underlying sonochemical action are also the basis of the extremely effective use of US to degas liquids. Once cavitation bubbles have

formed, they fill with any dissolved gas. Because the bubbles contain gas, they do not collapse easily in the compression cycle of the wave, so they will continue to grow on further rarefaction cycles, filling with more gas and eventually floating to the surface. Since rarefaction cycles take place extremely rapidly (around 40 000 times per second in an ultrasonic bath), the bubbles grow so quickly that degassing appears to be almost instantaneous.

A distinction should be made between the bubbles which are formed by cavitation and those which occur naturally in the parent liquid or are induced by ultrasonic action (sparging). Cavitation bubbles, which range in size from infinitesimal to visible (40 μm and above) appear only when the radiating surface is activated and vanish apparently instantaneously when the power is turned off (in fact, they vanish within a half-cycle or 25×10^{-6} s at 20 kHz). Naturally occurring bubbles of entrapped air or other gases are most evident in freshly poured hot tap water as cloudiness or in still water as small bubbles adhering to the undersurface and the vessel walls. Sparged bubbles, which are those induced mechanically by external means such as ultrasonic action at or near the gas–liquid interface (the surface), tend to float in the liquid and even produce foam.

Because bubbles must grow, rise and escape through the surface for degassing to be successful, variables such as temperature, viscosity, vapour pressures and surface tension have a critical influence. The distance bubbles must travel to reach the surface is especially influential and the process must be designed to allow for such a transit time. In order to provide for transit, the energy may be interrupted periodically by pulsing the activity of the radiator. To further complicate matters, because cavitation causes both sparging and coalescence, the energy level (intensity) must be carefully selected. These adjustments are done empirically.

The degassing of liquids and low-melting melts under the action of US was among the earliest effects revealed in the 1930s [96] and has been widely studied ever since. Theoretical treatments of the dynamics of a single bubble in a pressure field have been undertaken for many decades which have allowed a distinction to be made between stable and transient cavitation [97]; a high-frequency reactor to be designed to study the degassing effect [98]; and ultrasonic propagation through aqueous kaolin suspension during degassing to be studied [99].

Porosity is one of the major defects in aluminium alloy castings. The presence of porosity can be detrimental to the mechanical properties and corrosion resistance of the castings. Porosity in castings occurs as a result of the precipitation of gas from solution during solidification or of the inability of the liquid metal to feed through the interdendritic regions to compensate for the volume shrinkage associated with solidification. Hydrogen is the only gas that is appreciably soluble in molten aluminium. Figure 2.9 shows the effectiveness of ultrasonic treatment for the removal of hydrogen, which is further improved when performed in vacuum [100]. The dynamics of hydrogen evolution in aluminium alloys as a function of the processing time, melt temperature, and initial hydrogen concentration have been investigated by Xu *et al*. [101], and the mechanism of US degassing discussed. Naji Meidani and Hasan developed in two similar publications [102,103] a mathematical model combined with a physical model to simulate the growth characteristics of a single bubble in a liquid by rectified diffusion. The model is based on the coupled momentum, energy and mass transport equations. The effects of the initial bubble radius, initial concentration of dissolved gas in the liquid, and the amplitude and frequency of the imposed ultrasonic field on the process of rectified diffusion were numerically studied. Experimental results were compared with those of the mathematical model, and the two exhibited a quite reasonable overall consistency.
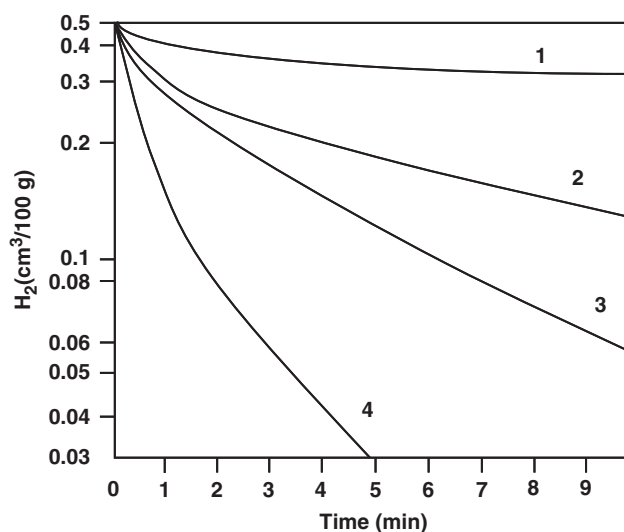
FIGURE 2.9. *Kinetics of hydrogen removal from the melt (an aluminium alloy) with different degassing techniques: (1) universal flux, (2) ultrasonic treatment, (3) vacuum treatment and (4) ultrasonic treatment in vacuo. (Reproduced with permission of Elsevier Ref. [100].)*

One salient example of the need for degassing in the clinical field and of the effective-ness of ultrasound for this purpose is a prototype of ultrasonic micro-degassing device for portable dialysis systems. The bubbles inside these systems reduce the effective exchange surface area, which is extremely important here [104].

Although degassing is a very common operation in analytical chemistry (particularly in liquid chromatography), it is rarely described in analytical procedures. Phrases such as "a previously degassed mobile phase (sample)" is the only description provided in the experimental section of papers. An unusual reference to this step can be found in an article on the ion chromatographic determination of trace levels of bromate by the use of large-injected volumes, which included the following sentence in its abstract: "With more than 1.5 ml injection volume, a sample pretreatment with a cartridge in Ag and H form, followed by a 10 min degassing in an ultrasonic bath, was needed" [105]. However, no further information about the degassing step or the type of US device used was provided in the Apparatus section.

2.6.3. Ultrasonic atomization

Atomization is the popular name given to the first step in a *spray-drying* operation, *viz*. the division of a liquid, suspension or emulsion into fine narrow-sized droplets or particles which can quickly lose the liquid phase under appropriate physical conditions. Liquids, suspensions and emulsions are usually atomized by forcing them at high velocity through

a small aperture; however, US is a more effective way for this purpose as it provides finer droplets with high sphericity and a uniform size distribution that ensure a lower momentum associated with ejected droplets relative to the droplets obtained by using conventional nozzles.

Bauckhage *et al*. [106] conducted an in-depth study on US standing-wave-assisted optimization by using two sonotrodes (20 kHz) oscillating against each other to disintegrate extremely viscous fluids (*viz.* synthetic resins and highly concentrated suspensions), or fluids with a high tension such as metal melts, into narrow-sized, extremely small droplets and from there the production of fine spherical powders. In this way, they obtained high solidification rates for metal powders (in particles with mean diameters of less than 10 μm) of up to 2×10^{-6} K/s. More recent research in this field has allowed correlations to be established with a view to predicting droplet size in US atomization, which accounts for the effects of the physico-chemical properties of the liquid (flow rate, viscosity, density and surface tension) and ultrasonic properties such amplitude, frequency and the area of the vibrating surface [107]; also, it has allowed analytical information about concentration characteristics to be derived from droplet diameter distributions [108].

Available knowledge of US atomization has enabled its use to enrich surfactants from aqueous solutions [109], and prepare lead–zirconate–titanate powders and ceramics *via* sol–gel and ultrasonic atomization hybrid methods [110]. The most important field of application of US atomization is probably the pharmaceutical industry, where the production of nanoparticles using supercritical CO_2 antisolvent is helped by US atomization, which also enhances mass transfer and prevents agglomeration through increased mixing. Nanoparticles as small as 130 nm in size have been obtained by using a power supply of 180 W [111]. Also, US atomization can be performed in a reduced pressure atmosphere for aseptic spray-drying for microencapsulation [112].

Dedicated portable atomization equipment has been patented [113] and an atomizer for the production of submicron, nanostructured metal powders with melting points up to 2000°C has been reported that testify to the interest of research in this area [114].

Although spray-drying is unusual in analytical chemistry, it is occasionally preferred to freeze-drying for sample conservation as it is faster and more economical — and also the only effective way of removing the liquid phase when the sample is fat-rich [115].

References

 1. A.M. Ure, L.R.P. Butler, R.O. Scott and R. Jenckins, *Pure Appl. Chem*., 60 (1988) 1461.
 2. A. Paschke, *Trends Anal. Chem*., 22 (2003) 78.
 3. P.D. Bièvre, *Accred. Qual. Assur*., 7 (2002) 181.
 4. S. Morales-Muñoz, J.L. Luque-García and M.D. Luque de Castro, *Crit. Rev. Environ. Sci*., 33 (2003) 391.
 5. S. Morales-Muñoz, J.L. Luque-García and M.D. Luque de Castro, *Anal. Chim. Acta*, 557 (2006) 278.
 6. H. Kataoka, *Anal. Bioanal. Chem*., 373 (2002) 31.
 7. E. Psillakis and N. Kalogerakis, *Trends Anal. Chem*., 22 (2003) 565.
 8. G. Theodoridis and I.N. Papadoyannis, *Mikrochim. Acta*, 136 (2001) 199.
 9. P. Bermejo, J.L. Capelo, A. Mota, Y. Madrid and C. Cámara, *Trends Anal. Chem*., 23 (2004) 654.
10. N.J. Miller-Ihli, *J. Anal. At. Spectrom*., 9 (1994) 1129.
11. T. Tekin, D. Tekin and M. Bayramoglu, *Ultrason. Sonochem*., 8 (2001) 373.
12. T. Tekin, *Hydrometallurgy*, 64 (2002) 187.
13. H.T. Dogan, A. Kurtbas and T. Tekin, *Chem. Eng. Technol*., 27 (2004) 87.
14. S. Chemat, A. Lagha, H.A. Amar and F. Chemat, *Ultrason. Sonochem*., 11 (2004) 5.

15. M. Chanon and J.L. Luche, Sonochemistry: Quo Vadis, in J.L. Luche (Ed.), *Synthetic Organic Chemistry*, Plenum Press, New York, 1998.
16. Q. Wang, M. Kuninobu, K. Kakimoto, H.I. Ogawa and Y. Kato, *Bioresource Technol*., 68 (1999) 309.
17. A. Tiehm, K. Nickel and U.Neis, *Water Sci. Technol*., 36(11) (1997) 121.
18. Y.C. Chiu, Ch. N. Chang, J.G. Lin and S.J. Huang, *Water Sci. Technol*., 36(11) (1997) 155.
19. T.I. Onyeche, O. Schäfer, H.Bormann, C. Schröder and M. Sievers, *Ultrasonics*, 40 (2002) 31.
20. C.P. Chu, D.J. Lee, B.V. Chang, C.S. You and J.H. Tay, *Water Res*., 36 (2002) 2681.
21. S. Lafitte and C.F. Forster, *Bioresource Technol*., 84 (2002) 113.
22. A.C. Íñigo, R. Alonso and S. Vicente-Tavera, *Ultrason. Sonochem*., 8 (2001) 127.
23. L.Wang and Y.J. Wang, *J. Cereal Sci*., 39 (2004) 291.
24. R. Al-Merey, M.S. Al-Masri and R. Bolou, *Anal. Chim. Acta*, 452 (2002) 143.
25. T.I. Trofimov, M.D. Saosonov, S.C. Lee, N.G. Smart and C.M. Wai, *J. Chem. Technol. Biotechnol*., 76 (2001) 1223.
26. M.C. Yebra, A. Moreno-Cid, R. Cespón and S. Cancela, *Talanta*, 62 (2004) 403.
27. M. Antunes Vieira, B. Welz and A.J. Curtius, *Spectrochim. Acta B*, 57 (2002) 2057.
28. C. Santos, F. Álava-Moreno, I. Lavilla and C. Bendicho, *J. Anal. At. Spectrom*., 15 (2000) 987.
29. J.L. Capelo, I. Lavilla and C. Bendicho, *J. Anal. At. Spectrom*., 13 (1998) 1285.
30. E. Priego-López and M.D. Luque de Castro, *Chromatographia*, 57 (2003) 513.
31. Y.C. Fiamegos, C.G. Nanos and C.D. Stalikas, *J. Chromatogr. B*, 813 (2004) 89.
32. M. Machado, P. Primo and C. Santos de Sousa, *Microchem. J*., 73 (2002) 273.
33. M. Sakakiraba, D. Wang, R. Takahashi, K.V. Takahashi and S. Mori, *Enzyme Microbial Technol*., 18 (1996) 444.
34. C. Turner, J.W. King and T. McKeon, *J. AOAC Int*., 87 (2004) 797.
35. M.P. Cañizares-Macías, J.A. García-Mesa and M.D. Luque de Castro, *Anal. Chim. Acta*, 502 (2004) 161.
36. Y.G. Adewuyi, *Ind. Eng. Chem. Res*., 40 (2001) 4681.
37. G.J. Price, *Current Trends in Sonochemistry*, Royal Soc. Chem., Cambridge, 1992.
38. L.A. Crum, T.J. Mason, J.L. Reisse and K.S. Suslick, *Sonochemistry and Sonoluminescence*, Kluwer Academic Publishers, Dordrecht, The Netherlands, 1999.
39. T.J. Mason and J.P. Lorimer, *Applied Sonochemistry*, Wiley-VCH, Weinheim, Germany, 2002.
40. T.J. Davies, C.E. Banks, B. Nuthakki, J.F. Rusling, R.R. France, J.D. Wadhawan and R.G. Compton, *Green Chem*., 4 (2002) 570.
41. Z. Liu, X. Quan, H. Fu, X. Li and K. Yang, *Appl. Catal*., 52 (2004) 33.
42. G. Cravotto, L. Boffa, M. Turello, M. Parenty and A. Barge, *Steroids*, 70 (2005) 77.
43. S. Baxter, S. Zivanovic and J. Weiss, *Food Hydrocol*., XX (2004) 1410.
44. M. Sivakumar, P. Senthilkumar, S. Majumdar and A.B. Pandit, *Ultrason. Sonochem*., 9 (2002) 25.
45. S. da Silva Borges, M. Korn and J.L.F. da Costa Lima, *Anal*. Sci., 18 (2002) 1361.
46. S. da Silva Borges and M. Korn, *Quím. Nova*, 25 (2002) 558.
47. J. Ruiz-Jiménez and M.D.Luque de Castro, *Anal. Chim. Acta*, 489 (2003) 1.
48. F. Priego-Capote and M.D. Luque de Castro, *Anal. Chim. Acta*, 489 (2003) 223.
49. S. Gupta and D.L. Feke, *Fluids Mechan. Transport Phenom*., 44 (1998) 1005.
50. R.Y. Wang, J.A. Jarratt, P.J. Keay, J.J. Hawkes and W.T. Coakley, *Talanta*, 52 (2000) 129.
51. J. Li, D.K. Hallbauer and R.D.Sanderson, *J. Membrane Sci*., 215 (2003) 33.
52. J.J. Hawkeks, D. Barrow, J. Cefai and W.T. Coakley, *Ultrasonics*, 36 (1998) 901.
53. R.S. Juang and K.H. Lin, *J. Membrane Sci*., 243 (2004) 115.
54. P. Cava-Montesinos, M.L. Cervera, A. Pastor and M. de la Guardia, *Anal. Chim. Acta*, 531 (2005) 111.
55. J. Booth, R.G. Compton, E. Hill, F. Marken and T.O. Rebbitt, *Ultrason. Sonochem*., 4 (1997) 1.
56. Y. Neuman, V. Rukshin, V. Tsang, S. Atar, T. Miyamoto, H. Luo, S. Kobal, T. Thompson, Y. Birnbaum, M. Horzewski, R. Siegel and S. Kaul, *Thrombosis Res*., 112 (2003) 99.
57. Y. Adler, A. Dagan, G. Golovchiner, Z. Iakobishvili, I. Matz, E. Lev, R.J. Siegel and Y. Birnbaum, *Ultrasound Med. Biol*., 29 (2003) 483.

58. V. Suchkova, E.L. Carstensen and C.W. Francis, *Ultrasound Med. Biol*., 28 (2002) 377.
59. A. Harder, R. Wildgruber, A. Nawrocki, S.J. Fey, P.M. Larsen and A. Görg, *Electrophoresis*, 20 (1999) 826.
60. S.G. Wang, Q. Zhang, S.F. Yoon, J. Ahn, Q. Wang, D.J. Yang, Q.F. Huang, E. Rusli, W.Z. Tang and F.X. Lu, *Diamond Rel. Mat*., 11 (2002) 1683.
61. H. Li, J. Wang, Y. Bao, Z. Guo and M. Zhang, *J. Crystal Growth*, 247 (2003) 192.
62. R. Chow, R. Blindt, R. Chivers and M. Povey, *Ultrasonics*, 43 (2005) 227.
63. M. Patrick, R. Blindt and J. Janssen, *Ultrason. Sonochem*., 11 (2004) 251.
64. T.J. Mason, L. Paniwnyk and J.P. Lorimer, *Ultrason. Sonochem*., 3 (1996) S253.
65. P.R. Lutwyche, J.P. Lorimer and T.J. Mason, unpublished results, final year undergraduate chemistry project, Coventry Polytechnic, 1985.
66. F. Priego-Capote and M.D. Luque de Castro, *Trends Anal. Chem*., 23 (10,11) (2004) 829.
67. O.N.M. McCallion, K.M.G. Taylor, M. Thomas and A.J. Taylor, *Intern. J. Pharmaceutics*, 129 (1996) 123.
68. D. Bemer and P. Tierce, *J. Aerosol Sci*., 27 (1996) S393.
69. S.V. Komarov, M. Kuwabara and M. Sano, *Ultrason. Sonochem*., 7 (2000) 193.
70. A.C. Dedhia, P.V. Ambulgekar and A.B. Pandit, *Ultrason. Sonochem*., 11 (2004) 67.
71. D. Hristozov, A.C. Domini, V. Kmetov, V. Stefanova, D. Georgieva and A. Canals, *Anal. Chim. Acta*, 516 (2004) 187.
72. M.S. Öncel, M. Ince and M. Bayramoglu, *Ultrason. Sonochem*., 12 (2005) 237.
73. S.C. Lee, S.C. Zou, K.F. Ho and L.Y. Chan, *Fresenius J. Anal. Chem*., 369 (2001) 166.
74. K.M. Swamy and K.L. Narayana, *Ultrason. Sonochem*., 8 (2001) 341.
75. B. Nienczewski, *Ultrason. Sonochem*., 6 (1999) 149.
76. E. Maisonhaute, C. Prado, P.C. White and R.G. Compton, *Ultrason. Sonochem*., 9 (2002) 297.
77. Y. Lu, N. Riyanto and L.K. Weavers, *Ultrason. Sonochem*., 9 (2002) 181.
78. J.O. Kim, S. Choi and J.H. Kim, *Appl. Acoustics*, 58 (1999) 211.
79. J. Foldyna, L. Sitek, B. Svehla and S. Svehla, *Ultrason. Sonochem*., 11 (2004) 131.
80. K. Kobayashi, M. Yamaguchi, S. Yoshihara, T. Kubota and J. Kudo, Assignor to TDK Corp. Tokyo. U.S. Patent 6 178 974. Jan. 30, 2001.
81. M.P. Pedziwiatr and E.A. Pedziwiatr, Cresskill, U.S. Patent 6 019 852. Feb. 1, 2000.
82. L. Jatzwauk, H. Schöne and H. Pietsch, *J. Hospital Infect*., 48 (2001) 580.
83. M. Tanomaru, M.R. Leonardo, K.C. Bonifácio, F.R. Dametto and I.A.B. Silva, *Internat. Endodontic J*., 34 (2001) 581.
84. I.J. Seymour, D. Burfoot, R.L. Smith, L.A. Cox and A. Lockwood, *Internat. J. Food Sci*., 37 (2002) 547.
85. N. Oulahal-Lagsir, A. Martial-Gros, E. Boistier, J.L. Blum and M. Bonneau, *Lett. Appl. Microbiol*., 30 (2000) 47.
86. P. Poesio and G.Ooms, *J. Petroleum Sci. Engin*., 45 (2004) 159.
87. J. Li, R.D. Sanderson and E.P. Jacobs, *J. Membrane Sci*., 205 (2005) 247.
88. M.O. Lamminen, H.W. Walker and L.K. Weavers, *J. Membrane Sci*., 237 (2004) 213.
89. I. Masselin, X. Chasseray, L. Durand-Bourlier, J.M. Lainé, P.Y. Syzaret and D. Lemordant, *J. Membrane Sci*., 181 (2001) 213.
90. T. Kobayashi, Ts. Kobayashi, Y. Hosaka and N. Fuji, *Ultrasonics*, 41 (2003) 185.
91. S. Muthukumaran, S. Kentish, S. Lalchandani, M. Ashokkumar, R. Mawson, G.W. Stevens and F. Grieser, *Ultrason. Sonochem*., 12 (2005) 29.
92. A.D. Farmer, A.F. Collings and G.J. Jameson, *Ultrason. Sonochem*., 7 (2000) 243.
93. A.D. Farmer, A.F. Collings and G.J. Jameson, *Intern. J. Mineral Proc*., 60 (2000) 101.
94. S.B. Awad, www.crest-ultrasonics.com
95. T. Sonoda, A. Watazu, J. Zhu, A. Kamiya, K. Ushiki, K. Naganuma and M. Kato, *Vacuum*, 60 (2001) 197.
96. G.I. Eskin, *Ultrason. Sonochem*., 2 (1995) S137
97. T.G. Leighton, *Ultrason. Sonochem*., 2 (1995) S123.
98. N. Gondrexon, V. Renaudin, P. Boldo, Y. Gonthier, A. Bernis and C. Petrier, *Chem. Eng. J*., 66 (1997) 21.
99. J.C. Austin and R.E. Challis, *Ultrasonics*, 37 (1999) 299.
100. G.I. Eskin, *Ultrason. Sonochem*., 8 (2001) 319.

101. H. Xu, X. Jian, T.T. Meek and W. Han, *Materials Lett*., 58 (2004) 3669.
102. A.R. Naji Meidani and M. Hasan, *Materials Proc. Technol*., 147 (2004) 311.
103. A.R. Naji Meidani and M.Hasan, *Appl. Mathem. Model*., 28 (2004) 333.
104. Z. Yang, S. Matsumoto and R. Maeda, *Sensors Actuators*, 95 (2002) 274.
105. S. Valsecchi, A. Isernia, S. Polesello and S. Cavalli, *J. Chromatogr*., 864 (1999) 263.
106. K. Bauckhage, O. Andersen, S. Hansmann, W. Reich and P. Schreckenberg, *Power Technol*., 86 (1996) 77.
107. R. Rajan and A.B. Pandit, *Ultrasonics*, 39 (2001) 235.
108. K. Yasuda, Y. Bando, S. Yamaguchi, M. Nakamura, A. Oda and Y. Kawase, *Ultrason. Sonochem*., 12 (2005) 37.
109. H. Takaya, S. Nii, F. Kawaizumi and K. Takahashi, *Ultrason. Sonochem*., 12 (2005) 483.
110. Z.J. Xu, R.Q. Chu, G.E. Li, X. Shao and Q.R.Yin, *Materials Sci. Eng*., 117 (2005) 113.
111. P. Chattopadyay and R.B. Gupta, *Intern. J. Pharm*., 228 (2001) 19.
112. S. Freitas, H. Peter and B. Gander, *J. Control. Release*, 95 (2004) 185.
113. Compaq Computer, USA Patent 6 259 971.
114. B. Clausen *et al*., www.metal-power.net
115. V. Fernández-Pérez, J. Tapiador, A. Martín and M.D. Luque de Castro, *Innov. Food Sci. Emerging Technol*., 5 (2004) 361.

CHAPTER 3

Ultrasound-Assisted Sample Digestion

3.1. INTRODUCTION

Direct solid analysis (*viz*. the detection of the target analytes in an untreated solid sample) is an area of limited scope in Analytical Chemistry. Only a few techniques such as infrared, Raman, photoacoustic and X-ray spectrometries and others that use some device of the electrothermal, laser ablation or glow-discharge type, for example, prior to sample insertion into an atomic spectrometer or a laser source to remove small portions of the solid sample for their subsequent analysis (*e.g*. laser–induced breakdown spectroscopy (LIBS)) are useful for this purpose. The greatest problem associated with the direct analysis of solid samples arises in the calibration step. Calibration can be done in various ways involving reference materials (RMs), synthetic solid standards, the method of standard additions and the use of aqueous standards. Reference materials are scant and are often replaced with synthetic solid samples mimicking the composition of the original sample. However, preparing synthetic solid standards is a difficult, time consuming process that is only justified when both the number of samples and that of analyses involved is quite large (*e.g*. in the steel industry). The method of standard additions has been used to suppress the influence of the bulk composition of solid samples; however, it relies on the assumption that the analyte contained in the solid sample and that of the added analyte will be identically affected by the matrix. Finally, the use of aqueous standards entails assuming that the instrumental signal will be independent of the bulk matrix and dependent on the analyte concentration alone. This requirement is rarely met owing to the presence of spectral and chemical interferences from the matrix [1].

Therefore, as noted in Chapter 2, most analytical methods involve some sample preparation step. Most often, such a step involves the transfer of the target analytes from the solid to a liquid phase. By exception, some techniques such as headspace or pervaporation involve the physical removal of volatile analytes from the solid sample.

One way of transferring a solid to a liquid phase is by sample dissolution, which, according to the IUPAC, is the process by which two phases are mixed to form a new homogeneous phase. Although IUPAC does not specify the nature of the two phases, its definition refers to the mixing of a solid phase and a liquid phase to obtain a solution. Based on this definition of dissolution, a solid can be dissolved in various ways, the simplest of which is by suspension in a solvent under agitation. Agitation can be provided by a vortex, magnetic stirrer, mixer or, simply, manual shaking. This operation is called "direct dissolution" and is not considered to be part of the analytical process, even though it can be a major source of error if it is not conducted properly. This operation can be performed in an efficient, reproducible manner by using robotic methods to avoid human intervention.

Sample dissolution can also be accomplished by using heat, chemical reagents and moisture. The underlying process is called "digestion" and involves decomposition of the sample matrix and the loss of its initial structure. Matrix decomposition is based on chemical processes ranging from complex reactions (*e.g*. destruction of organic matter by oxidation under drastic conditions) to the mere solvation of sample molecules for their dissolution. In addition to heating, chemical reagents and moisture, the pressure can be

modified in order to assist sample digestion. The use of high pressures allows the solvent to be maintained in a liquid state at a temperature above the boiling point. Calorific energy can be replaced or supplemented with other auxiliary energies such as microwaves or US in order to accelerate sample digestion. Each type of energy assists digestion differently; thus, microwaves raise the temperature very rapidly, whereas US increases it slowly to an equilibrium value. Ultrasound can assist digestion *via* mechanical and chemical effects.

3.2.   INFLUENCE OF ULTRASOUND ON SAMPLE DIGESTION

3.2.1. Effects involved in ultrasound-assisted sample digestion

As stated in Chapter 1, sonochemical studies have focused on the chemical effects of US. However, US is also known to have mechanical effects through super-agitation, the effects being especially significant at low frequencies. In digesting a suspension of a solid sample in a liquid phase, irradiation with US has several mechanical and chemical effects taking place simultaneously, all of which help dissolve the sample. The most important mechanical effects are microjetting and microstreaming. The former is a consequence of cavitation at or near any large solid surface, the resulting bubble collapsing in an asymmetric way. The large solid surface hinders liquid motion from the side concerned, so the major liquid flow into the collapsing bubble comes from the other side of the bubble [2–4]. As a result, a liquid jet is formed that implodes on particles, which collide between them, shearing, smoothing and pitting their surfaces, thus decreasing their size. The liquid jet can attain speeds above 100 m/s [5]. Microstreaming is a consequence of cavitation in the presence of suspended powder. When particles are small, they are mechanically disaggregated; this results in the dispersion of loosely held clusters and hence, in dissolution. Therefore, the mechanical effects of US act in combination as microjetting reduces particle size while microstreaming disperses particles and facilitates dissolution. It should be noted that microjetting and microstreaming are not the sole possible mechanical effects; ablation, erosion and interparticle collisions, among others, can also occur, albeit to a lesser extent.

Concerning chemical effects, US is known to increase the reactivity of some chemicals. The high temperature and pressure within a collapsing cavitation bubble produced by US irradiation causes the formation of free radicals and various other species. The primary chemical effects are therefore the promotion and acceleration of reactions involved in sample digestion.

Although the mechanical and chemical effects are simultaneous, their impact differs. The digestion conditions are strongly influential and the basis for the two digestion modes are depicted in Fig. 3.1. Ultrasound-assisted soft digestion (USASD) is usually the result of using US at an ambient or warm temperature and atmospheric pressure as the only auxiliary energy. Under these conditions, mechanical effects are the main agents responsible for sample digestion, even though chemical effects are also present. On the other hand, US-assisted strong digestion (USASTD) involves drastic conditions equivalent to those of an exhaustive sample treatment, including high temperatures and the use of highly reactive chemicals (*e.g.* pure or highly concentrated oxidants or reductants) in addition to ultrasonication.

The digestion approach of choice depends on particular sample composition. Provided the sample does not contain insoluble or refractory compounds, USASD may suffice to accelerate its dissolution. On the other hand, a complex matrix will normally have to be decomposed by drastic treatment, particularly if it contains refractory compounds.
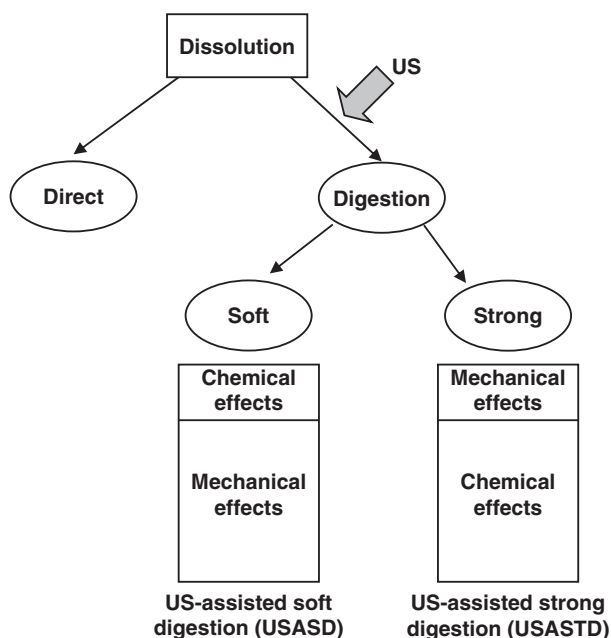
FIGURE 3.1. *Ultrasound digestion modes and effects involved.*

The digestion conditions to be used may alter some species, including the target analytes. Any such alterations which may result in analyte losses should be avoided. Some alterations have no effect on the final result; thus, atomic detectors provide the total concentrations of the target elements irrespective of their chemical form.

3.2.2. Variables affecting ultrasound-assisted sample digestion

Both ultrasonic baths and probes are useful for US-assisted digestion. When the ultrasonic energy provided by a bath suffices to accelerate dissolution of the sample, its use is preferred to that of a probe because baths are more commonplace in analytical laboratories. However, the increased power output of ultrasonic probes is often required to shorten digestion times. No comparison of the efficiency of the two types of ultrasonic source for US-assisted digestion appears to have been reported to date.

The procedure for performing US-assisted digestion is very simple. Although an ultrasonic bath can be used as the vessel, this is not a good option in order to avoid corrosion of its walls. Immersion of standard glasses, vessels or cells of different materials into it is therefore preferred. The procedure involves weighing the sample in the vessel, adding the liquid phase and immersing it into the bath for ultrasonic irradiation under appropriate conditions. With probes, the tip is usually immersed in the vessel containing the solid dispersed in the liquid phase. However, when some chemical reagents can attack the tip (*e.g.* in a metal probe), the probe and sample vessel should be placed in a transmitting liquid.

The performance of baths and probes in US-assisted digestion under soft or strong conditions depends on various factors that are rarely optimized for maximal efficiency and throughput in developing US-assisted digestion methods.

Variables affecting ultrasound-assisted digestion in both baths and probes

Ultrasound-assisted digestion is strongly influenced by a number of variables; however, most analytical chemists are unfamiliar with them and fail to optimize them and report their values. This is one of the main origins of poor precision and reproducibility in digestion procedures.

Vessel shape. One factor that is usually ignored in discrete analytical studies in general and digestion in particular is the shape of the vessel where the target chemical system is contained. Although round-bottomed flaks are the most commonly used vessels, flat-bottomed vessels (*e.g.* conical flasks) are preferred. This is because the transfer of energy is much more effective when the sound impinges directly on the flat bottom of a conical flask than when it hits the underside of a spherical container at an angle as this results in some energy being reflected away. One example is the digestion of potassium carbonate in dimethylformamide, which can be monitored *via* the decrease in particle size. As can be seen from Fig. 3.2, flat-bottomed conical vessels (*i.e.* vessels with a high base area to volume ratio) are more effective than round-bottomed flasks [2].
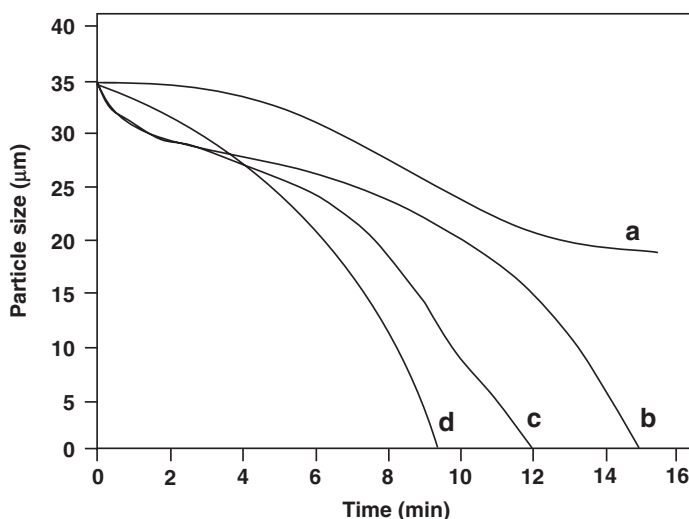
FIGURE 3.2. *Influence of vessel shape and stirring on the US-assisted digestion of potassium carbonate (1 g) in dimethylformamide in: (a) a 100 ml conical vessel without stirring; (b) a 100 ml round-bottomed vessel with stirring; (c) a 100 ml conical vessel with stirring; (d) a 250 ml conical vessel with stirring. (Reproduced with permission of Oxford Chemistry Press, Ref. [2].)*

The type of manifold to be used for continuous work should be thoroughly optimized once the power of the ultrasonic source has been checked to be adequate for the intended purpose.

Stirring of the solid–liquid system. As can be seen in Fig. 3.2, stirring the target suspension is highly advisable in batch work. This is particularly important in solid–liquid systems because the solid settles at the base of the vessel unless it is dispersed or agitated during the US-assisted step. The reason why additional stirring is so advantageous in this situation is that it ensures effective contact between the solid and liquid phases during sonication.

Temperature of the medium. Ultrasonic irradiation warms up the solid–liquid system. The resulting adverse effects of the temperature changes can be avoided in various ways, namely:

(a) By adopting the highest temperature reached during US application as the equilibrium temperature.
(b) By operating over very short periods and using cold water in the tank — the temperature can be assumed to remain essentially constant over short bursts of sonication.
(c) By circulating thermostated cooling water through the tank.

The currently available ultrasonic probes and baths are equipped with temperature control. There is an operational working alternative, particularly with US-probes, that is called "temperature mode" and involves applying US only until the sample reaches a preset temperature.

Pressure. The influence of this factor on digestion, both classical (*e.g.* wet digestion or dry ashing [6–8]) and otherwise (*e.g.* microwave-assisted digestion [9,10]), has been demonstrated, but scarcely studied in US-assisted digestion. There are only a few cases where high pressure has been applied using closed ultrasonic reactors for the acceleration of chemical reactions. These devices can also be used as ultrasonic digestors.

Characteristics of the solvent. Solvent properties affect US-assisted digestion as they impose the cavitation threshold above which sonochemical effects are "felt" by the medium. Also, any phenomenon altering some solvent property can modify such a threshold. Thus, any change in temperature results in a change in solvent properties such as the vapour pressure, viscosity or surface tension, which affect cavitation and their effects as a result.

Radiation amplitude. This variable is directly related to the amount of energy applied to the system. Exhaustive treatments require high irradiation amplitudes, for which probes are more suitable than baths.

Volume and nature of the transmitting liquid. The volume of transmitting liquid is another variable to be considered with ultrasonic baths and also when the sample reservoir is immersed in a thermostated bath in the case of probes. Small volumes of the transmitting liquid make direct impingement of the ultrasonic probe on the sample microcell redundant. With large volumes, US efficiency is decreased through scatter of the ultrasonic energy in the bulk solution.

The nature of the transmitting liquid must always be taken into account with ultrasonic baths, and also with probes when they are not to be dipped in the sample vessel. The nature of the liquid influences the cavitation phenomenon (*viz.* the estimation of the zones that will receive the maximum irradiation amplitude).

Particle size. Particle size is a key variable inasmuch digestion mechanisms are influenced by particle diameter. In fact, depending on particle size, simultaneous microstreaming and microjetting or some other effect can dictate the efficiency of US-assisted digestion to a variable extent.

Variables specific to ultrasonic baths: vessel position

The most important variable with ultrasonic baths is the position of the irradiated vessel with respect to the transducer. This is a consequence of non-uniform energy distribution in the bath owing to the formation of standing waves.

In the most common bath design, the ultrasonic transducer is attached to the underside of the metallic base of the bath and the strongest power level occurs directly above the transducer. However, the ultrasonic power profile in the bath liquid varies in a non-uniform manner with the distance from the base. This has been ascribed to the fact that US is driven through the liquid as waves, so there are points where the irradiation amplitude is maximal and others where it is zero. Maxima are always desirable and can be calculated as multiples of the half-wavelength of sound (λ) in the medium. Such distances can be calculated from the equation:

$$c = f \cdot \lambda \tag{3.1}$$

For example, the velocity of sound (c) through water is approximately 1500 m/s, so the wavelength of US in water for a transducer operating at a frequency (f) of 20 kHz will be 7.5 cm. The maximum effect expected will occur probably at distance intervals of 3.75 cm from the transducer position. These high-intensity positions can be accurately located by using a simple mapping technique involving sonicating a piece of aluminium foil placed vertically in the bath. After a preset irradiation time, a number of perforations will appear in the foil. Obviously, the vessel will have to be positioned at the point where the maximum irradiation is to be expected. For a bath with a single transducer on the base, this is a simple task: the vessel must be placed vertically above the transducer. For a bath with multiple transducers, application of a mapping technique is more difficult. The points of maximum irradiation can be located in other ways as described in Chapter 1.

Variables specific to ultrasonic probes

There are other specific physical variables that influence digestion assisted by an ultrasonic probe, namely:

Depth of immersion into the sample vessel or bath containing the transmitting liquid.
This variable has a decisive influence on the effect of ultrasonic probes. This is because virtually no sonication exists alongside or above the tip. Therefore, if the probe is only slightly immersed, it will cause foaming at the liquid surface and result in the loss of

US energy. On the other hand, if the probe is immersed to an excessive depth, the energy supplied will be inadequately transmitted through the liquid and the digestion efficiency will suffer as a result.

Probe tip–sample cell distance. This variable should be considered when the probe is not inserted into the sample vessel. The shorter the distance, the less attenuation occurs and the higher is the energy applied to the sample as a result.

Application of pulses and duration. This variable, which affects ultrasonic probes exclusively, comes into play when operating in a pulsed mode. In USASD, sample dissolution can be favoured by short or long pulses; in USASTD, the severity of the treatment requires using long pulses.

Variables affecting continuous ultrasound-assisted digestion

There are only two references to continuous US-assisted digestion, both by the same authors [11,12], who optimized the composition of the liquid phase, sonication time, temperature, volume of solvent and flow-rate. On the other hand, they failed to consider the potential effects of other important variables such as the shape of the container, the volume and nature of transmitting liquid, particle size and, especially, the position of the container in the ultrasonic bath.

All comments above about common and specific variables for ultrasonic baths and probes also apply to continuous US-assisted digestion, which additionally involves dynamic variables. The most influential dynamic variable is the flow-rate of the liquid phase, which should be set in such a way as to avoid compaction of the solid in the chamber and ensure effective contact of the two phases. Consequently, the flow-rate of choice in each case will depend on the particular solid–liquid system.

Other dynamic variables to be optimized include the direction of the liquid phase flow, combinations of static and dynamic cycles and use of straight or coiled tubes in the continuous manifold.

3.3.   ULTRASOUND-ASSISTED SOFT DIGESTION (USASD)

Ultrasonic energy is frequently used to accelerate the dissolution of solid samples under soft conditions of temperature, pressure and chemical reagents. Similar to direct dissolution by agitation, US-assisted soft digestion is not used to the same extent as other operations of the analytical process such as leaching, derivatization or detection. The simplicity of this operation with some types of samples and the operator's lack of awareness of its error contribution are responsible for the absence of optimization studies for this process. Inappropriately conducted soft digestion can result in major errors and affect the quality of the results.

3.3.1. Scope of ultrasound-assisted soft digestion

Dissolution is usually performed by suspending the solid sample in a vessel containing a solvent and agitating the mixture by manual or mechanical stirring or shaking to ensure complete transfer of the solid into the liquid phase. This operation is normally carried out

at room temperature but is facilitated by warming. Direct dissolution is applied to readily soluble samples.

Dissolution as a sample preparation step is preferred to leaching and the physical removal of analytes when the sample can be easily solubilized without the need for exhaustive or drastic treatment. There are obvious advantages in the simplicity of the dissolution operation (*e.g.* the need for no operator training and the ability to perform the dissolution in an automated way by, for example, using a robotic approach).

Dissolution can be virtually instantaneous or may take minutes or even hours — this being the longest step in the analytical process. One way of accelerating dissolution is by using auxiliary energy such as that of US. Ultrasound facilitates dissolution *via* mechanical effects and, to a lesser extent, chemical effects. A vast number of analytical methods use US energy to facilitate sample dissolution by soft digestion. However, optimization data and additional information about the mechanisms involved in each case are rarely reported. Obviously, the assistance of US to the dissolution of solid samples has been sought in those applications where substantially shortened analysis times were expected.

Ultrasound-assisted soft digestion is subject to the same shortcomings as other dissolution modes. Thus, the most serious shortcoming is the absolute lack of selectivity relative to other solid SP alternatives by effect of the whole sample being transferred to the liquid phase. This lack of selectivity is a major drawback for USASD as an alternative to other SP approaches in an analytical process and can dictate its exclusion in favour of a more selective choice involving removal of the target analytes and providing a less complex liquid, thereby reducing the risk of interferences. One way of circumventing the lack of selectivity of USASD is by using a determination technique selective for the target analytes. While this is always desirable, when unfeasible, additional steps can be performed to reduce or suppress the effects of interferents. There are several ways of increasing the selectivity of the analytical process, by chemical or biochemical reactions, such as complex formation, surface adsorption, electrochemical reactions, etc. The choice will depend on the particular analyte(s) and (or) interferent(s) [13]. One other drawback of USASD that detracts from sensitivity is the dilution effect of the liquid phase. This drawback can be overcome by using a subsequent concentration step that will additionally raise the selectivity of the method *via* the concomitant clean-up effect usually inherent in preconcentration steps.

Although clean-up and preconcentration help to improve the selectivity of dissolution and offset the dilution effect, they lengthen the analytical process. This drawback should always be borne in mind in view of the growing tendency to shorten the analytical process so as to analyse as many samples as possible in the shortest time. It is always preferable to use selective steps such as leaching, pervaporation or headspace to remove the analytes from a solid sample. However, very frequently, they fail to provide quantitative results owing to inadequate efficiency and (or) precision. In this situation, USASD is an effective alternative to ensure complete transfer of analytes to a liquid phase and hence the quality in the results.

Although USASD involves soft operating conditions, the absence of analyte changes caused by US should be checked whenever preserving the stability of the analytes is important. The high temperatures and pressures reached within a collapsing cavitation bubble produced by US induce the formation of free radicals, which can trigger reactions altering the concentrations of the target analytes.

As previously stated, both ultrasonic baths and probes can be used for USASD, both in discrete and continuous approaches. Thus, the choice of an ultrasonic bath or a probe will depend on the particular treatment to be applied. If a bath provides enough energy

for the intended purpose, then it should be preferred to a probe as it is more widely available and allows several samples to be treated simultaneously and in greater amounts. The absence of uniformity in the energy profiles emitted by baths can pose problems in digesting several samples simultaneously because the intensity can vary between them. Among others, this can affect the determination of volatile or labile analytes, which may be differently vaporized or degraded, respectively, depending on the position of the sample in the bath.

Probes supply more powerful energy; also, in the absence of highly reactive chemicals, the tip can be directly inserted into the digestion medium.

Most applications of USASD are discrete in nature. This can be ascribed to the fact that few research groups have so far worked on continuous approaches despite such major advantages as automation and reduced chemical consumption. Because automation is one of the main goals in developing continuous systems, the best way of performing batch digestion steps in an automated manner is by using a robot to mimic the operations carried out manually by an operator [14].

3.3.2. Experimental checking of USASD mechanisms

As previously stated, the principle behind USASD is based on the mechanical effects of US, which enhance the kinetics of some processes. Let us review such effects in the light of recent studies.

That soft digestion enhanced by US was first demonstrated by Kannan and Pathan [15], who soft-digested aqueous benzoic acid in the experimental device shown in Fig. 3.3. The cylindrical geometry for the sample was intended to ensure uniformity in the solid surface and improved accessibility by the liquid phase. The solid was immersed in a water bath with temperature control at 31°C. The ultrasonic source was a probe that was inserted vertically into the water bath. The device was rated at 500 W and 20 kHz frequency. Trial experiments of USASD without temperature control of the water bath
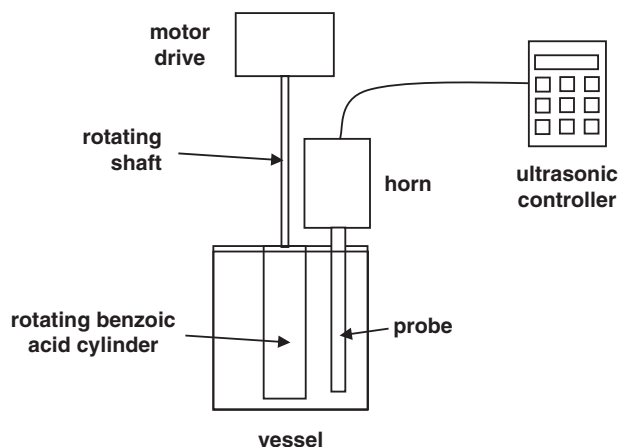
FIGURE 3.3. *Experimental set-up for the USASD of benzoic acid in water. (Reproduced with permission of Elsevier, Ref. [15].)*

resulted in a fast temperature rise and rapid solid digestion. With temperature control, the process was much slower, but developed in a more uniform way. The runs involving US assistance were of shorter duration than those without ultrasonic energy, which exhibited very low digestion rates. Thus, the runs involving no US assistance took 5 h at a low cylinder speed (50 rpm); with US at 70% of the nominal converter power, the run time needed to obtain approximately the same concentration of benzoic acid in the solution as in absence of US was 40 min. The application of US resulted in a mass transfer coefficient up to 5.5 times higher than in the absence of sonication. On the other hand, increasing the speed of rotation five times increased the mass transfer coefficient by approximately three times only. Therefore, US was much more effective than mechanical rotation, which testifies the strong influence of ultrasonic energy on the transfer of the solid to the liquid phase. The effect is probably a result of increased turbulence and a consequent reduction in mass transfer resistance when the solvent impinges on the solid.

Some authors have studied in depth the mechanical effects of US that produce the superagitation phenomenon upon application of US. Such effects can act simultaneously or separately depending on the characteristics of the sample (particularly its composition and particle size); also, the mechanism can change by effects of variations in particle size during the process. Lu *et al.* [16] studied the digestion in water of silica and alumina particles of various sizes and surface areas in the presence of US as compared with dissolution assisted by a rotating agitator at a speed of 120 rpm. Both processes were monitored *via* particle size changes using a Malvern Mastersizer laser light scattering particle size analyser. Two different ultrasonic processors were used to compare their efficiencies. An ultrasonic probe operating at 20 kHz with a power density of 460 W/l coupled to a glass Rosett cell was used in addition to a near-field acoustic processor (NAP) equipped with two water-cooled magneto-restrictive transducers fixed to each stainless steel parallel plate, operating at 16 kHz on one plate and 20 kHz on the other, with a total power density of 53.3 W/l. Figure 3.4 shows the kinetics of particle size reduction for the alumina particles in the presence of sonication (by the probe) and with agitation only. As can be seen, particle size exhibited no change with hydrodynamic mixing over a 1-h period; by contrast, sonication decreased the particle size according to a first-order kinetics regime. Regarding the results provided by the NAP, the particle size decreased under the effects of US and also with a decreasing rate according to a first-order regime. Interestingly, however, the efficiency of the NAP was much higher than that of the probe by virtue of the two ultrasonic transducers operating at different frequencies on opposite sides of the sonicated liquid, in contrast to the probe with a single transducer.

A complementary SEM study was conducted to analyse the structure of the particles before, during and after ultrasonic treatment. Figures 3.5A and B shows the images of silica particles (initial diameter 60 μm) before and after 60 min sonication, respectively. Compared to non-sonicated particles, the surface of US-treated particles was both smoothed and pitted. In addition, many new and small particles were formed by sonication as the initial particles were violently agitated and collided frontally and tangentially with the outcome being broken particles.

The concentrations of aluminium and silicon in the aqueous solution were measured using ICP-AES. Compared to agitation, the concentrations of the two elements in the aqueous phase increased with the sonication time. Figure 3.6 shows the variation of the aluminium concentration with time. Table 3.1 lists the concentrations of the particles after 60 min of sonication and agitation. As can be seen, the concentrations after sonication were 7–20 times higher than with agitation only due to the combined effect of microstreaming and microjetting. With alumina and silica, which exhibited marked changes in particle size and a comparatively small increase in the concentrations of Al and Si in the liquid phase, microjets and particle collisions appear to be more decisive
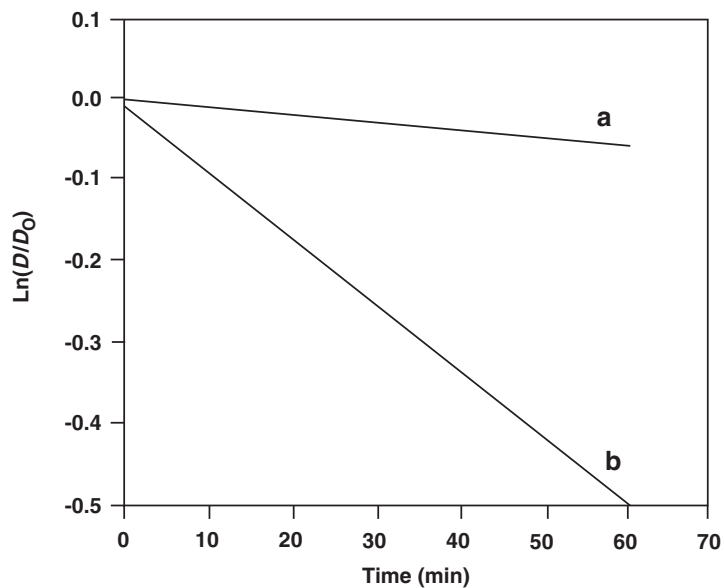
FIGURE 3.4. *Change in diameter of alumina particles with mechanical agitation (a) and sonication (b) demonstrating the progress of USASD. D_o (initial diameter) = 130 µm; SA_o (initial surface area) = 200 m^2/g; pH = 6; C_A (alumina concentration) = 2 g/l. (Reproduced with permission of Elsevier, Ref. [16].)*
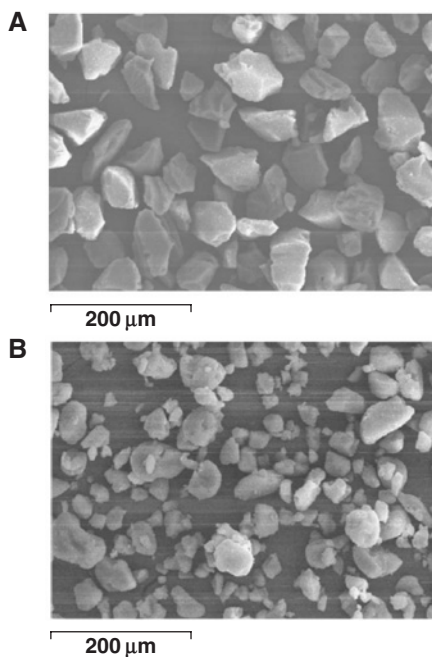
FIGURE 3.5. *SEM image for silica particles of D_o (initial diameter) = 60 µm: (A) before sonication and (B) after sonication for 60 min. (Reproduced with permission of Elsevier, Ref. [16].)*
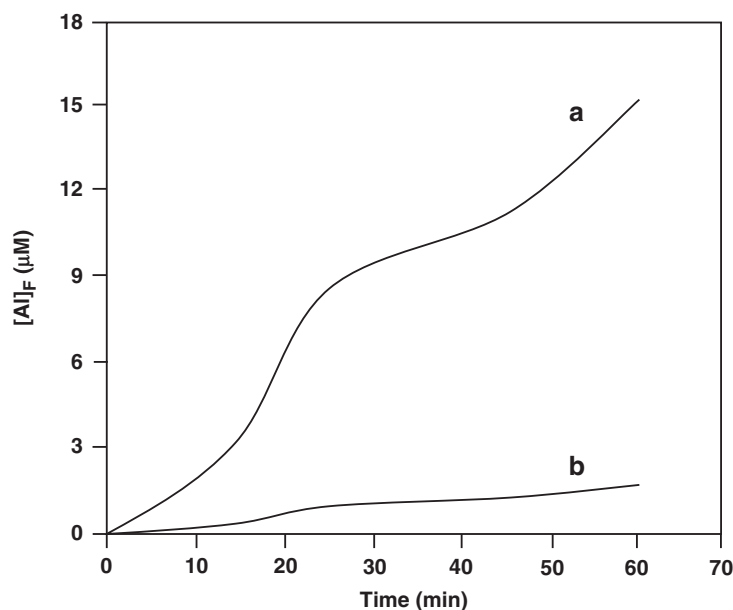
FIGURE 3.6. *Aluminium concentration in the filtrate (< 0.45 μm pore size) after (a) USAD and (b) mechanical agitation. D_o = 130 μm; SA_o = 200 m^2/g; pH = 6; Concentration (alumina) = 2g/l. (Reproduced with permission of Elsevier, Ref. [16].)*

than microstreaming. An additional mechanism to which other authors have ascribed the enhanced solubilization of particles under US is related to the increased temperature in the interfacial region of collapsing cavitation bubbles [17]. Under such a high temperature, bubbles may dissolve surfacial alumina and silica during cavitational collapse and formation. Thus, the increased concentration of silicon in the solution relative to aluminium may have resulted from the lower melting point of silica relative to alumina (1.873 K *versus* 2.288 K [18]).

TABLE 3.1. *Concentration of silicon and aluminium in the filtrate (< 0.45 μm) after sonication and with agitation only after 60 min (2 g/l concentration).*

Particle	C (with sonication) (μM)	C (without sonication) (μM)
Silica (D_O = 2 μm)	17	17
Silica (D_O = 60 μm)	58	3
Silica (D_O = 130 μm)	36	5
Alumina (D_O = 130 μm), SA_O = 155 m^2/g	24	2
Alumina (D_O = 130 μm), SA_O = 200 m^2/g	16	1

C — concentration; D_O — initial particle size; SA_O — initial surface area.
Reproduced with permission of Elsevier, Ref. [16].

3.3.3. Applications of USASD

Ultrasound-assisted soft digestion (USASD) has been applied to a variety of sample and analyte types in widely diverse fields. This section discusses its implementation in the analytical process and its principal uses. Ultrasonic soft digestion has been used in connection with both organic and inorganic analytes.

   The most common way of implementing USASD in the analytical process is as the first step, which is frequently the only sample treatment performed. This non-selective step can be used when a selective enough determination technique (*e.g.* atomic or mass spectrometry) is to be used or with samples of simple and (or) known composition. One example is the above-described ultrasonic soft digestion in a continuous way for 30 s prior to the determination of iron and zinc in milk powder and infant formulas by flame atomic absorption spectrometry (FAAS) [11,12]. The authors used the words "dissolution" and "leaching" indifferently when the proper term, according to IUPAC, would have been "digestion" as an auxiliary energy was used to accelerate dissolution. Figure 3.7 shows the manifold used to implement the two methods. The procedure involved weighing the sample in a glass minicolumn, which was connected to the continuous system and immersed in an ultrasonic water bath. Once the circuit was filled with solvent, the solvent was circulated through the manifold while the minicolumn was ultrasonicated. The direction of the flow was changed every 10 s in order to avoid accumulation of the sample at one end of the minicolumn and its clogging. Then, the switching valve was actuated in order to drive the solution to a flame atomic absorption spectrometer for determination. Water was used as the liquid phase, so the process was soft digestion based on mechanical effects. However, this procedure can also be used for strong digestion with highly concentrated chemical reagents and high bath temperatures only limited by the boiling point of the transmitting liquid. The reported throughput was 80 samples per hour, but cleaning of the
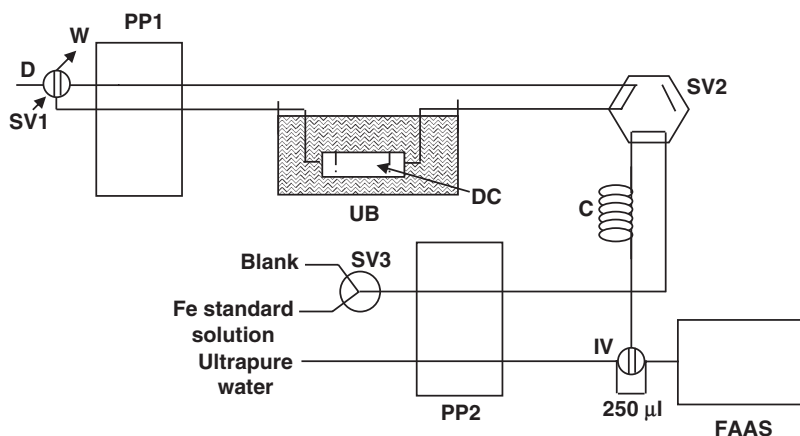
FIGURE 3.7. *Continuous USASD of milk powder and infant formula prior to the FAAS determination of iron and zinc. C — coil, D — digestant, DC — digestion chamber, FAAS — flame atomic absorption spectrometer, IV — injection valve, PP — peristaltic pump, SV — switching valve, UB — ultrasonic bath and W — waste. (Reproduced with permission of Elsevier, Ref. [11].)*

manifold between analyses and weighing of the sample and connection of the minicolumn to the continuous manifold were presumably excluded.

A number of samples with a simple and (or) known composition have been subject to USASD, particularly in the analysis of pharmaceutical formulations in diverse dosage forms such as tablets, capsules, suppositories and powder, with digestion times ranging from 5 to 30 min in most cases [19–32]. The nature of the solvents used depends on the composition of the sample and can range from toluene to sodium hydrogen sulphite. Other types of samples of known composition which have been digested with US assistance include sugar-containing foodstuffs [33,34], cosmetics [35], disinfectant products [36], plants [37] and packaging materials [38]; the ensuing applications testify the usefulness of this operation in routine analyses. Table 3.2 shows selected applications of USASD, which, in addition, has been used in robotic methods to facilitate complete automation of sample preparation prior to electrospray mass spectrometry detection. For this purpose, a Zymark robot was used to transfer sample cups from a rack to an ultrasonic bath to ensure rapid and complete digestion of the sample before placing the cup in a centrifuge in order to proceed with the analytical process [39]. This method demonstrates the feasibility of incorporating USASD into discrete automated methods for quality control in industrial and routine analyses, which require the processing of large numbers of samples without human intervention.

Ultrasound-assisted soft digestion can also be used to reconstitute a solid residue in a solvent resulting from a preconcentration and (or) clean-up step by evaporating the solvent on rotary-evaporator or with an N_2 stream, for example. Most often, the residue comes from an extract and the aim is usually to improve sensitivity and (or) selectivity. One example is the determination of the total cholesterol content in foods, which are previously saponified, extracted from an aqueous phase to an organic one, preconcentrated and US-assisted reconstituted in sodium cholate [40]. Another example is the determination of melatonin in biological samples following leaching with dichloroethane; the organic phase is then evaporated and the residue reconstituted in water with US assistance prior to CE–UV detection [41].

Ultrasound-assisted soft digestion has been used for other practical purposes from which analytical chemists can derive new applications. One case in point is in medicine, where ultrasound has been used as an adjunctive therapeutic treatment for clot dissolution of pharmacological thrombolysis. The combination of externally applied low-frequency high-intensity US with fibrinolytic therapy resulted in more rapid and complete reperfusion than the application of US or administration of fibrinolytic agents alone [42].

3.4.   ULTRASOUND-ASSISTED STRONG DIGESTION (USASTD)

3.4.1. Scope of USASTD

Strong digestion is characterized by the drastic conditions in terms of temperature, pressure and concentration of chemical reagents in order to effect sample dissolution, which is the most crucial step in this operation. The complexity of the matrix dictates the specific conditions to be used for its efficient decomposition so that the target analytes can be thoroughly released from it and solubilized in a form amenable to determination with the technique of choice. The stability of the analytes is important inasmuch as strong digestion can result in losses and in transformation into other species not compatible with the determination technique used. As a result, the principal field of application of USASTD is the determination of inorganic analytes with atomic detectors.

TABLE 3.2. *Selected applications of US-assisted soft digestion.*

Application field	Analytes	Sample	Digestion medium	Digestion time (min)	Reference
Pharmaceutical	Dimenhydrinate	Tablets	Chloroform	–	[19]
	Water-soluble vitamins	Tablets	DMSO	10	[20]
	Metronidazole and norfloxacin	Tablets	Acetic acid/acetonitrile (10/90%)	10	[21]
	Indapamide	Pills	Methanol	20	[22]
	Melatonin	Tablets	Ethyl acetate	15	[23]
	Fluoxetine hydrochloride	Capsules	H_2O	15	[24]
	Acetaminophen, caffeine and butalbital	Tablets	Methanol	30	[25]
	Catecholamines	Tablets	0.01M $NaHSO_4$ aqueous	–	[26]
	Aspirin and codeine	Tablets	30% Acetonitrile aqueous	2	[27]
	Paracetamol and isopropylphenazone	Tablets	H_2O	–	[28]
	Quetiapine fumarate	Tablets	Methanol	–	[29]
	Moxifloxacin	Tablets	0.1% H_3PO_4 aqueous	–	[30]
	Glycyrrhizic acid	Tablets	H_2O	10	[31]
	Amlodipine	Tablets	Methanol	30	[32]
Food	Toxic elements	Sugar and sugar–containing foodstuffs	H_2O	3	[33]
	trans–10–Hydroxy2–decenoic acid	Royal jelly	Acetonitrile/0.1% H_3PO_4 aqueous/THF (63/35/27%)	–	[34]
Hygiene	Sunscreen agents	Cosmetics	Methanol	5	[35]
	Triclosan	Disinfectants	Methanol/acetonitrile/ H_2O (40/40/20%)	30	[36]
Plant	Alkaloids	Poppy *Papaver somniferum*	5% Acetic acid aqueous	10	[37]
Polymer	Styrene	Polystyrene	Toluene	–	[38]

Strong digestion is a frequent step in official methods of analysis, which use both classical digestion procedures and modifications thereof intended to accelerate or automate this step. Classical strong digestion methods are of two main types, namely dry ashing and wet digestion. A third type of method, fusion, is used to a lesser extent. In fusion methods, the sample is mixed with an alkali metal hydroxide, carbonate or borate as melting reagent. The mixture is heated up to its melting point and then allowed to cool, the resulting fusion cake being dissolved in an appropriate liquid phase. Fusion is usually reserved for the determination of major matrix elements in acid-insoluble samples. Alkaline fusion is often used for geological and industrial purposes as it allows the subsequent efficient solubilization of both major and trace elements in the sample matrix. Fusion methods generally require four to eight times as much reagent as sample. The fluxing agents should be of a very high purity as they can be potential sources of contamination in trace element analyses.

Dry ashing or calcination are generally used to remove organic matter. Therefore, their use is restricted to inorganic analytes. Dry ashing at a high temperature and atmospheric pressure (*e.g.* in a muffle furnace) is the most widely used procedure in this context. The procedure consists of weighing the sample in a suitable crucible and heating in a muffle furnace at 400–550°C for several hours. A high pressure can also facilitate ashing. Dry ashing ensures the quantitative decomposition and removal of organic matter. The effect of the decomposition of organic matter is called "mineralization". This term is improperly used to refer to dry ashing, as mineralization can also be caused by other strong digestion procedures. The inorganic components of the matrix are transformed into carbonates or oxides that are then dissolved in an appropriate acid.

The other major group of strong digestion procedures is wet digestion, where the organic components of the sample are oxidized in the aqueous phase by heating in the presence of an oxidant (usually a combination of acid and hydrogen peroxide). Like dry ashing, wet digestion can be implemented in two ways depending on whether atmospheric or high pressure is used. The aim of using high pressure is to maintain the solvent in the liquid state above its boiling point [43].

Dry ashing and wet digestion have some disadvantages that detract from accuracy and precision in the results. Such disadvantages include long manipulation times, an increased consumption of chemicals, increased viscosity and losses of elements by volatilization and fume-hood emissions in addition to the risk of sample contamination. Also, reactions between some analytes and crucible materials can give rise to combustion residues.

Calorific energy can be replaced with other auxiliary energies, particularly microwaves, for wet digestion. Because heating occurs within the digestion medium, microwave digestion is more efficient than conventional heating. The use of microwaves often improves expeditiousness and efficiency in the decomposition of some types of samples that are difficult to solubilize otherwise. Also, it facilitates automation of the process. The advantages of microwave-assisted digestion have promoted its wide adoption as an effective sample pre-treatment, mainly for the determination of metals in a wide range of sample matrices; in fact, many of the ensuing methods are now used as references by several official bodies. An increasing number of laboratories are replacing conventional methods with others based on this technology, as reflected in the ever increasing amount of material published on the subject [44]. The principal restriction of these procedures is the long cooling times required before low or high-pressure pumps are opened [45]. Also, the amounts of acid and sample that can be used are limited by the vessel capacity — which detracts from the limits of detection — and the use of a

domestic microwave oven with closed systems involves serious safety and reproducibility problems [46].

Ultrasonic energy is also used to assist wet digestion, albeit to a much lesser extent than microwave-assisted digestion. As stated in Chapter 2, the term "digestion" is rarely used in connection with ultrasonic treatments. However, the proper term when ultrasonic energy is used in conjunction with a high temperature and (or) some chemical reagent is "strong digestion" as the matrix is decomposed and the whole solid transferred to the liquid phase. Partial digestion can also be produced owing to the presence or formation of insoluble compounds.

Ultrasonic strong digestion is based on mechanical and, especially chemical effects. The chemical effects result from the reactivity of the chemical agents (oxidants or reductants) promoted by the radicals generated by sonolysis of the solvents in the liquid phase (particularly in aqueous solutions). In fact, the radicals act as promoters of the chemical reactions involved in matrix decomposition.

The operational set-ups for ultrasonic strong digestion are identical to those used for discontinuous or continuous soft digestion. However, no USASTD methods based on continuous systems have to date been reported despite their technical feasibility. Thus, discrete strong digestion under the assistance of a US bath or probe in open or closed systems is the most common choice. One requirement with open devices is controlling the atmospheric emissions. Probes are more frequently used than baths by virtue of the higher energy they provide. Because strong digestion is an exhaustive treatment, the tip probe is normally immersed in the digestion vessel. A metallic tip can therefore corrode and contaminate the solution, thereby interfering with the determination of metallic elements. This problem can be avoided by using probes made from a specific material (particularly glass) [47], or by covering the probe tip with a Teflon band to avoid corrosion in the presence of oxidants [48]. One drawback of using a band is that it attenuates ultrasonic energy, so the energy emitted by the probe is not completely applied to the sample–liquid system.

The primary aim in using ultrasonic energy to accelerate the digestion of solid samples is to overcome the shortcomings of classical digestion procedures and microwave-assisted digestion. The salient advantage of US is that it enables operation at ambient temperature; by contrast, the previous choices involve high temperatures. This results in improved safety as compared with both conventional procedures and microwave-assisted digestion. Thus, complex reagent mixtures — even those unusable in classical procedures and microwave assisted digestion — can be used in USASTD with significantly reduced fume-hood emissions. Also, analyte losses by vaporization are generally absent, although losses can also be produced by alterations caused by the radicals generated by sonolysis of the liquid phase. Additional benefits include ease of use, availability of the experimental set-up, which requires no special vessels, relatively low costs and suitability for in-field digestion [49,50].

3.4.2. Digestion media

Similar to other digestion methods, the choice of digestion medium in USASTD is dictated by the particular type of treatment required. Thus, with clayey matrices, the digestion medium should contain HF; on the other hand, if the samples contain a high proportion of organic matter, then the digestion medium should include an oxidizing acid to eliminate it or an organic solvent to dissolve it. As stated before, USASTD can be used with any type of solvent; by contrast, safety reasons make some solvents unusable in classical procedures and microwave-assisted digestion.

The high significance of USASTD in spite of its scant use warrants some comments on the characteristics of the different reagents that can be employed in the process, whether acids or other types of substances.

Nitric acid

Nitric acid is the primary choice for strong digestion. It is an oxidizing acid that can dissolve most metals to soluble nitrates. Although it has a poor oxidizing strength below 2 M, it is a powerful oxidant in concentrated solutions. Also, its oxidizing power can be boosted by the addition of chlorate, permanganate, hydrogen peroxide or bromine, as well as by raising the temperature. Most metals and alloys are oxidized by nitric acid; however, gold and platinum are not, and some metals are passivated by concentrated solutions of this acid. Such metals can be dissolved by using a combination of acids or a dilute nitric solution. On the other hand, nitric acid at a high temperature can decompose most organic molecules and converts hydrocarbons into carbon dioxide and water.

Hydrochloric acid

Hydrochloric acid is a non-oxidizing acid that exhibits weak reducing properties during strong digestion. Concentrated HCl is an excellent solvent for some metal oxides and also for metals that are more readily oxidized than hydrogen. At high temperatures, many silicates and other refractory oxides, sulphates and fluorides are attacked by HCl to produce generally soluble chloride salts. Because it is not an oxidizing agent, concentrated hydrochloric acid is rarely used to digest organic materials. Nevertheless, it is an effective solvent for basic compounds such as amines and alkaloids, as well as for some organometallic compounds. The hydrolysis of natural products with HCl is a routine preliminary procedure for the analysis of amino acids and carbohydrates, and also for that of intracellular components.

Hydrofluoric acid

Hydrofluoric acid is a non-oxidizing acid, the reactivity of which is based on its strong complexing capacity. It is most commonly used in inorganic analysis because it is one of the few acids that can dissolve silicates. Its strong complexation capabilities prevent the formation of sparingly soluble products of various metals and increases their solubility and stability. Digestion with HF produces soluble fluorides mainly — by exception, the fluorides of alkaline earths, lanthanides and actinides are insoluble or sparingly soluble at most. In order to improve digestion, HF is routinely combined with another acid such as HNO_3. Insoluble fluorides may frequently be redissolved by removing the HF after digestion.

Phosphoric acid

Hot phosphoric acid has been successfully used to digest iron-based alloys when HCl would have volatilized specific trace constituents. Phosphoric acid can also digest a wide

range of aluminium slags, iron ores, chromium and alkali metals. Because of its low vapour pressure, it affords relatively high temperatures without disrupting the digestion.

Sulphuric acid

While dilute sulphuric acid exhibits no oxidizing properties, in concentrated form, the acid is capable of oxidizing many substances. In fact, concentrated H_2SO_4 is an effective solvent for a wide range of organic tissues, inorganic oxides, hydroxides, alloys, metals and ores. Sulphuric acid is commonly used with other acids and reagents. Two of the most frequent combinations are with perchloric acid and hydrogen peroxide. Sulphuric acid can act as a dehydrating agent and dramatically increase the oxidizing power of per-chloric acid. Mixtures of the two acids can cause problems in some classical procedures and microwave-assisted digestion as they can react explosively with organic matrices in closed vessels or if heated too rapidly.

Perchloric acid

Hot $HClO_4$ is a strong oxidant which attacks metals that are unresponsive to other acids. Perchloric acid also effects the thorough decomposition of organic materials. Because of its oxidizing capacity, the hot acid is frequently used to take elements to their highest oxidation state. Cold concentrated and hot diluted $HClO_4$ pose little hazard; however, very concentrated $HClO_4$ is potentially explosive when in contact with organic materials and easily oxidized inorganics. Extreme safety precautions are required when using this concentrated acid at high temperatures. Because of this potential hazard, expensive acid hoods, special scrubbers and duct work are needed to handle it.

Hydrogen peroxide

Typically, concentrations of about 30% of hydrogen peroxide are used for digestion. More recently, however, 50% solutions have become available. Hydrogen peroxide alone can react explosively with many organics, especially in the more concentrated form. Hydrogen peroxide is usually combined with an acid because its oxidizing power increases with increasing acidity. The combination of H_2O_2 and sulphuric acid forms monoperoxosul-phuric acid (H_2SO_5), which is a very strong oxidant. Because of its oxidizing power, hydrogen peroxide is frequently added after the primary acid has completed a pre-digestion of the matrix. The hydrogen peroxide can complete digestion and the potential safety hazards are minimized. In this respect, H_2O_2 is used similarly to $HClO_4$.

Basic media

Some applications require the use of a basic medium for ultrasonic digestion. Most such involve biological samples the matrix of which is decomposed by hydrolysis — which is more effective in a basic medium than in an acidic medium. One example is the digestion of tissues, where cells are disrupted in a basic medium such as that provided by tetramethylammonium hydroxide, sodium hydroxide, potassium hydroxide or sodium methoxide.

Type of treatment

Depending on the nature of the sample matrix and analytes, USASTD can be implemented in three different ways. The treatment of choice will be dictated by the following well-defined criteria:

Total attack is generally accomplished by using hydrofluoric acid in combination with other acids that allow all sample components except silica, which is volatilized during evaporation to dryness, to be solubilized. Some other components (*e.g.* boron) may be partially lost. This type for treatment is exclusive for inorganic analytes. Methods using this procedure are best validated with CRM.

Strong attack is generally performed by using a mixture of strong acids other than hydrofluoric acid. Better adapted to routine analysis, strong attack is easy to implement, but less complete in some cases (*e.g.* with soils or sediments) than total attack because of the presence of insoluble residues (silicates). Strong attack may be preferable in some cases such as the assessment of pollution levels in environmental samples. It is an unusual choice for organic analytes, except those with a high stability.

Moderate attack should in principle be used to simulate transfers of elements in the environment (*e.g.* the uptake by plants of trace elements from soil). This is the most usual type of attack in organic applications as the oxidizing power involved is more limited [43].

3.4.3. Applications of USASTD

As in classical digestion procedures and microwave-assisted digestion, the main field of application of USASTD is the determination of metals, particularly with a view to overcome analyte volatilization and safety problems. The inorganic applications involve environmental and industrial hygiene samples [50]. The applications to environmental samples include the determination of metallic elements in street dust samples and sediment reference materials. The results obtained by USASTD are in agreement with those provided by classical procedures based on acid digestion — with a reduction in analysis time from approximately 9 to 1 h — and reference values [51]. One other application of USASTD to environmental samples is the determination of metals in highly viscous waste oil, where the organic matter was eliminated by sonication with concentrated nitric acid as immiscible phase. The results obtained were comparable to those provided by microwave digestion, but the ultrasonic procedure was simpler, shorter and less labour-intensive [52].

Ultrasonic strong digestion has also been applied to biological samples (particularly tissues). In one application, USASTD of the sample with a strong basic medium, tetramethylammonium hydroxide–water mixture, for 2 min was followed by the determination of metals by microwave-induced plasma optical emission spectrometry (MIP-AES) [53]. In another, mussel samples were treated with concentrated hydrochloric acid prior to the determination of inorganic mercury [54]. Other seafood products have also been digested with ultrasonic assistance and high concentrations of an $HNO_3/HCl/H_2O_2$ mixture; the treatment was deemed ultrasonic-assisted-acid leaching, even though the composition of the liquid phase was typical of a strong digestion procedure — an incomplete one as a filtration step was required [55].

There are also some non-analytical uses of USASTD. One is in metallurgy, where minerals are subject to exhaustive dissolution treatments that can be used for analytical purposes. Such is the case with the digestion of phosphate rock in HCl [56] or HNO_3 [57], pyrite ores in sulphuric acid [58] or uranium oxides in supercritical carbon dioxide [59].

One other frequent application is the ultrasonic anaerobic digestion of waste-activated sludge for its degradation. Ultrasound-assisted sludge degradation has been extensively studied over the past 10 years on the laboratory and pilot scales and, recently, also on a full scale. Ultrasonic sludge digestion releases soluble organic cell compounds into the aqueous phase, which produces more biogas during digestion than does the same process in the absence of sonication [60,61]. Tests have shown that especially low (20 kHz) frequency ultrasound and relatively high ultrasonic intensity are well suited to the digestion of sewage sludge [62,63]. This has been ascribed to high mechanical shear forces exerted by jet streams during cavitation bubble implosion [64]. Sonication of secondary sludge results in a more pronounced release of chemical oxygen demand as compared to raw sludge treatment. The solid concentration of sludge influences the disintegration efficiency. There are few references to the chemical pretreatment of sludge in combination with US prior to anaerobic digestion. Sludge digestion was found to be improved by the use of NaOH and US in conjunction [65].

3.4.4. Synergistic effects of ultrasound and other auxiliary energies on strong digestion

The assistance of SP with other auxiliary energies is widely accepted to be the best way of accelerating and improving the efficiency of the different operations involved in SP. However, there is still room for research and innovation in this area. One of the most promising approaches in this context is the combination of various types of energy to assist SP steps. Of special interest here is the joint use of US and microwaves in order to combine their individual advantages and exploit new effects in addition to increasing the kinetics of the processes. A focus of much research in this respect has been strong digestion. Chemat *et al*. [67] put forward a mechanism to account for the effects of US and microwaves on digestion and developed a device for implementing digestion assisted by both microwaves and US, which has been used in various applications. The mechanism assumes particle fragmentation and molecule excitation induced by the high energy level of bubble cavitation under US, and also microwave polarization to induce dielectric volumetric heating and selective heating of solid particles. Figure 3.8 compares US (cavitation phenomena) and microwaves (dielectric heating) and shows the apparatus involved, which was based on a Prolabo Maxidigest 350 monomode microwave oven cavity with a power range from 0 to 300 W. A borosilicate reactor 20 to 150 ml in capacity was used as an open vessel operating at atmospheric pressure. The incident microwave power was controlled by a programmer which allowed operation in one or several steps depending on the duration of the experiment in minutes. The US system was a cup horn type Branson Sonifier 250 (diameter of the transducer tip 18 mm). Ultrasound waves (20 kHz) were emitted from the bottom of the reactor, and the US probe never came into direct contact with the reactive mixture in order to avoid interactions and short circuits with the electromagnetic field. Propagation of the US waves in the reactor was facilitated by the presence of decalin in the double jacket. Decalin has a low viscosity and allows US to propagate easily; also, it is inert towards microwaves.

Experiments involving digestion assisted by microwaves and US demand extreme safety measures and caution. In fact, the heating effect of microwaves and the use of strong acids and oxidants such as HNO_3 or H_2O_2 can be highly hazardous in inexperienced hands. Only approved equipment and scientifically sound procedures should be used.
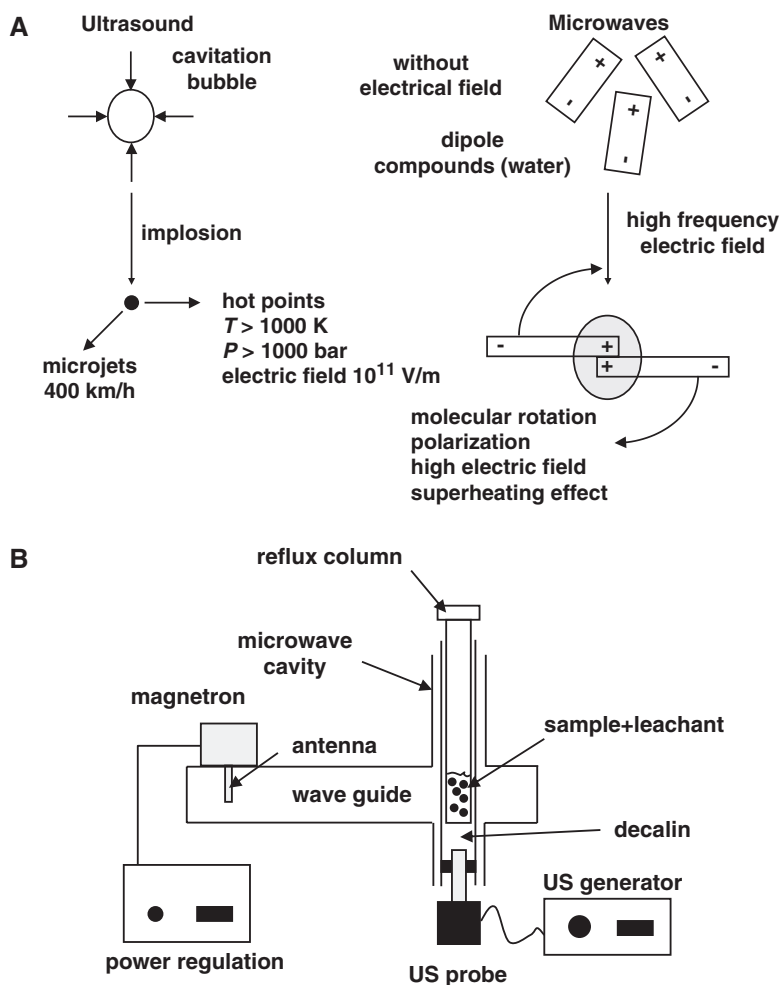
FIGURE 3.8. *(A) Analogy between ultrasound cavitation and microwave heating. (B) Scheme of the device for US-assisted microwave digestion. (Reproduced with permission of Elsevier, Ref. [67].)*

    The device proposed by Chemat *et al*. was used for the determination of total Kjeldahl nitrogen in food products (powdered milk, rice, corn, flour, beef, corned beef and chick pea); the digestion time, 10 min, was much shorter than in the classical Kjeldahl and microwave digestion (180 and 30 min, respectively). One other application was the diges-tion of mineral materials using nitric acid. Dissolution with the combined microwave–US device was six times faster than with classical heating. Under microwaves and US, the whole metal oxide was dissolved within only 1 hour; by contrast, the classical and the microwave method took 6 and 3 h, respectively. The device was also used to digest edible

oils for the determination of metals, which took 30 min as compared to 40 and 60 min, with the classical and the microwave methods, respectively [66,67].

3.5. ULTRASOUND-ASSISTED ENZYMATIC DIGESTION

3.5.1. Effect of ultrasound on enzymatic digestion

Ever since its inception in forensic toxicology [68], enzymatic digestion has been extensively used to isolate drugs from forensic samples. Carpenter [69] was the first to develop an analytical procedure in which subtilisin, a proteolytic enzyme, was used to determine Cd, Cu, Pb and Tl from human liver and kidney tissues.

The enzymes used for this type of digestion in Analytical Chemistry are mainly hydrolytic enzymes, the catalytic effect of which is based on the insertion of water at a specific bond of the substrate. The hydrolytic enzymes used in analytical applications include lipases (which hydrolyse fats into long-chain fatty acids and glycerol); amylases (which hydrolyse starch and glycogen to maltose and to residual polysaccharides); and proteases (which attack the peptide bonds of proteins and peptides themselves).

Enzymatic digestion has some advantages over conventional sample pretreatment procedures based on acid or alkaline digestion; thus, the former uses mild conditions as regards temperature and pH, which avoids potential analyte losses by volatilization or chemical transformation to other species, and reduces the risk of contamination. In addition, the selectivity of enzyme catalysis is a powerful tool for distinguishing between fractions of elements associated with different components of the matrix as enzymes act on certain chemical bonds only.

For most enzymes, catalytic activity is temperature-dependent to a maximum level, above which they lose their activity. Also, by analogy with other proteins, enzymes are stable only within a limited range of pH. Outside this range, enzymes are denatured by changes in the charges of ionizable amino acid residues that alter the tertiary structure of proteins. Enzyme activity reaches a peak or a plateau at a specific pH, so enzymatic digestion is usually performed in a buffered medium. The process is also affected by the enzyme concentration, which must therefore be optimized as well.

The selectivity of enzymes results in most enzymatic digestions leaving a solid residue consisting of substances that cannot be hydrolysed. The residue is usually separated by centrifugation and the liquid phase saved for further work. That is why some authors refer to enzymatic digestion as "extraction" or "leaching". However, the fact that enzymes release analytes by decomposing the sample matrix is more typical of a digestion, so, enzymatic processes should be regarded as partial digestion processes.

Incubation is the most widely used procedure to accomplish the enzymatic digestion of solid samples. A mixture of sample and enzyme is stirred or shaken in a buffered medium at 37°C. The incubation time can be: (a) short (4–6 h); (b) medium (10 h) or (c) long (24 h); the last is the most frequent choice [70].

Sonication has been used to improve digestion with enzymes; performance is influenced by the same factors as ultrasonic digestion in addition to those that can affect enzyme stability (*e.g.* pH, ionic strength or enzyme mass). However, studies on the effect of ultrasonication on enzyme reactions have revealed both enhanced activity and inactivation of the enzyme depending on the amplitude of sonication. Siwek *et al*. [71] reported an increase in enzymatic activity in the hydrolysis of Antarctic krill with ultrasound, allowing to quantitatively extract selenium organic compounds in 15 min compared with 24 h in the absence of ultrasound. Bracey *et al*. [72] found a reduction in particle size

of enzyme agglomerates from 51 to 2 μm after 30 min of sonication, which increased reaction rates.

3.5.2. Applications of ultrasound-assisted enzymatic digestion

Enzymatic digestion assisted by US has been used for the determination of organic and, especially, inorganic analytes. One of its most interesting uses is in metal — metalloid speciation, where enzymatic digestion in combination with ultrasonication enabled the determination of trace and ultratrace levels of metals and metalloids, and their species, while preserving their chemical integrity. Ultrasonic enzymatic digestion is a promising methodology with environmentally acceptable performance in this context. Enzyme probe sonication has proved a powerful choice for accelerating the digestion of yeast material, oyster and mussel tissues with proteolytic enzymes for the determination of Se [73]. Total Se was released within 15 s and complete dissolution of Se species in the yeast material (*viz*. Se–methionine) took 30 s. No buffered medium was required to use an ultrasonic probe, and no chemicals other than water were needed. One other typical application is the US-assisted enzymatic digestion of mussels for multielement determinations with ICP-AES, where the use of US energy shortens the long hydrolysis time of conventional thermostatic devices. In fact, the process takes only 30 min as compared to 12–24 h in conventional enzymatic hydrolysis [74].

Organic applications have focused on the digestion of solid samples by enzymatic hydrolysis under the assistance of ultrasonic energy for isolating target fractions. One example is the isolation of rice starch; analysis of the starch structure by high performance size-exclusion chromatography and scanning electron microscopy revealed no damage to the molecular structure or the starch granule surface [75]. One other example is the isolation of oil from *Jatropha curcas L*. seed kernels, where US-assisted enzymatic digestion took about 2 h as compared to 24 h for Soxhlet extraction [76]. The application of US for a short time (60 s or less) has also facilitated proteolytic digestion in both solutions and gels, thereby greatly reducing the operating time relative to conventional overnight incubation. In addition, it has enabled the identification of individual proteins by MALDI-TOF and HPLC–MS/MS [77].

3.6.   ULTRASOUND-ASSISTED CELL DISRUPTION

Cell disruption was one of the earliest uses of US in biology for releasing cells for *in vitro* study. In analytical methods, this treatment can be used in biological and biochemical applications where membranes act as barriers. The envelope of cells and microorganisms is a semi-rigid structure which provides sufficient intrinsic strength to protect them from osmotic lysis. These walls contain glycan strands cross-linked by peptide chains. The cross-linkage provides resistance to chemical and biological degradation. Ultrasonic energy in combination with some chemical reagents is an effective method for cell disruption, particularly in bioanalytical methods [78]. The US effects on cells involve both types of cavitation (transient and stable). In fact, the two types of cavitation have a wide range of biological effects on cell walls [79]. Thus, transient cavitation allows the formation of free radicals (*e.g*. from hydrogen peroxide) and other sonochemical compounds [80]. The formation of hydrogen peroxide and other compounds at high enough concentrations causes biochemical changes in living cells [81]. However, cells subjected to ultrasonic standing wave fields do not compromise

cell viability. Radel *et al*. [82] explained that, where propagating waves dominate, strong cell destruction is observed; with standing waves, however, cell destruction is negligible.

The effects of US on surviving cells may include structural changes and interactions with deoxyribonucleic acid (DNA) [83]. The biological effects observed *in vitro* include fragmentation of cell membranes caused by the collapse of cavitation bubbles, microstreaming near the boundary layer and formation of radicals, which promote chemical reactions leading to wall decomposition [84]. Carstensen *et al*. [85] found the extent of cell disruption to be inversely proportional to the cell concentration.

Cell disruption is a relatively frequent biological sample treatment. Applications include the purification of genomic DNA from *Mycobacterium bovis* Bacillus Calmette–Guérin by ion-exchange chromatography, where cell disruption was effected by an ultrasonic probe in conjunction with a NaCl/Tris-HCl/EDTA solution at pH 8.0 [86]; and the determination of glycosaminoglycans in human penis tissue, where the disruption was carried out with an ultrasonic bath containing a Tris-HCl/CaCl$_2$ solution at pH 8.0 [87]. Table 3.3 compares the advantages and shortcomings of selected treatments for cell disruption. As can be seen, US is the clear choice in terms of disruption efficiency.

Another use of cell disruption as a step in the analytical process is for obtaining a suspension of single cells — that can be used under optimal fermentation conditions — by ultrasonic disruption of cells manufactured in active dry wine yeast. Their potential was confirmed by comparing the elution profiles of non-sonicated and sonicated yeast sample dispersions obtained using two different field flow fractionation techniques [88].

TABLE 3.3. *Advantages and disadvantages of cell disruption treatments.*

Method	% Cell disruption	Advantages	Disadvantages
Seber colloid mill	50	Relatively simple	Energy dissipation — suspension heating
Ball mill shakers	90	High efficiency, relatively simple	Energy-intensive
High pressure homogenization	85	High efficiency, low energy levels	Complicated
Hydrodynamic cavitation	75	Excellent energy efficiency	Very little information and experience
Ultrasound	100	Complete disruption	Energy-intensive
Krepro	55	Recycling of all waste products, process flexibility	Corrosion and odour problems
Cambi	30		Relatively low efficiency, dependence on sample type
Thermochemical treatments	15–60	Relatively simple	Corrosion, odour, subsequent neutralization
Biological	5–50	Simple operation, low cost	Very low efficiency, odour
Vertech	95	High efficiency, no need for high pressure pumps	Corrosive, leakages, blockages in shaft
Loprox	90	High efficiency	Low pH, corrosive, high cost

The removal of metals and active compounds from the plant body for analytical purposes has also been accomplished in this way [89].

The disruption of microorganisms by ultrasonic cavitation has been extensively exploited for many years. Commercially available cell disrupters typically consist of half-wavelength probes about 15 cm long that are resonant at 20 kHz. The probes have titanium tips to minimize pitting damage by cavitation in the surrounding liquid. These sonicators are usually large laboratory-based units owing to the length of the probe used and are unsuitable for use in the field. Also, there is the inherent risk of hazardous aerosol formation in immersing the probe in a liquid sample containing any pathogens, and probe size dictates that only fairly large sample volumes can be disrupted. Commercial cell disruption devices operating at higher frequencies are more compact because of the shorter wavelengths associated with the higher frequencies. Ultrasonic disrupters operating at 20 and 40 kHz, and also at 1 MHz, have been used to treat small sample volumes as in the isolation of bacterial DNA for polymerase chain reaction (PCR) analysis [90–92]. These devices effectively disrupt bacterial cells but can cause substantial sample temperature increases (as high as 50 to 90 K). These temperature rises, however, are acceptable when the purpose of disruption is to isolate DNA for PCR analysis, but can be deleterious to the stability of some compounds such as proteins.

A tubular sonication device was recently reported by Borthwick *et al*. [93] (see Fig. 3.9). The device requires the addition of no chemical, enzyme or particles that might complicate the subsequent determination step. Furthermore, denaturation of target DNA or proteins for detection is minimized as the device tolerates moderate temperature rises; this allows the use of sensitive and specific immunological detection methods on sonicated biological materials. Because the tubular device is composed of a piezoelectric resonator made of several material layers, selection of an appropriate operating frequency is essential to ensure proper performance (*i.e.* acceptable cell disruption efficiency). This device can be used for batchwise treatment of small sample volumes or in flow systems without the risk of hazardous aerosol formation inherent in probe sonicators.
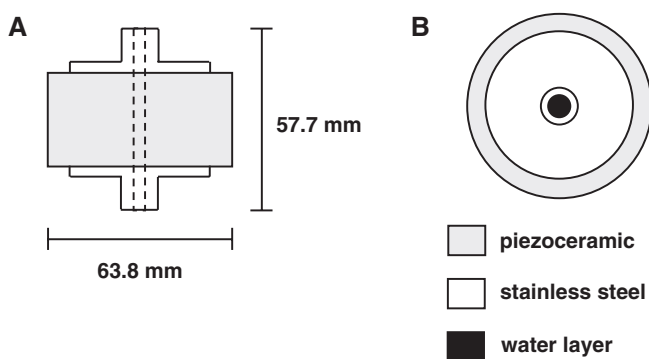
FIGURE 3.9. *Schematic views of the cell disrupter reported by Borthwick et al. (A) Side view with the sample chamber represented by dotted lines. (B) Plan view where the water layer represents the sample. (Reproduced with permission of Elsevier, Ref. [93].)*

References

1. M.D. Luque de Castro and J.L. Luque-García, *Acceleration and Automation of Solid Sample Treatment*, Elsevier, Amsterdam, 2002.
2. T.J. Mason, *Sonochemistry*, Oxford University Press, Oxford, 1999.
3. K.S. Suslick, The Yearbook of Science and the Future, in *Encyclopedia Britannica*, Chicago, 1994, pp. 138.
4. L.C. Hagenson and L.K. Doraiswamy, *Chem. Eng. Sci.*, 53 (1998) 131.
5. K.S. Suslick and G.J. Price, *Ann. Rev. Mater. Sci.*, 29 (1999) 295.
6. A. von Bohlen, R. Klockenkämper, J. Messerschmidt and F. Alt, *Anal. Chim. Acta*, 451 (2002) 279.
7. S. Zimmermann, C.M. Menzel, Z. Berner, J.D. Eckhardt, D. Stüben, F. Alt, J. Messerschmidt, H. Taraschewski and B. Sures, *Anal. Chim. Acta*, 439 (2001) 203.
8. W. Diegor, H. Longerich, T. Abrajano and I. Horn, *Anal. Chim. Acta*, 431 (2001) 195.
9. S. Ringmann, K. Boch, W. Marquardt, M. Schuster, G. Schlemmer and P. Kainrath, *Anal. Chim. Acta*, 452 (2002) 207.
10. J. Frank, M. Krachler and W. Shotyk, *Anal. Chim. Acta*, 530 (2005) 307.
11. M.C. Yebra, A. Moreno-Cid, R. Cespón and S. Cancela, *Talanta*, 62 (2004) 403.
12. M.C. Yebra, A. Moreno-Cid, R. Cespón and S. Cancela, *At. Spectrosc.*, 24 (2003) 218.
13. J. Vessman, R.I. Stefan, J.F. Van Staden, K. Danzer, W. Lindner, D. Thorburn Burns, A. Fajgelj and H. Müller, *Pure Appl. Chem.,* 73 (2001), 1381.
14. M. Valcárcel and M.D. Luque de Castro, *Automatic Methods of Analysis*, Elsevier, Amsterdam, 1988.
15. A. Kannan and S. K. Pathan, *Chem. Eng. J.*, 102 (2004) 45.
16. Y. Lu, N. Riyanto and L.K. Weavers, *Ultrason. Sonochem.*, 9 (2002) 181.
17. C.M. Preece and I.L. Hansson, *Adv. Mech. Phys. Surf.*, 1 (1981) 199.
18. D.R. Lide, *CRC Handbook of Chemistry and Physics*, 73rd edn, CRC Press, Boca Raton, FL, 1990.
19. Z. Bouhsain, B.A. Hasan, S. Garrigues and M. de la Guardia, *Quím. Anal.*, 14 (1995) 96.
20. C. Nsengiyumva, J.O. De Beer, W. van de Wauw, A.J. Vlietinck and F. Parmentier, *Chromatographia*, 44 (1997) 634.
21. S.V. Raj, S.U. Kapadia and A.P. Argekar, *Indian Drugs*, 34 (1997) 585.
22. T. Ozden, Z.H. Turker and A.U. Tosun, *Pharm. Pharmacol. Commun.*, 4 (1998) 397.
23. H.Y. Aboul-Enein, C. Doneanu and A. Covaci, *Biomed. Chromatogr.*, 13 (1999) 24.
24. A.H. Prabhakar, V.B. Patel and R. Giridhar, *J. Pharm. Biomed. Anal.*, 20 (1999) 427.
25. A. Haque and J.T. Stewart, *J. Liq. Chromatogr. Relat. Technol.*, 22 (1999) 2159.
26. P. Solich, C.K. Polydorou, M.A. Koupparis and C.E. Efstathiou, *J. Pharm. Biomed. Anal.*, 22 (2000) 781.
27. X.Y. Wang, F.D. Cui and R.M. Ma, *Shenyang Yaoke Daxue Xuebao*, 19 (2002) 31.
28. Q.C. Chu, X.H. Ding, X. Zhang and J.N. Ye, *Fenxi Ceshi Xuebao*, 21 (2002) 75.
29. C.M. Fu and R.Z. Wang, *Zhongguo Xinyao Zazhi*, 11 (2002) 144.
30. B. Zhu, C.Q. Hu, S.J. Jiang and L.H. Yin, *Zhongguo Kangshengsu Zazhi*, 27 (2002) 462.
31. Z.M. Du, Y. Liu, Y.F. Zhang and B.F. Yang, *Zhongcaoyao*, 33 (2002) 807.
32. T.F. Jiang, B. Liang, J.B. Li, C. Li and Q.Y. Ou, *Fenxi Kexue Xuebao*, 19 (2003) 33.
33. F.A. Chmilenko and L.V. Baklanova, *J. Anal. Chem.*, 53 (1998) 784.
34. M. Genc and A. Aslan, *J. Chromatogr.*, 839 (1999) 265.
35. J. Li, H.Y. Zhao, G.K. Peng, P.Y. Tian and C.Q. Li, *Sepu*, 20 (2002) 372.
36. Y. Li, C.Y. Wang, L. Liu, W.Y. Zhang and Z.J. Yang, *Fenxi Shiyanshi*, 22 (2003) 77.
37. K. Itenov, P. Moelgaard and U. Nyman, *Phytochemistry*, 52 (1999) 1229.
38. M.D. Geraldo, M.I. Montenegro and D. Pletcher, *Talanta*, 42 (1995) 1725.
39. R. Raso and H.W. Fehlhaber, *Rapid Commun. Mass Spectrom.*, 9 (1995) 1400.
40. O. Baticz and S. Tomoskozi, *Nahrung*, 46 (2002) 46.
41. Y.O. Kim, H.J. Chung, S.T. Chung, J.H. Kim, J.H. Park, S.Y. Han, K.S. Kil and D.H. Cho, *J. Chromatogr.*, 850 (1999) 369.

42. H. Luo, Y. Birnbaum, M.C. Fishbein, T.M. Peterson, T. Nagai, T. Nishioka and R.J. Siegel, *Thromb. Res.*, 89 (1998) 171.
43. M. Hoenig and A.M. de Kersabiec, *Spectrochim. Acta B*, 51 (1996) 1297.
44. J.A. Nóbrega, L.C. Trevizan, G.C.L. Araújo and A.R.A. Nogueira, *Spectrochim. Acta B*, 57 (2002) 1855.
45. M.V. Balarama Krishna and J. Arunachalam, *Anal. Chim. Acta*, 522 (2004) 179.
46. R.M. García-Rey, R. Quiles-Zafra and M.D. Luque de Castro, *Anal. Bioanal. Chem.,* 377 (2003) 316.
47. D. Hristozov, A.C. Domini, V. Kmetov, V. Stefanova, D. Georgieva and A. Canals, *Anal. Chim. Acta*, 516 (2004) 187.
48. H. Okur, T. Tekin, A. Kadir Ozer and M. Bayramoglu, *Hydrometallurgy*, 67 (2002) 79.
49. M. Demange, J.G. Gendre, B. Hervé-Bazin, B. Carton and A. Peltier, *Ann. Occup. Hyg.*, 34 (1990) 399.
50. C. Brunori, I. Ipolyi, L. Macaluso and R. Morabito, *Anal. Chim. Acta*, 510 (2004) 101.
51. A. Elik, *Talanta*, 66 (2005) 882.
52. T. Wang, X. Jia and J. Wu, *J. Pharm. Biomed. Anal.*, 33 (2003) 639.
53. H. Matusiewicz and B. Golik, *Microchem. J.*, 76 (2004) 23.
54. S. Río-Segade and C. Bendicho, *Ecotoxicol. Environ. Saf.*, 42 (1999) 245.
55. P. Bermejo-Barrera, O. Muñiz–Naveiro, A. Moreda-Piñeiro and A. Bermejo-Barrera, *Anal. Chim. Acta*, 439 (2001) 211.
56. T. Tekin, *Hydrometallurgy*, 64 (2002) 187.
57. T. Tekin, D. Tekin and M. Bayramoglu, *Ultrason. Sonochem.*, 8 (2001) 373.
58. H.T. Dogan, A. Kurtbas and T. Tekin, *Chem. Eng. Technol.*, 27 (2004) 87.
59. T.I. Trofimov, M.D. Samsonov, S.C. Lee, N.G. Smart and C.M. Wai, *J. Chem. Technol. Biotechnol.*, 76 (2001) 1223.
60. C. Bougrier, H. Carrère and J.P. Delgenès, *Chem. Eng. J.*, 106 (2005) 163.
61. A. Grönroos, H. Kyllönen, K. Korpijärvi, P. Pirkonen, T. Paavola, J. Jokela and J. Rintala, *Ultrason. Sonochem.*, 12 (2005) 115.
62. K. Nickel, Ultrasound in Environmental Engineering, *TUHH Reports on Sanitary Engineering*, 25 (1999) 217.
63. G. Lehne and J. Müller, Ultrasound in Environmental Engineering, *TUHH Reports on Sanitary Engineering*, 25 (1999) 205.
64. U. Neis, T. Tiehm and K. Nickel, *Ultrasound in Environmental Protection*, Jai Press Inc., New York, 2001.
65. Y.C. Chiu, C.N. Chang, J.G. Lin and S.J. Huang, *Water Sci. Tech.*, 11 (1997) 155.
66. A. Lagha, S. Chemat, P.V. Bartels and F. Chemat, *Analusis*, 27 (1999) 452.
67. S. Chemat, A. Lagha, H. Ait Amar and F. Chemat, *Ultrason. Sonochem.*, 11 (2004) 5.
68. M.D. Osselton, *J. Forensic Sci. Soc.*, 17 (1977) 189.
69. R.C. Carpenter, *Anal. Chim. Acta*, 125 (1981) 209.
70. P. Bermejo, J.L. Capelo, A. Mota, Y. Madrid and C. Cámara, *Trends Anal. Chem.*, 23 (2004) 654.
71. M. Siwek, A.B. Noubar, J. Bergmann, B. Niemeyer and B. Galunsky, *Anal. Bioanal. Chem.*, 384 (2006) 244.
72. E. Bracey, R.A. Stenning, B.E. Brooker, *Enzyme Microb. Technol.*, 22 (1998) 147.
73. J.L. Capelo, P. Ximénez-Embrún, Y. Madrid-Albarrán and C. Cámara, *Anal. Chem.*, 76 (2004) 233.
74. C. Peña-Farfal, A. Moreda-Piñeiro, A. Bermejo-Barrera, P. Bermejo-Barrera, H. Pinochet-Cancino and I. de Gregori-Henríquez, *Anal. Chem.*, 76 (2004) 3541.
75. L. Wang and Y.J. Wang, *J. Cereal Sci.*, 39 (2004) 291.
76. S. Shah, A. Sharma and M.N. Gupta, *Ind. Crops Prod.*, 20 (2004) 275.
77. D. López-Ferrer, J.L. Capelo and J. Vázquez, *J. Proteome Res.*, 4 (2005) 1569.
78. M.P.J. Weemaes and W.H. Verstraete, *J. Chem. Technol. Biotechnol.*, 73 (1998) 83.
79. M.W. Miller, D.L. Miller and A.A. Brayman, *Ultrasound Med. Biol.*, 22 (1996) 1131.
80. P.V. Riesz and T. Kondo, *Free Radical Biol. Med.*, 13 (1992) 247.
81. D.L. Miller and R.M. Thomas, *Ultrasound Med. Biol.*, 20 (1994) 193.

82. S. Radel, A.J. McLoughlin, L. Gherardini, O. Doblhoff-Dier and E. Benes, *Ultrasonics*, 38 (2000) 633.
83. D. Liebeskind, R. Bases and F. Elequin, *Radiology*, 131 (1979) 177.
84. D.L. Miller, *Ultrasound Med. Biol.*, 13 (1987) 443.
85. E.L. Cartensen, P. Kelly, C.C. Church, *Ultrasound Med. Biol.*, 19 (1993) 147.
86. W. Jing, S. Shuhan, H. Zhenlin, Z. Fengjuan and L. Yiling, *J. Chromatogr.*, 811 (2004) 103.
87. A. Goulas, E. Papakonstantinou, G. Karakiulakis, V. Mirtsou–Fidani, A. Kalinderis, D.G. Hatzichristou, *Int. J. Biochem. Cell Biol.*, 32 (2000) 975.
88. R. Sanz, S. Battu, L. Puignou, M.T. Galcer·n and Ph.J.P. Cardot, *J. Chromatrogr.*, 1002 (2003) 145.
89. F. Priego-Capote and M.D. Luque de Castro, *Trends Anal. Chem.*, 23 (2004) 644.
90. E.M. Fykse, J.S. Olsen and G. Skogan, *J. Microbiol. Methods*, 55 (2003) 1.
91. M.T. Taylor, P. Belgrader, B.J. Furman, F. Pourahmadi, G.T.A. Kovacs, M.A. Northrup, *Anal. Chem.*, 73 (2001) 492.
92. D.P. Chandler, M. Okuzumi, F. Pourahmadi, D.A. Borkholder and M.A. Northrup, *Anal. Chem.*, 73 (2001) 3784.
93. K.A.J. Borthwick, W.T. Coakley, M.B. McDonnell, H. Nowotny, E. Benes and M. Gröschl, *J. Microbiol. Methods*, 60 (2005) 207.

This page intentionally left blank

CHAPTER 4

Ultrasound-Assisted Leaching

4.1. INTRODUCTION

As noted in Chapter 2, "leaching" is the proper name for solid–liquid extraction by solubilization of the target analytes; also, leaching is most often favoured over dissolution and digestion for the treatment of solid samples on account of its higher selectivity (see Chapter 3). Like dissolution, leaching can be assisted by auxiliary energies in order to improve both its efficiency and to shorten treatment times. In contrast to digestion, where microwaves are more widely used than US, leaching is assisted by microwaves and US to a similar extent. This can be ascribed to microwave-assisted digestion which usually provides more drastic conditions than US-assisted digestion, the former thus being more effective in decomposing sample matrices. In leaching, selective solubilization of analytes can be accomplished with the assistance of either type of auxiliary energy.

Similar to "leaching", the word "leacher" should be reserved to the apparatus or approach used for leaching. Likewise "leachant" and "leachate" refer to the solvent used to dissolve the target analytes and the resulting solution containing the target analytes, respectively.

The duration of a leaching step is dictated by both solubility mechanisms and transport phenomena. Careful selection of the leachant plays a key role in three crucial steps of the leaching process, namely:

(1) The leachant is brought into contact with the surface and inside of the matrix, thereby starting the separation process.
(2) The retained analytes are removed by sweeping or displacement from the active sites of the matrix as a result of the higher affinity and (or) concentration of the leachant molecules. This is immediately followed by their dissolution (solvation) in the leachant.
(3) The analytes are transported from the inside of the matrix to its surface by essentially diffusional forces, and outside the matrix by primarily convective forces, provided leaching is performed in the dynamic or agitated mode.

The use of auxiliary energies is one way of increasing the leaching efficiency, mainly by boosting the transport phenomena. Swamy and Narayana developed a model to explain the mechanisms behind US-assisted leaching (USAL), which they compared with its equivalent in the absence of sonication [1] (see Fig. 4.1). Without US assistance, leaching is assumed to be caused by leachant penetration through the sample and diffusion of the analytes to the depleted outer region. The effects of US are primarily related with the cavitation phenomenon, which, as stated in Chapter 1, involves the implosion of bubbles formed during US application when they can no longer efficiently absorb more energy. The implosion generates rapid adiabatic compression of gases and vapours within the bubbles or cavities and, as a consequence, high effective temperature and pressure are generated. The high temperature results in increased solubility of the analytes in the leachant and in diffusivity of the analytes from the sample matrix to the outer region. The increased pressure favours penetration of the leachant into the sample matrix and

A　　　　　　　　　　　　　　　**B**

leached
zone

untouched core

surface pits within
which acoustic
effects can occur

solvent front
moving inwards

micro-cracks
giving greater
solvent penetration

solid–liquid interface
disturbed by cavitation
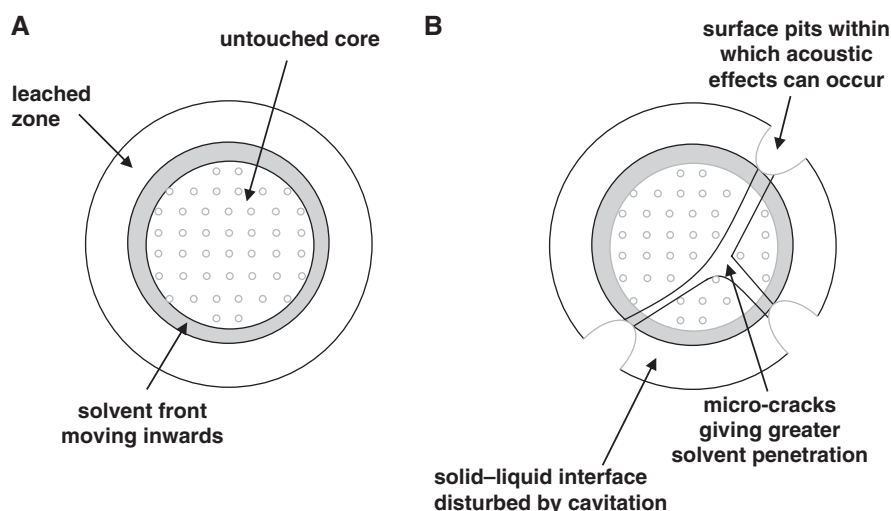
FIGURE 4.1. *Mechanisms of leaching in the absence (A) and presence of sonication (B).*

transport between the solid matrix and liquid phase at the interface [2]. Specifically, the following effects are involved:

(1) Collapse of bubbles generated in the proximity of the solid surface produces high-speed microjets which can raise transport rates and increase the surface area through surface pitting.
(2) Particle fragmentation through collision also increases the surface area and, in addition, it facilitates leachant penetration into the matrix.
(3) Acoustic streaming disrupts the diffusion layer on the surface.
(4) Ultrasonic energy facilitates diffusion of the analytes to the outer zone.

Phenomena 1 and 2 are the result of the microjetting effect described in Chapter 3, whereas phenomenon 3 can be identified with the microstreaming effect. One key difference in selecting the liquid phase for leaching or digestion is the primary purpose, namely: selective solubilization of the target analytes in the former and destruction of the sample matrix in the latter.

According to Romdhane and Gourdon [3], US energy accelerates the kinetics of leaching and improves its efficiency through increased diffusion of the analytes to the outer region, which is the limiting step of mass transfer. Although the last assertion is only true for those matrix–analyte combinations where the limiting step is analyte diffusion, US also plays a key role in leaching when the limiting step is breaking of the matrix–analyte bond.

Another factor that increases the efficiency of USAL is the presence of free radicals formed through cavitation. In fact, the oxidative energy of radicals created by sonolysis of the solvent dramatically improves the efficiency of leaching, at the expense of potential alteration in the stability of the target analytes.

4.2. USE OF ULTRASONIC BATHS *VERSUS* ULTRASONIC PROBES FOR LEACHING

Except in some special cases where the users themselves have designed and produced their own ultrasonic devices, US equipment for leaching consists of commercial ultrasonic baths or probes.

The US intensity received by the target sample in ultrasonic baths is strongly influenced by variables such as the level of transmitting liquid, US intensity, shape of the leaching vessel and position of the vessel inside the bath. In addition, not all cleaning baths operate at the same frequency and not always is such a frequency stated; this frequently hinders accurate reproduction of reported leaching methods.

As stated in Chapter 1, US probes avoid or minimize most of the shortcomings of US baths. Thus, the energy emitted by probes is more reproducible and remains constant for a longer time. On the other hand, probes generally result in lower sample throughput and are subject to decoupling phenomena. Decoupling occurs when cavitation only affects the radiating surface, so marginal US intensity is detected elsewhere in the surrounding liquid. This undesirable effect can be avoided by dipping the probe either in the sample vessel or very close to it [4].

Comparative studies have also revealed that probes allowed more expeditious leaching than did ultrasonic baths [5]. In any case, ultrasonic baths have been massively used for leaching on account of their accessibility.

4.3. DISCRETE *VERSUS* CONTINUOUS ULTRASOUND-ASSISTED LEACHING

The fact that US facilitates the removal of the target analytes from solid samples is clearly reflected in a large number of reported applications encompassing a broad range of species and sample types. Most USAL applications have been developed in discrete systems using a US bath or probe. Continuous approaches are less common, despite their superior performance [2]. This section discusses the general procedures for the development of both approaches, their advantages and shortcomings, and the common and specific variables that govern their performance.

4.3.1. Discrete and continuous ultrasound-assisted leaching

Ultrasound-assisted leaching involves irradiating a sample–leachant system in order to facilitate the transfer of the target analytes to the liquid phase.

The general procedure for developing discrete US-assisted leaching (DUSAL) is simpler than that of its dynamic counterpart (continuous US-assisted leaching or CUSAL), as the former requires no specific knowledge to design and construct the continuous manifold and optimize interrelated flow variables as in CUSAL.

In DUSAL procedures, the sample is weighed and poured into the leaching vessel together with an appropriate volume of leachant. Subsequently, US is applied in either of the two ways depending on the type of US device used. With a US bath, the sample vessel can only be dipped in the transmitting liquid to receive US energy through it. On the other hand, US probes allow the use of a transmitting liquid in a bath that can be thermostated, so both the probe and the sample vessel can be dipped in the bath or, alternatively, the probe tip can be directly inserted into the sample vessel. The latter choice provides stronger US action. In both, once leaching is completed, the resulting slurry must

be filtered or centrifuged to remove non-dissolved matter — centrifugation is always preferable because filtration can result in adsorption of the analytes on the filter — and the leachate is diluted to a given volume, if required, to proceed with the analytical process.

For CUSAL, the sample is weighed and placed in a leaching chamber both ends of which are tightly connected to the flow manifold in order to avoid leakage of the liquid phase and allow passage of the leachant. Two types of sample chamber have so far been used for this purpose, namely:

(1) The one-piece chamber, which consists of a small device with inlet and outlet orifices furnished with connectors for placing the container in-line in the dynamic manifold (Fig. 4.2A). Insertion of the solid sample into the chamber is time consuming owing to its small size and (or) the small diameter of the inlet and outlet orifices — the sample is inserted through one.
(2) The dismountable chamber of Fig. 4.2B, which consists of two halves, the lower of which is used to weigh the sample. Following weighing, the two halves are tightly joined together by screws which also act as connectors. Both types of cells can be made in stainless steel or methacrylate, the latter material enables viewing of the inside cell. Because US causes fragmentation of sample particles, the sample chamber must be fitted with appropriate filters on both ends to ensure that the solid will remain on the inside and avoid sample losses and (or) manifold blockage, and hence overpressure in the system or stoppage of the leachant flow, respectively. The filters are frequently made of stainless steel or cellulose — depending on particle size, small portions of glass wool can be used instead — to avoid interaction with the analytes.

For fine, very compact samples, the powder must be mixed with glass beads to avoid increasing compaction and pressure in the dynamic system. In addition, the presence of beads improves sample–leachant contact, as shown in the leaching of phenoxyacid herbicides from soil using water containing ethylenediaminetetraacetic acid (EDTA) as leachant [6]. The bead diameter should be chosen in terms of the cell dimensions. Another way of solving compaction problems and (or) avoiding ineffective sample–leachant contact (*e.g.* through formation of preferential channels in the bulk sample through which the extractant is circulated) in samples with a high moisture content is by mixing the sample with sea sand, as shown in the CUSAL of phenolic compounds from alperujo [7]. Alperujo is a semi-solid residue from olive oil production with a high moisture content (about 70%) that requires mixing with sea sand before introduction into the leaching chamber. The sea sand must be washed previously in order to remove impurities potentially interfering with subsequent steps. Special precautions should be exercised with respect to inorganic analytes as they can also be present in glass beads and sand. Washing with different acid mixtures until a blank analysis confirms that the analytes are absent from these materials is thus mandatory.

Once the leaching chamber containing the sample is closed, it is assembled to the dynamic manifold and dipped into a bath of transmitting liquid — usually water. Then, the dynamic system is filled with the leachant with the aid of a peristaltic pump or a similar device. Overpressure and concomitant shortcomings such as leaks should be checked during filling. The leachant is circulated through the sample for a previously determined optimum time under ultrasonic irradiation and appropriate operating conditions. When leaching is completed, the leachate is collected in a reservoir for the development of the subsequent steps of the analytical process. Neither filtration nor centrifugation is required to separate the leachate from non-dissolved matter after CUSAL, as the solid remains in the sample chamber whereas the leachate flows outside the dynamic system.
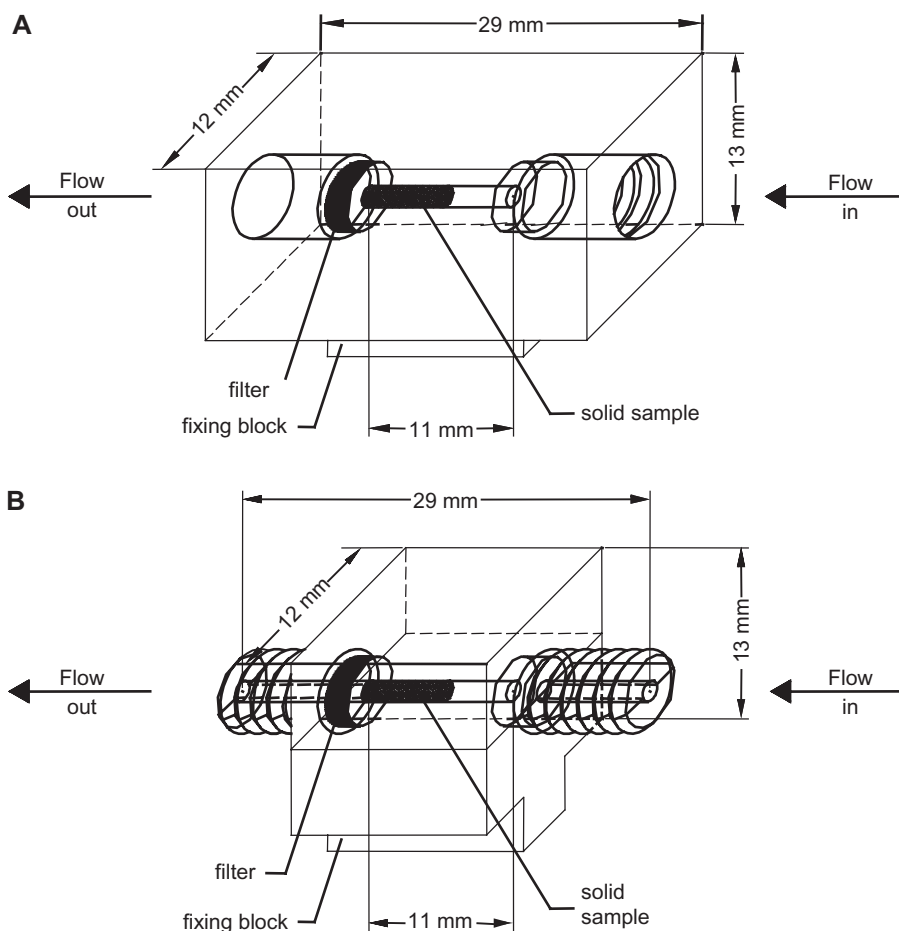
FIGURE 4.2. *Sample cells for continuous ultrasound-assisted leaching. (A) One-piece cell and (B) Dismountable cell. (Reproduced with permission of Elsevier, Ref. [2].)*

Before the next run, the system is flushed by circulating the leachant for a preset time in order to avoid cross-contamination.

4.3.2. Comparison of DUSAL and CUSAL

From the foregoing it follows that DUSAL is simpler than CUSAL. Thus, the former does not require skilled operator for proper implementation of leaching. On the other hand, CUSAL requires specific training in preparing the system before starting, during leaching and after leaching when this operation is connected on-line to others of the analytical process.

Both DUSAL and CUSAL can be assisted by ultrasonic baths and probes. Baths always require a liquid for transmitting the US energy. Probes can be dipped in the transmitting liquid, — which is always the case with CUSAL — but can also be directly dipped in the sample vessel in DUSAL. The presence of a transmitting liquid results in that of two media (namely, the transmitting liquid and the vessel walls) between the transducer emitting ultrasonic irradiation and the sample–leachant system. On the other hand, direct irradiation affords application of a higher energy, which can be important when drastic conditions are required.

Simultaneous treatment of several samples is possible in both discrete and continuous approaches, but is more frequent in DUSAL. Both US baths and probes can be used in either. When a transmitting liquid is involved, the sample vessel (DUSAL) or chamber (CUSAL) is placed in it, so special care must be taken in the number of sample devices that are immersed in the transmitting liquid as US wave reflections can reduce the sonication efficiency in different zones by factors from 5 to 12 [8]. Also, zones in the transmitting liquid differently affected by US can reach different temperatures. Homogenization of the transmitting liquid, continuous renewal or thermostation are convenient ways of ensuring reproducible US efficiency with all types of sample devices. The number of samples that can be treated simultaneously depends on the experimental US-assisted set-up used, which can vary widely in the case of US baths. Thus, the simultaneous treatment of up to nine samples in US bath without homogenization, renewal of the transmitting liquid or thermostation provided no statistically significant differences in analyte leaching at the 95% confidence level [5]; but this is not always the case, however. Concerning probes, all sample chambers should be placed at the same distance from the ultrasonic horn. A device such as that shown in Fig. 4.3 allows samples to be placed equidistant from the probe tip in DUSAL.

Continuous approaches outperform DUSAL in some respects. In the last two decades, automation has been one growing trend in technology and also in analytical chemistry [9]. The most salient advantages of automated analytical methods based on CUSAL over those relying on DUSAL are as follows:

(a) CUSAL saves reagents and samples. For example, hexavalent chromium has been leached from soil using both CUSAL [10] and DUSAL [11]. In the former, 1 g of soil was leached with 1 ml of leachant; in the latter, 2.5 g of soil required 50 ml of leachant.
(b) CUSAL can also be coupled to other continuous steps in order to automate the overall analytical process in a very easy and inexpensive manner, thereby reducing both errors and costs, and increasing the speed of the analyses in most cases [9]. On the other hand, the only way to automate DUSAL is by using robotic equipments, which is unaffordable to many analytical laboratories. One example of the use of robotics in this field is a method for the analysis of absorbing gel materials in diapers [12], where the use of a Zymate XP robot enabled complete automation of the analytical process (*viz*. USAL and acid–base titration) and it dramatically increased the sampling frequency. There is also a discrete method for the determination of cations in lichens, in which a burette was used to introduce a volume of leachant in the sample cell, which was sonicated for a preset time; then, the robot arm carried the leachate to a vial in a capillary electrophoresis (CE) autosampler [13].
(c) Unlike DUSAL, CUSAL requires no filtration or centrifugation.

Notwithstanding the advantages of CUSAL over DUSAL (automatability, mainly), the former has been less frequently used than the latter. In fact, few research groups have to date worked on CUSAL.
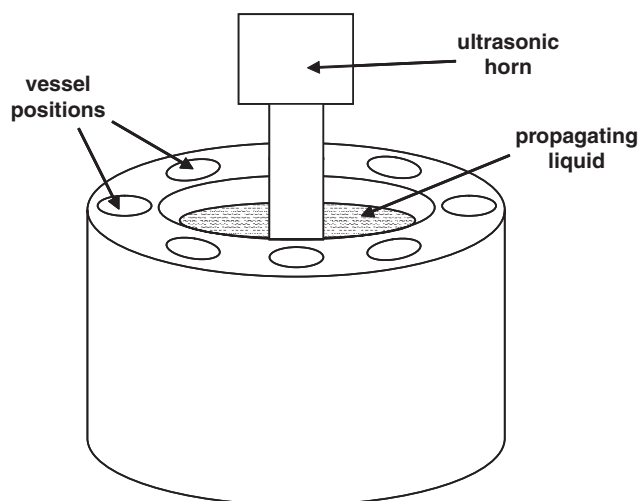
FIGURE 4.3. *Device for the simultaneous treatment of several samples in DUSAL using an ultrasonic probe.*

4.3.3. Variables affecting DUSAL and CUSAL

There are a number of common variables to be optimized in DUSAL and CUSAL. These variables, which are discussed in Chapter 3 as they also affect the efficiency of US-assisted digestion, are common to USAL and other processes assisted by this energy, and their effect has not been properly studied in the few US-assisted digestion methods reported so far. By contrast, most such variables have been optimized in USAL methods and classified as related or unrelated to the application of US energy. A distinction is made below between DUSAL and CUSAL when required in discussing their effects.

Variables related to ultrasonic assistance

The main variables related to the way in which US energy is applied to the sample–leachant system are the US amplitude, frequency, pulse mode operation, irradiation time, position of the vessel in the ultrasonic field, distance between the probe tip and sample vessel or chamber, and volume and nature of the transmitting liquid.

Ultrasound amplitude (power). This variable is directly related to the amount of energy applied and has similar effects with baths and probes. The former, however, are not powerful sources as most of them use modern piezoelectric transducers which provide a low-intensity power (in the region of 1–5 W/cm^2).
Leaching is accelerated mainly by high-amplitude US; however, medium- or even low-amplitude US can be a better choice when the decoupling effect makes near-maximum amplitudes impractical [14,15]. Such is the case with the removal of nitropolycyclic aromatic hydrocarbons from soil by CUSAL [16], which requires an output amplitude of

30% of 400 W as total power, and with the continuous leaching of cadmium and lead from plants [17] using an output amplitude of 10% of 400 W as total power.

Ultrasound frequency.   Raising the irradiation frequency entails increasing the irradiation amplitude in order to maintain an equivalent amount of cavitational energy in the system. Although the irradiation frequency influences the leaching efficiency, it is rarely optimized in USAL methods, as these ultrasonic devices usually operate at a single frequency. One example where the US frequency was optimized by using a transducer array is the leaching of tannins from *Salix phylicifolia* using water as leachant [18], where low-frequency US was found to be preferable for two reasons, namely: (a) cavitation was more easily generated and helped to destroy the cellular structure of the wood; and (b) multiple scattering and attenuation was low at low ultrasonic frequencies by virtue of the presence of small amount of solid suspended particles. The improved performance of low-frequency US is more apparent when sufficiently different settings (*e.g.* 20 and 40 kHz) are compared. Similar irradiation frequencies allow no accurate predictions in this respect. One exception is the USAL of active principles such as pyrethrines from pyrethrum flowers using hexane as leachant [3], where two very close frequencies from the same horn (20 000 and 20 223 Hz) resulted in a difference of 32% in leaching efficiency in favour of the higher one.

No commercial tunable frequency US devices, which could provide interesting conclusions about the influence of this variable on leaching, exist. Simultaneous irradiation with US at two different frequencies selected between 20, 40, 43 and 720 kHz was tested for metal leaching from ores [19]. Increased efficiency and significant savings in energy and operation time were obtained by simultaneously using the two sound wave sources, particularly those of the lower frequencies, to produce cavitation. The results obtained with single and dual frequencies are illustrated in Fig. 4.4 for copper leaching from ores. As can be seen, the efficiency of single-frequency USAL increased with decreasing frequency at a constant US intensity ($2 \ W/cm^2$); however, the use of single-frequency US for 20 min provided a maximum metal leaching efficiency of 62.5%, whereas the combined use of 20 and 40 kHz US at the same amplitude for the same time resulted in 92% metal leaching efficiency. Dual-frequency US irradiation increases grinding of ores during collision by causing size reduction, which facilitates the leaching of metals. Thus, when an ultrasonic power is distributed among the two transducers located co-axially arranged in opposite directions instead of being applied *via* a single transducer, higher energy density is produced by the effect of the larger amplitudes involved. The increased density gives rise to larger concentration gradients, which facilitate diffusion and accelerate leaching as a result.

Pulse mode operation.   Ultrasonic probes can operate in the pulse mode, where the variable to be optimized is the *duration of the pulse*, also known as the *duty cycle* (*viz.* the fraction of time US is applied within each second). The optimum pulse duration can range from a long time (US is emitted in an almost continuous manner) to a short one (0.1 s or less). One typical example of the use of a short duration and a low radiation amplitude is the above-described method for the removal of cadmium and lead from plants using 0.1 s and 10% of 400 W, respectively [17]. These values do not involve the favourable effects of US on leaching to be excluded, but the optimal operating conditions ensuring the most efficient cavitational effects are provided by short pulses of low-amplitude US energy. However, not always do low or high values of the two variables provide the best results. Thus, García-Rey *et al.* [20] found the optimum duty cycle and radiation amplitude for the DUSAL of metals from meat samples to be 0.1 s and 70% of the converter nominal
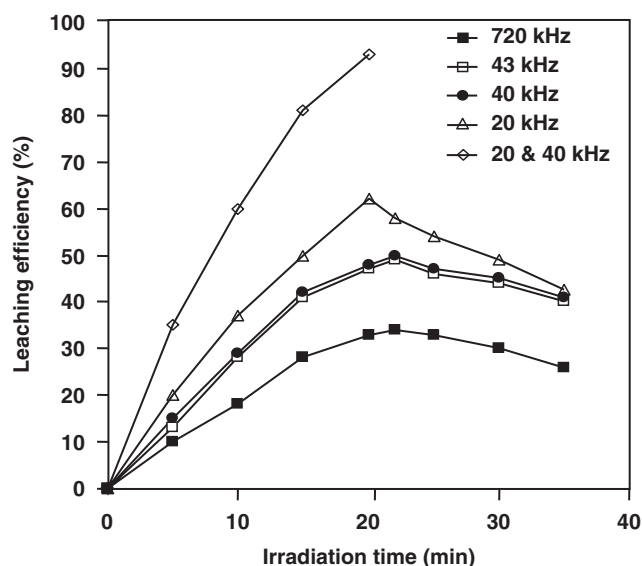
FIGURE 4.4. *Variation of the copper leaching efficiency with the sonication time at a variable ultrasonic frequency and a constant intensity of 2 W/cm². (Reproduced with permission of Elsevier, Ref. [19].)*

amplitude of 400 W at 20 kHz, respectively so, leaching was favoured by short US pulses of a high amplitude. Therefore, the optimum irradiation amplitude and pulse duration depend directly on the particular analytes to be leached and the type of matrix that contain them; as a result, both high and low settings for these parameters have been reported.

Position of the sample vessel. Although the position of the sample container with respect to the transducer is not a characteristic variable of US application, it determines the amount of energy that is received by the sample. This variable, exclusive of ultrasonic baths, should be optimized in both DUSAL and CUSAL methods. When only one sample is leached, the precision is not affected provided the sample vessel is always in the same position — cavitational effects can be maximal or not in this situation, however. If several samples are simultaneously treated, then the precision is probably affected because the irradiation profile is not uniform throughout the bath. One example is the DUSAL of cadmium and lead from foods, where the iodine method was used to locate the best position for cavitational effects [5]. This requires the use of mapping techniques.

Distance between the probe tip and the sample vessel or cell. This variable is equivalent to the vessel position in ultrasonic baths. Optimizing it entails testing different distances or using a mapping technique, as in the above-described leaching of active principles from flowers [3], where a thermoelectric probe allowed the position where cavitational effects were maximal to be located. When the ultrasonic probe is introduced in the transmitting liquid for DUSAL, the tip–vessel distance usually ranged from 1 to 10 cm; the energy supplied to the sample

can be increased by shortening the distance, but the effect also depends on whether an open or closed vessel is used. On the other hand, when the probe tip is dipped in the leaching medium — as is usually the case in strong treatments — this variable is substituted by the immersion depth of the probe tip in the leaching medium. The situation is similar in CUSAL, where the working distance usually ranges from 1 to 5 mm, however.

Volume and nature of the transmitting liquid. As stated in Chapter 3, the volume of the transmitting liquid must always be considered with ultrasonic baths and, also with probes when the tip is not directly dipped into the system to be sonicated. The purpose of optimizing the volume of the transmitting liquid is to facilitate efficient transmission through it. The nature of the transmitting liquid must be properly chosen as it influences cavitation. Both the volume and nature of the transmitting liquid used are frequently omitted in optimization tests. Their influence has been clearly demonstrated by Nascentes *et al*. [21] in their study of metal leaching (Ca, Mg, Mn and Zn) from vegetable samples in an ultrasonic bath. A volume of 1 000 ml of water containing 0.2% (w/v) of a detergent provided optimal results. Concentrations above 0.2% increased the presence of solid particles in the transmitting liquid and hindered propagation of ultrasonic energy.

Ultrasonication time. This variable, which is frequently included in optimization tests, is the period over which US is continuously applied (particularly with ultrasonic baths) or US pulses generated (with probes). Its optimum value depends on the particular operating conditions (*viz*. the US power, source, leachant), and also on the type of sample and analytes involved. Usually, the ultrasonication time ranges from few seconds to minutes (or even hours in specific applications requiring strong treatments or with the low-energy ultrasonic sources). The ultrasonication time can be optimized together with other important variables by using multivariate methodology and experimental designs (particularly with unstable analytes). When several leaching cycles are used, the ultrasonication time can refer to each individual cycle or to the overall leaching step. One example of the use of leaching cycles is a method for the removal of fat from bakery products, where fresh leachant was employed in cycles of ultrasound application and all sub-leachates were subsequently collected to quantify the removed species [22].

Once all variables have been optimized, a kinetic study of the leaching efficiency as a function of the ultrasonication time can be used to examine the course of the leaching process and determine the time required for complete removal of the target species.

Variables unrelated to ultrasonic assistance

Some operational variables not related to US application affect all leaching methods and therefore require optimization as well. The most important are discussed below.

Temperature. One of the main advantages of USAL is that it can be performed at ambient temperature, particularly in applications where this variable is restrictive owing to the presence of thermolabile analytes. During US application, the temperature increases as a function of the values of US variables such as the amplitude, pulse duration and irradiation time. For this reason, some ultrasonic devices are equipped with temperature control during leaching to stop the ultrasonic source if a preset maximum temperature is reached. This is frequently referred to as "the temperature mode" and is used mainly in leaching processes involving long irradiation times. The temperature is controlled *via* measurements of the transmitting liquid. Once the temperature falls below the preset maximum after US is

stopped, irradiation is resumed. When an appropriate temperature is the key to obtain a high leaching efficiency, its influence should be carefully examined in the optimization study [23,24]. Both the range over which the temperature can be optimized and the value adopted as optimal should fall below the highest working temperature recommended in the user's manual of the ultrasonic source in order to avoid damaging. The optimum value can range from 70°C required (*e.g.* in the USAL of hexavalent chromium from welding fumes [25]) to 20°C (*e.g.* in the removal of copper from mussels [26]). The optimum temperature is therefore dependent on the nature of the sample.

Leachant. The nature of the leachant is dictated by the properties of the analytes (particularly by their polarity). A pure solvent or a solvent mixture can be equally effective as leachants. The ability to use solvent mixtures is one major advantage of USAL over Soxhlet leaching. The importance of the leachant composition is apparent in applications such as the USAL of hexavalent chromium — a human carcinogen — in the presence of tervalent chromium — relatively non-toxic and an essential nutrient in the human diet to maintain effective glucose, lipid and protein metabolism — from solid samples [27,28]. Whereas Cr(VI) is usually leached at pH $\geq$ 7, where it is thermodynamically stable, Cr(III) is unstable in alkaline medium. Ammonia inhibits the oxidation of Cr(III) to Cr(VI) in aqueous alkaline media by complexation; therefore, an ammonium buffer [$(NH_4)_2SO_4$–NH_3] is used to leach Cr(VI).

Modifiers can be included in the leachant composition for improving the efficiency. One typical example is the use of surfactants as leachant components in USAL. Surfactants possess special properties such as ability to solubilize compounds of variable nature with a high efficiency and safety at a low cost. Low concentrations of these modifiers are usually employed, which facilitates their removal. Thus, Genapol X-080 has been effectively used for the USAL of active principles such as tanshinones from *Salvia miltiorrhiza bunge* (a Chinese plant) at 10% (w/v) in water [29]. The method provides a leaching efficiency similar to that obtained with methanol and dichloromethane–methanol and avoids the use of large amounts of toxic organic solvents. The micelle-assisted USAL of polycyclic aromatic hydrocarbons (PAHs) from marine sediments using 3.1% (w/v) polyoxyethylene-10-lauryl ether in water [30] provides a mean leaching efficiency of 99.5%; a comparison with its microwave-assisted counterpart revealed that the precision was dramatically improved by US assistance. In the previous two examples, the use of surfactants enabled subsequent preconcentration by cloud-point extraction with high concentration factors due to the reduction of the surfactant-rich phase volume. Micelle-assisted USAL has also been applied to inorganic compounds (*e.g.* in a method for the removal of trace elements from plants followed by ICP-AES detection [31]). Various surfactants including Triton X-100, didocecyldimethylammonium bromide and cetyltrimethylammonium bromide have revealed that quantitative efficiency in USAL with diluted acid (HCl), with and without the aid of low concentrations of surfactants, affects both ICP-AES signals and the nebulization process. However, the leaching efficiency depends on the type of surfactant, target element and sample matrix.

Another advantage of USAL is the need for little or no additional chemicals as compared to classical methods. Such is the case with the USAL of *trans*-fatty acids from bakery products [32]. This method uses *n*-hexane as leacher; by contrast, the Folch reference method requires a chloroform–methanol mixture and additional reagents including sodium chloride to remove non-fat contaminants such as sugars, amino acids and salts, which are co-extracted with the lipid fraction.

Particle size. Irradiating a suspension with US causes particle disruption to an extent dependent on both the initial particle size and the properties of the solid. Particle disruption in turn increases the surface area available for mass transfer and is thus one of the

most critical variables influencing USAL (through its effect on the contact surface area). The leaching efficiency strongly depends on how rigorously particle size is optimized. Filgueiras *et al*. studied the effect of variables including the extraction time, US amplitude, acid concentration in the leaching agent, leachant volume, amount of sample and particle size on the USAL of magnesium, manganese and zinc from plants prior to determination by flame atomic absorption spectrometry [33]. In previous research, particle size had proved a key variable. A small size (50 μm) was required to ensure quantitative leaching. In fact, the amount of metals leached increased with decreasing particle size. Beyond a certain particle size (≤ 50 μm), however, a further decrease in size was not accompanied by an increase in the amount extracted. Similar results were obtained in the leaching of metals (*viz*. copper, iron, zinc, calcium and magnesium) from animal feeds [34], where the optimum particle size was found to be in the range 0.25–0.50 mm. Smaller particle sizes resulted in decreased leaching efficiency for all metals, except calcium. Although particle size is rarely included among the optimized variables in USAL procedures, it is essential to examine its effects with a view to obtain reproducible results in routine USAL methods.

Sample–leachant ratio.   This variable should be optimized for two main reasons. First, the analytes must be at a suitable concentration in the leachate to allow their determination without the need for subsequent dilution or concentration, which lengthen the analytical process and are the sources of error. Second, the amount of sample and volume of leachant should be as small as possible while representative to avoid environmental problems and unnecessary expenses.

Agitation.   Agitation accelerates mass transfer through increased sample–leachant contact. In the method of Hristozov *et al*. [24] for direct USAL of heavy metals from sewage sludge, 10 min of agitation by magnetic stirring for a sonication time of 20 min was found to facilitate leaching. Bubbling into the leaching medium also improved the leaching efficiency by favouring sample–leachant contact and cavitation.

Shape of the sample container.   This variable is rarely examined despite its proven decisive influence, particularly when probes furnished with microtips are used in small vessels [35]. For small volumes, the smallest diameter vessel which allows the probe to be inserted without the risk of touching the vessel walls must be chosen. This minimized vessel diameter raises the height of the liquid sample, thereby exposing a higher surface area to the external cooling bath for more effective heat transfer; some energy, however, will be reflected back when the wave sound impinges directly on the bottom. In addition, when the leachant volume is minimized, the number of impacts between particles induced by cavitation is maximized and analyte leaching boosted as a consequence of the disrupting effect. Capelo *et al*. examined the influence of the sample vessel design on the USAL of PAHs from sediments on a small scale using a microtip [36] and found the Eppendorf-type vessel to provide the best results.

Dynamic variables.   These variables are characteristic of CUSAL, but unrelated to the way US is applied. The leachant flow-rate, whether straight or coiled tubes are used and merging points included for the *in situ* formation of unstable mixtures, among others, are well-known variables for users of dynamic manifolds.

4.3.4. Approaches for CUSAL

As stated earlier, the use of continuous systems for USAL provides substantial advantages such as a modest consumption of sample and reagents, expeditiousness,

avoidance of filtration and, obviously, the possibility of coupling with other steps of the analytical process. The last advantage allows the analytical process to be partly or fully automated and enjoy the additional benefits inherent in automation. Notwithstanding these advantages, few CUSAL methods exist in relation to batch leaching. CUSAL can be implemented in open or closed manifolds[1].

Continuous US-assisted leaching in open systems

These systems are very simple. In fact, they consist of open tubes connected to the inlet and outlet of the sample chamber (see Fig. 4.5A). For proper feeding of the chamber, the other end of the inlet tube is dipped in the reservoir holding the leachant, which is circulated through the manifold with the aid of a propelling unit. The outlet tube leads the leachate to the collection reservoir. Depending on the volume of leachant there are two types of manifolds:

In one-direction manifolds, the leachant is continuously pumped through the sample chamber always in the same direction; in this way the solid is continuously brought into contact with fresh leachant and the mass transfer equilibrium is displaced to the solubilization of the analyte into the liquid phase.

In two-direction manifolds, a given volume of leachant is introduced into the manifold and the direction of the flow is changed at preset intervals by programming the propulsion system. In this way, the leachant goes back-and-forth through the sample, thus avoiding both its compaction in the leaching chamber and raising the pressure inside the dynamic system. The leachant volume delivered is determined by the time the leachant is pumped into the manifold.

One-direction manifolds have the disadvantage that they cause leachate dilution, which, however, can be offset by implementing a concentration step after leaching. Two-direction manifolds afford more reproducible work as they allow more precise control of the leachant volume; however, mass transfer to the leachant may be incomplete if the solid–liquid partitioning equilibrium does not favour passage to the liquid phase. One way of circumventing the main shortcomings of the two types of open manifolds (namely, leachate dilution and non-quantitative removal) is by using a combination of both, that is, the sequential use of back-and-forth steps and cycles of leachate draining and filling of the dynamic system with fresh leachant [22].

Continuous US-assisted leaching in closed systems

Closed CUSAL systems consist of a circuit comprising the sample chamber and at least a switching valve for both introduction of the leachant and final collection of the leachate into a vial or reservoir (see Fig. 4.5B). The leachate can also be driven to a continuous

---

[1] In continuous manifolds (particularly flow injection manifolds), the word "open" is used to refer to those cases where the entire light or diameter of the tubing is occupied by liquids; by contrast, "packed" is used when the solid material (a sorbent, a support–enzyme conjugate, etc.) fills a portion of the tube. In the context of continuous leaching manifolds, "open" as opposed to "closed" is used to distinguish linear manifolds from manifolds in which the liquid is recirculated with the aid of valves that convert the manifold from closed to open and *vice versa*.
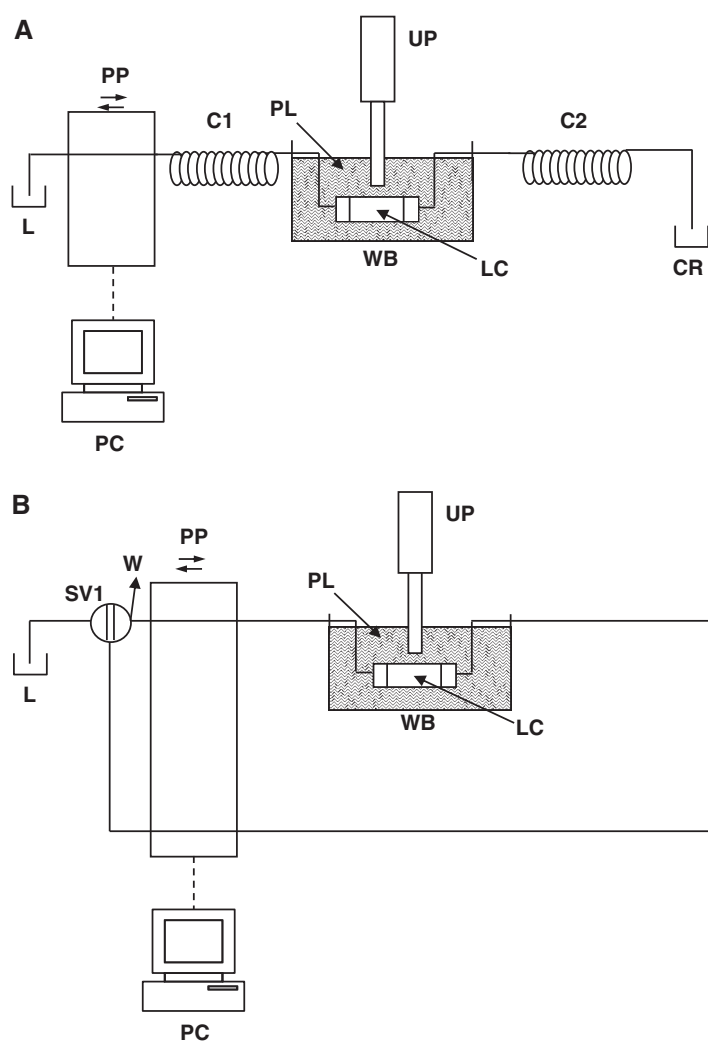
FIGURE 4.5. *Experimental set-up for continuous ultrasound-assisted leaching in an open (A) and closed manifold (B). C — coil, CR — collection reservoir, L — leachant, LC — leaching chamber, PC — personal computer, PL — propagating liquid, PP — peristaltic pump, SV — switching valve, UP — ultrasonic probe, W — waste and WB — water bath.*

manifold for on-line development of other steps of the analytical process, thus enabling full automation. Once leaching is completed, the switching valve is actuated to have the leachate swept by a carrier. The volume of leachant in the closed circuit is continuously circulated through the solid sample. There are two possible operational modes depending on the direction of the leachant, which can be continuously circulated in the same direction, — in contrast to open systems, a constant leachant volume is passed through the sample — or, similar to open manifolds, in alternate directions by programming the impulsion device. Closed systems have the advantages that they cause less marked dilution of the leachate and that they allow the leaching kinetics to be monitored either by withdrawing fractions of leachate for analysis or by inserting a flow cell in the circuit for continuous monitoring of the leaching process.

4.4. COUPLING CUSAL TO OTHER STEPS OF THE ANALYTICAL PROCESS

The designs described in Section 4.3.4 have been used either to leach the target analytes only and then proceed off-line with other steps of the analytical process, or to couple leaching on-line with other steps in order to automate the overall process as far as possible.

4.4.1. Off-line coupling of leaching to subsequent steps of the analytical process

Continuous ultrasound-assisted leaching is implemented off-line when the complexity of the subsequent steps hinders their development in a continuous manner. One of the few examples of continuous implementation is the analysis of phenolic compounds in strawberries [37], where the analytes were leached by CUSAL in an acetone solution containing 0.2 M hydrochloric acid and *tert*-buthyl-hydroquinone. After leaching, a rotary evaporator facilitated evaporation of acetone to near-dryness of the leachate, the residue being diluted with water adjusted to pH 8. Then, a clean-up preconcentration step was coupled on-line with individual separation and detection. Solvent exchange was the step most strongly hindering coupling to CUSAL. Another example also related to phenolics is their leaching from alperujo prior to separation–quantification by CE with diode array detection: a centrifugation step, which cannot be coupled on-line, was required after leaching [7]. The process can only be implemented in a discrete automated manner by using a robotic workstation.

In some cases, a given step can be coupled on-line with USAL but off-line development provides better results. Such is the case with a method for the determination of the *trans*-fatty acid content in bakery products [32]: following isolation of total fat, the fatty acids must be derivatized to methyl esters, which are volatile, for subsequent analysis by gas chromatography separation with mass spectrometry as detection system. The derivatization reaction must be complete, selective and sensitive enough, which is difficult to accomplish in a continuous manner as the procedure involves:

(a) reaction with sodium methylate, which is faster under agitation with a vortex instead of a mixing coil in a continuous system;
(b) centrifugation to separate the aqueous and organic phases, which is more effective than the use of a phase separator in continuous liquid–liquid extraction; and
(c) preconcentration in a rotary evaporator, which is also more efficient than solid-phase extraction coupled on-line with leaching for volumes in the region of 100 ml.

Because a commercial vortex, centrifuge or rotary evaporator can process several samples simultaneously, off-line batch derivatization is more practical, efficient and expeditious.

4.4.2. On-line coupling of leaching to subsequent steps of the analytical process

Leaching has been coupled to various steps of the analytical process in order to exploit their advantages. The coupling involves:

(a) direct detection when the leached species are sensitive to a given detector type;
(b) concentration (*e.g.* solid-phase extraction) prior to detection in order to overcome a dilution effect; or
(c) isolation of the individual target species by chromatography or CE. A derivatization step can also be included at any point of the overall process.

The situation can be as simple as coupling leaching to detection or as complex as linking a chain of steps, most often in an automated way.

On-line coupled leaching and detection

The leaching–detection couple is the simplest case enabling full automation of the analytical process. Depending on the particular continuous manifold used, the two operations can be coupled in different manner. In open systems, the detector can be placed at the end of an open manifold as shown in Fig. 4.6A; nevertheless, when these systems have been used for leaching purposes — one of their main applications — the subsequent steps of the analytical process have been performed off-line. In any case, in the one-way mode, fresh leachant is continuously pumped into the system, so the ensuing dilution decreases the sensitivity. One operational procedure here involves stopping the flow of leachant for a preset time during US application to facilitate analyte removal without significant dilution. When the direction of the leachant is changed at preset intervals, the location of the detector allows monitoring of the enrichment of the liquid phase with the leached analytes and hence the leaching kinetics. However, the most frequent choice is to allow leaching to complete and collect the leachate into a vial for subjecting it to subsequent steps.

Closed manifolds allow the detector to be placed inside or outside the open–closed circuit. Inserting the detector within the circuit (Fig. 4.6B) is only useful when the detector is sensitive to the target analytes or the leachant contains the derivatizing reagent. In both cases, the leaching process is continuously monitored and a rising signal is obtained, the slope of which reflects the leaching kinetics. Attainment of the mass-transfer equilibrium is signalled by the change from a rising segment to a plateau, after which the switching valve is opened to have the leachate driven to waste.

When the detector is placed outside the closed circuit, the valve that switches between an open and a closed system also acts as a connector with a dynamic manifold in which a derivatization reaction is conducted before the leachate reaches the detector. The two steps involved in the overall process (namely, leaching and derivatization–detection) are depicted in Figs. 4.7A and 4.7B.

Similar to other dynamic approaches, a variety of optical (spectroscopic and non-spectroscopic), electroanalytical (amperometric, potentiometric, conductimetric) and thermochemical detectors can be coupled to continuous US-assisted leachers to
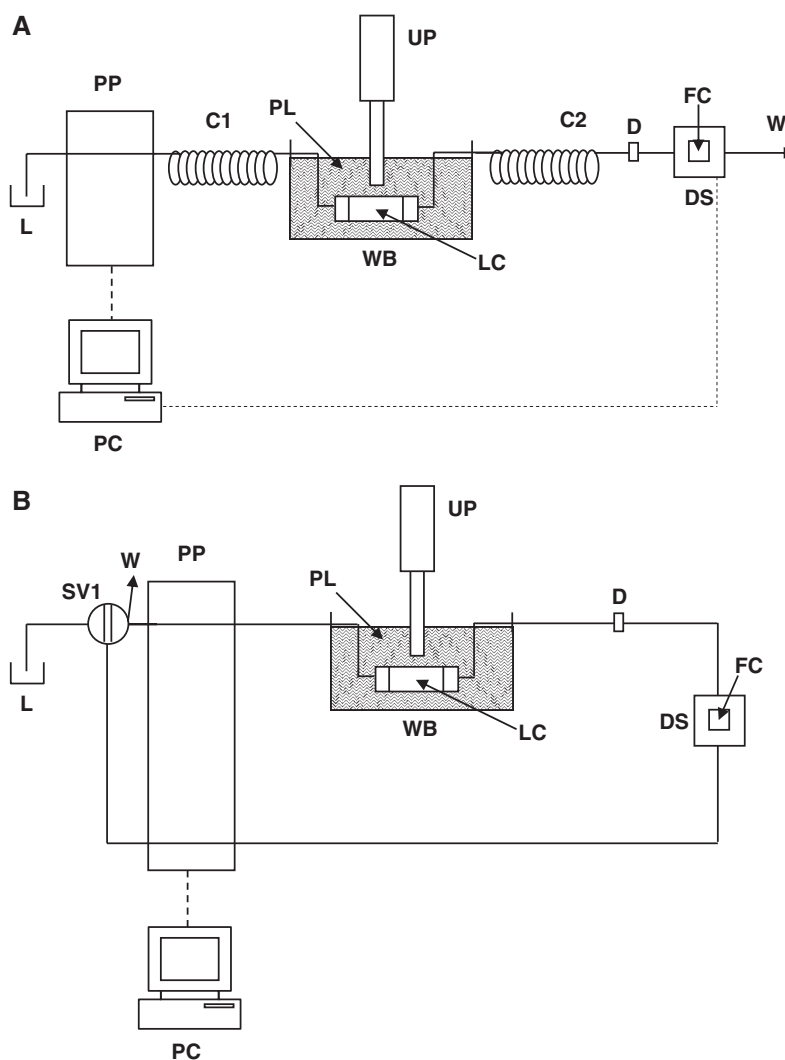
FIGURE 4.6. *Coupling of continuous ultrasound-assisted leaching and detection in an open (A) and a closed manifold with the detection system in the circuit for monitoring the leaching process (B). C — coil, D — debubbler, DS — detection system, FC — flow cell, L– leachant, LC — leaching chamber, PC — personal computer, PL — propagating liquid, PP — peristaltic pump, SV — switching valve, UP — ultrasonic probe, W — waste and WB — water bath.*
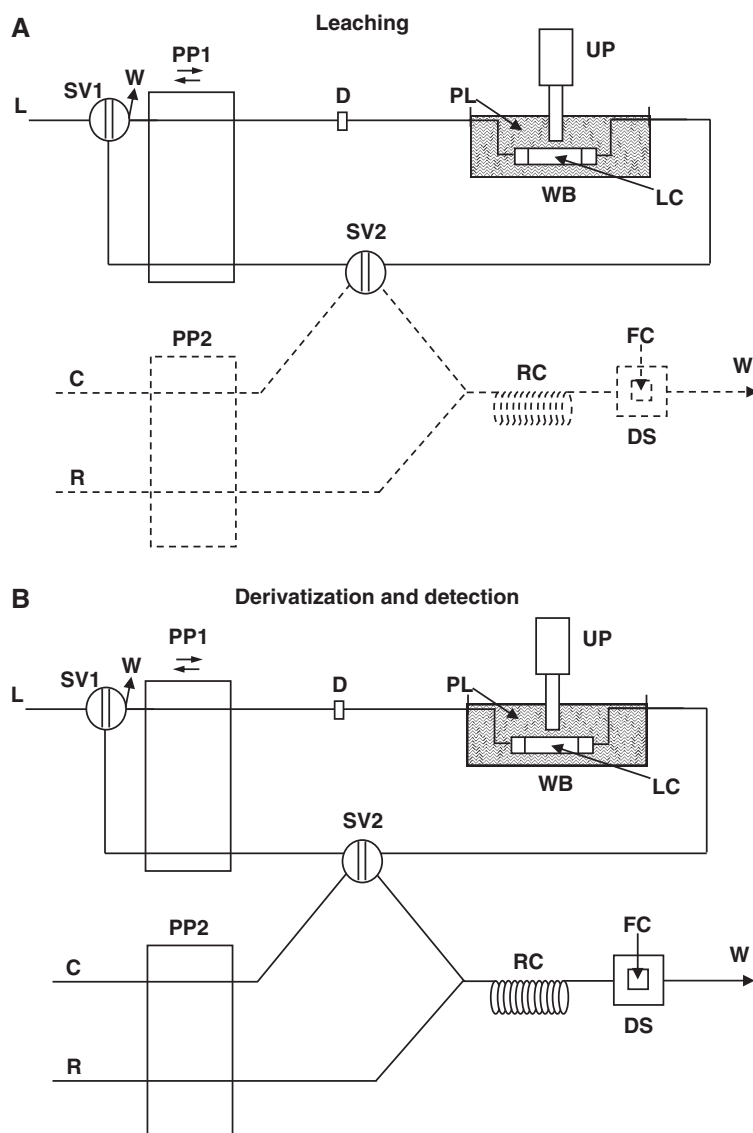
FIGURE 4.7. *Coupling of continuous ultrasound-assisted leaching in a closed manifold (A) and the derivatization–detection step (B). C — carrier, D — debubbler, DS — detection system, FC — flow cell, L — leachant, LC — leaching chamber, PL — propagating liquid, PP — peristaltic pump, R — derivatization reagent, RC — reaction coil, SV — switching valve, UP — ultrasonic probe, W — waste and WB — water bath. (Reproduced with permission of Elsevier, Refs. [38,39].)*

monitor leaching. However, only molecular and atomic optical detectors have to date been coupled to either open or closed leachers, always *via* FI manifolds. Molecular optical detectors are most frequently coupled to CUSAL, implemented through a flow cell, from which the leachate is led to waste after monitoring. Examples of the use of photometric detectors in this context include the methods for leaching iron from plant material for its subsequent determination following derivatization with 1,10-phenanthroline [38]; that of boron from soils using azomethine-H as derivatizing reagent and the manifold in Fig. 4.7 [39]; and that for the determination of hexavalent chromium [10], which was quantified by monitoring the absorbance of its complex with 1,5-diphenylcarbazide. Garrigues *et al*. [40] determined nicotine in tobacco by FTIR using a micro-flow cell with ZnSe windows and a pathlength of 0.457 mm. On the other hand, atomic detectors do not require a flow cell as the leachate is directly aspirated into the burner by nebulization. Such is the case with the method proposed by Yebra *et al*. for the determination of metals in meat or mussels [26,41–46] by using a continuous US-assisted leacher coupled on-line to a flame atomic absorption spectrometer (FAAS).

One type of unit most often required when a molecular detection system is coupled on-line with USAL is a debubbler. This device is useful in both closed and open manifolds as US usually produces bubbles that should be removed from the manifold to avoid parasitic signals at the detector.

On-line coupled leaching and filtration

Leaching and filtration are also often coupled in CUSAL. The main purpose is to remove suspended material from the leachate. Filtration should be avoided whenever possible as it can result in the retention of the target analytes on the filter; however, it may be the most effective way of removing particles that might cause problems in subsequent continuous steps. One case in point is the method of Cassella *et al*. for the determination of dithiocarbamate pesticides in commercial formulations and spiked solid samples [47] using the experimental set-up of Fig. 4.8. Samples were leached with the aid of an ultrasonic bath, after which filtration was required to prevent suspended material from reaching the detection system, which was a Fourier transform infrared (FTIR) spectrometer. In this way, all operations (namely, leaching, filtration and measurement) were integrated in order to minimize handling of samples and standards by the analyst — the analytes were toxic compounds that could cause skin and mucose membrane irritation, nerve and visual disturbances, and irreversible eye damage. The filtration unit was made by coupling an empty solid-phase extraction cartridge with a 0.45-μm nylon filter.

The filter can be easily cleaned if it is placed in the loop of an on-line injection valve so that, when filtration is completed, the flow of an appropriate rinsing solvent is passed through the filter in the upstream of the leachate in order to drag the solid retained on it.

On-line coupled leaching and concentration or clean up

Solid materials are commonly used to retain either analytes or interferents in solution in continuous analytical systems on account of their advantages. Thus, they afford efficient trace preconcentration in a convenient manner, thereby lowering detection and quantification limits and enabling the determination of the target analytes at the required levels. Also, they facilitate the removal of interferents (leachate clean-up) and the storage of analytes as the retained species remain unaltered over long periods due to the inert
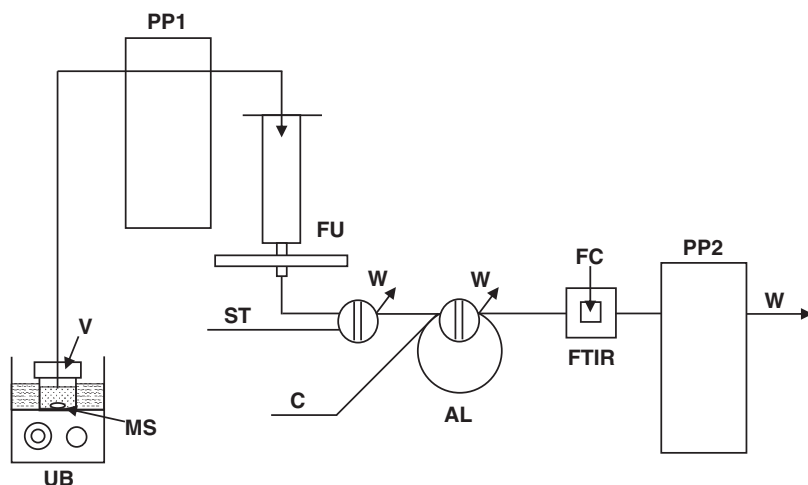
FIGURE 4.8. *On-line coupling of USAL and filtration for the determination of dithiocarbamate pesticides in commercial formulations. AL — analysis loop, C — carrier, FC — flow cell, FTIR — Fourier transform Infrared spectrometer, FU — filter unit, MS — magnetic stirrer, PP — peristaltic pump, ST — standard, UB — ultrasonic bath, V — sample vessel and W — waste. (Reproduced with permission of the Royal Society of Chemistry, Ref. [47].)*

nature of most sorbents. These materials prevent undesirable species, whether solid or liquid, from reaching the analyser or instrument and causing malfunctions with potential economic implications (filter effect). Finally, their on-line coupling poses no special technical difficulties [9]. Sorbent materials are usually packed either in cartridges or in short stainless steel or glass columns. Depending on the physical properties of the sorbent (particle size, bed length, etc.), the cartridge or column can be operated at room pressure, under gravity-flow conditions or at a high pressure. For the on-line implementation of a sorption step, a packed column cartridge is placed in the loop of an injection valve and the process conducted in two steps. First, with the valve in the filling position, the leachate coming from the US-assisted leacher is passed through the sorbent column in order to retain the target analytes and drive the remaining leachate to waste. In the second step, the valve is switched to the load position and an appropriate liquid phase is propelled to elute the analytes and bring them to the next step of the analytical process. Elution is performed upstream of retention, which avoids increased compaction of the solid material and hence overpressure problems in the dynamic manifold. The analytes are subsequently released from the column and driven to the instrument. Using air as the eluent carrier ensures minimal dilution. Reproducibility in the eluent volume can be achieved by confining it in the loop of an injection valve.

The retention material must be conditioned between uses in order to obtain reproducible results. The preconcentration factor is calculated as a function of the ratio between the leachate and elution volumes. A clean-up effect is usually obtained in the retention of the analytes as interferents are either not retained by the packed material or

retained but not eluted with the analytes if an appropriate eluent is used. A cleaning step involves selective retention of interferents in the column and passage of the analytes through it: the leachate is passed through the cartridge, the outlet of which is directly connected to the module where the next step of the analytical process is to take place while the column is regenerated. Regeneration is easier if the column is placed in the loop of an injection valve.

The choice of the sorbent is dictated by the characteristics of both the analytes and their potential interferences. The sorbents most frequently employed here are silica, alkylsilane-modified silica (bonded phases), alumina, porous polymers (with and without ion-exchange groups) and carbon-based materials. One typical application is a method for the determination of hexavalent chromium in soils [10] using the on-line system depicted in Fig. 4.9. After USAL, the analytes in the leachate were directly determined or preconcentrated depending on their concentration. Concentration was performed by on-line solid-phase extraction using a laboratory-made minicolumn packed with a strong anion-exchange resin. The absolute limits of detection were 4.52 and 1.23 ng without and with preconcentration, respectively.
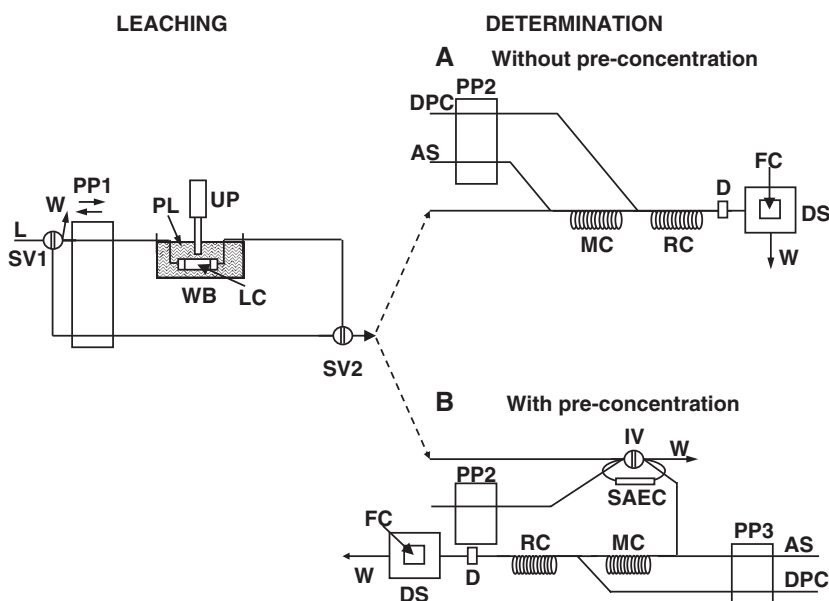
FIGURE 4.9. *On-line coupling of USAL and detection with (B) and without (A) an intermediate preconcentration–clean-up step for the determination of hexavalent chromium in soil. AS — acid stream, D — debubbler, DPC — diphenylcarbazide, DS — detection system, FC — flow cell, IV — injection valve, L — leachant, LC — leaching chamber, MC — mixing coil, PL — propagating liquid, PP — peristaltic pump, RC — reaction coil, SAEC — strong anion-exchange column, SV — switching valve, UP — ultrasonic probe, W — waste and WB — water bath. (Reproduced with permission of the Royal Society of Chemistry, Ref. [10].)*

On-line coupled leaching and individual separation

A flow manifold and continuous individual separation can be coupled *via* a variety of interfaces. However, only HPLC and GC have in fact been coupled to CUSAL, and only in a few applications. This is a logical consequence of the nature of US as vibrations from the ultrasonic source can affect sensitive parts of instruments. A CUSAL–HPLC interface can be as simple as a tube for transporting the leachate to the loop of the high-pressure injection valve of the chromatograph and filling it; the valve is then actuated to have the mobile phase drive the sample to the analytical column. One example of this coupling is a method for the determination of phenoxyacid herbicides in soils [6], which involves USAL in a closed manifold coupled on-line with a clean-up and concentration column packed with commercial C_{18} Hydra sorbent material and also with a chromatograph for individual separation and diode array detection of the analytes. The steps preceding chromatographic separation are conducted in the flow injection manifold, which allows the process to be fully automated.

The CUSAL–HPLC couple has been combined additionally with pre- or post-column derivatization. Thus, pre-column derivatization was used for the determination of colistin A and B in feeds; following USAL, the analytes were derivatized with *o*-phthaldialdehyde/2-mercaptoethanol and separated by HPLC for fluorimetric detection [48]. The experimental set-up used is depicted in Fig. 4.10A. Another application of CUSAL–HPLC is the determination of *N*-methylcarbamates in soils and food [49] (see Fig. 4.10B), where the analytes were also derivatized with *o*-phthaldialdehyde after separation for fluorescence-based monitoring. A number of steps of the process including leaching, filtration, solid-phase extraction, liquid chromatographic separation, post-column derivatization and fluorescence detection were performed on-line, all in an automated manner.

CUSAL can also be coupled to any other type of continuous separation by using an appropriate interface. Thus, CUSAL has been coupled to GC *via* a large-volume injection (LVI) module consisting of a programmed-temperature vaporizer (PTV) and the six-port injection valve shown in Fig. 4.11 to develop an on-line method for the determination of airborne organophosphate esters following their trapping on binder-free borosilicate fibre-glass filters [50]. The whole leached fraction — *viz*. 800 µl of 7:3 (v/v) hexane/methyl-*tert*-buthyl ether — was introduced without clean-up into the GC, which allowed the analytical process to be completed in less than 15 min.

4.5.   ULTRASOUND-ASSISTED LEACHING *VERSUS* OTHER LEACHING ALTERNATIVES

A number of alternatives to classical leaching methods ever since US was first used as auxiliary energy to assist a leaching process have been in use. The advantages of USAL over the classical leaching methods are obvious: frequently, the latter involve longer time preparation procedures under drastic conditions, the use of hazardous reagents and intensive intervention of the analyst, all with little room for automation. Similar to US, other auxiliary energies such as microwaves or the use of high pressures and temperatures have proved effective with a view to accelerate and automate leaching. The advantages and disadvantages of USAL as compared to three widely used leaching alternatives are discussed below. The three alternatives are classical Soxhlet leaching and two more recent techniques (namely, microwave-assisted extraction (MAE), and supercritical fluid extraction (SFE), which are increasingly competing with US-based methods in improved official methods of analysis.
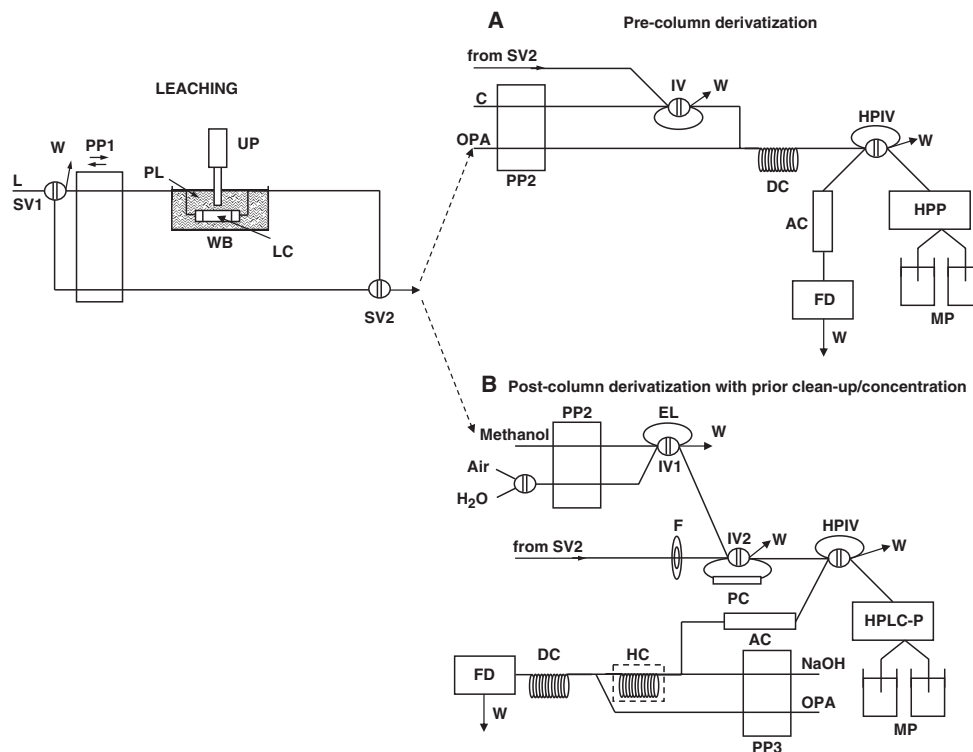
FIGURE 4.10. *On-line coupling of USAL and detection with derivatization: (A) in the pre-column mode for the determination of colistin A and B in feeds; (B) in the post-column mode for the determination of N-methylcarbamates in soil and foods. AC — analytical column, C — carrier, DC — derivatization coil, EL — elution loop, F — filter, FD — fluorimetric detector, HC — hydrolysis coil, HPIV — high-pressure injection valve, HPP — high-pressure pump, IV — injection valve, L — leachant, LC — leaching chamber, MP — mobile phase, OPA — o-phthaldialdehyde, PC — preconcentration column, PL — propagating liquid, PP — peristaltic pump, SV — switching valve, UP — ultrasonic probe, W — waste and WB — water bath. (Reproduced with permission of Elsevier, Refs. [48,49].)*

4.5.1. Ultrasound-assisted leaching versus conventional Soxhlet leaching

Soxhlet leaching has been traditionally used as a reference for comparing the efficiency of methods based on other principles, including US, with a view to their validation by use in routine analyses.

   The most salient advantages of USAL over conventional Soxhlet leaching are as follows:

(1) The cavitation phenomenon increases the polarity of the leachant, analytes and matrix. This increases the leaching efficiency, which is frequently similar to or greater than that provided by conventional Soxhlet leaching.
(2) Unlike Soxhlet leaching, USAL allows the addition of a co-leachant or a solvent mixture to further change the polarity of the liquid phase.
(3) The need for no high temperatures and pressures in USAL allows the use of mild operating conditions and enables the leaching of thermolabile analytes, which can be degraded by heat, or analytes prone to experiencing chemical transformations under the typical working conditions of Soxhlet leaching.
(4) The operating time in USAL is always shorter than in Soxhlet-based official methods, where it ranges from 8 to 24 h.
(5) The ability to fully automate the analytical process by coupling USAL with other steps is not shared by Soxhlet leaching, which cannot be coupled for unattended development of the analytical process.
(6) Leachant consumption is dramatically lower in USAL (usually a few millilitres as compared to 100–150 ml in most Soxhlet methods).
(7) The ability of water as leachant in USAL is of a high environmental interest; by contrast, water is difficult to use in Soxhlet leaching owing to its high boiling point.
(8) Moisture adjustment, which is very frequently required in Soxhlet leaching methods to ensure reproducible results, is unnecessary in USAL.
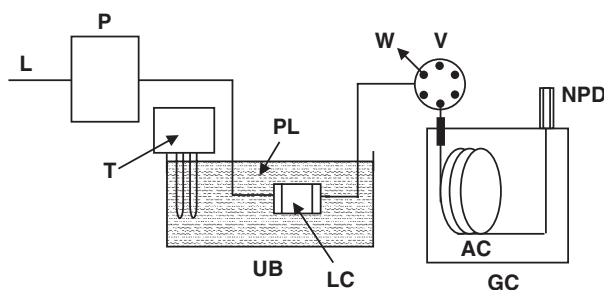
FIGURE 4.11. *On-line coupling of USAL and GC for the determination of airborne organophosphate esters in fibre filters. AC — analytical column, GC — gas chromatograph, L — leachant, LC — leaching chamber, NPD — nitrogen–phosphorous detection system, P — pump, PL — propagating liquid, T — thermostat, UB — ultrasonic bath, V — six-port injection valve and W — waste. (Reproduced with permission of Elsevier, Ref. [50].)*

On the other hand, USAL has the following disadvantages with respect to Soxhlet leaching:

(1) In batch methods (DUSAL), which are most widely used, the solvent cannot be renewed during the process, so the leaching efficiency is dictated by the solid–liquid partitioning equilibrium. The need for filtering and rinsing after leaching lengthens the duration of this step, increases solvent consumption and also the risk of losses and (or) contamination of the leachate.
(2) Ultrasound radiation produces free radicals in the solvent which can alter the chemical composition of analytes and hence the analytical results.

4.5.2. Ultrasound-assisted leaching versus supercritical fluid leaching

The US-based technique surpasses SFE in the following respects:

(1) The equipment needed is much simpler, so the overall cost of leaching is much lower. This can be of interest to routine laboratories with a limited budget, unable to afford a supercritical fluid extractor.
(2) USAL allows leaching of a wide variety of compounds, whatever their polarity, as it can be used with any solvent. On the other hand, supercritical fluid leaching uses almost exclusively CO_2 as leachant (with or without a co-leachant as a modifier), which restricts its scope to non-polar or low-polar analytes.
(3) The ability of USAL to operate under ambient conditions with respect to temperature and pressure ensures stability of thermolabile analytes.
(4) USAL is usually more expeditious than supercritical fluid leaching.

On the other hand, USAL falls short of supercritical fluid leaching in the following respects:

(1) Unlike the solvents used for sonication in some applications (*e.g.* cyclohexane, tetrahydrofuran and binary mixtures such as that of dichloromethane and acetone), supercritical CO_2 is not environmentally hazardous.
(2) The precision of SFE methods is similar to or slightly better than that of their US-assisted counterparts, especially when US baths are used.
(3) Leachant removal after depressurization in supercritical-CO_2 leaching allows the leached species to be dissolved in a fairly low volume of appropriate solvent.

4.5.3. Ultrasound-assisted leaching versus microwave-assisted leaching

Ultrasound-assisted leaching provides several interesting advantages over MAE, namely:

(1) Ultrasound-assisted methods are normally faster than those assisted by microwaves.
(2) The ultrasonic procedure is safer as it does not require high pressures or temperatures.
(3) In many cases, the whole procedure is simpler as it involves fewer operations and is thus less prone to contamination.
(4) Unlike many microwave-assisted leaching methods, USAL requires no moisture adjustment.

On the other hand, USAL is subject to the following shortcomings relative to microwave-assisted leaching:

(1) Particle size has a decisive influence on the USAL efficiency.
(2) Ultrasound-assisted methods are usually less robust than microwave-assisted ones because, as noted by Cencic-Kobda and Marcel [51], ageing of the US probe surface can alter the leaching efficiency.

4.6. APPLICATIONS OF USAL

USAL for sample pretreatment is being increasingly used in analytical laboratories all over the world. This section discusses the principal applications developed ever since the inception of US energy for sample leaching in the analytical laboratory. Only the most salient aspects are reviewed here in order to provide readers with a global picture of the potential of this auxiliary energy for leaching. Interested readers can delve deeper into specific aspects of each application in the corresponding references. A few special applications involving US assistance energy to other leaching techniques (particularly Soxhlet extraction and SFE) are also briefly discussed.

4.6.1. Discrete ultrasound-assisted leaching

This section discusses various applications of discrete ultrasonic leaching that are classified according to the nature of the leached species (inorganic, organometallic or organic) without regard to whether a bath or a probe was used.

Ultrasound-assisted leaching of inorganic species

Most of the applications of DUSAL to inorganic species involve the removal of metal elements from different types of matrices. The quantitative determination of metals at low concentration levels is one of the most frequent current tasks for routine analytical laboratories owing to their toxic effects on plants, animals and humans. One difference in toxicity between inorganic and organic species is that metals cannot be degraded, so they tend to accumulate in matrices such as sediments, soils, plants or animals, where they can produce even more toxic products such as organometals. Classical digestion procedures (*e.g.* dry ashing and wet digestion) and microwave-assisted digestion in either open vessels or closed systems are the most popular sample preparation modes prior to determining metals in solid samples. As noted in Chapter 3, these methods are subject to serious constraints. The use of slurries is one reliable alternative as it avoids the need for digestion and sample decomposition as a result. In addition, it dramatically reduces sample preparation times and costs, and minimizes sample contamination. However, this sample pretreatment frequently involves labour-intensive and time-consuming freeze-drying operations and the use of surfactants to maintain slurry stability. The latter can cause problems with some detection systems (*e.g.* in the determination of metals in onion [52] using total reflection X-ray fluorescence, where the surfactants exhibit X-ray self-absorption).

Alternative sample pretreatments have been developed to avoid the previous shortcomings. Some procedures based on the leaching of elements using diluted acids and (or) oxidants seem to be effective. These procedures are known as acid leaching, and they involve solubilization of metals in the leachant without causing sample matrix to decompose. Because organic matter need not be destroyed, a low acid concentration suffices; this reduces acid consumption, the production of nitrous vapours when nitric acid is used and pretreatment times (by effect of the need for no cooling) [53,54]. In this context, USAL has proved effective for the quantitative removal of a number of heavy metals from environmental, industrial and biological samples, and hence a useful alternative to drastic preparation procedures requiring concentrated acids and high temperatures and (or) pressures. One crucial advantage of USAL is that diminished matrix effects can be expected as a result of the analytes being isolated from non-leachable and potentially interfering matrix concomitants [55]. In addition, US energy provides leaching with significant advantages such as: (a) an increased throughput relative to classical leaching procedures; (b) greater simplicity; and, (c) avoidance of chemical emissions to the atmosphere, which helps comply with current policies for reducing environmental contamination [20].

Human activities often mobilize and redistribute natural compounds in the environment to an extent that they can cause adverse effects. Much attention has been paid to the determination of trace of pollutant elements on account of their significant effect on the environment. The potential of USAL has been put into use in environmental element analysis. Thus, the US leaching of cadmium from coals and pyrolysed oil shale prior to ETAAS [56] resulted in a twofold increase in precision, better detection limits and decreased background absorbance in relation to total digestion. Cadmium has also been successfully leached with US assistance from ash samples with subsequent flow-injection cold-vapour atomic absorption spectrometry [57]. Additional examples include the leaching of germanium from soils with an ultrasonic probe in 10 min [58] or that of lead from coal in 60 s [59].

In addition to the earlier examples, where only one element per sample was determined, ultrasonic extraction has proved effective as a prior step in the multi-element determination of heavy metals. One case in point is the study of Ashley *et al*., who developed various strategies employing ultrasonic leaching for sample preparation [60]. Dilute acids have been used for the USAL of a large number of metals from dusts and air filters, both in the laboratory and using field-portable equipment. The speciation analysis of various inorganic forms of a metallic element (namely, pentavalent and tervalent antimony) as citrate complexes from airborne particulate matter was facilitated by USAL [61]; the stability of the complexes in water prevented tervalent antimony from being oxidized to pentavalent antimony during leaching and alleviated the adsorption of antimony compounds on the sample surface. Another example of interest is a method for the USAL of Cr, Cu, Pb and Zn from sludge. A multivariate optimization study was performed using diluted acid as leachant for two main purposes, namely: to avoid risks associated with the use of pressurized digesters and reduce the treatment time [62].

Concerning the types of matrices from which the target analytes are removed, a large number of methods for the USAL of metals from soils, sediments and sewage sludge have exposed the significance of the sample preparation step in the environmental field. These samples are complex and possess physical, chemical and biological characteristics that vary with time and space. Metal accumulation in soils, sediments and sludge poses environmental risks through potential metal transfer to aquatic media or uptake by plants, which introduces the metals in the food chain. Examples of the use of USAL as a sample

preparation method for single-element analysis include the leaching of mercury from soils and sediments using diluted HNO_3 as leachant in the presence of KCl to improve the leaching efficiency by increasing the ionic strength and facilitating the formation of stable mercury halide compounds [63]; that of lead from reference sediment materials leached in only 20 s with an ultrasonic probe [64]; and the removal of radiochemical metals such as [210]Po and other natural radionuclides from soil and sediments [65]. In multi-element analysis, USAL has been used for the leaching of copper, lead and zinc from Syrian soils at low temperatures [66]; and that of cadmium, copper, lead, zinc, chromium, manganese and nickel from sewage sludge [24], where heating at 90°C was required for optimal leaching.

The total concentration of metals is not a measure of its toxicity; in fact, this depends on the bioavailability of the metal to plants or other organisms, which is determined mainly by its solubility. Therefore, in order to reliably estimate the bioavailability of metals and their toxicity one must determine not only its total concentration but also those of its different chemical forms or ways, whether free or bound to a solid matrix [67]. A number of existing sequential and single leaching procedures to assess the metal availability in soils are time consuming as they involve mechanical shaking for long times [68,69]. Sequential leaching is effective for the determination of various chemical forms of heavy metals. Various sequential leaching schemes have been developed to establish metal distribution in different fractions that include the widely used Tessier sequential leaching scheme [70] and the more recent scheme proposed by the Standards, Measurement and Testing Programme (SM&T) [71]. The fractions include exchangeable species and those associated with carbonates, Fe–Mn oxides (reducible), organic matter and sulphides (oxidizable) and residual fraction. Notwithstanding their shortcomings (*e.g.* re-adsorption between phases during leaching, poor reagent selectivity, a strong dependence of the leaching efficiency on the operating conditions and difficulty in comparing results from different methods), sequential methods have been widely accepted for metal fractionation in various types of samples with a view to determine the mobility and potential bioavailability of metals in the environment [72]. However, sequential leaching methods are labour intensive and time consuming, so they are scarcely used in routine analyses. Some authors have succeeded in reducing the lengthy treatment times involved by replacing the conventional procedures with others assisted by auxiliary energies such as microwaves [73,74] or US [75–78]. One of the main differences between these energies is bulk heat, which is produced by microwaves but not by US. Therefore, US affords more expeditious leaching than conventional methods and without significant bulk heating. Pérez-Cid *et al*. compared conventional and US-accelerated Tessier sequential leaching schemes for metal fractionation in sewage sludge and concluded that the most mobilizable fractions could be accurately determined by using the sonication procedure; Cr and Pb were largely associated with the oxidizable (last step) and residual (final residue) fractions, so they should exhibit a low mobility [77].

Single leaching methods involve replacing a sequential stepwise procedure with a single leaching step using the same reagents and operating conditions as the sequential procedure but a separate portion of sample for each reagent [79]. In this way, single leaching allows the leachable metal content to be more easily determined than with sequential methods, at the expense of using larger amounts of sample. This shortcoming can be circumvented by using small-scale single leaching. Filgueiras *et al*. compared the conventional method endorsed by SM&T in the presence and absence of US [68]. They found the assistance of US in substantially reducing sample and reagent consumption, and also in allowing all fractions to be simultaneously leached by using a separate sub-sample for each leachant. The leachable amounts of trace metals found were quite consistent.

The method was simple and expeditious, and uses sample and reagents sparingly, so it can be very useful when rapid assessment of metal mobility is required.

The determination of metals in biological tissues is of great interest on account of the toxic effects of many of them on humans. This has increased the need to establish a safe concentration range for each metal and elucidate its role in the food chain. Preparing biological samples is made difficult by the encapsulation of metals within cell walls, which can be disrupted by the combined effect of a dilute acid attack and ultrasonication in order to bring the metals into the leachant. The increasing use of soil fertilizers to boost agricultural production has raised the need to determine macroelements and microelements in plant and leaf tissues in order to optimize application conditions. The current need for new fast methods of analysis requires the development of simple, fast and quantitative sample preparation procedures for routine use in agronomical studies. USAL is especially useful for this purpose, as shown in the removal of metals from onion with results similar to those provided by classical methods based on wet digestion and dry ashing [52], albeit in a more simple and expeditious manner, and with reduced chemical consumption. Also, the USAL of Ca, Mg, Mn and Zn from vegetables such as lettuce, cabbage and spinach in an ultrasonic bath avoids the hazard and problematic handling involved in some wet digestion methods [21].

Plants can accumulate metals in, or on, their tissues by virtue of their ability to adapt to various chemical effects of the environment. Thus, plants are intermediate reservoirs for trace elements from the lithosphere, hydrosphere or atmosphere. For this reason, plants are often used as bio-indicators of pollution related to heavy metals in the environment *via* their bio-accumulative properties. Lichens and mosses, which rely on the surface absorption of nutrients, have been widely used in biomonitoring surveys [80,81]. As a result, the number of environmental samples subjected to analysis within the framework of routine monitoring or risk and sustainability assessment studies is growing continuously [82]. Variations in concentration of metals in plants can reflect changes in concentration of the metals in soil [83,84]. Moreover, the ability of plants to accumulate and concentrate heavy metals is responsible for the spreading of these elements in the food chain. USAL has been used as an alternative to sample digestion for the removal of Mg, Mn and Zn from various plant materials, using diluted HCl [33], and also for the leaching of trace and major elements from spruce needle samples [85]. In addition, USAL has been applied to various trace metals in tea and tobacco leaves that were subsequently quantified by ICP-AES [31], and to the determination of total arsenic and total inorganic arsenic in seaweed after high-temperature USAL with methanol in order to remove organometallic compounds. After leaching, total arsenic was quantified by ETAAS and inorganic arsenic by hydride generation atomic absorption spectrometry (HG-AAS). No alteration of analytes by US was found in two CRMs [23].

Similar to plants, animals can also be used as bio-indicators. Thus, the analyses of aquatic organisms have been increasingly used to obtain direct measures of abundance and availability of metals in the environment. Mussels can accumulate metals and thus be used to estimate pollutant levels in the environment. Cadmium and lead have been leached from mussels by using dilute nitric acid under US assistance [86]. Leaching was carried out in autosampler cups in order to minimize sample manipulation.

The determination of trace elements in foods is very important as some minerals are toxic whereas others are essential for vital processes in humans. In fact, the knowledge of the relationship between the mineral content in the diet and some diseases such as hypertension or osteoporosis has increased the interest in the mineral content — or the presence of metals, if toxic — in food. USAL has proved an effective choice for removing metals such as Pb, Cd, Cu and Ca from meat [20], chloride salts from various types of

meat products [87], Cd and Pb from food samples such as vegetables, pig kidney and fish [5] or major and trace elements from fats [88] and edible seaweeds [89].

In addition to its usefulness for environmental samples, USAL is a powerful tool for leaching metals from hygiene samples at workplaces [90]. One case in point is that of filters of various materials used to collect aerosol particulates. Such filters are frequently extracted with US assistance, as in the determination of Cr(VI) in welding fumes, whereas polycarbonate membrane filters were used to collect the aerosols for subsequent leaching in an ultrasonic bath [25].

USAL has also been used in the determination of trace impurities in high-purity materials. This type of analysis is mandatory with a view to controlling their quality and studying the synergistic action of, and correlation with, impurities. The accuracy and precision of the analytical results depend strongly on the particular separation procedure used before the determination step, as shown in the multi-element quantitative USAL of impurities such as iron, copper, lead and bismuth in high-purity silver metal. For this purpose, a silver sample was dissolved in nitric acid and treated with chloride, after which the solution was evaporated to dryness and the impurities were redistributed on the surfaces or in the interstitial spaces of agglomerates of matrix crystals. Then, the impurities were leached into 0.1 M nitric acid with the aid of ultrasonic irradiation [91].

The use of US energy for ore leaching has become increasingly popular in hydrometallurgy. Ultrasound assistance to classical methods has enabled the fast [92,93] and selective [94] removal of metals in this field. One case in point is silver, which can be leached almost completely from the solid waste of a silver ore beneficiating plant by using a USAL method involving thiourea [95], and so is the leaching of TiO_2 from red mud with sulphuric acid and the aid of ultrasonic energy, which causes particle rupture and increases the surface area available for leaching. Ultrasound increased the efficiency of leaching by 20% relative to identical conditions in its absence [96].

Ultrasound-assisted leaching of organometallic compounds

The analysis of organometallic compounds is of great interest from different points of view. Environmentally, these compounds are released into the atmosphere from anthropogenic sources or by species, the metabolism or transport mechanisms of which involve the formation of metal–carbon bonds *via* natural processes. Also, there is an increasing interest in the determination of metalloporphyrins, particularly in energy-related materials such as crude oils and gasoline. Finally, the monitoring of metal-containing drug metabolites and the study of the behaviour of metal proteins in humans have opened up new avenues for the application of USAL to clinical studies.

The key step in the analysis of organometallic compounds is sample preparation; specifically, their isolation from the matrix is very complex as the analytes must be separated with no loss, conversion between species or contamination and with minimal interferences. These compounds have been traditionally leached by mechanical stirring using a suitable leachant (*e.g.* relatively concentrated solutions of acetic, hydrochloric or hydrobromic acids in water or methanol). However, the use of pressurized solvents at high temperatures, microwaves or sonication has been proposed to reduce the leaching time [97]. The use of US to assist leaching is especially interesting here as it does not require high temperatures or pressures, and uses mild operating conditions. Degradation phenomena during application of high temperatures and pressures or microwaves can pose problems with some pollutants. The operating conditions and leachants that can be used for speciation analyses of organometallic compounds are restricted to those which preserve

the stability of all species. One example is the speciation of mobilizable arsenic — As(III), As(V), monomethylarsonic acid and dimethylarsinic acid — in river sediments, where leaching was carried out with water and phosphate buffer (pH 5.5–6.5) in two consecutive steps (corresponding to the soluble and exchangeable fractions) under probe sonication at 30% of the radiation amplitude for 1 min [98].

The determination of phenyltin species, which are quite stable under the anaerobic conditions prevailing in sediments, is also of great interest; so much so that the European Community has included triphenyltin (TPhT) on its list of priority pollutants. Analytical surveys of TPhT in sediments, and the monitoring of potential environmental degradation to less toxic species such as di- and monophenyltin (DPhT and MPhT, respectively) calls for rapid soft sample preparation procedures preserving the stability of this compound during analysis. Sonication of sediment samples in glacial acetic acid for a short time (4–10 min) allowed the simultaneous determination of phenyl and buthyltin species with efficiencies between 70 and 90% for phenyl compounds. The stability of TPhT in acetic acid decreases with increasing temperature, so any sample-leaching procedure using an acid medium in combination with high temperatures is unsuitable for the speciation of TPhT or any other phenyltin compound in sediments [99].

The determination of methylmercury in biological certified reference materials such as dogfish liver or tuna fish was accomplished following USAL with nonane in the presence of tetraethylborate for *in situ* derivatization [100]. In this way, methylmercury was leached with an efficiency higher than 90% and without artifact formation of methylmercury during sample preparation. Compared to classical methods such as acid and alkaline digestion or distillation, USAL dramatically shortens the sample preparation procedure and reduces sources of error as a result. Microwave-assisted leaching also shortens analysis times, from hours to a few minutes; however, it requires careful optimization of the operating conditions. Degradation of methylmercury to inorganic mercury and losses by evaporation as elemental mercury have been observed following acid leaching of biological materials subjected to microwaves [101]. In addition, the equipment required may increase the cost of analyses. The main shortcoming of the previous USAL method for the determination of methylmercury [100] is that it cannot be used with inorganic mercury. Río-Segade *et al*. developed a method that allows the separation of inorganic mercury and methylmercury in fish tissues in a short time without the need for chromatographic separation. For this purpose, USAL was combined with flow injection–cold vapour generation atomic absorption spectrometric determination of both mercury species, the separation of which was based on their disparate leachability in hydrochloric acid under US treatment [102]. Methylmercury was separately determined using sodium tetrahydroborate as reducing agent after selective leaching with 2 M hydrochloric acid, while inorganic mercury was determined by selective reduction with stannous chloride in 5 M hydrochloric acid in leachates containing both mercury species.

Ultrasound energy has also been used to accelerate the leaching of metal proteins (particularly metallothionein-isoforms and superoxide dismutase from liver samples) [103]. One of the main problems encountered in analysing these samples (namely, the need to preserve the species stability during leaching) is circumvented by USAL.

Ultrasound-assisted leaching of organic compounds

In addition to its high efficiency for dissolving metals from a wide variety of samples, US is also used for its ability to leach organics from various types of matrices. The wide range

of organic compounds that can be encountered precludes the establishment of standard conditions for efficient USAL, so different solvents and conditions are required depending on the particular target compounds. The risk of some organic compounds being altered by the radicals generated by solvent sonolysis must always be borne in mind. An optimization study based on a multivariate approach is the best method for avoiding or minimizing alterations during USAL.

Ultrasonic leaching of organic compounds has been used in virtually all fields, which testifies to its versatility. In the environmental field, USAL has proved effective for the removal of organic pollutants from various types of samples. One of the principal groups of organic pollutants is that of PAHs, which are widely distributed in the environment. These pollutants result from incomplete combustion of fossil fuels, as well as from diagenetic processes during fossil fuel formation and, in smaller amounts, from forest fires and, possibly, microbiological synthetic processes. Some PAHs possess carcinogenic and (or) mutagenic properties, and are included on the US Environmental Protection Agency and European Community lists of priority pollutants. The solids usually leached with the aid of US for the subsequent determination of these compounds are mainly soils and sediments [30,36,104–108], sewage sludge [109], and particulate matter [110,111], and also, to a lesser extent, food [112], vegetables [113,114], aerosols [115] and coal [116], among others. In addition to official methods for the isolation of PAHs from diverse matrices, USAL is widely used as a reference for checking the efficiency of alternative techniques such as MAE or SFE. Also, USAL has been compared in terms of performance with other leaching techniques. For instance, it was compared with MAE for the leaching of PAHs from sediments; although both techniques proved similarly efficient, the precision, expressed as the average relative standard deviation, was considerably higher in USAL [107]. Another comparison involved subjecting various samples to conventional Soxhlet extraction and pressurized liquid extraction (PLE) for the leaching of PAHs from sediments and mussels [106]; USAL was found to leach all analytes more efficiently and reproducibly from sediments than did Soxhlet and PLE. On the other hand, ultrasonication of mussel samples was similarly efficient to the other two techniques. One shortcoming of PLE was that the leachates were dirtier and required clean-up by alkaline digestion and SPE using alumina, which complicated the overall process.

Ultrasonic leaching is not always the best choice for PAHs leaching. Such is the case with their leaching from wooden sleepers and coal tar [117], where Soxhlet leaching was more efficient than USAL. The duration of the Soxhlet and ultrasonic leaching procedures was similar (24 h). This can be ascribed to the USAL method being used not under optimal conditions (*i.e.* to a decoupling effect) as most methods for US-assisted PAHs leaching provide significant improvements over their conventional and non-conventional counterparts.

The ability with which PAHs can be removed depends largely on the particular congener. Usually, the leaching efficiency for a given PAH is inversely proportional to the number of rings it possesses, so obtaining results comparable with those provided by other leaching techniques entails carefully adjusting the operational variables to the specific target analytes [118].

Polychlorinated biphenyls (PCBs) are also frequently included in pollutant monitoring programmes owing to their substantial persistence and accumulation in the environment. This has raised the need to develop methods for their routine analysis. USAL as a sample preparation method is an effective choice for the fast, efficient and straightforward removal of these compounds, as shown by the method for the determination of 146 PCBs in heron eggs [119], where ultrasonic leaching resulted in improved precision, efficiency and reliability under the operational conditions proposed. USAL was used prior to the

determination of PCBs in food in the analyses that followed the Belgian 1999 dioxin in food crisis [120]; fat was extracted by USAL and fractionated by matrix solid-phase dispersion prior to GC-ECD analysis. Concerning environmental samples, USAL has been used to leach PCBs from environmental waste [121], charcoal [122] and fly ash [123].

Pesticides are another major group of pollutants for which USAL is effective. These compounds can be decomposed or degraded by the action of sunlight, water, chemical agents or microorganisms such as bacteria when released into the environment. Degradation usually leads to the formation of less harmful breakdown products which, however, can generate even more toxic products under specific environmental conditions. Also, degradation-resistant pesticides remain in the environment over long periods [124]. The varied behaviour of these compounds makes it crucial to choose an appropriate method for their removal from solid samples for subsequent analysis. Traditional methods such as shake-flask and Soxhlet extraction are very time- and solvent-consuming for use to isolate pesticides; also, they occasionally require too high temperatures or provide very low efficiency for this purpose. A number of MAE, SFE, ASE (accelerated solvent extraction) and USAL methods have been developed in order to overcome these drawbacks that additionally reduce both solvent consumption and leaching time. MAE, SFE and ASE are unsuitable for thermolabile analytes; also, ASE and SFE use relatively expensive equipment and SFE cannot handle large sample amounts or provide high efficiencies for polar pesticides. USAL is quite flexible as it is not subjected to any restriction in the type of extractant (pure or mixed) that can be used for maximal efficiency and selectivity. In addition, USAL can be performed at ambient temperature and pressure [125]. Recently, there have been some attempts at using solid-phase microextraction (SPME) for the determination of pesticides in solid samples with advantages such as simplicity in sample handling, reductions in sample size and solvent volume, and no need for any additional clean-up procedures. The limited number of methods of this type reported so far can be ascribed to restrictions in fibre stability, analyte release or volatility.

Regarding matrix types, soil is the main environmental reservoir of pesticides, and constitutes a source from which these compounds and their metabolites can be released into the atmosphere, ground water or living organisms [126]. A number of methods for pesticide analysis in soils use ultrasonic energy to assist the isolation of the analytes [127–144]. Typical examples include the leaching of multi-residue carbamate pesticides in small polypropylene columns using low volumes of methanol (5 ml) [136]; that of antifouling pesticides from sediments, also with methanol [127]; or that of the fungicides vinclozolin and dicloran from soils [130]. In the last case, USAL was followed by a clean-up/ concentration step by SPE in order to remove interferents and bring the concentrations of the trace analytes within the linear determination range. Examples of the USAL of pesticides from food include that of honey [129] with better efficiencies (92% for atrazine and 94% for simazine) than the traditional shake-flask method; that of herbicides and insecticides belonging to different chemical groups from tomato crops [134]; the simultaneous leaching of pyrethroid, organophosphate and organochlorine pesticides from fish tissue using 90:10 (v/v) acetonitrile–methanol [141]; and that of fumigant residues from wheat with significantly decreased leaching times relative to classical leaching with or without heating [138].

Not only PAHs, pesticides and PCBs, but also other pollutants have been isolated with excellent results by USAL. One case in point is the leaching of total organic pollutants from particulate samples [145] by using a direct ultrasonic leacher, where the transducer was bonded directly to the bottom of the sample vessel (see Fig. 2.6A). The ultrasonic piezoelectric transducer was used at two different power settings (25 and 50 W). The transducer was tightly attached to the glass sample vessel and a condenser

was connected to avoid evaporation losses. After complete removal, the leachate was delivered through a valve at the bottom of the vessel. The performance of this ultrasonic system was compared with that of conventional Soxhlet extraction and the US-assisted leacher was found to be an effective choice for the leaching of particulate organic matter from airborne particulate. The main advantages of this method over Soxhlet extraction included significantly shortened leaching times (15 min *versus* 12 h) and dramatically reduced leachant volumes. Also, the USAL method was slightly more efficient and is not affected by moisture. The leacher can be assembled from readily available parts (*viz.* glassware, a high-frequency generator and a transducer).

Also of interest in this context are the leaching of explosives such as centralite from building materials [146]; plasticizers — some of which have been classified as endocrine disrupters by the European Union — from sediments [147] and plastics [148]; veterinary antibiotics from soils [149]; nitroaromatics from soils [150]; oestrogens and progestrogens in river sediments [151]; chemical warfare agents such as sarin and hydrolysis products from soil [152]; and alkylphenols from atmospheric samples [153] or surfactants from river sediments [154].

The low temperatures at which USAL can be performed make it a powerful tool for leaching natural products such as hemicellulose components and lignin from vegetable materials (seeds, fruits or leaves) [155,156]; active principles or oils [3]; saponins [157]; steroids and triterpenoids [158]; isoflavones [159]; volatile compounds [160]; carvone and limonene [161]; vitamin E isomers [162] or antioxidants [163]. Operating at ambient temperatures avoids thermal damage to leached species and the loss of volatile components; this makes USAL very useful for the isolation of natural compounds with pharmacological properties from plants. Similar to the leaching of metals from biological samples, the combined effect of dilute acid attack and ultrasonication breaks down cell walls, thus making this type of energy highly effective for disrupting cells.

USAL has also been used as a sample treatment in the analysis of foods and related products. For this purpose, similar to the removal of natural products from plants, US application to the leaching of organic compounds must be carefully evaluated because, during sonication, transient species such as radicals and the conditions produced by acoustic cavitation can result in undesirable oxidative changes in the isolated compounds. Typical applications include the leaching of lipids from marine mucilage samples (also with environmental connotations) [164]; tartaric and malic acids from grapes and by-products of winemaking [165]; date syrup from date fruits [166]; polyphenols from apple tissues [167]; and policosanol from rice [168].

Finally, USAL has been recommended as an excellent choice in clinical and drugs analysis for the removal of retinamide (an anticarcinogenic agent) from tissues [169]; DNA from animal bones [170]; tramadol from pharmaceutical formulations [171]; veterinary drug residues from animal tissues [172]; and anabolic steroids from hair [173]. Industrial applications of USAL in this context include the isolation of terpenoid aldehydes from cotton [174] and additives from poly(ethylene) [175], which are used to provide required properties to plastics during manufacturing and utilization, and therefore influence both the processing and durability of the end-products. Leaching poly(olefin) additives within a reasonable time is rather difficult because they tend to degrade upon heating. Thus, an increase in temperature can cause the polymer to undergo a transition from the glassy to the rubbery form at the glass transition temperature. The USAL of additives from polymers provides fast, quantitative recovery with no appreciable degradation or the need for additional evaporation of the solvent or re-dissolution of the additive. The structure of the target additives affects the extraction kinetics, which entails careful selection of both the extraction temperature and time.

4.6.2. Continuous ultrasound-assisted leaching

CUSAL has developed to a much lesser extent than batch USAL despite its outstanding advantages (see Section 4.3.2.). In any case, CUSAL has been applied to a variety of analytes in highly diverse matrices. The first two applications of CUSAL involved inorganic analytes (namely, iron from plant material and boron from soil [38,39]). In the former, formation of the well-known complex between the analyte and 1,10-phenanthroline provided results consistent with those of the conventional method based on AAS following hot-acid leaching. In the determination of boron in soil, the leaching time was reduced from 40 to 5 min by applying ultrasonic irradiation while the leachant was circulated through the solid (see Fig. 4.7). The temperature was found to have a crucial influence on the leaching step. Thus, the analytical signal for the leached analyte after derivatization increased by almost 50% on increasing the leaching temperature from 40 to 80°C. Clearly, higher temperatures favour dissolution of boron and increase the efficiency of US. The latter effect can be easily understood by considering that the distance between molecules in both solids and liquids increases with increasing temperature, thereby decreasing attenuation of ultrasonic irradiation and strengthening its effect at the interface between the circulating liquid and the static sample [176]. More recently, CUSAL has also been used for the determination of hexavalent chromium in soil [10]. The target analyte was leached in a much shorter time than that required by the reference EPA method 3060A. Also, the CUSAL method provided similar results while avoiding time-consuming manual operations and facilitating coupling to a preconcentration step in order to reduce the detection limit. The leaching of cadmium and lead in plants prior to electrothermal atomic absorption spectrometry reduced the extraction time by a factor of 3 and 10 relative to microwave-assisted and dynamic superheated water leaching, respectively [17]. Also, macro- and micronutrient metal elements were leached from animal feeds in a shorter time than that required by the reference AOAC Method 968.08 (18 min *versus* 4.5 h) with similar results but greater procedural simplicity as a consequence of the shorter number of operations involved [34]. The CUSAL of various metals from mussels and meat was compared with DUSAL and the sonication time found to be reduced by factors of 6–12 for mussels and 60 for meat [26,41–46].

In addition to metals, CUSAL has proved efficient for organics. Thus, nitropolycyclic aromatic hydrocarbons were extracted from natural contaminated soil with similar efficiency to that provided by the reference EPA method 3540 based on Soxhlet leaching but with dramatically reduced leaching times (10 min *versus* 24 h) and leachant volumes (less than 10 ml *versus* 100 ml) [16]. Also, *N*-methylcarbamates in soil and food were leached without any degradation of the target compounds and efficiencies higher than those provided by alternative techniques such as SFE or PLE and found to require longer leaching times and provide poorer efficiencies owing to the need to use mild conditions in order to preserve the structural integrity of the pesticides [49]. Phenoxyacid herbicides in soil and sediment were removed with excellent results by using water as leachant and EDTA as co-leachant, which is of special environmental importance [6]. On the other hand, the USAL of dithiocarbamate pesticides from solid formulations using chloroform as leachant is not recommended because the analytes are partially destroyed by the action of some radicals formed through sonolysis of the solvent [47]. However, this conclusion is limited to this particular solvent.

Concerning natural products, the leaching of phenolic compounds from alperujo (a residue generated in olive oil production) and strawberries [7,37] are two excellent examples of the capabilities of CUSAL. The latter application showed that, although these compounds are easily degraded and especially sensitive to temperature, the use of

appropriate operating conditions avoids degradation during CUSAL and the antioxidant capacity of the analytes to be preserved. The continuous ultrasonic leaching of nicotine from tobacco in a closed-flow system for 2 min coupled on-line with FTIR determination [40] constitutes an excellent example of both the efficacy of CUSAL and its availability for on-line coupling to other analytical steps.

Finally, the food industry has also taken advantage of CUSAL as in the case of the removal of fat from bakery products [22]. The ability of this technique to isolate the target analytes without degradation under optimal conditions allows the leachates to be used for the determination of *trans*-fatty acids after derivatization to esters [32]. GC-MS and MIRS (mid infrared spectrometry) with the aid of chemometrics were used to compare the leachates provided by CUSAL and the Folch method (a soft but time-consuming reference leaching method with which the absence of degradation in leached compounds has been extensively demonstrated) and no significant difference between the two was observed.

4.6.3. Ultrasound assistance to other leaching techniques

This section deals with those cases in which US has been used to help other leaching techniques — particularly Soxhlet and SFE — in order to improve their performance.

Soxhlet leaching has been the most widely used technique over the years for isolating a variety of analytes from all types of samples. However, new leaching techniques that overcome the drawbacks associated with Soxhlet extraction constitute one of the most active research lines in solid sample preparation at present. The most serious shortcomings of Soxhlet leaching are the long time required for leaching, the large amounts of organic solvent waste produced and the inability to automate the process. A variety of devices intended to circumvent these shortcomings while retaining the favourable characteristics of Soxhlet extraction have been developed, most of which use microwaves as auxiliary energy to accelerate leaching [176]. Thus, Luque-García *et al*. recently reported a Soxhlet leacher assisted by US energy for the leaching of total fat from oil seeds such as sunflower, rape and soyabean [177]. The leacher, which is depicted in Fig. 4.12, is based on the same principles as a conventional Soxhlet extractor, but has the Soxhlet chamber accommodated in a thermostatic bath through which US is applied by means of an ultrasonic probe. The application of US to the sample cartridge provides results similar to or even better than those obtained by conventional Soxhlet leaching (official ISO method); however, it enormously decreases the number of Soxhlet cycles needed for quantitative leaching, thereby reducing the leaching time to at least half that needed by conventional procedures. This approach constitutes a valuable choice for the extraction of easily compactable matrices such as seeds.

Ultrasonic energy has also been employed to boost mass transfer in supercritical fluid leaching *via* small-scale agitation. An ultrasonic transducer with an operating working frequency of about 20 kHz was placed inside a supercritical fluid leacher as shown in Fig. 4.13A for this purpose. The US–SFE leacher has been used to leach oil from particulate almonds [178]; US application was found to reduce the leaching time by 30% and raise the efficiency by 20% relative to the same process under silent conditions. Figure 4.13B illustrates the effect of US on the efficiency of oil leaching from particulate almonds 3–4 mm in size. As can be seen, the initial part of the efficiency curve was identical with and without US application; this suggests that this stage is mainly controlled by the solubility of the solute in the leachant, while it seems clear that the following stage is mainly determined by mass transfer mechanisms, where US plays a key role.
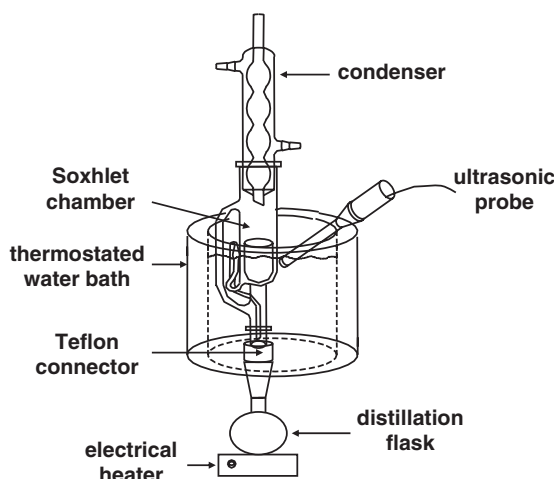
FIGURE 4.12. *Scheme of an ultrasound-assisted Soxhlet leacher. (Reproduced with permission of Elsevier, Ref. [177].)*

Electrokinetic remediation of soils contaminated by lead and phenanthrene has also been successfully enhanced by US. An increase in outflow, permeability and contaminant removal rate was observed in US-assisted electrokinetic tests that testifies to the technical feasibility of *in situ* electrokinetic ultrasonic remediation [179].

4.7. ULTRASOUND-ASSISTED BIOLEACHING

Bioleaching is the use of microorganisms to leach metals from sulphides and (or) iron-containing ores and mineral concentrates. Iron and sulphide are microbially oxidized to produce ferric iron and sulphuric acid, and these chemicals convert the insoluble sulphides of metals such as copper, nickel and zinc to soluble metal sulphates that can be readily recovered from the solution. Even though the bioleaching process is very slow, it is not energy intensive. Among various physical stimuli for accelerating the process, US has proved effective for rapidly boosting the performance of living biocatalysts. Although sonication is generally associated with damage to cells by disruption, there is evidence for the beneficial effects of sonication on the ability to leach metals under catalysis by cells. Thus, the bioleaching of lateritic nickel ore is enhanced by the growth of *Aspergillus niger* under US [180,181]. Bioleaching using *Aspergillus niger* by conventional means leached 60% of the copper from an oxidized mining residue, whereas ultrasonic pretreatment raised the leaching efficiency up to 80% [182].

Bioleaching has a number of advantages over chemical leaching, namely:

(a) It allows the exploitation of low-grade ores and mineral resources located in remote areas, which would otherwise be expensive for the mining industry.
(b) It is more environmentally friendly than conventional smelting as it uses less energy and does not produce any SO_2 emissions.
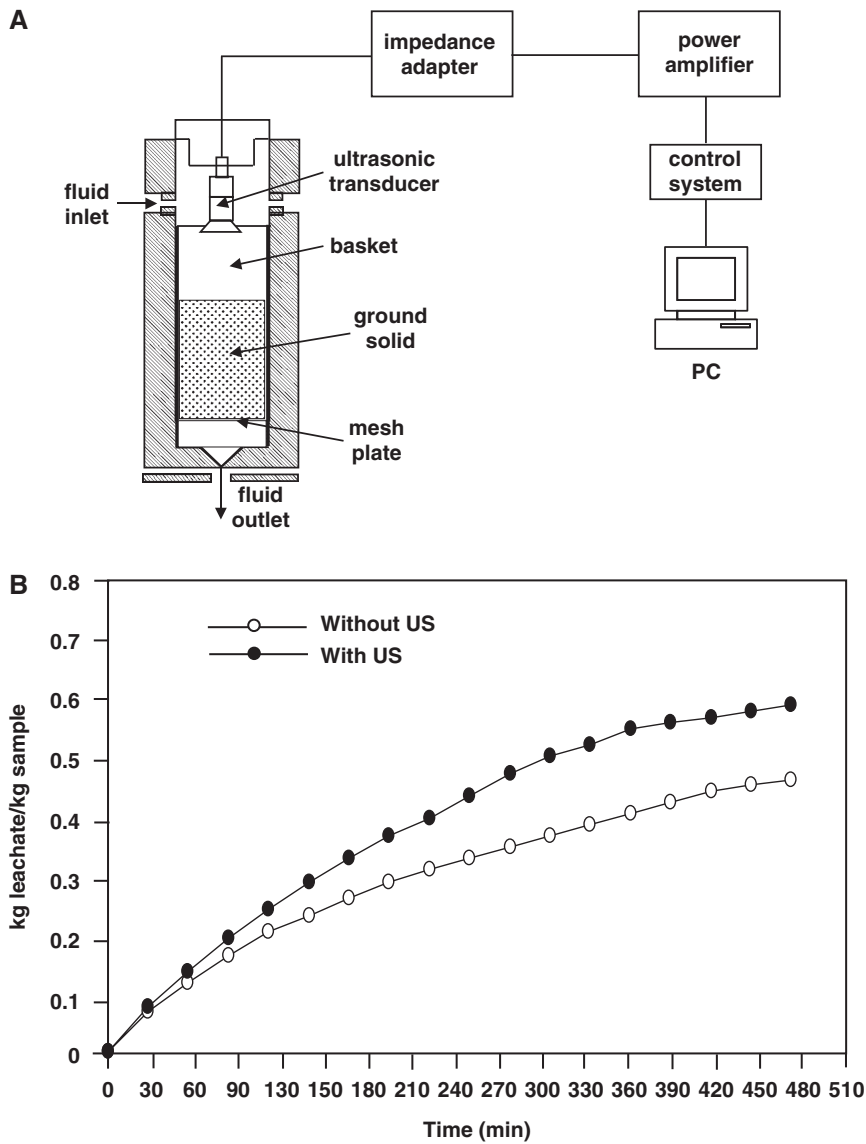
FIGURE 4.13. *Scheme of a supercritical fluid leacher assisted by ultrasound (A). Supercritical leaching efficiency of oil from almond for a 3–4 mm particulate size with and without ultrasound assistance (B). (Reproduced with permission of Elsevier, Ref. [178].)*

(c) Less landscape occurs as the bacteria grow naturally. Native bacteria can operate over a wide temperature range (–20 to 55°C). Also, the bacteria can be recycled.
(d) The bacteria are self-sustaining.
(e) Bioleaching is a less energy-intensive process.
(f) It is simpler and hence cheaper to operate and maintain, as skilled workers are not needed to operate complex chemical plants.

However, bioleaching also has some disadvantages as the bacterial process is slower than conventional techniques, which may raise processing costs. Also, not all ore types are amenable to extraction and no available method exists as yet to stop the bacteria from extracting minerals once bioleaching has started. The application of ultrasound expands the advantages of leaching while avoiding or lessening its shortcomings to an acceptable level. Thus, US irradiation allows to:

(a) stimulate microbes and facilitate rapid microbial growth;
(b) accelerate metal extraction;
(c) improve the metal leaching efficiency;
(d) enhance the selectivity of the bioleaching process;
(e) reduce the usual dependence of the bioleaching process on the origin of the ore; and
(f) control bacterial activity by using ultrasonic intensities higher than the threshold values killing all or some of the microorganisms.

In conclusion, sonobioleaching is an emerging technology providing the mining industry with the potential for more efficient leaching of metals from ores at significantly reduced costs, all with minimal environmental consequences and engineering operational problems. Future research should focus on the use of US for the bioleaching of organic analytes from various types of matrices and the development of analytical methods assisted by this technology [183].

References

1. K.M. Swamy and K.L. Narayana, Ultrasonically Assisted Leaching, in *Ultrasound in Environmental Protection*, Elsevier, Amsterdam, 2001.
2. J.L. Luque-García and M.D. Luque de Castro, *Trends Anal. Chem.*, 22 (2003) 41.
3. M. Romdhane and C. Gourdon, *Chem. Eng. J.*, 87 (2002) 11.
4. T.J. Mason, *Sonochemistry*, Oxford University Press, Oxford, 1999.
5. P.C. Aleixo, D.S. Júnior, A.C. Tomazelli, I.A. Rufini, H. Berndt and F.J. Krug, *Anal. Chim. Acta*, 512 (2004) 329.
6. A. Caballo-López and M.D. Luque de Castro, *Chromatographia*, 58 (2003) 257.
7. F. Priego-Capote, J. Ruiz-Jiménez and M.D. Luque de Castro, *J. Chromatogr. A*, 1045 (2004) 239.
8. C.C. Nascentes, M. Korn, C.S. Sousa and M.A.Z. Arruda, *J. Braz. Chem. Soc.*, 12 (2001) 57.
9. M. Valcárcel and M.D. Luque de Castro, *Automatic Methods of Analysis*, Elsevier, Amsterdam, 1988.
10. J.L. Luque-García and M.D. Luque de Castro, *Analyst*, 127 (2002) 1115.
11. B.R. James, J.C. Petura, R.J. Vitale and G.R. Mussoline, *Environ. Sci. Technol.*, 29 (1995) 2377.
12. K. Ida, S. Ishigami and N. Nakagawa, *Lab. Robot. Autom.*, 10 (1998) 125.
13. M. Arhoun, J.L. Martín-Herrera, E. Barreno and G. Ramis-Ramos, *Lab. Robot. Autom.*, 11 (1999) 121.
14. G.J. Price, *Currents Trends in Sonochemistry*, Royal Society of Chemistry, Cambridge, 1992.

15. L.A. Crum, T.J. Mason, J.L. Reisse and K.S. Suslick, *Sonochemistry and Sonoluminiscence*, Kluwer Academic Publisher, Dordrecht, The Netherlands, 1999.

16. E. Priego-López and M.D. Luque de Castro, *J. Chromatogr. A*, 1018 (2003) 1.

17. J. Ruiz-Jiménez, J.L. Luque-García and M.D. Luque de Castro, *Anal. Chim. Acta*, 480 (2003) 231.

18. M. Mäntysalo and E. Mäntysalo, *Ultrasonics*, 38 (2000) 723.

19. K.M. Swamy and K.L. Narayana, *Ultrason. Sonochem.*, 8 (2001) 341.

20. R.M. García-Rey, R. Quiles-Zafra and M.D. Luque de Castro, *Anal. Bioanal. Chem.*, 377 (2003) 316.

21. C.C. Nascentes, M. Korn and M.A.Z. Arruda, *Microchem. J.*, 69 (2001) 37.

22. J. Ruiz-Jiménez and M.D. Luque de Castro, *Anal. Chim. Acta*, 502 (2004) 75.

23. O. Muñiz-Naveiro, A. Moreda-Piñeiro, A. Bermejo-Barrera and P. Bermejo-Barrera, *At. Spectrosc.*, 25 (2004) 79.

24. D. Hristozov, C.E. Domini, V. Kmetov, V. Stefanova, D. Georgieva and A. Canals, *Anal. Chim. Acta*, 516 (2004) 187.

25. R. Milacic, J. Scancar and J. Tusek, *Anal. Bioanal. Chem.*, 372 (2002) 549.

26. A. Moreno-Cid and M.C. Yebra, *Spectrochim. Acta B*, 57 (2002) 967.

27. J. Wang, K. Ashley, E.R. Kennedy and C. Neumeister, *Analyst*, 122 (1997) 1307.

28. K. Ndung'u, N.K. Djane, F. Malcus and L. Mathiasson, *Analyst*, 124 (1999) 1367.

29. Z. Shi, J. He and W. Chang, *Talanta*, 64 (2004) 401.

30. V. Pino, J.H. Ayala, A.M. Alfonso and V. González, *Fresenius J. Anal. Chem.*, 371 (2001) 526.

31. J. Borkowska-Burnecka, U. Jankowiak, W. Zyrnicki and K.A. Wilk, *Spectrochim. Acta B*, 59 (2004) 585.

32. J. Ruiz-Jiménez, F. Priego-Capote and M.D. Luque de Castro, *J. Chromatogr.*, 1045 (2004) 203.

33. A.V. Filgueiras, J.L. Capelo, I. Lavilla and C. Bendicho, *Talanta*, 53 (2000) 433.

34. F. Priego-Capote and M.D. Luque de Castro, *Anal. Bioanal. Chem.*, 378 (2004) 1376.

35. J.L. Capelo and A.M. Mota, *Current Anal. Chem.*, 1 (2005) 193.

36. J.L. Capelo, M.M. Galesio, G.M. Felisberto, C. Vaz and J. Costa-Pessoa, *Talanta*, 66 (2005) 1272.

37. M.C. Herrera and M.D. Luque de Castro, *Anal. Bioanal. Chem.*, 379 (2004) 1106.

38. F. Lázaro, M.D. Luque de Castro and M. Valcárcel, *Anal. Chim. Acta*, 242 (1991) 283.

39. D. Chen, F. Lázaro, M.D. Luque de Castro and M. Valcárcel, *Anal. Chim. Acta*, 226 (1989) 221.

40. J.M. Garrigues, A. Pérez-Ponce, S. Garrigues and M. de la Guardia, *Analyst*, 124 (1999) 783.

41. M.C. Yebra, M.F. Enríquez, A. García and A. Moreno-Cid, *Fresenius J. Anal. Chem.*, 370 (2001) 64.

42. M.C. Yebra and A. Moreno-Cid, *J. Anal. At. Spectrom.*, 17 (2002) 1425.

43. A. Moreno-Cid, M.C. Yebra, S. Cancela and R.M. Cespón, *Anal. Bioanal. Chem.*, 377 (2003) 730.

44. M.C. Yebra and A. Moreno-Cid, *Anal. Chim. Acta*, 477 (2003) 149.

45. M.C. Yebra, A. Moreno-Cid and S. Cancela-Pérez, *Talanta*, 66 (2005) 691.

46. M.C. Yebra, S. Cancela-Pérez and A. Moreno-Cid, *Anal. Chim. Acta*, 533 (2005) 51.

47. A.R. Cassella, R.J. Cassella, S. Garrigues, R.E. Santelli, R.C. de Campos and M. de la Guardia, *Analyst*, 125 (2000) 1829.

48. S. Morales-Muñoz and M.D. Luque de Castro, *J. Chromatogr.*, 1066 (2005) 1.

49. A. Caballo-López and M.D. Luque de Castro, *J. Chromatogr.*, 998 (2003) 51.

50. C. Sánchez, M. Ericsson, H. Carlsson and A. Colmsjö, *J. Chromatogr.*, 993 (2003) 103.

51. Z. Cencic-Kobda and J. Marcel, *Chromatographia*, 49 (1999) 21.

52. J. Alvarez, L.M. Marcó, J. Arroyo, E.D. Greaves and R. Rivas, *Spectrochim. Acta B*, 58 (2003) 2183.

53. E.M.L. Lorentzen and H.M. Kingston, *Anal. Chem.*, 68 (1996) 4316.

54. P. Bermejo-Barrera, O. Muñiz-Naveiro, A. Moreda-Piñeiro and A. Bermejo-Barrera, *Anal. Chim. Acta*, 439 (2001) 211.

55. H. Méndez, F. Alava, I. Lavilla and C. Bendicho, *Anal. Chim. Acta*, 452 (2001) 217.
56. J.L. Brasil, E.C. Lima, R. Cataluña-Veses and M.M. Tisott, *At. Spectrosc.*, 25 (2004) 94.
57. M. Liva, R.M. Olivas and C. Cámara, *Talanta*, 51 (2000) 381.
58. I. López-García, N. Campillo, I. Arnau-Jerez and M. Hernández-Córdoba, *Anal. Chim. Acta*, 531 (2005) 125.
59. M.M. Silva, M. Goreti, R. Vale and E.B. Camarao, *Talanta*, 50 (1999) 1035.
60. K. Ashley, R.N. Andrews, L. Cavazos and M. Demange, *J. Anal. At. Spectrom.*, 16 (2001) 1147.
61. J. Zheng, A. Iijima and N. Furuta, *J. Anal. At. Spectrom.*, 16 (2001) 812.
62. S.R. Segade, M.C.D. Albor, E.F. Gómez and E.F. López, *Int. J. Environ. Anal. Chem.*, 83 (2003) 343.
63. A. Collasiol, D. Pozebon and S.M. Maia, *Anal. Chim. Acta*, 518 (2004) 157.
64. E.C. Lima, F. Barbosa and F.J. Krug, *J. Anal. At. Spectrom.*, 14 (1999) 1913.
65. M.S. Al-Masri, A. Al-Hamwi and H. Mukallati, *Environmental Radiochemical Analysis*, Royal Society of Chemistry, Cambridge, 1999.
66. R. Al-Merey, M.S. Al-Masri and R. Bozou, *Anal. Chim. Acta*, 452 (2002) 143.
67. Y. Ge, P. Murray and W.H. Hendershot, *Environ. Pollut.*, 107 (2000) 137.
68. A.V. Filgueiras, I. Lavilla and C. Bendicho, *Anal. Bioanal. Chem.*, 374 (2002) 103.
69. A. Marín, A. López-Gonzálvez and C. Barbas, *Anal. Chim. Acta*, 442 (2001) 305.
70. A. Tessier, P.G.C. Campbell and M. Bisson, *Anal. Chem.*, 51 (1979) 844.
71. P. Quevauviller, G. Rauret and B. Griepink, *Int. J. Environ. Anal. Chem.*, 51 (1993) 231.
72. A. Fernández-Alborés, B. Pérez-Cid, E. Fernández-Gómez and E. Falqué-López, *Analyst*, 125 (2000) 1353.
73. B. Pérez-Cid, M. de Jesús-González and E. Fernández-Gómez, *Analyst*, 127 (2002) 681.
74. P. Pazos-Capeáns, M.C. Barciela-Alonso, A. Bermejo-Barrera and P. Bermejo-Barrera, *Talanta*, 65 (2005) 678.
75. C.M. Davidson and G. Delevoye, *J. Environ. Monit.*, 3 (2001) 398.
76. B. Pérez-Cid, I. Lavilla and C. Bendicho, *Anal. Chim. Acta*, 360 (1998) 35.
77. B. Pérez-Cid, I. Lavilla and C. Bendicho, *Fresenius J. Anal. Chem.*, 363 (1999) 667.
78. B. Pérez-Cid, I. Lavilla and C. Bendicho, *Int. J. Environ. Anal. Chem.*, 73 (1999) 79.
79. F.M.G. Tack, H.A.H. Vossius and M.G. Verloo, *Int. J. Environ. Anal. Chem.*, 63 (1996) 61.
80. M.E. Conti and G. Cecchetti, *Environ. Pollut.*, 114 (2003) 471.
81. M. Aceto, O. Abollino, R. Conca, M. Malandrino, E. Mentasti and C. Sarzaanini, *Chemosphere*, 50 (2003) 333.
82. M.V. Balarama-Krishna and J. Arunachalam, *Anal. Chim. Acta*, 522 (2004) 179.
83. I. Novazamski, T.M. Lexmon and V.J.G. Houba, *Int. J. Environ. Anal. Chem.*, 51 (1993) 47.
84. A.P. Murphy, M. Coudert and J. Barker, *J. Environ. Monit.*, 2 (2000) 621.
85. A. Lesniewicz and W. Zyrnicki, *Int. J. Environ. Anal. Chem.*, 83 (2003) 735.
86. I. Lavilla, J.L. Capelo and C. Bendicho, *Fresenius J. Anal. Chem.*, 363 (1999) 283.
87. E. Sucman and J. Bednar, *Electroanalysis*, 15 (2003) 866.
88. F. Anwar, T.G. Kazi, R. Saleem and M.I. Bhanger, *Grasas Aceites*, 55 (2004) 160.
89. N. Ladra-Ramos, R. Domínguez-González, A. Moreda-Piñeiro, A. Bermejo-Barrera and P. Bermejo-Barrera, *At. Spectrosc.*, 26 (2005) 59.
90. K. Ashley, *Trends Anal. Chem.*, 17 (1998) 366.
91. M. Hiraide, Y. Mikuni and H. Kawaguchi, *Fresenius J. Anal. Chem.*, 354 (1996) 212.
92. B. Pesic and T. Zhou, *Metall. Trans.*, 23B (1992) 3.
93. K.L. Narayana, K.M. Swamy, K.S. Rao and J.S. Murty, *Min. Proc. Ext. Met. Rev.*, 16 (1997) 239.
94. J.A. Barrera-Godinez, T.J. O'Keefe and J.L. Watson, *Miner. Eng.*, 5 (1992) 1365.
95. M. Salim-Öncel, M. Ince and M. Bayramoglu, *Ultrason. Sonochem.*, 12 (2005) 237.
96. E. Sayan and M. Bayramoglu, *Hydrometallurgy*, 71 (2004) 397.
97. J.L. Gómez-Ariza, E. Morales, I. Giráldez, D. Sánchez-Rodas and A.Velasco, *J. Chromatogr. A*, 938 (2001) 211.
98. A. Huerga, I. Lavilla and C. Bendicho, *Anal. Chim. Acta*, 534 (2005) 121.
99. J. Carpinteiro, I. Rodríguez and R. Cela, *Fresenius J. Anal. Chem.*, 370 (2001) 872.

100. Q. Tu, J. Qian and W. Frech, *J. Anal. At. Spectrom.*, 15 (2000) 1583.
101. C.M. Tseng, A. de Diego, F.M. Martin, D. Amouroux and O.F.X. Donard, *J. Anal. At. Spectrom.*, 12 (1997) 743.
102. S. Río-Segade and C. Bendicho, *J. Anal. At. Spectrom.*, 14 (1999) 263.
103. V. Nischwitz, B. Michalke and A. Kettrup, *Analyst*, 128 (2003) 109.
104. T. Watanabe, S. Ishida, M. Kishiji, Y. Takahashi and A. Furuta, *J. Chromatogr. A*, 839 (1999) 41.
105. M.N. Kayali-Sayadi, S. Rubio-Barroso, C.A. Diaz-Diaz and L.M. Polo-Diez, *Fresenius J. Anal. Chem.*, 368 (2000) 697.
106. E. Martínez, M. Gros, S. Lacorte and D. Barceló, *J. Chromatogr.*, 1047 (2004) 181.
107. V. Pino, J.H. Ayala, A.M. Alfonso and V. González, *Talanta*, 54 (2001) 15.
108. Y.F. Song, X. Ping, S. Fleischmann and B.M. Wilke, *Chemosphere*, 48 (2002) 993.
109. C. Miege, J. Dugay and M.C. Hennion, *J. Chromatogr.*, 995 (2003) 87.
110. P.A.P. Pereira, J.B. de Andrade and A.H. Miguel, *Anal. Sci.*, 17 (2001) 1229.
111. A. Christensen, C. Ostman and R. Westerholm, *Anal. Bioanal. Chem.*, 381 (2005) 1206.
112. M.J. Nieva-Cano, S. Rubio-Barroso and M.J. Santos-Delgado, *Analyst*, 126 (2001) 1326.
113. A. Hubert, P. Popp, K.D. Wenzel, W. Engewald and G. Schueuermann, *Anal. Bioanal. Chem.*, 376 (2003) 53.
114. A. Dugay, C. Herrenknecht, M. Czok, F. Guyon and N. Pages, *J. Chromatogr. A*, 958 (2002) 1.
115. R.K. Bentsen, K. Halgard, H. Notoe, H.L. Daae and S. Oevreboe, *Sci. Total Environ.*, 212 (1998) 59.
116. A. Domínguez, R. Alvarez, C.G. Blanco and M.A. Diez, *J. Chromatogr.*, 719 (1996) 181.
117. M. Ochsenkühn-Petropoulou, A. Lampropoulou, H. Becker and W. Spyra, *Mikrochim. Acta*, 136 (2001) 185.
118. W.H. Griest and B.A. Tomkins, *Anal. Chem.*, 60 (1988) 2169.
119. S.G. Chu, C.S. Hong, B.A. Rattner and P.C. McGowan, *Anal. Chem.*, 75 (2003) 1058.
120. P. Sandra and F. David, *J. Chromatogr. Sci.*, 40 (2002) 248.
121. W. Sulkowski and A. Rosinska, *J. Chromatogr. A*, 845 (1999) 349.
122. J.S. Yang, D.H. Kim, D.H. Kim, D.W. Lee and Y.S. Chang, *J. Liq. Chromatogr. Relat. Technol.*, 24 (2001) 2293.
123. J.S. Yang, J.H. Jeong, D.W. Lee and Y.S. Chang, *J. Liq. Chromatogr. Relat. Technol.*, 24 (2001) 2815.
124. D.A.J. Weed, R.S. Kanwar, D.E. Stoltenberg and R.L. Pfeiffer, *J. Environ. Qual.*, 24 (1995) 68.
125. V. Andreu and Y. Picó, *Trends Anal. Chem.*, 23 (2004) 10.
126. L.C. Luchini, T.B. Peres and M.M. de Andrea, *J. Environ. Sci. Health*, B35 (2000) 51.
127. K. Martínez and D. Barceló, *Fresenius J. Anal. Chem.*, 370 (2001) 940.
128. C. Gonçalves and M.F. Alpendurada, *Talanta*, 65 (2005) 1179.
129. I. Rezic, A.J.M. Horvat, S. Babic and M. Kastelan-Macan, *Ultrason. Sonochem.*, 12 (2005) 477.
130. D.A. Lambropoulou and T.A. Albanis, *Anal. Chim. Acta*, 514 (2004) 125.
131. A. Otterbach and B.W. Wenclawiak, *Fresenius J. Anal. Chem.*, 365 (1999) 472.
132. M.A. Ali and P.J. Baugh, *Int. J. Environ. Anal. Chem.*, 83 (2003) 909.
133. A. Bouaid, L. Ramos, M.J. González, P. Fernández and C. Cámara, *J. Chromatogr.*, 939 (2001) 13.
134. J.L. Tadeo, J. Castro and C. Sánchez-Brunete, *Int. J. Environ. Anal. Chem.*, 84 (2004) 29.
135. S. Stipicevic, S. Fingler, L. Zupancic-Kralj and V. Drevenkar, *J. Sep. Sci.*, 26 (2003) 1237.
136. C. Sánchez-Brunete, A. Rodríguez and J.L. Tadeo, *J. Chromatogr. A*, 1007 (2003) 85.
137. C. Sánchez-Brunete, E. Miguel and J.L. Tadeo, *J. Chromatogr.*, 976 (2002) 319.
138. Y. Ren and S.E. Allen, *J. AOAC Int.*, 84 (2001) 1551.

139. G. Gatidou, A. Kotrikla, N.S. Thomaidis and T.D. Lekkas, *Anal. Chim. Acta*, 505 (2004) 153.
140. N. Rosales-Conrado, M.E. León-González, L.V. Pérez-Arribas and L.M. Polo-Diez, *Anal. Chim. Acta*, 470 (2002) 147.
141. J. You and M.J. Lidy, *Int. J. Environ. Anal. Chem*., 84 (2004) 559.
142. C. Sánchez-Brunete, B. Albero and J.L. Tadeo, *J. Agric. Food Chem*., 52 (2004) 1445.
143. S. Navarro, N. Vela, C. García and G. Navarro, *J. Agric. Food Chem*., 51 (2003) 7359.
144. B. Albero, C. Sánchez-Brunete and J.L. Tadeo, *J. Chromatogr*., 1007 (2003) 137.
145. S.C. Lee, S.C. Zou, K.F. Ho and L.Y. Chan, *Fresenius J. Anal. Chem*., 369 (2001) 166.
146. A. Keszler, B. Kazinczy and L. Kotai, *Fresenius J. Anal. Chem*., 364 (1999) 328.
147. R.A. Gimeno, R.M. Marcé and F. Borrull, *Chromatographia*, 58 (2003) 37.
148. X. Li, Z. Zeng, Y. Chen and Y. Xu, *Talanta*, 63 (2004) 1013.
149. P.A. Blackwell, H.C. Holten Lützhoft, H.P. Ma, B. Halling-Sorensen, A.B.A. Boxall and P. Kay, *Talanta*, 64 (2004) 1058.
150. T. Bausinger, U. Dehner and J. Preuß, *Chemosphere*, 57 (2004) 821.
151. M.J. López de Alda, A. Gil, E. Paz and D. Barceló, *Analyst*, 127 (2002) 1299.
152. P.A. d'Agostino, J.R. Hancock and L.R. Provost, *J. Chromatogr*., 912 (2001) 291.
153. S. Berkner, G. Streck and R. Herrmann, *Chemosphere*, 54 (2004) 575.
154. H.F. Sun, T. Hase, N. Hata, I. Kasahara and S. Taguchi, *Anal. Sci*., 17 (2001) 1291.
155. Z. Hromádková and A. Ebringerová, *Ultrason. Sonochem*., 10 (2003) 127.
156. R. Sun and J. Tomkinson, *Ultrason. Sonochem*., 9 (2002) 85.
157. J. Wu, L. Lin and F. Chau, *Ultrason. Sonochem*., 8 (2001) 347.
158. E.C. Schinor, M.J. Salvador, I.C.C. Turatti, O.L. Zucchi and D.A. Dias, *Ultrason. Sonochem*., 11 (2004) 415.
159. M.A. Rostagno, M. Palma and C.G. Barroso, *J. Chromatogr*., 1012 (2003) 119.
160. E. Alissandrakis, D. Daferera, P.A. Tarantilis, M. Polissiou and P.C. Harizanis, *Food Chem*., 82 (2003) 575.
161. S. Chemat, A. Lagha, H. Aitamar, P.V. Bartels and F. Chemat, *Flavour Fragr. J*., 19 (2004) 188.
162. R. Bruni, A. Guerrini, S. Scalia, C. Romagnoli and G. Sacchetti, *Phytochem. Anal*., 13 (2002) 257.
163. S. Albu, E. Joyce, L. Paniwnyd, J.P. Lorimer and T.J. Mason, *Ultrason. Sonochem*., 11 (2004) 261.
164. M. Mecozzi, M. Amici, G. Romanelli, E. Pietrantonio and A. Deluca, *J. Chromatogr. A*, 963 (2002) 363.
165. M. Palma and C.G. Barroso, *Anal. Chim. Acta*, 458 (2002) 119.
166. M.H. Entezari, S.H. Nazary and M.H. Haddad Khodaparast, *Ultrason. Sonochem*., 11 (2004) 379.
167. R.M. Alonso-Salces, A. Barranco, E. Corta, L.A. Berrueta, B. Gallo and F. Vicente, *Talanta*, 65 (2005) 654.
168. G. Cravotto, A. Binello, G. Merizzi and M. Avogadro, *Eur. J. Lipid Sci. Technol*., 106 (2004) 147.
169. J. Vratilova, T. Frgala, B.J. Maurer and C.P. Reynolds, *J. Chromatogr. B*, 808 (2004) 125.
170. M. Prado, C.M. Franco, C.A. Fente, A. Cepeda, B.I. Vázquez, J. Barros-Velázquez, *Electrophoresis*, 23 (2002) 1005.
171. M. Pospisilova, M. Polasek and V. Jokl, *J. Pharm. Biomed. Anal*., 18 (1998) 777.
172. R.J. McCracken, D.E. Spence and D.G. Kennedy, *Food Addit. Contam*., 17 (2000) 907.
173. Y. Gaillard, F. Vayssette, A. Balland and G. Pepin, *J. Chromatogr. B*, 735 (1999) 189.
174. C.G. Benson, S.G. Wyllie, D.N. Leach, C.L. Mares and G.P. Fitt, *J. Agric. Food Chem*., 49 (2001) 2181.
175. N. Haider and S. Karlsson, *Analyst*, 124 (1999) 797.
176. M.D. Luque de Castro and J.L. Luque-García, *Acceleration and Automation of Solid Sample Treatment*, Elsevier, Amsterdam, 2002.
177. J.L. Luque-García and M.D. Luque de Castro, *J. Chromatogr*., 1034 (2004) 237.

178. E. Riera, Y. Golás, A. Blanco, J.A. Gallego, M. Blasco and A. Mulet, *Ultrason. Sonochem*.,
     11 (2004) 241.
179. H.I. Chung and M. Kamon, *Eng. Geology*, 77 (2005) 233.
180. K.L. Narayana, K.M. Swamy, V.V. Panchanadikar, R.N. Kar and L.B. Sukla, *Acoust. Lett*.,
     18 (1995) 227.
181. K.M. Swamy, L.B. Sukla, K.L. Narayana, R.N. Kar and V.V. Panchanadikar, *Acoust. Lett*.,
     17 (1993) 43.
182. C.N. Mulligan and R. Galvez-Cloutier, *Water Sci. Technol*., 41 (2000) 255.
183. K.M. Swamy, K.L. Narayana and V.N. Misra, *Ultrason. Sonochem*., 12 (2005) 301.

CHAPTER 5

Ultrasound Assistance to Heterogeneous Systems

5.1. INTRODUCTION

The systems dealt with in this chapter can be classified according to the nature of the phases involved and the number of phases present before sonication:

   There are three types of US-assisted heterogeneous systems according to the nature of the phases involved, namely: (a) solid–liquid systems (*e.g.* slurry formation, solid–liquid filtration, sonophoresis, crystallization and solid–liquid agglomeration or aggregation); (b) gas–liquid systems, which encompass foaming–defoaming operations, nebulization (aerosolization and spraying or atomization) and degassing; and (c) solid–gas systems (*e.g.* solid–gas agglomeration and filtration).

   Depending on the number of phases present before US is applied, heterogeneous systems can be of two types, namely: (a) two-phase systems, which encompass slurry formation, solid–liquid and solid–gas agglomeration, solid–liquid and solid–gas filtration, sonophoresis, defoaming and degassing; and (b) one-phase systems, which include crystallization, foaming, nebulization (aerosolization and spraying or atomization). Group (a) can be further divided into solid–liquid systems (slurry formation, agglomeration and filtration), liquid–solid systems (sonophoresis), solid–gas systems (filtration), and gas–liquid systems (defoaming and degassing). On the other hand, group (b) can be split into several systems according to the nature of the second phase formed under US irradiation into solid-phase (crystallization) and gas-phase (atomization, foaming, nebulization–aerosolization and spraying or atomization) systems.

   This chapter initially deals with those solid–liquid systems in which the solid phase exists before US is applied, namely: slurry formation, agglomeration and filtration, which are followed by sonophoresis, a special type of liquid–solid filtration. Then, a system where formation of the second phase is favoured by US (crystallization) is discussed, and so are systems involving a gas phase into which a liquid phase is included (nebulization), or from which it is removed (defoaming and degassing) with the aid of US complete the chapter.

5.2. ULTRASOUND-ASSISTED SLURRY FORMATION

The use of slurry formation in analytical chemistry is virtually restricted to sample preparation prior to insertion into atomizers — including ionization, if required — for subsequent atomic (or mass) detection. Slurries for this purpose are prepared by adding a liquid to a solid sample that is previously ground, sieved, weighed and placed in a container ensuring stability of the slurry during the time required to withdraw an aliquot for manual or automatic transfer to the measuring instrument. The amount of sample to be weighed depends on the analyte concentration, the final volume of slurry, and the sample homogeneity.

   Slurry formation is widely regarded as a sampling mode [1], which is incorrect as the sample exists as such before it is suspended in the liquid. In fact, as stated in the previous paragraph, the sample is usually ground, sieved and weighed, so slurry formation is a sample preparation step rather than a sampling procedure. In any case, slurry formation is highly reliable for automating the insertion of solid samples into atomic detectors.

Slurries can be inserted into an atomic spectrometer by hand, *via* an autosampler or through a flow injection manifold. When autosampler cups are used to weigh the solid sample, the maximum volume of slurry that can be inserted is limited to the cup volume (about 2 ml), which in turn dictates the maximum amount of material that can be suspended. Once the solid sample and the liquid are brought into contact, the solid must distribute evenly in the volume of liquid.

Slurry formation for sample preparation gained widespread acceptance over the 1990s as a means for dealing with various types of samples with practical advantages over alternative procedures including the ability to use conventional liquid autosamplers, process several replicates in a single aliquot, handle increased amounts of sample and alter the slurry concentration. Additional assets include improved analytical performance as a result of the combined benefits of solid and liquid sampling and the ability to use liquid standards for direct calibration or standard-addition calibration. At present, isotopic dilution constitutes another effective calibration alternative with mass detectors. This choice dispenses with the need for effective extraction into the liquid phase and equilibration in spiked solid samples or sample slurries, except in the vapour phase of vaporization cells [2]. On the other hand, the large number of variables to be considered — which are often interrelated — complicate optimization of analytical processes involving slurry formation and usually require the use of chemometric approaches [3–6]. One especially critical variable is slurry stability, which can be improved by using stabilizing agents and an appropriate device to maintain particles in suspension.

Low frequency, high energy, power ultrasound in the kHz range is typically used to assist slurry formation, so the mechanical and chemical effects of cavitation are significant. However, the overall effect of US is widely regarded as mere agitation [7] or, at most, as "dispersion" (the effect observed by Fuyi and Zuncheng by using a non-specified US device for 60 min [8]). In fact, the overall phenomenon is more complex and its nature depends mainly on the type of US device used, the time during which US is applied, the type of liquid phase involved, and the nature of the matrix and analyte(s).

5.2.1. Types of devices for ultrasound-assisted slurry formation

Most US-assisted slurry formation procedures use an ultrasonic cleaning bath and ordinary analytical glassware (*e.g.* a beaker vessel). Although energy in US baths is known to be uneven [9], the influence of the position on cavitational effect has never been studied or special recommendations in this respect to obtain better reproducibility have been made. Placing the vessel containing the solid–liquid system at random in the US bath or simultaneously processing up to 20 samples [10] can influence reproducibility to a variable extent dependent on the time US energy is applied to the system.

The use of a US probe [11,12] or the sequential use of a US bath and a probe to assist slurry formation [11] is much less frequent. Treated slurries can be transferred to an autosampler or atomizer in various ways ranging from manual pipetting of aliquots to automated dynamic procedures. Once an aliquot has been transferred to an autosampler cup, it can be homogenized by manual shaking, vortexing, with a microprobe, an inert gas stream, etc.

The earliest use of a small ultrasonic probe to prepare slurries from coal fly ash directly in the autosampler cups was reported by van Loenen and Weers [13]. They found ultrasonic stirring not to ensure slurry homogeneity during the time required for the autosampler to withdraw each sample aliquot unless the analyte was completely leached.

A subsequent design by Carnrick *et al*. [14] was marketed by Perkin-Elmer under the trade name of USS-100 (from Ultrasonic Slurry Sampler). This sampler, out of the market at present, consisted of an ultrasonic probe, a power supply and control unit for the probe, a mounting system for direct attachment to Perkin-Elmer AS-60 or AS-70 furnace autosamplers and the connecting cabling and parts required for installation. The power and homogenization time used by the USS-100 were controlled by the same AA instrument software used for conventional operation of the autosampler, which also afforded automatic standard preparation and automatic matrix modification. During use, the USS-100 probe and autosampler capillary are rinsed, and the latter is moved to a standby position. The probe is then inserted into the appropriate sample cup, where the sample is ultrasonicated for the user-specified time (typically 10–15 s). After mixing, the probe is rapidly removed from the cup, the autosampler capillary withdrawing an aliquot of the slurry from the cup for transfer to the furnace. The greatest shortcomings of the USS-100 were its high purchasing costs, its low homogenization efficiency — up to a maximum volume of 2 ml — and its incompatibility with HF as the probe was made of a Ti alloy.

Hoenig and Cilissen reported a laboratory made automated device for attachment to any Varian SpectraAA system furnished with a graphite furnace and a programmable sampler dispenser [15].

5.2.2. Variables influencing ultrasound-assisted slurry formation

Slurry formation is strongly affected by diverse physical and chemical variables including particle size, slurry concentration and the factors governing slurry stability.

Particle size

The particle size of the solid material used to prepare slurries can influence their stability, deposition and atomization efficiency, which in turn can affect accuracy and precision. Various types of solid-grinding devices including mixer mills, other ball mills, and bottle and bead mills have been used to prepare slurries. The appropriate particle size varies among materials depending on various parameters such as the homogeneity of the original material with respect to the analyte, the amount of sample used for analysis and the particular liquid phase employed. Particle size can also influence the slurry homogeneity through the rate of particle sedimentation and the amount of analyte transferred to the liquid phase. The presence of large particles in a slurry can pose problems arising from discrimination of the larger particles by the autosampler and irreproducible injection of the sample into the atomizer. In addition, large particles vaporize slowly and can result in incomplete atomization of the analytes, and sedimentation is also less marked in low-density particles.

Notwithstanding the decisive importance of particle size in the materials used to prepare slurries, specific information about particle size distribution is rarely reported in connection with slurry formation. Also, when particle size is reported, the sample has usually been ground to pass through a given mesh dimension and only the maximum particle size of the material is stated. Wibetoe *et al*. [12] studied the potential of using a Coulter particle analyser with a view to developing a method for measuring the effect of grinding solid materials for slurry formation. Such a method would allow particle size distributions to be plotted and (or) quantified in various ways including number-size and volume-size plots, size being expressed as a volume, surface area or — most often — diameter. Plotting volumes of particles against size is advantageous as detailed information about the larger particles is lost
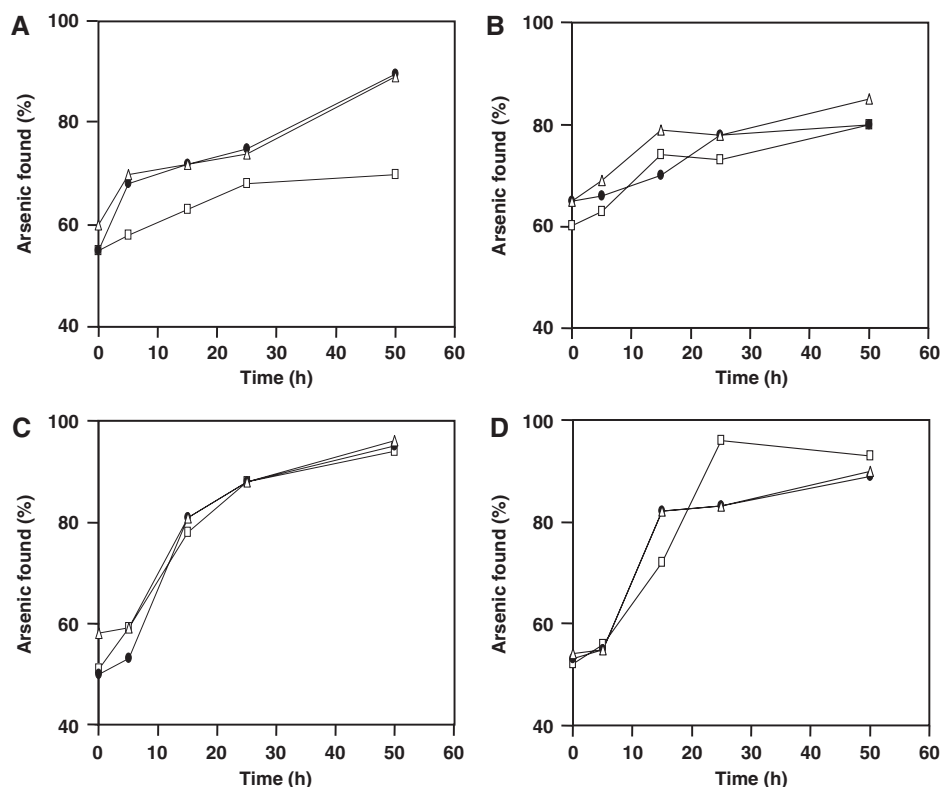
FIGURE 5.1. *Effect of particle size and the slurry standing time on the recovery of As compared to the certified value. (□) 36 µm, (●) 50 µm and (△) 77 µm. (A) Slurry of marine sediment, (B) aqueous phase of the sediment slurry, (C) slurry from a coal, (D) aqueous phase of the coal slurry. All data points are the averages of four independent experiments. (Reproduced with permission of Elsevier, Ref. [16].)*

when the distribution is expressed in terms of number-percentage. Thus, grinding the plant material for as long as 60 min has been shown not to be necessary always as the precision and accuracy obtained after 5 min of grinding is more than adequate in many cases.

The effect of particle size cannot be generalized as it depends on the specific type of matrix and analyte, their interaction, the aggressiveness of the liquid phase, the liquid–solid contact time, the effectiveness of US action in modifying the particle size — which clearly depends on the US power, intensity and application time — and the slurry standing time, among others. Figure 5.1 illustrates the effect of some variables for slurries formed in *aqua regia*+HF after 30 min of sonication in an ultrasonic bath. The optimum standing time prior to hydride generation of As was found to be 48 h, with very little difference between using the slurry or the aqueous phase after application of such highly drastic conditions [16], which caused virtually complete leaching of the target analyte in the slurry preparation.

Not always does the lowest particle size provide the best results. The decreased detector response obtained from a particle size ≤ 36 μm relative to ≤ 50 and ≤ 77 μm was ascribed to the increased co-extraction of interferents with the analyte for sediments [16] or to the coagulation of particles in the case of plant material [17].

The fact that particle size does not influence slurry behaviour in many cases [2,18–20] has been ascribed to the volatility and mobility of the analytes (*e.g.* Cd, Se, Tl) facilitating passage into the liquid phase.

Slurry concentration

One other key factor in preparing a slurry is concentration. Samples with high analyte contents are easier to analyse with the slurry technique than by direct solid sampling as the slurry can be readily diluted. However, the slurry can only be diluted to a certain extent because precision degrades with a high dilution as a result of only a small number of particles remaining in the slurry. On the other hand, when the analyte content in the original sample is very low, the slurry concentration can be increased accordingly — the pipetting efficiency, however, can deteriorate with more concentrated slurries. One other factor to be considered is that increasing the slurry concentration can boost matrix effects. In food analyses, the RSD is typically less than 4% when using particles less than 50 μm in diameter — provided the slurry concentration is below 10% m/v. Accuracy deteriorates when the slurry concentration exceeds 5% as a result of matrix effects. In fact, slurry concentrations above 5% result in deposition of the slurry aliquot [21]. The errors associated with slurry formation have been characterized and found to arise from uncertainty in the sample volume and the number of particles it contains, as well as from variations in the mass of individual particles. These errors can be minimized by using small particles, concentrated slurries and narrow particle size distributions. Some authors have even proposed a minimum number of particles in the aliquots for insertion into atomizers, which should never be less than 50 [22].

Some authors [23] claim that using slurry nebulization is only advisable when no efficient alternative digestion procedure is available. The dilution factor in slurry nebulization is at least as high as in normal solution nebulization. The concentrations of dissolved solids in analytical solutions are even higher as the dispersing agents alone account for 0.5 to 1%. In addition, contamination from impurities in the grinding agents may result in analytical errors. Polyatomic ions formed from the components of the grinding agents or the dispersants can also cause interferences.

Slurry stability

The stability of slurries obtained with US assistance depends mainly on the ultrasound characteristics and the presence of stabilizing agents. The effect of the former is equivalent to magnetic stirring, vortexing, bubbling a gas — usually argon — or electric dispersion in metallic samples, etc.

Stabilizing agents

Preparing slurries in aqueous solutions is rarely effective because most powdered materials undergo rapid sedimentation. This occurs immediately after the solid and liquid

phases are brought into contact and can be quantified *via* Stokes' law. The sedimentation rate depends on the relative densities of the liquid and solid phases, the viscosity of the liquid medium and the radius of the sample particles. The slurry can be stabilized using a highly viscous liquid medium such as Viscalex, glycerol, a non-ionic surfactant, an organic solvent or a thixotropic thickening agent, among others. The stabilizing capacity of these agents depends largely on their concentration, as well as on the characteristics and particle size of the sample. By way of example, 10% glycerol was found to ensure optimum homogenization of slurry herbal medicine samples [17,24]. On the other hand, the maximum slurry concentration that can be used depends on the concentration of the stabilizing agent. The time interval between effective suspension of the slurry and removal of an aliquot for analysis can be extended by using a highly viscous medium similar in density to the sample particles. Problems have been noted regarding the use of viscous media to prepare slurries, such as the sample aliquot being inefficiently pipetted into the atomizer when a high concentration of stabilizing agent is used. Also, the sample can remain around the dosing hole, which can degrade precision with both micropipettes and autosamplers. The use of the latter additionally requires flushing the capillary between successive determinations. Also, it requires pyrolysis to remove excess stabilizing agent. Stabilizers are usually inefficient when the slurry contains particles of high density. Apart from stabilizing agents, the addition of wetting and antifoaming substances such as Triton X-100 can improve slurry dispersion and increase homogeneity, thereby resulting in better precision and more symmetric peaks for the target analyte [25]. Stabilizing agents are the preferred choice when the samples are to be inserted *via* an autosampler as the slurry can be allowed to stand in the sampling cups without further homogenization. Other reagents deemed stabilizers (*e.g.* H_2O_2) are in fact used to avoid carbonaceous residues in the atomizer.
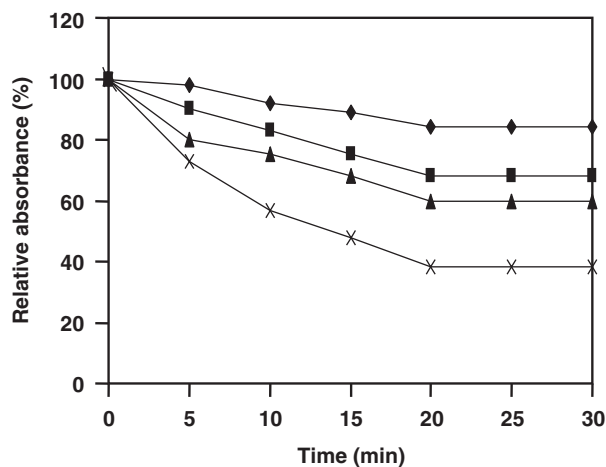
FIGURE 5.2. *Effect of various stabilizing conditions on the sedimentation time of lead slurries. (♦) 5% nitric acid + 0.1 % Triton X-100, (■) 0.5% nitric acid + 0.1 % Triton X-100, (▲) 5% nitric acid and (✕) 0.5% nitric acid. Each slurry was subjected to US radiation only before injection of the first aliquot. (Reproduced with permission of Elsevier, Ref. [26].)*

Figure 5.2 illustrates the effect of various stabilizers on the slurry sedimentation time after stopping US application in the determination of lead from lake sediments in particle sizes ≤ 2 mm [26]. The presence of nitric acid has the twofold effect of stabilizing slurries and increasing analyte leaching. The latter effect is a function of both the acid concentration and the nature of the target analyte [10].

5.2.3. Analytical applications of ultrasound-assisted slurries

The use of ultrasound-assisted slurry is a simple, efficient alternative to circumvent problems associated to digestion of samples with complex matrices derived from the required hazardous conditions, but also to leaching when efficiencies are not quantitative. Applications involving slurries prepared by ultrasonic assistance are continuously proposed with different detection systems, which demonstrate the versatility of slurries for metallic elements determination.

Ultrasound-assisted slurry formation followed by cold-vapour or hydride generation

Ultrasonic slurry formation has been frequently used prior to cold-vapour and hydride generation. Both procedures usually involve a drastic treatment of the slurry to ensure complete transfer of the target species to the liquid phase for subsequent formation of the gas phase — after a normally long standing time — which is the only phase reaching the atomizer in the case of hydride generation and the detection point in the case of mercury vapour formation. The gaseous analytes or their hydrides are most often obtained in a commercial or laboratory-made dynamic flow injection manifold.

Thus, the treatment of soils and sediments usually requires exhaustive conditions, which are characteristic of partial or total digestion processes according to the final aspect of the treated sample. Antunes et al. [27] treated sediments with aqua regia, HF and HCl in an US-bath prior to insertion of the slurry into a flow injection system for the determination of Cd, Hg, Pb and Se. Following 30 min pretreatment at 90°C in a US bath, a standing time of 12 h was required to vaporize the analytes (either by hydride generation or cold vapour formation) in the on-line system for their subsequent ICP-MS detection. After such a drastic pretreatment, the appearance of the slurry remaining after vapour generation was similar to that of the initial slurry, so dissolution of solid particles was incomplete. The standing time can be shortened by using isotopic dilution for calibration. On the other hand, lengthy US-assisted treatment of slurries was found to be required to determine hydride-forming elements in reference sediment materials [28]. The slurry treatment involved sonication for 30 min in a US bath, standing for 24 h under occasional shaking, another 30 min in the US bath and heating of the slurry in a water bath at 90°C for 15 min. These treatments are actually partial digestion or leaching treatments as the slurry itself never reached the detector; also, they could be expedited substantially by using one of the continuous or discrete approaches described in Chapters 3 and 4 [29].

One other case is the method for the determination of As in sediments and coal, where the powder obtained by grinding the samples to a particle size ″50 μm was mixed with *aqua regia* and hydrofluoric acid in an ultrasonic bath for 30 min. Following dilution with hydrochloric acid, the slurry was allowed to stand for 48 h, after which an aliquot was used for hydride generation [16]. According to its proponents, this "simple" treatment dispenses with sample digestion. However, it is dubious that the action of US under the drastic conditions provided by *aqua regia*+HF only produced a mixture of the ingredients

and not a real digestion; nevertheless, the authors tailed to comment on the state of the slurry (*viz.* whether it contained a solid phase) after treatment.

No standing time, but manual stirring for 30 s in a batch system was required after sonication in a US bath to form slurries from milk powder samples using 8% (v/v) *aqua regia,* 2% (v/v) antifoam and 1% (m/v) hydroxylamine hydrochloride for the subsequent determination of mercury [30]. Following sonication the slurry was treated with KBr and KBrO$_3$ in a hydrochloric acid medium to digest organic mercury, the treated sample being inserted into a multicommutated system to drive the resulting gas phase to an atomic fluorescence detector. After these steps, the target analyte should be in solution, so the process can be called "leaching". In any case the concentration of mercury in the liquid phase was not compared with that obtained by direct vaporization of the target analyte from the slurry.

One other example dealing with samples different from sediments and soils was that proposed by dos Santos *et al.* [31]. Five different slurry preparation procedures were tested for the determination of mercury by axial view ICP-OES using on-line cold vapour generation in biological and environmental certified reference materials. In all cases, samples were first grinded to a particle size ≤53 μm. The procedures were as follows: (1) using *aqua regia*+HF with 30 min sonication, standing time for 24 h followed by another 30 min of sonication and dilution with water up to 10% *aqua regia* (v/v) and 2% (v/v) HF; (2) same as the previous one, except that the standing time and the second ultrasonic treatment were omitted and dilution with water was performed after first sonication step; (3) same as the previous one, except that HF was not used; (4) same as the previous one, except that the *aqua regia* was replaced by nitric acid; (5) same as the previous one, except that the acid nitric was replaced by tetramethylammonium hydroxide. The results provided by the first three procedures were in agreement with the certified values. However, procedure (3) was recommended by authors because of the shortest process time and no use of HF. In contrast, the conditions used in procedures (1) and (2) were more characteristic of digestion processes.

In other cases, the drastic conditions provided by the reagents and US action have been held as simply a procedure for obtaining a specific oxidation state of the analytes, which can hardly remain in the solid particles after the US assisted treatment. Such is the case with the determination of hydride-forming elements (As, Sb, Se and Sn) and Hg in geological reference materials by FI coupled to a hydride generation system prior to ICP-MS detection. Two procedures differing in the liquid medium (*viz.* concentrated hydrochloric acid or aqua regia plus hydrochloric acid) were used to sonicate the slurry at a frequency of 40 kHz in a US bath. According to Schwingel Ribeiro *et al*. [28] these harsh conditions only pursued to reduce the hydride forming analytes to their lower oxidation states. The acid concentration in the solution can also dramatically influence the signal obtained, as shown in Fig. 5.3 [10].

Probably, the very long time used in most cases could be significantly reduced by using a multivariate optimization approach focusing on interrelated variables. Figure 5.4 shows a surface response from a central composite design for [HCl]-ultrasound exposure for the determination of tin in coal acidified slurries [6].

Ultrasound-assisted slurry formation prior to its introduction into the atomizer

When the slurry itself is to be fed to the atomizer or vaporizer, the duration of the previous ultrasonication step is dictated by the nature of the sample matrix. Thus, samples for the determination of As, Pb, Se and Sn in sediments by electrothermal vaporization
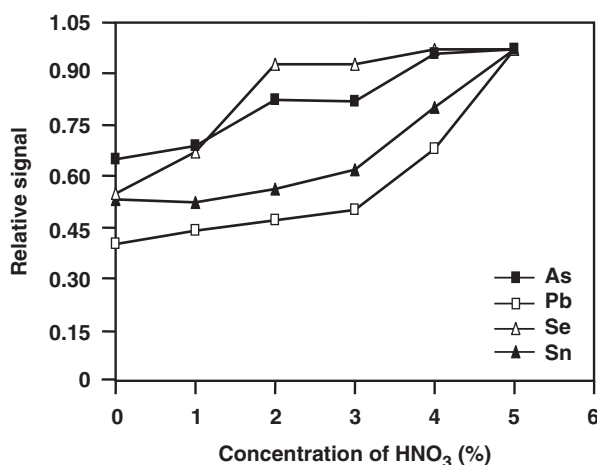
FIGURE 5.3. *Effect of the concentration of nitric acid on the peak intensities of several metals in sediment slurry using Ru as permanent modifier. (Reproduced with permission of Elsevier, Ref. [10].)*

inductively coupled plasma mass spectrometry were ground to a particle size ≤50 mm and suspended in 5% v/v nitric acid and 1% v/v hydrofluoric acid after sonication in a cleaning bath for 30 min. Following standing for 8 h, the slurry was shaken immediately before pouring into an autosampler cup [32].

Less drastic conditions — which were also bound to cause partial leaching, however — were used for other authors for US-assisted slurry treatment involving $NH_4NO_3 + H_2O_2 +$ Triton X-100 and sonication in a US bath for 10 min, after which suspended particles were vortexed to withdraw aliquots for analysis [25].

Matrices such as seafood, compost, medicinal herbs or fine ambient aerosols require shorter ultrasonication times (5–15 min) in US baths, less aggressive liquid solutions
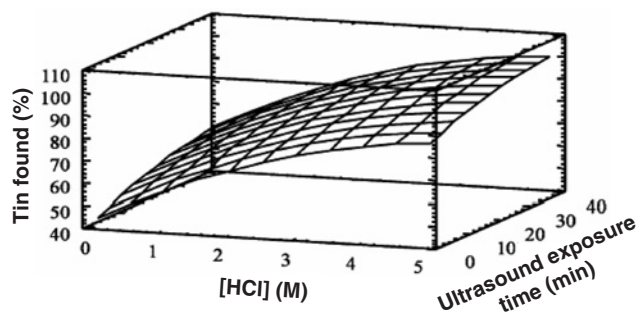
FIGURE 5.4. *Response surface estimated from the central composite design obtained for the pair [HCl]–US exposure time in the determination of tin in coal acidified slurries. (Reproduced with permission of Elsevier, Ref. [6].)*

and no standing time [10,17,33,34]. The resulting slurries are usually transferred to a USS-100 for determination.

Filtration — which can be done in a continuous manner in a dynamic system — after a drastic slurry treatment would avoid the need to insert the slurry into the detector as the target analytes would be in solution. This US-assisted leaching procedure is frequently preferred to slurry insertion and involves centrifugation after leaching in batch methods [33].

Only homogenization — and slight leaching if any — occurs when ground samples are poured into the cups of a USS-100 system or a similar device. Usually, the suspension is sonicated with a US probe for 10–20 s [35,36]. The ensuing methods should be thoroughly checked before application to natural samples; also, they should not be applied to matrices or analytes other than those used in their development.

5.2.4. *Ultrasound-assisted slurry formation* versus *other sample preparation methods*

Ultrasound-assisted slurry formation has been compared mainly with microwave-assisted digestion of various matrices and analytes. A distinction should be made here between methods using a cleaning US bath and those employing a probe.

The 10-min treatment in a cleaning US bath proposed by Bermejo-Barrera *et al*. for seafood products provided results that departed from those obtained by acid microwave-assisted digestion in a domestic oven for Fe and Se, but were in agreement for 9 other metals [33]. On the other hand, sonication of a compost slurry in a US bath (5% v/v Triton X-100 + 1% v/v nitric acid) for 15 min, followed by transfer of an aliquot to an autosampler cup and sonication with a USS-100 probe for 10 s provided the same results for chromium as did wet microwave-assisted digestion with 3 ml concentrated HNO_3 + 1 ml H_2O_2 + 1 ml concentrated HF. The latter procedure involved three steps in a commercial Perkin-Elmer digestor, namely: 700 W for 6 min, 1000 W for 15 min and 15 min cooling and making to volume [34].

A more significant comparison, where US-assisted slurry formation was the clear winner, was made by Felipe-Sotelo *et al*. in the determination of cobalt in geological samples [37]. Direct slurry homogenization with aqueous solution of 0.5% nitric acid, 5–20 mg sample, for 10 s with the aid of a USS-100 microprobe sufficed to obtain similar results to those for microwave digested samples (*viz*. a four-step digestion programme involving 0.3 g sample, 3 ml of concentrated HNO_3 and 0.5 ml H_2O_2). Also, US-assisted leaching, microwave-assisted digestion under very drastic conditions, and US-assisted slurry formation were found to provide very similar results for As in seafood — particularly when the solid particles were allowed to settle in the last case [5].

Overall methods using either different or no sample preparation procedures and various detection techniques have also been compared. Thus, fine ambient aerosol was analysed for 11 elements by using US-assisted slurry formation for 15 min prior to AAS, as well as by X–ray fluorescence spectroscopy and laser ablation ICP-MS. Sample treatments were found to provide similar results. However, the detection techniques compared the number of target analyte elements to be determined, detection limits and purchase costs [10].

5.2.5. *Non-analytical ultrasound-assisted slurry formation*

Its unique combination of excellent physical and chemical properties make diamond one of the most technologically advanced materials available today. Most uses of diamond require depositing a highly adherent thin diamond film onto a non-diamond substrate.

In particular, diamond is attractive as a coating for alumina ceramic electronic package and wear-resistant components [38,39]. Diamond films are also desirable as hard, highly transparent protective coatings for optical components such as sapphire or quartz [40]. Generally, diamond coatings suffers from three major problems, namely low nucleation density, poor adhesion and large residual compressive stress. Among the solutions to these problems [41], US-assistance for preparing slurries for film deposition has proved to be an excellent tool for enhancing and controlling diamond particle density in coatings. The most effective slurries with a view to obtaining high diamond particle densities (DPD) are those consisting of small (<0.25 μm) and larger particles (>3 μm) of diamond, alumina or titanium, for example [42–46]. Whereas, US abrasion with a mono-dispersed diamond slurry results in DPD of *ca*. 10^8 particles/cm^2, treatment with poly-dispersed slurries provides DPD above 10^{10} particles/cm^2. The increased diamond nucleation has been ascribed to a "hampering" effect whereby the larger particles insert very small debris onto the treated surface, thus increasing the density of nuclei onto which diamond growth can take place during chemical vapour deposition. In this way, continuous diamond films of less than about 100 nm thickness can be grown after only 5 min deposition; by contrast, 2 h is required to obtain similar results with a mono-dispersed diamond slurry. Particle size also differed markedly; thus, it was 1–2 μm for mono-dispersed diamond after 2 h of deposition and *ca*. 300 nm for mixed slurries after about 40–50 min [46,47]. These, mainly mechanical, effects of US may be of interest to analytical chemists.

5.3. ULTRASOUND-ASSISTED AGGLOMERATION OR AGGREGATION

The removal of fine particles from gases and liquids is a subject of permanent industrial interest. By contrast, only solid–liquid systems are analytically or clinically relevant in this respect. Ultrasound power may help improve the efficiency and performance of analytical separation methods. The specific mechanisms by which separation processes can be ultrasonically enhanced vary with the nature of the medium to be treated.

In gas suspensions, where very fine particles have to be removed, US action involves agglomeration of particles in order to increase their size and, consequently, to improve the collection efficiency of conventional filters (*e.g.* electrostatic precipitators, cyclone separators). These filters, while effective for large particle separation, are inefficient for retaining particles smaller than 2.5 μm. Therefore, acoustic agglomeration provides a means for separating fine particles released from industrial, domestic or vehicle sources, which, analytically, constitutes an excellent method for sampling in environmental analysis.

In solid–liquid separations, particle agglomeration can also be used to prevent filter clogging and increase the separation efficiency; in general, however, the procedure is less efficient than with gases.

Ultrasonic standing waves (*viz*. waves that vary spatially in pressure amplitude in the direction of wave propagation), usually within the MHz region, of high pressure amplitude and high power have most often been used to effect agglomeration. A comparison of the effect of standing waves with that of propagating waves (*viz*. waves that do not vary spatially in pressure amplitude as the wave travels in a medium with negligible attenuation) revealed the former to perform better, particularly with biochemical systems [48].

The capabilities of ultrasonic radiation forces for manipulating suspended particles have been the subject of a broad spectrum of experimental research. The effectiveness of particle–liquid separation by ultrasonic radiation forces depends on the acoustic distribution in a standing-wave field. In a US standing wave, suspended particles of appropriate

density and compressibility collect near pressure nodal positions to form bands parallel to the transducer, out of the acoustic field, thus providing a way for agglomeration. The energy distribution in a US particle-separation device analysed from measurements of the energy-density distribution in the liquid carried out using a microscope-based imaging system were compared to laser interferometer measurements of the velocity–amplitude distribution on the transducer and reflector surfaces of the ultrasonic separator. The energy density was found to follow the same trend as the surface velocity, being higher near the resonator centre and approaching zero near the walls. These results suggest that the energy-density distribution in the liquid is a defined function of the dimensions, imposed boundary conditions and physical properties of the reflector and transducer, thus providing a practical basis for developing a mathematical model of cell aggregation and retention, and enabling the design of resonators with predetermined energy density distributions for specific particle, separation, and fractionation applications.

5.3.1. Basic mechanisms of ultrasound-assisted agglomeration

Solid–gas systems

Acoustic agglomeration is a process in which acoustic forces cause particles to interact and, eventually, to collide. The complex mechanisms behind this process involve orthokinetic and hydrodynamic interactions. The orthokinetic interaction is founded on the hypothesis that collisions are produced due to the different acoustic entrainments experienced by particles of different size and weight. In order to describe this mechanism, an agglomeration volume is defined around each particle as a volume where another particle can be captured [49]. However, this mechanism, which constitutes the basis for most existing interaction models, can explain neither the agglomeration of monodispersed aerosols nor the way in which the agglomeration volume is refilled once the initial particles are captured.

Hydrodynamic mechanisms are those which produce particle interactions through the surrounding fluid due to hydrodynamic forces and the asymmetry of the flow field around each particle. These mechanisms, which are not dependent on the relative differences in acoustic particle entrainments, can act from distances larger than the acoustic displacement and have to be considered as the main mechanism in the agglomeration of monodispersed aerosols, where particles are equally entrained. There are two main types of hydrodynamic mechanisms, namely mutual radiation pressure [50] and the acoustic wake effect [51,52]. The radiation pressure is a second-order effect which produces a force on a particle immersed in an acoustic field due to the transfer of momentum from the acoustic wave to the particle. This force moves the particles towards the pressure node or antinode planes of the applied standing wave, depending on the size and density of the particles. The mutual radial pressure can be computed from the primary wave as well as from other wave fields of nearby scatters. In fact, it gives rise to particle interactions as the result of forces produced on two adjacent particles by a non-linear combination of incident and scattered waves.

The acoustic wake effect is based on the asymmetry of the flow field around a moving particle at moderate Reynolds numbers (Oseen regime). If two closely spaced particles are oscillating, the leading particle will disturb the fluid and generate a wake behind itself. If the second particle is located close enough, in the first semi-cycle it will travel within the wake. The wake leads to a pressure reduction behind the leading particle so that the trailing particle moves with higher speed. The same effect occurs in the second semi-cycle, but the roles of the leading and trailing particles are exchanged.

As a consequence, particles on the acoustic axis converge during a number of cycles and eventually collide. Equations for the dynamics of particles under standing waves that include the mass, radius and velocity of the particles, the kinetic and dynamic velocities of the fluid and its velocity due to the acoustic wave have been derived [53].

The orthokinetic effect has been shown to occur mainly in solid–gas systems and to be irrelevant in liquid suspensions. The radiation pressure seems to be the most important effect in the latter case with a view to agglomerating particles or at least bringing them together.

Solid–liquid systems

A standing wave can induce three types of acoustic forces, namely:

(1) The axial component of the primary acoustic radiation forces, which is parallel to the *z*-direction of the coordinates and accelerates the particles towards the pressure nodal planes of the standing wave field.
(2) The lateral components of the primary acoustic radiation forces, which drive the particles within the pressure nodal planes towards areas of local maximum acoustic intensity.
(3) The so-called "secondary force", or Bjerknes force, which is generated as particles scatter the sound waves, and thus represents an additional source of sound. The secondary force can be repulsive or attractive, depending on the angle between the particle-connecting line and the sound wave direction. For an angle of 90° (*viz.* for particles arranged within the acoustic pressure nodal planes), the secondary force is an attracting, interparticle force, strongly dependent on the distance between the particles. The attracting characteristic of secondary forces results in the formation of associated within the acoustic pressure nodal planes.

The agglomeration of particles in an acoustic field is also explained as the result of two mechanisms, namely: first, the particles can move to the nodes or antinodes of a standing acoustic wave, where they can concentrate and aggregate [54]. Then, an acoustic pulse can make small particles in close proximity to each other move with different velocities and agglomerate. It has been shown [45] that 5–50-μm-sized metal particles suspended in a hydrocarbon liquid collide and fuse when irradiated with US. The particle size of activated sludge is in the same range; its size distribution is bimodal, comprising 25–100 μm flocs and 0.5–5 μm free colloids [56].

5.3.2. Variables influencing ultrasound-assisted agglomeration

Not all factors potentially influencing agglomeration have been identified; also, their effects differ depending on the organic, inorganic or biochemical nature of the particles to be aggregated and the particular dispersive medium. The most salient, best known variables influencing US-assisted agglomeration are discussed below.

Size of the initial particle

Acoustic agglomeration is seemingly much more efficient for large particles than for small ones, especially in solid–gas systems. In fact it is difficult to achieve a high agglomeration

rate in aerosols exhibiting a *quasi*-monodisperse particle size distribution. The boundary for this behaviour lies in the range 70–100 nm; however, the exact threshold depends on the presence of moisture in the dispersive medium [57].

Nature of the dispersive medium

The polarity of the dispersive medium greatly affects agglomeration, in a way that must be studied on a case-by-case basis. In a study on ultrasonic agglomeration of submicron particles in diesel exhaust, the presence of moisture was found to raise the agglomeration rate by decreasing the number of particles by up to 56% [57]. On the other hand, with inorganic particles (*e.g.* TiO_2 or ZnS suspensions), the presence of a polar medium such as water adversely affected the formation and stability of aggregates of fine particles. In fact, most particulate substances acquire a surface electric charge (electric double layer) upon contact with water and generate dispersive forces opposing acoustic agglomeration forces. Enomoto *et al*. obtained contradictory results in this respect; thus, they ascribed the increased agglomeration of Si-components in a sonicated medium to the formation of OH radicals that would attack OH groups in surface spheres. They supported this assertion on the results of an experiment involving diphenyl-picrylhydrazyl, a known scavenger for OH radicals that distorted the spheres formed [58].

Ultrasound frequency and intensity

Some contradictory effects have been reported concerning the influence of US frequency on various dispersion systems, initial particle sizes, and characteristics of the US device other than frequency; this has precluded the accurate elucidation of the effects of this variable on agglomeration. Thus, by using frequencies of 20, 1740 and 4000 kHz and intensities <25.4 W/cm^2 on spherical silica, Enomoto *et al*. found the sphere size to increase with increasing US intensity and 20 kHz sonication to induce agglomeration among spheres [58]. They assumed agglomeration to reduce the apparent surface area of the particles and hence to potentially increase the deposition thickness on the assumption that the amount of precipitated Si component would be the same. At high frequencies, agglomeration was scant, but the increase in sphere size was significant. The variation of the size of agglomeration as a function of the vibration amplitude (*viz*. ξ = vibration amplitude = $(2\pi f)^{-1} (2I/\rho c)^{1/2}$, where I is the ultrasonic intensity, f the frequency and ρc the acoustic impedance of the liquid) exposed a strong effect of this variable and its low values at frequencies in the MHz range (see Fig. 5.5). This result has more recently been supported by research on the sonochemical agglomeration of monodispersed nanoparticles under high-intensity US irradiation (at 20 kHz, 100 W/cm^2) without thermal post-treatment, as required for obtaining three-way catalytic converters [59].

Recently, new methods for controlling particle retention involving changing the intensity and frequency of US waves by effectively coupling acoustic-gravity fields have been developed on the basis of the Yoshioka–Kawashima theory [60]. The relationship between the acoustic radiation force on a particle in a standing wave, the wavelength of the radiation, the distance of the particle from the node and the particle radius was established with a view to controlling elution by using a coupled acoustic-gravity field and orthogonal laminar flow. Based on such relationship, Masudo and Okada used a dynamic system at a variable US frequency. The mobile phase flow was stopped for 10 min to allow
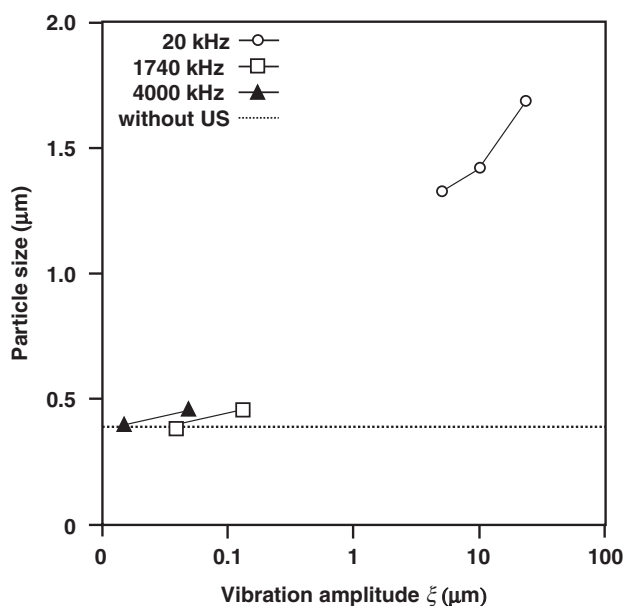
FIGURE 5.5. *Variation of particle size as a function of the US vibration amplitude at 20°C, using an irradiation time of 90 min. (Reproduced with permission of Elsevier, Ref. [58].)*

the particles inserted into the channel to migrate to their equilibrium positions, after which separation was started. If particles aggregated near the channel walls, they actually did not move because the local flow-rate is almost zero. By contrast, particles aggregating at the centre of the channel should flow down to the channel outlet at the maximum flow-rate. The operating frequencies used to change the nodal positions were 463, 500 and 774 kHz. Simple calculations showed that the node must form at the upper wall surface at 500 kHz and at the bottom wall surface at 774 kHz. A large peak appeared near the void peak at f = 463 kHz suggesting that particle aggregation occurred near the centre of the channel. No peaks were detected while the transducer was excited at 774 or 500 kHz, which strongly suggests that the particles accumulated in the vicinity of either wall. When the electric voltage supplied to the transducer was switched off, a large peak was detected at 500 kHz, but not at 774 kHz. Since the resonant frequency of the transducer was *ca*. 500 kHz, the US intensity at this frequency should be larger than that obtained at 774 kHz. It can thus be reasonably inferred that particles accumulated on the upper channel wall at f = 500 kHz and then settled down to the mobile phase stream when the US force is removed. On the other hand, particles accumulated on the bottom channel wall at f = 774 kHz, so they were not eluted even in the absence of US force. The distance of the aggregated particles from the bottom or upper channel can be altered by linearly changing the supplied electric voltage with time and keeping the US frequency constant. In this way,

particle retention is externally controllable and theoretically predictable [61]. This is the basis for filterless US-assisted filtration, which is discussed later.

Haake and Dual have developed models for calculating the transmitted wave as a function of the applied electric voltage and incident wave. They found application of an electrical impedance to the piezo-device to allow the reflection coefficient to be altered in amplitude and phase, and hence the characteristics of the reflected wave to be controlled [62].

Another method recently developed for manipulating small particles uses the forces created by a two- or three-dimensional sound field that is excited by a vibrating plate, the surfaces of which move sinusoidally and emit an acoustic wave into a layer of fluid. Such a wave is reflected by a rigid surface and generates a standing sound field in the fluid, the forces of which act on particles by displacing them in one, two or three dimensions. In this way, particles of sizes between one and several hundred microns can be simultaneously manipulated in a contactless manner. Equations describing this behaviour have been reported [63].

Large-scale streaming and thermal convection

Ultrasound can also have an adverse effect on disturbing the manipulation or aggregation of suspended particles. Large-scale streaming is one of the major undesirable phenomena that may occur during ultrasonic aggregation. The effect is known as "quartz-wind" or "Eckart streaming"; however, thermal convection also plays a prominent role here as a result of acoustic energy being absorbed by the bulk medium and heating caused by losses in the transducer and reflector. In experiments under microgravity conditions, thermal convection has been identified as the major limiting mechanism for 1.3 μm latex and 5 μm yeast particles banding in a 5.4 ml tubular chamber at 1 and 3 MHz [64]. In addition to these bulk types of streaming, small-scale Schlichting (scale $<< \lambda$) and Rayleigh (scale $\approx \lambda$) type streaming can also occur in a US field [65]. Their influence on suspended particle behaviour in US-standing waves has not been fully investigated so far. Streaming, in general, causes drag and stress on particles and particle clusters. Large-scale streaming, in particular, may drive particles out of the desired positions, prevent particle aggregation or even disrupt aggregates. The generation of large-scale streaming has been investigated theoretically and experimentally, mostly for travelling waves [65,66]. With standing wave fields, streaming can be ascribed to a travelling component in the real standing wave that appears from sound absorption and produces a net force on every single fluid element. This is the driving force for bulk fluid motion. Provided Stokes' law holds, which is a reasonable assumption at $Re < 1$ (*i.e.* for spherical particles < 50 μm with a maximum streaming velocity of 20 mm/s in water), the streaming drag force on a particle is proportional to its diameter, d; on the other hand, the radiation force is proportional to d^3 [67]. Therefore, the importance of the streaming phenomenon increases with decreasing particle diameter.

Conditioning the US suspensions effectively entails favouring the effects of radiation force and US-induced particle interactions while minimizing streaming. One common measure here is to cool the transducer and reflector by means of separate cooling water loops. Air-cooling the outer transducer and reflector surface may also be useful [68]. Streaming can additionally be controlled by exciting the transducer with tone bursts [69]. The appearance and speed of acoustically driven bulk streaming have been found to depend on the free pathlength for streaming: the shorter the pathlength, the slower the streaming. No large-scale streaming is detected at a certain threshold, however [70,71].

5.3.3. Applications of ultrasound-assisted agglomeration

Although analytical chemists have so far unexploited US for agglomeration purposes, many existing applications in the inorganic, organic and, especially, biochemical field can be extended to the analytical domain. The main advantages of US-agglomeration as a separation technique are that particles of diameter between one and a few hundred micron can be manipulated in a contactless manner and that a large number of particles can be manipulated simultaneously using the repetitive structure of the sound field. The selected examples described below illustrate the potential of this unexplored field for analytical chemists.

Inorganic applications

The synthesis of novel materials (particularly multicomponent materials) with unusual properties for uses as catalytic converters is gaining interest [72]. Thus, nanoporous structures of materials obtained by high-US agglomeration of monodispersed nanoparticles exhibit excellent properties and do not require the thermal post-treatment usually needed for the crystallization of amorphous materials or removal of surfactants [73].

Bentonite has been used to study the behaviour of US-fields [71], so its results can be used by analytical chemists for new inorganic applications.

Organic applications

Some by-products of coal combustion (*viz*. high carbon fly ashes) contain three forms of carbon (namely inertinite particles and isotropic and anisotropic coke) which are commonly agglomerated for use by the cement industry or for dumping in landfills. This, in fact, constitutes an environmental cleaning step. A comparative study of three processes (namely triboelectrostatic separation, US column agglomeration and column flotation) for proper agglomeration of these unburnt particles showed US to be an interesting energy source for this purpose, which was only slightly surpassed in efficiency by column flotation [74]. The US agglomeration of submicron particles in diesel exhaust has also proved to be highly efficient for environmental cleaning purposes, particularly in the presence of moisture [57].

Biochemical applications

This is the only analytical field where high-US agglomeration has been tested and its potential as an efficient separation method — which some authors deem "filtration" or "filterless US-assisted filtration mode" — exploited [75].

Thus, Bhaskar *et al*. developed a novel US-enhanced latex agglomeration test for the detection of serum antibodies against *Mycobacterium tuberculosis*. The use of US enabled the detection of low levels of antibodies in serum by increasing the sensitivity of the test. The rate of particle–particle collisions under an oscillator frequency of 100 kHz was raised to such an extent that the sensitivity for samples diluted up to 20 times exhibited agglutination, which was visible to the naked eye [76]. Figure 5.6 clearly shows the advantage in using US for this purpose.

The identification of proteins by MALDI–MS following in-gel digestion in a low-salt, non-volatile buffer of the proteins was simplified by collecting the resulting peptides in a small volume under sonication for 5 min; this facilitated automation of the overall process [77].
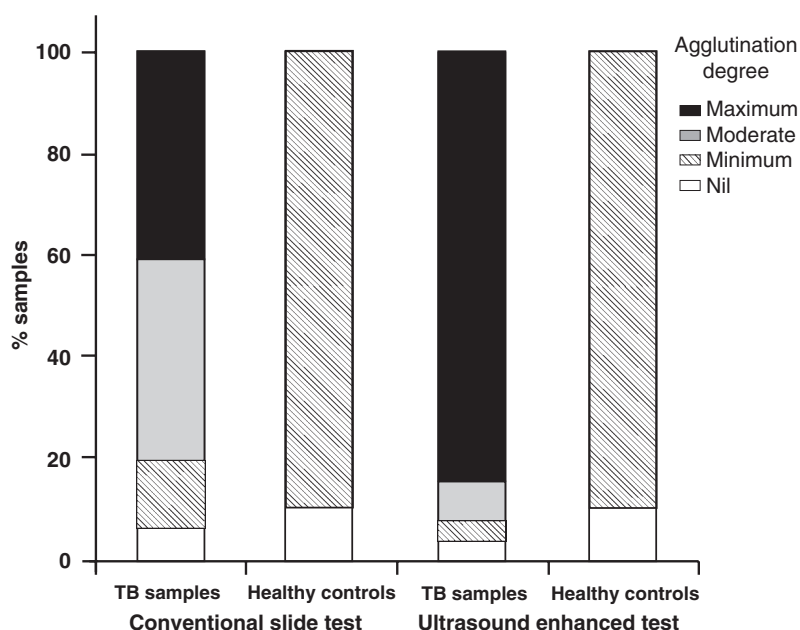
FIGURE 5.6. *Percentage of samples from* Mycobacterium tuberculosis *(TB) patients and healthy controls exhibiting different degrees of agglutination when tested using the conventional slide procedure or the US-enhanced latex agglutination test. (Reproduced with permission of Elsevier, Ref. [76].)*

Fractionation of different cell populations in a suspension can be accomplished by subjecting the suspension to a resonant US field and a laminar flow field propagating in orthogonal directions within a thin, rectangular chamber. The steady, laminar flow transports the cell suspension along the chamber, while the US field causes the suspended cells to migrate to the mid-plane of the chamber at rates related to their size and physical properties. A thin flow splitter positioned near the outlet divides the effluent cell suspension into two product streams, thereby allowing cells that respond faster to the US field to be separated from those that respond more slowly. Modelling the trajectories of individual cells through the chamber revealed that fractionation could be controlled by altering the strength of the flow relative to that of the acoustic field [78].

New US devices and gravity conditions have been assayed with a view to obtaining better separation of biological materials. Such is the case with an h-shaped ultrasonic resonator used to separate biological particulates under terrestrial gravity and microgravity conditions [79]. Based on the results, gravity can hinder the removal of cells from pressure-nodal planes provided the resonator is properly oriented relative to the gravitational field. The gravitational effects can be employed to overcome the lateral acoustic forces associated with cell trapping. The optimum separation frequency varies with the specific composition and particle size distribution in the cell suspension.

Also, acoustic forces cannot be increased arbitrarily without the risk of reducing cell viability, or causing cavitation in the suspension, which may decrease the overall separation efficiency and cause cell destruction.

Microfluidic channels have also been used under US irradiation for agglomeration–separation purposes. Thus, Nilsson *et al*. tested two microchannels of different width. The width of one microchannel, 750 μm, coincided with the wavelength of the applied US; this gave rise to a standing wave with two pressure nodes and three pressure anti-nodes [80]. Five-micron polyamide spheres inserted into the channel moved into the pressure nodes and remained there throughout the length of the channel because of the laminar flow properties. The end of the channel was split into three outlets and the particles were collected *via* the side outlets while the main part of the particle-free medium exited through the central outlet. The results showed that 90% of the particles to gather in 2/3 of the original fluid volume. The smaller channel, 350 μm wide, and a standing wave with only one pressure node were used with the aim of gathering particles in the central outlet while the main part of the medium exited through the side outlets. The smaller channel width allowed the use of the same high actuation frequency, even if operating at a half wavelength mode — which should produce a strong acoustic force on the particles. Another advantage is that two types of particles can be separated from each other provided their physical properties are appropriate in relation to the carrier fluid. This effect can be used in medicine to remove lipid particles from blood collected during open-heart surgery [81]. In fact, when erythrocytes and lipid particles suspended in blood plasma are exposed to a half standing wave field orthogonal to the direction of flow as they pass through the channel, the differences in compressibility and density of the two particle types cause them to move in a different direction, namely erythrocytes towards the centre of the channel and lipid particles towards the side walls. Splitting the channel into three outlets allows erythrocytes to be driven to the central outlet and lipid particles to the side outlets thanks to the laminar flow profile. More than 80% of lipid particles can thus be removed and approximately 70% of erythrocytes collected in one-third of the original fluid volume. Figure 5.7, which depicts the functioning of two of these filterless approaches, illustrates their foundation.

When a suspension of biological sludge is sequentially subjected to underwater sparks of 3 kV, 50 kA and US energy, it has been found to produce a synergistic effect. Thus, the sparks helped the suspension consolidate, decreased the charge density on the solids and increased their settling rate. The amount of cake solids increased, but only by one percentage point; however, high-speed video images showed that the spark generated a steam bubble, the dynamics of growth of which can be estimated via the Rayleigh model. The bubble collapsed into an acoustic field which then agglomerated the particles and resulted in faster settling [82].

5.4.   ULTRASOUND-ASSISTED FILTRATION

Filtration is the separation of a particulate phase (solid or liquid) and a continuous phase (liquid or gaseous) by using a porous medium. Most often, filtration involves solid–liquid systems and is intended to either provide a solid-free liquid or isolate a solid from its mother liquor.

Conventional filtration methods for separation generally use physical devices such as membranes, sieves or filtration beds and force-driven methods such as settling, flotation or centrifugation. Some involve the assistance of external (electric or magnetic) fields.
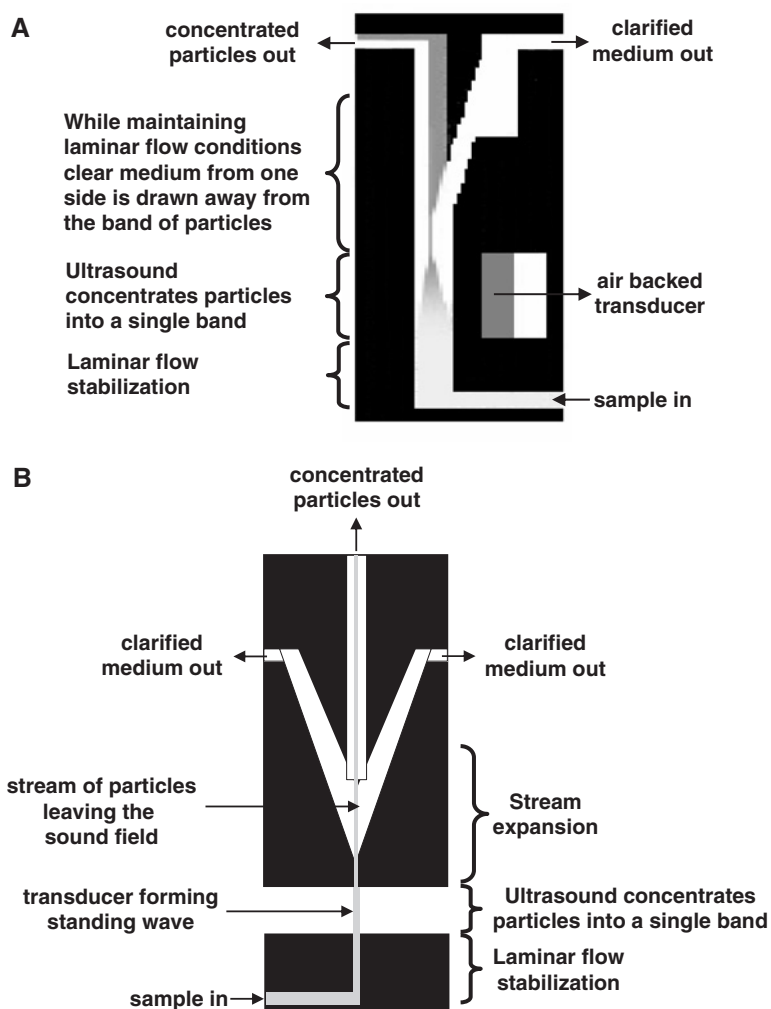
FIGURE 5.7. *Filterless filtration chamber. (A) Cross-sectional view showing the filter construction layers. (B) Development-phase filter. (Reproduced with permission of Elsevier, Ref. [82].)*

Ultrasonic filtration of particulate matter from a liquid has aroused some interest since the fact that the rate of flow through a filter can be increased substantially by US has been demonstrated. Acoustic fields thus possess a great potential for improving the efficiency of conventional separation process (see the previous section, which discusses the advantages of agglomeration). The use of acoustic energy to assist solid–liquid separation processes has been explored in different ways, mostly aimed at obtaining drying

effects. In fact, the authors pioneering the use of acoustic energy to remove moisture from a product employed air-borne US and assumed that the main effect was to increase the rate of evaporation [83]. However, they also claimed that the compressive and expansive effects of the acoustic waves inside the material might additionally result in water release from the product (a pumping effect). The usefulness as a separation tool of an acoustic field resonating within a porous mesh having a pore size much larger than the particle diameter was later demonstrated [84]. It has been widely checked that suspensions can flow through an acoustic chamber with no significant pressure drop — because of the large pore size of the mesh — and particles be trapped within the mesh, when an acoustic field is applied [83–85]; also, overall particle retention efficiencies as high as 90% have been obtained. In addition, laboratory experiments have exposed a number of interesting phenomena associated with the motion of particles through the filter mesh. These include the focusing of particles along specific trajectories within the mesh and the stable levitation of clusters of particles at positions that do not contact any part of the solid mesh despite the continued fluid flow. These phenomena are closely related to aggregation, but possess special connotations resulting from the proximity of the filter.

Acoustic and hydrodynamic effects can combine in various ways to cause particles to be retained within the filter mesh. In one, individual particles may simply collide and stick to an element of the mesh. It has been observed experimentally that, in some regions, particles can be focused along specific trajectories and that this results in the formation of dendritic structures attached to fixed points on the mesh. Also, interaction of the acoustic field with the porous medium may create points where particles are held in the fluid solely by acoustic forces, a phenomenon that has been observed in some experiments. Finally, particles may be trapped by agglomerating with other particles and form temporary flocs too large to pass through the interstices between pores. This last interpretation almost coincides with that of Mason *et. al.* [86], who believe that, following US-assisted agglomeration of particles (*i.e.* more rapid filtration), the US vibrational energy supplied to the system helps keep particles partly suspended, thereby leaving more free channels for solvent elution.

5.4.1. Mechanisms of ultrasound-assisted filtration

A number of models have been proposed to predict the motion of particles in response to the acoustic and flow forces present within the filter mesh and explain the effects of variables influencing the filtration process. Thus, Grossner *et al*. used the experimental chamber of Fig. 5.8 to develop a mathematical model to predict the motion of particles and explain the experimentally observed phenomena. The chamber was a Plexiglas structure supporting a piezoelectric transducer and a glass reflector. A US plane wave resonating at a frequency near 1 MHz was established in the enclosed volume, which also accommodated the porous mesh [87]. Because the geometry of the mesh is complex, the authors adopted the standard modelling practice of studying the region surrounding one element of the porous mesh and picturing the mesh as an assembly of cylinders. The model was intended to provide two-dimensional trajectories of particles in the vicinity of one mesh element, which was assumed to be an infinite circular cylinder. The axis of the cylinder fibre was normal both to the upstream flow direction and to the direction of the incident ultrasonic plane wave. The angle between the directions of the approach flow and the acoustic field, however, was arbitrary. The flow fluid was described in terms of (x, y) coordinates — with the approach flow always in the $+x$ direction when describing the hydrodynamic flow field — and the angle between the acoustic field
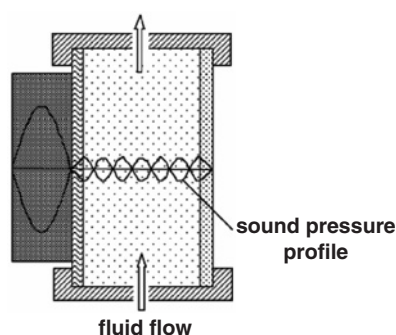
FIGURE 5.8. *Experimental chamber for the development of mathematical models for predicting the response of particles to US. (Reproduced with permission of Elsevier, Ref. [87].)*

and the hydrodynamic flow field. At each point in the fluid, a balance between acoustic and drag forces determined the direction and magnitude of the particle velocity. Because particles were small, the net force on them was assumed to be zero. Other major assumptions included creeping flow around the cylinder, no interparticle hydrodynamic or acoustic interaction and steady state particle velocities. Under these assumptions and conditions, the authors established mathematical equations which describe particle motion for the case of orthogonal approach flow and incident acoustic field [87]. Such equations allow particle motion to be computed at each point in space, and motions to be integrated with a view to predicting particle trajectories in the vicinity of the cylinder. A simple substitution method can be used to solve the set of differential equations needed to determine the trajectories. The stopping conditions include a particle imping-ing upon the fibre element, leaving the selected area of interest or levitating at a point in space.

The effectiveness of the filter element has been evaluated in terms of capture perform-ance. For a cross-sectional area normal to the bulk flow direction and upstream from the filter element, a "capture window" exists in this plane through which all particles that even-tually collide with the cylinder pass. The width of the capture window can be calculated from the cylinder radius and acoustic energy density, and used as an experimental measure of capture efficiency.

Recently, Grossner *et al*. used their previous findings to develop an overall transport model to predict macroscopic performance criteria such as breakthrough times and dynamics of filtration performance [88]. The model compared favourably with experi-mental studies on filtration phenomena by Gupta and Feke [89] (using the multi-layer resonance model of Rusinko [90]), and also with data from Grabenstetter [91].

5.4.2. Variables influencing ultrasound-assisted filtration

The most influential parameters on US-assisted filtration can be identified from experi-mental studies and the fitting of theoretical models to experimental results.

Ultrasound frequency and intensity

Because primary and secondary acoustic forces increase with increasing frequency, improved filter performance can be expected if a filtration chamber is operated at an increased harmonic frequency provided the power is kept constant and the acoustic wavelength remains larger than the particle size, so that primary acoustic forces prevail. However, experimental evidence suggests the opposite. The captured particles form a finer, crispier dendritic structure that is consistent with the finer spatial variation in the acoustic field expected at the higher frequencies. Thus, at the higher harmonic of two frequencies, the porous medium was found to saturate faster than at the lower frequency; however, the rate of particle capture in the initial filtration period was the same at both (1103 and 1852 MHz) [85]. The results can differ depending on particle-size distribution and feed rate. Thus, a higher frequency may be more efficient for removing smaller particles.

Tests conducted at three low frequencies (namely 28, 45 and 100 kHz) at a constant intensity of 2.5 W/cm^2 by using a polyacrylonitrile (PAN) ultrafiltration membrane and a 1 wt% dextran aqueous solution (Fig. 5.9A) showed that the highest frequency does not affect the permeate flux and that the effect increased with decreasing frequency [92]. The effect can be explained in terms of cavitation, which was especially marked at 28 kHz and insubstantial at 100 kHz. The effect of US on the permeate flux of the dextran solution exhibited an induction period that was the shortest at the lowest frequency. As can be seen in Fig. 5.9A, US had no effect on membrane permeability, as found by using the previous frequencies and pure water for filtration.

Figure 5.9B shows the influence of US intensity over the range 2.5 to 3.4 W/cm^2 as measured after 30 min of cross-flow filtration in order to surpass the longest induction period (28 min at 45 kHz). At 100 kHz, the permeate flow of the dextran solution did not change with the US intensity and was virtually identical with that observed in the absence of US. At 28 and 45 kHz, however, the US intensity clearly influenced the results.

Ultrasound power

A similar response to intensity changes was obtained by changing the applied US power at high US frequencies and variable powers for a heterogeneous system consisting of polystyrene particles in water. Filtration improved as the power was increased from 20 to 40 W, but not significantly from 40 to 50 W [85].

Ultrasound propagation direction

A simplified particle-trajectory analysis has been used to explain the essential features of US-assisted filtration. Acoustic forces can cause particle trajectories to deviate from hydrodynamic pathlines towards particle collectors, thereby enhancing their collection efficiency in comparison to pure hydrodynamic interception.

Figure 5.10A shows three of the possible directions for membrane irradiation with US for the previously discussed dextran aqueous solution and Fig. 5.10B shows the resulting permeate flow as compared with the absence of US. An orthogonal direction of the flow relative to the US radiation was found to provide the best results; on the other hand, a minimal effect was observed when the direction of US propagation opposed that of the permeate flow.
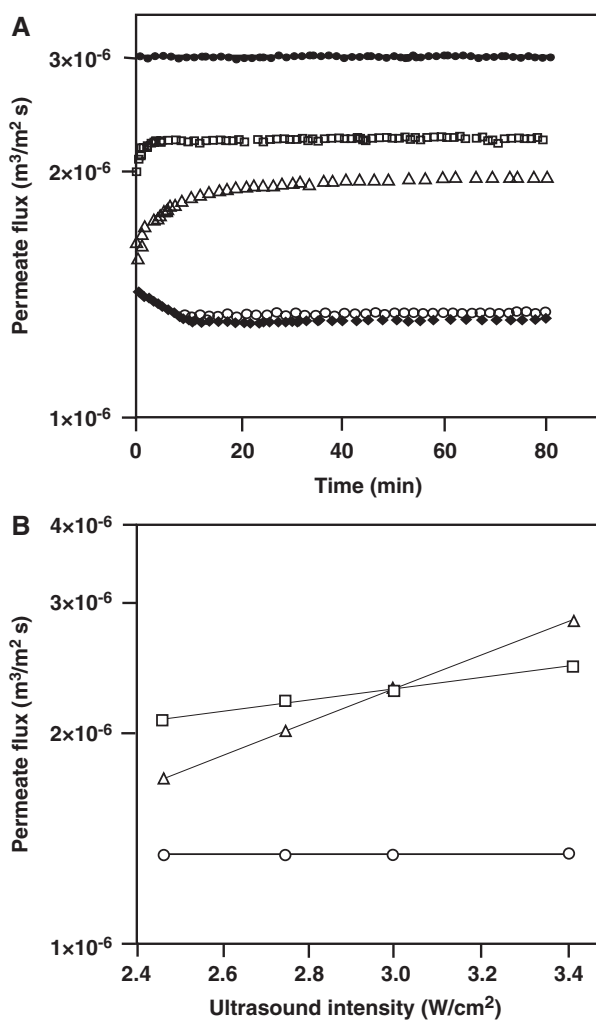
FIGURE 5.9. *Influence of US frequency (A) and intensity (B) on the permeate flux of a 1 wt% dextran aqueous solution at an operating pressure of 30 kPa and a feed flow-rate of 325 ml/min. (□) 28 kHz, (△) 45 kHz, (○) 100 kHz, (♦) without US and (●) for water irrespective of the frequency. (Reproduced with permission of Elsevier, Ref. [92].)*

Osmotic pressure

The effect of this variable depends strongly on the nature of the particles and their ability to rapidly form a gel layer [93]. In general, US effectively decreases the osmotic pressure of concentrated polymers; in practice, however, the phenomenon may be much more complex [94].
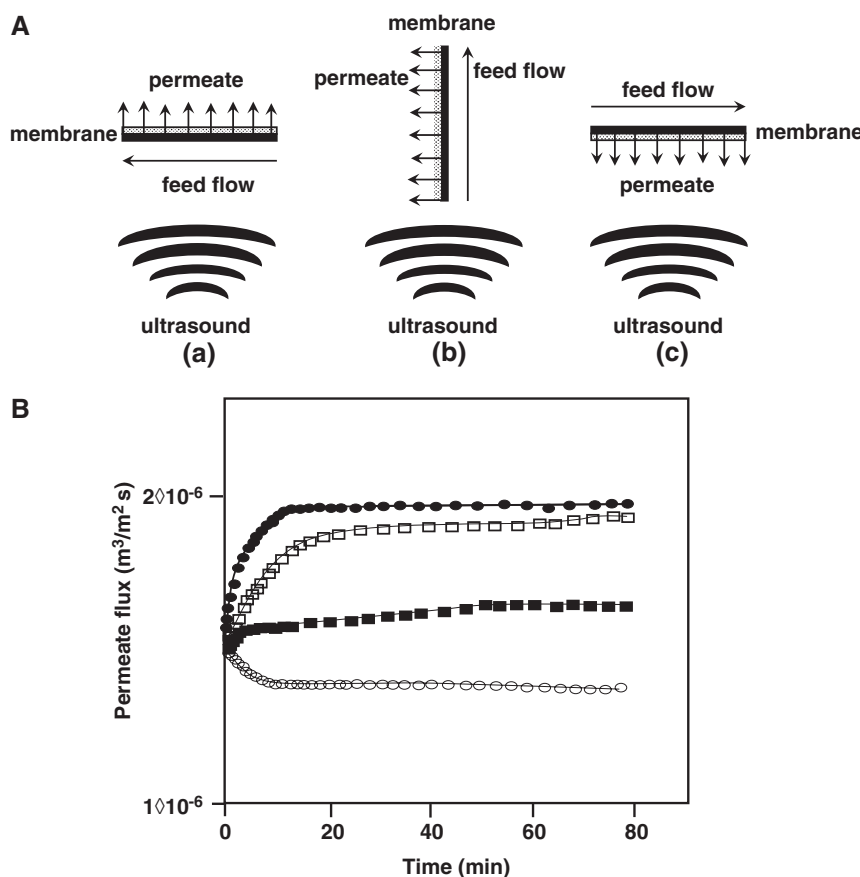
FIGURE 5.10. *(A) Experimental set-up of membrane and US wave. (B) Permeate flux change with the filtration time for (a-to-c) filtration. The working frequency for (a) (●), (b) (□) and (c) (■) was 45 kHz. (○) corresponds to an experiment in configuration (a) without US. The feed flow-rate of 1 wt% dextran solution was 325 ml/min. (Reproduced with permission of Elsevier, Ref. [92].)*

Feed flow and particle concentration

When the filter pore size is greater than the diameter of the particles, these pass through the porous barrier and the suspension flows through the chamber unimpeded by the barrier. When a high-frequency acoustic field of 20–40 W is energized, retention of particles within the porous barrier is apparent and their collection into dendritic or globular configurations is observed. A distinct trapping zone is observed if a suspension is continuously fed to the chamber; the front of this zone moves from the bottom of the chamber to the top and forms a saturated region within the porous barrier. If the acoustic field is deactivated, the organized collection of particles breaks down and the particles can immediately be flushed out with continued fluid flow.

Since the acoustic field is activated only after the suspension flow is established, the particle concentration in the effluent matches that of the feed concentration at the start of a given experiment. The effluent concentration drops down to one-fifth of the feed concentration within a given time depending on the concentration of the suspension. This suggests that substantial particle retention occurs within the porous medium. The cumulative retention efficiency can be 80–90%. Saturation is observed after a critical amount of solids has been collected within the porous medium. Abrupt changes in concentration are observed in the effluent stream for short bursts and, in the intervening periods, additional particle collection occurs within the porous barrier.

With an increase in the feed rate, the residence time of the suspension in the acoustic field is reduced, and the filtration efficiency correspondingly declines. In addition, the time to saturation diminishes with increased flow-rate, which suggests that filtration is limited to the space available for particle retention in the porous medium.

The saturation time is roughly inversely proportional to the feed concentration. Thus, for a suspension of polystyrene particles in water, the saturation time changes from 10 to 4 min when the concentration changes from 0.5 to 1.0 mass/mass% feed [85].

A comparison of the previous results with the cleaning effect of ultrasound irradiation at the frequencies in the kHz range, which decreases the fouling conditions of filtration and ultrafiltration membranes (see Section 2.6.1), clearly reveals that this effect does not apply to high-frequency US [95].

Nature of the membrane

The membrane material strongly influences the effect of US energy on filtration. Water permeation through a polyacrylonitrile (PAN) membrane from a dextran [96], that of NaCl through a nylon membrane coated with amphiphiles [97], the transport of organic compounds across a polymer membrane suspension, and that of hydrocortizone and benzoic acid through a cellulose membrane and poly-dimethylsiloxane membrane, respectively [98], illustrate the influence of the membrane material on the type of particles it can retain optimally.

5.4.3. Dewatering: a broad application field of ultrasound-assisted filtration

"Deliquoring" or "dewatering" are used to designate the removal of a liquid from a product without changing its phase. More specifically, deliquoring refers, as a kind of filtration process, to the reduction of moisture content of filter cakes by mechanical means.

Recent research on acoustic dewatering and drying testifies to the high potential of this approach; however, industrial applications are scant and analytical applications remain to be developed. It is therefore time to pay some attention to this energy when dewatering and drying — otherwise rather commonplace in the analytical laboratory –are required.

The main effects involved in the use of high-intensity US for deliquoring are (a) alternating acoustic stresses, (b) radiation pressure, (c) acoustic streaming, (d) interface instabilities and (e) cavitation.

Ultrasonic energy is useful to dewater fine-particle high-concentration suspensions such as slurries and sludges. In fact, US stresses produce a kind of sponge effect and facilitate the migration of moisture through natural channels or other channels created by wave propagation. Other US effects such as acoustic streaming, local heating, interface instabilities, agitation and cavitation may also be beneficial for solid–liquid separation.

The combined effect of vacuum filtration and sonication in the presence of surface active agents is very effective for dewatering fine particles such as those of coal. Under the optimal working conditions, a residual cake mixture was found to be substantially reduced from 21 to 10% and the filtration rate increased from 4.3×10^3 to 10.5×10^3 l/m^2/h [99]. Also, the synergistic effect of US and an electrical field produced a more open cake with a higher porosity and lower specific resistance for filtration of rutile suspensions. This was a consequence of the acoustic field significantly increasing the measured conductivity of electrolytic and rutile suspensions. Thus, US enhances the effect of an applied electric field close to the isoelectric point of the suspension by reducing the effective particle size and increasing electrophoretic velocities [100].

5.4.4. Filterless ultrasound-assisted filtration

As noted in Section 5.3.3, the ability of US to agglomerate particles enables efficient solid–liquid separation without a filter [75–81]. Thus, when ultrasonic standing waves of megahertz frequency and laminar flow are combined in a chamber such as those in Fig. 5.7, effective solid–liquid separation is accomplished in such a way that the chambers have been named "filter chambers" [101]. One pre-requisite for these filters is that the sedimenting particles should be brought together to form clumps that will be subject to opposing forces from gravity and the upward flow. This principle of operation becomes ineffective at low concentrations, where there is insufficient mass for sedimentation, and also for microscaling, where the shear forces between particles and the fluid are significant. The chamber in Fig. 5.7A is made of stainless steel and consists of a 115-mm long channel with a 4 mm long side channel exiting through a slot cut at an angle of 9° by wire erosion. Both channels have a cross-section of 10 mm × 0.25 mm. The chamber in Fig. 5.7B has similar dimensions and two Perspex side windows to view the suspension in the region of the flow division [102]. The *pseudo*-filters have a 0.25 mm (single half wavelength) acoustic pathlength. Standing wave radiation pressure on suspended particles drive them towards the centre of the acoustic pathlength, and the clarified suspending phase from the region closest to the filter wall is drawn away through the downstream outlet. Experimental tests with these chambers provided >1000-fold clearance of 5 μm yeast cells, at a sample flow-rate of 6 ml/min, from which the clarified aliquot was 1 ml/min. At such a flow-rate, the average residence time in the sound field was <1 s. Latex particles of 25, 9, 5.7, 2.8 and 1.5 μm diameter were also tested. These *pseudo*-filters operate at flow-rates and efficiencies similar to those provided by other methods based on centrifugation or membrane filters, with the advantages of very short residence times, continuous flow without blocking or refilling and no moving parts other than the flow chamber and the pump. In addition, these chambers can be interfaced to other microfluidic devices (*e.g.* dielectrophoretic particle analysers [103], flow injection analysers [104], micro-pumps [105], mixers [106], DNA chips [107], heat exchangers [108]).

Silicon microfluidic ultrasonic separators [109] and copper–epoxy laminate-based printed circuit boards [110] can also be used for microscale separation.

An early comparison of US and dielectrophoretic separations revealed the lower size limits of microparticles (0.65 μm for single particles and 14 nm for particle ensembles) manipulated by dielectrophoresis to be similar to those for ultrasonic fields (0.25 μm in intermediate volume suspensions to 40 nm in microchamber assemblies). Unlike US-assisted separations, dielectrophoretic separations require either very low volumes to avoid heating in salt-containing suspensions or desalination prior to separation in the field [111].

5.5.   SONOPHORESIS

Transdermal drug delivery constitutes a key advance in painless delivery of drugs to be frequently given to patients (*e.g.* those for insulin-dependent diabetes). However, transdermal drug delivery is limited to a short list of drugs owing to the low permeabiliy of many through the stratum corneum — the primary barrier of the skin. Various approaches including chemical enhancement [112], iontophoresis and electroporation [113], and sonophoresis [114], have been tested with a view to improving drug transport through the skin. Sonophoresis has received special attention on account of its characteristics and has so far provided very promising results. Recently, the use of "reverse sonophoresis" has opened up new avenues for sampling with monitoring and (or) diagnostic purposes [115].

5.5.1. Mechanism of ultrasound action in transdermal transport

Notwithstanding the large number of studies conducted towards its elucidation over the past 20 years, the mechanism of US action in transdermal transport remains poorly understood. As suggested by several research groups, one possible way by which US improves percutaneous transport is through interaction with structural lipids in the intercellular channels of the stratum corneum, similar to some chemical transdermal enhancers, which act by disordering lipids. Also, US is believed to increase transdermal permeability through the transfollicular and transepidermal routes; microscopic bubbles formed by cavitation at the surface of the skin under US vibration might generate a rapid liquid flow, thereby increasing skin permeability.

The role played by various US-related phenomena, including cavitation, thermal effects, generation of convective velocities and mechanical effects, has led some authors to hypothesize that transdermal transport during low-frequency US application occurs across keratinocytes rather than through hair follicles; therefore, cavitation will be the source of disorder of the stratum corneum lipids and result in significant water penetration into the disordered lipid region, which may lead to the formation of aqueous channels through which permeants can move. Studies aimed at elucidating the transport pathway enhanced by low-frequency sonophoresis, the relationship between solvent [tritiated water (^3H_2O)] and flux in µl and solute transport clearance across the hairless rat skin, have recently been reported. The basis for elucidation was the relationship between solute clearance and solvent (water) flux, which were monitored by confocal microscopy. Based on the results, the transdermal transport induced by convective solvent flow probably occurs *via* corneocytes and stratum corneum lipids; however, US also potentially pushes a vehicle such as water into the skin by asymmetric collapse of transient cavitation bubbles on the liquid–solid interface [116].

In heat-stripped stratum corneum exposed to US, convection plays a key role and the effective pore radius produced in the skin is much larger than that in full-thickness skin.

The definitive role that cavitation plays in the enhancing mechanism has been described and predicted by using suitable mathematical models, which have also been employed to evaluate three modes of bubble cavitation (namely shock-wave emission, microjet penetration and microjet impact) on the stratum corneum. Both microjets and spherical collapses were found to be potentially responsible for the enhancing effect [117].

5.5.2. Biological effects of ultrasound

Low-frequency US, such as that used in sonophoresis, has various effects (thermal, cavitational, acoustic streaming, dermal) on biological tissues.

Thermal effects

Absorption of US by a medium invariably increases its temperature. Those materials that possess high US absorption coefficients (*e.g.* bone) experience severe thermal effects compared with, for example, muscle tissue, which has a low absorption coefficient. The increase in temperature upon US exposure at a given frequency varies directly with the US intensity and exposure time. The absorption coefficient of a medium increases with increasing US frequency and so does the temperature as a result. In this context, the time threshold (TT) indicates the time after which a threshold temperature rise is exceeded and hence how long a piece of tissue can be safely exposed to US provided the safe TT is known.

Cavitational effects

Collapse of cavitation bubbles releases a shock wave that can cause structural alteration in the surrounding tissue. Tissues contain air pockets that are trapped in the fibrous structures and act as nuclei for cavitation upon US exposure. The cavitation effect varies inversely with US frequency and directly with US intensity.

Acoustic streaming effects

The shear stresses developed by streaming velocities may affect the neighbouring tissue structures. Acoustic streaming may be important when the medium has an acoustic impedance different from that of its surroundings, the fluid in the biological medium is free to move or continuous waves are applied.

Effect of ultrasound on skin

A study of the effect of US at variable frequencies and intensities (namely, 1 MHz, 2 W/cm^2; 48 kHz, 0.5 W/cm^2; and 20 kHz, 12.5–225 mW/cm^2) on animal skin revealed that no damage to the epidermis or underlying living tissues occurred provided the application parameters (*e.g.* application duration, frequency and intensity) were properly controlled.

5.5.3. Variables influencing sonophoresis

In vitro and *in vivo* studies on sonophoresis have allowed the variables to be optimized in developing sonophoretic experiments to be identified. Such variables pertain mainly to the irradiation source (namely, US frequency and intensity, application time and pulse length, and also the distance of the horn to the skin); others such as the nature of the permeant should also be considered, however.

Ultrasound frequency and intensity

Clinical applications use three different US regions, namely: high-frequency (3–20 MHz) or diagnostic US for clinical imaging; medium-frequency (0.7–3.0 MHz) or therapeutic US in physical therapy, and low-frequency (18–100 kHz) or power US for lithotripsy, cataract emulsification, liposuction, cancer therapy, dental descaling and US scalpels. The three regions have been assayed for enhancing transdermal drug delivery. While diagnostic US has insubstantial sonophoretic effects, therapeutic US under identical operating conditions is about 10 times more efficient, and power US enhancements are up to 1000 times higher than therapeutic US. In addition, low-frequency US reduces skin resistance by up to 50% and increases the permeability resistance to tritiated water by a factor of 4.5; this suggests that US causes some degree of structural alteration [116].

An intensity threshold exists for each individual system below which US has no effect on transdermal delivery. Thus, the transdermal delivery of insulin to hairless rats under 20 kHz-US for 60 min at three different intensities (2.5, 5.0 and 10 W/cm^2) with 0.1 s pulses each 6 min revealed the following: no significant change in the blood glucose level relative to the control was observed at 2.5 W/cm^2; only a slight change was found at 5 W/cm^2; and a significant reduction (*ca.* 40%) was observed at 10 W/cm^2 [118].

At a constant frequency of 41 kHz, increasing the US intensity stepwise over the range 60–300 mW/cm^2, increased transport in tritiated water by a factor of up to 140 in an intensity-dependent manner, normal transport levels being recovered on stopping US application. The water flux induced by 41 kHz US at 300 mW/cm^2 was 1465 ± 512 µl/h, which is roughly 100 times higher than that obtained by iontophoresis at 1.5 mA/cm^2 [116].

Skin conductivity enhancement and cavitation depend on the US intensity and frequency. The relationship between cavitation and intensity is complex (see Chapter 1). The skin conductivity enhancement is proportional to the US intensity up to 14 W/cm^2 at a frequency of 20 kHz and distance between the horn and the skin of 1 cm; however, the linear relationship does not hold good at higher intensities owing to the formation of a cavitation cloud near the US source that reduces the amount of energy delivered to the skin. The intensity providing the greatest skin conductivity enhancement depends on the particular US frequency.

The dependence of the enhancement on US intensity, pulse length and application time can be combined into a single parameter, namely the total density delivered by the transducer (E = intensity × application time × pulse duration). There is a threshold energy density for skin permeability to be affected, which is approximately 200 J/cm^2 at the applied frequency [119].

Ultrasound application time

Sonophoresis can be implemented in two different ways, namely: (a) by simultaneously applying the drug and US to the skin, and (b) with a US pre-treatment. The former is more effective than the latter as it enhances transdermal transport in two ways (namely, by enhancing diffusion through structural alterations of the skin, and by inducing convection). Sonophoretically induced transdermal transport enhancement decreases after US is switched off. Although this method can be used to achieve temporal control over skin permeability, it requires patients to use a wearable US device for drug delivery. The US pre-treatment enhances skin conductivity to a variable extent. The effect is illustrated in Fig. 5.11A, which was obtained at a frequency of 20 kHz, a distance of the horn to the skin of 1 cm, and an intensity of 7.44 W/cm^2, using pulses of 30 s each 1 min.
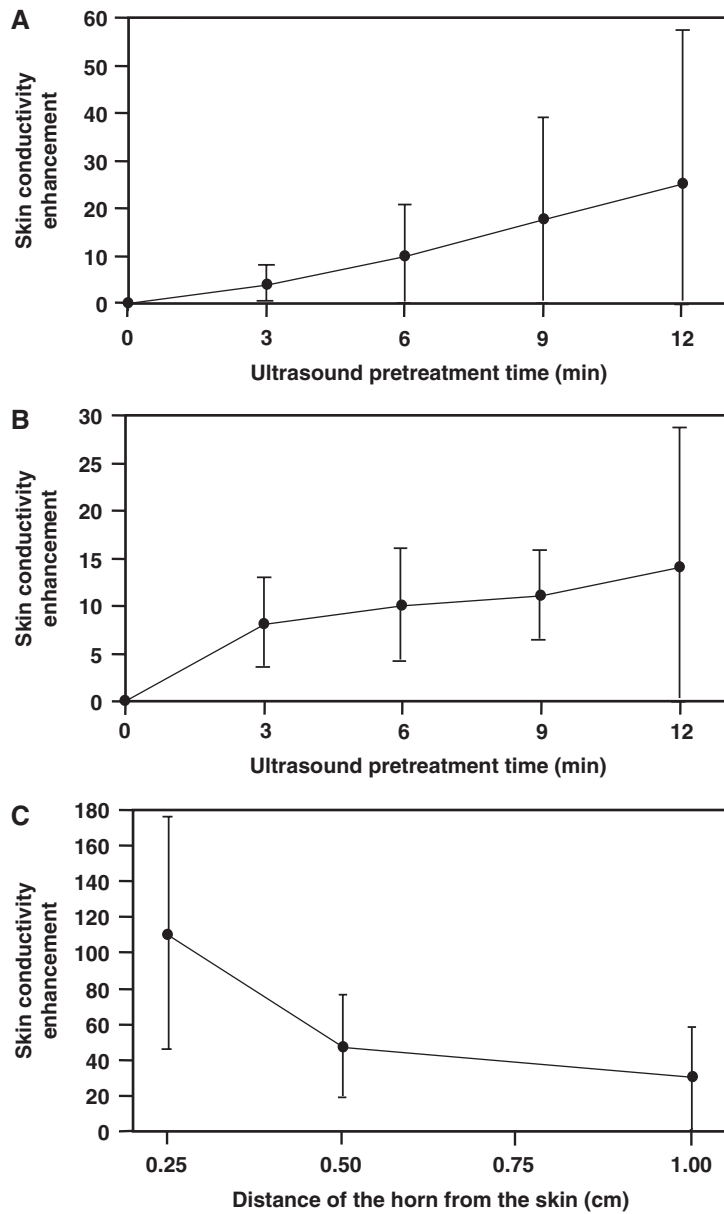
FIGURE 5.11. *(A) Variation of the skin conductivity enhancement with time during US exposure. (B) Variation of the ^{3}H-mannitol skin conductivity enhancement for 24 h with the US pre-treatment time (20 kHz, 7.44 W/cm^2 and 5 s pulses applied every 10 s). (C) Variation of the skin conductivity enhancement with the distance of the horn from the skin (application time, 12 min). Vertical bars indicate SD values for n = 3. (Reproduced with permission of Elsevier, Ref. [119].)*

Figure 5.11B, obtained under the same operating conditions, shows that the skin conductivity enhancement for mannitol as measured after 24 h of US pre-treatment was proportional to the pre-treatment time [119]. Also, increasing the overall US-application time and pulse length in the transdermal delivery of insulin to hairless rats enhanced transport of the drug and lowered the blood glucose level as a result [118].

Distance of the horn to the skin

Figure 5.11C illustrates the dependence of the skin conductivity enhancement on the distance of the horn from the skin at an application time of 12 min, a frequency of 20 kHz, and an intensity of 7.44 W/cm^2, using pulses 5 s out 10 s. As can be seen, skin conductivity increased with decreasing distance of the horn from the skin.

Contribution of thermal effects to ultrasound-enhanced transport

There is a proportional — albeit not purely linear — relationship between the amount of energy delivered by a US device and the increase in temperature of the vehicle in contact with the skin. At a 20 kHz US frequency, US intensities above 8 W/cm^2 significantly increases the temperature of the vehicle, *viz*. about 10–20°C for intensities from 8.1 to 15 W/cm^2 at the end of a 2-h treatment — interestingly, half of the temperature rise occurs within only 10 min of US application. Tests under isothermal control have revealed that about 25% of the skin permeability enhancement produced by sonophoresis can be ascribed solely to a thermal effect [120].

Physico–chemical characteristics of the permeants and barrier effects

Studies on the clearance (μl/h) of model hydrophilic solutes such as calcein (MW 623) and dextrans FD-4 (MW 4400) and FD-40 (MW 38000) in tritiated water across the skin under the influence of US have revealed a good flux correlation with ^3H_2O. Unexpectedly, the slopes obtained by linear regression of the plots were consistent for all solutes examined [116]. In other words, the permeability coefficients of the solutes were comparable with those of tritiated water and independent of molecular size up to 40 kDa under the effect of US. This can be ascribed to the above-described asymmetric collapse of transient cavitation bubbles at the liquid–solid interface, which can produce transport routes for hydrophilic solutes in the stratium corneum.

The lipophilicity of the permeant is one other factor influencing the US transdermal enhancement; its precise effect has not yet been clearly established, however.

Unlike iontophoresis, which acts on the transporting molecules and ions, US has been shown to act on the skin barrier itself. The effects of sonophoresis depend on the "quality" of the barrier that is subject to US treatment; thus, barriers which are intrinsically more permeable will be more liable to physical perturbation by US and *vice versa*. This may explain why the most successful attempts at the US-assisted extraction of glucose across the skin involved the use of a surfactant or chemical enhancer to better "normalize" the increased transport effects observed. One of the challenges in pretreatment-type sonophoresis is that the degree of skin permeability must be determined prior to drug placement.

When new US devices for sonophoresis are designed and constructed, their effects are checked on artificial membranes. The use of silicone membranes and over-saturated

lidocaine solutions to study the performance of a new device revealed that the structure of the sonicated membranes was irreversibly damaged [121].

5.5.4. Ultrasound devices for sonophoresis

One of the key issues for the success of sonophoresis technology remains the development of US devices that enable transdermal transport with a low cost, and small enough physical size and weight. Although low-frequency sonophoresis has been extensively studied over the past ten years, no commercial devices are available to date. The principal difficulty lies in developing a miniaturized low-frequency device that is powerful enough to create pathways within the skin. Two prototypes of low-frequency sonophoresis devices have been subjected to preliminary human pilot trials. One is a US skin-permeation apparatus (the SonoPre^R [122]), which was used in a Phase I clinical study on patients with diabetes [123] and for rapid cutaneous anesthesia [124]. The other (the EX1-4), which comprises a four-element transducer array containing a special cymbal transducer, was developed by Encapsulation Systems [125] and also used for transdermal insulin delivery. Various devices using horn- or disk-type transducers have been patented [122, 126–128].

A sonophoresis device with a flat flextensional US transducer has also been reported [121]. Vibration plates made of three different materials were simulated with the finite element method before fabrication and subsequent investigation of their properties. Compared to other types of flextensional US transducers, they have a simple structure, provide intensities at par with those of commercial sonicators and are easier and more inexpensive to produce.

5.5.5. Synergistic effects of ultrasound on transdermal transport

Ultrasound may enhance transdermal transport by inducing skin alteration and active transport (forced convention) in the skin. Various other means of transport enhancement, including chemicals, iontophoresis and electroporation, may enhance transport synergistically with US. Thus, the evaluation of the synergistic effect of low-frequency US with chemical enhancers and surfactants for permeation of mannitol revealed that application of US or sodium lauryl sulfate (SLS) alone, both for 90 min, increased skin permeability about 8 and 3 times, respectively. However, the combined use of US and a 1% SLS solution increased the skin permeability 200 times to mannitol [129].

Ultrasound also reduces the threshold voltage for electroporation and increases transdermal transport at a given electroporation voltage. The enhancement of transdermal transport induced by their combined use is greater than their combined individual enhancements [130]. Similar conclusions have been obtained by combining US and electric current. Because US reduces skin resistivity, a lower voltage is required to deliver a given current during iontophoresis compared to the controls. This results in lower power requirement and less skin irritation [131].

5.5.6. Future trends in sonophoresis

Sonophoresis is a very promising technique in a number of fields, the most salient of which are discussed below.

In recent years, the potential of using the skin for vaccination purposes has received a great deal of attention [132]. One of the more promising ways of enhancing skin permeability to enable transdermal transport of large molecules or complexes for transcutaneous immunization is sonophoresis.

Another potential future application of US as a topical enhancer lies in topical gene therapy [133,134]. Gene therapy is a technique for correcting defective genes that are responsible for disease development, most commonly by replacing an "abnormal" disease-causing gene with the "normal" gene. A carrier molecule (vector) is commonly used to deliver the therapeutic gene to the target cell. Topical delivery of the vector–gene complex can be used for target cells within the skin, as well as for systemic circulation. Additional applications may include the healing of cutaneous wounds such as severe burns and skin wounds of diabetic origin. Topical gene therapy requires the penetration of a large complex to or through the skin, which can be efficiently assisted by US to ensure adequate skin permeability.

The most salient analytical application of sonophoresis at present is for sampling through the skin. Studies on transdermal transport of glucose have been promoted by the growing interest in developing non-invasive technologies for monitoring blood sugar levels in diabetics. Because the enzymatic biotransformation of glucosylceramides by β-glucocerebrosidase produces an endogenous glucose "depot" within the skin and exogenous glucose can also be metabolized during its transdermal passage, an unequivocal interpretation of sonophoretically enhanced glucose transport is complicated [120,135].

One of the points requiring in-depth research as regards the medical uses of US is safety. The use of US as both a technical tool and a therapeutic agent in medicine has raised much concern about US bioeffects and safety. The World Federation for Ultrasound in Medicine and Biology has issued several publications on the safety of US bioeffects, specifically addressing thermal bioeffects [136] and non-thermal bioeffects [137] in an attempt at reaching an international consensus and adopting a common policy on safety guidelines. The use of ultrasound as an aid to increase skin permeability relies on its non-thermal bioeffects — mostly cavitation. In view of this, much attention should be paid to the issue of US affecting the structure of the skin. The reversibility or irreversibility of the changes experienced by the skin and the role of the free radicals generated during the cavitation process within the skin require further research with a view to establishing acceptable US parameter values for safe exposure.

5.6. ULTRASOUND-ASSISTED CRYSTALLIZATION (SONOCRYSTALLIZATION)

Crystallization is a process used in many industrial domains including chemical, pharmaceutical and pretrochemical industries. Research into the influence of US on crystallization processes conducted over the last 70 years has revealed that the nucleation of solid crystals from a number of liquids ranging from organic fluids to metals is affected by the presence of US waves. However, the precise mechanisms for US action on crystallization remain to be established. Nucleation processes — *viz.* production of microscopic crystals — are classified in Fig. 5.12. The so-called "primary nucleation" occurs when a crystal is nucleated in a solution containing no pre-existing crystals. On the other hand, nucleation induced in the bulk of a liquid in the absence of solid surfaces is called "homogeneous nucleation". If a solid interface — whether a container wall or a pre-existent crystal — is involved, the process is called "heterogeneous nucleation". Finally, nucleation induced by pre-existing crystals is called "secondary nucleation" and results
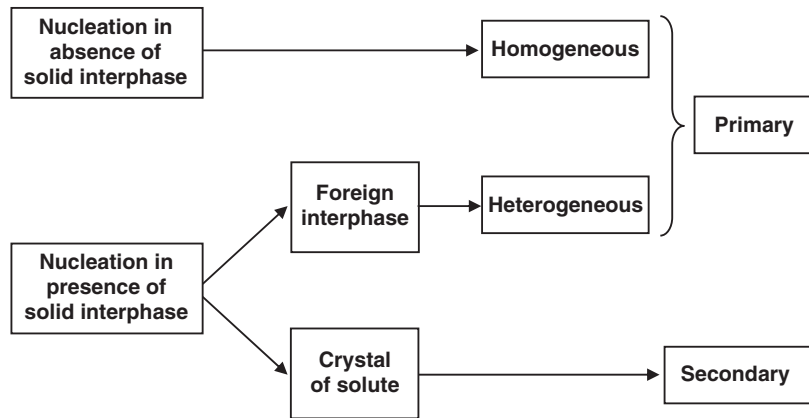
FIGURE 5.12. *Classification of nucleation processes.*

from the crystals either acting as templates for new crystal nuclei or fragmenting to pro-
duce more nucleation sites.

Crystallization in the presence of an ultrasonic wave (sonocrystallization) exhibits a
number of features specific to the US wave that clearly distinguishes it from crystallization
in its absence. For most materials, such features include, (a) faster primary nucleation,
which is fairly uniform thorough the sonicated volume; (b) relatively easy nucleation in
materials which are usually difficult to nucleate otherwise; (c) the initiation of secondary
nucleation; and (d) the production of smaller, purer crystals that are more uniform in size.

Ultrasound has been shown to significantly influence the reduction of agglomeration
under given conditions. Three US effects may contribute to this phenomenon. Thus, the
shock wave, which is caused by cavitation, can shorten contact between crystals to an
extent precluding their bonding together. Also, some agglomeration invariably occurs at
the nucleation stage. Nuclei possess a high surface area to volume ratio; this results in
a high surface tension, which the nuclei tend to lower by adhering to one another. The
surface tension decreases as crystals grow larger and become more stable, which hinder
agglomeration. Finally, the excellent mixing conditions created by US also reduce agglom-
eration through control of the local nucleus population. In fact, US decreases the nucle-
ation rate and probability of contact between nuclei, thereby significantly reducing
agglomeration.

5.6.1. Effects of ultrasound on crystallization

Both types of US effects (namely physical, which facilitate mixing–homogenization, and
chemical, resulting from radical formation through cavitation) influence crystallization by
altering the principal variables involved in this physical process (namely induction period,
supersaturation concentration and metastable zone width). These effects vary in strength
with the nature of the US source and its location; also, their influence is a function of the
particular medium to which this form of energy is applied.

Induction period and supersaturation conditions

This parameter (t_{ind}) is defined as the time elapsed between the creation of supersaturation and the appearance of crystals, and decreases as supersaturation increases. Mathematical equations for the induction time that hold for all nuclei forming and growing in a saturated solution have been reported [138]. The induction time is usually determined from conductivity measurements. Thus, the formation of crystals is signaled by a drop in the solution conductivity. The crystallization time is taken to be the time where the derivative of the conductivity with respect to time becomes negative.

The induction time is dramatically reduced by the presence of US; the effect, however, depends on the particular medium and working conditions. Thus, at an absolute supersaturation of 0.0156 g K_2SO_4/g water, the induction time in the absence and presence of US was found to be 9000 and 1000 s, respectively. Also, the conductivity decreased faster with US than without US. Because the conductivity was proportional to the potassium sulphate concentration, this difference suggests that more crystalline matter was formed in the presence of US [139].

The effect of US on t_{ind} is especially significant at low absolute supersaturations; thus, contradictory results have been obtained for highly supersaturated solutions [140]. Figure 5.13 illustrates the effects for the anti-solvent crystallization of roxithromycin in an acetone–water mixture [141]. As can be seen in Fig. 5.13A, the induction time decreased as supersaturation increased, whether or not US was applied. However, US significantly reduces the induction time, particularly at low supersaturations. Therefore, the effect of US on nucleation is stronger than that of high supersaturation levels [142].

Figure 5.13B shows the variation of $\ln(t_{ind})$ with $\ln(\sigma)$ (σ being relative supersolubility) in the presence and absence of US. The slope and intercept of the straight line obtained with US were 2.01 and 9.04, respectively, and those obtained in its absence were 1.95 and 7.59. The apparent nucleation orders were very similar and suggestive of a diffusion-controlled mechanism. The nucleation constant (k_N) was increased 4.25 times by US as a result of the significantly increased nucleation. Although the shortening of the induction time by US has been ascribed to a wall temperature effect, it results largely from the strong specific effect of US on nucleation [139].

Figure 5.13C shows the linear relationship between $\ln(t_{ind})$ and $\ln^{-2}(S)$ (S being the supersaturation ratio), consistent with the typical results for crystallization processes. As can be seen, the slopes are high; the supersaturation ratio is relatively high and the lines exhibit no inflection points. This suggests the prevalence of homogeneous nucleation. The temperature at which absolute supersaturation (calculated as the difference between the actual concentration and the saturation concentration) occurs is also influenced by US. In the previous experiment, the maximum cooling time in the absence of US, about 900 s, shortened to 450 s in the presence of US.

Metastable zone width

The metastable zone width can also be reduced by the application of US. The apparent order of nucleation or growth is decreased by US. Based on available evidence, the metastable zone width can be reduced simply by applying a low US power. Thus, US decreases the apparent order of the primary nucleation rate and increases the rate of appearance of the solid. Seemingly, US modifies the mechanism of nucleation itself as its presence strongly reduces the apparent order of nucleation.
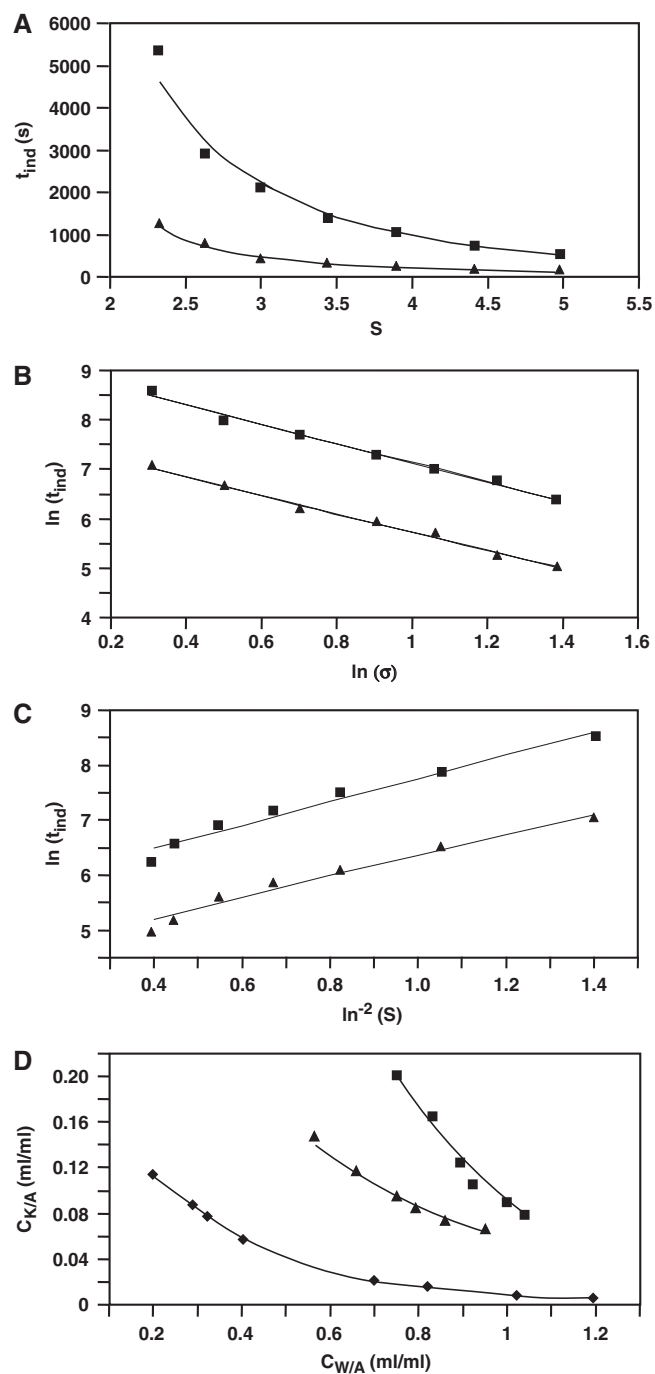
FIGURE 5.13. *Effects of US on crystallization parameters. (A) Influence of US on the induction period of roxithromycin. (B) Variation of the induction time as a function of the relative supersolubility. (C) Variation of the induction time as a function of the supersaturation ratio. (D) Effect of US on the metastable zone of roxithromycin. (▲) with US, (■) without US, (♦) solubility curve (Reproduced with permission of Elsevier, Ref. [141])*

The increase in the nucleation rate can be ascribed to the presence of shock waves in the solution. In fact, the waves can raise the probability of collision of a molecule and a molecular aggregate.

The fact that US decreases the supersaturation limit has been ascribed to its raising the nucleation temperature. Thus, during nucleation, the cooling rate remains roughly constant; under silent conditions, however, a temperature rise is observed. After nucleation, the cooling rate decreases as the US power is raised. Two opposing effects are involved, namely cooling is decelerated by the crystallization heat, but heat exchange is improved.

Ultrasound can induce nucleation under conditions where spontaneous primary nucleation cannot occur in its absence. Also, US can prevent seeding and hence foreign particles from reaching the solution.

Figure 5.13D shows the effect of US on the metastable zone of roxithromycin [141]. As can be seen, US significantly reduces the metastable zone width; therefore, a supersaturated solution is much more unstable under a US field.

5.6.2. Ultrasound-related variables and their effects on crystallization

The contradictory effects of US-related variables on crystallyzation occasionally reported can be ascribed to considerable differences in working conditions and the nature of the studied systems.

Effect of ultrasound frequency

The ultrasound typically used in common crystallization media (mainly aqueous media) falls in the low-frequency range.

Low-frequency US waves of variable frequency (namely, 15, 20, 25 and 30 kHz) used for sonocrystallization were found to result in no substantial differences in shape, mean size or size distribution in the resulting crystals. Therefore, these wavelengths seem to have the same influence on nucleation and crystal growth. One possible explanation is that they are much larger than the size of the nuclei and crystals.

High-frequency US has been used to assist crystallization around the glass transition temperature for metallic glass; dramatic effect has been found which has been ascribed to rapid crystallization caused by a stochastic resonance in which the jump frequency of atoms matches the frequency of the interatomic potential change by the US vibration [143].

Effect of ultrasound intensity, power and horn tip size

Increasing the *US intensity* and *diameter of the horn tip* increases the crystallization rate. Figure 5.14 illustrates the individual and combined effects of these variables in the crystallization of calcium carbonate at different US intensities and horn tip diameters of 3, 14 and 22 mm. As can be seen in Fig. 5.14A, increasing the US intensity decreased the Ca^{2+} concentration in the medium and increased the amount of crystallized matter formed. A similar effect was observed by increasing the diameter of the horn tip or the product of the US intensity and the square root of the horn tip area, which additionally increased the crystallization rate (see Figs. 5.14B and 5.14C). These two effects physically contribute to
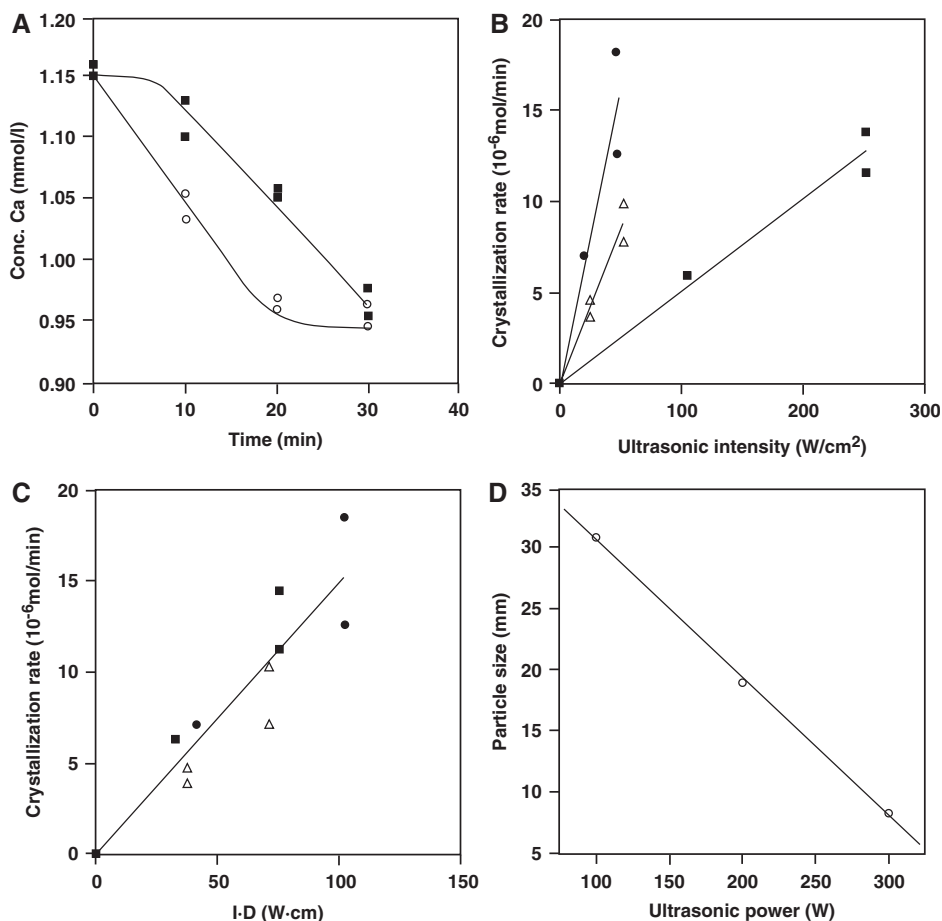
FIGURE 5.14. *(A) Influence of US intensity on calcium carbonate crystallization expressed as free [Ca²⁺]. US intensity: (■) 250 W/cm², (o) 105 W/cm² (horn tip diameter and immersion depth 3 mm and 3 cm, respectively). (B) Variation of the crystallization rate of calcium carbonate with the US intensity at variable horn tip diameters: (■) 3 mm, (△) 14 mm, (●) 22 mm (horn immersion depth 3 cm). (C) Variation of the crystallization rate of calcium carbonate with the product of the US intensity and square root of the horn tip area. Horn tip diameter and immersion depth as in B. (D) Variation of the particle size of hydroxyapatite as a function of the US power (Reproduced with permission of Elsevier, Refs. [142], [144].)*

the liquid flow patterns in the reaction vessel. An increase in US intensity is expected to result in heavier flow, while one in horn tip diameter should lead to more uniform flow patterns. From these patterns, it can be concluded that the effect of cavitation known as "microstreaming" contributes little to crystallization, and it is more markedly affected by macrostreaming [142].

As can be seen in Fig. 5.14D for crystallization of hydroxyapatite (HAp), increasing the *US power* decreases the particle size [144]. No HAp crystals formed above 300 W; below

this threshold, however, the particle size of the crystals formed increased with decreasing US power. Therefore, the particle size of the crystal can be controlled through the US power applied. With other inorganic and organic crystals, raising the US power produces shorter, thicker crystals; this can be ascribed to mass transfer in the mixture being effectively accelerated and the driving force of crystallization — the driving force excepted — increasing as a result. With large kinetic energies and speeds, the solute molecules will have an increased opportunity to collide with each other, penetrate the stagnant film and hence insert themselves into the crystal lattice more uniformly and easily. As the shape of the crystal depends on the growth rate at each face of the crystal, one may assume that the speed of insonated molecules is fast enough for them to approach each side of the crystal to compensate partly for differences in growth rate on each side in conventional crystallization, where diffusion control may occur. If so, one can expect a crystal insonated with a larger energy to be shorter and thicker [145]. In this way, sonocrystallization provides a method for obtaining small crystals similar to supercritical fluid micronization, but with lower equipment costs and the ability to operate under ambient conditions.

The effect of US power on formed crystals was studied at 0, 10 and 100 W by suspending potash alum crystals in a potash alum saturated solution for 3 h. Conductivity measurements showed that there was neither dissolution nor crystallization, but electron scanning microscopy revealed that the shape of the crystals changed due to erosion. Also, crystal size decreased with increasing US power. Size analysis confirmed the appearance of small particles upon application of US. The amount of smaller crystals formed was modest at a low power (10 W) but increased dramatically with increasing US power; an abrasion effect was therefore clearly involved [146].

Effect of horn immersion depth

With a US homogenizer, the flow pattern of the liquid depends on the distance from the horn tip. Since flow pattern (mixing) is the physical effect of US irradiation, any change in the flow pattern due to horn immersion may affect the crystallization rate. There is an optimal, specific horn immersion depth for each US device and irradiated medium which must be established experimentally on a case by case basis.

Effect of the volume of ultrasonicated solution

The mean crystal size is known to increase with increasing the volume of the insonated mixture. One explanation for this behaviour is that a fixed US wave in a larger container produces weaker penetrating and reflecting waves, so vibration and cavitation at some point in the liquid are lower. This results in fewer nuclei, and hence in larger crystals being formed. Also, increased liquid volumes provide larger free spaces for crystals to reduce collision and abrasion with each other.

Effect of ultrasound duration

Increasing the US irradiation time gives rise to the following sequence: at short times, the US wave fails to blend the solution and precipitant uniformly, so little precipitate is obtained after insonation; longer times produce apparent crystals, the size of which decreases under continuous sonication [147].

Effect of ultrasound on crystal characteristics

Whether US irradiation affects the characteristics of the crystals formed seemingly depends on the particular system. Thus, some authors have obtained similar crystals in the presence and absence of US [140,142], whereas others have reported substantial differences [148,149]. In the antisolvent crystallization of roxithromycin in an acetone–water mixture, the crystals exhibit a hexagonal and rhombus shape in the absence and presence of US, respectively [141]. This has been ascribed to an increased or decreased growth rate of some crystal faces under the influence of hot spots, which can alter the crystal lattice; on the other hand, abrasion may have some effect on the crystal habit.

Induction time models have shown that the principal mechanism behind US effect is heterogeneous primary nucleation. Based on various models for classical primary nucleation, US seems to decrease the activation energy and reduce the critical radius as a result.

5.6.3. Special ultrasound-assisted crystallization systems

Ice and oil are affected in a special manner by US as regards crystallization.

Sonocrystallization of ice

The phase diagram of ice is very unusual. Thus, its freezing point decreases as the ambient pressure increases to about 2 kbar. Eight different phases of ice have been observed, depending on the temperature and pressure conditions. Also, unlike most materials, water expands during freezing. While the melting temperature of ice is constant at a given pressure, the nucleation of water to form ice can occur within a temperature range called the "supercooling range", depending on some physico-chemical properties of the sample such as volume, purity and gas content. The supercooling range of water spans temperatures from 0 to — 40 °C (at ambient pressure); the addition of other molecules such as sucrose to water can be used to decrease the nucleation temperature under normal (control) conditions. Ice crystals grown in sucrose solutions also usually exhibit more dendritic ice structures.

The earliest work on the sonocrystallization of ice was published in 1964 [150]; primary nucleation of ice was found to occur at higher temperatures in the presence of a US wave — consistent with the expansion of water upon freezing. Since then, experimental research on the effects of US has focused on the primary nucleation temperature and the effect of a US field on the growth of an ice crystal or on the final crystal morphology has scarcely been studied. Although some attempts have been made to assess the degree of reproducibility of the experiments, the actual results have varied between authors. In any case, it appears that some link between the nucleation of ice crystals and that of cavitation can be expected because the general circumstances under which they occur are broadly similar. Even some probability that US-induced ice nucleation increases when the solution is supersaturated with air bubbles has been shown [151]. Studies of both primary and secondary nucleation of ice in sucrose solutions have shown that both can be achieved at higher nucleation temperatures in the presence of US. These nucleation temperatures can be reproduced with a lower standard deviation and a greater

precision than under the control conditions — without US. Increasing the US output level and pulse duration raises the nucleation temperature [152].

Sonocrystallization of oil

The key effect of cavitation on crystallization and the widely documented effect of this phenomenon on the production of free radicals have restricted the use of US with crystallization systems involving fats — and oil in particular. Fats are known to easily produce free radicals that lead to "off-flavours" when high power US devices are used [153]. For this reason, although the structure of the final product might be improved, the presence of "off-flavours" has prevented US from being a viable choice for the crystallization of edible fats. Studies on oils of variable oxidant stability (that is, with variable ability to produce free radicals under US action), such as palm and sunflower oils, under different US conditions (namely variable intensity, power and application time, both below and above the cavitational threshold), led to the following conclusions for palm oil: (1) below and far from the cavitational threshold, a sample subjected to US became viscous and the crystals it formed were of a more uniform size and heavier than in the control sample, the matrix surrounding the crystals appearing as if it had been filled with a network of hairs or needles. (2) Increasing the intensity — still below the cavitation threshold — led to a different product (namely crystals mainly at the base of the cell with some floating at the top of suspension in the liquid). (3) At an intensity even below, but very close to the threshold, the sample was very smooth and similar to face cream in consistency; also, the crystals were uniform and small, with no liquid present, thus suggesting the presence of many nucleation sites that produced crystals simultaneously. (4) The crystals formed at intensities above the threshold were similar to those obtained under silent conditions. (5) Far below the threshold intensity of US, the crystal structures of the control and ultrasonicated samples were very different, but there was little difference in crystallization time or temperature — this suggests that a threshold exists below which the crystallization kinetics is not altered. (6) There was a minimum time and a maximum temperature at which crystallization started when the US intensity was close to but below the cavitational threshold.

In short, for a given fat, once the range of crystal structures has been determined, it is possible to select a particular texture by choosing an appropriate US intensity. In this way, under a constant cooling regime, it is possible to vary the structure of the final product from a material looking similar to cottage cheese through to a fine cream simply by varying the US intensity below the threshold [154].

5.7. ULTRASOUND-ASSISTED NEBULIZATION

Ultrasound assisted aerosol formation or nebulization prior to sample insertion into an atomic detector is dealt with in Chapter 8 on the grounds of its close relationship to the instrument in spatial and temporal terms. Also, as a step of spray drying, known as "atomization ", is discussed in Chapter 2 inasmuch it can be used for sample conservation purposes and hence as an analytical operation preceding sample preparation. This section is concerned with other non-analytical uses of US-assisted aerosol formation that are closely related to the analytical field and can open new avenues for the development of previously unexplored analytical uses.

Ultrasound-assisted nebulization is largely used in the clinical field, where the word "aerosolization" or "aerosoling" is used preferentially over "nebulization", and industrial field, where "US-assisted nebulization" and "US-assisted spraying" are preferred.

5.7.1. Ultrasound-assisted aerosolization

Pulmonary administration of pharmaceutical compounds using aerosols is a common clinical practice due to its relatively easy use. It is generally accepted that aerosol particles of 1–5 µm in size are required for deposition in the alveolar region of the lung, which exhibits the highest systemic absorption; however, particles less than 1 µm in diameter are more easily incorporated into the "respirable percentage" of aerosolized droplets.

The particle size distribution of an aerosol can vary significantly by effect of temperature and concentration changes in the aerosolized droplets over time. The two most common types of commercial aerosolization devices, *viz.* air-jet and ultrasonic nebulizers, are known to result in an increase in concentration of dissolved drugs during aerosoling. Also, the latent heat of evaporation is known to lower the temperature of the nebulizing solution in an air-jet nebulizer. By contrast, the temperature rise in a drug solution in a US nebulizer increases the drug concentration.

Aerosol droplet size is influenced by physical variables such as surface tension, viscosity, saturated vapour pressure and temperature. A decrease in the first three decreases droplet size. Because a decrease in temperature increases all three variables, it also increases the difficulty of aerosol formation. Droplet diameter is related to the US frequency [155] and other physical parameters by the following equation:

$$D_g = \alpha \, (8\pi \, \sigma/\rho)^{1/3} \, f^{-2/3} \qquad\qquad (5.1)$$

where D_g is the droplet diameter, α is an experimental constant, σ and ρ are the surface and density of the liquid, and f the US frequency. As can easily be inferred from the equation, effective aerosol formation requires the use of high-frequency US.

The use of surfactants to modify the surface tension of an aerosol and alter its droplet size distribution has shown that their influence depends strongly on the characteristics of the solution to be aerosoled. The span, defined as 90% undersize — 10% undersize/50% undersize, gives a measure of the width of the volume distribution relative to the median diameter of the droplets formed in the aerosoling process. Comparative studies performed with commercial air-jet and US nebulizers have shown that, under similar working conditions, the latter provide less heterodispersed aerosols, with span values ranging from 1.50 to 1.75, which are similar for aqueous drug solutions in the presence and absence of surfactants [156].

One undesirable size-effect of aerosolization is droplet aggregation, which has been shown to result from increased hydrophobicity in the nanoparticles formed in an air-jet device, but not in US-assisted devices, whether particles are hydrophobic or hydrophilic [157].

Recent studies on aerosol formation by using air-jets and ultrasonication prior to the determination of complex size and zeta potential revealed that neither type of device destabilized the compounds studied (*viz.* polyethylenimines), even though droplet size was found to increase upon air-jet aerosoling [158].

Although some laboratory-scale US devices for aerosol formation have been developed [159], most of the aerosoling equipments used in clinical applications are of the commercial type.

5.7.2. Ultrasound-assisted spraying

Thin films of widely variable composition (mainly rare earth oxides, nickel, iron and other metal oxides, but also other simple and complex compounds) have been used for a variety of purposes (namely in semiconductor technology, optical and electronic applications

such as optical waveguides, optical filters, capacitors, etc.) and constitute a topical focus of materials research. The efficient formation of micro and nano drops is the key to obtain a film as thin as required on a given support. The formation of a spray to facilitate deposition can be successfully assisted by US. The variables influencing US-assisted spraying are similar to those affecting US-assisted aerosol formation and hence strongly dependent on the particular medium; this entails optimizing the variables related the target system, in addition to those typical of US. Thus, the pulse time [160,161] and US frequency [162] have been found to influence the properties of the resulting films as characterized by a number of analytical techniques such as X-ray diffraction, scanning electron microscopy, atomic force microscopy and X-ray photoelectron spectroscopy.

5.8.   ULTRASOUND-ASSISTED DEFOAMING

Foam is a dispersion of a gas in a liquid where the distances between individual bubbles are very small. In a foam system, the volume ratio of gas to liquid is very large and the bulk density approaches that of a gas. Depending on the particular context, foaming can be desirable or undesirable.

Interesting studies on foaming, foam films, antifoaming and defoaming were discussed at length by Pugh in the 1990s [163], particularly as regards the need for foam avoidance, formation and (or) control in specific areas. Thus, foams occur as an undesirable phenomenon in many industrial applications when liquids with a foaming tendency are aerated (*e.g.* in bioreactors, sewage treatment plants) or when gases are released under conditions of sudden pressure relief in a chemical reactor. Such undesirable foaming, if uncontrolled, can lead to a number of problems including losses of liquid contents, contamination, fouling of sensors, environmental pollution, reduction in working volume or suppression of gas–liquid mass transfer. Unwanted foaming is commonly controlled by the addition of chemical antifoams or defoamers. These additives, however, are expensive and contaminating. Also the use of antifoams in some areas such as the production of food and pharmaceutical products is legally restricted.

On the other hand, controlled bubble formation is required in a number of industrial fields (*e.g.* in the production of microcellular polymers). These polymers contain bubbles around 10 μm in diameter and have higher dimensional accuracy, higher impact strength, higher specific modulus and greater specific strength than foamed plastics containing larger bubbles. In order to produce microcellular structure, a high nucleation rate must be obtained and bubble growth must be controlled and stopped before bubbles coarsen. Theoretical predictions of bubble number and size have shown that US-assisted bubble control allows the results to conform to the predictions [164]. High-intensity US is efficient at destabilizing static foams, but is also effective at controlling dynamic foaming resulting from Newtonian and non-Newtonian liquids; this makes it suitable for processes requiring continuous defoaming [165]. The effectiveness of US in destabilizing and controlling foams seems to be governed by vibrational amplitude, frequency and foam structure [166].

Analytically, foam can cause problems in analytical operations such as chromatographic separations and molecular spectrometric detection, among others, where it must thus be avoided or removed.

5.8.1. Mechanism of ultrasound-assisted defoaming

The exact mechanism by which foam is destroyed under US radiation is still obscure. Various attempts have been made at explaining why foam collapses faster under

US vibrations. Foam destruction by large-amplitude sound wave can be ascribed to (a) periodically collapsing forces of the propagated sound waves (acoustic waves), (b) unidirectional pressure, (c) induced resonant vibration in the bubbles or (d) turbulence produced by the "sonic wind". A combination of these forces causes acoustic defoaming and, in general, radiation pressure forces prevail at medium and high frequencies. High-power sound waves, like electromagnetic waves, can exert a radiation pressure against any obstacle upon which they impinge.

Another theory concerning the effect of US on foam destruction is based on the mechanism of marginal regeneration proposed by Stein [167], which is considered to be triggered by squeezing mode surface waves along the film-plateau border boundaries. Such surface waves tend to stimulate thickness fluctuation that leads to faster drainage and film rupture. Thus, the US vibration would first increase the drainage of liquid from the foam, which would lead to its collapse. By correlating only the initial collapse rate of foam in the presence of US vibration in terms of various influential parameters such as the surface tension of the surfactant solution, ratio of horn diameter to column diameter and initial liquid hold-up, an equation has been established for predicting the initial collapse ratio [168].

5.8.2. Variables influencing ultrasound-assisted defoaming

Although no comprehensive study of the variables influencing US-assisted defoaming has been conducted, some interesting conclusions can be drawn from available evidence.

Ultrasound frequency, intensity and amplitude

There is some controversy concerning the frequency of US capable of causing defoaming. Thus, according to Komarov *et al*. low-frequency sound (< 1.3 kHz) is more effective in slag foaming suppression than are higher frequency waves (1.3–12 kHz); also, the steady-state foam height decreases abruptly when the sound pressure reaches a threshold value that depends on the sound frequency and liquid viscosity [169]. However, high-amplitude airborne sound waves over a wider frequency range (0.7 to 29 kHz) enable effective control of foams of medium viscosity [170].

More recent studies by Pandit *et al*. using a horn (20 kHz) to study the effect of the ratio of horn to column diameter on the foam drainage and collapse rate have revealed that high-intensity US can destabilize the static foam structure [168]. The efficiency of the US horn has been related to the position of its tip; also, the use of periodic ultrasound vibrations has proved more efficient (*viz*. to save energy and operating expenses) than continuous application [167].

Acoustic transducers operating at 10 and (or) 20 kHz are capable of defoaming liquids provided the acoustic source is placed above the liquid surface upon which the foam is being generated.

No dedicated analytical acoustic defoamers have been reported as defoaming is not a frequent problem in analytical laboratories; rather, they have been developed for technical applications.

5.9.   ULTRASOUND-ASSISTED DEGASSING

Although the analytical uses of US-assisted degassing are virtually restricted to the stages preceding sample preparation, a number of analytical methods produce a gas

at some point in the process. There are few references to the use of US for accelerating effi-cient gas removal. One case in point is the ion chromatography method for the determina-tion of bromate in drinking water. Reduction of chloride and carbonate with on-guard Ag and H cationic columns provides an eluate containing CO_2 and H_2 bubbles that are effectively removed by a 10-min sonication in an ultrasonic bath. No mention of the type of bath used or the necessity of a long sonication time for degassing was made by the proponents, so one can conclude that excess US irradiation was used to ensure the absence of gases [171]. In designing applications of US during sample preparation one should bear in mind the following two requirements: (a) the US application time should be optimized to reduce the overall analysis time; and (b) the effect of US irradiation on the target system should be considered in order to avoid analyte losses and the formation of potential interferents.

A US-assisted micro-degasser prototype for portable dialysis is one of the very few ana-lytical devices of this type reported so far [172]. The prototype consists of a degassing chamber formed in a glass wafer and gas-venting channels formed in a silicon wafer encap-sulated by the anodic bonding of Si to the glass wafer. A diaphragm of 6 mm $\times$ 6 mm $\times$ 0.1 mm was etched on the Si side for oscillation when excited by a 49 kHz square wave. The use of water to demonstrate the degassing process and monitoring it by using a micro-scope equipped with a video camera revealed that 38% of dissolved oxygen was removed.

References

1. M.D. Luque de Castro and J.L. Luque-García, *Acceleration and Automation of Solid Sample Pretreatment*, Elsevier, Amsterdam, 2002.
2. L.F. Dias, G.R. Miranda, T.D. Saint'Pierre, S.M. Maia, V.L.A. Frescura and A.J. Curtius, *Spectrochim. Acta B*, 60 (2005) 117.
3. M.J. Cal-Prieto, A. Carlosena, J.M. Andrade, S. Muniategui, P. López-Mahía, E. Fernández and D. Prada, *J. Anal. At. Spectrom.*, 14 (1999) 703.
4. M.J. Cal-Prieto, A. Carlosena, J.M. Andrade, S. Muniategui, P. López-Mahía, E. Fernández and D. Prada, *Quím. Anal.*, 18 (1999) 137.
5. C. Santos, F. Álava-Moreno, I. Lavilla and C. Bendicho, *J. Anal. At. Spectrom.*, 15 (2000) 987.
6. J. Moreda-Piñeiro, P. López-Mahía, S. Muniategui-Lorenzo, E. Fernández-Fernández and D. Prada, *Anal. Chim. Acta*, 461 (2002) 261.
7. C. Bendicho and M.T.C. de Loos-Vollebregt, *J. Anal. At. Spectrom.*, 6 (1991) 353.
8. W. Fuyi and J. Zuncheng, *Anal. Chim. Acta*, 391 (1999), 89.
9. P.C. Aleixo, D. Santos Jr., A.C. Tomazelly, I.A. Rufini, H. Berndt and F.J. Krug, *Anal. Chim. Acta*, 512 (2004) 329.
10. J.P. Pancras, J.M. Ondov and R. Zeisler, *Anal. Chim. Acta*, 538 (2005) 303.
11. S.M. Maia, J.B. Borba da Silva, A.J. Curtius and B. Welz, *J. Anal. At. Spectrom.*, 15 (2000) 1081.
12. G. Wibetoe, D.T. Takuwa and W. Lund, *Fresenius J. Anal. Chem.*, 363 (1999) 46.
13. D.C. van Loenen and C.A. Weers, *Fortshr. Atomspektrom. Spurenanal.* 2 (1986) 635.
14. G.R. Carnrick, G. Daley and A. Fotinopoulos, *At. Spectrosc.* 10 (1989) 170.
15. M. Hoenig and A. Cilissen, *Spectrochim. Acta B*, 48 (1993) 1303.
16. M. Antunes Vieira, B. Welz and A.J. Curtius, *Spectrochim. Acta*, 57 (2002) 2057.
17. M.N. Amin, S. Kaneco, T. Suzuki and K. Ohta, *Microchem. J.*, 74 (2003) 181.
18. R. Falciani, E. Novaro, M. Marchesini and M. Gucciardi, *J. Anal. At. Spectrom.*, 15 (2000) 561.
19. D. Pozebon, V.L. Dressler and A.J. Curtius, *At. Spectrosc.* 19 (1998) 80.
20. G. Tao, Y. Fujikawa, M. Mitsui and R. Yamada, *J. Anal. At. Spectrom.*, 17 (2002) 560.
21. S. Lynch and D. Littlejohn, *J. Anal. At. Spectrom.*, 4 (1989) 157.
22. N.J. Miller-Ihli, *Fresenius J. Anal. Chem.*, 345 (1993) 482.
23. H. Baumann, *Fresenius J. Anal. Chem.*, 342 (1992) 907.

24. M.N. Amin, S. Kaneco, T. Suzuk, Y. Taniguchi and K. Ohta, *Anal. Bioanal. Chem*., 373 (2002) 205.
25. S.J. Huang and S.J. Jiang, *Analyst*, 125 (2000) 1491.
26. D. Baralkiewicz, *Talanta*, 56 (2002) 105.
27. M. Antunes Vieira, A. Schwingel Ribeiro, L.F. Dias and A.J. Curtius, *Spectrochim. Acta*, 60 (2005) 643.
28. A. Schwingel Ribeiro, M. Antunes Vieira and A.J. Curtius, *Spectrochim. Acta*, 59 (2004) 243.
29. R. Japón, J.M. Luque-Rodríguez and M.D. Luque de Castro, *J. Chromatogr*., 1108 (2006) 76.
30. P. Cava-Montesinos, E. Ródenas-Torralba, A. Morales-Rubio, M.L. Cervera and M. de la Guardia, *Anal. Chim. Acta*, 506 (2004) 145.
31. E.J. dos Santos, A.B. Herrmann, M. Antunes Vieira, V.L. Azzolin Frescura and A.J. Curtius, Spectrochim. Acta B, 60(2005) 659.
32. L.F. Dias, T.D. Saint´Pierre, S.M. Maia, M.A. Mesquita da Silva, V.L.A. Frescura, B. Welz and A.J. Curtius, *Spectrochim. Acta B*, 57 (2002) 2003.
33. P. Bermejo-Barrera, A. Moreda-Piñeiro and A. Bermejo-Barrera, *Talanta*, 57 (2001) 969.
34. F. Laborda, M.P. Górriz and J.R. Castillo, *Talanta*, 64 (2004) 631.
35. M. Felipe-Sotelo, A. Carlosena, E. Fernández-Fernández, S. Muniategui, P. López-Mahía and D. Prada, *Anal. Chim. Acta*, 524 (2004) 329.
36. F. Barbosa Jr., E.C. Lima and F.J. Krug, *Analyst*, 125 (2000) 2079.
37. M. Felipe-Sotelo, A. Carlosena, E. Fernández, P. López-Mahía, S. Muniategui and D. Prada, *Talanta*, 63 (2004) 735.
38. M. Yaowu, X. Yiben, H. Xiaoqin and W. Hong, *Thin Solid Films*, 305 (1997) 266.
39. W.D. Fan, H. Wu, K. Jagannadham and B.C. Goral, *Surf. Coat. Technol*., 72 (1995) 78.
40. R.K. Singh, D.R. Gilbert and J. Laveige, *Appl. Phys. Lett*., 69 (1996) 2181.
41. Z. Fang, Y. Xia, L. Wang, Z. Wang, W. Zhang and Y. Fan, *J. Phys. D: Appl. Phys*., 35 (2002) L57.
42. Y. Chakk, R. Brener and A. Hoffmann, *Appl. Phys. Lett*., 66 (1995) 2819.
43. Y. Chakk, R. Brener and A. Hoffmann, *Diamond Relat. Mater*. 5 (1996) 286.
44. Y. Avigal and A. Hoffmann, *Diamond Relat. Mater*., 8 (1999) 127.
45. R. Shima, Y. Chakk and A. Hoffmann, *Carbon*, 38 (2000) 1839.
46. R. Akhvlediani, I. Lior, Sh. Michaelson and A. Hoffmann, *Diamond Relat. Mat*., 11 (2002) 545.
47. S.G. Wang, Q. Zhang, S.F. Yoon, J. Ahn, Q. Wang, D.J. Yang, Q.F. Hunag, Rusli, W.Z. Tang and F.X. Lu, *Diamond Relat. Mater*., 11 (2002) 1683.
48. S. Radel, A.J. McLoughlin, L. Gherardini, O. Doblhoff and B. Benes, *Ultrasonics*, 38 (2000) 633.
49. E.P. Mednikov, *Acoustic Coagulation and Precipitation of Aerosols*, Consultants Bureau, New York, 1965.
50. L. Song, *Modeling of Acoustic Agglomeration of Aerosols Particles*, PhD Thesis, Pennsylvania State University, 1990.
51. T.L. Hoffmann, *Visualization of particle interaction and agglomeration in an acoustic field*, PhD Dissertation, Pennsylvania State University. 1993.
52. I. González, *Estudio de las Interacciones Hidrodinámicas de Origen Viscoso en la Aglomeración Acústica de Partículas*, PhD Thesis, Universidad Complutense, Madrid, Spain, 1998.
53. E. Riera-Franco de Sarabia, J.A. Gallego-Juárez, G. Rodríguez-Corral, L. Elvira-Segura and I. González-Gómez, *Ultrasonics*, 38 (2000) 642.
54. J. Spengler and M. Jekel, *Ultrasonics*, 38 (2000) 624.
55. S.J. Doktycz and K.S. Suslick, *Science*, 247 (1990) 1067.
56. L.H. Mikkelsen and K. Keiding, *Water Res*., 36(12) (2002) 2931.
57. E. Riera-Franco de Sarabia, E. Elvira-Segura, I. González-Gómez, J.J. Rodríguez Maroto, R. Muñoz-Bueno and J.L. Dorronsoro-Areal, *Ultrasonics*, 41 (2003) 277.
58. N. Enomoto, T. Koyano and Z. Nakagawa, *Ultrason. Sonochem*., 3 (1996) S105.
59. Y.C. Yu, L. Zhang and J. Lin, *Colloid Interfacial Sci*., 260 (2003) 240.
60. K. Yoshioka and Y. Kawashima, *Acustica*, 5(1955) 167.
61. T. Masudo and T. Okada, *Anal. Sci*., 20 (2004) 753.
62. A. Haake and J. Dual, *Ultrasonics*, 40 (2002) 317.
63. A. Haake and J. Dual, *Ultrasonics*, 42 (2004) 75.

64. J.J. Hawkes, J.J. Cefai, D.A. Barrow, W.T. Coakley and L.G. Briarty, *J. Phys. D: Appl. Phys.* 31 (1998) 1673.
65. W.L. Nyborg and W.P. Mason (Eds.), *Phys. Acoust. 2. Pat B*, (1965) 265.
66. H. Mitome, *Electr. Comm. Jpn.*, 81 (3) (1998) 1.
67. L.P. Gorkov, *Sov. Phys.*, 6 (1962) 773.
68. M. Göschl, *Acust. Acta Acust.*, 84 (1998) 632.
69. H. Mitome, *J. Acust. Soc. Am.*, 100 (1996) 2589.
70. K. Beissner, *Forts. Akust. DAGA*, (1982) 479.
71. J. Spengler and M. Jekel, *Ultrasonics*, 38 (2000) 624.
72. W.T. Coakley, *Trends Biotechnol.*, 15 (1997) 506.
73. Z. Mandralis, W. Bolek, W. Burger, E. Benes and D.L. Feke, *Ultrasonics*, 32 (1994) 113.
74. M.L. Gray, K.L. Champagne, Y. Soong, R.P. Killmeyer, M.M. Maroto-Valer, J.M. Andrésen, M.V. Ciocco and P.H. Zandhuis, *Fuel Proc. Technol.*, 76 (2002) 11.
75. J.J. Hawkes and W.T. Coakley, *Enzyme Microbial Technol.*, 19 (1996) 57.
76. S. Bhaskar, J.N. Banavaliker, K. Bhardwaj and P. Upadhyay, *J. Immun. Meth.*, 262 (2002) 181.
77. M. Fountaulakis and H. Langen, *Anal. Biochem.*, 250 (1997) 153.
78. M. Kumar, D.L. Feke and J.M. Belovich, *Biotechnol. Bioeng.*, 89 (2005) 129.
79. H. Böhm, L.G. Briarty, K.C. Lowe, J.B. Power, E. Brenes and M.R. Davey, *Biotechnol. Bioeng.*, 82 (2003) 74.
80. A. Nilsson, F. Petersson, H. Jönsson and T. Laurell, *Lab. Chip*, 4 (2004) 131.
81. F. Petersson, A. Nilsson, C. Holm, H. Jönsson and T. Laurell, *Analyst*, 129 (2004) 938.
82. J. Yang, B. Hartong, J. Carletton and S. Banerjee, *Water Res.*, 39 (2005) 1374.
83. Brun and R.M.G. Boucher, *J. Acoust. Soc. Am.*, 29(5) (1957) 573.
84. S. Gupta and D.L. Feke, *Ultrasonics*, 35 (1997) 131.
85. S. Gupta and D.L. Feke, *AIChE J.*, 44 (1998) 1005.
86. T.J. Mason, L. Paniwnyk and J.P. Lorimer, *Ultrason. Sonochem.*, 3 (1996) S252.
87. M.T. Grossner, A.E. Penrod, J.M. Belovich and D.L. Feke, *Ultrasonics*, 41 (2003) 65.
88. M.T. Grossner, J.M. Belovich and D.L. Feke, *Chem. Eng. Sci.*, 60 (2005) 3233.
89. S. Gupta and D.L. Feke, *Ultrasonics*, 35 (1998) 1005.
90. D. Rusinko, M.D. Thesis, Case Western Reserve University, Cleveland, OH, USA, 2001.
91. P.J. Grabenstetter, unpublished results.
92. T. Kobayashi, X. Chai and N. Fujii, *Sep. Purif. Technol.*, 17 (1999) 31.
93. M. Cheryan, *Ultrafiltration Handbook*, Technomic, Lancaster, 1996.
94. M. Mulder, *Basic Principles of Membrane Technology*, 2nd edition, Kluwer Academic, Dordrecht, 1996.
95. T. Kobayashi, Ts. Kobayashi, Y. Hosaka and N. Fujii, *Ultrasonics*, 41 (2003) 185.
96. X. Chai, T. Kobayashi and N. Fujii, *J. Membrane Sci.*, 148 (1998) 129.
97. Y. Okahata and H. Noguchi, *Chem. Lett.* (1983) 1517.
98. T.N. Julian and G.M. Zentner, *J. Pharm. Pharmacol.*, 38 (1986) 871.
99. B.P. Singh, *Minerals Eng.*, 12(4) (1999) 437.
100. M.C. Smythe and R.J. Wakeman, *Ultrasonics*, 38 (2000) 657.
101. J.J. Hawkes and W.T. Coakley, *Sens. Actuators B*, 75 (2001) 213.
102. J.J. Hawkes, D. Barrow, J. Cefai and W.T. Coakley, *Ultrasonics*, 36 (1998) 901.
103. P.M. Hughes and H. Morgan, *Anal. Chem.*, 71 (1999) 3441.
104. R.Y. Wang, J.A. Harratt, P.J. Keay, J.J. Hawkes and W.T. Coakley, *Talanta*, 52 (2000) 129.
105. L.S. Jang, C.J. Morris, N.R. Sharma, R.L. Bardell and F.K. Forster, *ASEM International Engineering Congress and Exposition*, Nashville, USA, 14–19 Nov. 1999.
106. K. Yasuda, *Sens. Actuators B*, 64 (2000) 128.
107. Z.H. Fan, S. Mangru, P. Heaney, W. Ho, Q.P. Dong and R. Kumar, *Anal. Chem.*, 71 (1999) 4851.
108. A.Weisberg, H.H. Bau and J.N. Zemel, *Int. J. Heat Transfer*, 35 (1992) 2465.
109. N.R. Harris, M. Hill, S. Beeby, Y. Shen, N.M. White, J.J. Hawkes and W.T. Coakley, *Sens. Actuators B*, 95 (2003) 425.
110. T. Lilliehorn, U. Simu, M. Nilsson, M. Almwvist, T. Stepinski, T. Laurell, J. Nilsson and S. Johansson, *Ultrasonics*, 43 (2005) 293.

111. W.T. Coakley, *TIBTECH*, 15 (1997) 506.
112. B. Barry, *J. Control. Rel.*, 6 (1987) 85.
113. A. Banga, S. Bose and T. Ghosh, *Int. J. Pharm.*, 179 (1999) 1.
114. S. Mitragotri, D. Blankschtein and R. Langer, *Pharm. Res.*, 13 (1996) 411.
115. J. Kost, S. Mitragotri, R.A. Gabbay, M. Pishko and R. Ranger, *Nat. Med.*, 6 (2000) 347.
116. Y. Morimoto, M. Mutoh, H. Ueda, L. Fang, K. Hirayama, M. Atobe and D. Kobayashi, *J. Control. Rel.*, 103 (2005) 587.
117. A. Tezel and S. Mitragotri, *Biophys. J.*, 85 (2003) 3502.
118. A. Boucaud, M.A. Garrigue, L. Machet and L. Vaillant, *J. Control. Rel.*, 81 (2002) 113.
119. T. Terahara, S. Mitragotri, J. Kost and R. Langer, *Intern. J. Pharm.*, 235 (2002) 35.
120. G. Merino, Y.N. Kalia, M.B. Delgado-Charro, R.O. Potts and R.H. Guy, *J. Control. Rel.*, 88 (2003) 85.
121. H.Y. Zhang and S.H. Yeo, *Sens. Actuators A*, 115 (2004) 133.
122. Sontra Medical, www.sontra.com
123. H. Chuang, *Diabetes Technol. Therm.*, 6 (2004) 21.
124. N. Katz, *Anesth. Analg.*, 98 (2004) 371.
125. Encapsulation Systems, www.encsys.com
126. J.E. Ogden, U.S. Patent 5,656,016. 1997.
127. J. Shimada and J.E. Shapland, U.S. Patent 5,267,985. 1993.
128. R.T. Bock, U.S. Patent 5,618,275. 1997.
129. S. Mitragotri, *J. Pharm. Sci.*, 89 (2000) 892.
130. J. Kost, *Pharm. Res.*, 13 (1996) 633.
131. L. Le, *Pharm. Res.*, 17 (2000) 1151.
132. I. Lavon and J. Kost, *DDT*, 9 (2004) 670.
133. T. Cao, *Hum. Gene Ther.*, 11 (2000) 2297.
134. J.C. Vogel, *Hum. Gene Ther.*, 11 (2000) 2253.
135. S. Mitragotri and J. Kost, *Ad. Drug Deliv.*, 56 (2004) 589.
136. Anon., *Ultrasound Med. Biol.*, 24 (Suppl. 1) (1998) S1.
137. Anon., *J. Ultrasound Med.*, 19 (2000) 149.
138. D. Kashchiev, D. Verdoes and A.G. Van Vermolen, *J. Crystal Growth*, 110 (1991) 373.
139. N. Lyczko, F. Espitalier, O. Louisnard and J. Schwartzentruber, *Chem. Eng. J.*, 86 (2002) 233.
140. E. Dalas, *J. Crystal Growth*, 125 (1992) 27.
141. Z. Guo, M. Zhang, H. Li, J. Wang and E. Kougoulos, *J. Crystal Growth*, 273 (2005) 555.
142. I. Nishida, *Ultrason. Sonochem.*, 11 (2004) 423.
143. T. Ishitsubo, E. Matsubara, S. Kai and M. Hirao, *Acta Materialia*, 52 (2004) 423.
144. C. Li-yun, Z. Chuan-bo and H. Jian-feng, *Mat. Lett.*, 59 (2005) 1905.
145. H. Li, J. *Crystal Growth* 247 (2003) 192.
146. N. Amara, B. Ratsimba, A.M. Wilhelm and H. Delmas, *Ultrason. Sonochem.*, 8 (2001) 265.
147. H. Li, J.Wang, Y. Bao, Z. Guo and M. Zhang, *J. Crystal Growth*, 247 (2003) 192.
148. N. Enomoto, M. Katsumoto and Z. Nakagawa, *J. Ceram. Soc. Jpn.*, 102 (1994) 1105.
149. N. Enomoto, J. Akagi and Z. Nakagawa, *Ultrason. Sonochem.* 3 (1996) S97.
150. B. Chalmers, in: *Principles of Solidification*, John Wiley & Sons, N.Y. 1964, pp. 62–90.
151. X. Zhang, T. Inada and A. Tezuka, *Ultrason. Sonochem.*, 10 (2003) 71.
152. R. Chow, R. Blindt, R. Chivers and M. Povey, *Ultrasonics*, 41 (2003) 595, and 43 (2005) 227.
153. M.P. Cañizares, J.A. García-Mesa and M.D. Luque de Castro, *Anal. Chim. Acta*, 502 (2004) 161.
154. M. Patrick, R. Blindt and J. Janssen, *Ultrason. Sonochem.*, 11 (2004) 251.
155. D. Bemer and P. Tierce, *J. Aerosol Sci.*, 27 (1996) S393.
156. O.N.M. McCallion, K.M.G. Taylor, M. Thomas and A.J. Taylor, *Intern. J. Pharm.*, 129 (1996) 123.
157. L.A. Dailey, T. Schmehl, T. Gessler, M. Wittmar, F. Grimminger, W. Seeger and T. Kissel, *J. Control. Reles.*, 86 (2003) 131.
158. L.A. Dailey, E. Kleemann, T. Merdan, H. Petersen, T. Schmehl, T. Gessler, J. Hänze, W. Seeger and T. Kissel, *J. Control. Reles.*, 100 (2004) 425.
159. R. Paneva, G. Temmel, E. Burte and H. Ryssel, *Sens. Actuators*, 62 (1997) 765.

160. S. Wang, W. Wang and Y. Qian, *Materials Res. Bull*., 35 (2000) 2057.
161. S. Wang, Z. Qiao, W. Wang and Y. Qian, *J. All. Comp*., 305 (2000) 121.
162. S. Wang, W. Wang, W-Z. Wang and Y-W. Du, *Materials Sci. Eng.*, B90 (2002) 133.
163. R.J. Pugh, *Adv. Coll. Interface Sci*., 64 (1996) 67.
164. J.R. Youn and H. Park, *Polym. Eng. Sci*., 39 (1999) 457.
165. M.D. Morey, N.S. Deshpande and M. Barigou, *J.Collid. Inter. Sci*., 219 (1999) 90.
166. M. Barigou, *Chem. Eng. Technol*., 24 (2001) 6.
167. H.N. Stein, *Adv. Colloid Interface Sci*., 34 (1991) 175.
168. A.C. Dedhia, P.V. Ambulgekar and A.B. Pandit, *Ultrason. Sonochem*., 11 (2004) 67.
169. S.V. Komarov, M. Kuwabara and M. Sano, *Ultrason. Sonochem*., 7 (2000) 193.
170. R.M.G. Boucher and A.L.Weiner, *Br. Chem. Eng*., 8(12) (1963) 802.
171. S. Valsecchi, A. Isernia, S. Polesello and S. Cavalli, *J. Chromatogr*., 864 (1999) 263.
172. Z. Yang, S. Matsumoto and R. Maeda, *Sens. Actuators A*, 95 (2002) 274.

CHAPTER 6

Ultrasound Assistance to Analytical Heterogeneous Liquid–Liquid Systems

6.1. INTRODUCTION

Heterogeneous liquid–liquid systems are quite common place in analytical chemistry, which uses them for a variety of purposes, including the following in relation to sample preparation: (1) analyte transfer from one phase to another, followed by (a) phase separation in order to feed only the phase enriched with the analyte to the detector or subject it to some other operational step prior to detection, or (b) continuous monitoring of the enriched phase without phase separation; (2) the formation of a heterogeneous medium, — small droplets of one phase in another — which is the usual purpose of homogenization and emulsification. Ultrasound (US) has been used to improve the outcome of (1) and (2), albeit with rather disparate results and frequency.

   Although mass transfer between two immiscible phases (*i.e.* liquid–liquid extraction) is an old separation technique, the potential and effects of US on it (*viz.* acceleration of the transference and (or) displacement of the equilibrium) have been scarcely studied.

   By contrast, dispersion of a phase as small droplets into another under US assistance until the initial heterogeneous liquid–liquid system is made uniform, which is known as "homogenization" or "emulsification", is a well-documented process in both the analytical and industrial fields. Depending on the operating conditions and the type of ultrasound used, both emulsion formation and destruction can be favoured.

   One emergent field for US application involves liposomes, the formation of which and (or) their performance can be improved by this type of energy. The peculiar structure of liposomes and the growing interest of analytical chemists in them warrant their discussion here.

6.2. ULTRASOUND-ASSISTED LIQUID–LIQUID EXTRACTION

Whether US facilitates mass transfer between two immiscible phases is arguable if one considers the ability of this form of energy to facilitate emulsification. Probably for this reason, analytical chemists have been reluctant to test US as a means for improving liquid–liquid extraction (LLE). In fact, US application most often produces stable emulsions that result in long phase-separation times; therefore, US favours mass transfer between phases — provided that the partitioning equilibrium involved facilitates the transfer. Efficient, fast LLE entails avoiding or minimizing the former effect and maximizing the latter. These are the two major factors to be optimized in ultrasound-assisted liquid–liquid extraction (USALLE).

6.2.1. *Variables influencing ultrasound-assisted liquid–liquid extraction*

Maximizing the extraction efficiency and minimizing emulsification of the immiscible phases in USALLE entails optimizing both the typical US-related variables and those characteristic of LLE. In addition, the specific US-related variables to be optimized depend on whether

(1) a discrete or continuous experimental approach is implemented, (2) a bath or a probe is used and (3) direct immersion or a transmitting liquid (if a probe and a discrete approach are used) is employed.

The effect of US variables is discussed in detail in Chapters 3 and 4, so this section focuses on the sole difference from the effects described in them (*viz*. not only the extraction efficiency, but also the undesirable emulsification effect of US must be considered). However, most existing discrete USALLE methods have been optimized without provision for emulsification (*i.e.* for the time needed for the phases to separate). This is not the case with continuous methods, where emulsification is avoided or restricted to the interface, which is not monitored.

The influence of the variables pertaining to LLE (*e.g.* the aqueous-to-organic phase volume ratio, partition coefficient of the target species between the two immiscible phases) is outside the scope of this book and is discussed in detail elsewhere [1,2].

6.2.2. Discrete ultrasound-assisted liquid–liquid extraction approaches

Most of the USALLE approaches reported are of the discrete type and use an ultrasonic bath. Usually, a vessel containing the sample and the immiscible, acceptor phase is immersed in the transmitting liquid held in a bath and the process involves application of US for a preset time, phase separation and repetition of the extraction cycle, if required. With slight differences, this procedure has been used to extract aroma compounds from grape must, wine [3–5], aged brandies and aqueous alcoholic wood extracts [6], or specific compound families such as monoterpenoids [7] as well as volatiles [8] both from wine, pesticides from honey [9] and methylmercury from biological materials [10].

In 1995, Cocito *et al*. demonstrated the usefulness of USALLE for extracting aromas from wine [3]. Four years later, Hernanz Vila *et al*. [4] used the method of Cocito *et al*. in combination with a factor design to optimize extraction-related variables such as the sample and extractant volumes, and extraction time; however, improvements over the original method were insubstantial (*e.g.* the sample and immiscible solvent volumes were lowered from 125 to 100 ml and from 60 to 50 ml, respectively, with similar precision in both cases). Note that no US-related extraction variables, but only sample and extraction volumes, and the extraction time were optimized. A determination of aromas in wine from seven clones of Monastrell grapes [5] using the Cocito method provided coefficients of variation that were somewhat higher than those obtained by Cocito *et al*. Nevertheless, the authors concluded that volatiles provide a valuable tool for classifying and distinguishing grape clones and that the sensory properties of wines may differ not only among varieties, but also among clones.

An interesting comparative study of aroma compounds in aged brandies and aqueous alcoholic wood extracts involving US-assisted extraction was carried with a view to identify the components of brandy aroma already present in grapes and wines, those formed in the distillation step and those coming from the oak wood [6]. After three extraction cycles with 30, 10 and 10 ml of dichloromethane in an ultrasonic bath, the volume of the overall extract was reduced to 100–200 µl in a rotary evaporator and the individual components quantified by GC–FID. The relatively high standard deviations obtained in some cases (0.1–18.4%) can be ascribed mainly to both irreproducibility in the US energy provided by the bath and the low final extract volumes.

The LLE temperature was controlled in none of the previous methods. This, together with the typical decline in power of US baths, might be the origin of the high imprecision.

The discrete USALLE of monoterpenoids has been compared with direct immersion SPME of these compounds from wine [7]. A modification of the method from Cocito *et al.* was used because dichloromethane replaced 1:2 *n*-pentane-diethylether as the extractant. Samples were extracted three times under US application for 10 min, using 30, 10 and 10 ml of organic extractant and at a constant temperature of 20°C. For an unconvincing reason (namely, the chromatographic resolution was reduced through overlap of major compounds with minor ones with a greater number of cycles), the authors chose to use only three extraction cycles; however, the adverse effect of using more cycles could have been avoided by diluting the extracts, with the additional advantage that useful information about the extraction kinetics of the different compounds could have been obtained. The conclusions of this study were as follows:

(1) both methods are suitable for the extraction of the target compounds from wines with subsequent gas chromatographic (GC) individual separation with a view to classify wines produced in different geographical zones;
(2) both provide similar sensitivity and precision (CV < 5.5%);
(3) US extraction is more efficient (95.1% *versus* 82.5%) and provides richer qualitative–quantitative flavour profiles;
(4) the SPME method is faster (the greatest weakness of US extraction was the long time required to concentrate the extract under an inert atmosphere, 12 h) and uses less sample volume (7 ml *versus* 100 ml).

The usefulness of US for accelerating the LLE of compounds from honey lies mainly in the ability to operate at ambient temperature; by contrast, some techniques such as simultaneous distillation–extraction [11] and purge and trap [12] are subject to thermal artifacts. USALLE has been used to extract volatile compounds from citrus flowers and citrus honey with a view to discriminate honey according to its botanical origin [8], and also pesticides [9]. In this context, USALLE is faster than conventional methods and has the added advantage that it extracts compounds of molecular weight up to 220, which helps to determine the origin of honey; this, however, calls for improved repeatability as the RSD values for some compounds exceed 20%.

Pesticides such as atrazine and simazine have also been extracted from honey with the aid of an ultrasonic bath. In addition to the type of extractant, variables such as the extractant volume, sonication time and number of extraction cycles were optimized, the temperature and the height of the transmitting liquid in the bath being kept constant. A comparison of the ensuing method with its shake-flask extraction counterpart showed the former to be faster and more efficient, and provide relatively lower standard deviations [9].

One major criticism of all previous US-assisted methods is that they have not been compared with their unassisted counterparts, so the influence of US on the results has not been quantified. This, however, is not the case with the method for pesticides in honey and that for the determination of mercury in biological materials proposed by Tu *et al.*, which is based on acid leaching for 5 min, followed by simultaneous *in situ* derivatization and LLE for 40 min in the presence of sodium tetraethylborate and nonane, buffered at pH 7.0, under US [10]. The mixture was shaken by hand and sonicated at 40°C at a fixed US amplitude of 100%; however, the characteristics of the US bath used were omitted. Phase separation was effected by centrifugation at 5400 rpm for 5 min. The improvement provided by US assistance is apparent from Fig. 6.1.

Another criticism of the previous methods is that their proponents have failed to state the type of US device used as they seemingly believe that ultrasonic baths are the sole available choice for this purpose. In fact, only one USALLE method using a probe appears
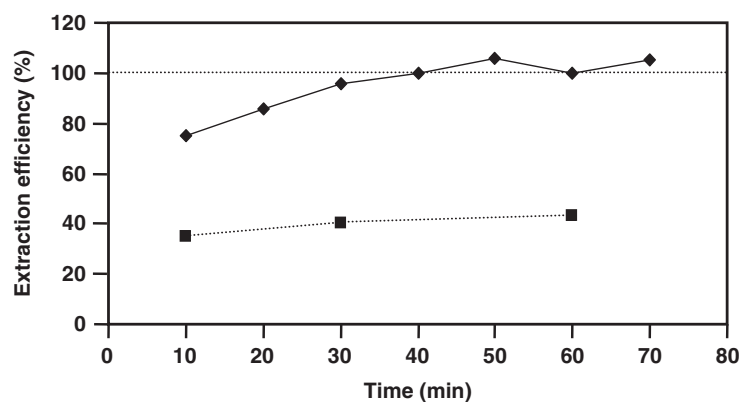
FIGURE 6.1. *Influence of time on the extraction efficiency of methylmercury from CRM-463 sample (biological material) with (♦) and without (■) US assistance. (Reproduced with permission of Elsevier, Ref. [10].)*

to have been reported; the method was used to extract iron from largely organic solvents. Although the proponents gave no optimization details, they specified the depth of the US probe in the extraction system, the ultrasonication and silent periods, and the time required for phase separation. The use of a US probe rather than a conventional US bath was found to significantly improve the rate of emulsification — which was the aim pursued in this case for proper mass transfer — as the system became turbid within few seconds of starting the probe-based sonication step. However, neither temperature control was used, nor the typical variables of US probes (namely, power, pulse duration, amplitude) were optimized; also, the authors failed to distinguish sample and extract and used the word "sonoemulsification" to refer to the US-assisted step leading to iron extraction. The efficiency of US-assisted extraction (100.2%) was reduced to 21% under silent conditions [13].

Some authors have used US to ensure homogenization of the sample and an acid solution. This homogenization dramatically reduces the time needed for subsequent conventional liquid–liquid extraction in a separatory funnel [14]; others have used US to accelerate an oxidation step preceding or following conventional LLE [15].

6.2.3. Continuous ultrasound-assisted liquid–liquid approaches

Dynamic approaches to USALLE have been scarcely explored even though manifolds for mass transfer from an organic phase to an aqueous and *vice versa* have been designed (see Fig. 6.2) and successfully applied [16,17] since the earliest attempts of the authors' group in the 1980s [18].

Continuous LLE is briefly introduced here before the functioning of these manifolds is explained in order to justify the choice of specific operational modes.

Conventional continuous LLE requires the use of three basic units (*viz.* a segmenter, an extraction coil and a phase separator, in order to achieve the sequential formation of aqueous–organic phase segments, mass transfer between the two types of segments and clean separation of the acceptor phase to be led to the detector, respectively, [2]).
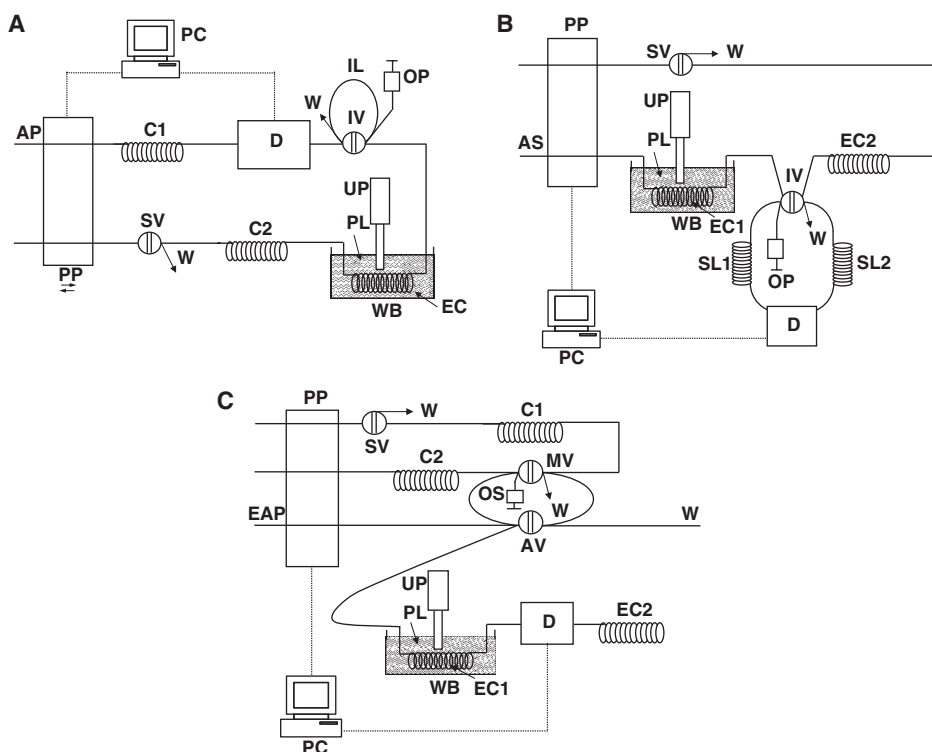
FIGURE 6.2. *Flow injection manifolds for continuous US-assisted liquid–liquid extraction without phase separation. (A) Monitoring one interface. (B) Sequential monitoring of the two interfaces in a chemical system involving extraction from an aqueous to an organic phase. (C) Sequential monitoring of the two interfaces in a chemical system involving extraction from an organic to an aqueous phase. AP — aqueous phase, AS — aqueous sample, AV — auxiliary valve, C — coil, D — detection system, EAP — extractant aqueous phase, EC — extraction coil, IL — injection loop, IV — injection valve, MV — main valve, OP — organic phase, OS — organic sample, PC — personal computer, PL — propagating liquid, PP — peristaltic pump, SL — sub-loop, SV — selection valve, UP — ultrasonic probe, W — waste and WB — water bath. (Reproduced with permission of Elsevier, Refs. [16,17].)*

The shortcomings of phase separators can be circumvented by avoiding phase separation. This simplified mode can be implemented in various ways, namely:

(a) By using none of the three usual devices. Instead, the sample can be bubbled through a cell containing the extractant. When the solute is to be transferred to an organic phase, such a phase must be the heavier one; the sample is bubbled at the bottom of the cell and mass transfer occurs in the way of the drops through the organic layer. This method is not very effective and the use of an organic phase heavier than the aqueous phase is a highly restrictive condition [19,20].

(b) By using both a segmenter and an extraction coil. In this way, longer, more extensive contact between the sample and the extractant is achieved, and mass transfer is

accomplished by using a coil as long as required. The enrichment of the extractant with the solute can be monitored in two ways, namely: (1) by increasing the length of the segments in an expansion chamber [21], thus enabling transient alternate passage of only organic phase and only aqueous phase through the flow cell; or (2) by using a dynamic manifold with iterative change of the flow direction [22]. In this way, only the extractant phase — a single, relatively long segment — is monitored by changing the flow direction when the interface between the two immiscible liquids is close to the detection point, but has not yet reached it [22,23]. The detector can be accommodated in the loop of an injection valve or in the transport tube (see Fig. 6.2). The extraction process is thus similar to the conventional shaking in separation funnels except for the major differences that it can be fully automated and allows continuous monitoring of solute transfer.

The manifolds in Fig. 6.2, which differ in the chemical system involved and whether one or both interfaces are monitored, are based on the last approach. Thus, manifold in Fig 6.2A can be used when only one of the interfaces is to be monitored. The procedure is as follows: initially, the injection loop (IL) of valve IV is filled with sample and the extractant phase is circulated through the manifold to establish the detector baseline. Switching of IV to the inject position is synchronized with the iterative change of the flow direction in such a way that the injected zone (the sample) never reaches the flow cell in the detector — thus avoiding parasitic signals resulting from changes in refractive index or viscosity — but approaches it as much as possible; as a result, the extract is monitored at the most analyte-enriched zone. Such a zone is transported to the extraction coil (EC) in each cycle, where it is subject to US radiation for an interval depending on the flow rate and EC length. Then, the zone, which is very close to the interface, is led to the detector and gives a peak in each cycle; the final result is thus a multi-peak recording such as that of Fig. 6.3A. Circulation of the liquids through the flow system is accomplished by using the peristaltic pump in propelling–aspiration cycles to ensure reproducible operation. After extraction, the system is unloaded and rinsed through switching valve (SV) to avoid passage of organic solvents through the pump tubes.

This manifold has been used for the USALLE of paracetamol from suppositories [17]. Hydrolysis of the analyte prior to reaction with *o*-cresol in the alkaline extractant medium was also favoured by US (the entire sample plug was irradiated in EC). Hydrolysis and formation of the reaction product displaced the extraction equilibrium, thus favouring extraction into the aqueous phase. The influence of the variables related to the dynamic manifold (namely, flow rate and sample volume), chemical variables (namely, NaOH and *o*-cresol concentrations) and temperature was studied using the univariate method on account of their independence; on the other hand, those related to US (namely, probe position, radiation amplitude and pulse duration) were the subject of a multivariate study in which the latter two exhibited an insignificant but positive effect. Positioning the probe closest to the extraction coil was found to maximize extraction efficiency. The positive effect of US on extraction and analyte hydrolysis provides the overall enhancement shown in Fig. 6.4A, which shows the results obtained in the presence and absence of US. The time required for the development of the method was significantly shorter than that required by the United States Pharmacopoeia (USP) method. In addition, the latter produces emulsions that need about 30 min for phase separation after extraction.

Sequential monitoring of the two interfaces in each cycle is also possible. This can be exploited for two purposes, namely: (a) the simultaneous monitoring of the extraction process with and without US assistance by using a sample plug long enough to ensure irradiation of only one interface; (b) the simultaneous monitoring of the extraction process
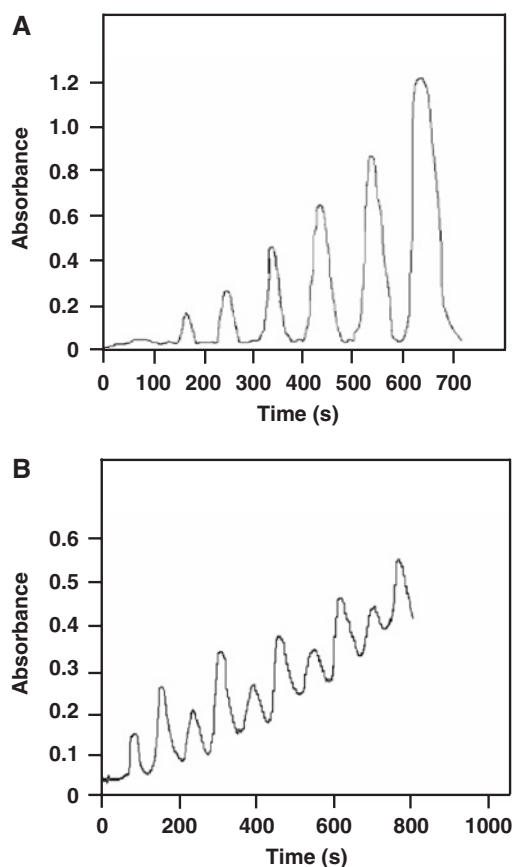
FIGURE 6.3. *Multi-peak recordings obtained from continuous US-assisted liquid–liquid extraction. (A) Monitoring one of the interphases for the extraction of paracetamol into a basic aqueous phase containing o-cresol. (B) Monitoring the two interphases for the extraction of polyphenols from olive oil into a basic aqueous phase. (Reproduced with permission of Elsevier, Refs. [16,17].)*

under assistance by a different type of energy (*e.g.* US and microwaves) at each interface. The manifold required differs depending on the nature of the donor and acceptor phases. Manifolds of both types have been designed for (a).

The manifold in Fig. 6.2B is the only available choice for the sequential monitoring of the two interfaces in a chemical system involving extraction from an aqueous phase to an organic one. The operational procedure is as follows: the loop of the injection valve (IV) accommodating the flow cell is filled with the clean organic, extractant phase to establish the detector baseline and the aqueous sample is then propelled by the peristaltic pump to fill the manifold. Then, the extraction is started by switching IV to the unload position and the process is monitored in one flow direction until the corresponding interface is as close as possible to the detection point — without reaching it to avoid parasitic signals — in order
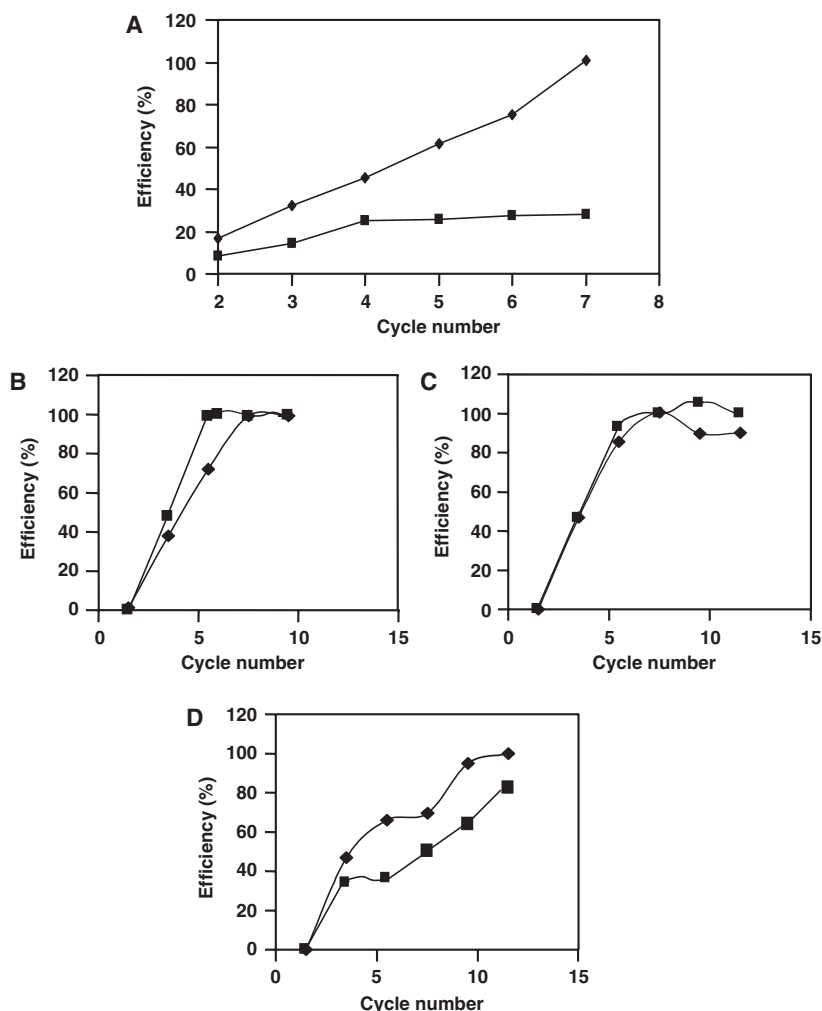
FIGURE 6.4. *Comparison of the continuous liquid–liquid extraction with (♦) and without (■) US assistance. (A) Paracetamol in alkaline medium with the manifold shown in Fig.6.2A. (B) I_2 in dichloromethane with the manifold shown in Fig. 6.2B. (C) Fe^{2+} in dichloromethane with the manifold shown in Fig. 6.2B. (D) Polyphenols in a basic aqueous phase with the manifold shown in Fig. 6.2C. (Reproduced with permission of Elsevier, Refs. [16,17].)*

to monitor virtually the entire organic plug. Such a plug must be long enough to allow one of the interfaces reaching reactor EC1 to be ultrasonicated while the other is outside the transmitting liquid and far enough from it to avoid its influence. Each interface is circulated through a tubing length (EC + SL) large enough to avoid the loss of liquid in the cycles and facilitate monitoring of both interfaces. Absorbance changes in the organic phase, which result from extraction of the analytes, are monitored at an appropriate wavelength to obtain

multi-peak recording consisting of alternate peaks for the ultrasound-assisted (USA) and non-ultrasound-assisted (NUSA) interface (see Fig. 6.3B). This allows the processes occurring at the two interfaces to be compared in a single experiment.

The manifold in Fig. 6.2B has been used to develop two methods for the extraction of two analytes from an aqueous phase, with or without a chemical reaction (*viz.* extraction of Fe(II) into a dichloromethane/*o*-phenanthroline phase with the formation of the well-known red complex, and extraction of I_3^- into dichloromethane) [16]. Because both chemical systems are well known, chemical and flow-related variables were set at their reported optimum values, and US-related variables (namely, probe position, radiation amplitude and cycle duration) were optimized by using a multivariate approach. The temperature was kept constant throughout the experiments. The results for iodine (Fig. 6.4B) reveal that the presence of US results in poorer extraction of this analyte. On the other hand, those for the water Fe(II)/*o*-phenantholine dichloromethane system reveal that the presence of US improves the extraction after several cycles (see Fig. 6.4C); however, the improvement is very slight, so it does not justify the use of ultrasound here.

The manifold in Fig. 6.2C was designed for the sequential monitoring of the two inter-faces of a chemical system involving extraction from an organic phase to an aqueous one. The key element of this manifold is an internally coupled valve system that serves two main purposes, namely: (1) to enable passage of virtually all aqueous extractant contained in the loop of the auxiliary valve by the detection point while avoiding that of the interfaces; and (2) to dispense with the need to circulate the organic phase — the sample in this case — through the peristaltic pump and hence with the use of special pump tubes. The extraction coils (ECs) must be long enough to allow ultrasonication of one interface without affecting the other and must be suited to the particular application; on the other hand, the length of the coils (Cs) is not crucial but must be large enough to avoid liquid losses during the back-and-forth cycles. The functioning of the system is as follows: the loop of the auxiliary valve is filled with aqueous phase modified as required (*e.g.* pH adjustment, derivatization reagents), and the detector baseline established. Then, the loop of the main valve is filled with organic sample (preferably with a syringe, hypodermic needle and adapter to avoid the use of special pump tubes) and an aqueous phase that acts as a carrier in the back-and-forth movement of the donor and acceptor plugs is circulated through C. Next, both valves are switched to the unload position and, simultaneously, the programme controlling the pump is started. EC1 is sonicated while it contains one of the interfaces. After each run, the manifold is flushed. To this end, the loop of the main valve is filled with an appropriate organic solvent, which is circulated in both directions through the manifold before going to waste through valve SV — which avoids passage through the pump tubes. Finally, the manifold is rinsed with water.

The previous manifold and procedure have been used for the extraction and determina-tion of polyphenols from extra virgin olive oil [16]. The method is based on the standard for this type of analytes and samples, which involves extraction of organic compounds into a Folin–Ciocalteu reagent solution, with monitoring of the product at 725 nm. Figure 6.3B shows the multi-peak recording obtained. The peaks correspond alternately to sonicated and unsonicated interfaces and show that US is more effective than no sonication. The treat-ment to be applied to the peaks in order to obtain an appropriate analytical signal can differ depending on the sensitivity of the monitored product. Thus, if the absorbance is relatively high, measurements of the first peak close to each interface can be used as the analytical signal. With low absorbances, the combined absorbance of a number of peaks can be used as the analytical signal. For comparison with the two previous methods for the extraction from an aqueous phase to an organic one (Figs. 6.4B and C), Fig. 6.4D shows the efficiency of the corresponding USA and NUSA processes.

The peristaltic pump in all these manifolds operates in a propulsion–aspiration mode in order to ensure more reproducible flow rates.

6.2.4. Conclusions

Reported evidence for USALLE allows the following conclusions to be drawn:

(1) Ultrasound does not always favour mass transfer between two immiscible phases.
(2) Transfer from an organic phase to an aqueous one is more markedly favoured by US than the transfer from an aqueous phase to an organic one.
(3) The effect of US can be more significant when a chemical reaction occurs simultaneously with extraction. The influence of US on mass transfer and chemical reaction should be discriminated in order to select the latter.
(4) Available information is too scant to allow general rules on the behaviour of chemical systems under USALLE to be established.

6.3.   ULTRASOUND-ASSISTED HOMOGENIZATION AND EMULSIFICATION

Homogenization is commonly defined as a chemical or physical treatment by which the composition or structure of a substance (solid, liquid or gas) or mixture of substances is made uniform. The ability of US to effectively stir, mix or agitate a system without altering its chemical characteristics has been widely demonstrated and used in both laboratory and industry. At the laboratory scale, the use of homogenization in the analytical process is not restricted to key or optimized steps as the target system is sonicated for a time exceeding that strictly required to ensure adequate homogenization. However, homogenization is included in most types of US-assisted processes described in Part I of this book (dissolution, digestion, leaching, etc.) by virtue of the stirring, mixing and agitating capabilities of US.

Most applications of US-assisted homogenization whether analytical and non-analytical, involve liquid systems. Food processing industries have exploited US homogenization [24] as a key step in the processing of milk, yogurt and ice cream because it helps avoid creaming during incubation and storage. In fact, homogenization increases the stability, consistency and body of yogurt. The purpose of this phenomenon in the case of milk is to reduce fat globules and clumps to a size such that they will no longer rise to the top of the liquid when milk is consumed. High-amplitude US provides highly effective homogenization of milk relative to conventional homogenization procedures. Long US exposure times increase the effect (*e.g.* sonicating after inoculation reduces the total fermentation time by 0.5 h) and increasing the US amplitude before inoculation significantly improves the water holding capacity and viscosity while reducing syneresis. While sonication after inoculation does not decrease syneresis, it increases the water holding capacity and viscosity [25]. Bioprocesses also benefit from the use of US for continuous homogenization; this, coupled to immobilized metal affinity expanded bed adsorption, provides a new method for on-line purification of histidine-tag-enhanced green fluorescent protein with yields close to 100% [26]. The pharmaceutical industry has used US during the tableting of powders [27].

Analytically, the most interesting systems are those formed by two or more immiscible liquids, homogenization of which is known as "emulsification" and dealt with separately on account of its importance.

6.3.1. Ultrasound-assisted emulsification

According to Becher, an emulsion is a heterogeneous system consisting of two immiscible liquids one of which (the dispersed phase) is intimately dispersed in the other (the continuous phase) in the form of small droplets whose diameters generally exceed 0.1 μm [28]. Although emulsions are heterogeneous systems, — they consist of two immiscible phases — emulsification is intended to produce a homogeneous system in terms of chemical structure.

The type of emulsion formed (normally water-in-oil or oil-in-water, commonly expressed as *w/o* or *o/w*, *w* denoting the aqueous phase and *o* the organic phase) is determined by the volume ratio of the two liquids and also by the phase addition sequence and the nature of any additives used to promote emulsification [29]; the affinity of emulsifiers for oil and water is measured on the hydrophile–lipophile balance (HLB) scale [30]. Oil-in-water emulsions are most common in all application fields.

Milk, cream, mayonnaise, butter, margarine, skin lotions, formulated cosmetics, pharmaceutical ointments, varnishes, paints and lubricants are among the most typical examples of emulsions. Also, emulsions are commonplace in a wide range of technologies and play a key role in materials processing, from metal working to textile finishing [31].

Emulsions occur naturally in the vegetable and animal kingdoms (*e.g.* in rubber tree latex and milk, respectively). However, mixing two immiscible liquids to produce an emulsion almost always requires the assistance of energy; also, the resultant emulsion is usually unstable. The stability is especially low for those liquid–liquid dispersions with a high interfacial area. In this respect, the use of additives helps obtain stable emulsions from two immiscible liquids. There are two main types of emulsion additives, namely: emulsifiers and stabilizers, the effects of which are based on different principles. Emulsifiers belong to the class of surface active substances. Thermodynamically, emulsifiers reduce the surface free energy required to increase any interfacial area A ($\Delta G = \gamma \Delta A$) by lowering the interfacial tension (γ), and allow finely dispersed media to be easily created. The most common class of emulsifiers is that of surfactants, which can form monolayers or liquid crystals. By virtue of their amphiphilic molecular structure, surfactants are adsorbed at the interface between two phases thereby helping to stabilize the droplets of the dispersed phase of an emulsion. Depending on the stabilizing properties of the system, coalescence (*viz.* irreversible formation of large drops leading to less stable emulsions and eventually to phase separation) of droplets after disruption influences the final droplet size distribution. Highly efficient emulsifiers and low volume fractions of the dispersed phase can reduce coalescence considerably. Additional emulsifiers include starch, lignin, lignite, finely divided solids, synthetic emulsifiers (*e.g.* polymers, sulphonated hydrocarbons, ethyoxylated nonylphenols, etc.) and proteins.

The other major class of emulsion additives is that of stabilizers. In contrast to emulsifiers, stabilizers are non-surface active macromolecules which are added to emulsions in order to increase the viscosity of the continuous phase, thus reducing the mobility of the droplets in order to prevent emulsification from coalescence [32].

Even if some additive is used, the assistance of US is usually needed to disperse a liquid phase into the continuous phase and produce metastable mixtures, as reducing large droplets to smaller ones involves additional shear forces, and the viscous resistance during agitation absorbs most of the applied energy [33]. Figure 6.5 illustrates a continuous mechanical emulsification process [32,34]. Initially, unstable interfacial waves form at the oil–water interface that produces large oil droplets (*ca.* 50–100 μm in size) in the continuous phase. Subsequently, the droplets in the pre-mix emulsion are disrupted in the dispersion zone by mechanical energy input. Then, the new droplets formed must be stabilized against coalescence, where, as noted earlier, additives play a prominent role.
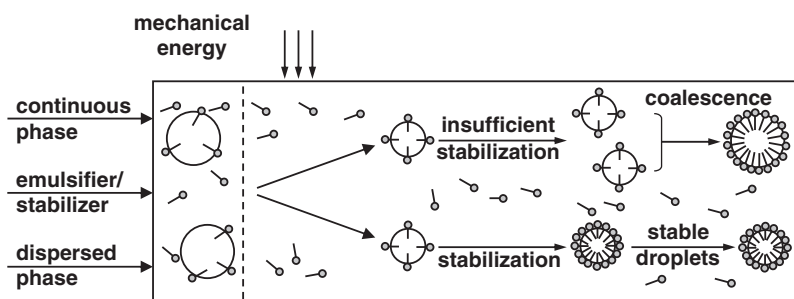
FIGURE 6.5. *Mechanical emulsification process. (Reproduced with permission of Elsevier, Ref. [32,34].)*

Finally, excess applied energy is dissipated as heat and as a result the temperature of the emulsion is raised.

Emulsification can take place in a single or several, consecutive steps [35,36]. Industrial emulsifications are normally made by valve homogenizers or colloid mills, which use large amounts of materials and are often inefficient. At the laboratory scale, mechanical energy can be provided by a variety of apparatus among which rotor–stator systems and high-pressure homogenizers are most widely used. Droplets of the dispersed phase in these systems are broken up under the action of shear or inertial forces in laminar or turbulent flow. In membrane emulsification, the dispersed phase is pressed through the pores of a microporous membrane to form small droplets in the continuous phase after reaching the other side of the membrane surface [37].

Ultrasound-assisted emulsification was initially developed by Wood and Loomis [38]. The first patent of an ultrasonic emulsifier was granted in 1944 in Switzerland. Since then, research on US-assisted emulsification and underlying mechanisms has grown in parallel due to interest in the process [32].

Mechanisms of ultrasound-assisted emulsification

The increasing demand for products with well-defined composition and properties has aroused much interest in elucidating the basic mechanisms behind emulsion production and stabilization under different conditions [39].

Several possible mechanisms have been proposed to explain the influence of US energy on droplet formation and disruption. One assumes the formation of droplets as a consequence of unstable oscillations at the liquid–liquid interface. Such oscillations contribute to droplet disruption only if the diameter of droplets is considerably larger than the oscillation wavelength, which is about 10 µm for oil–water systems. Therefore, this mechanism, which is known as the "capillary waves mechanism" and rarely used to explain US-assisted emulsification, is only valid for droplets larger than 10 µm (first steps of the process).

One mechanism similar to that of capillary waves is based on the oscillation and subsequent disruption of droplets under US action. The corresponding resonance radius at a frequency of 20 kHz (common for ultrasonic sources) is about 10 µm. This mechanism must be considered as one source of US-assisted emulsification, but can only be applied to immiscible liquid–liquid systems with a diameter within the established range for most of the droplets. In fact, most immiscible liquid–liquid systems are formed by droplets with

a broad size distribution. Therefore, this mechanism can only be the principal one when a wide range of sound frequencies are used [40].

The most widely accepted mechanism for US-assisted emulsification is based on the effects of cavitation, which are deemed crucial for the process to develop. However, this mechanism is based on the implosion bubbles generated by cavitation, which produce intensive shock waves in the liquid surrounding the ultrasonic source and liquid jets of a high velocity. Such microjets can cause droplet disruption in the vicinity of collapsing bubbles [41–43]. Those factors favourably affecting cavitation in liquid media generally improve emulsification in terms of a smaller droplet size of the dispersed phase right after disruption. Behrend *et al*. investigated the onset and distribution of cavitation in w/o emulsions using vegetable oil with a semi-continuous approach and a low-volume flow cell [32]. For this purpose, a sequence of pictures were taken with a high-speed camera shortly after the US source was switched on. As can be seen in Fig. 6.6, at 3 ms small bubbles were visible near the emitting surface that propagated downwards into the liquid at a speed of about 1 m/s. The velocity of sound in the system was approximately 1500 m/s (*viz*. roughly three orders of magnitude higher than the velocity of gas bubble propagation). As a result of local cavitation, bubbles are thus generated only in the immediate vicinity of the surface. Under the action of sound, the bubbles are not disrupted as expected because of their small distance from the probe. They are not even significantly deformed, but transported downwards with the liquid flow.

6.3.2. Continuous and discrete ultrasound-assisted emulsification

Ever since the earliest uses of US energy to assist emulsification were reported, many scientists — analytical chemists included — and industrialists have used various types of US devices to make emulsions in a continuous or discrete manner.

Although discrete emulsification can be accomplished with ultrasonic baths, probes are more frequently used for this purpose because they can directly transmit US energy to a liquid–liquid system. Figure 6.7A illustrates a straightforward procedure for obtaining an ultrasonic emulsion. The sonotrode is immersed either into the continuous phase and the phase to be dispersed is gradually added or into the two-phase system while ultrasonic energy is applied. In the latter case, the tip of the probe can be positioned at the interface [44] between the two immiscible liquids or in the continuous (or dispersed) phase, irrespective of their
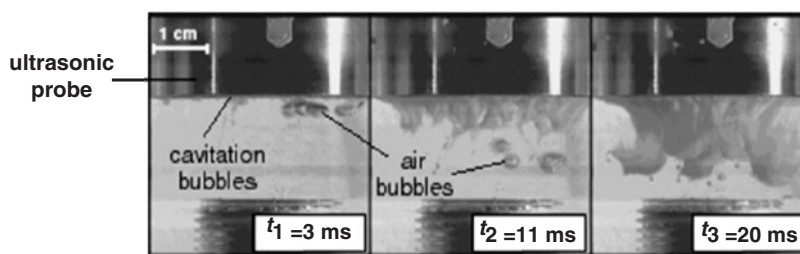

FIGURE 6.6. *Propagation of gas bubbles in sonified vegetable oil. Frame frequency 1000 s^{-1}, velocity of sound in vegetable oil about 1500 m/s. (Reproduced with permission of Elsevier, Ref. [32].)*
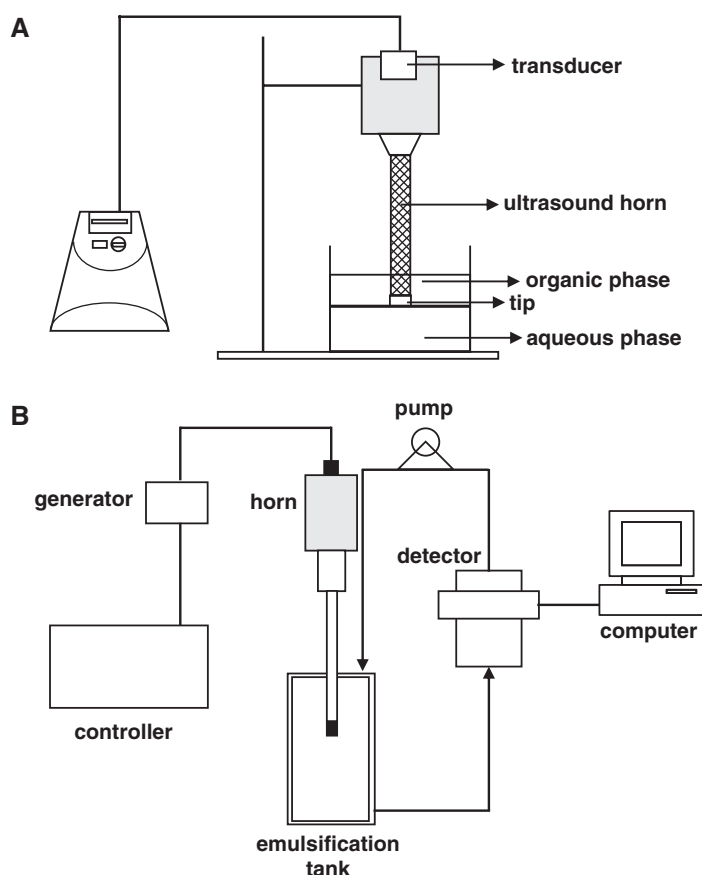
FIGURE 6.7. *Discontinuous approaches for US-assisted emulsification. (A) Production of w/o emulsions. (B) Production and monitoring of emulsions. (Reproduced with permission of Elsevier, Refs. [46,56].)*

organic or aqueous nature [45]. The influence of the sonotrode position, which can be optimized, is discussed in the section dealing with the variables affecting US-assisted emulsification process. Ultrasound-assisted emulsification in discrete systems allows the emulsification process to be monitored by withdrawing small portions of the liquid–liquid system [46] (see Fig. 6.7B). Also, operators do not any require special training. The main shortcoming of discrete emulsification approaches is that large volumes may not be properly emulsified as a result of US intensity in the liquid–liquid system, which rapidly decreases with increasing distance from the ultrasonic emitter. For this reason, many applications require stirring the two-phase system [47]. Thus, discrete approaches are useful for small batches; on the other hand, scale-up is difficult despite the increasing commercial availability of powerful industrial ultrasonic sources. In any case, little research on US emulsification processes with conditions similar to those of industrial practice has been published.

Dynamic US-assisted emulsification can be accomplished in completely continuous and stopped-flow systems. Both use a pre-mixing reservoir circuit in which the two immiscible liquids are pumped, a mixing point and a small reservoir near the flow cell to sonicate the two-phase system. The dimensions and characteristics of the pre-mixing dictate the differences between stopped-flow and continuous approaches (see Figs. 6.8A and B, respectively). Thus, in stopped-flow systems, the pre-mixer is a larger vessel furnished with pressure control. Valve V2 in Fig. 6.8A is closed during the pre-mixing time, so that the two-phase system does not circulate through the dynamic manifold. After pre-mixing, V2 is switched to the open position, the volumetric pump is started and valve V3 is open or closed depending on whether atmospheric pressure or a higher level within the dynamic system is required to facilitate emulsification [48]. In completely continuous approaches, the pre-mixer is a well-stirred glass cell where the two phases merge and are stirred in their way from the inlets to the outlet. The pre-mixing step is particularly important with viscous fluids, which can produce unstable interfacial waves [49]. This step provides a coarse emulsion that can be readily broken up further by ultrasonic energy.

Continuous and stopped-flow emulsification systems are preferred for analytical and non-analytical laboratory work because the liquid volume to be treated is very small. This allows the same ultrasonic intensity to be received throughout the volume, and as a result the efficiency and precision of the emulsification process improved. In addition, continuous stopped-flow emulsification can be coupled to other physical and chemical operations (*e.g.* previous or subsequent steps of the analytical process). Unlike discrete systems, however, dynamic systems do not allow monitoring of the emulsification process. Industrial applications can also exploit continuous and stopped-flow approaches in order to improve the efficiency of the process and connect emulsification to other steps in the production line.

Similar to discrete systems, the most common choice of ultrasonic source in dynamic systems is a probe in direct contact with the two-phase system (see Fig. 6.8A). Alternative choices use one or several ultrasonic transducers and reflectors accommodated in the walls of the manifold tubing. Such is the case with the continuous approach depicted in Fig. 6.8B. This system was reported by Freitas *et al*. [49] and it included an ultrasonic flow cell designed by the authors. The flow cell (Fig. 6.8C) consists of a glass tube of 2 mm inner diameter wrapped in a cylindrical steel jacket. A sonotrode attached to a piezoelectric transducer was welded to the outside wall of the steel jacket for irradiation with US energy. Pressurized water was passed between the glass tube and steel jacket for sound conduction. As noted in Chapter 1, no cavitational effects are produced when a liquid is pressurized above a specific pressure threshold that depends on temperature and the physico-chemical characteristics of the fluid. Above such a pressure (*ca.* 4.5 bar for water in this ultrasonic cell), cavitation in the transmitting water is suppressed and acoustic energy is efficiently transferred *via* the glass tube into the emulsion. When the emulsion is not pressurized, cavitation occurs and droplets are disrupted. The residence time of the emulsion in the ultrasonic field is calculated from the dead volume of the flow cell divided by the corresponding emulsion flow-rate. These ultrasonic flow cells are suitable for uses requiring clean, sterilized equipment such as the emulsification of aseptic processes (*e.g.* pharmaceutical emulsions for the delivery of therapeutic agents, fat emulsions for parenteral nutrition or liposomes). Emulsification with direct sonication is unsuitable for aseptic processes as ions and particles can contaminate emulsion by cavitational abrasion of the sonotrode, which is frequently made of a metal alloy.

Another type of mechanical transducer which is frequently used for emulsification is the liquid whistle. Unlike the more conventional whistle, which operates on gas motion,
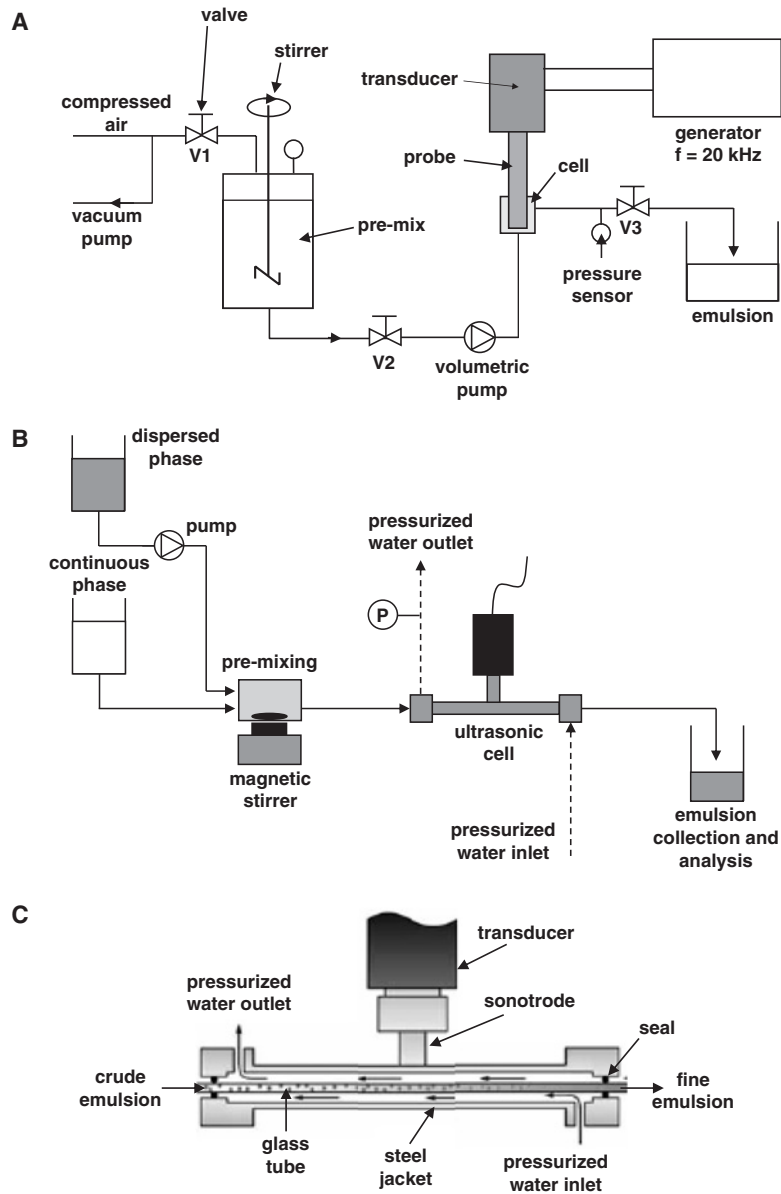
FIGURE 6.8. *Stopped-flow (A) and continuous (B) approaches for US-assisted emulsification. (C) Design of the ultrasonic flow-through cell for continuous US assisted emulsification. (Reproduced with permission of Elsevier, Refs. [37,49].)*
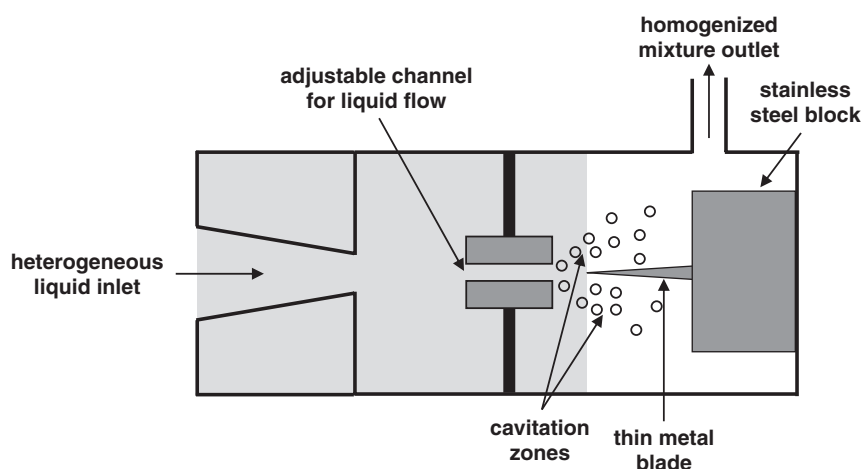
FIGURE 6.9. *Liquid whistle emulsifier. (Reproduced with permission of Elsevier, Ref. [24,50].)*

this device (Fig. 6.9) allows liquid motion to be converted into sound [50]. For this purpose, a liquid is forced at a high speed from a jet across a clamped thin metal blade vibrating at a frequency, which is dependent on the flow rate. The flow is adjusted to obtain ultrasonic frequencies; under these conditions, the liquid undergoes cavitation as it passes across the blade. Similarly, when two immiscible liquids are forced across the blade of the liquid whistle, the resulting cavitational mixing produces extremely efficient emulsification. In liquid whistle devices, the power depends on the medium (by mechanical flow across the blade); by contrast, in the more common sources of US (baths and probes), an external source transfers energy to the medium. The liquid whistle can be used for on-line processing in industrial applications with a large capacity.

Performance of various emulsification approaches

The emulsification efficiency can be measured in various ways. One is based on the ratio between the volume of emulsified dispersed phase, V_e, and the initial volume of the dispersed phase, V_0:

$$E(\%) = \frac{V_e}{V_0} \times 100 \qquad (6.1)$$

In continuous mechanical emulsification systems based on turbulent flow, the power density P_V (*viz.* power dissipated per unit volume of the emulsion) and residence time, t_r, in the dispersing zone have been found to influence the result of emulsification as measured by the mean droplet size $d_{3,2}$ which is called the "Sauter diameter". This dependency is in most cases described by the following expression:

$$d_{3,2} \sim P_v^{-a} \, t_r^{-b}, \qquad (6.2)$$

where the Sauter diameter, $d_{3,2}$, is a measure of the specific interfacial area of the emulsion:

$$d_{3,2} = \frac{\sum n_i d_i^3}{\sum n_i d_i^2} = 6 \cdot \frac{V}{A}$$

(6.3)

where i being the index, n_i the number of droplets in interval i ($d_i \leq d < d_{i+1}$), d_i the mean droplet size in interval i, V the volume of the dispersed phase and A the interfacial area.

Because exponents a and b are often quite similar, their product is used to describe the energy input per unit volume of emulsion (energy density, E_V); such a product can be easily calculated by dividing the total power input, P, by the volume flow-rate V_f of the emulsion:

$$d_{3,2} \sim (P_v t_r)^{-c} = E_V^{-c} = \left(\frac{P}{V_f} \right)^{-c}.$$

(6.4)

This concept of energy density allows one to compare different types of continuous or semi-continuous mechanical emulsification devices in terms of efficiency and is a helpful tool for scaling-up purposes in practical applications.

The Sauter diameter or mean droplet size is also used to compare the efficiency of emulsification process. Comparisons are based on emulsion stability: small diameter corresponds to a stable emulsion.

The efficiency of US-assisted emulsification has been compared with that of other mechanical alternatives in several studies. The most important conclusion is that, with US assistance, the size of emulsions is much smaller than with mechanical agitation under the same conditions; this makes sonicated emulsions more stable. One of these comparative studies was conducted by Behrend *et al*. with a view to prepare oil-in-water emulsions. Ultrasound-assisted emulsification in a semi-continuous approach was compared with various mechanical alternatives, particularly the toothed colloid mill and three high-pressure homogenizers (*viz*. the standard valve, sharpened edge valve and Microfluidizer®). The comparison, illustrated in Fig. 6.10, provided qualitative and quantitative information about the potential of semi-continuous US emulsification in relation to conventional mechanical emulsification systems. The conclusion was that the results of US emulsification are comparable with those of the Microfluidizer® and other highly efficient high-pressure homogenizers such as the sharpened edge valve. These high-pressure systems and membrane emulsification for special purposes are the most efficient choices currently available [32].

Abismaïl *et al*. compared the efficiency of US-assisted emulsification of kerosene-in-water with mechanical agitation, using an Ultra-Turrax system. Ultrasonic emulsification was carried out in a discrete manner. Simple visual inspection revealed longer stability in the ultrasonic emulsions; thus, an identical extent of creaming was observed 6 days after sonication but only 1 day after mechanical emulsification. In addition, measurements of backscattering intensity changes revealed that the main difference was the greater extent of clearing by coalescence at the bottom of the vessel used for mechanical agitation in relation to the sonicated sample [51].

The main drawback of ultrasonic emulsification is the need to take special precautions to avoid surfactant degradation. During sonication, the surfactant accumulates at the interface of cavitation bubbles, where it can be chemically degraded by radicals produced by thermal decomposition of the solvents involved [52]. Water, the most common solvent, produces H and OH radicals [53,54]. In especially problematic situations where surfactant
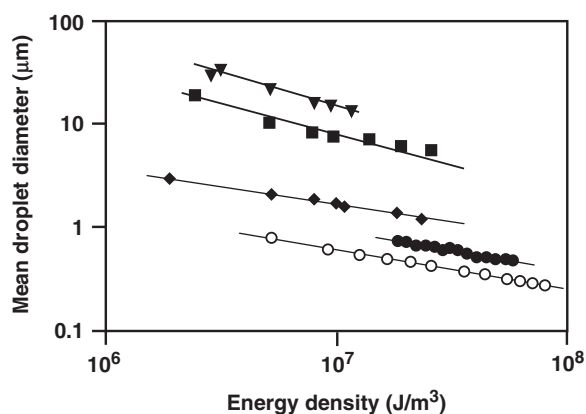
F IGURE 6.10. *Comparison of different mechanical emulsification techniques with US assisted emulsification. (▼) toothed colloid mill, (■) standard valve, (♦) sharpened edge valve, (○) Microfluidizer® and (●) US-assisted emulsification. (Reproduced with permission of Elsevier, Ref. [32].)*

degradation can be anticipated, highly stable acoustic w/o emulsions (with a very low volume fraction of oil) containing no surfactant can be prepared [55].

6.3.3. Variables influencing ultrasound-assisted emulsification

Obtaining highly stable emulsions efficiently entails optimizing a number of variables. Because the applications of emulsions are mainly industrial, processes are first optimized at the laboratory scale and then scaled up for commercial production. The optimization procedure can also be used in analytical applications involving an emulsification operation.

Irradiation power

The irradiation power is an important parameter for US-assisted emulsification; the higher the power is, the higher will be the stability of the resulting emulsion or the lower its Sauter diameter. These relationships were demonstrated by Abismaïl *et al.* [46], who tested variable irradiation powers from 30 to 238 W to prepare o/w emulsions of kerosene-in-water and compared sonication with gentle stirring. As can be seen in Fig. 6.11A, raising the ultrasonic power increased emulsion stability. However, the improvement in stability was negligible above 130 W as the increase in energy was not accompanied by a significant decrease of the Sauter diameter. The only hindrance to the application of a high ultrasonic power in emulsification is the potential degradation of some phase or additive. This is why ultrasonic baths are rarely used for emulsification.

In another study conducted at irradiation power values of 32, 25 and 17 W, reducing the sonication power from 32 to 25 W decreased emulsion stability (the Sauter diameter increased from 0.54 to 0.73 µm). At 32 W, the 10 and 90 percentiles of the droplet size distribution corresponded to 0.26 and 1.88 µm; at 25 W, they corresponded to 0.30 and 3.69 µm. Further reducing the sonication power (to 17 W) provided a highly inhomogeneous
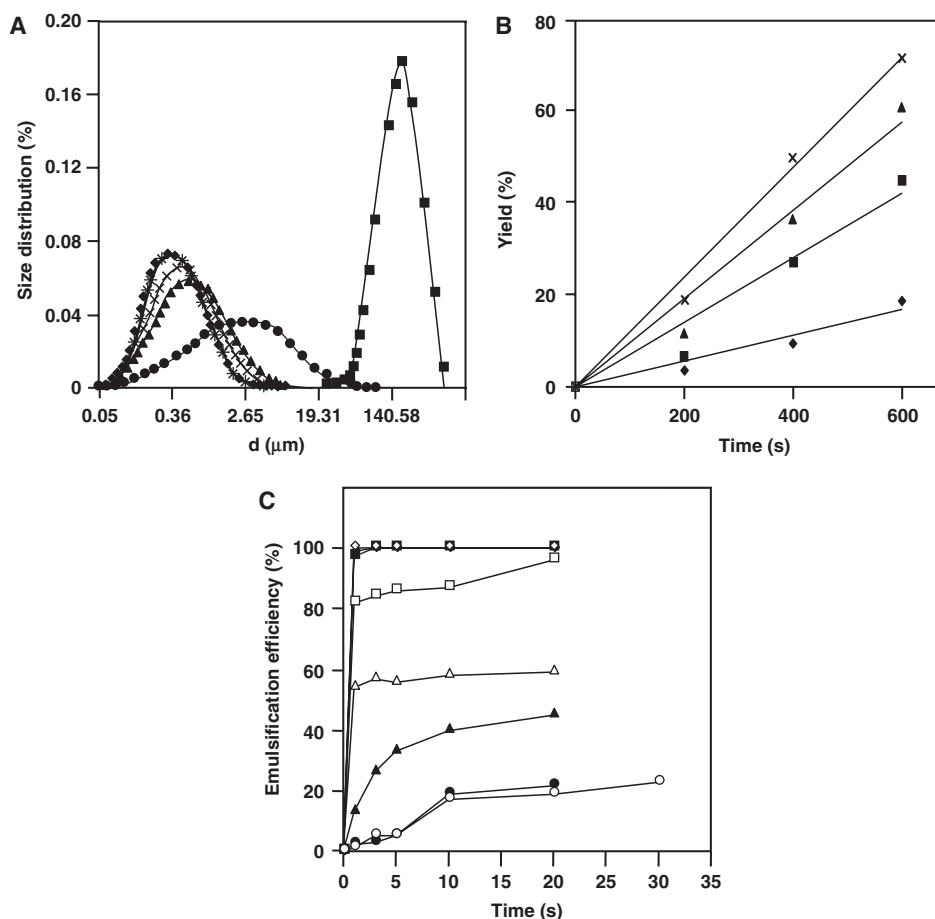
FIGURE 6.11. *(A) Influence of ultrasonic power on drop size distribution and comparison with gentle stirring. (♦) 238 W, (∗) 198 W, (×) 130 W, (▲) 75 W, (●) 30 W and (■) gentle stirring. Conditions: t (irradiation time) = 30 s, C (concentration) = 10 g/l, ϕ (volume ratio of phases) = 0.25 and γ (interfacial tension between kerosene and aqueous solution = 9.5 mN/m). (Reproduced with permission of Elsevier, Ref. [46].) (B) Effect of position of ultrasonic horn on the yield of benzoic acid as a consequence of US-assisted emulsification of methyl benzoate in aqueous sodium hydroxide. (♦) 5 mm from interface into the aqueous layer, (■) at the interface, (▲) 8 mm from interface into the organic layer and (×) 5 mm from interface into the organic layer. Mole ratio of ester to NaOH 1:2 and concentration of NaOH 10% w/w. (Reproduced with permission of Elsevier, Ref. [45].) (C) Influence of tip diameter on the efficiency of US-assisted emulsification at different powers. 19.1 mm: (●) 15 W, (▼) 33 W, (■) 63 W and (♦) 93 W; 12.7 mm: (○) 15 W, (▽) 33 W, (◇) 63 W and (♦) 93 W. (Reproduced with permission of Elsevier, Ref. [56].)*

emulsion with a large number of macroscopically visible droplets larger than 1 mm in size and, so the test was not repeated. Sonication below 17 W failed to produce proper emulsification [49].

Position of the ultrasonic source with respect to the liquid–liquid interface

This is a crucial variable affecting both emulsification and the kinetics of the process. This was demonstrated by Sivakumar *et al*. for the US-assisted emulsification of methyl benzoate in an alkaline aqueous sodium intended to facilitate hydrolysis of the ester [45]. The effect of the position of the ultrasonic horn was examined by keeping the horn in the organic layer, at a distance of 5 or 8 mm from the liquid–liquid interface, right at the interface and in the aqueous layer (at a distance of 5 mm). Figure 6.11B shows the influence of the position of the US source in terms of yield of benzoic acid. As expected, inserting the horn in the aqueous layer (the continuous phase) did not favour emulsification, so the reaction rate and yield were low. This suggests that the primary reason for the increased rate of the biphasic hydrolysis reaction in the presence of US is the generation of very high interface areas for mass transfer as a consequence of the emulsification process. Moving the ultrasonic horn from the interface into the organic layer (the dispersed phase) increased the yield of benzoic acid to a maximum value at a distance of 5 mm from the interface. For this specific case, the US intensity that reached the interface at greater distances from it was severely attenuated by the organic liquid, so the emulsification process became inefficient.

Tip diameter

The influence of this variable was studied by Juang and Lin for the preparation of w/o emulsions of water-in-kerosene at variable ultrasonic power values, particularly, 15, 33, 63 and 93 W [56]. Figure 6.11C compares the emulsification efficiencies obtained by using two horns with different tip diameters (19.1 and 12.7 mm). Differences were small with a high (93 W) or too low (15 W) ultrasonic power. With intermediate power values (33 and 63 W), the differences in emulsification efficiency were highly significant at short irradiation times, but much less at long times. As can be seen in Fig. 6.11C, the horn with the 19.1 mm tip diameter provided high emulsification efficiency in a short time, the efficiency increasing very slightly or remaining constant at longer times. The increase in efficiency with the 12.7 mm tip diameter was more gradual.

Vessel size

The influence of the vessel size in the preparation of emulsions under ultrasonic energy in discrete systems has been established in terms of parameter *R*, which is the ratio of the height of the liquid–liquid mixture in the vessel to the diameter of the vessel. Two cylindrical vessels of different size (specifically with an *R* value of 1 and 2.5) were used under the same working conditions. Similar to the tip diameter, the differences in emulsification efficiency between the two vessels were small at a high (93 W) or very low (15 W) ultrasonic power. On the other hand, at 33 and 63 W, the efficiency was higher for the vessel with *R* = 1 (*viz*. a cylindrical vessel) [56].

Irradiation time

The irradiation time is the period during which ultrasonic energy is applied to the liquid–liquid system. However, this variable must be examined differently in discrete and continuous approaches. For the former, the entire liquid–liquid system is irradiated simultaneously; in continuous and semi-continuous approaches, however, only the portion of volume filling the flow cell is sonicated. Abismaïl *et al.* studied the effect of the irradiation time in preparing o/w emulsions using discrete approaches and compared it with mechanical agitation [46]. As can be seen in Fig. 6.12A, the Sauter diameter decreased with increasing irradiation time; however, the strongest effect was observed within the first 15 s. After 30 s, the slope approached zero. The US technique provided smaller droplet sizes than mechanical agitation by a factor of 3 in all instances.

The residence time is the equivalent parameter for ultrasonic emulsification in continuous and semi-continuous approaches. This parameter can be controlled by varying the flow rate of both the dispersed and continuous phases. In the above-described study of Freitas *et al.* [49], the mean droplet size decreased at longer residence times of the emulsion in the ultrasonic field down to a value beyond which sonication resulted in no further improved emulsification. Thus, the limiting Sauter diameters for 33, 20 and 11% olive oil-in-water emulsions under ultrasonic energy were found to be 0.65, 0.50 and 0.47 µm, respectively. At a fixed residence time, the droplet size of the emulsion medium increased with increasing oil content. Thus, the droplet size of an 11% olive oil-in-water emulsion varied over the range 0.30–2.98, 0.24–1.67 and 0.23–1.39 µm at a residence time of 7, 14 and 28 s, respectively. Also, consistent with previous studies [37,47,51], droplet size decreased with increasing sonication power and residence time. Increasing both variables increases the amount of energy that is transferred to the emulsion and also the intensity of cavitation events, thereby resulting in more effective droplet size reduction. However, there exists an optimal power input above which coalescence prevails and re-increases droplet diameter [57]. The way the droplet size distribution changes when both sonication power and residence time are increased depends on the susceptibility of the larger droplets to breaking by cavitation as the smaller droplets are more resistant or even stable. Increasing the number of cavitation events by increasing either the power or residence time mainly affects the larger oil droplets and causes accumulation of fine droplets.

Volume ratio of phases

The volume ratio of the dispersed phase to the continuous phase, ϕ, is another key variable in the preparation of emulsions. Juang and Lin studied the effect of this variable in the w/o model of water-in-kerosene by changing this ratio from 1 to 10 at a constant volume of aqueous phase [56]. Figure 6.12B shows the influence of volume ratio on the emulsification efficiencies obtained at a constant ultrasonic power of 93 W. As expected, the emulsification efficiency increased with decreasing ϕ_W. However, it was relatively low (about 80%) at $\phi_W = 4$ and decreased markedly at higher ratios. This was a result of the amount of organic phase not being large enough to enclose the whole dispersed phase. Some authors have established a threshold ratio that depends mainly on the composition of the organic phase.

At a certain volume ratio between the phases, the dispersed phase is converted into the continuous phase and *vice versa*. In the water/kerosene/polyethoxylated sorbitan monostearate system, when this phenomenon, which is known as "phase inversion", occurs identical volumes of both phases are used to obtain o/w emulsions with an US horn at 20 kHz [51].
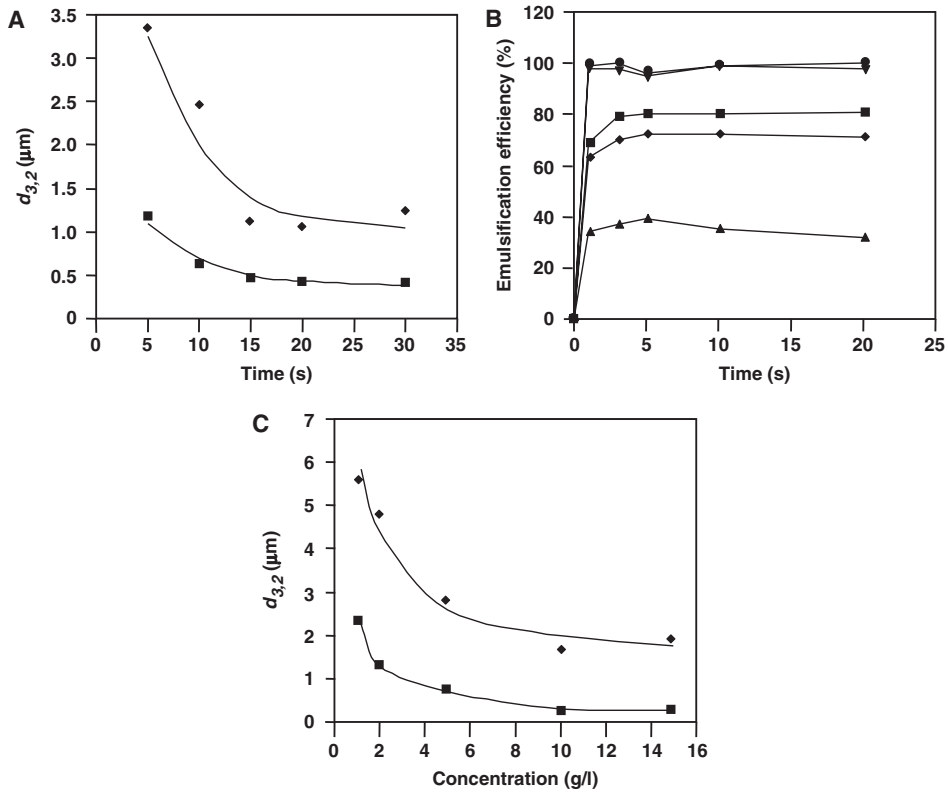
FIGURE 6.12. *(A) Variation of the Sauter diameter $d_{3,2}$ with the irradiation time. (♦) mechanical agitation and (■) US-assisted emulsification. C (concentration) = 10 g/l, ϕ (volume ratio of phases) = 0.25, P_{ma} = 170 W and P_{US} = 130 W. (Reproduced with permission of Elsevier, Ref. [51].) (B) Influence of the volume ratio on the efficiency of US-assisted emulsification. (●) ϕ = 1, (▼) ϕ = 2, (■) ϕ = 4, (♦) ϕ = 8 and (▲) ϕ = 10. P = 93 W, volume of aqueous phase = 100 ml and C_S (surfactant concentration) = 3%. (Reproduced with permission of Elsevier, Ref. [56].) (C) Variation of the Sauter diameter d_{32} with the surfactant concentration. (♦) mechanical agitation and (■) US-assisted emulsification. t = 30 s, ϕ = 0.25, P_{ma} = 170 W and P_{US} = 130 W. (Reproduced with permission of Elsevier, Ref. [51].)*

Viscosity

The viscosity of a liquid has been reported to affect the onset of acoustic cavitation. Viscosity is a qualitative measure of molecular interaction in a liquid. The higher the viscosity is, the higher are the attractive forces between the molecules and hence, the higher is the threshold intensity of US where cavitation starts. Based on experimental evidence, Briggs *et al*. [58] developed a quantitative relation between liquid viscosity η and the experimental value of the cohesive pressure p_{co}, which is defined as the difference between the hydrostatic pressure p_O — which coincides with ambient pressure when no

external pressure is applied — and the threshold pressure p_{th} for the onset of cavitation. Cohesive pressure describes the resistance of the liquid to the formation of cavities through expansion.

A study on the influence of the viscosity of the dispersed phase in the preparation of emulsions of vegetable oils (olive, soyabean and linseed) in water with US assistance revealed that replacing the oil with the highest viscosity and interfacial tension — olive oil — with soyabean oil, which has slightly lower viscosity and interfacial tension, caused virtually no reduction in droplet size. Linseed oil, with much lower viscosity and interfacial tension than olive oil, exhibited a much smaller Sauter diameter than the latter (*viz.* 0.47 µm *versus* 0.62 µm). Breaking low-viscosity droplets requires less vigorous cavitation shock waves than breaking more viscous ones [49].

The effect of the viscosity of the continuous phase was studied theoretically in o/w emulsions containing water-soluble stabilizers and also in w/o emulsions of various oils [32]. In the former, droplets were larger in the absence of a stabilizer than in its presence. However, there was no clear-cut correlation of the viscosity of the continuous phase with droplet size. This can be ascribed to the increased amount of energy dissipated in the immediate vicinity of the droplets relative to the bulk liquid, which may result in more efficient disruption than if the energy dissipation occurs evenly throughout the continuous phase. The addition of a stabilizer possibly alters and partly suppresses cavitation in the bulk liquid, the cavitation threshold and viscosity being related similarly as in pure liquids [58]. The energy may subsequently dissipate preferentially at the surface of droplets and result in more efficient use in terms of droplet disruption.

A study of w/o emulsions consisting of various oils revealed that the viscosity of the continuous phase could be changed by about three orders of magnitude without the need for additional soluble components. This study was conducted at a variable energy density. In all cases, the mean droplet size was found to decrease with increasing energy density. At low ratios (about 1%) of the dispersed-to-continuous phase, the viscosity of the continuous phase had little influence on droplet size at a constant energy density. Under these conditions, the emulsification efficiency was found to depend solely on the amount of energy per volume dissipated by cavitation. Also, physical liquid properties proved less important relative to pure liquids as a result of dispersed particles acting as "weak spots" in the system. The droplet sizes of the emulsions of the less viscous oils containing about 10 and 1% water were similar. The droplets of the emulsions of the highly viscous oils were slightly larger; however, their Sauter diameters were still below 1 µm.

At a constant energy density, droplet disruption is not expected to depend on the viscosity of the continuous phase. However, coalescence is especially significant at high water contents. The effect may be stronger in the more viscous oils as small droplets will separate more slowly, shortly after disruption, thus increasing contact times and hence the likelihood of coalescence [32].

Further research is needed on the influence of the viscosity of the continuous phase on US emulsification with a view to assess the significance of cavitation as a droplet disruption mechanism.

Surfactant concentration

The emulsification efficiency can be increased by increasing surfactant concentration in the medium; in fact, emulsion droplets find it difficult to disperse and tend to grow large at low concentrations of surfactant. Figure 6.12C shows the variation of droplet size (expressed as the Sauter diameter, $d_{3,2}$) in a w/o water-in-kerosene emulsion at variable

surfactant concentrations [51]. As can be seen, $d_{3,2}$ decreased significantly with increasing surfactant concentration up to a specific value (6% in this case). Surfactants are known to form an adsorbed monolayer onto the emulsion droplets. At surfactant concentrations below 6%, the transient interface was incompletely covered, so droplets coalesced and resulted in higher $d_{3,2}$ values. At surfactant concentrations above 6%, $d_{3,2}$ decreased only slightly, as it does in other systems. This can be ascribed to the excess surfactant or micelles being adsorbed onto the surface of the emulsion droplets and causing the droplets to coalesce [56].

Hydrostatic pressure

Cavitation in a high-intensity ultrasound field is the controlling mechanism of energy dissipation. The ambient pressure created by the pressure amplitude of the US wave may have two different effects on the magnitude of the cavitational effects. First, as stated in Chapter 1, applying an external pressure raises the cavitation threshold. However, the intensity of cavitation collapse produced by bubbles increases with increasing ambient pressure. Behrend and Schubert studied the influence of the hydrostatic pressure on emulsification using vegetable oil-in-water emulsions as model systems in a semi-continuous approach [37]. For this purpose, emulsions were processed at a constant flow-rate and variable pressures. They found droplet size to increase with increasing pressure and ascribed it to partial suppression of cavitation in the system. These authors also used variable energy densities. The highest energy densities were obtained at moderate pressure, where cavitation intensities peaked. No clear-cut effect of the hydrostatic pressure in the system was observed at a constant energy density. Therefore, the application of an external pressure may neither influence the magnitude of cavitational effects per unit volume, nor the intensity of cavitation collapse, the effect on droplet disruption depends on the particular experimental range.

Dissolved gas

The effect of the presence of dissolved or dispersed gas in a sonicated liquid on ultrasound-induced cavitation is well documented. Some authors deem the dissolved gas indispensable for cavitational effects to occur as gas molecules or microbubbles provide the basis for bubble formation and growth. However, a higher content of gas in the liquid will increase the gas–vapour ratio inside the bubbles. By virtue of its dissolution kinetics, the gas acts as a buffer, cushioning bubble collapse and reducing shock wave intensity as a result. Behrend and Schubert studied the effect of the gas content in the liquid and found the highest energy densities to be exhibited by the non-pretreated system. Both degassing and gas saturation led to reduced peak energy intensities. However, similar to external pressure, the gas content has no clear-cut effect on the droplet disruption at a constant energy density [37].

6.3.4. Applications of ultrasound-assisted emulsification

For the interest of analytical chemists, a large number of methods have been developed where ultrasonic emulsification is a key step in the determination of the target analytes. Most such methods are concerned with the determination of metallic elements in liquid

samples by the use of an atomic detector. Ultrasonic emulsification can be implemented in two ways in the analytical process depending on the sample composition: organic or aqueous. Organic samples require previous LLE as direct analysis with atomic detectors can pose problems such as the following facts: (1) calibrating with aqueous standards is inappropriate and dissolving metal in organic solvents can be difficult; (2) evaporation of the organic solvent can alter analyte concentrations; (3) some system components such as nebulizers can wear or clog; (4) sample insertion into graphite furnace is poorly reproducible; and (5) losses of plasma ionization power in ICP can turn it off. One effective alternative is emulsification of the organic sample with an aqueous phase containing an acid or a ligand, as the method of Murillo *et al*. [59], who determined Mg, Ca and Zn in organic matrices such as lubricating oils with ultrasonic emulsification of the sample in water containing ethoxy nonylphenol as a surfactant. After emulsification, the analytes were determined by ICP-AES with RSDs between 3 and 5%. The aqueous phase should not contain any strong oxidants in order to avoid decomposition of the organic phase; thus, Wang *et al*. found mixing the organic phase with a powerful oxidant such as concentrated nitric acid as aqueous phase caused sample digestion [60].

Ultrasound-assisted emulsification in aqueous samples is the basis for the so-called "liquid membrane process" (LMP). This has been used mostly for the concentration and separation of metallic elements or other species such as weak acids and bases, hydrocarbons, gas mixtures and biologically important compounds such as amino acids [61–64]. LMP has aroused much interest as an alternative to conventional LLE. An LMP involves the previous preparation of the emulsion and its addition to the aqueous liquid sample. In this way, the continuous phase acts as a membrane between both the aqueous phases (*viz*. those constituting the droplets and the sample). The separation principle is the diffusion of the target analytes from the sample to the droplets of the dispersed phase through the continuous phase. In comparison to conventional LLE, the emulsion-based method always affords easier, faster extraction and separation of the extract — which is sometimes mandatory in order to remove interferences from the organic solvents prior to detection. The formation and destruction of o/w or w/o emulsions by sonication have proved an effective method for extracting target species.

LMP has been used for trace analysis by impregnation of emulsion globules with chelating agents, as in the determination of traces of cobalt, nickel and copper from a previously dissolved aluminium matrix [65]. A water-in-oil emulsion was prepared with diluted hydrochloric acid as a dispersed phase, thenoyltrifluoroacetone as a chelating agent, Span-80 as a non-ionic surfactant and toluene as a continuous phase. The mixture was sonicated and the resulting emulsion added to 25 ml of sample solution and dispersed by stirring as tiny globules. Traces of heavy metals diffused through the toluene layer into the small droplets of hydrochloric acid encapsulated into the emulsion. This method was also used to determine metallic elements in sea water. An oxine-impregnated emulsion was prepared by dissolving the oxine and a non-ionic surfactant (Span-80) in toluene as a continuous phase, which was mixed by sonication with diluted hydrochloric acid. The water-in-oil emulsion was added to the water sample and dispersed as numerous small globules (0.1–0.5 mm in diameter) by stirring for 10 min. The metallic elements diffused through the toluene layer into the small droplets of hydrochloric acid. After collection, the tiny globules were demulsified by flotation and heating to separate the aqueous and organic phases while metals remained in the aqueous phase and were determined by atomic absorption spectrometry. In this way, a preconcentration factor of 100 was obtained [66].

One salient advantage of LMP is that it affords discrimination between different species of a given element by using emulsions containing a surfactant. This has been demonstrated

for copper and iron in river water [67,68]. Iron is the most abundant heavy metal in river water; its most usual oxidation state, Fe(III), reacts with coexisting organic and inorganic matter to form complicated colloidal and suspended particles. The chemical speciation of iron aided by emulsion globules is based on discriminating between collectable species and those which do not penetrate into the emulsion globules. Collectable species include hydrated iron(III) oxide of size smaller than 1 μm and, if present, hydroxo complexes and hydrated ions. On the other hand, non-collectable species include humic complexes, hybrid particles of hydrated Fe(III) oxide and humic substances, as well as suspended solids in particle sizes higher than 1 μm. This discrimination ability can be attributed to the surfactant layer at the oil–water interface. The method was compared with the conventional LLE, which provides no such selectivity because all Fe(III) species are extracted simultaneously into the organic phase under vigorous shaking. This example testifies to the ability of emulsion globules to discriminate physico-chemical forms of trace elements.

Ultrasonic-assisted emulsification is commonplace in the pharmaceutical, cosmetic, food, chemical and other industries. The target process is first studied at the laboratory scale in order to maximize emulsification efficiency at the lowest possible cost. To this end, analytical methods are frequently developed to examine the influence of variables or new ultrasonic emulsifiers tested for this purpose. When favourable results are obtained, the process is scaled-up to industrial level.

Ultrasonic emulsification can be used in different situations ranging from normal conditions to others requiring manufacturing equipment that can be readily cleaned and sterilized. This is especially important in the food or pharmaceutical fields, where the use of ultrasonic processing systems with aseptic production is indispensable with a view to avoid product contamination. New ultrasonic processing systems are continuously designed for this purpose [49].

The pharmaceutical field is among those most widely exploiting ultrasonic emulsification (mainly for the preparation of emulsion-based drugs). Thus, US emulsification has been recently used to prepare biodegradable nanoparticles that can in turn be used to obtain drug-loaded biodegradable microspheres. The method involves ultrasonic emulsification in a continuous flow system to obtain suspended nanoparticles, followed by collection of the particles, solvent extraction and evaporation [49].

Ultrasound has also been employed to obtain non-aqueous emulsions, which are of great interest for non-analytical applications such as the preparation of sol–gels with hydrolysable metal alkoxides in organized media, or the incorporation of hydrolysable drugs. Analytical applications in which the presence of water is undesirable can also take advantage of non-aqueous emulsions. These emulsions may be of pharmaceutical or cosmetic interest if they are primarily composed of edible and non-toxic ingredients; also, they can be formulated to exhibit a wide range of physical properties. Potential uses are as topical dermatological bases — particularly for labile drugs — as emollient bases for cosmetic preparations and as nutrient preparations. Stable non-aqueous emulsions can be obtained in two general ways. One involves surfactants consisting of two incompatible blocks selectively soluble in each of the immiscible liquids. Thus, diblock copolymers of polystyrene and polyisoprene can stabilize DMF/hexane emulsions for almost 24 h [69]. The main drawback of this approach is the need to develop new surfactants tailored to the particular liquid combination. The other choice is to find an appropriate oil-immiscible polar liquid that can substantially replace water as a surfactant solvent. A liquid capable of replacing water in an emulsion should possess an appreciable polarity to make it immiscible with oils and a good solvent for the solvophilic part of the surfactant molecules [70].

6.4.   JOINT USE OF ULTRASOUND AND LIPOSOMES: AN ANALYTICAL TOOL

Liposomes are spherical vesicles formed by the aggregation of amphiphilic phospholipid molecules in a bilayer structure. Liposome formation occurs when phospholipids are dispersed into an aqueous medium — usually water — as a result of interactions between phospholipids and water. Thus, liposomes encapsulate part of the aqueous medium in which they are suspended. The amphiphilic character of phospholipids allows them to form closed structures where hydrophobic and (or) hydrophilic molecules can be entrapped or anchored.

Liposomes occur in nature, but can also be easily synthesized in the laboratory. Depending on the preparation method used, which influences their size — in relation to the number of bilayer shells — and physical properties, liposomes are classified as small unilamellar vesicles (SUVs, 25–50 nm), large unilamellar vesicles (LUVs, 100 nm to 1 μm), giant unilamellar vesicles (GUVs, 1.0–200 μm) multilamellar vesicles (MLVs, 0.1–15 μm), and multi-vesicular vesicles (MVVs, 1.6–10.5 μm); the last consists of several small vesicles. Bicelles, which contain surfactant molecules in the lipid bilayer, constitute a special type of liposome.

The mechanical and chemical properties of liposomes can be altered by incorporating a great variety of compounds into their structure. Thus, hydrophilic molecules can be entrapped in the aqueous cavity, hydrophobic molecules can be entrapped within the organic chains of the bilayer and amphiphilic compounds can be anchored to the polar head groups or inserted into the organic chains depending on the particular functional group.

The nature and properties of liposomes are directly related to the preparation method used (specifically, to the phospholipid composition) and on the presence of other chemical species in the liposome structure. Thus, mixtures of egg phosphatidylcholine are primarily used by virtue of their low cost and neutral charge; other neutral phospholipids such as sphingomyelin and phosphatidylethanolamine are also frequently used. Charged liposomes can be prepared by the addition of negatively charged amphiphiles (*e.g.* diacetylphosphate, phosphatidyldiglycerol, phosphatidic acid, phosphatidylserine, polymers and DNA) or positively charged amphiphiles (*e.g.* stearylamine, sphingosine). Cholesterol, which is naturally present in biological membranes, is frequently used to synthesize liposomes. The inclusion of cholesterol in liposomes plays a prominent role in controlling the fluidity and permeability of the artificial vesicles.

Liposomes have aroused interest in a great variety of areas from biochemistry and molecular biology to cosmetics and food technology. One of the most salient applications of liposomes has been promoted by their high similarity to natural cell membranes, for which they are extensively used as substitutes in medical and pharmaceutical research. Since their inception, liposomes have often been used as models for studying the nature of cell membranes, the structure and functions of which they can mimic quite closely. One example is the determination of membrane distribution coefficients of drugs with a view to estimate their ability to penetrate cells. Interactions between analytes and phospholipid membranes depend on the characteristics of both the analytes and the membrane.

Liposomes can play two different roles in analytical chemistry [71]:

(1) as target analytes or matrices for the target analytes, and
(2) as analytical tools for some step in the analytical process.

Liposomes and their constituents have been determined as target analytes by using current analytical techniques — usually, they require some separation. Some liposomal

determinations have exploited the advantages of US energy discussed at length in Chapters 3–8. Typical examples include the determination of phosphatidylcholine in liposome suspensions using ICP-AES with an ultrasonic nebulizer [72] and that of the phospholipid–lipophilic compound ratio in liposomes by thin-layer chromatography scanning densitometry — which involves US-assisted preliminary extraction [73].

This section focuses mainly on the use of liposomes as analytical tools as these aggregates — the formation of which can be greatly favoured by US — can play major roles towards improving analytical properties such as sensitivity and selectivity in some analytical steps. The increased sensitivity achieved normally results from their ability to amplify signals; such is the case with fluorescent liposomes in fluorescence-based immunoassays [74–76]. Concerning selectivity, liposomes are frequently used as transport devices or active phases in separations. In both cases, the experience acquired in other research areas has been exploited in the analytical field. Ultrasound has also been used in combination with liposomes to increase the efficiency of analytical steps involving their presence. Applications in this area range from the preparation of liposomes or encapsulation of various types of compounds in the liposome structure to special processes in which US enhances the actuation of liposomes.

6.4.1. Ultrasound-assisted liposome preparation

There are various methods for preparing liposomes in different sizes, membrane compositions and layer structures. Their outcome is greatly influenced by the particular treatment and temperature used to form the liposomes. Temperature is an essential parameter in dealing with both liposomes and with biological membranes. Membrane bilayers exist in a fluid state above the main phase-transition temperature (T_m) and in a well-ordered gel state below T_m. Under normal conditions (*i.e.* at body temperature), biological membranes will be generally in a fluid state. The phase-transition temperature of the phospholipids depends on variables such as the length of the acyl chains, degree of saturation, structure of the polar head group and water content.

Although liposomes can form spontaneously, they are rarely thermodynamically stable, so they usually require some auxiliary energy such as mechanical agitation, electric energy, US or combination of mechanical treatments. The main advantage of US assistance here is that it does not raise the temperature significantly. Ultrasonic energy has been used to assist the two most common methods of liposome preparation, namely:

(1) The reversed-phase evaporation method, in which the lipids are previously dissolved in an organic solvent (usually chloroform). The solvent is evaporated and the lipid residue dissolved in ethyl ether. Then, an aqueous electrolyte solution (*e.g.* Tris/HCl buffer at pH 7.8) is added and the solution purged with He. After sonication for 5 min at 20°C under a He atmosphere, the organic solvent is evaporated until the mixture becomes a gel-like suspension. Each individual step of the production process requires appropriate optimization (sonication included). This method was used to prepare liposomes containing sulphorhodamine B and labelled with atrazine; it provided reproducible LUVs of diameter 654 ± 109 nm [77]. Also, liposomes thus prepared were used to determine alachlor in environmental samples by immunoanalysis [78]. For this purpose, samples were mixed with dipalmitoyl phosphatidylethanolamine using *N*-succinimidyl-*S*-acetylthioacetate. The mixture, where the alachlor was covalently bonded to the lipids, was then dissolved in a non-specified organic solvent. After sonication and removal of the organic solvent, the liposome suspension was reacted

with potassium ferrocyanide, filtered, gel filtered and, finally, dialysed to proceed with the analytical process.

(2) The dry lipid film method, which involves dissolving the lipids in an organic solvent (usually chloroform). The solvent is removed by evaporation under an argon atmosphere in a 50°C water bath with constant rotation until a thin film of lipids was formed on the recipient walls. The resulting lipid film is then placed in a desiccator under vacuum for complete drying. Next, the lipid film is rehydrated and the resultant dispersion sonicated until the mean size of the liposomes reaches the desired value. Liposomes are then frozen at –70°C, lyophilized and finally stored at 4°C or used immediately. This method has been frequently used for the production of acoustically active liposomes, the uses of which are discussed in the application section, and the encapsulation of substances (usually by rehydration with a solution of the compound concerned). In combination with mannitol and an intermediate sonication step, it provided excellent results in the encapsulation of a hydrophilic solute such as calcein [79]; the encapsulation efficiency, about 15%, was significantly improved (up to 20%) by increasing the number of freeze–thaw cycles. The method has also been used to prepare antibody-conjugated liposomes using a phospholipid containing a maleimide group in the liposomes for conjugation to the antibodies [80].

6.4.2. Ultrasound-assisted applications of liposomes

Interest in analytical uses of liposomes is growing steadily as shown by the publication of large number of articles on this topic [71,81]. Applications have used various techniques including liquid chromatography, capillary electrophoresis, immunoassay and sensors. The results warrant some interesting conclusions from the bioanalytical, medical and pharmaceutical points of view.

Those analytical systems where liposomes are used as artificial cell membranes to study body distribution mechanisms as efficient drug-delivery systems, controlled drug delivery, the synthesis of new biomaterial for tissue engineering and gene therapy are worthy of special mention.

Ultrasound-assisted preparation of liposome-based sensors

Immobilizing a sensing reagent in the host matrix of an optochemical sensor greatly affects its stability. Immobilization by the formation of covalent bonds between the sensing reagent and the support is usually the preferred method because it avoids leakage of dye molecules from the host matrix [82,83]. The presence of an appropriate functional group in the sensing reagent is indispensable for covalent immobilization. Thus, if functionalization is required, the structural and spectral properties of the sensing reagent may be altered. Physical immobilization of the sensing reagent overcomes these shortcomings; however, dye leakage and functionalization problems decrease sensor stability [84]. Alternatively, the sensing reagent can be encapsulated in the internal compartment of liposomes, usually entrapped in a sol–gel film (which is extensively used as a matrix for fluorescence sensors [85,86]). Sol–gel supports have some advantages including mechanical and chemical stability, lack of spectral interferences, minimal quenching of fluorescence reagents and ease of fabrication.

Ultrasound can play a prominent role in the preparation of sensors such as that developed by Nguyen *et al.* [87], which required sonication of a mixture of tetramethylorthosilicate,

water and 0.1 N HCl for 2 h to make it clear, colourless and monophasic. The ensuing solution was stored at –20°C for 7 days to ensure complete hydrolysis of the unreacted silicate. Then, it was mixed with the liposomes encapsulating the sensing reagent until gelation. This procedure is effective in preventing dye leakage and increasing the chemical stability of sol–gel-based optochemical sensors. Encapsulating water-soluble fluorescent dyes in liposomes is easy; also, the presence of conjugating functional groups is not necessary. A pH sensor obtained with this immobilization method is more stable than those prepared by physical immobilization. The method has also been used to immobilize liposome-encapsulated enzymes in sol–gel matrices for the preparation of biosensors [88].

The two previous examples testify to the effectiveness of US for liposome preparation without degradation problems. Its advantages can be extended to other analytical techniques such as liquid chromatography and capillary electrophoresis, where US can help in the immobilization of liposomes to be used as stationary phases.

Other fields of application of ultrasound-assisted formation of liposomes

The similarity of liposome structure to cell membranes has promoted a large number of studies in various fields. The analytical chemist can also exploit the characteristics of liposomes to develop new analytical methods or contribute to expand their use in other fields such as medicine, pharmaceutics or biochemistry.

One open field for liposome application where US plays a crucial role is as vehicles for carrying compounds. Thus, liposomes have been explored as non-toxic, biodegradable and non-immunogenic drug-delivery vehicles. They are suitable for delivering both hydrophilic and lipophilic drugs. When a drug is incorporated into liposomes, its pharmacokinetics is markedly changed; as a result, its systemic toxicity is lowered and its premature degradation or inactivation reduced [89]. Ideally, liposomes are able to carry an appropriate drug dose, remain stable in circulation and then release their drug contents up to a relatively high concentration in order to exert its intended therapeutic effect at the target site. In order to deliver a high local dose, triggerable release would be desirable. However, few triggering procedures have so far been reported; all are based on the application of electric or magnetic fields, variations of temperature or pH and irradiation with ultrasonic energy. Some advantages such as its non-invasive character and the ability to penetrate into the body make US an interesting choice for controlled release applications. In addition, US can be focused on targeted sites and increase the permeability of blood–tissue barriers and cell membranes [90].

One requirement for liposomes to respond to US stimulation is the presence of a US-sensitive vehicle. Thus, early research showed that acoustically active liposomes can be used as contrast agents for US image enhancement [91]. Also, subsequent studies revealed that such liposomes encapsulate air — which is responsible for their acoustic activity — in their structure [92]. These acoustically active liposomes have the potential to carry drugs and their acoustic activity allows them to respond to US stimulation by releasing their contents.

The effect of US on content release is attributed to the rarefaction phase of the sound wave. Thus, when the negative US wave impinges upon the liposomes, the air pocket expands and stresses the bounding monolayers and also those in the adjacent bilayer. If the pressure drop is large enough, then the stress exceeds the elastic limit of the weakest surface and, at some point, either the bilayer or the monolayer rends. When the integrity of the vesicle is lost, some or all contents are released. If the air in the pocket is expanded faster than it is diffused to the external aqueous phase, then, the monolayer

or bilayer reaches the lysis threshold and most liposomes release some contents. The ultrasonic frequency used for the delivery of compounds is about 1–2 MHz [79].

Similar to drugs, liposomes could be conjugated with antibodies, peptides and genes, among others, to expand the existing range of analytical and non-analytical applications of US.

References

1. R. Cela, R.A. Lorenzo and M.C. Casais, *Técnicas de Separación en Química Analítica*, Editorial Síntesis, Madrid, 2002.
2. M. Valcárcel and M.D. Luque de Castro, *Non-chromatographic Continuous Separation Techniques*, Royal Society of Chemistry, Cambridge, 1991.
3. C. Cocito, G. Gaetano and C. Delfini, *Food Chem.*, 5 (1995) 311.
4. D. Hernanz Vila, F.J. Heredia Mira, R. Beltrán Lucena and M.A. Fernández Recamales, *Talanta*, 50 (1999) 413.
5. E. Gómez-Plaza, R. Gil-Muñoz, J. Carreño-Espín, J.A. Fernández-López and A. Martínez-Cutillas, *Eur. Food. Res. Technol.*, 209 (1999) 257.
6. I. Caldeira, R. Pereira, M.C. Clímaco, A.P. Belchior and R.B. de Sousa, *Anal. Chim. Acta*, 513 (2004) 125.
7. R.M. Peña, J. Barciela, C. Herrero and S. García-Martín, *Talanta*, 67 (2005) 129.
8. E. Alissandrakis, D. Daferera, P.A. Tarantilis, M. Polissiou and P.C. Harizanis, *Food Chem.*, 82 (2003) 575.
9. I. Rezic, A.J.M. Horvat, S. Babic and M. Kastelan-Macan, *Ultrason. Sonochem.*, 12 (2005) 477.
10. Q. Tu, J. Qian and W. Frech, *J. Anal. At. Spectrom.*, 15 (2000) 1583.
11. G.B. Nickerson and S.T. Likens, *J. Chromatogr. A*, 21 (1966) 1.
12. M.D. Luque de Castro and J.L. Luque García, *Acceleration and Automation of Solid Sample Treatment*, Elsevier, Amsterdam, 2002.
13. A.J. Wain, N.S. Lawrence, J. Davis and R.G. Compton, *Analyst*, 127 (2002) 8.
14. A. González Casado, E.J. Alonso Hernández and J.L. Vílchez, *Water Res.*, 32 (1998) 3168.
15. J.L. Capelo, C.D. dos Reis, C. Maduro and A. Mota, *Talanta*, 64 (2004) 217.
16. J. Ruiz-Jiménez and M.D. Luque de Castro, *Anal. Chim. Acta*, 489 (2003) 1.
17. F. Priego-Capote and M.D. Luque de Castro, *Anal. Chim. Acta*, 489 (2003) 223.
18. P. Linares, F. Lázaro, M.D. Luque de Castro and M. Valcárcel, *Anal. Chim. Acta*, 200 (1987) 51.
19. M. Agudo, A. Ríos and M. Valcárcel, *Analyst*, 119 (1994) 2097.
20. J.M. López-Fernández, A. Ríos and M. Valcárcel, *Fresenius J. Anal. Chem.*, 356 (1996) 49.
21. F. Ortiz-Boyer, J.A. García-Mesa and M.D. Luque de Castro, *Anal. Chem.*, 66 (1994) 2794.
22. F. Cañete, A. Ríos, M.D. Luque de Castro and M. Valcárcel, *Anal. Chem.*, 60 (1988) 2354.
23. J.A. García-Mesa, P. Linares, M.D. Luque de Castro and M. Valcárcel, *Anal. Chim. Acta*, 235 (1990) 441.
24. T.J. Mason, L. Paniwnyk and J.P. Lorimer, *Ultrason. Sonochem.*, 3 (1996) S253.
25. H. Wu, G.J. Hulbert and J.R. Mount, *Innov. Food Sci. Emerging Technol.*, 1 (2001) 211.
26. A.M. Noubhani, W. Dieryck, S. Chevalier and X. Santarelli, *J. Chromatogr.*, 968 (2002) 113.
27. I. Caraballo, M. Millán, A. Fini, L. Rodríguez and C. Cavallari, *J. Control. Release*, 69 (2000) 345.
28. P. Becher, *Emulsions, Theory and Practice*, Reinhold, New York, 1965.
29. S.E. Friberg and S. Jones, Kirk-Othmer *Encyclopedia of Chemical Technology*, vol. 9, Wiley, New York, 1994.
30. P. Becher, *J. Disp. Sci. Technol.*, 5 (1985) 81.
31. J.C. Johnson, *Emulsifiers and Emulsifying Techniques*, Noyes Data, Park Ridge, NJ, 1979.
32. O. Behrend, K. Ax and H. Schubert, *Ultrason. Sonochem.*, 7 (2000) 77.
33. P. Walstra, *Chem. Eng. Sci.*, 48 (1993) 333.
34. H. Karbstein, *Untersuchungen zum Herstellen und Stabilisieren von Öil-in-Wasser-Emulsionen*, PhD Thesis, University of Karlsruhe, Germany, 1994.

35. Z. Haque and J. Kinsella, *J. Food Sci.*, 54 (1989) 39.
36. U. Einhorn-Stoll, M. Weiss and H. Kunzek, *Nahrung*, 46 (2002) 294.
37. O. Behrend and H. Schubert, *Ultrason. Sonochem.*, 8 (2001) 271.
38. R.W. Wood and A.L. Loomis, *Phil. Mag.*, 4 (1927) 417.
39. H. Schubert, Mechanical Production and Quality Aspects of Food Emulsions, *PARTEC'98, Reprints of 1st European Symposium on Process Technology in Pharmaceutical and Nutritional Sciences*, Nürenberg, Germany, 10–12 March, 1998.
40. E.S. Rajagopal, *Principles of Emulsion Formation: Sonic and Ultrasonic Emulsification*, Emulsion Science, Academic Press, London, 1968.
41. W. Lauterborn and C.D. Ohl, *Ultrason. Sonochem.*, 4 (1997) 65.
42. M.K. Li and H.S. Fogler, *J. Fluid Mech.*, 88 (1978) 499.
43. M.K. Li and H.S. Fogler, *J. Fluid Mech.*, 88 (1978) 513.
44. N.P. Vichare, P.R. Gogate, V.Y. Dindore and A.B. Pandit, *Ultrason. Sonochem.*, 8 (2001) 23.
45. M. Sivakumar, P. Senthilkumar, S. Majumdar and A.B. Pandit, *Ultrason. Sonochem.*, 9 (2002) 25.
46. B. Abismaïl, J.P. Canselier, A.M. Wilhelm, H. Delmas and C. Gourdon, *Ultrason. Sonochem.*, 7 (2000) 187.
47. Y.F. Maa and C.C. Hsu, *Pharm. Dev. Technol.*, 4 (1999) 233.
48. H. Hielscher, *Flow Vessel for a Disintegrator*, UK Patent Application 2 250 930. 1991.
49. S. Freitas, G. Hielscher, H.P. Merkle and B. Gander, *Ultrason. Sonochem.*, 13 (2006) 76.
50. Branson, Fairview Estate, Clayton Road, Hayes, Middlesex UB31AN, UK.
51. B. Abismaïl, J.P. Canselier, A.M. Wilhelm, H. Delmas and C. Gourdon, *Ultrason. Sonochem.*, 6 (1999) 75.
52. A.E. Alegria, Y. Lion, T. Kondo and P. Riesz, *J. Phys. Chem.*, 93 (1989) 4908.
53. K. Makino, M.M. Mossoba and P. Riesz, *J. Am. Chem. Soc.*, 104 (1982) 8537.
54. K. Makino, M.M. Mossoba and P. Riesz, *J. Phys. Chem.*, 87 (1983) 1369.
55. S.R. Reddy and H.S. Fogler, *J. Phys. Chem.*, 84 (1980) 1570.
56. R.S. Juang and K.H. Lin, *Colloids and Surfaces A: Physicochem. Eng. Aspects*, 238 (2004) 43.
57. J.P. Canselier, H. Delmas, A.M. Wilhelm and B. Abismaïl, *J. Disper. Sci. Technol.*, 23 (2002) 333.
58. H.B. Briggs, J.B. Johnson and W.P. Mason, *J. Acoust. Soc. Am.*, 19 (1947) 664.
59. M. Murillo, A. González, A. Ramírez and N. Guillén, *At. Spectrosc.*, 15 (1994) 90.
60. T.B. Wang, X.J. Jia and J. Wu, *J. Pharm. Biomed. Anal.*, 33 (2003) 639.
61. G. Schulz, *Desalination*, 68 (1988) 191.
62. C. del Cerro and D. Boey, *Chem. Ind.*, 21 (1988) 681.
63. M.P. Thien and T.A. Hatton, *Sep. Sci. Technol.*, 23 (1988) 819.
64. F. Nakashio, *J. Chem. Eng. Jpn.*, 26 (1993) 123.
65. M. Nakao, H. Matsumiya and M. Hiraide, *Bunseki Kagaku*, 53 (2004) 975.
66. H. Matsumiya, T. Kageyama and M. Hiraide, *Anal. Chim. Acta*, 507 (2004) 209.
67. M. Hiraide and K. Hasegawa, *Fresenius' J. Anal. Chem.*, 363 (1999) 261.
68. M. Hiraide, M. Ogoh, S. Itoh and T. Kageyama, *Talanta*, 57 (2002) 653.
69. A. Imhof and D.J. Pine, *J. Colloid Interface Sci.*, 192 (1997) 368.
70. T. Sakthivel, V. Jaitely, N.V. Patel and A.T. Florence, *Int. J. Pharm.*, 214 (2001) 43.
71. A. Gómez-Hens and J.M. Fernández-Romero, *Trends Anal. Chem.*, 24 (2005) 9.
72. T. Kamidate, T. Suita and H. Watanabe, *Anal. Biochem.*, 241 (1996) 264.
73. S. Rodríguez, M.V. Cesio, H. Heinzen and P. Moyna, *Lipids*, 35 (2000) 1033.
74. A.K. Singh, P.K. Kilpatrick and R.G. Carbonell, *Biotechnol. Prog.*, 12 (1996) 272.
75. S.J. Lim and C.K. Kim, *Anal. Biochem.*, 247 (1997) 89.
76. Y. Okabayashi and I. Ikeuchi, *Analyst*, 123 (1998) 1329.
77. R. Dams, W.E. Lambert, F. Comhaire and A.P. de Leenheer, *Anal. Chim. Acta*, 399 (1999) 185.
78. A.J. Edwards and R.A. Durst, *Electroanalysis*, 7 (1995) 838.
79. S.L. Huang and R.C. MacDonald, *Biochim. Biophys. Acta*, 1665 (2004) 134.
80. S.M. Demos, H. Alkan-Onyuksel, B.J. Kane, K. Ramani, A. Nagaraj, R. Greene, M. Klegerman and D. McPherson, *J. Amer. Coll. Cardiol.*, 33 (1999) 867.
81. S.K. Wiedmer, M.S. Jussila and M.L. Riekkola, *Trends Anal. Chem.*, 23 (2004) 562.
82. W. Liu, Y. Wang, J. Tang, G. Shen and R. Yu, *Analyst*, 123 (1998) 365.
83. R.A. Potyrailo and G.M. Hieftje, *Anal. Chem.*, 70 (1998) 3407.

84. B.G. Healey and D.R. Walt, *Anal. Chem.*, 69 (1997) 2213.
85. A.M. Hartnett, C.M. Ingersoll, G.A. Baker and F.V. Bright, *Anal. Chem.*, 71 (1999) 1215.
86. P. Lavin, C.M. Mcdonagh and B.D.J. Maccraith, *Sol-Gel Sci. Technol.*, 13 (1998) 641.
87. T. Nguyen, K.P. McNamara and Z. Rosenzweig, *Anal. Chim. Acta*, 400 (1999) 45.
88. V. Vamvakaki, D. Fournier and N.A. Chaniotakis, *Biosens. Bioelectron.*, 21 (2005) 384.
89. T.M. Allen, *Drugs*, 54 (1997) 8.
90. R.J. Price, D.M. Skyba, S. Kaul and T.C. Skalak, *Circulation*, 98 (1998) 1264.
91. S.L. Huang, A.J. Hamilton, A. Nagaraj, S.D. Tiukinhoy, M.E. Klegerman, D.D. McPherson and R.C. MacDonald, *J. Pharm. Sci.*, 90 (2001) 1917.
92. S.L. Huang, A.J. Hamilton, E. Pozharski, A. Nagaraj, M.E. Klegerman, D.D. McPherson and R.C. MacDonald, *Ultrasound Med. Biol.*, 28 (2002) 339.

CHAPTER 7

Ultrasound-Assisted Analytical Chemical Reactions

7.1. INTRODUCTION

The enormous influence of US on chemical reactions, particularly in organic syntheses, has been widely exploited for more than two decades, as reflected in the large number of books devoted to this specific use of US over this period [1–7]. However, the earliest uses in this field date from 1938 [8]. Industrially, US is largely used to accelerate chemical reactions (especially organic syntheses) and also in degradation and hydrolysis reactions. By contrast, US has been only sparingly used to assist analytical reactions despite the proven high potential of this form of energy for their acceleration.

Preliminary studies conducted in the 1980s by the authors' research group [9] using continuous flow injection approaches clearly exposed the following effects of US on analytical systems:

(1) US dramatically increases dispersion of an injected volume in the carrier, which adds to the effects of, especially, the flow-rate, reactor length, inner diameter of the transporting tubes, viscosity and temperature.
(2) Homogeneous uncatalysed reactions (*e.g.* the formation of the Co–salicylaldehyde thiosemicarbazone complex, which requires the prior oxidation of Co(II) to Co(III)) are less markedly affected by US than are homogeneous catalysed reactions (*e.g.* the copper-catalysed oxidation of 2,2′-dipyridylketone hydrazone by hydrogen peroxide). The yield of these reactions increases by 28 and 300%, respectively, relative to unsonicated blanks.
(3) Heterogeneous reactions are most strongly influenced by US. One case in point is the Griess reaction, which can be boosted by inserting a redox or catalytic reactor in line with a dynamic system to reduce the previous nitrate to nitrite. Another reaction is the above-mentioned oxidation of a hydrazone by hydrogen peroxide, but catalysed in this case by a solid copper reactor instead. Despite the promising initial results, this research line was not re-started by the authors' group until very recently. Contributions in this area therefore remain scant.

This chapter deals mainly with the types of analytical reactions assisted by US so far (namely, derivatization, oxidation and hydrolysis reactions). Also, it examines the importance of sonochemistry in other fields and potential applications of the experience gained in other areas such as US-assisted synthesis, hydrolysis, degradation and polymerization for analytical purposes are briefly discussed.

7.2. ULTRASOUND-ASSISTED DERIVATIZATION

Ultrasound-derivatization reactions involve inorganic, organic and organic–inorganic species, and are implemented in discrete or continuous systems. Most have exploited existing experience in non-analytical areas. They are discussed below according to chemical type.

7.2.1. Depolymerization reactions

The very long experience with the depolymerizing effect of US on high polymers such as starch, gelatine and arabic gum [10–12] can be used in analytical chemistry to boost reactions involving a slow, limiting depolymerization step (*e.g.* the determination of phosphate using the Molybdenum Blue method [13]). Molybdenum Blue forms in two steps involving (1) the reaction of *o*-phosphate with molybdate ions in an acid medium to give molybdophosphoric acid, and (2) reduction to the blue heteropolyacid by a suitable reductant (usually ascorbic acid). Application of US in both steps showed that ascorbic acid was degraded *via* an oxidation reaction promoted by free radicals formed during irradiation. Also, application of US for 15 min during the formation of the heteropolyacid was found to increase the absorbance of the solution by about 20%; however, US application to the molybdate solution for 1 min provided the same improvement, so the limiting step was depolymerization of molybdate ions, which occurred rapidly in the presence of US.

7.2.2. Redox reactions

The formation of OH and H radicals in sonicated aqueous media accelerates or facilitates redox reactions which are slow or unlikely in the absence of US. Such is the case which the photometric determination of nickel by complexation with dimethylglyoxime, which involves the oxidation of Ni(II) by bromine, iodine, hydrogen peroxide or persulphate. The oxidant is mixed with the Ni(II) solution prior to adding the chelating agent; however, replacing the oxidant with US irradiation under reproducible conditions as regards the position of the reaction vessel — in the centre of the US bath — and continuous renewal of the bath water at 400 ml/min substantially increases the absorbance and precision relative to the strongest oxidant among those commonly used for this purpose (*viz*. persulphate), as shown in Fig. 7.1. In addition, the absence of an oxidant reduces interferences from Fe(II), Cu(II), Co(II), particularly when air is continuously bubbled into the solution, as a result of the formation of nitrite and nitrate ions in aqueous solutions saturated with air or nitrogen upon exposure to low-frequency US [14]. As noted earlier, the oxidation of Co(II) to Co(III) prior to complexation with salicylaldehyde thiosemicarbazone in a continuous manifold is also accelerated by US [9].

Not all redox reactions are favoured by US. One that is not is the basis for the determination of polyphenols in extra virgin olive oil by the extraction of the target analytes into a basic aqueous medium containing the Folin–Ciocalteu reagent. Mass transfer of the polyphenols to the aqueous phase is doubly displaced by the conversion of the analytes into their polyphenolates and subsequent oxidation by the Folin–Ciocalteu reagent. The overall process is greatly enhanced by US irradiation; however, tests examining the influence of US on each step separately by applying US for 3 min in each revealed no difference in the oxidation reaction relative to an insonated blank [15]. The method, implemented in a continuous manifold, has been discussed in Chapter 6; the experimental set-up and the recordings obtained — which expose the influence of US on the extraction process — are shown in Figs. 6.2 and 6.3.

7.2.3. Esterification reactions

Resolving enantiomers usually requires the use of a derivatization reaction that is of the esterification type when α-hydroxy acids are to be derivatized with (+)-1-(9-fluorenyl)
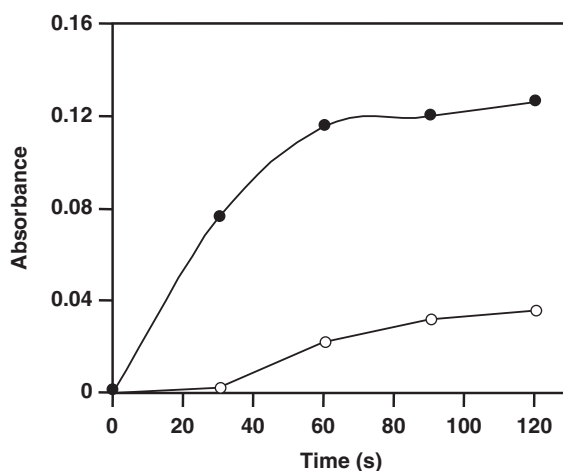
FIGURE 7.1. *Comparison of the absorbance of Ni–dimethylglioxime complex in an ultrasonicated solution (●) and in one containing persulphate (○). [Ni(II)] = 1.0 mg/l. (Reproduced with permission of Elsevier, Ref. [14].)*

ethyl chloroformate. Fransson and Ragnarsson [16] used reverse phase liquid chromatography (RPLC) to separate the analytes, and a US bath to implement the derivatization reaction; however, they did not provide any details about the gains in using this type of energy.

The conversion of amino acids into *N*(*O*,*S*)-ethoxycarbonyl amino acid ethyl esters is significantly improved by US assistance. The derivatization reaction, developed at a microscale, constitutes the step prior to single-drop microextraction, which is followed by GC–MS. Single-drop microextraction (SDME) is a relatively new sample preparation mode which enables extraction of the analytes or their derivatization products into a small volume of organic solvent. It uses a small drop of water-immiscible solvent for sample preparation, combines extraction and preconcentration in a single step [17–19], is expeditious and can be implemented with simple equipment usually available in analytical laboratories. The derivatization step involves mixing 1 ml of sample (urine) with 400 µl of 4:1 ethanol–pyridine and 100 µl of ethylchloroformate. The reaction vial is ultrasonicated — no information about the characteristics was reported in the original article — for 10 min, followed by the addition of 50 mg of NaCl and vigorous stirring for 2 min until all suspended air and CO_2 produced by the reaction are removed. Comparative tests of the derivatization reaction of 12 amino acids assisted by stirring at room temperature, at 70°C and under ultrasonication only provided the results shown in Fig. 7.2, which can be summarized as follows:

(1) the reaction involving stirring at room temperature took a long time to complete and barely levelled off after 80 min;
(2) heating and ultrasonication considerably accelerated the reaction, the latter clearly being a better choice for fast completion of the reaction;
(3) ultrasonication can expose subtle interactions and special effects of entropic and enthalpic origin;
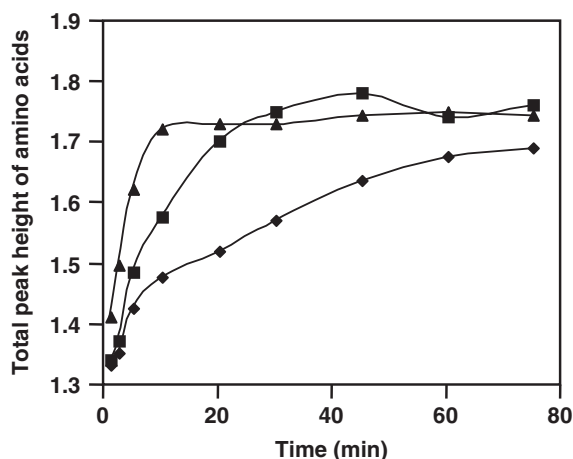
FIGURE 7.2. *Progress of the derivatizing reaction of 12 amino acids under stirring (♦), heating (■) and ultrasonication (▲), expressed as the sum of all peak heights. (Reproduced with permission of Elsevier, Ref. [20].)*

(4) the efficient removal of bubbles from the bulk solution by US is of paramount importance as bubbles are detrimental to the SDME process — by attaching to drops, they reduce the surface available for extraction and facilitate dislodgement. Ultrasonication for 10 min following 2 min of vigorous stirring increased the yields of the corresponding derivatives by 20–35%, depending on the particular amino acid [20].

7.2.4. Alkylation reactions

Although gas chromatography (GC) affords the separation and quantification of phenols, the results are often poor by the effect of the high polarity and low vapour pressure of these compounds [21]. Because isomeric compounds with almost identical properties (*e.g. o*-, *m*- and *p*-cresols) are difficult to separate [22,23], derivatization reactions involving the formation of ethers [24] and esters [25], and (or) bromine [26] and silyl derivatives [27] are frequently used to improve the chromatographic characteristics of the analytes [24]. One simple, efficient derivatization reaction is acetylation by acetic anhydride in an alkaline aqueous medium [28,29], which has been used for the automated determination of phenolic compounds (*viz.* phenol and *o*-, *m*- and *p*-cresol). The procedure, depicted in Fig. 7.3, involves three main steps, namely: (a) ultrasound irradiation to accelerate the derivatization reaction; (b) pervaporation [30] to remove the products of the target analytes from the aqueous matrix; and (c) GC to separate the individual products, followed by flame ionization detection (FID) [31]. The sample was pumped into the reaction chamber together with the reagent and stopped in it for US irradiation for the required time; then, the mixture was led to the lower chamber of the pervaporation unit for transfer of the volatile products to the upper chamber, from which a He stream was used to transfer the pervaporated species to the separation column. The multivariate optimization design used in step (a) showed the probe distance to the reaction chamber to be the most
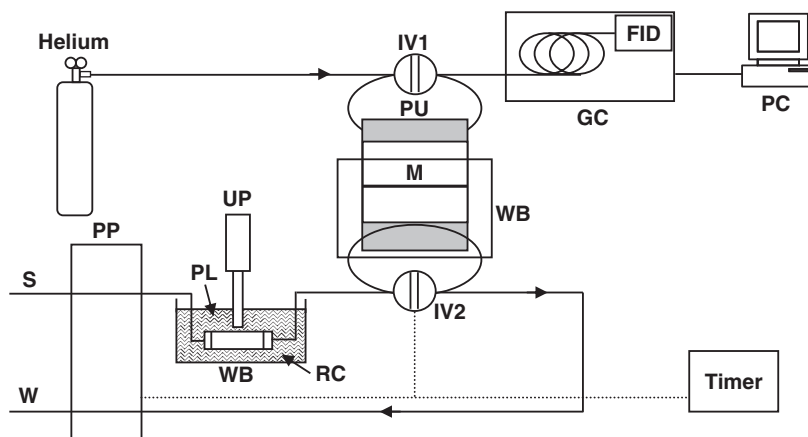
FIGURE 7.3. *Experimental set-up for the fully automated continuous determination of phenols. FID — flame ionization detector, GC — gas chromatography, IV1 — HPLC injection valve, IV2 — low-pressure injection valve, M — membrane, PC — personal computer, PL — propagating liquid, PP — peristaltic pump, PU — pervaporation unit, RC — reaction chamber, S — sample, UP — ultrasonic probe, W — waste and WB — water bath. (Reproduced with permission of Springer-Verlag, Ref. [31].)*

important factor, followed by the pulse duration and radiation amplitude. The reaction time was more than halved relative to the absence of US irradiation and to the use of microwaves under optimal conditions.

7.2.5. Addition reactions

Although the earliest examples of the use of US as a substitute for phase transfer catalysts in organic addition reactions were reported more than two decades ago and a number of such reactions have since been improved as a result [1–7], the sole analytical application exploiting this potential is a method for the determination of paracetamol where the drug is derivatized by hydrolysis to *p*-aminophenol, which reacts with *o*-cresol in an alkaline medium to form the Indophenol Blue dye, according to the following reaction:

$$(7.1)$$
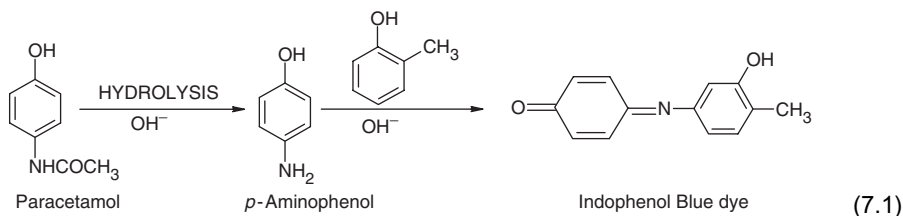
The method was developed for determining the analyte in suppositories, so extraction from a toluene solution to an aqueous phase was required prior to hydrolysis and the

addition reaction. All these steps were performed in the continuous manifold of Fig. 6.2. Figures 6.3 and 6.4 show the multi-peak recordings obtained by continuously monitoring the aqueous extractant phase during the liquid–liquid extraction (LLE) without phase separation and comparison of the results in the presence and absence of US, respectively [32]; as can be seen, the use of US had an enormous influence on the overall process.

Multivariate optimization of the variables influencing the method (namely, dynamic, chemical variables and US-related) revealed a negligible favourable effect of the US amplitude and pulse duration and an adverse effect of the distance of the probe to the reactor — the best results were obtained with the probe in contact with the reactor. A series of tests were conducted with a view to clarify the influence of US on each of the reactions taking place simultaneously with the extraction process; thus, 3-tube sets containing the following were prepared: (1) *o*-cresol in an alkaline medium; (2) paracetamol in toluene; and (3) previously formed Indophenol Blue dye. Because temperatures below 25°C failed to improve the monitored instrumental signal, all triplicate tubes were subject to US at different temperatures (namely, 25, 35 and 55°C) in the water bath where the probe was dipped for 3 min. The spectra thus obtained were compared with those for non-irradiated, blank tubes. The results clearly showed that:

(1) The *o*-cresol solutions were unstable (the solution was colourless after 24 h), but even more so in the presence of US. The effect is not perceptible during an experiment under the usual working conditions, but increases dramatically as the temperature is raised.
(2) The yield of the derivatization reaction was higher when the hydrolysis step was assisted by US (the absorbance was five times higher than without US).
(3) The end product was stable to US irradiation, and slightly decomposed below 55°C. These results explain why the amplitude and the pulse duration should be as high as possible but the temperature not higher than 55°C.

One of the main advantages of the use of US for enhancing processes implemented in a continuous fashion over that of microwave energy is the small temperature rise involved in the former case, which avoids the presence of undesirable air bubbles in the dynamic system and hence of parasitic signals at the detector.

7.2.6. Ethylation of organometallic compounds

Ethylation by sodium tetraethylborate has become an attractive choice for the speciation analysis of organometallic compounds [33,34]. With this reagent, ethylation takes place even in an aqueous phase, which makes it possible to simplify the pre-treatment process by combining derivatization and extraction in one step. This has been the case with the determination of methylmercury in biological materials by GC–MIP-AES or GC–ICP-MS. Following leaching in an automatic shaker for 5 min, addition of the reagent — an appropriate volume of an immiscible phase, nonane — to the suspension and pH adjustment, the system was ultrasonicated in a bath for 40 min. Although the differential effects of US on the derivatization reaction and on LLE have not been experimentally established, its combined effect is clearly apparent from Fig. 6.1 [35].

7.2.7. Complex formation

Although US seemingly facilitates complex formation reactions (*e.g.* in the method for the determination of Ni by the formation of the Ni–DMG complex, where US favours Ni(II)

oxidation [14], or that for phosphate based on the formation of the heteropolyacid complex, where US accelerates the depolymerization [13]), the potential effect of US on this type of equilibrium has not yet been examined. The only reported example to the authors' knowledge deals with the LLE of Fe(II) from an aqueous sample to an *o*-phenanthroline–dichloromethane phase, which is not significantly improved by US assistance (see Fig. 6.4) [15].

7.3. ULTRASOUND-ASSISTED OXIDATION REACTIONS

Oxidation reactions in analytical chemistry usually constitute a step preceding derivatization, if present, intended to make the analyte amenable to derivatization or, less frequently, direct detection. One can expect US to favour any oxidation reaction taking place in an aqueous medium through the well-known radical formation process. This assumption has been verified with a small, but representative, number of examples. In other cases, aqueous solutions saturated with a solvent of higher vapour pressure than water have been found to favour oxidation reactions.

Four major application fields of oxidation reactions widely used in analytical chemistry have exposed the gains in using US, which include increased efficiency and shortened times in reactions such as the oxidation of inorganic species in CCl_4-saturated aqueous media, the degradation of organometallic compounds prior to the determination of the target metal, oxidation of organic matter for the determination of the chemical oxygen demand (COD), and the fast oxidation of oils for correlating the time required with long-time oxidative stability. As shown below, processing times were dramatically shortened by US assistance in all instances.

7.3.1. Oxidation of inorganic species

Inorganic compounds can be oxidized in an easy, fast, controlled way under the influence of US. This analytical use of US, only examined by Korn *et al.* [36–39] so far, constitutes an underexplored field which can provide analytical chemists with great benefits. Their work has focused on the generation of species by exploiting the oxidative effect of chlorine radicals formed by the sonolysis of CCl_4 in aqueous solutions. The principle behind this use is that when water is sonicated in the presence of a solvent with a higher vapour pressure, preferential sonolysis of the molecules of the latter occurs. Thus, when water saturated with CCl_4 is subject to US, CCl_4 can migrate to the bubbles formed by cavitation and C–Cl bonds be broken by the energy generated in the collapse phenomenon to give $CCl_3^{\cdot}$ and $Cl^{\cdot}$. This hypothesis is supported by the proven fact that an aqueous solution saturated with CCl_4 that was irradiated with a US device of 40 kHz and 200 W for 4 min exhibited a pH decrease from 4.6 to 2.6 (Fig. 7.4). This can be ascribed to the production of HCl and, possibly, also HClO, as a result of the interaction between chlorine radicals and water according to the following reactions:
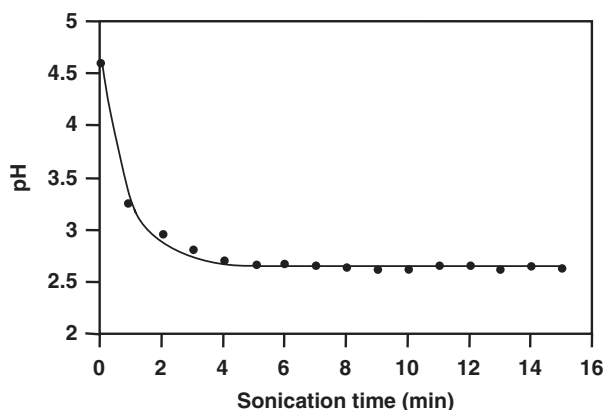
$$CCl_4 \rightarrow Cl^{\cdot} + CCl_3^{\cdot} \tag{7.2}$$

$$Cl^{\cdot} + H_2O \rightarrow HCl + OH^{\cdot} \tag{7.3}$$

$$2Cl^{\cdot} + H_2O \rightarrow HCl + HClO \tag{7.4}$$

FIGURE 7.4. *Variation of the pH of a CCl₄-saturated water solution with the sonication time. (Reproduced with permission of the Brazilian Society of Chemistry, Ref. [38].)*

The amount of chloride ions produced after 3 min of sonication was 12.19 μmol.

Another hypothesis for the generation of chlorine acids is related with the interaction of dissolved oxygen with water and CCl_3^- to produce phosgenium, which would then decompose to CO_2 and Cl_2 at temperatures above 100°C [40].

Reactions involving OH· and H· produced by water sonolysis may also yield chlorine acids from dissolved CCl_4. However, this mechanism is less likely for the following reasons: (1) the increased vapour pressure of CCl_4 favours diffusion of these molecules into bubble cavities, (2) the energy needed to break a C–Cl bond (73 kcal/mol) is lower than that for an O–H bond in water (119 kcal/mol). Thus, aqueous solutions saturated with CCl_4 that are sonicated for tens of seconds contain oxidant species such as those from reactions 7.2–7.4, or even Cl_2 formed as follows:

$$2Cl \rightarrow Cl_2 \qquad (7.5)$$

Ultrasound-assisted generation of iodine and other
oxidized-iodine species from iodide

Oxidation of iodide to iodine ($E_o = -0.615$ V) promoted by sonication was one of the earliest tests demonstrating the sonochemical effects on solutions. The following effects were detected in water-sonicated systems with and without CCl_4 and (or) iodide:

(1) In an aqueous solution containing only iodide ions, oxidation resulted from the action of the hydroxyl radicals produced by water sonolysis, albeit with a poor yield.
(2) In a water–CCl_4 two-phase system under sonication, turbidity appeared through both emulsification and Cl_2 formation.
(3) In the presence of KI, a pink colour appeared due to the oxidation of iodide to iodine and extraction of I_2 into the organic phase.

(4) No pink colour or turbidity was observed in a water solution of KI saturated with CCl_4 under sonication, but subsequent addition of CCl_4 to extract the I_2 formed provided a pink organic phase, the absorbance of which at 520 nm varies with the sonication time as shown in Fig. 7.5A. Under these conditions, enough radicals were formed during 2-min sonication to ensure complete oxidation of a 0.476 M iodide solution.

(5) Iodide oxidation can also be monitored at 352 nm through the formation of the I_3^- complex (Fig. 7.5B), which completes within 2 min under sonication.

(6) Formation of HIO, which justifies the decrease in the absorbance with time in Fig. 7.5A, occurs, as shown in Fig. 7.5C, by selective oxidation of *leuco* Violet Crystal by HIO, with maximum absorption at 592 nm [38,41].

Ultrasound-assisted oxidation of Fe(II)

Exposing an aqueous solution of Fe(II) to ultrasonication results in its oxidation (E_o for the Fe(II)/Fe(III) couple is –0.771 V). Under these conditions, Fe(II) interacts with the OH radicals generated by water sonolysis to form Fe(III) and OH^-, according to:

$$Fe^{2+} + OH\cdot \rightarrow Fe^{3+} + OH^- \qquad (7.6)$$

Prior sonication of pure water and subsequent mixing with a Fe(II) solution does not ensure significant oxidation of ferrous ions. On the other hand, sonication of a CCl_4-saturated aqueous solution prior to mixing with a Fe(II) solution provides quantitative oxidation of Fe(II). The amount of Fe(III) produced by mixing variable concentrations of Fe(II) with aqueous solutions saturated with CCl_4 and sonicating for 1 min was determined by absorption monitoring of the complex formed with 5-sulphosalycilic acid. The results are shown in Table 7.1 together with those provided by solutions of Fe(III) of identical concentration. Total oxidation of Fe(II) to Fe(III) was thus demonstrated.

Figure 7.6 illustrates the effect of US on the oxidation of Fe(II) under different working conditions. As can be seen, prior sonication of pure water results in no significant oxidation (<1.3%). When ferrous ion is present during sonication, oxidation is slightly more marked, which confirms that hydroxyl radicals resulting from water sonolysis take part in the oxidation of Fe(II). The addition of Fe(II) to a sonicated CCl_4-saturated water solution increases the amount of Fe(III) formed and produces complete oxidation after 40 s of sonication. Oxidation is faster with direct sonication of a CCl_4-saturated aqueous solution containing Fe(II), possibly because the ferrous ion interacts directly with the chlorine radicals formed.

Ultrasound-assisted oxidation of Cr(III)

The photometric determination of chromium by reaction with 1,5-diphenylcarbazide is selective for Cr(VI) [42]. Chromium(III) can also be determined in this way following quantitative oxidation to Cr(VI) by sonication in a carbonated aqueous solution saturated with CCl_4. Under the optimal working conditions, 1 μg of Cr(III) takes less than 60 s to be oxidized [37]. The environmental and health hazards associated with the use of CCl_4 are minimal due to the small amount used. Thus, 2000 l of CCl_4-saturated aqueous solution is prepared from 1 l of CCl_4. This solution volume affords more than 50000 determinations of Cr(III) in water [37].
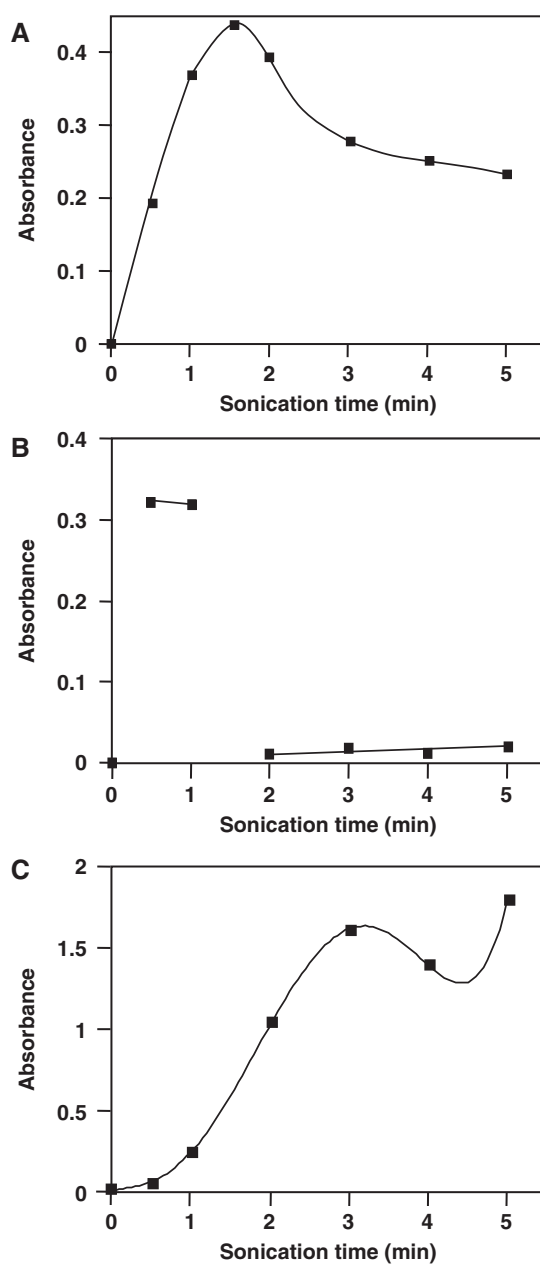
FIGURE 7.5. *Oxidizing effect of a CCl_4-saturated water solution on iodide as determined by monitoring: (A) the I_2 formed and extracted by CCl_4, at 520 nm; (B) the formation of I_3^- at 352 nm; (C) the selective oxidation of the leuco form of Violet Crystal by the HIO formed under US, at 592 nm. (Reproduced with permission of the Brazilian Society of Chemistry, Ref. [38].)*

TABLE 7.1. *Absorbance at 490 nm of aqueous solutions of Fe^{3+} and Fe^{2+} after derivatization with 5-sulphosalicylic acid.*

	Absorbance	
Amount of Fe (µg)	Fe^{3+}	Fe^{2+}/US*
0	0.003	0.003
2.5	0.021	0.021
5.0	0.040	0.038
7.5	0.054	0.056
10.0	0.071	0.071
12.5	0.085	0.086

*The Fe^{2+} solution was previously mixed with a CCl_4-saturated aqueous solution sonicated for 2 min. (Reproduced with permission of the Brazilian Society of Chemistry, Ref. [38].)

Ultrasound-assisted reagent generation

Another use of the oxidative effect of CCl_4-saturated water solutions is the generation of the strong reductants required to obtain arsine from As(III). A factorial design was used to optimize the overall process for the determination of this toxic element in urine. The sample was acidified with 1×10^{-4}–1×10^{-1} M HCl, placed in a reactor vessel containing 0.1–1 g of Zn and sonicated for 1–10 min while air was circulated through the solution to remove the volatile hydride for transfer to the detector [38].
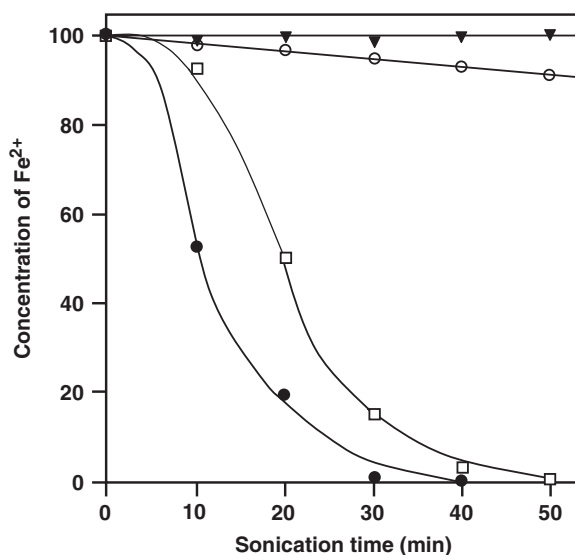
FIGURE 7.6. *Residual amounts of Fe(II) at different ultrasonication times under variable conditions. (▼) Water sonication before mixing with the Fe(II) solution; (○) direct sonication of an aqueous solution of Fe(II); (□) prior sonication of a CCl_4-saturated water solution followed by mixing with the Fe(II) solution; and (●) direct sonication of a CCl_4-saturated water solution containing Fe(II). (Reproduced with permission of the Brazilian Society of Chemistry, Ref. [38].)*

Analyte oxidation and reagent generation in flow systems using tubular ultrasonic reactors have so far been unsuccessful [39]. This is another under-explored area for analytical chemists.

7.3.2. Degradation of organometallic compounds prior to metal determination

Research in this field, conducted by Capelo *et al*., has focused on organomercurials in water and urine, and involved US probes and batch approaches in all instances [43–46]. Because these compounds are usually accompanied by inorganic mercury in natural samples, organic and inorganic mercury in water are determined separately. The process is more complex for urine as the presence of other organic matter entails isolating the target analytes after oxidation to ensure proper derivatization and detection.

Organomercurials (*viz*. methylmercury and phenylmercury) in water can be readily oxidized within 3 min by a 100-W power probe of 20 kHz frequency at 40% amplitude in a 1 M HCl medium. As can be seen in Fig. 7.7, the influence of both sonication time and amplitude on the oxidation of both compounds is very similar. Complete oxidation of the target analytes requires the presence of HCl in the medium. Also, replacing US with an oxidant such as H_2O_2 or HNO_3 precludes reaching 100% efficiency [47]. The principal advantage of US assistance to this process is the need for no chemical oxidants, high temperatures or pressures, which avoids the generation of hazardous waste and decrease the risk of Hg loss by volatilization. Oxidation is more efficient — the yield is up to 15% higher — at low temperatures (*viz*. with the sonication cell immersed in an ice bath) than at uncontrolled temperatures. An additional advantage is the tolerance of concentration up to 1000 mg/l of OH radical scavengers, which facilitates application to wastewater with a COD of up to 1000 mg/l without diminishing the oxidation efficiency [43].

Oxidizing the organic matter of organomercurials in urine requires the use of a chemical oxidant in addition to US. Depending on the nature of the auxiliary oxidant, speciation analysis of organic and inorganic mercury may be possible. Thus, the use of ozone in addition to US (*viz*. "sonozone" [43]) ensures oxidation of the organic matter and the target inorganic analyte to its higher oxidation state (Hg(II), the appropriate form for subsequent reduction to the elemental mercury required for atomic detection) without altering organic mercury. Three 10-min steps (namely, (1) sonication, (2) ozonization and (3) ozonization + sonication) produce a treated urine sample ready for derivatization and detection.

The determination of total mercury, and that of the organic forms as the difference between total and inorganic mercury, requires the use of a strong oxidant such as $KMnO_4$. The main shortcoming of this reagent is that it forms MnO_2 instead of Mn(II); the MnO_2 forms a film on the walls of vessels or tubing in batch or continuous approaches, respectively, in which mercury is adsorbed [44]. The use of US here avoids precipitation of manganese dioxide due to the low concentration of $KMnO_4$ required (0.01%) and oxidation is completed between 30 s and 8 min, depending on the complexity of the urine sample; this is much shorter than the 30 min required in unsonicated media. The time for US-assisted urine oxidation is a function of that needed to fulfil the recommendations for efficient development, *viz*. the absence of, (1) a precipitate (MnO_2), (2) colour from permanganate and (3) yellow colour from urine. The step sequence to be followed is depicted in Fig. 7.8. The solution is thus made ready for direct derivatization (by reduction with an appropriate reagent such as $SnCl_2$ or $NaBH_4$ prior to atomic detection) or for LLE by complex formation with dithizone and subsequent destruction of the complex after back-extraction into
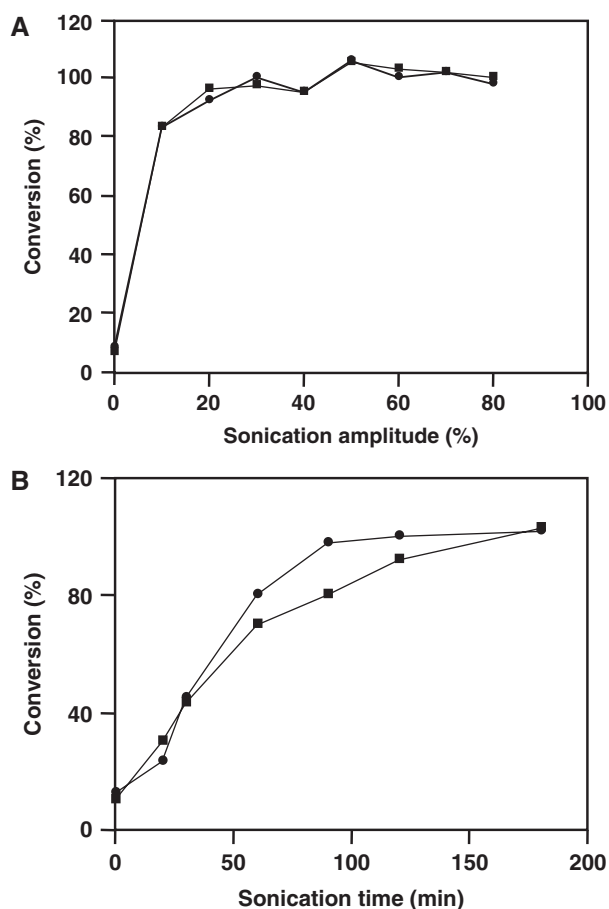
FIGURE 7.7. *Influence of the sonication amplitude (A) and sonication time (B) on the yield of Hg from MeHg⁺ (■) and PhHg⁺ (●). Oxidation conditions: 1 mol/l HCl, 5 ml sample and NaBH₄ as the reducing agent, 3-min sonication time in (A) and 60% amplitude in (B). (Reproduced with permission of the American Chemical Society, Ref. [43].)*

an aqueous phase. The increased complexity introduced by this step is offset by the ability to preconcentrate the target analytes, if required, and the avoidance of problems arising from the introduction of organic solvents into a graphite furnace. Back-extraction and destruction of the complex can also be assisted by 15-s US irradiation [45]; this has provided recoveries between 86 and 98% of phenylmercury and ethylmercury compounds in spiked urine. The influence of interrelated variables was recently examined using full factor designs [46].

The improved oxidation of organomercurials under cold-controlled temperature conditions (usually in ice baths) has been ascribed to decreased cavitation and an increased risk of volatilization of Hg at increased temperature.
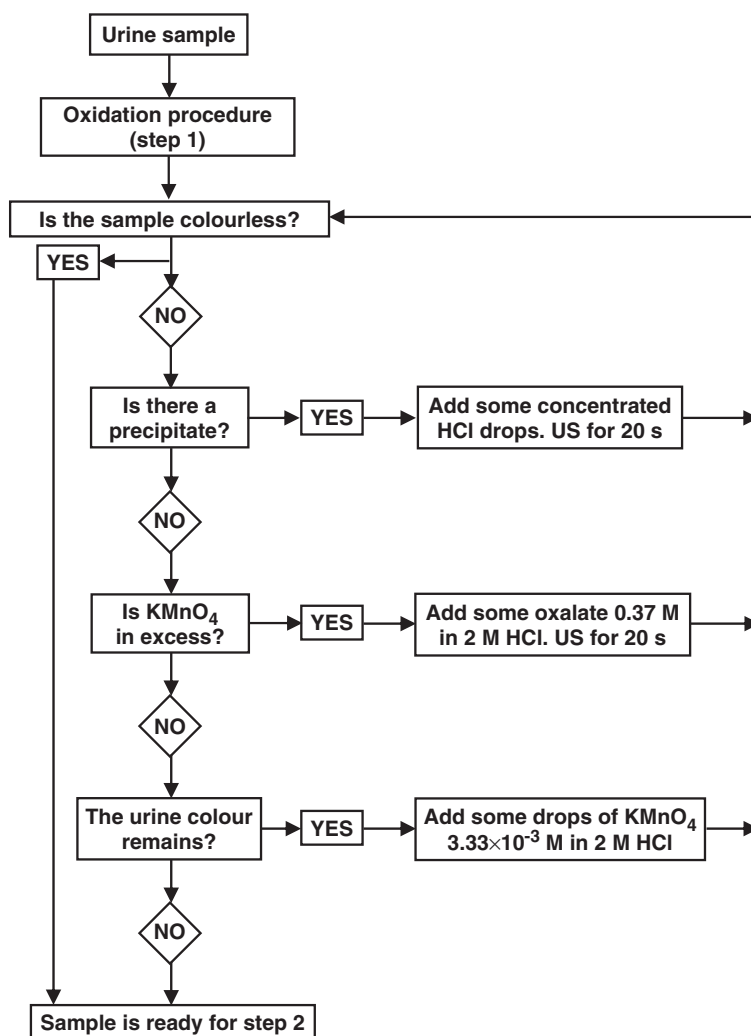
FIGURE 7.8. *Step sequence for the determination of total and organic mercury in urine. (Reproduced with permission of the Royal Society of Chemistry, Ref. [44].)*

Using the word "focused" to designate the action of US on the oxidation of organomercurials with a sonotrode dipped in the transmitting liquid can be misleading as nothing is used to "orientate" US in a given direction.

7.3.3. Oxidation of organic matter for chemical oxygen demand determination

Since degradation of organic matter requires the presence of oxygen, the content of organic matter in a given aqueous system can be estimated from the amount of oxygen

needed to oxidize the organic matter it contains. When the oxidation is chemical in nature, the result is named "COD". Usually, COD ranges from 20 to 50 mg/l in slightly contaminated water (*e.g.* surface water, domestic sewage) to over 100 000 mg/l in an extremely contaminated industrial wastewater. A fast, precise and accurate method for determining COD is therefore essential for environmental analyses. The reference semi-micro method for COD determination involves the oxidation of organic matter of the sample by — usually — adding a known amount of oxidant (dichromate in sulphuric acid), refluxing at a high temperature in an open container and titrating excess oxidant with ferrous ammonium sulphate [47]. This method is subject to some serious drawbacks, namely: (1) it is time consuming (digestion and titration take 2 h); (2) it requires skilled operators as the likelihood of error is high; (3) it uses large amounts of expensive, toxic chemicals; (4) the selectivity is diminished by the presence of inorganic interferents such as Cl^-, NO_2^- or Fe^{3+}. Several modifications have been developed towards circumventing these shortcomings, those based on flow injection and segmented flow systems being the ones most markedly reducing the digestion time (from 2 h to few minutes) [48–52].

The digestion of organic matter for COD determination can be assisted by US, which shortens the time required to 3 min [53,54]. A conventional US bath cannot provide the amount of energy needed, as does a probe dipped in a transmitting liquid; so direct insertion of the probe into the sample is mandatory for proper development of the oxidation. Also, the presence of an oxidant in a very acid medium severely shortens the lifetime of alloy-based probes, so glass probes should be used in their place [55]. Using a plastic or polyethylene round-bottomed test tube to accommodate an alloy probe (see Fig. 7.9) can also be more efficient than using a conventional transmitting bath [56]. Figure 7.10 illustrates the influence of two typical US variables (pulse duration and sonication time) on a model organic matter (*viz.* potassium hydrogen phthalate (KHP)) as determined using one such probe. As can be seen, pulses of 0.9 s applied over 1-s periods ensure total oxidation of KHP within 2 min.
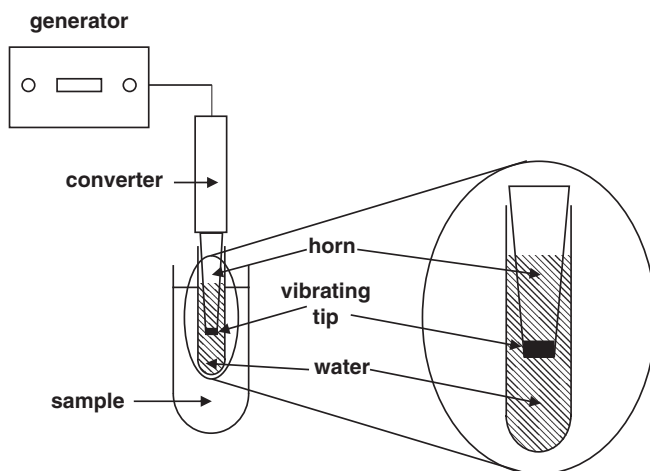

FIGURE 7.9. *Experimental set-up for the US-assisted determination of COD. (Reproduced with permission of Elsevier, Ref. [56].)*
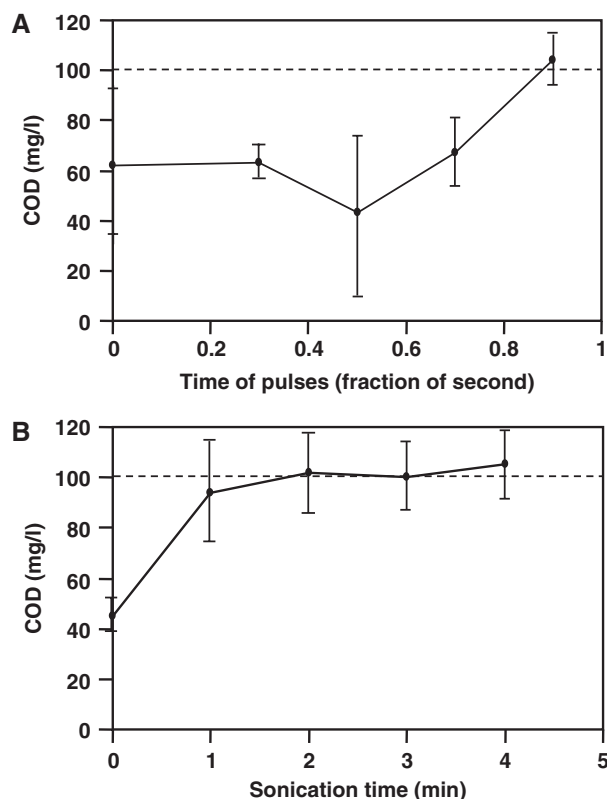
FIGURE 7.10. *Effect of pulse length (A) and sonication time (B) on the US-assisted determination of COD. Amplitude 55%, tip depth 0.7 cm from the liquid surface, (H_2SO_4) 56% (v/v), theoretical oxygen demand 100 mg/ml, temperature 27±2°C, sonication time in (A) 2 min, pulse length in (B) 0.9 s/s. (Reproduced with permission of Springer-Verlag, Ref. [55].)*

As in other oxidation processes, increased temperatures have an adverse effect which also ascribed to the resulting increased vapour pressure leading to easier cavitation, but less violent collapse, as a consequence of the decreased viscosity and surface tension. As the temperature approaches the solvent boiling point, a large number of cavitation bubbles are formed concurrently that act as a barrier to sound transmission and dampen the effective US energy from the source to enter the liquid medium. A temperature close to room level is easy to maintain and ensures proper development of the process.

Bubbling a gas through an oxidizing medium subjected to US had a favourable effect on the process; no differences, however, were observed in the use of monoatomic (*e.g.* Kr, Ar, He) or diatomic gases (*e.g.* N_2, O_2, air), or in the manner the gas was bubbled (before or during sonication).

Concerning interferences with the oxidation of organic matter in water, US-assisted oxidation tolerates the presence of chloride ions up to 7000 mg/l for 100 mg/l COD as

KHP, which is lower than the levels allowed by FI- [51] and Ce(IV)-based methods [57] (*viz*. 30 000 and 10 000, respectively).

Unfortunately, as with the conventional method, the ratios of measured and theoretical COD values depend on the particular target compounds. The applicability of US in this context was assessed by using six organic compounds of known theoretical oxygen demand (ThOD). As can be seen in Table 7.2, the ratios of measured to theoretical COD ranged from 0.22 for pyridine to 1.01 for dextrose. These results warrant the following conclusions:

(1) Readily oxidized compounds such as dextrose are completely oxidized by US under the working conditions used.
(2) Volatile compounds such as ethanol or 1-butanol provide experimental COD values from 52 to 62% of the theoretical values, which may be a result of the heat produced by both the addition of sulphuric acid to the sample in the open container and the high-temperature microzones created by cavitation, which will promote the loss of these compounds before they are oxidized by dichromate.
(3) Aromatic derivatives such as phenols are completely oxidized under the experimental conditions, as are straight-chain carboxylic acids such as acetic acid, which are normally not oxidized in the absence of a catalyst and might not be completely oxidized even in the presence of one [58,59].
(4) Pyridine and compounds difficult to oxidize even with highly efficient methods [57,60] are poorly oxidized. The relative standard deviation of the method was below 20%, except for pyridine (24%), ethanol (22%) and 1-butanol (27%).

7.3.4. Fast oxidation of oil for correlation with its oxidative stability

Measuring the resistance to oxidation is one way of establishing oil quality inasmuch as this property determines storage and usage stability. The length of the stability period (*viz*. the interval between oil production and the oil becoming rancid) depends both on intrinsic features (*e.g.* the contents in fatty acids and natural antioxidants such as tocopherols and biophenols) and environmental conditions (temperature, light, air exposure, type and material of the container, trace metal content) and the time the oil is exposed to them.

Chemical and physical tests for oxidative stability are based on the determination of either precursor hydroperoxides or oxidation end-products [61–64], and on oxygen

TABLE 7.2. *Determination of COD for various organic compounds using the ultrasound-assisted method.*

Organic compound	ThOD* (mg/l)	COD (mg/l)	RSD (%)
Dextrose	102	103	19
Ethanol	158	98	22
1-Butanol	119	62	27
Phenol	114	114	15
Acetic acid	107	101	17
Pyridine	133	29	24

*ThOD: theoretical oxygen demand. (Reproduced with permission of Springer Verlag, Ref. [55].)

absorption and gravimetric monitoring of the losses of volatile products [65,66]. Some methods based on the peroxide value [67,68] or biophenol concentration [69] have been automated.

The stability of edible oils varies widely depending on seed type, one of the most stable being virgin olive oil. Stability also varies widely depending on both the olive variety (*e.g.* picual, manzanilla, arbequina, hojiblanca) and the production process. Because extra virgin olive oil is stable for several months under optimal storage conditions, its stability is traditionally determined in the laboratory using an accelerated oxidation test involving raising the temperature and exposing the oil to oxygen or air bubbled through it.

Most common choices for assessing the oxidative stability of oils are the active oxygen method (AOM) [70] and the Rancimat method [71]. Commercial automated equipment for implementation of the latter — which essentially involves bubbling air through the sample under heating, collecting the volatile compounds formed into an appropriate solution and monitoring its changes in conductivity — affords continuous monitoring, but has two main shortcomings, namely: (1) it requires a long time to establish the target oxidative stability, especially in virgin olive oils; and (2) only up to eight samples can be treated simultaneously in each batch. Large number of samples can be simultaneously treated by using a robotic method based on oxygen absorption and gravimetric monitoring of the volatile losses [66]. Up to 150 samples can be included in each batch. The equipment needed, however, is very expensive. The use of microwaves to accelerate oxidation reduces by 60–68% the time required by the Rancimat method [72] (from 19, 30 and 129 h to 7, 12 and 43 h, respectively, for different olive oils); however, because the microwave-based method is not automated, monitoring for 7, 12 or 43 h is impracticable.

Ultrasound irradiation of an edible oil (particularly direct irradiation of the sample) causes fast oxidation of biophenols present and produces a rancid smell as a result, mainly with easily oxidized oils such as those from sunflower [73]. Ultrasound energy allows Rancimat times from 129 h to be reduced to 50 min; therefore, the overall time required for the determination of oil stability, even for highly stable virgin olive oils, is less than 1 h.

The oxidation process is usually monitored photometrically and expressed using parameters K_{232} and (or) K_{270} (*viz.* absorbance at 232 and (or) 270 nm/olive oil concentration — g per 100 ml), according to the CE Norm L24813–1991. The oxidative stability is related to the induction period, which is the time within which the absorbance does not change significantly. Subsequently, marked increase in absorbance is observed as the oxidation products formed absorb strongly in the UV region, with maxima at 232 and 270 nm.

The influence of US variables on the oxidation of oils from various types of seed or fruit has been determined by using a multivariate method, as the variables are interrelated. With virgin olive oil, the use of a probe dipped in a transmitting liquid did not cause any significant oxidation of the samples, so direct insertion of the probe into the oil (1 cm beneath the surface) was the preferred choice. Figure 7.11 shows the influence of radiation amplitude for a total irradiation time of 5 min distributed in cycles of 30 s with a 1-min interval between cycles, a 3-mm diameter tip and 3 g of sample per assay. As can be seen, the influence of radiation amplitude on K_{232} conformed to no clear-cut pattern. On the other hand, K_{270} drastically increased above an amplitude of 40%. Figure 7.12 shows the variation of K_{270} with time at a variable radiation amplitude; also, it illustrates the effect of bubbling air during the oxidation process.

The strong influence of temperature on US-assisted oxidation reactions entails placing the sample containers in a thermostated bath in order to ensure reproducible results.
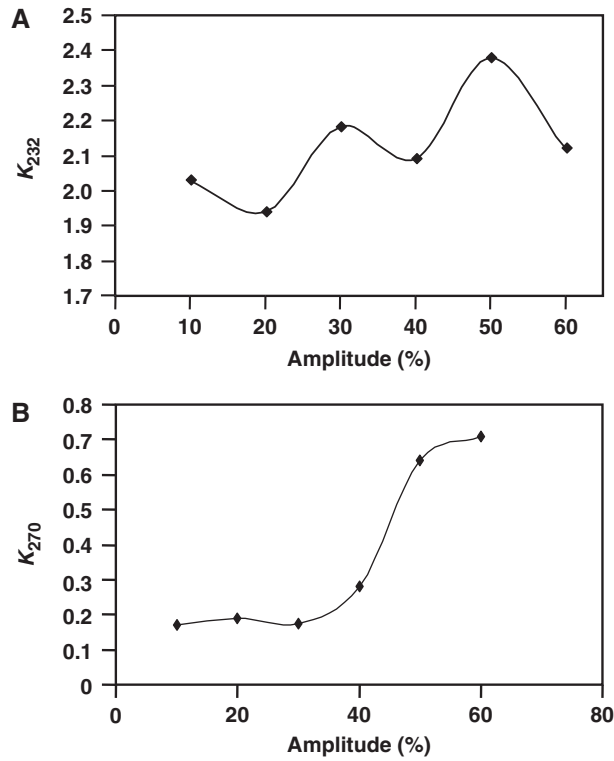
FIGURE 7.11. *Influence of radiation amplitude on the oxidation of olive oil as determined by monitoring the absorbance at 232 nm (A) and 270 nm (B), and plotting the US variable against K. (Reproduced by permission of Elsevier, Ref. [74].)*
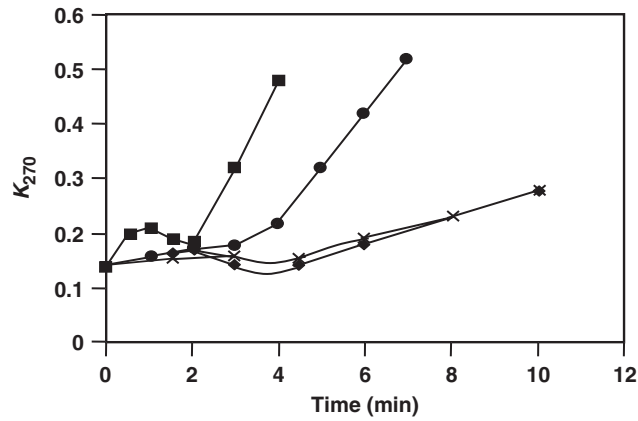

FIGURE 7.12. *Plot of parameter K_{270} as a function of time at a variable US radiation amplitude. 3% (♦), 40% (●) and 50% (■). The effect of bubbling air during the oxidation process was studied at a radiation amplitude of 30% (x). (Reproduced with permission of Elsevier, Ref. [74].)*

Figure 7.13 shows the oxidative stability of virgin olive oils from diverse olive varieties. Figure 7.14 exposes the excellent correlation of the US method with the conventional Rancimat method, and the drastic reduction in operating time (from, for example, 129 h to 50 min [74]).

This research has opened up new avenues in food analysis for accelerating the oxidation step in existing methods for the determination of the oxidative stability of edible fats.

7.4.   ULTRASOUND-ASSISTED HYDROLYSIS REACTIONS

Hydrolysis reactions in analytical chemistry are mainly used to convert the target analytes into easily derivatized and detected forms. Whereas the accelerating effect of US on these reactions has been widely proven and thoroughly studied in organic chemistry under different chemical (pH, aqueous–organic media) and US conditions [75–77], few analytical studies on them have been reported. By contrast, US-assisted enzymatic hydrolysis reactions have received considerable attention from analytical and bioanalytical chemists; such reactions, however, are discussed in Chapter 3 as the processes are better known as enzymatic digestions.

7.4.1. Hydrolysis of phenol compounds

One of the few recent examples of this reaction is the hydrolysis of paracetamol simultaneously with its LLE into an alkaline medium from suppositories [32]. Separate development of each step showed the yield of the derivatizing reaction to be higher when the hydrolysis step is assisted by US (absorbances were five times higher than with non-sonicated hydrolysis).
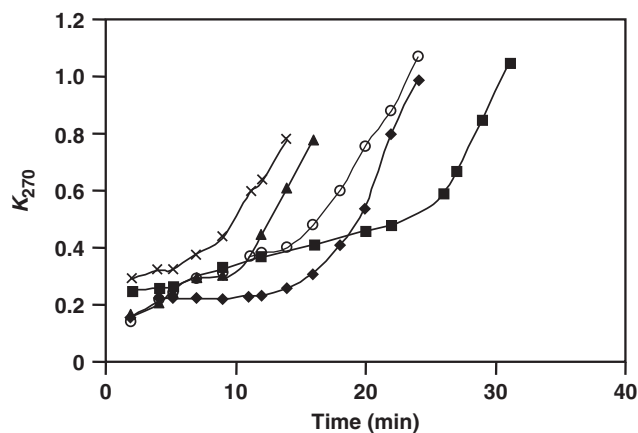

FIGURE 7.13. *Study of the stability of four virgin olive oils from different olive seed varieties obtained in the first extraction and from repaso oil (second extraction) using the US-assisted method. Olive variety: arbequina (♦), hojiblanca (○), manzanilla (▲), picual (■) and repaso (**x**). (Reproduced with permission of Elsevier, Ref. [74].)*
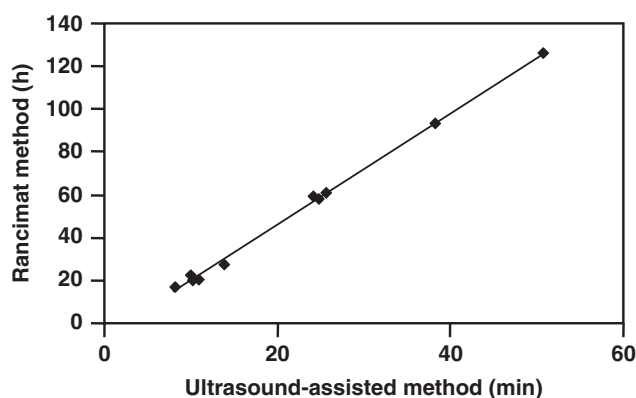
Figure 7.14. *Comparison of the results of the US-assisted and conventional Rancimat methods (Reproduced with permission of Elsevier, Ref. [74].)*

The US-assisted leaching of phenol compounds from strawberries with an acetone solution containing 0.2 M HCl and 2 g/l *ter*-butyl-hydroquinone facilitates the hydrolysis of the target phenols and their dissolution in the leachant, thus accelerating their removal from the matrix. A titanium alloy probe (2.54 mm in diameter) was used to develop three 30-s cycles; the operating conditions included 50% US amplitude and 0.8-s pulses over 1 s for an overall time of 30 s. The resulting yields were similar to those obtained by maceration at 85–90°C for 20 h, with no appreciable degradation [78] — which is one of the major shortcomings of long leaching times [79].

7.4.2. Hydrolysis of carbohydrates

One of the most common hydrolysis reactions is that required to convert polysaccharides into monosaccharides prior to the determination of total carbohydrates in food and environmental samples. The use of highly acid media (*e.g.* 12 M sulphuric acid) and elevated temperatures (≈100°C) for 20 min produced partial oxidation of carbohydrates [80]. Using room temperature to avoid oxidation resulted in incomplete hydrolysis [81], and so did lowering the concentration of sulphuric acid to 0.5 M while keeping the temperature at 100°C for 8 h [82–84]. One of the most accurate ways of determining total carbohydrates is by using 1 M HCl at 100°C for 20 h [85,86].

Existing studies on the US-assisted hydrolysis of carbohydrates have failed to clarify the behaviour of chemical systems upon US irradiation [87]. Thus, Dubois *et al*. used a US bath at a frequency of 35 kHz — further details were not reported — as, in their opinion, a probe increases the temperature of the irradiated system significantly. They found very acid conditions (12 M sulphuric acid) to cause total degradation of carbohydrates — the sonicated solution did not exhibit any absorption at 485 nm after the addition of phenol for the development of the Dubois method [88]. They concluded that promoting hydrolysis in an acid medium — it is unclear whether they assayed different acid concentrations — is not feasible and performed the ultrasonicated hydrolysis step in pure water for 3 h, after which they added the acid to develop the derivatizing reaction. Further research on this topic is clearly required in order to clarify such an uncommon behaviour.

The above examples clearly show that the experience on hydrolysis largely acquired in dealing with organic compounds for non-analytical purposes [1–7] has been under-exploited in the analytical field.

7.5. EXPERIENCE IN SONOCHEMISTRY TO BE EXPLOITED IN ANALYTICAL CHEMISTRY

The long time during which research in sonochemistry has been conducted and the fact that no special equipment requirements are involved in using ultrasonic energy — other, by contrast, "older" technologies such as electrochemistry require a conducting medium, photochemistry the presence of a chromophore and microwaves of dipolar species — have promoted the development of a large number and variety of applications which analytical chemists could exploit. Most such applications have been developed by using US devices present in most analytical laboratories (*e.g.* power ultrasonic devices with frequencies in the range 20–100 kHz); others, however, use unusual frequencies.

7.5.1. Ultrasound-related variables and their effects on chemical reactions

As shown in the previous sections, most analytical applications of US-assisted reactions have been developed without optimizing US variables; such a simple sentence as "ultra-sound is applied for *x* min" has been the only detail given in most cases. Past experience with US-assisted reactions makes it advisable to consider the following variables in developing new analytical applications.

Ultrasound frequency

It has been widely demonstrated that low frequencies, close to 20 kHz, enhance cavitation, which is the source of the dramatic effect of ultrasonic power on chemical reactivity. However, higher frequencies are advantageous when radical formation is the key to facilitating, accelerating or making possible a given reaction.

Ultrasound power and intensity

The first requirement for attaining the level of US required to cause chemical effects on a reaction is that sufficient acoustic energy be supplied in order to overcome the cavitation threshold of the medium. Once the threshold has been exceeded, the region of cavitation around the radiating source, the "cavitational zone", will increase with increasing intensity; also one might expect the sonochemical rate to increase in parallel. In fact, the observed increase in the rate of hydrolysis of methyl ethanoate in the presence of US was found to be directly proportional to intensity. A limiting value was reached, however, beyond which the sonochemical rate decreased with increasing power [89,90]. A further example is provided by the effect of power on the release of iodine by sonolysis of aqueous KI [91], where the initial response of iodine appears to be proportional to power, but the effect decreases beyond 40 W and drops dramatically above 100 W. The explanation for these effects of US power lies in the production of a large number of cavitation bubbles on and near the acoustic source that act as a "cushion" to dampen the efficiency of energy transmission into the medium.

Solvent, temperature and pressure

The choice of solvent and the bulk working temperature are two significantly important, often interrelated variables. An increased solvent vapour pressure decreases the maximum bubble collapse temperature and pressure. Hence, for a reaction where cavitational collapse is the primary source of sonochemical activation, a low bulk temperature is to be preferred — particularly if a low-boiling solvent is used. Conversely, for a reaction requiring elevated temperatures, a high-boiling solvent will be more appropriate. For heterogeneous reactions where the effect of sonication is exerted on the surface of either a catalyst or an inorganic solid reagent, a balance must be struck to ensure enough cavitation to activate the reagent without overly disturbing the thermodynamics of the reaction.

Application of an external pressure to a reaction system, which increases the hydrostatic pressure of the liquid, increases the energy required to initiate cavitation. In practical terms, if such a threshold energy can be exceeded with the available irradiation source, then raising the hydrostatic pressure will increase the sonochemical effect as the maximum temperatures and pressures experienced during bubble collapse will be higher under these conditions.

7.5.2. Homogeneous and heterogeneous reactions

The disparate US requirements of homogeneous and heterogeneous reactions have also been rarely considered by analytical chemists conducting research in this field.

Homogeneous reactions

In homogeneous liquid systems, sonochemical effects generally occur either inside the collapsing bubble, — where extreme conditions are produced — at the interface between the cavity and the bulk liquid — where the conditions are far less extreme — or in the bulk liquid immediately surrounding the bubble — where mechanical effects prevail. The inverse relationship proven between ultrasonically induced acceleration rate and the temperature in hydrolysis reactions under specific conditions has been ascribed to an increase in frequency of collisions between molecules caused by the rise in cavitation pressure gradient and temperature [92–94], and to a decrease in solvent vapour pressure with a fall in temperature in the system. This relationship entails a multivariate optimization of the target system, with special emphasis on the solvent when a mixed one is used [95–97]. Such a commonplace hydrolysis reaction as that of polysaccharides for the subsequent determination of their sugar composition, whether both catalysed or uncatalysed, has never been implemented under US assistance despite its wide industrial use [98].

Homogeneous non-aqueous sonochemistry is another unexplored area for analytical chemists that might provide very interesting results [99].

Heterogeneous reactions

This type of US-assisted reaction, which is very common in organic chemistry (particularly organometallic chemistry), has not yet been used as such in the analytical field, where US could be applied to common organic reactions preceding GC separation that could be implemented in a continuous manner by placing the solid catalyst in a minicolumn subjected

to US at appropriate times. Also, these reactions can be used to amplify the favourable effect of US on leaching processes, which would act on both the reaction and leaching.

The effects of US on these reactions are the results of: (1) transient bubble collapse on or near the solid surface causing a jet of liquid to impinge on it; and (2) acoustic streaming, by which US waves cause the liquid to move and aid mass transfer. The variables boosting these actions must be optimized on a case-by-case basis.

The Barbier [100,101], Bouveault [102] and Reformatsky reactions [103], to name a few of the many that can be accelerated by US, have not yet been addressed in analytical sono-chemistry. Models of controlled and calculable time averaged rate of mass transfer to and from the interface [104] can be highly useful in this context.

Ultrasound-assisted degradation

Destruction of undesirable pollutants is a common practice in the environmental field that has taken wide use of US for accelerating degradation processes. Thus, the mechanisms of US action on cellular material have been clarified [105] and the effect on its destruction demonstrated as efficient. Unfortunately, the need for high US intensities makes the technique expensive to use for general microbiological decontamination. However, this degradation method can be analytically useful with a view to identify and (or) determine key components after fast sample preparation.

Recent reports on research in this field — concerned with dye [106–111], phenolic contaminants [112–115], fluoro or sulphonate compounds [116] and volatile species degradation [117,118] — testify to the interest raised in this area from which analytical chemists can obtain interesting analytical information.

The combined use of US of highly different frequencies and inorganic catalysts [119–122], ultraviolet light [123], photocatalysts [124] and biocatalysts [125], and that of US and electrochemistry [126,127], has also been widely exploited, but not for analytical purposes [128].

The use of US to reduce the antioxidant activity of olive mill wastewater can be of interest to analytical chemists with a view to characterize the degradation products [129].

Ultrasound-assisted anaerobic digestion, which yields characteristic products that are easier to identify and quantify than those from aerobic digestion, is another unexplored area for analytical chemists.

Ultrasound-assisted degradation reactions are not exclusive of the environmental field; in fact they have also been used in polymer studies. There is no universal consensus regarding the influence of US frequency on this process. Thus, Schmid's hypothesis that degradation is the result of solvent movement past the macromolecule, so, a decreased frequency should allow a rigid macromolecular structure more time to accommodate the impact of the solvent (*i.e.* degradation ought to decrease with decreasing frequency [130]) contradicted by the fact that degradation increases with decreasing frequency or is unaffected by this variable [131,132]. There is also some debate over the effect of external pressure; whereas an increased solvent vapour pressure reduces depolymerization, and so does an increased temperature, the US intensity must be empirically optimized for each individual polymer–solvent system.

A number of chemical analyses require prior depolymerization of the original sample (*e.g.* starch, lignin, chitosan, carbohydrates). This process is occasionally very slow and has scarcely been subjected to US, despite the proven accelerating effect of this form of energy on these polymers [133,134] and others such as polystyrene [135] and poly(ethylene oxide) [136], or even on pharmaceutical precursors [137].

7.6. CONCLUSIONS

Past success in the use of organic reactions (*e.g.* depolymerization [13], esterification [16,20], alkylation [31], addition [32], ethylation [35]) for analytical purposes should encourage analytical chemists to explore the benefits of sonochemistry.

Also, analytical chemists could monitor such reactions to facilitate their optimization and subsequently implement them with available equipment [138]. This would provide an improved knowledge of the underlying mechanisms and facilitate the development of modern sample preparation techniques for clean-up and preconcentration [139].

Careful selection of the type and characteristics of the US device will always be required as it can be the key to successful development of US-assisted methods involving organic reactions [140].

References

1. K.S. Suslick, Ed., *Ultrasound: Its Chemical, Physical and Biological Effects,* VCH, Weinheim, Germany, 1988.
2. T.J. Mason and J.P. Lorimer, *Sonochemistry. Theory, Applications and Uses of Ultrasound in Chemistry,* Ellis Horwood, Chichester, England, 1989.
3. S.V. Ley and C.M.R. Low, *Ultrasound and Synthesis,* Springer-Verlag, Heidelberg, Germany, 1989.
4. T.J. Mason, Ed., *Advances in Sonochemistry,* JAI Press, London, England, 1990.
5. T.J. Mason, *Practical Sonochemistry. A Users Guide to Applications in Chemistry and Chemical Engineering,* Ellis Horwood, Chichester, England, 1991.
6. T.J. Mason, *Sonochemistry,* Oxford University Primer Series, No.70, Oxford Science Publications, Oxford, England, 1999.
7. T.J. Mason and J.P. Lorimer, *Applied Sonochemistry,* Wiley-VCH, Weinheim, Germany, 2002.
8. C.W. Porter and L. Young, J. Am. Chem. Soc., 60 (1938) 1497.
9. P. Linares, F. Lázaro, M.D. Luque de Castro and M. Valcárcel, *Anal. Chim. Acta,* 200 (1987) 51.
10. E.W. Flosdorf and L.A. Chambers, *J. Am. Chem. Soc.*, 55 (1933) 3051.
11. A. Szalay, *Phys. Chem. A*, 164 (1933) 234.
12. A.S. Gyorgi, *Nature* (London), 131 (1933) 278.
13. M. Korn, P. Machado Primo and C. Santos de Sousa, *Microchem. J.*, 73 (2002) 273.
14. C. Santos de Sousa and M. Korn, *Anal. Chim. Acta*, 444 (2001) 309.
15. J. Ruiz-Jiménez and M.D. Luque de Castro, *Anal. Chim. Acta*, 489 (2003) 1.
16. B. Fransson and U. Ragnarsson, *J. Chromatogr.*, 827 (1998) 31.
17. L. Liu and P.K. Dasgupta, *Anal. Chem.*, 68 (1996) 1817.
18. M.A. Jeannot and F.F. Cantwell, *Anal. Chem.*, 68 (1996) 2236.
19. E. Psillakis and N. Kalogerakis, *Trends Anal. Chem.*, 21 (2002) 54.
20. Y.C. Fiamegos, C.G. Nanos and C.D. Stalikas, *J. Chromatogr.*, 813 (2004) 89.
21. A. di Corcia, *J. Chromatogr.*, 80 (1973) 69.
22. P. Buryan, J. Macak and J. Hrivna, *J. Chromatogr. A*, 137 (1977) 425.
23. Y. Hoshika, *J. Chromatogr. A*, 144 (1977) 181.
24. J.N. Seiben, D.G. Crosby, H. Fonda and C.J. Soderquist, *J. Chromatogr. A*, 73 (1972) 89.
25. R.J. Agauer, *Anal. Chem.*, 40 (1968) 122.
26. Y.I. Korenman, I.V. Gruzdev, B.M. Kondratenok and V.N. Fokin, *Anal. Chem.*, 54 (1989) 1134.
27. S. Nakamura, M. Takino and S. Dasihima, *Analyst*, 126 (2001) 3089.
28. L.E. Sojo and J. Djauhari, *J. Chromatogr.*, 840 (1999) 21.
29. I. Turnes, I. Rodríguez, C.M. García and R. Cela, *J. Chromatogr.*, 743 (1996) 283.
30. M.D. Luque de Castro and A. Jurado López, Pervaporation, *Encyclopedia Anal. Sci.*, (2005) 538.

31. E. Priego-López and M.D. Luque de Castro, *Chromatographia*, 57 (2003) 513.
32. F. Priego-Capote and M.D. Luque de Castro, *Anal. Chim. Acta*, 489 (2003) 223.
33. S. Rapsomanikis, O.F.X. Donard and J.H. Weber, *Anal. Chem.*, 58 (1986) 35.
34. N. Bloom, *Can. J. Fish. Aquat. Sci.*, 46 (1989) 1131.
35. Q. Tu, J. Qian and W. Frech, *J. Anal. At. Spectrom.*, 15 (2000) 1583.
36. S. da Silva Borges and M. Korn, *Quim. Nova*, 25 (2002) 558.
37. S. da Silva Borges, M. Korn and J.L.F. Costa Lima, *Anal. Sci.*, 18 (2002) 1361.
38. M. Korn, M.V.A.S. Andrade, S. da Silva Borged, C.S. Sousa and F.S. Oliveira, *J. Braz. Chem. Soc.*, 14 (2003) 254.
39. M. Korn, private communication.
40. F. Battin-Leclerc, F. Baronnet, G. Paternotte, J.P. Leclerc and R. Gourhan, *J. Anal. Appl. Pyrolysis*, 53 (2000) 95.
41. G.L. Hatch, *Anal. Chem.*, 56 (1984) 2238.
42. Z. Marczenko, *Spectrophotometric Determination of Elements*, Wiley & Sons, New York, 1976.
43. J.L. Capelo, I. Lavilla and C. Bendicho, *Anal. Chem.*, 72 (2000) 4979.
44. J.L. Capelo, C. Maduro and A.M. Mota, *J. Anal. At. Spectrom.*, 19 (2004) 414.
45. J.L. Capelo, C.D. dos Reis, C. Maduro and A.M. Mota, *Talanta*, 64 (2004) 217.
46. J.L. Capelo, C. Maduro and A.M. Mota, *Ultrason. Sonochem.*, 13 (2006) 98.
47. J.T. Creed, T.D. Martin and C.A. Brockholl, *J. Anal. At. Spectrom.*, 10 (1995) 443.
48. B. Welz, D.L. Tsalev and M. Sperling, *Anal. Chim. Acta*, 261 (1992) 91.
49. T. Korenaga and H. Ikatsu, *Analyst*, 106 (1981) 653.
50. T. Korenaga and H. Ikatsu, *Anal. Chim. Acta*, 141 (1982) 301.
51. T. Korenaga, X. Zhou, O. Kimido, T. Moriwake and S. Shinoda, *Anal. Chim. Acta*, 272 (1993) 237.
52. M. Goto, *Trends Anal. Chem.*, 2 (1983) 92.
53. J.M.H. Appleton, J.F. Tyson and R.P. Mounce, *Anal. Chim. Acta*, 179 (1986) 269.
54. L. Tian and A. Wu, *Anal. Chim. Acta*, 261 (1992) 301.
55. A. Canals and M.R. Hernández, *Anal. Bioanal. Chem.*, 374 (2002) 1132.
56. A. Canals, A. Cuesta, L. Gras and M.R. Hernández, *Ultrason. Sonochem.*, 9 (2002) 143.
57. A. Cuesta, J.L. Todolí, J. Mora and A. Canals, *Anal. Chim. Acta*, 372 (1998) 399.
58. J.R. Baker, M.W. Milke and J.R. Mihelcic, *Water Res.*, 33 (1999) 327.
59. Y.C. Kim, S. Sasaki, K. Yano, K. Ikerbukuro, K. Hashimoto and I. Karube, *Analyst*, 125 (2000) 1915.
60. A. Cuesta, J.L. Todolí and A. Canals, *Spectrochim. Acta B*, 51 (1996) 1791.
61. K. Robards, A.F. Kerr and E. Patsalides, *Analyst*, 113 (1988) 213.
62. J. Tsaknis, S. Lalas, M. Hole, G. Smith and V. Tychopoulos, *Analyst*, 123 (1988) 325.
63. T. Chiba, M. Takazawa and K. Fujimoto, *JAOCS*, 66 (1989) 1588.
64. E.K. Strochkova, Y. Turyan and I. Kuselman, *Talanta*, 54 (2001) 411.
65. J.A. García-Mesa, M.D. Luque de Castro and M. Valcárcel, *Lab. Robotics Autom.*, 5 (1993) 29.
66. J.A. García-Mesa, M.D. Luque de Castro and M. Valcárcel, *Talanta*, 11 (1993) 1595.
67. P.G. Nouros, C.A. Georgiou and M.G. Polissiou, *Anal. Chim. Acta*, 389 (1999) 239.
68. J.A. García-Mesa, M.D. Luque de Castro and M. Valcárcel, *Analyst*, 118 (1993) 891.
69. M.P. Cañizares and M.D. Luque de Castro, *Anal. Chim. Acta*, 323 (1996) 55.
70. AOCS Active Oxygen Method, CD 12–57 (1981).
71. M.W. Laubli and P.A. Bruttel, *JAOCS*, 63 (1986) 772.
72. M.P. Cañizares, J.A. García-Mesa and M.D. Luque de Castro, *Anal. Biochem. Chem.*, 378 (2004) 479.
73. F. Chemat, I. Grondin, A.S.C. Sing and J. Smadja, *Ultrason. Sonochem.*, 11 (2004) 13.
74. M.P. Cañizares, J.A. García-Mesa and M.D. Luque de Castro, *Anal. Chim. Acta*, 502 (2004) 161.
75. J.N. Chen and W.M. Kalback, *Ind. Eng. Chem. Fundam.*, 6 (1967) 175.
76. S. Fogler and D. Barnes, *Ind. Eng. Chem. Fundam.*, 7 (1968) 222.
77. E.C. Couppis and G.E. Klinzing, *AJChE J.*, 20 (1974) 485.
78. M.C. Herrera and M.D. Luque de Castro, *Anal. Biochem. Chem.*, 379 (2004) 1106.

79. M.D. Luque de Castro and J.L. Luque García, *Acceleration and Automation of Solid Sample Treatment*, Elsevier, Amsterdam, 2002.
80. B. Josefsson, L. Uppstrom and G. Ostling, *Deep-Sea Res.*, 19 (1972) 385.
81. J.D. Pakulsky and R. Benner, *Marine Chem.*, 40 (1992) 143.
82. A. Compiano, J. Romano, F. Garabetian, P. Laborde and I. de la Giraudière, *Marine Chem.*, 42 (1993) 237.
83. M. Kakuta and A. Misaky, *Agric. Biol. Chem.*, 43 (1979) 993.
84. M. Kakuta and A. Misaky, *Agric. Biol. Chem.*, 43 (1979) 1269.
85. S.M. Myklestad, E. Skanoy and S. Hestmann, *Marine Chem.*, 56 (1997) 279.
86. C.M. Burney and J.Mc.N. Sieburth, *Marine Chem.*, 5 (1977) 15.
87. M. Mecozzi, M. Amici, E. Pietrantonio and R. Acquistucci, *Ultrason. Sonochem.*, 6 (1999) 133.
88. M. Dubois, K.A. Gilles, J.K. Hamilton, P.A. Rebers and F. Smith, *Anal. Chem.*, 28 (1956) 350.
89. E.C. Coupis and G.E. Klinzing, *AIChE J.*, 20 (1974) 485.
90. S. Folger and D. Barnes, *Ind. Eng. Chem. Fundam.*, 7 (1968) 222.
91. A. Helglein, Contributions to Various Aspects of Cavitation Chemistry, in T.J. Mason (Ed.), *Advances in Sonochemistry*, JAI Press, London, 1993, p. 17.
92. P. Riesz, Free Radical Generation by Ultrasound in Aqueous Solutions of Volatile and Non-Volatile Solutes, T.J. Mason (Ed.), *Advances in Sonochemistry*, JAI Press, London, 1993, p. 23.
93. J.W. Chen and W.M. Kalback, *Ind. Eng. Chem. Fundam.*, 6 (1967) 175.
94. A. Tuulmets and P. Raik, *Ultrason. Sonochem.*, 6 (1999) 85.
95. T.J. Mason and J.P. Lorimer, *J. Chem. Soc. Chem. Commun.*, (1980) 1135.
96. A. Tuulmets and S. Salmar, *Ultrason. Sonochem.*, 8 (2001) 209.
97. M. Sivakumar, O. Senthilkumar, S. Majumdar and A.B. Pandit, *Ultrason. Sonochem.*, 9 (2002) 25.
98. M. Sakakibara, D. Wang, R. Takahashi and S. Mori, *Enz. Microb. Technol.*, 18 (1996) 444.
99. A. Henglein and C.H. Fisher, *Ber. Bunsenges Phys. Chem.*, 88 (1984) 1196.
100. D.H. Yang, J. Einhorn, C. Einhorn, M.J. Aurell and J.L. Luche, *J. Chem. Soc. Chem. Commun.*, (1994) 1815.
101. M.J. Aurell, C. Einhorn, J. Einhorn and J.L. Luche, *J. Org. Chem.*, 60 (1995) 8.
102. C. Petrier, A.L. Gemal and J.L. Luche, *Tetrahedron Lett.*, 23 (1982) 3361.
103. B.H. Han and P. Boudjouk, *J. Org. Chem.*, 47 (1982) 5030.
104. J. Booth, R.G. Compton, E. Hill, F. Marken and T.O. Rebbitt, *Ultrason. Sonochem.*, 4 (1997) 1.
105. D.E. Hughes and W.L. Nyborg, *Science*, 138 (1962) 108.
106. G. Tezcanli-Guyer and N.H. Ince, *Ultrason. Sonochem.*, 10 (2003) 235.
107. A. Rehorek, M. Tauber and G. Gübitz, *Ultrason. Sonochem.*, 11 (2004) 177.
108. K.T. Byun and H.Y. Kwak, *J. Photochem. Photobiol. A*, 175 (2005) 45.
109. J. Wang, B. Guo, X. Zhang, Z. Zhang, J. Han and J. Wu, *Ultrason. Sonochem.*, 12 (2005) 331.
110. K. Okitsu, K. Iwasaki, Y. Yobiko, H. Bandom, R. Nishimura and Y. Maeda, *Ultrason. Sonochem.*, 12 (2005) 255.
111. A.O. Martins, V.M. Canalli, C.M.N. Azevedo and M. Pires, *Dyes Pigments*, 68 (2005) 227.
112. Y. Lu and L.K. Weavers, *Environ. Sci. Technol.*, 36 (2002) 232.
113. H. Hao, M. Wu, Y. Chen, Y. Yin and Z. Lu, *Environ. Toxicol.*, 18 (2003) 413.
114. H. Hao, Y. Chen, M. Wu, H. Wang, Y. Yin and Z. Lü, *Ultrason. Sonochem.*, 11 (2004) 43.
115. Y. Kojima, T. Fujita, E.P. Ona, H. Matsuda, S. Koda, N. Tanahashi and Y. Asakura, *Ultrason. Sonochem.*, 12 (2005) 359.
116. H. Moriwaki, Y. Takagi, M. Tanaka, K. Tsuruho, K. Okitsu and Y. Maeda, *Environ. Sci. Technol.*, 39 (2005) 3388.
117. O. Ayyildiz, P.R. Anserdon and R.W. Peters, *J. Hazards Mat. B*, 120 (2005) 149.
118. H. Shemer and N. Narkis, *Ultrason. Sonochem.*, 12 (2005) 495.
119. D. Drijvers, H. van Langenhove and M. Bekers, *Water Res.*, 33 (1999) 1187.
120. A.N. Nikolopoulos, O. Igglessi-Markopoulou and N. Papayannakos, *Ultrason. Sonochem.*, 11 (2004) 183.

121. M.H. Entezari, A. Meshmati and A. Sarafraz-yazdi, *Ultrason. Sonochem*., 12 (2005) 137.
122. N.B. Abderrazik, A. Azmani, C. R'Kiek, W. Song and K.E. O'Shea, *Catal. Today*, 101 (2005) 369.
123. R.A. Sierka and G.I. Amy, *Ozone Sci. Eng*., 6 (1985) 275.
124. E. Selli, C.L. Bianchi, C. Pirola and M. Bertelli, *Ultrason. Sonochem*., 12 (2005) 395.
125. M.H. Entezari and C. Pétrier, *Ultrason. Sonochem*., 12 (2005) 283.
126. F. Trabelsi, *Les ultrason de haute frequence: Etude d'un reacteur, application a la degradation de composes organiques par sonochimie et sonoelectrochimie,* PhD Thesis, ENSIGC, Toulouse, France, 1995.
127. Y. Zhao, Z.L. Zhu and X.F. Huang, *Guangpuxue Yu Guangpu*, 24 (2004) 867.
128. Y.G. Adewuyi, *Environ. Sci. Technol*., 39 (2005) 3409.
129. D. Atanassova, P. Kefalas, C. Petrakis, D. Mantzavinos, N. Kalogerakis and E. Psillakis, *Environ. Intern*., 31 (2005) 281.
130. G. Schmid, P. Paret and H. Pfleider, *Kolloidn. Zh*., 124 (1951) 150.
131. G. Schmid and W. Poppe, *Z. Elektrochem*., 53 (1949) 28.
132. H.H. Jellinek, *J. Poly. Sci*., 37 (1959) 485.
133. R. Czechowska-Biskup, B. Rokita, S. Lotfy, P. Ulanski and J.M. Rosiak, *Carbohydrates Polym*., 60 (2005) 175.
134. S. Baxter, S. Zivanovic and J. Weiss, *Food Hydrocolloids*, 19 (2005) 821.
135. J. Li, S. Guo and X. Li, *Poly. Degrad. Stab*., 89 (2005) 6.
136. S.P. Vijayalakshmi and G. Madras, *Poly. Degrad. Stab*., 90 (2005) 116.
137. R.J. Emery, M. Papadaki, L.M. Freitas dos Santos and D. Matzavinos, *Environ. Intern*., 31 (2005) 307.
138. S. Hassoon, V. Bulatov, Y. Yasman and I. Schechter, *Anal. Chim. Acta*, 512 (2004) 125.
139. E. Psillakis, D. Matzavinos and N. Kalogerakis, *Chemosphere*, 54 (2004) 849.
140. J.L. Luche, C. Petrier, J.P. Lansard and A.E. Greene, *J. Org. Chem*., 48 (1983) 3837.

CHAPTER 8

Ultrasound Assistance for Improving Detection Techniques

8.1.   INTRODUCTION

In Chapters 2–7, we have discussed the use of US to facilitate preliminary operations of the analytical process such as cleaning or degassing (Chapter 2); sample dissolution (Chapter 3); removal of target analytes from solids (Chapter 4); specific processes in heterogeneous solid- and gas–liquid (Chapter 5) or liquid–liquid systems (Chapter 6); or chemical reactions (Chapter 7), in increasing closeness to detection.

This chapter deals with US assistance to operations that are even closer to the detection step such as nebulization or spray formation immediately before the insertion of sample into atomic or mass detectors, respectively; levitation to obtain a sample droplet (usually for *in situ* detection, with or without preconcentration or previous derivatization) and electroanalytical determinations (either to facilitate preparation of the electrode or influence the electroanalytical step itself). In nebulization and levitation, US competes — most often advantageously — with alternative choices having a similar effect; in electroanalytical methods, US has a characteristic effect. Both traditional and novel detection techniques can therefore benefit from US assistance in some way.

The US frequencies used to assist the operations discussed in this chapter fall in the range of kilohertz to megahertz; however, the underlying phenomena for each application differ. Thus, the effects involved in US-assisted electroanalytical techniques and nebulization are related to cavitation (*viz*. acoustic streaming, microstreaming and microjetting). Acoustical levitation in turn is based on the production of a standing wave between an ultrasonic radiator and a solid reflector.

The ultrasonic devices used to assist levitation and nebulization are typically conventional US transducers. Their simple design and operation have facilitated the development of widely available commercial equipment. On the other hand, the absence of US-assisted commercial electroanalytical cells has promoted the construction of laboratory-made units that are usually furnished with commercial probes or, less frequently, baths.

8.2.   ULTRASOUND-ASSISTED NEBULIZATION

Liquid nebulization as a means of obtaining aerosols is commonly used for activities such as drug administration, hair spraying or perfume application [1,2]. Direct nebulization of a liquid phase containing the target analytes has been widely used in analytical chemistry for sample insertion into some detection systems (particularly atomic spectrometers). The main purpose of analytical nebulizers is to insert the maximum possible amount of sample, and hence of analyte, in the form of aerosol consisting of very small droplets, into the detection system.

Aerosol generation by nebulization requires the liquid bulk to be assisted with energy. The characteristics of the aerosol formed are greatly dependent on the amount of energy supplied and the efficiency with which it is transferred [3]; this allows nebulizers to be classified according to the type of energy they use into:

(a) those assisted by the kinetic energy of a high-velocity gas stream (pneumatic nebulizers) or the liquid itself (hydraulic nebulizers);
(b) those assisted by mechanical energy applied through a rotating (rotating nebulizers) or vibrating device (ultrasonic nebulizers) and;
(c) those where the energy is generated by mutual repulsion of charges accumulated on the surface (electrostatic nebulizers).

For many years pneumatic nebulizers of the V-groove, Meinhard and cross-flow type have been the most widely used sample insertion devices for aerosol generation. The interaction geometry between the gas and liquid sample streams allows pneumatic nebulizers to be classified into two major groups, namely: (a) pneumatic concentric nebulizers, which involve concentric interaction; and (b) cross-flow nebulizers, which involve perpendicular interaction between the liquid and gas streams. Pneumatic nebulizers are well established and widely used on account of their simplicity, robustness, ease of use and low cost; however, they provide low transport efficiency and tend to be clogged by high salt-content solutions [4].

The search for more efficient systems for aerosol generation has led to an increasing use of thermal, hydraulic and ultrasonic nebulizers over the last two decades. The greatest disadvantages of these high-efficiency nebulizers are their high cost and difficulty of use [5]. Ultrasound has been used to assist sample insertion into detection systems ever since the earliest ultrasonic nebulizers (USNs) were reported in the 1980s [6]. The energy required to obtain an aerosol with a narrow droplet size distribution is emitted by a vibrating transducer. Once formed, the aerosol is carried to the detector by the nebulizer gas stream [7].

The analytical performance of atomic detectors in terms of sensitivity, selectivity and resolution has been markedly improved by the use of USNs. However, the utility of these nebulization systems is not exclusive of atomic detectors as, in fact, USNs have been successfully implemented in electrospray formation devices, which are employed as interfaces between separation techniques such as CE or HPLC and mass detection [8].

8.2.1. Use of ultrasonic nebulizers with atomic spectrometers

As noted earlier, USNs have been employed for sample insertion into atomic spectrometers such as flame atomic absorption spectrometry (FAAS) [9,10], electrothermal atomic absorption spectrometry (ETAAS) [11], atomic fluorescence spectrometry (AFS) [12,13], inductively coupled plasma-atomic emission spectrometry (ICP-AES) [14,15], inductively coupled plasma-mass spectrometry (ICP-MS) [16,17] and microwave induced plasma-atomic emission spectrometry (MIP-AES) [18,19]. Most of the applications of ultrasonic nebulization (USNn) involve plasma-based detectors, the high sensitivity, selectivity, precision, resolution and throughput have fostered their implementation in routine laboratories despite their high cost [4].

Ultrasonic nebulization devices for atomic spectrometers

Except for a few laboratory-made units and some devices marketed by other firms, most applications of ultrasonic nebulization (USNn) in atomic spectrometry have been developed with two commercial devices from CETAC Technologies (*viz.* the U-5000AT+ and U-6000AT+). It should be noted that these two commercial ultrasonic devices were originally designed for ICP instruments but have been used with other types of detectors [20].
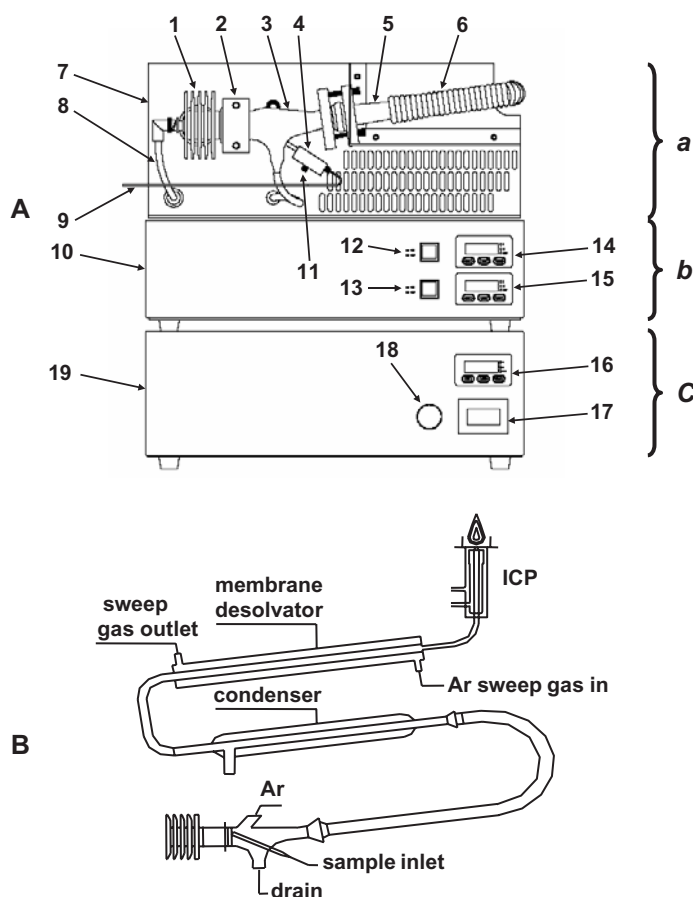
FIGURE 8.1. *(A) CETAC ultrasonic nebulizers U-5000AT+ (1–15) and U-6000AT+ (1–19). 1 — transducer, 2 — aerosol chamber stand, 3 — aerosol chamber, 4 — sample/rise adapter, 5 — U-tube, 6 — heat cords, 7 — glassware module, 8 — transducer radio frequency (RF) cable, 9 — sample inlet tubing, 10 — electronics module, 11 — auxiliary rinse port, 12 — operate switch, 13 — fast pump switch, 14 — heater controller (nebulizer), 15 — cooler controller (nebulizer), 16 — heater controller (desolvator), 17 — flow meter, 18 — flow control and 19 — membrane desolvator controller. (B) Detailed scheme of the U-6000AT+ glassware module. (Reproduced with permission of CETAC Technologies.)*

The U-5000AT+ model consists of two main modules, namely, glassware and electronics (*a* and *b* in Fig. 8.1A). The glassware comprises a piezoelectric transducer operating at 1.4 MHz, an aerosol chamber, a temperature-controlled heated U-tube evaporator and a thermo-electric condenser. The piezoelectric transducer converts rf energy into ultrasonic oscillations and nebulizes the liquid sample to a fine, dense aerosol which is received by the aerosol chamber and mixed with argon gas before entering the U-tube for vaporization; once vaporized, it is passed through a thermoelectric condenser where the solvent is

removed by a drain pump. The remaining sample consists of a dry, analyte-enriched aerosol for insertion into the detector. However, additional devices may be required with plasma-based detectors when the solvent vapour, whether aqueous or organic, cannot be efficiently removed. In order to solve this problem, the U-6000AT+ includes a membrane desolvator (see Fig. 8.1B) controlled by module *c* in Fig. 8.1A, consisting of a micro-porous PTFE tubular membrane where the solvent is retained while the analytes are sent to the detector through the tube. An argon flow removes the solvent vapour from the outer wall of the membrane. Whether the desolvator is required depends on the particular analytes and technique. Thus, in MIP-based techniques, matrix effects exhibited a strong influence in a systematic study of 35 analytes involving the use of USN without a desolvation system [21]. In some cases, the operation of the desolvation membrane can be hampered by the analysis conditions (*e.g.* in the determination of platinum in urine, where the membrane is prone to frequent blocking by the urine matrix [22]).

Liquid samples are inserted into the two commercial USNs through the inlet tubing by pumping with, for example, a peristaltic pump. For this reason, these nebulizers are frequently said to operate in the continuous mode [23]. The inlet tube also allows the USN to be used as an interface between a flow system, where other steps of the analytical process can be developed, and the detector. CETAC USNs have been used in official methods of analysis such as US-EPA Method 200.15 for the determination of metals and trace elements in water by USN-ICP-AES [24].

Ultrasound nebulizers can also be operated in the geyser mode [25,26], which involves using a nebulizing cell coupled to the ultrasonic transducer *via* a water transmitting bath. This nebulizer is scarcely used in quantitative analysis owing to its poor precision. However, it has the advantage that it does not produce any waste as any products condensing on the walls of the spray chamber are recycled into the sample cell. Joannon *et al*. modified a commercially available continuous USN, as shown in Fig. 8.2, to operate in the batch mode by coupling the ultrasonic transducer horizontally with a sample cell made of silica glass *via* a water bath [26]. The precision was thus improved and the
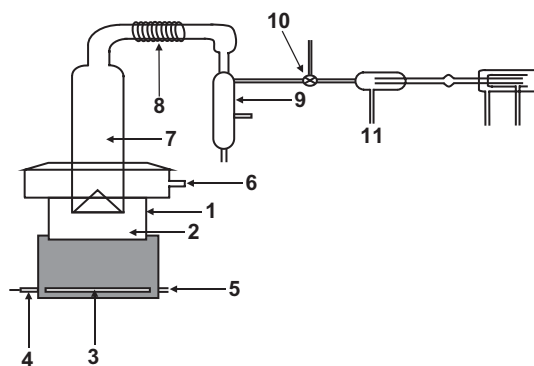

FIGURE 8.2. *Scheme of a geyser-type ultrasonic nebulizer. 1 — interchangeable nebulizing cell, 2 — sample solution and geyser-like aerosol plume, 3 — piezoelectric transducer, 4 — ultrasonic generator, 5 — transducer cooling circuit, 6 — PTFE base with argon carrier gas inlet, 7 — spray chamber, 8 — heated tube (150°C), 9 — condenser (1°C), 10 — 3-way valve and 11 — argon sheath gas. (Reproduced with permission of Elsevier, Ref. [26].)*

repeatability was similar to that obtained with pneumatic nebulization. In any case, geyser-type USNs have so far been scarcely accepted by analysts.

The high efficiency of USNs intended for dosage of pharmaceuticals has also been useful for sample insertion into atomic spectrometers. Thus, Hayashi *et al*. used one such nebulizer equipped with a vibrating metal mesh with a low-pressure helium ICP-MS instrument to remove argon-related interferences. One drawback was the low tolerance of solvent loading, which required the use of a desolvation system [27].

The relatively high cost of commercial USNs has promoted the development of custom-made prototypes. Thus, some authors have modified commercial humidifiers to obtain batch USNs for use with atomic spectrometers. However, these custom-made nebulizers are impractical and feature a severely limited throughput. Thus, Yeon *et al*. used a humidifier to make a continuous USN for ICP-AES with a configuration similar to that of the CETAC units [23]. The prototype exhibited improved sensitivity relative to a pneumatic nebulizer, but also impaired precision owing to signal instability.

Jankowski *et al*. used two prototypes of low-flow USNs differing in the configuration of the MIP excitation source [7]. One, designed by Jankowski's group, used a transducer operating at 2.6 MHz and 10 W, and horizontal conduction to the plasma source. The other, designed by Plazmatronika, was equipped with acoustic power adjustable up to 50 W and 2.65 MHz. A spherical spray chamber made of PTFE was used to couple the connection to the plasma source in a vertical configuration. Unlike most high-flow USNs for MIP-AES, neither nebulizer used a desolvation unit.

Variables involved in ultrasonic nebulization

Optimizing the major variables influencing USNn operation has been a crucial step in the development of some analytical methods; however, US energy variables such as frequency and intensity, which have proved influential in other processes such as digestion, leaching or emulsification, have rarely been considered in optimization studies. Thus, the two main variables influencing signal intensity during USNn are the nebulizer gas flow-rate and the temperature inside the heating, desolvation and cooling areas. The nebulizer gas flow-rate determines the velocity at which the sample can be inserted into the detector; however, it can also affect plasma stability in plasma-based detectors. For the CETAC USNs, this parameter is recommended to be set at 0.6–2.0 ml/min, depending on the particular application [20]. In ICP-MS, the dwell time, defined as the time taken by the instrument to measure the signal at each mass during repetitive scans, can be regulated *via* the flow rate of the nebulizer gas and sweep gas — which is an argon flow used to remove the solvent vapour from the exterior of the membrane desolvator when one is used. Figure 8.3 shows the influence of the sweep gas flow-rate of the USN on the signal intensity for Sb(V) and trimethylantimony chloride (TMSbCl$_2$) as obtained by ICP-MS [28].

Temperatures in a USN range from 140 to 160°C in the heating and desolvation zones, and are in the region of 2°C in the cooling area. However, the exact values depend on both the solvents employed and the sample composition, so, they should be optimized for each particular application. When a desolvation tube is used, its temperature is one crucial operating parameter for the USNn. Thus, if the temperature of the tube is too high, the water and organic solvent evaporate completely and the aerosol particulate may be too small to be carried by the nebulizer gas flow, thereby decreasing the transport efficiency; if the temperature is too low, then too much water and organic vapour may be introduced and the plasma overcooled as a result. One example for the influence of temperature is provided by Sb speciation analysis by HPLC–USN-ICP-MS, where lowering
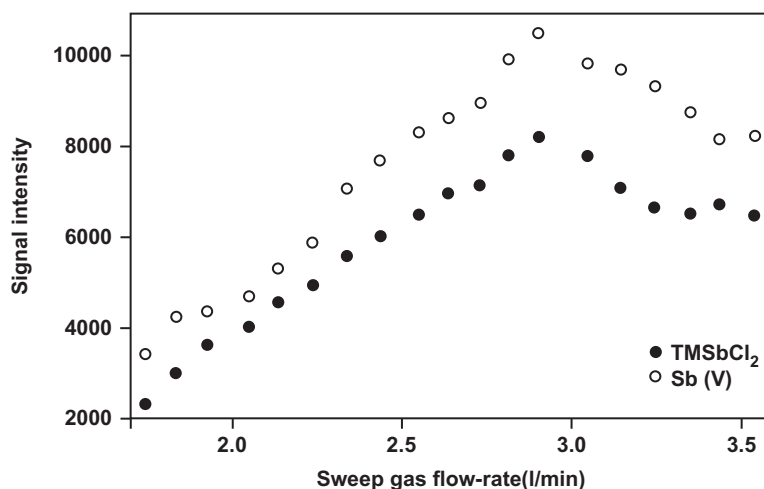
FIGURE 8.3. *Influence of the sweep gas flow-rate of the USN on the signal intensities of Sb(V) and TMSbCl$_2$. (Reproduced with permission of Elsevier, Ref. [28].)*

the temperature of the USN heating and desolvation regions from 160 to 80°C increased the sensitivity by approximately 25%, probably as a result of the absence of condensation of the aspirated mobile phase at 80°C in the tube connecting the outlet of the USN and the plasma torch [28]. Another example is the determination of trace elements in crude oil and fractions, where the heater system of the USN had to be disconnected in order to avoid deposition of asphaltenes and adherence of oil residues onto the quartz tube [29].

During the desolvation process in a USN, the sample is exposed to a large glass surface area; the analytes are often retained on the extensive glass surface and then released slowly throughout the following analysis, thereby increasing the background signal for these analytes. In order to remove the memory effect, an optimized washing protocol normally based on HCl and HNO$_3$ must be used to clean the equipment properly [30].

The solvent where the sample is diluted is another significant variable to be optimized (in terms of the detection system, sample stability, etc.) in order to ensure the best possible operating conditions.

Alternatives to ultrasonic nebulization

Ultrasonic nebulization is known to provide a higher analyte transport efficiency than pneumatic nebulization (normally 8–15 times higher); this results in improved sensitivity and lower detection limits, which is especially important for the analysis of species at trace or ultratrace levels [31–35]. Ultrasound-assisted generation of smaller drops and the use of a desolvation system to remove most of the solvent load allow the production of fine, dry analyte-enriched aerosol for insertion into a detection system; some authors, however, ascribe most of the sensitivity increase of USNs to the desolvation system alone [36].

Matrix effects in ultrasonic nebulization cause more problems than in pneumatic nebulization [37]. The matrix effects of USNn with heavy matrices have been ascribed to: (a) differences in matrix composition between standards and samples often leading to changes in the efficiency of aerosol formation due to changes in viscosity or salt content

of the sample and responsible for various evolution phenomena occurring in the plasma; (b) changes in aerosol transport, mainly during the condensation step; and (c) changes in analyte dissociation and (or) excitation in plasma-based detectors. All these phenomena decrease analyte signals. In theory, correction with a classical internal standard should allow these effects to be offset; occasionally, however, this conventional method fails. Thus, Hoenig *et al*. found the determination of boron and copper by USN-ICP-AES in the presence of calcium and nitric acid — which were added to both standards and samples — to be hampered by chemical reactions occurring in the condensation stage of the USNn and resulting in subsequent analyte losses to the waste [38,39]. In this situation, more sophisticated corrective means such as multivariate techniques are required. In common with other high-efficiency nebulizers (*e.g.* high-pressure or concentric high-efficiency nebulizers), USNs are only useful for significant matrix effects if an efficient desolvation system is employed. Another shortcoming of USNs — similar to all high-efficiency nebulizers — is their susceptibility to acid concentrations above 10%, which can cause erosion of the sampler cone. By contrast, conventional pneumatic nebulizers can operate at acid concentrations as high as 50% v/v, except for HF [40].

Concerning sample consumption, USNn reduces the sample insertion rate and results in longer measurement times, which is important in the analysis of semi-micro amounts of sample. However, sample consumption with USNn is high relative to microconcentric high-efficiency nebulizers, which can provide excellent results with as little as 100 µl of sample [41].

Applications of atomic spectrometers with ultrasonic nebulization for sample insertion

The widespread use of USNn for sample insertion in atomic spectrometers is apparent from the number of reported applications. As noted earlier, the atomic techniques benefiting to the greatest extent from USN are plasma-based techniques [4,19]. By contrast, FAAS- and ETAAS-based detectors have scarcely been used with USNn [9–11].

Laser-excited AFS with flame atomization or laser-induced plasma as atom source have also benefited from direct USNn. One example is the method used to obtain on-line and size-segregated information on the elemental chemical composition of ultrafine aerosols [12]. In contrast to plasma-based detectors, laser-excited AFS instruments afford miniaturization for field applications.

Microwave-induced plasma atomic emission spectrometry is a useful analytical technique for the determination of alkali and alkaline earth metals (*e.g.* that of sodium in water-soluble organic pharmaceuticals [42] with detection limits of 0.91–3.0 ng/ml). Also, it allows samples with organic contents up to 5% to be inserted without a desolvation system. Beryllium in spiked water samples was determined in this way with detection limits at the level of parts per trillion (ppt) and a precision of 1.8% as relative standard deviation (RSD) [43].

The USN-ICP-AES combination has been used in place of the time-consuming ETAAS for the determination of trace elements in biological and environmental matrices (*e.g.* As and B in plant matrices or plant-derived foods [44]); detection limits, however, were poorer than those provided by ETAAS. The same USN-ICP-AES combination has also been used for sequential trace multi-element determination of metals other than Cd in Argentinian wines — the presence of low cadmium concentration required the use of ETAAS instead [45].

Simultaneous determinations of several analytes at trace or ultratrace levels with a high resolution require the use of a highly sensitive multi-elemental technique such as

ICP-MS. Ultrasonic nebulization not only increases the sample introduction efficiency, and hence the analytical sensitivity, but also reduces the effects of problematic spectral interferences from different polyatomic species (oxides, hydroxides, argides). Typical examples include the determination of trace elements in food matrices, where USNn reduced the effect of interferences relative to pneumatic nebulization [46] and that of platinum group elements and gold in geological samples with resolvable signals above background in the femtogram per gram range [30]. However, spectral interferences from matrix constituents of the sample alter the quantification of some trace elements by low-resolution quadrupole ICP-MS in sample solutions with a high matrix complexity and salt load — the latter resulting from decomposition by melting with fluxes — in the absence of a desolvation system [17]. The use of high-resolution sector field ICP-MS allows the elimination of most polyatomic interferences, with improved sensitivity resulting from the improved ion transmission and low detection noise. Ultrasonic nebulization with magnetic sector field ICP-MS has enabled the determination of Pt, Pd and Rh at very low levels in urine samples relative to the low-resolution quadrupole ICP-MS, which proved ineffective to quantify the target analytes [47].

Organic samples have also been analysed with atomic detectors using USN without the need for sample preparation step. However, the insertion of organic solvents into the plasma of an ICP-MS instrument is critical since the plasma may be destabilized or even extinguished as a result. Thus, unoxidized carbon atoms may recombine to form graphite on the relatively cold interface cones and the ionic lens, thereby obstructing the cone orifices or changing the optimum voltage of the ionic lens. In addition, carbon polyatomic ions may be formed and interfere with the determination of some analytes [48]. Ultrasonic nebulizers — with or without a desolvation membrane — allow the amount of organic vapour that reaches the plasma to be restricted. Other miscellaneous approaches have been proposed to reduce the organic vapour content of the plasma such as the addition of oxygen to the plasma gas [49,50] in the determination of trace elements in crude oil and fractions by USN-ICP-MS, dilution with toluene being the sole treatment required. Carbon build-up at the interface and ion lenses was minimized by optimizing the argon-to-oxygen ratio in the plasma and by the desolvation system of the USN [29].

Ultrasonic nebulizers have also been employed in continuous flow systems as interfaces between sample preparation steps in the analytical process and detection by virtue of their suitability for operating in a continuous mode. Thus, preconcentration devices have commonly been coupled to atomic spectrometers in order to increase the sensitivity of some analytical methods. An enhancement factor of 100 (10 due to USNn and 10 due to preconcentration) was obtained in the determination of platinum in water using a column packed with polyurethane foam loaded with thiocyanate to form a platinum–thiocyanate complex [51]. An enhancement factor of 216 (12 with USNn and 18 with preconcentration) was obtained in the determination of low cadmium concentrations in wine by sorption of metallic complexes with pyridylazo reagents on the inner walls of a PTFE knotted reactor [52]. One special example is the sequential determination of As(III) and As(V) in water by coupling a preconcentration system to an ICP-AES instrument equipped with a USN. For this purpose, two columns packed with two different resins selective for each arsenic species were connected *via* a 16-port valve in order to concentrate them for their subsequent sequential elution to the spectrometer [53].

Separation equipment such as HPLC or CE has been coupled to atomic spectrometers *via* USNs to enable the determination of inorganic and organometallic analytes. Thus, antimony speciation analysis — inorganic Sb(III) and Sb(V), as well as $TMSbCl_2$ — was accomplished by separation by anion exchange chromatography and subsequent insertion of the eluent into the plasma of an ICP-MS instrument using USNn [28].

Selenium speciation analysis has been performed with on-column preconcentration HPLC–AFS and USN as the interface, with detection limits of 8.6 and 30 ng/ml for Se(IV) and Se(VI), respectively, in spiked water [13]. The high resolution and small sample consumption of CE have also been used in combination with ICP-MS *via* USN for efficient trace element speciation analysis in environmental and biological samples. Thus, metallothioneins were separated and detected using CE–USN-ICP-MS with resolution similar to that obtained with a concentric-glass nebulizer, but improved signal intensity (from 3.6 to 8.4 times) and signal-to-noise ratio (from 1.3 to 2.8 times) [54]. The CE–USN-ICP-MS combination has also been employed for the determination of inorganic anions and cations in aqueous solutions with detection limits in the low parts per billion (ppb) to ppt range [55].

In the case of solid samples, the usual procedure is the off-line transfer of the target analytes to a liquid phase. Such is the case with the determination of lead in *Ilex paraguariensis* (mate tea) samples, where the leachate was introduced into a continuous system for on-line preconcentration–determination using USN as an interface [56]; or that of platinum group elements in impact breccias by USN-ICP-MS following digestion and anion exchange concentration [57]. However, operations involving solid samples (*e.g.* leaching, digestion, pervaporation) can indeed be performed in continuous flow systems, so there should not be any problem to couple them with atomic spectrometric detection *via* a USN interface.

8.2.2. Ultrasound-assisted electrospray formation

Electrospray ionization (ESI) is a soft ionization method which allows the formation of gas phase ions through a gentle process that enables the sensitive determination of non-volatile and thermolabile compounds. The use of ESI sources in MS has greatly facilitated the study of large biomolecules, pharmaceutical drugs and their metabolites; this has revolutionized the field of biomedical analysis and contributed to the growth of proteomics and drug discovery research. ESI has been successfully used with virtually all types of mass spectrometers including quadrupole, magnetic, Fourier transform, ion trap and time-of-flight equipment [58].

The evolution of the ESI source has been marked by the use of electrospray devices as interfaces between the separation systems such as HPLC or CE and MS detectors, the earliest instances of which were reported by Yamashita and Fenn [59] and Aleksandrov *et al*. [60] in the mid-1980s. Because ESI–MS is used in many areas of chemistry, a vast number of articles reporting specific modifications of the electrospray interface has been published so far. Also, instrument manufacturers have provided innovative solutions for more sensitive and reliable mass spectrometers.

Controlling spray formation is crucial with a view to obtain a stable spray and an optimal signal. Because a small droplet contains less solvent, desolvation and ionization can be more efficient. In addition, with smaller droplets, analytes that are not surface active will have a greater chance of being transferred to the gas phase rather than being lost in the bulk of the parent droplet residue. The use of an ESI interface has been limited in practice by severe restrictions on solvent composition and volumetric flow-rate. Thus, when the volumetric flow-rate is in the range 0.05–3 ml/min, which is typical of HPLC, sensitivity can be an issue owing to the decreased ionization efficiency resulting from a large droplet size. In this case, some type of post-column flow splitting can be used in order to remove most part of mobile phase or buffer [8]. A better established alternative is the use of orthogonal nebulizers in order to sample the spray from a region peripheral

to the main droplet trajectory, where the droplets are smaller. Flow-rate restrictions make ESI amenable to capillary liquid chromatography at rates of nano or microlitres per minute. Concerning solvent composition, electrospray efficiency becomes particularly difficult when the mobile phase composition changes during gradient elution, which is required in many HPLC–MS applications. Coupling CE to ESI–MS is also complicated owing to the large variety of solvent compositions required for separation, including problems posed by the high conductivity of buffer solutions [58].

In order to improve the efficiency of the electrospray interface, researchers have sought a means to decouple as much as possible the spray formation and ionization processes so as to facilitate the production of fine spray of droplets required for successful ion evaporation in the source. For this purpose, spray formation should be made relatively independent of the physical and chemical properties of the liquid phase and its flow rate. One alternative is producing the spray by ultrasonic vibration nebulization instead of applying an electric field [61]. Figure 8.4 depicts an electrospray source equipped with a USN. This device is capable of producing the fine spray of droplets required for ESI by purely mechanical means, which is less dependent on the influence of applied electrical fields than conventional ESI. In addition, droplets generated by ultrasonic-assisted electrospray formation have proved more uniform in size than those provided by an electrospray interface equipped with a pneumatic nebulizer [62]. A USN has been coupled to a multiple channel ESI source to generate multiply charged (both positively and negatively) peptides and protein ions in order to obtain more information. For this purpose, a CETAC U-5000AT — suitable for ICP-based detectors — was connected to a seven-channel ESI–MS [63].

The widespread acceptance of ultrasonic-assisted electrospray formation has promoted the commercial production of a device of this type by Analytica of Branford, Inc. However, most applications of US-assisted electrospray formation are based on custom-made designs.

8.3.   ULTRASOUND-ASSISTED LEVITATION

The interest aroused by micro and nanotechnology in the scientific, chemical, biochemical, pharmaceutical, biological, biomedical and biotechnological fields, among others,
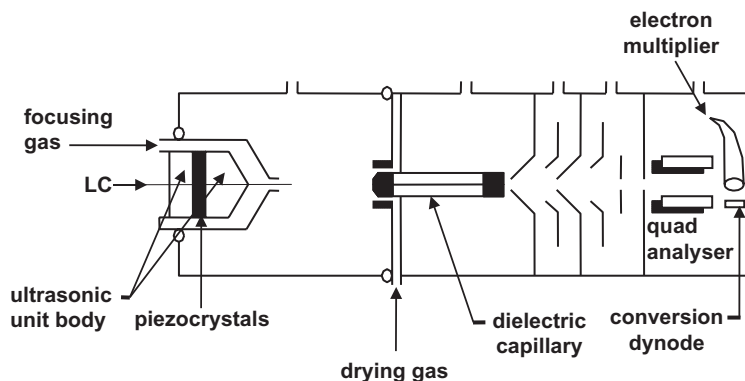
FIGURE 8.4. *Scheme of electrospray source with an ultrasonic nebulizer. (Reproduced with permission of the American Chemical Society, Ref. [61].)*

is indisputable. In this context, the miniaturization of analytical instruments has become a key trend by virtue of their wide applicability. However, miniaturization and nanotechnology are steadily growing in use, but there continues to be a lack of analytical systems capable of producing high-quality information at a high throughput.

The main advantages of miniaturized systems are reduced costs, short separation times, high throughput, system integration and multiplexing capabilities, increased reaction yields, expeditious operation and sample preparation, and reduced waste generation — which is crucial from an environmental point of view. Many of these advantages can be ascribed to the significantly increased surface-to-volume ratio of miniaturized analytical systems relative to large, conventional analytical systems, which enhances heat and mass transfer; as shown below, however, the increased surface-to-volume ratio can be disadvantageous in some cases. In addition, portable miniaturized systems afford simple, efficient integration of several steps lying close to one another in the time sequence of the overall analytical process, thereby facilitating automated handling of reduced amounts of samples [64,65].

In theory, the previous advantages could make miniaturization a panacea; in practice, however, they do not. Thus, when a system is scaled down, some characteristics such as lengths, areas and volume ratios can differ so markedly from those of macroscopic systems as to affect the development of the process concerned. The new behaviour will be dominated by material confinement in small structures, a large interfacial volume fraction and various unique properties, phenomena and processes. In fact, many current theories of matter at the microscale level have critical gaps for nanometer dimensions and fail to describe the new phenomena observed at the nanoscale level accurately [66]. Also, scaling-down can be problematic with samples containing low analyte concentrations as their determination will require larger amounts of sample.

Recent breakthroughs in miniaturized analytical instrumentation include fully integrated "lab-on-a-chip" and micro total analysis systems. The former have had only moderate success as many analytical chemists have been reluctant to accept them [67]. At present, chip-based analytical systems are subject to major shortcomings such as the risk of analyte adsorption on walls and at interfaces — which is important especially in low-volume analytical systems — and optical interference at the walls of the chips hampering detection. Further research in this field is required in order to effectively circumvent these shortcomings [68].

Levitation of small amounts of sample can be used to avoid contact with solid walls around the sample in a gas-surrounding medium (air in most cases). Levitation provides advantages similar to those of miniaturization in chip-based methods (basically, low reagent and sample consumption). In addition, levitation avoids contamination between samples and external objects, and also adverse effects of sample–wall contact on detection [69].

Sample levitation can be accomplished in different ways, one of which is by using ultrasonic energy. The phenomenon by which small samples of solids, liquids or suspensions can be levitated at the nodal points of a standing ultrasonic wave was first described by Bücks and Müller in 1933 [70]. The flexibility and potential of acoustic levitation in various fields are widely documented, mainly by studies in the analytical and bioanalytical fields [71–73]. Therefore, levitation can be considered a mature technique. Its development warrants inclusion of a dedicated section in this chapter to describe its fundamentals and compare the advantages and limitations of acoustic levitation with other levitation modes. The devices used for this purpose and the potential applications of each mode are also discussed.

8.3.1. Levitation techniques

There are various techniques enabling free matter floatation or levitation; because they rely on different physical principles, they have their own advantages and shortcomings. Thus, in addition to acoustic levitation, one has magnetic, electrical, optical and aerodynamic levitation, each in turn having several variants (see Fig. 8.5) [68,80]. The fundamentals of each levitation technique are briefly discussed and compared below, with special emphasis on acoustic levitation. The scope of each technique is difficult to gauge precisely, the choice of one over the others being strongly influenced by the system under study. For example, using levitation in bioanalytical chemistry involves combining biological compatibility with easy sample handling, stable sample positioning, ready access to the sample, the ability to process a wide range of sample volumes, and low supply and operational costs.

Magnetic levitation

Levitation can be accomplished without any energy input by using a magnetic field generated by a permanent magnet, electromagnet or superconducting magnet. Magnetic levitation can be carried out in the electromagnetic (EM) or electrodynamic (ED) mode. In the former, an attractive force is generated between normal electromagnets and a ferromagnetic guide. A feedback control loop is required to ensure adequate stability. EM levitation can only be used with high-electrical conductivity materials at ambient temperature [74–76]. ED levitation is based on the induction of eddy currents in conducting materials by a magnetic field. One variant of the ED mode relies on the force acting between the magnetic field generated by superconducting magnets and stationary coils located in the wave guide. Field changes are induced by the relative motion between the superconducting magnets and stationary coils. Another option is based on the force generated by magnetic field variations inducing time-varying currents. This type of ED levitation is considered to be electrical levitation in some cases.

Magnetic levitation is often used in combination with other types of levitation to increase stability (particularly with permanent magnets) [77–79].
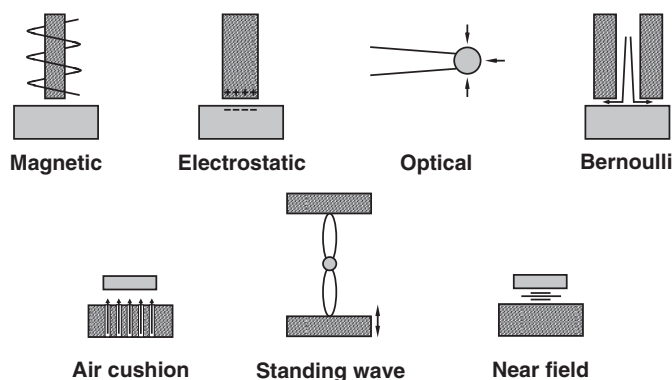
FIGURE 8.5. *Main levitation techniques. (Reproduced with permission of Elsevier, Ref. [80].)*

Electrostatic levitation

In electrostatic levitation, a charged drop is levitated by applying electrostatic fields from a set of properly arranged electrodes which allow conductive, semiconductive and dielectric materials to be levitated. The difference from ED levitation is that the electrical fields used to manipulate the sample in electrostatic levitation are of the static type. This technique can also be used to levitate small uncharged particles by inducing polarization in the sample. Similar to magnetic levitation, the attractive forces produced require the use of closed-loop control to ensure stability. Also, the suitability of electrostatic levitation has so far been demonstrated at ambient temperature only because static charges gradually decay with time at high temperatures. A large levitation force is required to offset the gravitational pull, which in practice requires large sample charges and strong applied electric fields (or a large potential difference between the electrodes). The high voltage required constitutes a serious drawback, but has the advantage that it affords levitation of relatively large particles [80]. Electrostatic levitation has found use in protein crystal growth [81] and X-ray scattering studies of metallic liquids [82], among others.

Optical levitation

Optical levitation, first demonstrated by Ashkin in 1970 [83], can be accomplished by using a large number of aperture lenses to focus a laser beam sharply onto a sample, which is thus subjected to a scattering force that pushes it forward in the direction of the energy flux. A gradient force is also exerted to pull the sample towards regions with a high electrical density (generally, the focal region). In regions where two forces cancel each other, the sample may be suspended at a stable three-dimensional (3D) position [84]. The main shortcoming of optical levitation is the presence of thermal forces caused by temperature gradients induced in the medium surrounding the sample. Such forces make levitation positions unstable, but can be avoided by suspending relatively transparent particles in transparent surrounding media (water, oil or air) [80].

Other optical-based levitation methods use two or more laser beams to generate only one stable equilibrium point below the beam-crossing point [85]. Typical applications include 3D cellular and intracellular micromanipulation [86], and cell sorting [87].

Aerodynamic levitation

Aerodynamic levitation uses a flow of gas or liquid to apply a force in order to raise spherical specimens. Depending on the flow direction, one has air cushion levitation (pressurized air flows upwards through several holes leading to a repulsive levitation force that counterbalances the sample weight) or Bernoulli levitation (compressed air from a high-pressure supply flows downwards through a nozzle and, after lifting up the sample, flows outwards) [80]. There are also some hybrid variants of aerodynamic levitation based on the two previous principles, namely: simultaneous upward suction force and downward air cushion levitation [88]. Aerodynamic levitation has found much use in industrial applications and for levitating solid spheres. Some vibrational instability has been encountered in aerodynamic levitation with liquids [89].

Acoustic levitation

Although the fundamentals of acoustic levitation have been established by now, some complex theories of non-linear acoustics remain unclear [80]. Acoustic levitation is based on the production of a standing wave with equally spaced nodes and antinodes by multiple reflections between an ultrasonic radiator and a solid reflector; this allows the levitation of small samples in the pressure nodes of the acoustic standing wave (see Fig. 8.6). However, not all nodes are useful for stable levitation, those lying directly in front of the transducer and the reflector being preferable [90]. The mode using a transducer and a reflector (known as "standing wave levitation") is most widely documented and used in analytical applications; hence, the following section is devoted to it. So-called "near-field levitation" or "squeeze film levitation" replaces the reflector with the levitated object and is better suited to guiding or transferring systems.

In near-field levitation, the sample is lifted through direct radiation within the near field of a high-intensity ultrasonic transducer, so the levitation height is normally quite short because the levitation force is inversely proportionally to the square of the levitation distance [91,92] and depends on the intensity of the sound transducer. The high-intensity US generates strong forces, so it can levitate samples of any weight provided the sample and vibrating plate are kept at an appropriate distance.
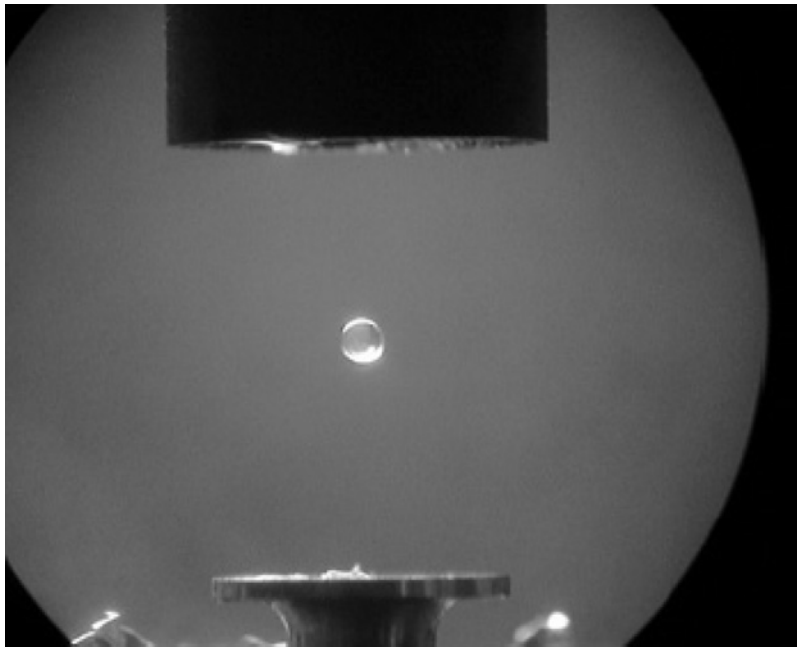
FIGURE 8.6. *A 500-nl water drop levitated in a node of a standing wave created between an ultrasonic transducer (bottom) and a solid reflector (top). (Reproduced with permission of Springer-Verlag, Ref. [68].)*

Acoustic levitation can be accomplished in a gaseous atmosphere not only under ambient conditions, but also under microgravity conditions or in a liquid environment; most often, however, it involves levitating the small amounts of sample used with the increasingly ubiquitous miniaturized systems. The maximum diameter a levitated sample can have depends on the ultrasonic wavelength used; in fact, it is a multiple of a half-wavelength under ambient atmospheric conditions. Acoustic levitators usually operate at US frequencies from 15 to 100 kHz (*i.e.* at wavelengths over the range 2.2–0.34 cm). However, with ultrasonic wavelengths above *ca*. 8 mm the maximum volume of a levitated liquid drop cannot be estimated from the wavelength as it is determined by the ratio of hydrostatic pressure to the capillary pressure generated by surface tension inside the drop. If such ratio, which is called the "Bond number", exceeds 1.5, then the drop will disintegrate. Therefore, the two variables dictating the maximum volume of a levitated drop are the surface tension and the specific density of the liquid [93,94]. With solids, the main requirement derives from the density of the material; however, the limits for this parameter depend on the particular acoustic levitator. Thus, the APOS BA10 from Dantec Dynamics is specially designed for applications involving liquid and solid samples with densities over the range 0.5–2.0 g/ml, but short levitation times are also possible with samples of a higher density (below 8 g/ml) [68].

Figure 8.7 depicts an ultrasonic levitator and the distribution of the acoustic pressure and velocity, and the levitation force, in a standing acoustic wave. Under microgravity conditions, a particle can be positioned exactly in the pressure node, where both the acoustic pressure and levitation force are zero, whereas the acoustic velocity is maximal. Therefore, stable levitation is possible at such a position. In the remaining space, however, levitation forces act in the direction of the nearest pressure node in order to produce a stable levitation by upward or downward flow, depending on the experiment. For this purpose, ultrasonic irradiation of relatively high power must be applied as variables such as density or ultrasound velocity only contribute to scale the forces. Nevertheless, some surface properties such as roughness can influence the fluid flow and as a result alter the acoustic field slightly [80].
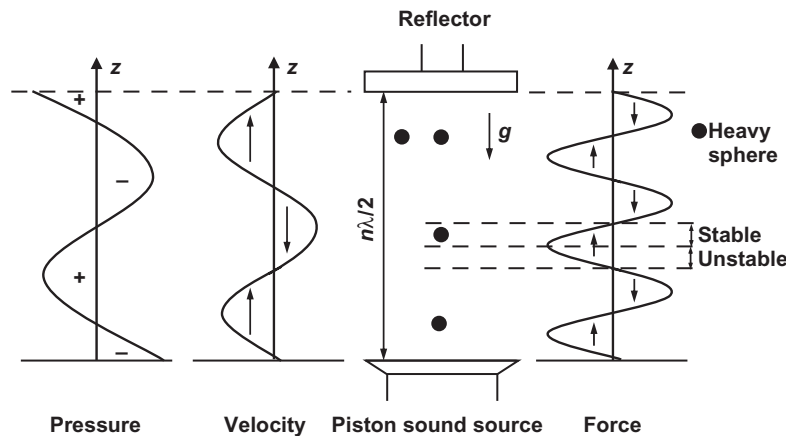
FIGURE 8.7. *Levitation of samples in an acoustic standing wave. (Reproduced with permission of Elsevier, Ref. [80].)*

Comparison of levitation techniques

A comparison of the above-described levitation techniques allows one to conclude that (1) electric and magnetic levitation can only be applied to specific materials and always require strict control in order to ensure stability; (2) optical levitation is restricted to very small, relatively transparent particles in a transparent surrounding liquid — in addition, the forces it generates are too small to allow samples larger than 150 μm to be handled, although this limit is dependent on the particular optical levitator; (3) aerodynamic levitation exhibits poor lateral stability and requires a more complex experimental set-up (one including an external source of pressurized air) than does ultrasonic levitation [80].

The main advantage of acoustic levitation in relation to other levitation techniques is that materials in different states of aggregation (solids, liquids, suspensions and gases) can be levitated by using acoustic forces irrespective of their physical properties (*viz*. whether they are insulators or conductors, magnetic or non-magnetic) [72], with the sole exception of the restrictions imposed by the density of the material. Although US can, in theory, be used to levitate any type of material, applications of acoustic levitation to solids have so far been restricted to a few studies in analytical chemistry and related areas, largely as a result of the unavailability of appropriate devices for sample positioning and detection systems for extracting information from solids; the latter problem stresses the significance of sample preparation. Finally, gas levitation has essentially been limited to basic studies.

The main problems of acoustic levitation are acoustic streaming and non-uniformity in the force field. The energy density distribution induces an acoustic convection flow which enhances heat and mass transfer; this can be an advantage or a disadvantage with a view to position the samples stably as slight asymmetries in the acoustically induced convective flow field can result in undesired, uncontrolled sample rotation. This situation is particularly important in applications where heat and mass transfer are decisive, especially with strong acoustic fields. Therefore, strict control of the field flow around an acoustically levitated sample is extremely important [95–97]. A compromise solution must usually be adopted as the acoustic field should be strong enough to overcome gravity and prevent the drop from falling down, but not so strong as to cause the drop to disintegrate into small droplets by the effect of capillary forces, which are produced by the surface tension of the curved drop surface, becoming too weak to keep the drop intact [94].

8.3.2. Approaches to acoustic levitation

This section discusses the most interesting acoustic levitation approaches for use in analytical chemistry and describes devices for sample positioning in the levitator and reagent delivery, ultrasonic levitators and the coupling of acoustic levitators to detection and separation systems. Also, it discusses future prospects for acoustic levitation.

Sample and reagent delivery devices

The importance of sample delivery is frequently overlooked in the studies on acoustic levitation, even though precision in the analyses relies heavily on an appropriate choice of the sample volume. Delivery systems are closely related to the nature of the sample (liquid, suspension, solid or gas). Any type of system (*e.g.* a micropipette, capillary, or microsyringe) can be used to position a drop from a liquid or slurry sample in an ultrasonic levitator.

When the needle or tip holding the drop is positioned in the ultrasonic field, the US ampli-tude must be raised in order to overcome the adhesion forces which attach the drop to the needle or tip. Alternatively, the needle or tip can be introduced into the acoustic field through a small hole in the reflector plate [98]. Drop detachment from a microsyringe tip can be facilitated by coating the tip with a hydrophobic substance (*e.g.* paraffin in *n*-hexane or silicone) provided it does not alter the sample composition; drop detachment is more difficult for liquids with a low surface tension and (or) viscosity. Thus, levitation of solvents such as diethylether is virtually impossible; by contrast, ethanol, methanol and toluene can be readily detached by virtue of their weak adhesion to the needle tip. Table 8.1 lists selected organic and inorganic liquids used for acoustic levitation and their relevant properties. Capillaries can be coated with glass or polymers, but should be as thin as possible in order to reduce adhesion forces [72]. Also, the use of high ultrasonic power during sample positioning facilitates drop detachment; the droplet can be easily stabilized by adjusting the distance between the transducer and the reflector, and setting an appropriate ultrasonic power [68]. The microsyringe has so far proved the best choice of delivery system in terms of precision, which is about ± 0.05 µl [99].

Another effective choice is the use of piezoelectric micropumps, which, depending on the applied voltage (up to 80 V), pulse length (from 1 µs to 500 ms), droplet emission frequency (max. 1000 Hz), distance to the acoustic levitator and nature of the pumped liquid, can provide nanodroplets of sizes between 0.25 and 1.5 nl. The pumps are always operated in the burst mode, — continuous and cyclic burst modes are also possible, however — and the number of droplets to be used in each experiment is programmed on an individual basis. Micropumps can be mounted on adjustable holders at a certain distance from the ultrasonic field. Errors in measuring the sample volume can arise from droplet impact during the pumping process. The repeatability of this system with distilled water has been found to be about 1–5% as relative standard deviation. Micropumps constitute a good choice for acoustic levitation below 0°C as they avoid immediate freezing. In this way, a number of microdroplets can be accumulated until the desired droplet size is reached [100].

TABLE 8.1. *Maximum diameter (d_{max}) and volume (V_{max}) for levitated drops of fluids of variable surface tension (σ_S) and specific density (ρ_S).*

Liquid	σ_S (dyn/cm)	ρ_S (g/cm^3)	d_{max} (mm)	V_{max} (µl)
Ethanol	22.3	0.7894	4.16	37.6
Acetone	23.3	0.7910	4.24	40.0
Benzene	28.9	0.8790	4.48	47.0
Glycerine	65.7	1.2610	5.64	94.1
Methanol	22.6	0.7915	4.17	38.1
Mercury	465	13.546	4.58	50.3
CS$_2$	26.8	1.2630	3.95	32.2
CCl$_4$	26.8	1.5940	3.20	17.2
Toluene	28.5	0.8669	4.48	47.0
Water	72.75	0.9982	6.67	155
Xylol	30.1	0.8802	4.57	50.0
Cyclohexane	25.0	0.7784	4.43	45.6

Reproduced with permission of Springer-Verlag, Ref. [72].

One of the problems concerning micropumps is caused by the formation of gas bubbles inside the pump head, which can be avoided by adjusting the viscosity and surface tension of the solution (*e.g.* by adding 2–5% m/v glycerol [90]).

Another choice of non-contact delivery device is the flow-through droplet dispenser developed in-house at the Department of Electrical Measurements, Lund University, Sweden [73,101,102], which is shown in Fig. 8.8. This device features high precision, a wide droplet size range (up to picolitre volumes, which facilitate miniaturization), high frequency for droplet ejection (up to 9 kHz) and the ability to dispense samples from a flowing liquid (*e.g.* in a flow-injection system). Flow-through droplet dispensers are fabricated by using silicon micromachining methods. Droplets are ejected from a flow-through channel formed by joining two microstructured silicon plates with a protruding pyramid-shaped nozzle in the centre of the channel and a multilayer piezoelectric element connected to a push-bar in the channel wall opposing the nozzle. By applying a short-voltage pulse across the piezoelectric element, this is elongated and pushed into the channel, thereby generating a pressure pulse in the liquid, the increased pressure accelerating the liquid in the nozzle causing the ejection of a droplet as a result. This process can be repeated over a frequency range of up to several kilohertz. The volume of the ejected droplet, typically in the range 40–100 pl, is dependent on the size of the nozzle, the shape of the voltage pulse and various properties of the liquid such as its surface tension, viscosity and density.

There is a viscosity limit for liquids to be ejected by the dispenser that depends on the nozzle dimensions. Thus, liquids of viscosity higher than the dispenser limit exhibit poor accuracy in droplet formation and volume; this problem, however, can be overcome by heating the dispenser to a maximum temperature of 100°C restricted by the particular
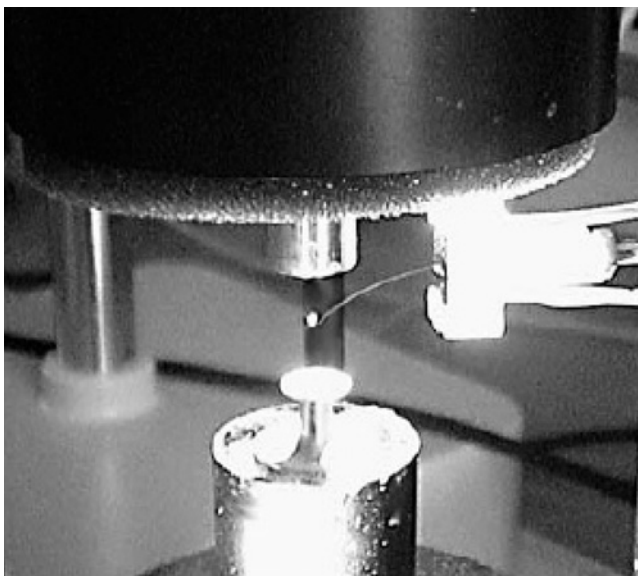
FIGURE 8.8. *Flow-through microdispenser addition to a levitated droplet. The dispenser trajectory is seen as the thin white line connecting the dispenser nozzle with the levitated droplet. (Reproduced with permission of Springer-Verlag, Ref. [68].)*

constituent material of the dispenser. Dispensing highly concentrated salt solutions can also cause problems due to salt crystallization in the nozzle, which can be avoided by using a dispenser furnished with a second layer of a salt-free liquid to cover the primary liquid upon ejection [103].

One advantage of micropumps and flow-through microdispensers is that droplet evaporation can be controlled accurately by adding a solvent in order to keep the droplet volume constant, which is essential for quantification purposes. Because US increases the temperature of the medium, it can facilitate solvent evaporation. This requires using a system such as an imaging detector to continuously monitor the droplet volume in order to determine the evaporation rate during acoustic levitation. Both micropumps and microdispensers can be coupled *via* FI manifolds to other units for the development of different steps of the analytical process.

Most of the research on analytical acoustic levitation has focused on liquid samples; ultrasonic levitation of solids has been used for containerless processing or material transportation in industrial applications. The few analytical applications of acoustic levitation to solids involve dissolution or suspension in a suitable liquid, the resulting solution or suspension being subsequently treated in accordance with the detection system used. Thus, if the detector system is suitable for liquid samples or suspensions, the best choice is to develop the analytical process directly in the solution or suspension. One obvious shortcoming is the resulting sample dilution, which, however, can be overcome by concentration through controlled droplet evaporation prior to detection. On the other hand, if the detection system is suitable for solids, the solvent can be completely evaporated in the droplet in order to accomplish levitation of solid particles.

Acoustic levitation of gas samples is an uncommon application where the best choice for sample delivery appears to be coupling a flow system to a closed acoustic levitation chamber.

Ultrasonic levitators

The earliest experiments of Bücks and Müller in acoustic levitation [70] have been followed by a number of studies and developments in acoustic levitators. Especially prominent among such studies are those by Kawahara *et al.*, who established the fundamentals of acoustic levitation [96]. These authors used a modified acoustic levitator from Tec 5, Sensorik u. Systemtechnik Gmb H. The levitator was operated at a frequency of 58 kHz, corresponding to a nominal wavelength of 5.93 mm at an ambient temperature of 293 K. The flat reflector was positioned 1.5 cm above the transducer to create five pressure nodes in the standing wave between the transducer and the reflector; the distance between them was accurately adjusted *via* a micrometer screw (with an uncertainty of about 20 μm). The modifications of the original acoustic levitator included placing a cylindrical glass tube of 12 mm i.d. around the acoustic transducer and reflector in order to form a closed chamber inside of which the acoustic standing waves were generated. This type of levitator, called the "tube levitator", enabled accurate control of the temperature and humidity inside the tube. A slight air flow was additionally blown into the tube to control air humidity and vapour concentration (from the droplet) in the tube. The relative humidity of the air in the tube was adjusted to 4.8% and the temperature was *ca.* 23°C at the beginning of each experiment. The air temperature close to the evaporating surface was measured with a thermocouple.

In 1997, Welter and Neidhart [72] developed one of the earliest applications of ultrasonic levitation in analytical chemistry by using an Apos BA 5 acoustic levitator from

Dantec Invent (Erlangen, Germany) at an ultrasonic frequency of 58 kHz with the configuration shown in Fig. 8.9; the wavelength at ambient temperature and pressure was thus *ca*. 5.7 mm. The optimum sample diameter was 2.4 mm and the maximum volume for water drops was 6.5 μl, the maximum levitated volume for other liquids being determined by their surface tension and specific density. The distance between the ultrasound transmitter and the reflector ranged from 1.43 to 1.70 cm; although the standing wave had five nodal points, only two were suitable for levitation of analytical samples for operational reasons. The transmitter and reflector were placed inside a closed glass tube 7 cm in diameter fitted with two gas suppliers and one opening 2.5 cm in diameter for positioning and removing samples that was closed with a rubber plug in order to maintain levitated samples in an arbitrary, non-corrosive, well-defined atmosphere. This system was in turn placed on two micrometer benches which allowed horizontal and vertical adjustment of the position relative to the detection systems, micropump and optical fibres [90].

Simultaneously, Nilsson *et al*. reported an airborne system, which was used to develop analytical methods [73] and patented in 1999 [104]. This system uses an APOS BA10 acoustic levitator from Dantec Dynamics (Erlangen, Germany) operating at a frequency of 100 kHz and temperatures of 0–70°C. Although the optimum volume of a levitated droplet at a frequency of 100 kHz seemed to be between 500 nl and 1 μl, the maximum droplet volume tested was 2.3 μl and the minimum volume positioned in the levitator was 50 pl; however, the droplet evaporated almost immediately after positioning [69].

Especially interesting in this context is the acoustic trap proposed in 2001 by Jacob *et al*. [100], who designed and constructed an acoustic levitator for use at temperatures down to –55°C. The mechanical part of the acoustic levitator consists of a resonator with a stepped-horn amplitude transformer and two piezoceramic transducers cemented to an aluminium cylinder. Opposite to the acoustic transducer, a curved reflector is mounted on a micrometer adjustment screw. The best performance as regards droplet positioning stability and energy was achieved in a gaseous medium. The vibrating plate and the lower
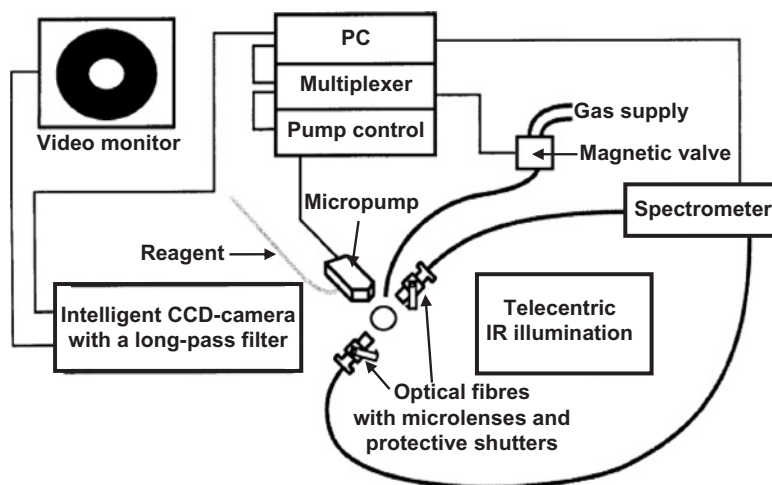
FIGURE 8.9. *Acoustic levitator used by Neidhart et al. for quantitative purposes. (Reproduced with permission of Springer-Verlag, Ref. [90].)*

aluminium cylinder were kept at a constant temperature by means of a brass cooling jacket with a 0.3 mm gap in between. In this way, any dumping and reduction in levitation force were avoided. The previous components were surrounded by a double-wall chamber filled with a cooling liquid (ethanol) and furnished with four round windows for observation, sample introduction, and temperature and humidity control. Dry air or nitrogen was blown in order to prevent condensation of water vapour during observation. The acoustic transducer in the cryo-levitator was thermostated to a stable temperature down to $-15°C$ in order to ensure a reproducible, stable resonance frequency. Temperatures below $-20°C$ caused an irreversible change in the cement used for fixing and also, occasionally, separation of the ceramics and cylinder. One way of working at lower temperatures is by keeping the transducer at $-15°C$ and the observation chamber cooled separately at the desired temperature. Alternatively, one can use a resonator with piezoceramic rings in which the aluminium cylinder is compressed by a central bolt. No temperature restriction down to $-55°C$ exists for this arrangement.

Hybrid acoustic levitators are especially useful for some applications. One case in point is the aero-acoustic levitator of Gustafson *et al*. [105], which consists of an O_2 jet (pre-heated at 400°C) coupled with an acoustic levitator. The gas jet can also be regulated *via* a mass flow controller [97]. Another example is the ultrasonic–electrostatic levitator developed by Chung and Trinh for containerless protein crystal growth [81], which consists of an ultrasonic levitator with a transducer and reflector that are also used as the ground and high-voltage electrodes required by an electrostatic levitator. This system can be operated as an ultrasonic or electrostatic levitator by altering the strength of the ultrasonic or electric field as the two effects are unrelated.

Units for sample or aliquot transfer to the detector

With detection techniques coupled to separation techniques such as GC, LC and CE, one choice is transferring the whole sample to the detector. This can be carried out with the above-described devices for sample positioning (*e.g.* microtips, micropipettes, capillaries, micropumps, flow-through microdispensers). One can also transfer sample aliquots instead of the whole drop using a very thin tip. Micropipettes prepared by etching fused silica capillaries in hydrofluoric acid and mounted on micropositioning devices have provided reproducible results in this respect. Adjusting the ultrasonic field can help the previous systems and provide a non-contact method for aliquot sampling by splitting each droplet into two. This requires shortening the distance between the transducer and the reflector, and causes droplet to change from spherical to ellipsoid in shape and eventually to split into two as shown in Fig. 8.10. One of the droplets can then be taken from the levitator without the risk of contaminating previous ones [69].

Another choice is blowing the sample out of the ultrasonic field by feeding a nitrogen stream into a Dewar flask containing liquid nitrogen. In this way, the frozen sample can be easily withdrawn with Teflon forceps. This requires a high skill from the analyst [72]. The use of aliquots entails continuous monitoring of the drop volume in order to accurately determine the aliquot volume taken — similar to control systems for solvent evaporation. Alternatively, an internal standard can be used to correct the inaccuracy derived from taking aliquots without volume control.

Robotic systems (*e.g.* those equipped with micro or nanopumps) can no doubt be highly useful for acoustical levitation of solid and liquid samples, and their subsequent transfer to a detection system with improved precision and automation.
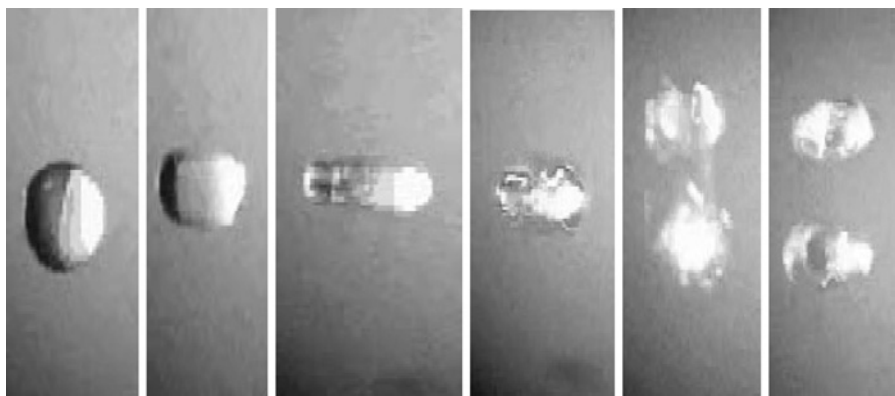
FIGURE 8.10. *Image sequence showing how sample aliquots can be obtained in a non-contact way by using the ultrasonic field to split a sample droplet into two. (Reproduced with permission of Ref. [69].)*

Detection systems

One additional advantage of acoustic levitation for sample handling is the ability to perform *in situ* detection in order to expedite the analytical process and continuously monitor the course of various processes on the levitating sample. The capabilities for *in situ* detection depend on the properties and operating conditions of the detection system concerned. Thus, optical detectors are especially capable in this respect as they can operate under remote and non-intrusive conditions. Various configurations involving diverse detectors have been developed for this purpose, one of which uses a charge coupled detector (CCD) camera to record video images from the droplet in order to monitor the acoustic levitation process (*e.g.* deformations, other undesirable processes) [106]. This experimental set-up is completed by a suitable irradiation source such as a laser, a light emitting diode (LED), or a UV, visible or IR lamp operated in a continuous or pulsed mode. Scattered light is collected at the entry of a double monochromator which is directly attached to the CCD. When a laser or LED is used, the diameter of the illuminating beam should be higher than the droplet diameter (about 10 times) in order to minimize the influence of the Gaussian profile of the irradiation source beam.

Ordinary and intensified CCDs have also been used with other configurations such as that for fluorescence imaging reported by Santesson *et al*. [107], which consists of a mercury lamp, an optical quartz fibre and the corresponding optics (lenses and interference filters in a 90° configuration). Each droplet image consisted of 109×91 pixels with recorded intensities (the droplet in each image typically had a diameter of ~35 pixels). The main advantage of this configuration is that it enables monitoring of dynamic processes in addition to analyte quantification. Both native and indirect fluorescence can be used for either monitoring or quantification of the target analytes. One example is the use of pH-dependent fluorophores to measure the fluorescence resulting from a pH change depending on the analyte concentration. The mercury lamp used can be replaced with a laser irradiation source in order to improve the sensitivity and selectivity. All laser-based detectors share the requirement that the laser focus must be set at an optimum distance from the drop in order to avoid signal fluctuations caused by drop movements. Omrane *et al*. used an

Nd:YAG laser for the simultaneous measurement of elastic, fluorescence and phosphorescence signals from droplets in order to determine droplet diameter, temperature and species concentrations [108]. An imaging stereoscope was required to combine the visualization of the signals emitted by the different detectors. Laser-induced phosphorescence (LIP) possesses the advantages of higher temperature sensitivity and longer lifetime; the latter property can be used to avoid interferences from background and undesirable elastic scattering signals by setting a small delay prior to data acquisition. In addition, LIP is insensitive to quenching (*e.g.* from oxygen) and to pressure changes of up to 1 GPa. However, the greatest asset of this approach is the ability to measure several signals simultaneously.

The scattering signal is especially interesting on account of the wealth of information it can provide. One specific right-angle light scattering detector is composed of a microscope equipped with a CCD for continuous control of the drop volume. The signal scattering intensity depends on many factors including insoluble particle concentration, size, size distribution and the presence of particulate aggregates. One requirement is that the measured area should be smaller than the smallest drop size throughout the experiment in order to avoid regions with reflections from the irradiation source. This detection technique is especially interesting with a view to monitor droplet processes [109].

Another approach, proposed by Rohling *et al*. [90], uses two diode array detectors suitable for absorption, fluorescence and phosphorescence measurements instead of a CCD. A 1.2-mm core diameter optical fibre is connected to a Xe–Hg lamp and a microlens is used to focus light onto the levitated drop; also, a 0.6-mm core diameter optical fibre is connected to the diode array detector, which is furnished with an appropriate microlens in order to collect emitted or unabsorbed light. Although coupled charge and diode detectors are the most common choices in this context, simpler configurations including a monochromator for collecting irradiation at a specified wavelength — which is of special interest in routine applications — can also be used.

Raman spectroscopy is another remote detection technique which has been successfully coupled to acoustic levitation. The approach allows quantification of analytes and the *in situ* study of dynamic processes, thus providing selective information for structural elucidation. The acoustic levitation–Raman spectroscopy couple improves scattering signals through increased deformation of the drop (about 50%). One shortcoming of this approach arises from the change in stability of ultrasonically levitated droplets on altering the operating conditions and results in decreased accuracy of measurements [106].

The low sensitivity of conventional Raman spectroscopy restricts its utility with dilute systems. However, substantial improvements in this respect have been achieved by using surface-enhanced Raman scattering (SERS); thus, some authors have reported sensitivity enhancements greater than 10^{12}, including the possibility of single-molecule detection [110,111]. In SERS spectroscopy, a laser is used as irradiation source to excite the sample adsorbed on a roughened metallic surface, thus enabling the high-sensitivity Raman scattering of molecules close to the surface. The origin of the enhancement is basically the increased electrical field strength, which decays rapidly into the adjacent solution. As a consequence, only the first molecular layers contribute to the observed SERS signal, making the measured signal virtually independent of the available volume. Acoustic levitation has been coupled to SERS spectroscopy in order to exploit the sensitivity enhanced by positioning the powdered sample on a metal plate at the node in the levitator where the drop is to be subsequently placed [112]. In addition to the enhanced sensitivity obtained with SERS, the signal-to-noise ratio for SERS can be improved by adjusting the drop environment (*e.g.* by adding electrolytes, changing the solvent, altering the colloid density) or by altering the irradiation conditions (*e.g.* by changing the wavelength

or intensity). One shortcoming of SERS spectroscopy in combination with acoustic levitation is that most of the metallic nanostructures employed for SERS detection (namely, colloidal solutions of silver or gold) are unsuitable for levitated drops. Some authors have proposed the *in situ* synthesis in the acoustic levitator of highly active SERS sols by reducing silver nitrate with alkaline hydroxylamine hydrochloride [113]. This has enabled SERS substrate preparation at room temperature in a short time. The *in situ* prepared silver sol has been used for the trace analysis of various organic molecules injected into the levitated SERS-active droplet by using a microdispenser; this allows the use of fresh substrate for each analysis and avoids problems related to analyte carry-over and sol instability.

Cerenius *et al*. [114] evaluated the use of acoustic levitation to keep a droplet of liquid in an X-ray beam long enough to acquire X-ray diffraction spectra. Solid samples can be studied additionally by suspension in a suitable solvent. The most salient advantage of X-ray diffraction here is that it can provide more detailed information and a higher quality than the Raman spectroscopy.

8.3.3. Applications of acoustic levitation

As shown by the applications developed so far, the characteristics of acoustic levitation make it especially suitable for use in analytical and bioanalytical chemistry — however, the earliest applications focused on the determination of mechanical and physical properties of materials such as specific density, viscosity and surface tension [93,115,116]. Ohsaka *et al*. developed a method for determining the viscosity of highly viscous liquids (particularly, undercooled liquids, which exist at temperatures below their freezing points [117]). Weiser and Apfel used acoustic levitation to measure mechanical properties such as density, compressibility and sound velocity in biological materials [71].

The earliest applications of acoustic levitation in analytical chemistry were concerned with the development of various steps of the analytical process. Thus, Welter and Neidhart [72] studied the preconcentration of *n*-hexanol in methanol by solvent evaporation and the liquid–liquid extraction of *n*-hexanol from water to toluene in a levitated droplet, which they found to be efficient when using GC–FID with *n*-pentanol as internal standard. Solvent exchange of fluorescein from methylisobutyl ketone to aqueous sodium hydroxide was also accomplished. Sample concentration in an acoustically levitated droplet prior to injection into a CE equipped with an LIF or UV detector has also been accomplished [73,118]. The target analytes (namely, dansylated amino acids) were concentrated in the levitated drop and a limit of detection of 15 nM — much lower than the 2.5 µM achieved by hydrodynamic injection without preconcentration — was achieved following CE separation and quantification. For this purpose, 36 000 sample droplets 2.3 µl in volume each were sequentially positioned in the acoustic levitator and evaporated. This example illustrates the potential of acoustic levitation for coupling to any type of detector for micro- or nanotrace analyses.

Derivatization of target analytes has also been performed in acoustically levitated droplets for the determination of mono-, di-, tri- and tetrabutyltin [119]. The target analytes were extracted simultaneously from acetate buffer to hexane and derivatized using $NaB(C_2H_5)_4$. Then, the organic phase was transferred for separation—determination by GC–AES. The results were comparable to those provided by conventional derivatization.

Acoustic levitation has also been used for microtitration with absorptive and fluorescent indicators. The addition of titrant was efficiently controlled *via* a piezoelectric micropump. This application testifies to the possibility of using this technique in routine laboratories where sample and (or) reagent availability may be a limiting factor [90].

A portable Raman spectrometer coupled to an acoustic levitator (Fig. 8.11) has been used for environmental monitoring and taxonomic identification of microorganisms in their native environments from spectra for living cells. The high signal-to-noise ratio achieved by suspending the cells in air without attenuation from surfaces provides an advantage over conventional Raman measurements in a conventional cuvette [120].

Leopold *et al.* reported a system for on-line monitoring of chemical reactions in ultrasonically levitated, nanolitre-sized droplets by Raman spectroscopy consisting of a flow-through microdispenser connected to an automated flow injection system which enabled on-line coupling to other steps of the analytical process [113].

Another field of application of acoustic levitation also related to reaction monitoring is cryo-enzymology studies, which use low temperatures in order to facilitate the investigation of enzymes by slowing the rates of enzymatic reactions, or trapping intermediate states in order to identify the pathways of specific reactions. Using supercooled liquid water at –6°C — small volumes of water can remain liquid down to about –42°C, but its viscosity increases significantly, being an ideal medium to slow down enzymatic reactions without disruption of enzymes or addition of antifreeze, water-in-oil emulsions or narrow capillaries — was found to decrease the rate of the alkaline phosphatase-catalysed hydrolysis of 4-methylumbelliferone phosphate 6 times relative to saturating conditions (a high substrate concentration) at 22°C [121]. The latter proved similar to bulk solution conditions, which suggests that levitation does not disrupt enzyme kinetics.

The study of living cells and intracellular biochemical reactions in microdroplets is another interesting field for acoustic levitation. This is particularly interesting in pharmaceutical, biological and medical sciences. Improved knowledge of the chemical composition and dynamics of single cells should lead to a better and broader understanding of how individual cells function in their natural environment. Thus, the addition of β-adrenergic agonists into acoustically levitated droplets (500 nl) containing adipocytes was found to
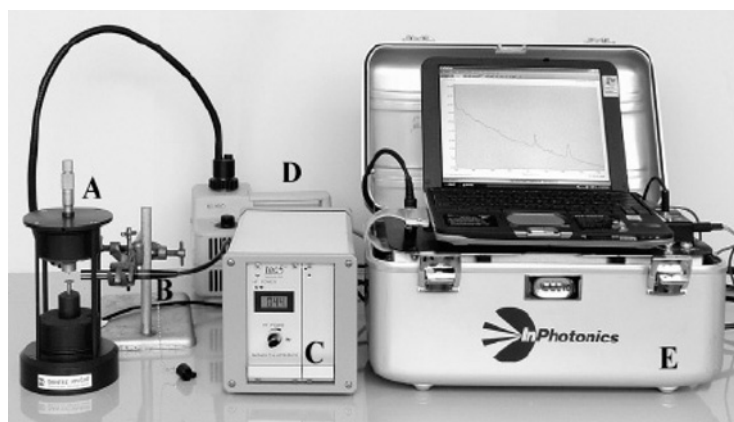
FɪGURE 8.11. *Portable Raman spectrometer coupled to an acoustic levitator. A — Dantec ultrasonic acoustic levitation device, B — Raman fibre-optic probe, C — control unit for the acoustic levitation device, D — quartz halogen light source and E — InPhotonics portable 785-nm Raman spectrometer. (Reproduced with permission of the American Chemical Society, Ref. [120].)*

stimulate adipocyte lysis and lead to free fatty acid release and a consequent pH decrease in the surrounding buffer; the addition of insulin antagonized lipolysis and hence also the pH decrease. pH changes caused by the cell response in the droplet were continuously monitored by using a pH-dependent fluorophore and fluorescence imaging detection [107]. Studies of cell-to-cell communication between adipocytes and pancreatic β-cells in ultrasonic levitated droplets have also been carried out. Stimulation of insulin secretion by β-cells by virtue of acetylcholine administration to a levitated drop containing adipocytes and insulin-producing β-cells was found to inhibit the isoprenaline-induced lysis of adipocytes present in the same drop [122].

Ultrasonic levitation and Raman spectroscopy have been used to elucidate inter- and intra-molecular structures, and to determine rates of transformation during phase change with a view to elucidate the reaction mechanisms of solidification of *o*-terphenyl crystals after melting, undercooling and seeding — all steps being developed in the acoustic levitator [123]. The pharmaceutical field can take advantage of this approach in order to shorten the time for the development of new pharmaceuticals. Thus, crystallization studies of benzamide and indomethacin have revealed the formation of two crystal modifications for each compound, which suggests that acoustic levitation can be useful to investigate polymorphs [112].

Levitation has also attracted substantial interest for protein crystallization as the growth of suitable protein crystals is an essential step in the determination of protein structures by X-ray crystallography. At present, crystals are mostly grown using trial-and-error procedures, which waste large quantities of valuable material; this can be avoided by using acoustically levitated drops for crystallization in protein precipitation studies in order to establish the nucleation conditions resulting in the minimum possible consumption of protein material. Attempts in this direction have been made by using levitated drops of protein at a given concentration that was injected with crystallizing agents and monitoring the crystallization process by right-angle light scattering [109].

Another bioanalytical application is the development of miniaturized biospecific affinity two-phase partitioning in an acoustically levitated drop for the study of biotinylated liposomes in aqueous poly(ethylene glycol)–dextran using NeutrAvidin-dextran as the affinity ligand. A two-phase drop was trapped and manipulated in a node of a standing ultrasonic wave; then, phase mixing was achieved by adjusting the ultrasonic field. The NeutrAvidin-dextran redistributed the biotinylated liposomes from the poly(ethylene glycol)-rich phase into the dextran phase. In this way, an entire affinity two-phase separation procedure including mixing of the phases and incubation to allow affinity interactions under constant volume, followed by phase separation by controlled evaporation, was performed in a single levitated drop [124]. This miniaturized method could also allow the separation of biologically active membranes or organelles from individual cells for analysis.

Environmental monitoring has also taken advantage of acoustic levitation for the investigation of physico-chemical processes relevant to the troposphere — mainly at temperatures below 0°C. Gas–liquid transfer of H_2O_2 from the gas phase to the levitated droplet was studied from *in situ* chemiluminescence measurements. Also, freezing of stably positioned droplets was observed by means of a microscope and a video camera, and the usefulness of this technique for simulation and investigation of cloud processes thus demonstrated. *Ex situ* microanalysis of sub-microlitre droplets by the use of an optical fibre luminometer also proved an effective means for investigating important physico-chemical processes at the micro scale [100].

Analytical chemistry can derive greater benefits from acoustic levitation more widely than it has so far by exploiting its three most powerful features, namely: (i) the ability to perform

contactless measurements, which is important with hazardous materials; (ii) the avoidance of undesired contamination from the container, which provides a promising method for preparing high-purity materials; and (iii) the avoidance of container wall-induced heterogeneous nucleation in order to facilitate massive undercooling in a melt prior to solidification.

8.4. ULTRASOUND ASSISTANCE TO ELECTROANALYTICAL TECHNIQUES

The current status of electroanalytical techniques is reflected in its decreased instrumental development relative to optical techniques and mass spectrometry. Some authors have pointed out that, despite the extensive work conducted on model systems, electroanalytical techniques have not yet reached full development [125].

The use of electroanalytical techniques in routine analyses, particularly those involving samples with organic constituents, has been traditionally curtailed by two main shortcomings, namely: (a) fouling and passivation of the electrodes by species depositing on their surface, which affects all electroanalytical techniques; and (b) slow mass transport to the electrode and slow kinetics of electron transfer, which affect the sensitivity of redox-based techniques.

Minimizing or avoiding these shortcomings has been an important goal for electroanalytical chemists, particularly for techniques based on redox processes. One alternative is the use of sound waves and, especially, US waves, based on the chemical and physical effects of cavitation (including solvent sonolysis, acoustic streaming, microstreaming and microjetting) [126] when this type of energy is applied to the electrolyte–electrode interface in much the same way to any type of liquid–solid interface.

Ultrasound assistance can be provided before and (or) during analysis. In those techniques which do not involve any electron exchange at the solution–electrode interface, US is normally applied prior to analysis in order to activate the electrode surface and hence in the absence of sample; in electron-exchange processes, US can be applied as a pretreatment, but also during analysis. In the latter case, US can be applied during the measurement step and, in stripping techniques, during deposition of the analyte of interest on the electrode, either electrochemically or by physisorption.

The assistance of US to electroanalytical techniques during analysis is known as s*onoelectroanalysis*. This should also include the use of low-frequency sound (below 20 kHz), which has been found to significantly increase mass transport and the limiting current (and sensitivity as a result) [127–130].

This section discusses the potential of sonoelectroanalysis, expansion of which is currently at a standstill owing to the few groups working on it. With few exceptions involving baths, probes are the ultrasonic sources used to assist electroanalytical processes with US. Some authors have pointed that the low, spatially variable distribution of ultrasonic intensity provided by baths is a major hindrance for using these devices with electroanalytical techniques [131]. Therefore, most of the examples described in this section involve the use of probes as US sources.

8.4.1. Influence of ultrasound on electroanalytical processes

Despite its beneficial effects on electroanalytical techniques, which include avoiding electrode passivation, enhancing mass transport and current intensity, and the ability to modify process kinetics, US assistance has not yet gained widespread acceptance in routine analytical laboratories [132,133].

Electrode depassivation

The ability of US to clean dirty surfaces has been discussed earlier in the section dealing with US assistance to steps preceding sample preparation in Chapter 2. However, the cleaning of passivated electrodes is worth special attention here by virtue of its importance for electroanalytical techniques. The depassivating or cleaning effect of US is a consequence of cavitational collapse when ultrasonic energy is applied to the electrode–solution interface. Specifically, the key cause is the mechanical effect known as microjetting (see Chapter 3), by which liquid jets implode on the electrode surface and remove adsorbed species. However, microjetting can produce pits on the electrode surface and damage it to some extent depending on variables such as the acoustic frequency and intensity applied, composition and temperature of the liquid phase and, obviously, the electrode material [133,134]. This surface pitting effect has been demonstrated in a polished platinum electrode in acetonitrile–tetrabutylammonium perchlorate (NBu_4ClO_4) by comparing its surface before and after sonication at 20 kHz at 60 W/cm^2 for 2 min [135]. This slow — but significant — roughing effect was monitored by atomic force microscopy (AFM), which revealed an electrode to be damaged by increased surface roughness [136], and also by AC impedance spectroscopy, using fractal dimensions as a measure of surface roughness [137].

Removing species adsorbed on an electrode surface requires a stress stronger than their cohesive force to the electrode surface. Depassivation assisted by US is governed by parameter α according to:

$$\alpha = \frac{\sigma R_p}{1.5 W_A},\qquad\qquad (8.1)$$

where σ is the tangential stress acting on the surface, R_p the radius of the spherical particle and W_A the work of adhesion of the particle. When α tends to very low values, US energy can only remove adsorbed species at frequencies and intensities above the usual levels. This situation is also dependent on the particular type of electrode. Thus, ascorbic acid adsorbed on platinum electrodes cannot be removed by sonication at 20 kHz [138]; also, sonicating carbon and gold electrodes for 10 s to 10 min at a horn–electrode distance of 7 mm after adsorption of phenanthrenequinone was found to only alter the current — through an increased electrode area caused by pitting [139].

Depassivating electrodes with US is not always possible; in fact, the high current densities induced by US can block electrodes rather than depassivate them in some cases [140,141]. This is a result of increased mass transport (see next section) producing a passivation effect and requires lowering the concentration of electroactive species in order to avoid it.

Nevertheless, electrode depassivation is of paramount importance in electroanalytical processes (particularly in highly passivating media, where silent electrochemical detection could fail and sonication can transform small signals into large, quantifiable ones). Typical examples involve biological and environmental samples — usually with complex matrices — from which large molecules such as proteins or surfactants can be readily removed with the aid of ultrasonic energy assistance (*e.g.* in the determination of dopamine in egg homogenate by sonovoltammetry [142], which was used as a model system to study the effects of electrode contamination and its subsequent reactivation by ultrasonic irradiation as illustrated in Fig. 8.12). No ultrasonic irradiation was used during

the measurement step in order to check for an increase in the voltammetric signal exclusively due to ultrasonic pre-activation of the electrode. Images obtained by AFM exposed such a depassivation on comparing the electrode surface after exposure to egg homogenate for 2 h and after *in situ* ultrasonic cleaning at 20 kHz. The ability to clean the electrode, combined with a potentially fast response, proved attractive for routine screening applications.

The passivating effect cannot be ascribed to organic species alone. Thus, Lorimer *et al*. showed 20-kHz sonication of a copper electrode surface prior to silent cyclic voltammetry to greatly increase peak current and sharpness in the copper voltammogram, which suggested an effective activation of the metal surface by US through increased surface roughness (and an increased effective electrode area as a result [143]). Oxidation was produced at the same potentials as without US activation; however, the reduction scan exhibited an additional peak to those for the reduction of cupric oxide to cuprous oxide and the further reduction of the latter to metallic copper. The new peak was ascribed to the formation of active sites during presonication of the copper surface.

Enhanced mass transport and increased current intensities

Mass transport induced by US is a key aspect of sonoelectrochemistry as confirmed by several authors who have identified the underlying physical processes [140,144–148]. Enhanced mass transport to the electrode displaces the redox process equilibrium and as a result increases the analytical signal. The influence of US is closely related to the use of continuous agitation or rotating disk electrodes [145,146]. The effect was demonstrated by
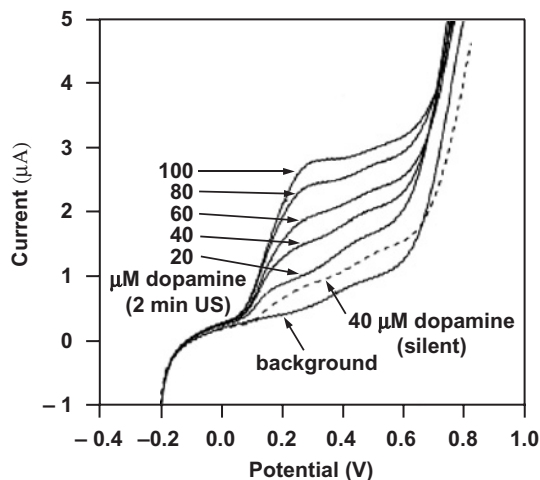
FIGURE 8.12. *Linear sweep voltammograms detailing the effect of US assistance for 2 min on electrode depassivation for the oxidation of dopamine in the range 20–100 µM at a glassy carbon electrode within egg homogenate. pH 7, scan rate 50 mV/s. (Reproduced with permission of Elsevier, Ref. [142].)*

Compton *et al*. for the oxidation of 2-mM ferrocene in acetonitrile containing 0.1 M NBu_4ClO_4 at a 2-mm diameter Pt disk electrode [149]. Ultrasound assistance (20 kHz, 50 W/cm^2, 40 mm electrode-to-horn distance) during the measurement step provided a limiting current that was ten times higher than under silent conditions.

The primary origin of enhanced mass transport is thought to be acoustic streaming, which is the mechanical effect of cavitation realizing as a turbulent flow (above 10 m/s) induced by a US source near a surface. The effect of acoustic streaming, first reported by Moriguchi in 1934 [150], is based on decreased thickness of the Nernst diffusion layer. As can be seen in Fig. 8.13, the diffusion layer model provides a very simple explanation for mass transport at the electrode–liquid phase interface by assuming a laminar sub-layer close to the solid surface and an approximately linear concentration gradient across a thin layer adjacent to the electrode. The equation best describing transport to a sonicated electrode is based on the uniformly accessible electrode model:
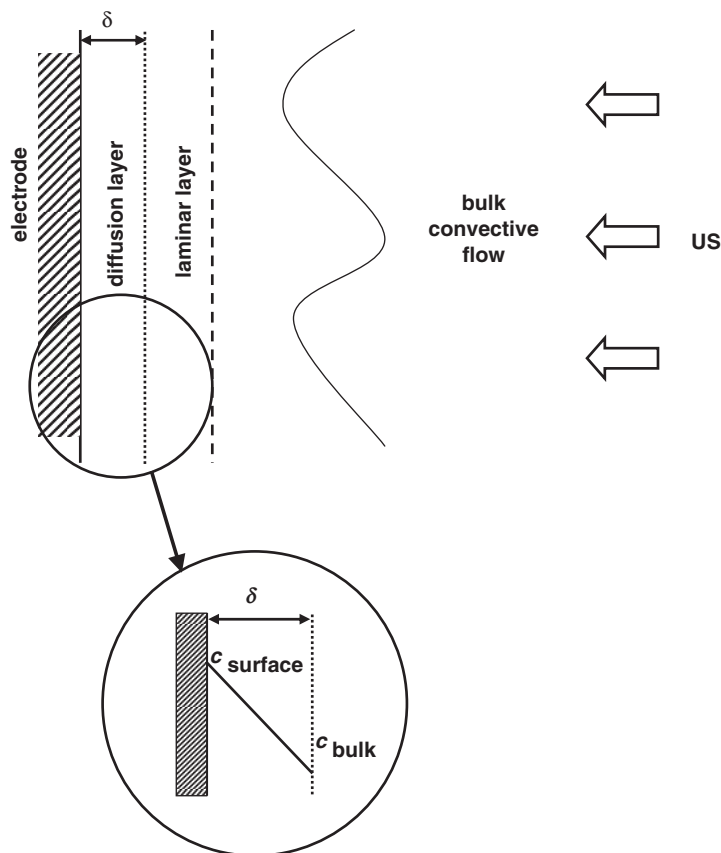
FIGURE 8.13. *Scheme of the Nernst diffusion layer model at an electrode surface in the presence of US. (Reproduced with permission of Elsevier, Ref. [133].)*

$$I_{lim} = \frac{nFDAc_{bulk}}{\delta},$$ (8.2)

where the limiting current I_{lim}, is related to the number of transferred electrons n, the Faraday constant F, the diffusion coefficient D, the electrode area A, the concentration c_{bulk}, and the diffusion layer thickness δ. In those cases where the electrode is positioned opposite to the ultrasonic horn (a face-on configuration) in aqueous media, proportionality between I_{lim} and $D^{2/3}Ac_{bulk}$ has been found [133]. Therefore, the diffusion layer thickness will be proportional to $D^{1/3}$. This ratio is a general feature of convective systems (as is the case of hydrodynamic electrodes), which are characterized by a not completely rigid diffusion layer as suggested by the Nernst model [151,152]. Acoustic streaming, however, can have adverse effects due to faster passivation or surface contamination [136].

The distance between the probe tip and the electrode is a key variable here as it affects the diffusion layer thickness (see Fig. 8.14A). The diffusion layer thickness tends to approximately the same limit for two different ultrasonic intensities at short horn–electrode
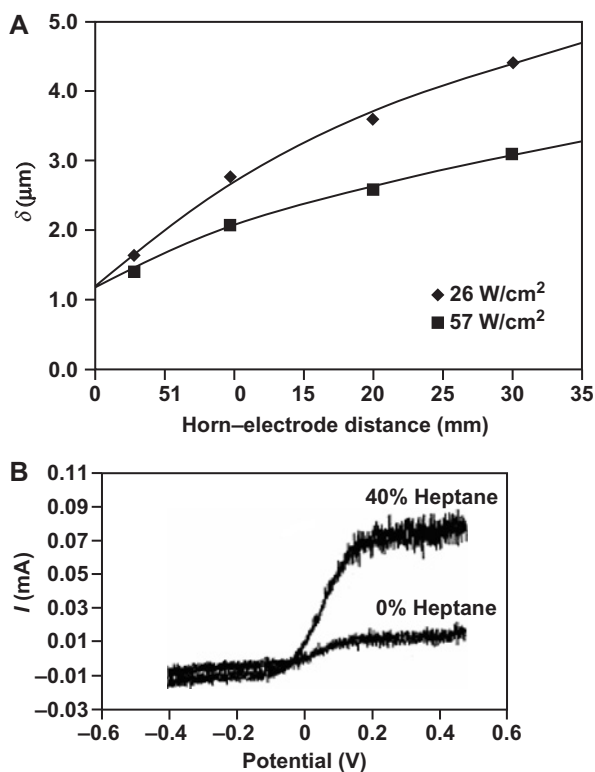
FIGURE 8.14. *(A) Variation of diffusion layer thickness as calculated from Eq. 8.2 with the probe tip–electrode separation for two different ultrasonic intensities. The solution was 1 mM [Fe(CN)$_6$]$^{3-}$/0.1 mM KCl and the working electrode a 4-mm-diameter Pt disc. (B) Influence of the addition of 40% heptane in the electrolyte (aqueous 0.1 M KCl) on the limiting current of 1 mM N,N,N′,N′-tetramethyl-p-phenylenediamine. (Reproduced with permission of Elsevier, Refs. [153,156].)*

distances [153]. Therefore, the effect of ultrasonic intensity is less significant at short distances between the electrode and the ultrasonic horn.

The effect of US frequency on mass transport is not very clear, so, medium-frequency values (20–100 kHz) are usually employed. According to Lorimer *et al*., US frequencies over the range 20–800 kHz have little or no influence on the limiting current [154]. However, the ultrasonic devices used by these authors (*viz*. two ultrasonic baths at 38 and 800 kHz, and a probe at 20 kHz) do not allow one to assert that the limiting current is not affected by US in the range 20–800 kHz. Del Campo *et al*. [155] used high-frequency US (about 500 kHz) to assist electroanalytical techniques and detected some effects that were governed by processes considerably different from those involved at lower frequencies. Specifically, the mass transport model for high frequencies has been suggested to be based on microjetting and microstreaming. High frequencies, however, are impractical for portable use.

Ultrasound in combination with an organic solvent facilitates the formation of binary systems with an aqueous electrolyte, thereby increasing the current intensity. Figure 8.14B shows this effect on the sono-voltammogram of *N,N,N′,N′*-tetramethyl-*p*-phenylenediamine (TMPD) in 0.1 M aqueous KCl with and without the addition of 40% v/v heptane [156]. The increased current in the acoustically emulsified media was ascribed to enhanced transport of electroactive material in heptane droplets towards the electrode surface, and related to the analyte solubility in the organic phase. The ratio of the current increase to the volume fraction of organic solvent (ϕ) can be expressed as:

$$I_{\lim} = I_{\lim\phi\to0}[1 + A\phi]. \tag{8.3}$$

Finally, US-enhanced mass transport has also been found to influence the rate of metal deposition (*e.g.* that of cobalt on glassy carbon electrodes by cyclic and stripping voltammetry, and chronoamperometry [157]).

Modification of process kinetics

The fact that US influences the mechanism of chemical reactions *via* the action of highly reactive radicals such as OH· and H· formed during solvent sonolysis is well known (see Chapter 7). Solvents sensitive to thermolysis or sonolysis (*e.g.* dimethylformamide [158], dimethylsulphoxide [159]) decompose slowly in the presence of intense US. Thus, radical species formed by cavitation are highly reactive and may participate as activators or enhancers in the electrode process [160]. In fast, *quasi*-reversible or irreversible systems, however, the only effect of US is to enhance mass transport without any direct effect on the rate of simple electron transfer processes.

The adsorption of species involved in an electrochemical reaction on an electrode is another type of process kinetically modified by US energy, as in the voltammetry of copper in alkaline solution using a copper electrode [161]. While the silent response was only slightly altered at pH 9 relative to pH 7, that assisted by US was significantly different. Thus, US greatly increased the rate of the anodic process in an alkaline solution, but produced inhibitory species at potentials above + 0.8 V (*versus* SCE) which deactivated the metal electrode. Removing such species by reversing the sweep to less anodic potentials reactivated the electrode and gave anodic currents during the reduction sweep. Similar results were obtained by using 20- and 38-kHz US during the electrochemical oxidation of thiosulphate in aqueous KCl, which increased the oxidation peak current

through enhanced mass transfer; however, it also shifted the oxidation peak potential anodically with increasing ultrasonic power [162]. Such a shift may have resulted from the formation of hydroxyl radicals, changes in electrode surface composition and complex adsorption phenomena.

In addition to enhancing the mass transport of metals for deposition on electrodes, US has been found to affect the mechanism of cobalt deposition on glassy carbon electrodes from aqueous sulphate solutions, and also the morphological details of the surface deposits [157]. The effect observed was a significant increase in the deposition and growth rates of cobalt on the electrode, and a switch from a complex, irreversible mechanism to a simple, reversible one. The ability to control the characteristics of the deposited layer *via* US application is similar to that of organic additives [163,164]. Similarly, sonication during preconcentration in stripping techniques allows intermetallic compounds to be formed and better stripping responses being obtained as a result. This effect has been checked in the sono-anodic stripping voltammetry of Pb^{2+} and Cu^{2+} in aqueous solutions to which Hg^{2+} was added in order to facilitate the formation of lead–copper amalgams in the preconcentration step [165].

8.4.2. Experimental devices used for ultrasound assistance to electroanalytical techniques

Ultrasonic energy can be used in various ways to enhance the performance of an electrochemical cell. Most of the electrochemical cells used for this purpose have been developed for sonovoltammetry, but can be modified for use in other electrochemical techniques. Bard in 1963 [166], and Klima *et al.* in 1994 [145], proposed electrochemical cells for coulometric and voltammetric studies, respectively, where the ultrasonic transducer was mounted at the bottom. The working electrode has also been used in the centre of the cavitation region generated in the cell electrolyte by a vertically arranged titanium-tipped horn probe [135,146]. The main problem with these cells is their large volume (150–200 ml), which is a major hindrance for bioelectrochemical studies or when expensive or scant samples or reagents are involved. Cells with small volumes and efficient coupling between ultrasonic energy and the electroanalytical process provide the best results.

The simplest way to assist electrochemical techniques with US is by using a bath to immerse the electrochemical cell, as proposed by Lorimer *et al*. [154] (see Fig. 8.15A). These authors used a three-compartment thermostated voltammetric cell consisting of a platinum flag (the counter electrode), a saturated calomel electrode (the reference electrode) and a rotating disc (the working electrode). Although an ultrasonic bath affords less accurate control of US irradiation, it affords a tenfold current increase in sonovoltammetry [167].

Ultrasonic probes have been more commonly coupled to electrochemical cells by virtue of the high amplitude they can provide. Various types of sonoelectrochemical cells using ultrasonic probes have been reported, especially interesting among which for analytical purposes are the sonovoltammetric cells independently proposed by Compton *et al*. [168] and Brett and Matysik [126] in 1996. In both cases, the tip of the 20-kHz probe was immersed into the cell at a fixed distance from the working electrode with special care in order to operate under controlled potential conditions (see Fig. 8.15B). Electrical isolation of the irradiating zone from the solution (for example, by the combined use of a PTFE spacer and connecting screw [142]) is of crucial importance, even though it decreases the irradiation amplitude, which is undesirable for some applications. The alternative for some techniques (sonovoltammetry, mainly) is bipotentiostatic control (particularly in high-frequency

A

counter electrode
(platinum flag)

working electrode
(rotating disc)

digital thermometer

electrochemical cell

reference electrode
(saturated calomel
electrode)

to and from
a thermostated
bath

redox couple
electrolyte

ultrasonic
bath

ultrasound
transducer

B

sonic
horn

to control unit
of sonic horn

reference electrode
(saturated calomel
electrode)

graphite counter
electrode

Pt resistance
thermocouple

Ar inlet for
degassing

Ti tip

Pyrex
reservoir

cooling coil
connected to
thermostated
water bath

disc electrode

FIGURE 8.15. *Thermostated electrochemical cells employed for sonovoltammetry. (A) With an ultrasonic bath. (B) With an ultrasonic probe (Reproduced with permission of Elsevier, Refs. [133,154], respectively.)*

US applications, where the ultrasonic field can induce potential oscillations [169]). Somewhat less common is the use of split cell arrangements where a glass separator [145] or a polymer coating [170] is used to separate the compartments in which the ultrasonic tip and the electrodes are immersed.

Another variable in sonoelectrochemical cells is the relative position of the ultrasonic tip and working electrode, which can be arranged in various ways, namely (see Fig. 8.16 [133]): (a) face-on, where the working electrode is opposite to the ultrasonic tip; and (b) side-on, where the electrode surface is normal to the ultrasonic tip. The former generates a very high mass flow depending on the electrode-to-tip distance, amplitude of the ultrasonic transducer and electrode area in the case of microelectrodes [171]. This configuration was used by Brett and Matysik for sonovoltammetry [126], the noise produced by US being minimized by accumulating and averaging sonovoltammetric sweeps. Variable tip–electrode angles provided a 50% increase in limiting current at a 45° angle with respect to the face-on configuration [172].

The flow generated by US application in the side-on position is similar to that observed at a channel electrode with the mass transport of electroactive material similar to that of a convective flow over a stationary plate. This geometry provides well-defined sonovoltammetric signals for quantitative purposes. The speed of the flow passing over the electrode has been measured to be between 50 and 170 cm/s [173,174].

Another possibility is adapting the titanium tip of the US transducer (Fig. 8.16C) for use as a working electrode (a "sonotrode"). The simplest case is the use of the titanium tip itself as electrode [175]; however, anodic currents are not possible owing to the formation of a TiO_2 layer [176]. More recently, sonotrodes have been prepared by directly embedding a platinum electrode into the horn tip; this provides extremely high limiting currents for diffusion layer thicknesses of less than 1 μm, even at low US intensities [133]. The operation

A Face-on   **B Side-on**   **C Sonotrode**

electrode

electrode   **electrode**
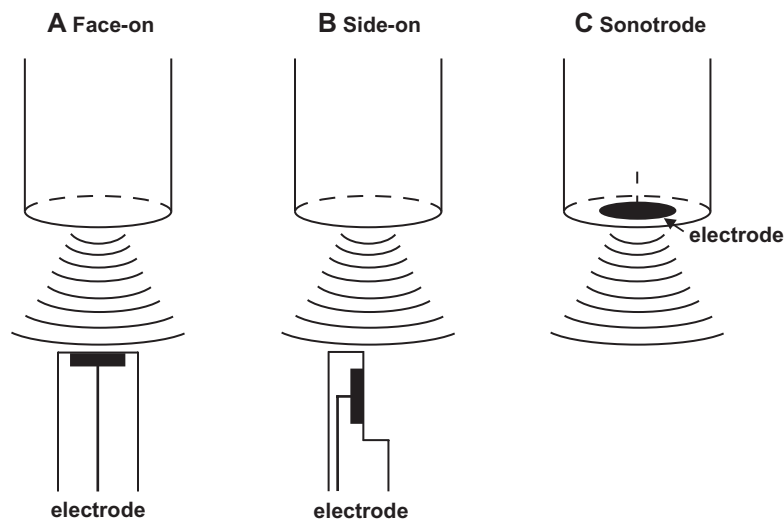
FIGURE 8.16. *Ultrasonic tip–working electrode positions employed in sono-electroanalytical cells. (Reproduced with permission of Elsevier, Ref. [133].)*

with sonotrodes is similar to the face-on position [140]; however, the ultrasonic amplitude must be controlled in order not to damage the electrode. Compton *et al*. compared both types of sonotrodes and concluded that the sonotrode with the platinum layer enhanced mass transport to a greater extent [176]. In addition, platinum sonotrodes can be mercury plated in order to extend the cathodic electrochemical window in aqueous solutions, and also to form a metallic amalgam in a plating step with a view to increase the sensitivity in anodic stripping voltammetry. Table 8.2 compares the efficiency of the different tip–electrode positions through the results of Compton *et al*. [174].

A special experimental technique operating at low temperatures (–70 to –35°C) known as "cryosonoelectrochemistry" was developed by Del Campo *et al*. [177]. The platinum disc electrode–US horn (20 kHz), in a face-on position, was immersed in liquid ammonia, which has proved an effective solvent for chemical and electrochemical processes at low temperatures and under mild conditions. Measurements must be made under dry conditions in an inert atmosphere.

8.4.3. Applications of ultrasound-assisted electroanalytical techniques

Ultrasound is currently regarded as a valuable tool for developing new electroanalytical methods and innovative chemically modified electrodes. Ultrasound can be applied to an electroanalytical cell either as a pretreatment or during the electrode process. This type of energy has proved efficient for pretreating electrodes; the interest on this type of application, however, is somewhat limited. One example is the determination of insulin by amperometric detection using glassy carbon electrodes that were pre-activated by sonication for 30 s in methanol and deionized water [178].

The use of US during the electrode process has focused on voltammetry for the determination of inorganic species in different types of samples, where the sensitivity of silent classical voltammetric techniques is normally decreased by electrode fouling. Typical applications of anodic stripping sonovoltammetry include the determination of lead and cadmium in aqueous solutions [179], copper and lead in fish gill mucosa [180], copper in beer [181], lead in wine [153] and copper in blood [182]. On the other hand, cathodic stripping sonovoltammetry has been applied to the determination of manganese in sea water [183] or instant tea [184] and nickel in industrial samples [185]; adsorptive stripping sonovoltammetry has been used for the determination of vanadium and nickel in aqueous media [186]; and linear sweep sonovoltammetry for that of nitrite in eggs [187]. Virtually all these applications involved using a 20-kHz ultrasonic probe and an optimized ultrasonic intensity that increased with increasing complexity of the sample matrix. It should be noted that total contents (including ions bound to complex organic matrices) were determined without the need for any sample treatment. The results provided by these US-assisted methods have been frequently compared with those obtained with atomic techniques such as AAS and ICP-MS and found to be highly consistent; however, sonoelectroanalysis involved lower costs and shorter analysis times.

The methods for organic analytes are less common. Thus, sonovoltammetry has been used to determine dopamine in egg homogenate [142]; riboflavine [186] and guanine and guanosine in aqueous solutions [188]; and ascorbic acid in commercial fruit drinks [189]. The few existing examples testify to the limited applicability of sonovoltammetry to organic analytes.

Electroanalysis in biphasic systems is a scarcely explored area owing to the difficulty of producing and maintaining an emulsion without the electrochemical process being

TABLE 8.2. *Comparison between tip–electrode positions from results obtained by Compton et al.*

Property	Face-on geometry	Side-on geometry	Ti-sonotrode	Pt-sonotrode
Position of the electrode	Opposite to the tip	Perpendicular to the tip	The tip is the working electrode	The tip is the working electrode
Shape of the electrode	Disc	Square	Same shape as the tip	Disc or square
Range of electrode sizes	Flexibility (macro and microdimensions)	Limited to macrodimensions	Limited by the size of the tip	Limited by the size of the tip
Range of ultrasonic intensities	0–70 W/cm^2	0–70 W/cm^2	0–70 W/cm^2	Limited as the Pt electrode can be ejected even with a strong cement
Quality of the voltammetry on sonication	Good sigmoidal-shaped voltammograms	Good sigmoidal-shaped voltammograms	Poor sigmoidal-voltammograms due to the TiO$_2$ layer formed on the electrode	Good voltammetry using the Pt insert

Reproduced with permission of Elsevier, Ref. [174].

altered by emulsifiers and stabilizers. The use of US to form emulsions ensures continuous contact of the sample with the electrode surface during the electrochemical process irrespective of the densities of their components. Two methods based on biphasic sono-voltammetry for lead in petrol (sonication at 20 kHz, 200 W/cm^2) [190] and vanillin in food flavouring solubilized in ethyl acetoacetate (sonication at 20 kHz, 52 W/cm^2) [191] have been reported in which ultrasonic energy was applied to the sample–aqueous electrolyte system in order to form the emulsion, transfer the analytes from the sample droplets to the aqueous electrolyte and effect the electrode process.

Indirect sonovoltammetry has enabled the determination of some species by their effect on electrochemically initiated reactions. For instance, Cu(II) can be determined by inhibiting the electrochemical reaction between *N,N*-diethyl-*p*-phenylenediamine and homocysteine through complexation of the latter [192].

Sonovoltammetry has also been combined with other steps of the analytical process (*e.g.* in US-assisted liquid–liquid extraction or digestion). Thus, US was found to aid copper extraction from blood (sample volume 100 µl) into an organic phase containing *N*-benzoyl-*N*-phenyl-hydroxylamine as ligand, from which it was then back-extracted into a fresh clean aqueous phase prior to analytical determination by sonovoltammetry [193]. Sediments were digested with a 4:1 nitric–perchloric acid mixture with US assistance for the subsequent determination of lead by sonovoltammetry with results similar to those of classical digestion combined with ICP-MS, but with significant time savings [194].

When steady currents cannot be obtained by sonovoltammetry, the use of Discrete Fourier Transform (DFT) analysis of chronoamperometric currents obtained under US assistance constitutes an effective alternative. Acquiring current signals at a high sampling rate (10 MHz) and processing by DFT allows one to determine analyte concentrations at specific frequencies by reducing the deviation in limiting currents. However, this technique is still at an initial state of development as it has only been applied to the model system $[Fe(CN)_6]^{3-}/[Fe(CN)_6]^{4-}$ [195]. Wavelet transform in pulsed ultrasonic modulation voltammetry is also at an incipient stage [196]. The current components corresponding to pulse-on and pulse-off can be recorded separately without an external data acquisition system. The difference between the two states has been found to be proportional to the concentration of the electroactive species.

Finally, US has been used for the characterization of new electrodes in electroanalytical experiments [197–200], and also for the preparation of new electrodes exploiting the enhancement of mass transport provided by US [201].

References

1. S.P. Newman, G. Goodman and S.W. Clarke, *Thorax*, 43 (1988) 318.
2. J.Y. Ding, M.J. Brooker, M.J. Andre, J.C. Andre, W.C. Zimlich, A.R. Imondi and M.E. Placke, *Resp. Drug Deliv.*, VII (2000) 349.
3. A.H. Lefebvre, *Atomization and Sprays*, Hemisphere Publishing Corporation, New York, 1989.
4. J. Mora, S. Maestre, V. Hernandis and J.L. Todolí, *Trends Anal. Chem.*, 22 (2003) 123.
5. J. Mora, J.L. Todolí, A. Canals and V. Hernandis, *J. Anal. At. Spectrom.*, 12 (1997) 445.
6. M.D. Luque de Castro and J.L. Luque-García, *Acceleration and Automation of Solid Sample Treatment*, Elsevier, Amsterdam, 2002.
7. K. Jankowski, D. Karmasz, A. Ramsza and E. Reszke, *Spectrochim. Acta B*, 52 (1997) 1813.
8. J.F. Banks, S. Shen, C.M. Whitehouse and J.B. Fenn, *Anal. Chem.*, 66 (1994) 406.
9. Y. Ren, W. Shi and Q. Jin, *Guangpuxue Yu Guangpu Fenxi*, 10 (1990) 32.
10. Y. Ren, W. Shi and Q. Jin, *Guangpuxue Yu Guangpu Fenxi*, 10 (1990) 36.

11. J. Stupar and W. Frech, *J. Chromatogr.*, 541 (1991) 243.
12. R.E. Neuhauser, U. Panne, R. Niessner, G.A. Petrucci, P. Cavalli and N. Omenetto, *Anal. Chim. Acta*, 346 (1997) 37.
13. Z. Mester and P. Fodor, *Anal. Chim. Acta*, 386 (1997) 89.
14. T.S. Conver and J.A. Koropchak, *Spectrochim. Acta B*, 50 (1995) 341.
15. B. Budic, *J. Anal. At. Spectrom.*, 16 (2001) 129.
16. R.C. Richter, K. Swami, S. Chace and L. Husain, *Fresenius J. Anal. Chem.*, 361 (1998) 168.
17. J.A.C. Broekaert, *Fresenius J. Anal. Chem.*, 368 (2000) 15.
18. D. Das and J.W. Carnahan, *Anal. Chim. Acta*, 444 (2001) 229.
19. J.A.C. Broekaert and V. Siemens, *Spectrochim. Acta B*, 59 (2004) 1823.
20. http://www.cetac.com
21. K. Jankowski and M. Dreger, *J. Anal. At. Spectrom.*, 15 (2000) 269.
22. S. Hann, G. Koellensperger, K. Kanitsar, G. Stingeder, M. Brunner, B. Erovic, M. Müller and C. Reiter, *Anal. Bioanal. Chem.*, 376 (2003) 198.
23. P.H. Yeon, Y.M. Cho and Y.N. Pak, *Bull. Korean Chem. Soc.*, 20 (1999) 1277.
24. http://www.epa.gov/
25. M.B. Denton, J.M. Freelin and T.R. Smith, Ultrasonic, Babington and Thermospray Nebulization, in J. Sneddon (Ed.), *Sample Introduction in Atomic Spectroscopy*, Elsevier, Amsterdam, 1988.
26. S. Joannon, P. Telouk and C. Pin, *Spectrochim. Acta B*, 52 (1997) 1783.
27. H. Hayashi, S. Furuzawa, T. Tanaka and M. Hiraide, *J. Anal. At. Spectrom.*, 19 (2004) 773.
28. M. Krachler and H. Emons, *Anal. Chim. Acta*, 429 (2001) 125.
29. C. Duyck, N. Miekeley, C.L. Porto da Silveira and P. Szatmari, *Spectrochim. Acta B*, 57 (2002) 1979.
30. J.C. Ely, C.R. Neal, J.A. O'Neill Jr. and J.C. Jain, *Chem. Geology*, 157 (1999) 219.
31. I.B. Brenner, P. Bremier and A. Lemarchand, *J. Anal. At. Spectrom.*, 7 (1992) 819.
32. R.I. Botto, *J. Anal. At. Spectrom.*, 8 (1993) 51.
33. R.I. Botto and J.J. Zhu, *J. Anal. At. Spectrom.*, 9 (1994) 905.
34. J.C. Ivaldi and J.F. Tyson, *Spectrochim. Acta B*, 50 (1995) 1207.
35. D.H. Sun, J.K. Waters and T.P. Mawhinney, *J. Anal. At. Spectrom.*, 12 (1997) 675.
36. M. Grotti, C. Lagomarsino and R. Frache, *Spectrochim. Acta B*, 59 (2004) 1001.
37. E. Vassileva and M. Hoenig, *Spectrochim. Acta B*, 56 (2001) 223.
38. M. Hoenig, H. Docekalova and H. Baeten, *Analusis*, 28 (2000) 419.
39. M. Hoenig and H. Docekalova, *4th EFS (European Furnace Symposium)*, Podbanske, Slovakia, 2000, p. 51.
40. H. Wildner and G. Wünsch, *Fresenius J. Anal. Chem.*, 354 (1996) 807.
41. W. Kerl, J.S. Becker, H.J. Dietze and W. Dannecker, *Fresenius J. Anal. Chem.*, 359 (1997) 407.
42. K. Jankowski, *Talanta*, 54 (2001) 855.
43. Y. Su, Z. Jin, Y. Duan, M. Koby, V. Majidi, J.A. Olivares and S.P. Abeln, *Anal. Chim. Acta*, 422 (2000) 209.
44. D. Sun, J.K. Waters and T.P. Mawhinney, *J. AOAC Int.*, 80 (1997) 20.
45. R. Lara, S. Cerutti, J.A. Sajonia, R.A. Olsina and L.D. Martínez, *Food Chem. Toxicol.*, 43 (2005) 293.
46. F. Cubadda and A. Raggi, *Microchem. J.*, 79 (2005) 91.
47. M. Krachler, A. Alimonti, F. Petrucci, K.J. Irgolic, F. Forastiere and S. Caroli, *Anal. Chim. Acta*, 363 (1998) 1.
48. M.A. Mesquita da Silva, V.L. Azzolin Frescura and A.J. Curtius, *Spectrochim. Acta B*, 55 (2000) 803.
49. D. Hausler, *Spectrochim. Acta B*, 42 (1987) 63.
50. E.H. Evans and L. Ebdon, *J. Anal. At. Spectrom.*, 5 (1990) 425.
51. S. Cerutti, J.A. Salonia, S.L.C. Ferreira, R.A. Olsina and L.D. Martínez, *Talanta*, 63 (2004) 1077.
52. R.F. Lara, R.G. Wuilloud, J.A. Sajonia, R.A. Olsina and L.D. Martínez, *Fresenius J. Anal. Chem.*, 371 (2001) 989.
53 S. Karthikeyan and S. Hirata, *Anal. Bioanal. Chem.*, 375 (2003) 139.
54. Q. Lu and R.M. Barnes, *Microchem. J.*, 54 (1996) 129.

55. P.W. Kirlew, M.T.M. Castillano and J.A. Caruso, *Spectrochim. Acta B*, 53 (1998) 221.
56. P.F. Marchisio, A. Sales, S. Cerutti, E. Marchevski and L.D. Martínez, *J. Hazard. Mater*., 124 (2006) 113.
57. X. Dai, C. Koeberl and H. Fröschl, *Anal. Chim. Acta*, 436 (2001) 79.
58. I. Manisali, D.D.Y. Chen and B.B. Schneider, *Trends Anal. Chem*., 25 (2006) 243.
59. M. Yamashita and J.B. Fenn, *J. Phys. Chem*., 88 (1984) 4451.
60. M.L. Aleksandrov, G.I. Barama, L.M. Gall, N.V. Krasnov, Y.S. Kusner, O.A. Irgorodskaya, V.I. Nikolaiev and V.A. Shkurov, *Bioorg. Khim*., 11 (1985) 700.
61. J.F. Banks, J.P. Quinn and C.M. Whitehouse, *Anal. Chem*., 66 (1994) 406.
62. C.M. Whitehouse, J.B. Fenn, S. Shen and C. Smith, U.S. Patent 5 306 412. *Method and Apparatus for Improving Electrospray Ionization of Solute Species*, 1994.
63. J. Shiea, D.Y. Chang, C.H. Lin and S.J. Jiang, *Anal. Chem*., 73 (2001) 4983.
64. N. Lion, F. Reymond, H.H. Girault and J.S. Rossier, *Curr. Opin. Biotechnol*., 15 (2004) 31.
65. J. Khandurina and A. Guttman, *Curr. Opin. Chem. Biol*., 7 (2003) 595.
66. P.A. Gröning, *Adv. Eng. Mater*., 7 (2005) 279.
67. M.J. Felton, *Anal. Chem*., 75 (2003) 505A.
68. S. Santesson and S. Nilsson, *Anal. Bioanal. Chem*., 378 (2004) 1704.
69. S. Santesson, *Miniaturized Bioanalytical Chemistry in Acoustically Levitated Droplets*, PhD Thesis, University of Lund, 2004.
70. K. Bücks and H. Müller, *Z. Phys*., 84 (1933) 75.
71. M.H. Weiser and R.E. Apfel, *J. Acoust. Soc. Am*., 71 (1982) 1261.
72. E. Welter and B. Neidhart, *Fresenius J. Anal. Chem*., 357 (1997) 345.
73. S. Nilsson, J.S.E. Johansson, M.I. Petersson, L. Schweitz and T.L.L. Johansson, *36th Annual Eastern Analytical Symposium & Exposition*, Somerset, NJ, 1997, p. 96.
74. B.J. Kang, L.S. Hung, S.K. Kuo, S.C. Lin and C.M. Liaw, *Mechatronics*, 13 (2003) 677.
75. K.H. Park, S.K. Lee, J.H. Yi, S.H. Kim, Y.K. Kwak and I.A. Wang, *Mechatronics*, 6 (1996) 591.
76. www.hfml.sci.kun.nl/froglev.html
77. B. Bona, E. Brusa, S. Carabelli, M. Chiaberge, C. Delprete, G. Genta, F. Maddaleno and A. Tonoli, *Mechatronics*, 7 (1997) 413.
78. X.J. Zheng, J.J. Wu and Y.H. Zhou, *J. Sound Vib*., 279 (2005) 201.
79. H. Karl, J. Fetzer, S. Kurz, G. Lehner and W.M. Rucker, Problem 28: An Electrodynamic Levitation Device, *Testing Electromagnetic Analysis Methods (TEAM) Workshop*, International Computing Society, Tucson, AR, 1998.
80. V. Vandaele, P. Lambert and A. Delchambre, *Precision Eng*., 29 (2005) 491.
81. S.K. Chung and E.H. Trinh, *J. Cryst. Growth*, 194 (1998) 384.
82. K.F. Kelton, G.W. Lee, A.K. Gangopadhyay, R.W. Hyers, T.J. Rathz, J.R. Rogers, M.B. Robinson and D.S. Robinson, *Phys. Rev. Lett*., 90 (2003).
83. A. Ashkin, *Phys. Rev. Lett*., 24 (1970) 156.
84. Y.K. Nahmias and D.J. Odde, *IEEE J. Quantum Electron*, 38 (2002) 131.
85. K. Taguchi, M. Tanaka and M. Ikeda, *Optics Commun*., 194 (2001) 67.
86. K. Konig, *Cell Mol. Biol*., 44 (1998) 721.
87. S.C. Grover, A.G. Skirtach, R.C. Gauthier and C.P. Grover, *J. Biomed. Opt*., 26 (2001) 14.
88. F. Erzincanli, *A Non-contact End-effector for Robotic Handling of Non-rigid Materials*, PhD Thesis, University of Salford, 1995.
89. E.H. Brandt, *Science*, 243 (1989) 349.
90. O. Rohling, C. Weitkamp and B. Neidhart, *Fresenius J. Anal. Chem*., 368 (2000) 125.
91. G. Reinhart and J. Hoeppner, *CIRP Ann*., 49 (2000) 5.
92. Y. Hashimoto, Y. Koike and S. Ueha, *Trans. IEEE Jpn*., 117 (1997) 1406.
93. E.G. Lierke, *Acoustica*, 82 (1996) 220.
94. A.V. Anilkumar, C.P. Lee and T.G. Wang, *Phys. Fluids A*, 5 (1993) 2763.
95. E.H. Trinh and J.L. Robey, *Phys. Fluids*, 6 (1994) 3567.
96. N. Kawahara, A.L. Yarin, G. Brenn, O. Kastner and F. Durst, *Phys. Fluids*, 12 (2000) 912.
97. A.L. Yarin, G. Brenn, J. Keller, M. Pfaffenlehner, E. Ryssel and C. Tropea, *Phys. Fluids*, 9 (1997) 3300.

98. A.L. Yarin, G. Brenn, O. Kastner and C. Tropea, *Phys. Fluids*, 14 (2002) 2289.
99. A.L. Yarin, D.A. Weiss, G. Brenn and D. Rensink, *Int. J. Multiphase Flow*, 28 (2002) 887.
100. P. Jacob, A. Stockhaus, R. Hergenröder and D. Klockow, *Fresenius J. Anal. Chem.*, 371 (2001) 726.
101. P. Önnerfjord, J. Nilsson, L. Wallman, T. Laurell and G. Marko-Varga, *Anal. Chem.*, 70 (1998) 4755.
102. T. Laurell, L. Wallman and J. Nilsson, *J. Micromech. Microeng.*, 9 (1999) 369.
103. J. Nilsson, J. Bergkvist, S. Ekström, L. Wallman and T. Laurell, Compound Microdispensing, in J. M. Ramsey and A. Van Den Berg (Eds.), *Micro Total Analysis Systems 2001*, Kluwer Academic Publishers, Monterrey, CA, 2001.
104. T. Laurell, J. Nilsson, S. Santesson, S. Nilsson, R. Zivin, R. Thurmond and L. Patel, U.S. Patent WO 99/44 746. *System for Performing Assays on a Levitated Droplet*, 1999.
105. D.E. Gustafson, W.H. Hofmeister, R.J. Bayuzick, K. Nagashio and K. Kuribayashi, *Mater. Sci. Eng. A*, 341 (2003) 1.
106. C. Esen, T. Weigel, V. Sprynchak and G. Schweiger, *JQSRT*, 89 (2004) 79.
107. S. Santesson, M. Andersson, E. Degerman, T. Johansson, J. Nilsson and S. Nilsson, *Anal. Chem.*, 72 (2000) 3412.
108. A. Omrane, S. Santesson, M. Aldén and S. Nilsson, *Lab on a Chip*, 4 (2004) 287.
109. S. Santesson, E.S. Cedergren-Zeppezauer, T. Johansson, T. Laurell, J. Nilsson and S. Nilsson, *Anal. Chem.*, 75 (2003) 1733.
110. S.M. Nie and S.R. Emery, *Science*, 275 (1997) 1102.
111. K. Kneipp, Y. Wang, H. Kneipp, L.T. Perelman, I. Itzkan, R. Dasari and M.S. Feld, *Phys. Rev. Lett.*, 78 (1997) 1667.
112. S. Santesson, J. Johansson, L.S. Taylor, I. Levander, S. Fox, M. Sepaniak and S. Nilsson, *Anal. Chem.*, 75 (2003) 2177.
113. N. Leopold, M. Haberkorn, T. Laurell, J. Nilsson, J.R. Baena, J. Frank and B. Lendl, *Anal. Chem.*, 75 (2003) 2166.
114. Y. Cerenius, A. Oskarsson, S. Santesson, S. Nilsson and L. Kloo, *J. Appl. Crystallogr.*, 36 (2003) 163.
115. E.H. Trinh, *Rev. Sci. Instrum.*, 56 (1985) 2059.
116. E.H. Trinh and H. Chaur-Jian, *J. Acoust. Soc. Am.*, 79 (1986) 1335.
117. K. Ohsaka, A. Rednikov, S.S. Sadhal and E.H. Trinh, *Rev. Sci. Instrum.*, 73 (2002) 2091.
118. M. Petersson, J. Nilsson, L. Wallman, T. Laurell, J. Johansson and S. Nilsson, *J. Chromatogr. B*, 714 (1998) 39.
119. R. Eberhardt, *Entwicklung einer Ultraschall-Levitations-Apparatur für die Probenvorbereitung in der Mikro- und Spurenanalyse*, PhD Thesis, Philipps University of Marburg, 1999.
120. B.R. Wood, P. Heraud, S. Stojkovic, D. Morrison, J. Beardall and D. McNaughton, *Anal. Chem.*, 77 (2005) 4955.
121. D.D. Weis and J.D. Nardozzi, *Anal. Chem.*, 77 (2005) 2558.
122. S. Santesson, T. Johansson, J. Nilsson, E. Degerman, P. Rorsman, P. Viberg, P. Spegel and S. Nilsson, *49th ASMS Conference on Mass Spectrometry and Allied Topics*, Chicago, IL, 2001.
123. A. Biswas, *J. Cryst. Growth*, 147 (1995) 155.
124. S. Santesson, I. Barinaga-Rementería Ramírez, P. Viberg, B. Jergal and S. Nilsson, *Anal. Chem.*, 76 (2004) 303.
125. M.E. Hyde, C.E. Banks and R.G. Compton, *Electroanalysis*, 16 (2004) 345.
126. A.M. Oliveira Brett and F.M. Matysik, *Electrochim. Acta*, 42 (1997) 945.
127. O. Mikkelsen and K.H. Schroder, *Electroanalysis*, 11 (1999) 401.
128. O. Mikkelsen and K.H. Schroder, *Electroanalysis*, 12 (2000) 1201.
129. O. Mikkelsen and K.H. Schroder, *Electroanalysis*, 13 (2001) 687.
130. A.O. Simm, C.E. Banks and R.G. Compton, *Anal. Chem.*, 76 (2004) 5051.
131. T.J. Mason and J.P. Lorimer, *Practical Sonochemistry*, *User's Guide to Applications in Chemistry and Chemical Engineering*, Ellis Horwood, Chichester, UK, 1989.
132. A.J. Saterlay and R.G. Compton, *Fresenius J. Anal. Chem.*, 367 (2000) 308.

133. R.G. Compton, J.C. Eklund, F. Marken, T.O. Rebbitt, R.P. Akkermans and D.N. Waller, *Electrochim. Acta*, 42 (1997) 2919.
134. W.J. Tomlinson, *Adv. Sonochem.*, 1 (1990) 173.
135. R.G. Compton, J.C. Eklund, S.D. Page, G.H.W. Sanders and J. Booth, *J. Phys. Chem.*, 98 (1994) 12410.
136. C.E. Banks and R.G. Compton, *Electroanalysis,* 15 (2003) 329.
137. F. Marken, S. Kumbhat, G.H.W. Sanders and R.G. Compton, *J. Electroanal. Chem.*, 414 (1997) 95.
138. R.P. Akkermans, M. Wu, C.D. Bain, M. Fidel-Suárez and R.G. Compton, *Electroanalysis*, 10 (1998) 613.
139. C.E. Banks and R.G. Compton, *Chem. Phys. Chem.*, 4 (2003) 169.
140. F. Marken, R.P. Akkermans and R.G. Compton, *J. Electroanal. Chem.*, 415 (1996) 55.
141. R.G. Compton, F. Marken and T.O. Rebbitt, *J. Chem. Soc.*, *Chem. Commun.*, (1996) 1017.
142. E.L. Beckett, N.S. Lawrence, Y.C. Tsai, J. Davis and R.G. Compton, *J. Pharm. Biomed. Analysis*, 26 (2001) 995.
143. J.P. Lorimer, T.J. Mason, M. Plattes and D.J. Walton, *J. Electroanal. Chem.*, 568 (2004) 379.
144. S.A. Perusich and R.C. Alkire, *J. Electrochem. Soc.*, 138 (1991) 708.
145. J. Klima, C. Bernard and C. Degrand, *J. Electroanal. Chem.*, 367 (1994) 297.
146. C.R.S. Hagen and L.A. Coury Jr., *Anal. Chem.*, 66 (1994) 399.
147. F.J. Del Campo, J. Melvilla, J.L. Hardcastle and R.G. Compton, *J. Phys. Chem. A*, 105 (2001) 666.
148. E.L. Cooper and L.A. Coury Jr., *J. Electrochem. Soc.*, 1998 (1994) 145.
149. R.G. Compton, J.C. Eklund, S.D. Page, T.J. Mason and D.J. Walton, *J. Appl. Electrochem.*, 26 (1996) 775.
150. N. Moriguchi, *J. Chem. Soc. Jap.*, (1934) 55.
151. R.G. Compton, J.C. Eklund and F. Marken, *Electroanalysis*, 9 (1997) 509.
152. C.M.A. Brett and A.M. Oliveira Brett, *Electrochemistry: Principles*, *Methods and Applications*, Oxford University Press, Oxford, 1993.
153. R.P. Akkermans, J.C. Ball, T.O. Rebbitt, F. Marken and R.G. Compton, *Electrochim. Acta*, 43 (1998) 3443.
154. J.P. Lorimer, B. Pollet, S.S. Phull, T.J. Mason, D.J. Walton and U. Geissler, *Electrochim. Acta*, 41 (1996) 2737.
155. F.J. Del Campo, B.A. Coles, F. Marken, R.G. Compton and E. Cordemans, *Ultrason. Sonochem.*, 6 (1999) 189.
156. C.E. Banks, N.V. Rees and R.G. Compton, *J. Electroanal. Chem.*, 535 (2002) 41.
157. S. Floate, M. Hyde and R.G. Compton, *J. Electroanal. Chem.*, 523 (2002) 49.
158. V. Misik, L.J. Kirschenbaum and P. Riesz, *J. Phys. Chem.*, 99 (1995) 5970.
159. T. Kondo, L.J. Kirschenbaum, H. Kim and P. Riesz, *J. Phys. Chem.*, 97 (1993) 522.
160. F. Marken, J.C. Eklund and R.G. Compton, *J. Electroanal. Chem.*, 395 (1995) 335.
161. J.P. Lorimer, T.J. Mason, M. Plattes, S.S. Phull, J. Iniesta and D.J. Walton, *Ultrason. Sonochem.*, 11 (2004) 223.
162. B.G. Pollet, J.P. Lorimer, J.Y. Hihn, S.S. Phull, T.J. Mason and D.J. Walton, *Ultrason. Sonochem.*, 9 (2002) 267.
163. R.J. Nichols, W. Beckmann, H. Meyer, N. Batina and D.M. Kolb, *J. Electroanal. Chem.*, 330 (1992) 381.
164. R.J. Nichols, C.E. Bach and H. Meyer, *Ber. Bunsenges Phys. Chem.*, 97 (1993) 1012.
165. R.P. Akkermans, J.C. Ball, F. Marken and R.G. Compton, *Electroanalysis*, 10 (1998) 26.
166. A.J. Bard, *Anal. Chem.*, 35 (1963) 1125.
167. D.J. Walton, S.S. Phull, A. Chyla, J.P. Lorimer, T.J. Mason, L.D. Burke, M. Murphy, R.G. Compton, J.C. Eklund and S.D. Page, *J. Appl. Electrochem.*, 25 (1995) 1083.
168. R.C. Compton, J.C. Eklund, S.D. Page and T.O. Rebbitt, *J. Chem. Soc.*, *Dalton Trans.*, 389 (1995).
169. F. Marken and R.G. Compton, *Ultrason. Sonochem.*, 3 (1996) S131.

170. H. Huck, *Ber. Bunsenges. Phys. Chem.*, 91 (1987) 648.
171. C.W. Lee, R.G. Compton, J.C. Eklund and D.N. Waller, *Ultrason. Sonochem.*, 2 (1995) S59.
172. B.G. Pollet, J.P. Lorimer, S.S. Phull, T.J. Mason and J.Y. Hihn, *Ultrason. Sonochem.*, 10 (2003) 217.
173. R.G. Compton, R.A.W. Dryfe and J.C. Erklund, *Res. Chem. Kinet.*, 1 (1994) 239.
174. J.C. Eklund, F. Marken, D.N. Waller and R.G. Compton, *Electrochim. Acta*, 41 (1996) 1541.
175. J. Reisse, H. Francois, J. Vandercammen, O. Fabre, A. Kirsch-de Mesmaeker, C. Maerschalk and J.L. Delplancke, *Electrochim. Acta*, 39 (1994) 37.
176. R.G. Compton, J.C. Eklund, F. Marken and D.N. Waller, *Electrochim. Acta*, 41 (1996) 315.
177. F.J. Del Campo, A. Neudeck, R.G. Compton and F. Marken, *J. Electroanal. Chem.*, 477 (1999) 71.
178. M. Zhang, C. Mullens and W. Gorski, *Anal. Chem.*, 77 (2005) 6396.
179. F.M. Matysik, S. Matysik, A.M. Oliveira Brett and C.M.A. Brett, *Anal. Chem.*, 69 (1997) 1651.
180. J.L. Hardcastle and R.G. Compton, *Electroanalysis*, 13 (2001) 89.
181. C. Agra-Gutiérrez, J.L. Hardcastle, J.C. Ball and R.G. Compton, *Analyst*, 124 (1999) 1053.
182. J.L. Hardcastle, G.G. Murcott and R.G. Compton, *Electroanalysis*, 12 (2000) 559.
183. A. Goodwin, A.L. Lawrence, C.E. Banks, F. Wantz, D. Omanovic, S. Komorsky-Lovric and R.G. Compton, *Anal. Chim. Acta*, 533 (2005) 141.
184. A.J. Saterlay, J.S. Foord and R.G. Compton, *Analyst*, 124 (1999) 1791.
185. J. Davis, D. Huw Vaughan, D. Stirling, L. Nei and R.G. Compton, *Talanta*, 57 (2002) 1045.
186. C. Agra-Gutiérrez and R.G. Compton, *Electroanalysis*, 10 (1998) 603.
187. J. Davis and R.G. Compton, *Anal. Chim. Acta*, 404 (2000) 241.
188. A.M. Oliveira Brett and F.M. Matysik, *Bioelectroch. Bioener.*, 42 (1997) 111.
189. R.P. Akkermans, M. Wu and R.G. Compton, *Electroanalysis*, 10 (1998) 814.
190. A.N. Blythe, R.P. Akkermans and R.G. Compton, *Electroanalysis*, 12 (2002) 16.
191. J.L. Hardcastle, C.J. Paterson and R.G. Compton, *Electroanalysis*, 13 (2001) 899.
192. J.A. Kershaw, O. Nekrassova, C.E. Banks, N.S. Lawrence and R.G. Compton, *Anal. Bioanal. Chem.*, 379 (2004) 707.
193. J.L. Hardcastle and R.G. Compton, *Analyst*, 126 (2001) 2025.
194. A.J. Saterlay, C. Agra-Gutiérrez, M.P. Taylor, F. Marken and R.G. Compton, *Electroanalysis*, 11 (1999) 1083.
195. L.E and D. Zhou, *Electroanalysis*, 16 (2004) 442.
196. X. Zhang. T. Tanaka and J. Jin, *Ultrason. Sonochem.*, 13 (2006) 133.
197. C. Agra-Gutiérrez, M.F. Suárez and R.G. Compton, *Electroanalysis*, 11 (1999) 16.
198. Y.C. Tsai, J. Davis, R.G. Compton, S. Ito and N. Ono, *Electroanalysis*, 13 (2001) 7.
199. C.E. Banks, J. Kruusma, M.E. Hyde, A. Salimi and R.G. Compton, *Anal. Bioanal. Chem.*, 379 (2004) 277.
200. J. Kruusma, C.E. Banks and R.G. Compton, *Anal. Bioanal. Chem.*, 379 (2004) 700.
201. S. Ward-Jones, A.O. Simm, C.E. Banks and R.G. Compton, *Ultrason. Sonochem.*, 13 (2006) 261.

This page intentionally left blank

CHAPTER 9

Ultrasound-Based Detection Techniques

9.1. INTRODUCTION

Most of the analytical methods for the characterization and analysis of liquids, solids, gases, suspensions, sample surfaces, coatings, etc., that have been developed over the past few decades are based on measurements of waves propagating through the test sample. For a long time, electromagnetic waves have prevailed in the field of analytical instrumentation, with well-established techniques such as those based on optical measurements in the ultraviolet, visible and infrared regions, fluorescence, circular dichroism, light scattering, nuclear magnetic resonance or electron microscopy, among others. Other types of waves that can propagate through materials are those caused by mechanical deformations. Ultrasonic techniques rely on measurements of low-intensity waves or mechanical deformations at frequencies higher than 50 kHz (mostly in the megahertz region, but also in the gigahertz region). The relationships between the properties of a material and its ultrasonic characteristics have been extensively studied and ultrasonic techniques used in non-destructive testing and imaging applications for decades. Ultrasound as an analytical tool has revolutionized medical diagnostics with powerful recent applications such as 3D and 4D imaging, distant palpitation or image enhancement with contrast agents; by contrast, the application of US to material analysis has been held back by problems with ultrasonic design, electronics and size of sample handled, complicated measuring procedures and inadequate resolution.

Analytical chemists have been reluctant to use ultrasound-based detection techniques, which have been widely employed in other research fields — particularly in physical chemistry, where they have enabled complex theoretical developments with which the analytical chemist is usually unfamiliar. Ultrasound-based detection can be a useful tool for analytical chemists provided they acquire the required basic knowledge about it. This chapter summarizes such basic knowledge for both potential and incipient users of batch [1–3] and continuous approaches [4–6] to leading the samples to a US detector.

The literature on US-based detection uses the words "method", "technique" and "measurement" indiscriminately; also the word "spectrum" is used to designate a plot where the *x* axis does not represent wavelength or frequency, and even more general concepts such as "hydrodynamic" instead of "dynamic" when the target system is non-aqueous or the indifferent use of "interphase" and "interface". This warrants some preliminary clarification and making the terminology uniform. In this respect a parallel can be established between molecular UV–visible spectroscopic techniques (most common in analytical laboratories) as a whole and US spectroscopic techniques, the latter of which share the feature that they use the spectral zone beyond the sound wavelength (commonly expressed as a frequency). In the former group, individual techniques are distinguished by the instrumental quantity or datum representing the phenomenon they measure (namely, absorbance, fluorescence emission and phosphorescence emission, which have given rise to absorptiometry, fluorimetry and phosphorimetry, respectively); these are generally used when fixed-wavelength measurements are made, the name of the phenomenon preceding the word "spectrometry" if measurements span a range of wavelengths. Ultrasound-based detection techniques can be further classified according to whether they are based on, (a) "primary responses", that is,

on measurements of quantities or data that change as US travels through the test material (*e.g.* the velocity in ultrasonic velocity spectroscopy, attenuation in ultrasonic attenuation spectroscopy or impedance in ultrasonic impedance spectroscopy); (b) measurements of a component of a more general phenomenon (*e.g.* absorption, scattering or even diffraction, in the case of attenuation); (c) measurements made under specific conditions such as reso-nance, interference, diffraction; (d) others based on the time of degradation of the absorbed energy into heat. The responses for types (b)–(d) can be deemed "modified" or "secondary" responses, and have given rise to techniques the names of which specify the particular measurement conditions (*e.g.* resonance US spectrometry). In addition, when some special device is used or typical measurements are provided (*e.g.* images in the case of acoustic microscopy), the approach is also deemed a technique even though the US parameter modified by the presence of a given frequency and material (the sample) falls in the category of primary responses (*e.g.* velocity, attenuation).

The scheme in Fig. 9.1 is intended to introduce analytical chemists into the world of US-based detection. It specifies the steps involved in detection and the possibilities in each case, namely: *ultrasound generation and detection*, which summarizes the most common principles behind transducers; *type of radiation produced* as a function of the radiation frequency (*f*), application time (*t*) and the path (*x*) the radiation follows to reach the sample; *types of waves* according to angle of incidence (or special waves resulting from the phonon–photon interactions); *response of the sample to the US force*, which is related to the nature of the sample and gives rise to different techniques based on a direct, primary response such as velocity or attenuation, a component of the overall primary response (absorption, scattering, diffraction) or special conditions such as resonance. The sections in this chapter follow the sequence as the steps of US-based detection. Thus, a brief descrip-tion of the most common types of devices for generating and detecting US over appropriate ranges is followed by description of the time and the way US radiation is used. Then, the ways in which US radiation can interact with a sample and produce different types of waves, which in turn provide different types of information, are examined. The types of responses — and hence measurements — behind the different ultrasonic techniques, and the basic theoreti-cal principles on which they rely are discussed next. Finally, the most salient US-based detection techniques are discussed and an overview of commercial and laboratory-made instruments is provided. Note that the development of these techniques has produced a number of specialized books, so only a very brief discussion of each is provided in this chapter. Some recent developments are commented on and recent references included to illustrate the continuous growth of research in this field.

Analytical chemists are encouraged to find ways to apply the continuous advances in US-based detection reported in the medical literature (mainly ultrasonic imaging and signal processing [7]) in pure analytical chemistry.

9.2. ULTRASOUND GENERATION AND DETECTION
IN ULTRASOUND-BASED DETECTION TECHNIQUES

The ultrasound intensity employed in US-based detection is so low (typically <1 W/cm^2) that it causes no physical or chemical alteration of the properties of the material through which the wave propagates; the amplitude of deformations is therefore extremely small, so ultrasonic spectroscopic techniques can be deemed non-destructive.

Unlike light waves, ultrasonic waves can propagate through opaque samples — in fact through most types of materials. Another advantage of ultrasonic waves is that their wavelength is fairly easy to change; unlike optical techniques, where waves originate from
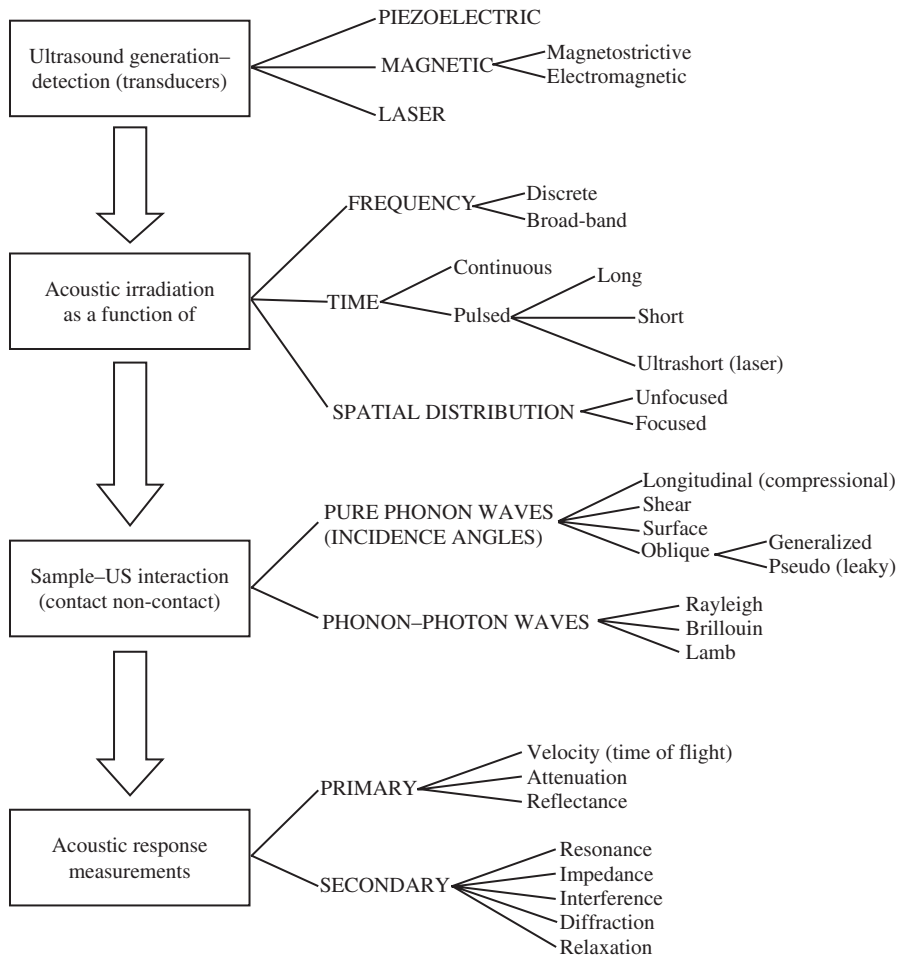
a light source and therefore require special effort to ensure an adequate spectral purity, ultrasonic waves are synthesized electronically, so a typical ultrasonic spectrometer can operate over a broad range of wavelengths spanning one, two or even more orders of magnitude; the process can be described as probing the inside of the analysed sample with a set of fingers differing in size by more than one order of magnitude.

Most types of ultrasonic measurements can be made with the general experimental set-up depicted in Fig. 9.2. A generator produces an electrical or light signal of appropriate frequency, duration and amplitude. The signal is applied to an ultrasonic transducer which converts it into pressure oscillations — the ultrasonic wave — which propagate through the sample, held in a suitable measurement cell. After passing through the sample, the ultrasonic signal is detected by the same or a different ultrasonic transducer and converted back into an electrical signal which is digitized by an analogue-to-digital converter and
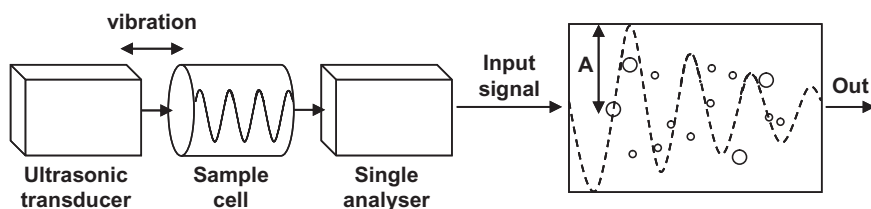
displayed on the screen of an oscilloscope or personal computer for analysis of the ultrasonic properties of the sample. The precise details of the analysis depend on the specific ultrasonic parameter measured.

   As can be seen in Fig. 9.1, there are three main types of US transducers, namely: piezoelectric, electromagnetic and optical. Depending on the extent of contact between the sample and the transducer these devices can be classified into high contact, two-point contact, one-point contact and contactless transducers. Sample–transducer contact can also be established *via* a couplant solution. The couplant solution should be stable enough to ensure highly reproducible measurements. In addition, when the couplant is water in contact with air, the solution volume decreases with time — particularly when the US beam is highly focused, as in acoustic microscopy.

9.2.1. *Piezoelectric ultrasound generators and detectors*

The most commonly employed US transducers are thin platelets of piezoelectric (mainly ceramic) materials with metallic electrodes on both surfaces (see Section 1.4). Such transducers have resonance frequencies determined by the interference of the ultrasonic signals created at both surfaces and internal reflections. The interferences cause distortions (broadening) in the echo pattern in pulse-echo measurements. The resonances also introduce phase shifts in the signals and lead to restrictions in the bandwidth. The frequency range can be expanded by using concave, cylindrical or spherical piezotransducers.

   The advent of piezoelectric transducers other than ceramic ones significantly boosted advances in medical US applications. Thus, ultrasound probes made of PVDF polymer have provided evidence that acoustic waves propagating through tissues undergo non-linear distortion and its associated generation of harmonics. Before PVDF material became available, the solid piezoelectric ceramic probes occasionally used to probe the field featured too narrow bandwidths and dynamic ranges to faithfully reproduce non-linear waveforms. The arrival of piezoelectric composite transducers, together with the use of spherical gas voids or microbubbles as contrast agents, greatly improved image quality. The conclusion that the harmonics of the bubble resonance frequency provided optimum image enhancement prompted the development of imaging transducers capable of operating at both fundamental and harmonic frequencies.

   Piezoelectric transducers can be of the high contact, two- or one- point contact types. The contact force between the sample and the transducer has been found to affect resonance spectra. Thus, resonant peaks increase with decreasing contact force; also, the resonant frequency is dependent on the contact force [8]. Electrical and mechanical cross-talk between

two transducers can be avoided and the force applied to the sample controlled by using various transducer configurations [9,10]. The simplest configuration, which was designed by Ledbetter *et al.* [11], can be used to measure frequencies in the 10 kHz to 5 MHz range. Two "pinducers" [12] are held axially aligned on an aluminium block by means of four rubber "O" rings, which avoids acoustic cross-talk at room temperature. By replacing the rubber "O" rings with Teflon sleeves, this configuration can be used down to cryogenic temperatures. The Curie temperature of the piezoelectric transducers and the stability of polymeric bonds restrict the highest temperature at which these configurations can be used. Using small lithium niobate transducers held by thin metallic membranes allows working at up to 750 K [13]; also using alumina buffer rods to separate the transducers from the hot sample allows the usable temperature range to be expanded up to 1820 K [14].

For measuring elastic moduli of millimetric samples, a 30-MHz $LiNbO_3$ transducer disc 1.5 mm in diameter has torsional resonances beginning below 200 kHz and many other resonances between this and the first compressional mode at 30 MHz; this makes it useless for some US techniques such as resonance ultrasound spectroscopy (RUS). However, by making a metallic diffusion bond to a single-crystal diamond disc 1.5 mm in diameter and 1 mm thick, a structure is produced with negligible damping to minimize noise, a lowest resonance of about 4.3 MHz and the ability to operate from below 1 K to above 1000 K. Ordinary epoxy bonds can also be used for this purpose; by restricting the maximum temperature to about 350 K and using a pair of similar (1.5-mm diameter) transducers attached to thin supporting diaphragms of polymer film, the resonances of a 1-mm rectangular parallelepiped sample can be measured by making contact with diagonally opposite corners without using any coupling fluids. Such point contact preserves the free-surface boundary conditions to less than 1 part in 10^5 if the contact force is below 1 *g*. Using drive levels of less than 1 V and electronics such as the previous one allows signal-to-noise ratios (SNR) better than 30 dB to be easily achieved.

In order to minimize the problem faced in separating the specimen response from the as-measured spectra of a resonator by minimizing sample–transducer contact, a one-point contact design was developed by replacing the receiving transducer with an optical interferometer and measuring elastic wave speeds in a 1-mm diameter ceramic ball [15].

The new generation of silicon technology imaging transducers combined with ongoing electronic miniaturization and the availability of extremely fast and powerful portable laptop computers will lead to the development of portable or even wearable high-resolution scanners affording wireless data transfer. This technology will help to make communication with remote locations and advanced medical applications more affordable.

9.2.2. Electromagnetic ultrasound generators and detectors

The resonant spectrum of a specimen can be acquired without physical contact between the sample and transducers. The instruments designed for this purpose facilitate the characterization of samples that must be kept in controlled atmospheres. Non-contact US measurements can rely on magnetic coupling, which can be accomplished by coating the sample with a thin film of a magnetostrictive material (*e.g.* nickel) or exciting eddy currents in the presence of a constant magnetic field; this is the basis for the two main types of electromagnetic US transducers, namely: magnetostrictive and electromagnetic.

Magnetostriction is the dimensional change (strain) which accompanies the domain movement and rotation of magnetization. When the magnetic field vibrates so does magnetostriction, and as a result ultrasonic waves are produced. A magnetostrictive transducer (MART) is a transducer in a non-contact US instrument where the coated sample

is placed inside two coaxial solenoids (S_1 and S_2) that act as a driving and receiving transducer, respectively (Fig. 9.3A). An AC voltage of amplitude *V* and frequency ω is applied to the excitation coil S_1 to generate a sinusoidal magnetic field $H(\omega t)$ at the sample. The magnetostrictive field responds to the applied field by generating a periodic stress which drives the sample into one of its mechanical resonances, — in the case of RUS — which are detected by solenoid S_2. The detection solenoid S_2 consists of two identical coils wound clockwise and counter-clockwise; this reduces direct magnetic coupling between S_1 and S_2. The resonances are detected because the permeability of the magnetostrictive film decreases when the sample approaches a resonant frequency and the magnetostrictive film changes from a strain-free state (away from the resonance) to a stress-free state (at resonance). These instruments afford RUS measurements between cryogenic temperatures and approximately 1000 K. The Curie temperature of the magnetostrictive material determines the upper temperature limit.
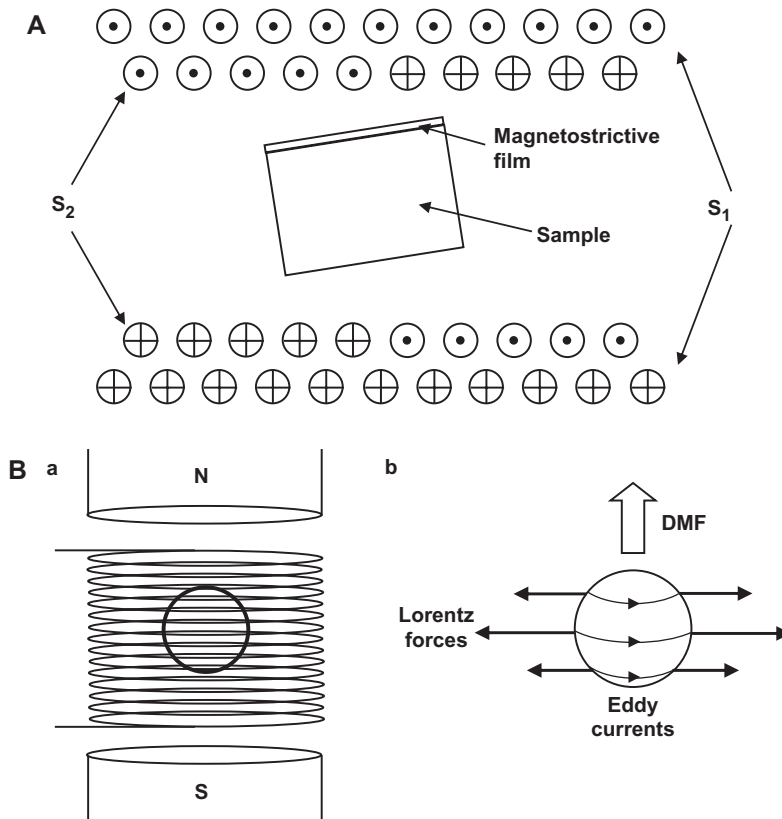
FIGURE 9.3. *Operation of non-contact transducer performance. (A) Magnetostrictive and (B) electromagnetic type. (a) The sample, wrapped in a solenoid, is placed inside a magnetic field. (b) Lorentz forces generated on the sample surface. DMF — direction of the magnetic field and S — solenoid. (Reproduced with permission of Elsevier, Ref. [16].)*

An electromagnetic-acoustic transducer (EMAT) is composed of electromagnets and operates simultaneously as a transmitter and receiver. Its design depends on the particular object geometry, the elastic wave mode used and whether the metal is ferrous or non-ferrous. In an EMAT non-contact RUS instrument, for example, the conductive sample is placed inside a permanent magnetic field of $H_0 \approx 1500$ Oe (see Fig. 9.3B) and the sample is wrapped in a solenoid. Bursts of AC current at frequency ω are sent to the solenoid and induce AC currents of frequency ω in the sample surface. The AC current interacts with the field H_0 to generate alternating Lorentz forces near the sample surface. Mechanical resonances are excited at appropriate ω values. The same solenoid is used to detect the resonances by measuring the induced signal during the time intervals in between successive excitation current bursts. In addition, the temporal decay of the signal is a measure of internal losses in the sample. "Trapped" torsional resonant modes in aluminium bars have been used to develop high-resolution load transducers [16,17].

It should be noted that many of the former studies on US-based detection were carried out by using piezoelectric transducers in contact with the sample [18,19]. Some, however, used non-contact electromagnetic transducers [20] and eddy current testing [21]. The greatest restrictions of the latter are that they require an electrically conductive sample and highly precise positioning of the transducer near the sample.

9.2.3. Optical ultrasound generators and detectors

Laser-ultrasound-based generators

Ultrasonic-laser instruments can use short-pulse lasers (a few nanoseconds long) to generate ultrasound and long-pulse (tens of microseconds long) or continuous lasers, coupled to an optical interferometer for the detection of US (*i.e.* the corresponding mechanical displacements) [22].

A laser source can be used in two ways to generate US, namely: (1) directly on the sample to obtain acoustic waves optically generated in the sample by thermoelastic or ablative stresses; or (2) by impingement of the light on, for example, an optical parametric oscillator (*e.g.* a high-pressure polyethylene film), which will deliver the US energy to the sample at the repetition rate of the laser source. The mode and frequency content of the acoustic waves generated in either case depend primarily on the temporal frequency content of the laser light and the spatial distribution of the light on the material (sample) surface. High optical powers afford relatively high acoustic amplitudes; however, they can easily damage most types of materials through ablation or melting. Surface damage need not be important in many experiments — in some cases, surface effects can even be beneficial.

The fact that laser-ultrasonics relies on light beams for US transduction provides a practical solution for remote testing at large distances, inspection of fast-moving parts on production lines and inspection in hostile environments [23,24]. The use of fibre optics to guide the laser light provides enormous flexibility for achieving virtually any desired configuration on the sample surface; also, it allows the generation of time delays for properly phasing the heating taking place on the sample surface, thereby creating an array effect that improves the SNR of the laser-generated wave in a particular direction. This, together with the use of appropriate lenses, enables spatial and temporal control of the laser light and hence of the US generated. On the other hand, light filters allow the energy to be manipulated over wide ranges (*e.g.* from 260 to 20 mJ [25]). The array effect can also be accomplished by using a transmission grating.

Unfortunately, laser-ultrasonics is inadequately sensitive for some material and process combinations. Averaging signals compensates for this lack of sensitivity at the expenses of increased inspection times and decreased savings.

The pulse duration and optical penetration depth play very prominent roles in laser-ultrasonics generation. For example, changing the generation wavelength from 10.6 µm to the 3–4 µm range can significantly raise the generation efficiency (for some type of samples such as painted materials, a 0.1-µm change in the source wavelength — from 3.4 to 3.3 µm — increases the amplitude of the generated US echo more than five times [26]). An increase in the amplitude of the generated ultrasonic waves increases the sensitivity. Also, measurements can be made more precise by dividing US amplitudes into the pulse energy produced to offset the variation of the output energy as a function of wavelength. The optical penetration depth can be increased by using an appropriate US frequency which, however, may also lead to thermal damage of the sample.

Laser-ultrasound-based detectors

The detectors commonly used in laser ultrasonics include various types of interferometers, which are sensitive to the displacement or velocity of the surface, and of knife-edge (*e.g.* photoelectromotive force receivers) detectors, which are sensitive to the tilt of the sample surface [27].

Acoustic aberrations can pose serious problems in many areas of ultrasonics as they result in significant signal losses and acoustic speckle. The effects are especially significant at high frequencies and in inhomogeneous materials such as polycrystalline metals. They often restrict the upper frequency range of techniques before the intrinsic absorption of the material does [28], although this can be offset by using adaptive approaches.

Worthy of special mention is the use of laser for phonon detection, as in Brillouin spectroscopy, which is especially suitable for detecting surface acoustic waves (SAWs). Generalized SAWs can be used to obtain Brillouin spectra with a 5-pass Fabry–Perot interferometer [29]; on the other hand, *pseudo*-SAWs, which are weaker than the previous ones, require a tandem $(3 + 3)$-pass Fabry–Perot interferometer system [30].

9.3. WAYS OF USING ULTRASOUND IN ULTRASOUND-BASED DETECTION TECHNIQUES

In dealing with the ways ultrasound can be used for detection purposes (Fig. 9.1), one must consider the specific range of US frequencies to be used, the time US is to be applied to the sample and the potential focusing of the US in its way to the sample.

Concerning frequency, the two most common ways of interrogating a sample by US are to apply a discrete US frequency or a broad-band pulse. There are single and dual transducer versions for both modes. Discrete US frequencies use a tone-burst, the duration of which is made long enough to obtain a central frequency that is well defined, but short enough to avoid interference from multiple reflections within the sample.

In relation to application duration, most ultrasonic instruments utilize either pulsed (tone-burst or broad-band pulses) or continuous-wave US (Fig. 9.4). Ultrasound pulses are by far the most widely used choice as pulses are easily applied, measurements are rapid and non-invasive, and the ultrasound device can be readily automated. Continuous-wave techniques have been traditionally used for highly accurate measurements in specialized research laboratories.

In pulse-echo-based techniques, the time of flight in a sample cannot be determined simply from the observation of the time span between adjacent echoes in the echo pattern if plane parallel transducers operated at resonant frequencies are employed. Transducers introduce substantial errors if the velocity is derived from such measurements, especially if relatively short samples are used. Various correction approaches have so far been developed in order to consider the influence of resonant transducers and the effects of diffraction [31–33]. The need for corrections can be avoided and a broad operational bandwidth obtained by using short pulses of duration equal to or shorter than the transduction [34]; this requires a time resolution better than the transit time in the transducer. This short-pulse excitation (*e.g.* the maximum for a 10-MHz transducer is 50 ns) requires a high-power wide-band ultra-linear amplifier to ensure the detection of US signals with sufficient resolution under non-resonant conditions.

Broad-band ultrasonic laser spectroscopy can also rely on the production of short acoustic pulses during absorption of laser emission in optophone, irradiation of the sample surface and recording of ultrasonic disturbances passing through the sample at a high temporal resolution. A comparison of complex spectra of the probing acoustic pulse and the signal transmitted through the sample makes it possible to determine, for example, the attenuation spectrum.

Focusing the acoustic waves onto the detection point increases the detection signal by combining all the generated amplitude into a small area or volume. This is most easily done by shaping the generating light into an arc.

9.4. SAMPLE–ULTRASOUND INTERACTION IN ULTRASOUND-BASED DETECTION TECHNIQUES

The interaction between samples and US generators depends on the way the US wave impinges on the sample and the presence or absence of contact between the two. The influence of the latter factor is discussed in Section 9.2, devoted to transducers. This section
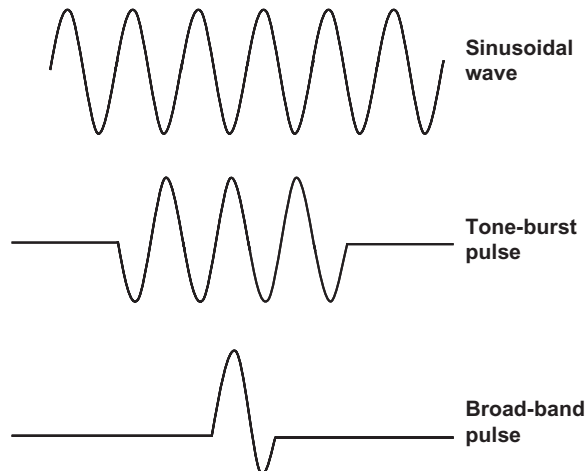
FIGURE 9.4. *Different types of input signal used in ultrasonic detectors to excite the ultrasonic transducer in order to generate an ultrasonic wave propagation into a sample.*

examines the types of wave formed depending on the particular impingement angle (see Fig. 9.1). The interaction of phonons and photons in techniques such as Brillouin scattering spectroscopy is discussed in Section 9.6.

9.4.1. Sample–ultrasound interaction

Before the ways in which US can be applied to a sample in order to obtain a response in the form of a signal are described, the concept of standing wave introduced in Chapter 1 warrants some additional explanation. In this respect, Fig. 9.5 can help understand the nature of these waves. Consider a vibrating string that is fixed on both ends, so its only stable vibrations will be those with "nodes" at its ends. Such a wave state is called a "standing wave". If a series of snapshots are taken of a string vibrating in a particular standing wave, it may look like Fig. 9.5A; thus, at times 0.5 and 1.5 the vibration amplitude is zero everywhere, and at time 2 the vibration begins to repeat. The set of situations in Fig. 9.5A can be represented in a single graph such as that of Fig. 9.5B: the positions where the string does not move are called "nodes", and those where the vibration amplitude is maximal are called "antinodes". At positions other than the nodes, the string oscillates at a frequency f that is a function of the wavelength λ through the travelling velocity, c. If the string is fixed on one end and free on the other — say left and right end, respectively — ideally without frictions, the standing waves formed will have a node on the left and an antinode on the right. The reason why standing waves occur is that, when a sine wave travelling, say, to the right, strikes the fixed end of the string, it is reflected back to the left. In the course of the reflection, the amplitude is reversed. The standing wave is actually the interference pattern between the incident and reflected waves.
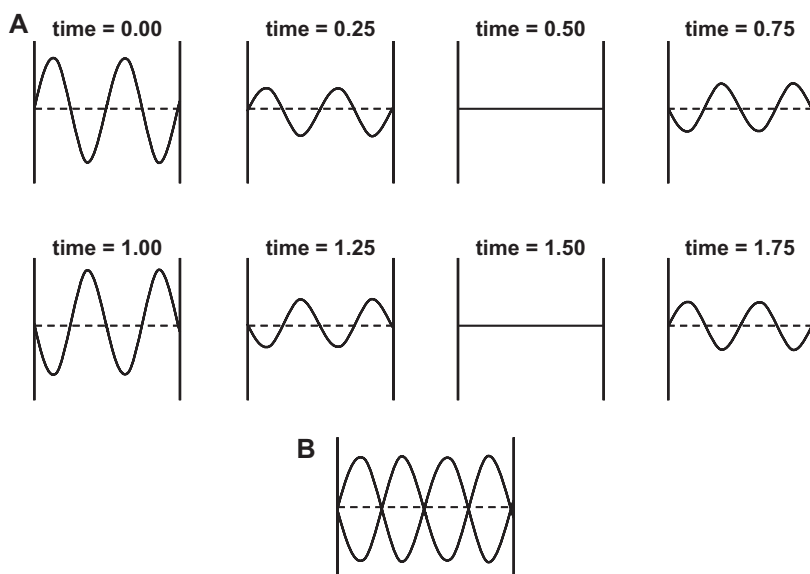
FIGURE 9.5. *Production of a standing wave. (A) Individual steps and (B) overall phenomenon.*

Ultrasonic waves can be produced in a number of different forms (*e.g.* as compressional waves, shear waves or surface waves) by applying a sinusoidal force $F(t)$ to the surface of a material. Compressional waves are most frequently used for ultrasonic non-destructive evaluation; shear waves and surface waves are also fit for this purpose in some cases [35]. If the force $F(t)$ is applied normal to the surface, a compression wave is generated; if it is applied parallel to it, a shear wave is produced. The force can also be applied along the surface (SAWs) or at a given angle to the surface (oblique waves). The amplitude of the applied pulse dictates whether the distortion caused in the material is linear or non-linear, and also the type of wave produced; thus, variable pulse amplitude causes non-linear distortion because the speed of sound in a liquid is pressure amplitude-dependent. Interactions between photons and phonons give rise to other types of waves (Rayleigh, Brillouin) and can be used to derive information about the interaction of US with the test specimen by examining changes in the light waves.

SAWs can be of the generalized (GSAW) or *pseudo*-SAW (PSAW) types. The latter, also referred to as "leaky" waves, are characterized by the facts that energy radiates into the bulk of the medium and that they experience little attenuation and are thus experimentally observable. This type of wave is especially amenable to analysis by Brillouin scattering spectroscopy.

SAWs have been extensively used as one of the leading candidates for non-destructive characterization of surface materials on account of their ability to probe material properties at different penetration depths depending on the inspection frequency. The SAW velocity has for long been the target parameter for techniques such as acoustic microscopy and Brillouin scattering spectroscopy. Presently, SAWs dispersion is also used for surface characterization with relative errors in the region of 0.1%; this has been facilitated by the ability to separate the contribution of surface roughness, which is unaffected by thermo-mechanical relaxation, from those of near-surface material variations (*e.g.* the primary residual stress effect and secondary cold work effects such as those of anisotropic texture and an increased dislocation density), all of which significantly decay during relaxation.

Ultrasonic Rayleigh surface waves are produced when an ultrasonic broad-band beam impinges obliquely on the surface of a specimen immersed in water. A pulse-echo response is produced at the liquid–solid boundary by the effect of the phenomenon called "ultrasonic backscattering of propagating Rayleigh surface waves". This type of waves become dispersive in the presence of a gradient in physical properties in the subsurface region, so the ultrasonic backward radiation is closely related to the properties of the subsurface region.

9.4.2. Contact and non-contact sample–ultrasound interaction as a function of the type of ultrasonic wave

Those techniques that use contact sample–US interaction suffer from couplant perturbation or are restricted by the transducer dimensions. Although Brillouin scattering is a non-contact interaction, it requires a high-quality sample surface and usually features rather poor SNRs by the effect of low proportion of Brillouin-scattered photons resulting in extremely long measurement times. Exploring the transient SAW pulse generated by a short laser pulse has been found to allow the phase velocity to be accurately determined [36,37]; however, obtaining high temporal resolution requires using high-energy laser pulses, which can damage the sample. In addition, the sensitivity is relatively low because the ensuing SAWs are broad-band signals. The phase velocity and angular dispersion of both surface and *pseudo*-surface waves can be measured with a precision of 0.2% by using an optical grating produced by an electronically addressable spatial light modulator

(SLM) imaged onto the sample surface in order to generate SAWs, the frequency and wavefront of which are controlled by the SLM. When the grating period matches the surface acoustic wavelength, the surface wave is strongly excited, so the wavelength, and hence the phase velocity, can be readily determined [38].

In many situations, it is desirable to generate ultrasonic waves in a solid without having any transducer directly in contact with the surface of the sample under investigation. Such circumstances may arise, for instance, in the non-destructive testing of materials in unfriendly environments (*e.g.* very hot, or highly radioactive, or simply not easily accessible). The initial work of White in 1963 [39] showed that bulk waves could be generated by a harmonic heat flow on the surface of a sample. Since then, the excitation of longitudinal, shear and Rayleigh waves by illuminating the target sample with a short laser pulse has been widely demonstrated, and the literature on the laser generation of ultrasonic waves has grown extensively and exposed the enormous flexibility of this source of US. Thus, issues such as illumination of the sample surface with an annulus of light in order to produce a stronger signal at the focal point with gains of more than 20 dB at the centre of the annulus; that of a line source configuration; the use of a periodic mask over the surface of the sample with a periodicity of a Rayleigh wavelength in order to force the generation of Rayleigh waves on the surface of the sample; the principles of ultrasonic array synthesis using laser beams and either transmission gratings or optical fibres to guide the laser light and accomplish convenient spatial and temporal control [40] helped establish the foundations of the present US–laser combination more than two decades ago.

Laser ultrasonic transducers are truly non-contact devices which effectively avoid acoustic coupling problems (*e.g.* damping in the transducer and couplant; reflection and transmission losses at the interface). Most laser ultrasonic devices have been used for excitation and detection of bulk elastic waves in point source or planar geometry, but also surface acoustic (Rayleigh or Brillouin) waves. Unlike the bulk wave regime, only one sample side is needed for excitation and detection when surface waves are used. This not only renders the measurements easier, but also avoids the need for an accurate knowledge and uniformity of the sample thickness. In addition, the excitation laser can be focused using cylindrical lenses in order to obtain an excitation line.

9.5. TYPES OF RESPONSES AND MEASUREMENTS IN ULTRASOUND-BASED DETECTION TECHNIQUES

An ultrasonic wave travelling across a material can be described in terms of the amplitude displacement of its layers (Fig. 9.6) from their equilibrium position. At a fixed position within the material, the displacement varies sinusoidally with time, the distance between successive maxima constituting the period (T). At any time t, the amplitude A decreases with increasing distance through attenuation by the sample. The distance between successive maxima is equal to the wavelength (λ).

9.5.1. *Basic principles of ultrasonic primary responses in ultrasound-based detection techniques*

Most ultrasonic material analyses rely on measurements of some characteristic of ultrasonic waves propagating through the sample that provides information on the interaction of ultrasonic waves with the inside of the sample, thus enabling analysis of its physical and chemical properties.
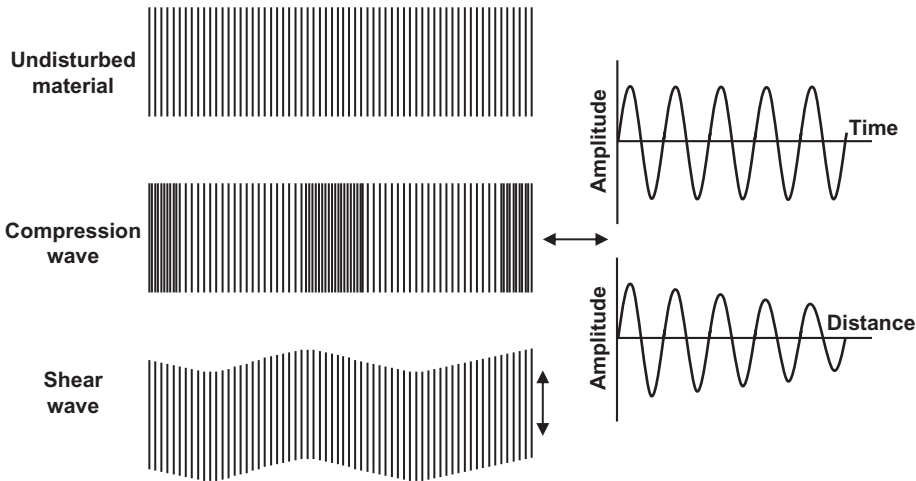
FIGURE 9.6. *Distortion caused depending on whether a sinusoidal force is applied normal or parallel to the surface of a material, thereby producing compression or shear waves, respectively. The time required for the wave to travel the distance between successive maxima is the period (T). The amplitude A at any time decreases with increasing distance through attenuation by the sample. The distance between successive maxima is equal to the wavelength (λ).*

Ultrasonic waves produce oscillating pressure and associated longitudinal deformations. Their propagation is determined by ultrasonic velocity and ultrasonic attenuation; hence, the two parameters most frequently measured in US spectroscopy are the ultrasonic velocity and attenuation coefficient. In addition, a number of measurements are related to or influenced by the velocity (*e.g.* impedance) or attenuation (particularly scattering, — the different components of which give rise to specific measurement modes — absorption and diffraction). These parameters are typical of each material and can be related to physical properties such as elastic constants, density, composition and microstructure in solids, and adiabatic compressibility, intermolecular free length, molar sound velocity, molar compressibility, specific acoustic impedance and molar volume in liquids. A variety of techniques exist for determining the ultrasonic properties of materials, the choice of a particular one being dictated by the material under study and the requirements of the researcher. Well-established techniques in this context are of interest mainly for routine measurements and for inexperienced users of ultrasound-based detection techniques; on the other hand, the newer techniques and modes can be more interesting for research purposes. The general principles on which each type of measurement among the most common ones rely are discussed below.

Equation of motion

A plane ultrasonic wave can be described in terms of the displacement of a particle from its equilibrium position as a function of the distance the wave has travelled as follows:

$$\frac{\partial^2 \xi}{\partial t^2} = \left(\frac{\omega}{k} \right)^2 \frac{\partial^2 \xi}{\partial x^2}, \tag{9.1}$$

where t denotes time, x distance, ξ particle displacement, k wave number (= ω/c — $j\cdot\alpha$), ω angular frequency (= $2\pi f$), f frequency, c velocity and α the attenuation coefficient and j is $\sqrt{-1}\cdot$ A convenient solution of this equation for sinusoidal waves is:

$$\xi = \xi_o \cdot \exp\cdot j(\omega t - kx),\tag{9.2}$$

where ξ_o is the initial amplitude of particle displacement. Ultrasonic waves often propagate through materials in the form of pulses rather than as sinusoidal waves. In any case, Eq. 9.2 still holds as pulses can be resolved into sinusoidal waves using Fourier analysis. The ωt term describes how the wave varies with time, and the kx term describes the way it varies with distance.

Ultrasonic velocity

Ultrasonic velocity (the speed of ultrasound) is determined by the elasticity and density of the propagation medium. Generally, the elastic response, which is extremely sensitive to molecular organization and intermolecular interactions, prevails. Solids exhibit the strongest interactions between molecules, followed by liquids and gases; therefore, solids are more rigid (*i.e.* they have higher elastic moduli) than liquids and gases. For this reason, sound travels faster in solids than it does in liquids and gases. Based on the forces acting on a homogeneous material as an ultrasonic wave passes through it, one can write [41]:

$$\frac{\partial^2 \xi}{\partial t^2} = \frac{\varepsilon}{\rho} \cdot \frac{\partial^2 \xi}{\partial x^2},\tag{9.3}$$

where ε is the appropriate elastic modulus of the sample and ρ its density. The measurable ultrasonic properties of a material can therefore be related to its physical properties by combining Eqs. 9.1 and 9.3:

$$\left(\frac{\omega}{k}\right)^2 = \frac{\varepsilon}{\rho}\tag{9.4}$$

In materials which are highly attenuating, the particle velocity and particle displacement are out of phase, so the elastic modulus and density of the material are complex and dynamic (*i.e.* frequency dependent). For many materials, the attenuation coefficient is fairly small (*i.e.* $\alpha \ll \omega/c$), so the particle velocity and displacement are in phase and Eq. 9.4 can be replaced with:

$$c^2 = \frac{\varepsilon}{\rho}\tag{9.5}$$

The speed of sound is directly proportional to the elastic moduli and inversely proportional to the density of the sample.

For compressional waves propagating in a liquid or gas, the appropriate modulus is the bulk modulus, K (which is the reciprocal of the adiabatic compressibility, κ); for bulk solids, it is $K + 4G/3$, where G is the shear modulus. Shear waves will propagate through most solids ($\varepsilon = G$), but are highly attenuated, and usually do not travel far enough to be detected ($\approx$ micrometre) by liquids and gases. Emulsions and suspensions have liquid continuous phases, so only compressional waves can usually propagate in them. The moduli and densities of materials depend on their structure, composition and physical state; consequently, ultrasonic velocity can be used to provide information about these properties.

Ultrasonic velocity is determined by the density and elastic response of the sample to the oscillating pressure in the ultrasonic wave, and can thus be expressed in terms of compressibility or storage modulus. This is extremely sensitive to the molecular organization, composition and intermolecular interactions in the analysed medium, and is the basis for most applications of ultrasonic spectroscopy to the determination of chemical properties of materials.

The ultrasonic velocity of a material can be determined by measuring (a) the US wavelength at a known frequency ($c = \lambda f$) or (b) the time t taken by a wave to travel a known distance d ($c = d/t$).

The equations to be used with leaky SAWs in acoustic microscopy can be found elsewhere [42].

Ultrasonic attenuation

Ultrasonic attenuation is caused by a loss of energy in an ultrasonic wave as it travels through a sample. It characterizes the ultrasonic transparency of the sample and can be seen as a reduction of amplitude of the wave. Attenuation is caused mainly by *absorption* and *scattering*, but also by *diffraction*. Absorption occurs to some extent in all materials by the effect of thermodynamic relaxation mechanisms which convert energy from the ultrasonic wave into some other form — ultimately heat and elastic hysteresis in the case of solids. In gases and liquids, the most important mechanisms of absorption are shear and bulk viscosity, thermal conduction and molecular relaxation [43]. In solids, the situation is more complex and a greater variety of mechanisms can contribute to the overall absorption. Scattering is often the predominant form of attenuation in heterogeneous materials such as emulsions, suspensions and foams, when an ultrasonic wave impinging on a discontinuity (*e.g.* a particle) is scattered in directions other than that of the incident wave. Scattering losses constitute a major form of attenuation in heterogeneous systems at high frequencies and when the size of the droplet is approximately equal to the US wavelength. Unlike absorption, the energy is still stored as US, but its propagation direction and phase have been altered. Measurements of US absorption and scattering can provide valuable information about some physico-chemical properties of materials including concentration, viscosity, and molecular relaxation and microstructure.

With homogeneous samples, periodic compressions and decompressions in the ultrasonic wave lead to an oscillation of the equilibrium position for the chemical process (*e.g.* A + B $\longleftrightarrow$ AB). A delay in the relaxation of the process to the equilibrium state causes absorption of energy. In non-homogeneous samples, the ultrasonic wave loses amplitude (energy) through scattering of the wave on particles, thus decreasing the amplitude of the wave (ultrasonic attenuation) and the dispersion of the ultrasonic velocity. The contribution of ultrasonic scattering is determined by the volume fraction of dispersed particles.

The attenuation coefficient (α) of a material is a measure of the decrease in amplitude of an ultrasonic wave as it travels through it and can be expressed, in nepers per metre (Np/m), as follows:

$$A = A_o \cdot \exp(-\alpha x), \tag{9.6}$$

where x is the distance the wave has travelled through the material (in metres), A_o the initial peak amplitude of the wave and A the peak amplitude at position x. The attenuation coefficient is determined from the relationship of the amplitude of an ultrasonic wave to the travelled distance following "fitting" of measurements to Eq. 9.6. The attenuation coefficient can also be given in decibels per metre (dB/m), where 1 Np = 8.686 dB.

Ultrasonic attenuation is determined by energy losses in ultrasonic waves and can be expressed in terms of the high-frequency viscosity of the medium or its longitudinal modulus. This allows the analysis of the kinetics of fast chemical reactions and the microstructure of materials in terms of particle sizing, aggregation, gelation, crystallization and other typical processes.

Transmission and reflection at boundaries

When an ultrasonic compressional wave impinges normally on a boundary between two materials of different acoustic impedances, it is partly reflected and partly transmitted. The ratio of the amplitude of the reflected wave (A_r) to that of the incident wave (A_i) is called the *reflection coefficient* (R), and the ratio of the amplitude of the transmitted wave (A_t) to that of the incident wave the *transmission coefficient* (T). The appropriate coefficients when particle velocity amplitudes are used are [41]

$$T = \frac{A_t}{A_i} = 2 \cdot \frac{Z_1}{(Z_1 + Z_2)} \tag{9.7}$$

and

$$R = \frac{A_r}{A_i} = \left(\frac{Z_1 - Z_2}{Z_1 + Z_2} \right) \tag{9.8}$$

The subscripts 1 and 2 refer to the material the wave travels in and the material that is reflected by or transmitted into, respectively. These equations show that the maximum transmission of ultrasound occurs when the impedances Z_1 and Z_2 of the two materials are identical. The materials are then said to be *acoustically matched*. If the materials have very different impedances, then most of the US is reflected. The reflection and transmission of ultrasound at boundaries has important implications on the design of ultrasonic experiments and the interpretation of their results. In addition, measurements of the reflection coefficient are often used to calculate the impedance of a material.

Like the ultrasonic velocity and attenuation coefficient, the acoustic impedance is a fundamental physical characteristic which depends on the composition and microstructure of the material concerned. Measurements of acoustic impedance can therefore be used to obtain valuable information about the properties of materials.

Ultrasonic propagation in non-scattering systems

Homogeneous liquids do not scatter ultrasound because they do not contain any discontinuities. Attenuation in these systems is solely due to absorption caused by thermodynamic relaxation processes. In a pure homogeneous liquid, which is not highly attenuating (*i.e.* $\alpha \ll \omega/c$), the velocity of ultrasound is simply related to the adiabatic compressibility and the density by the equation

$$c^2 = \frac{1}{\kappa\rho} \qquad (9.9)$$

If a second phase is added, then the values of κ, ρ and α are modified. If an emulsion or suspension is assumed to behave like an ideal mixture, then the volume-average of the compressibility (κ_o) and density (ρ_o) is used:

$$\kappa = \kappa_o = (1-\Phi)\kappa_1 + \Phi\kappa_2 \qquad (9.10)$$

$$\rho = \rho_o = (1-\Phi)\rho_1 + \Phi\rho_2 \qquad (9.11)$$

Here Φ is the dispersed phase volume fraction and the subscripts 1 and 2 refer to the continuous and dispersed phase, respectively.

The attenuation coefficient of a two-phase non-scattering system is equal to the volume average of the attenuation coefficients of the component phases:

$$\alpha = \alpha_o = (1-\Phi)\alpha_1 + \Phi\alpha_2 \qquad (9.12)$$

In non-scattering systems, ultrasonic properties and the volume fraction of the disperse phase are related in a simple manner. In practice, many emulsions and suspensions behave like non-scattering systems under certain conditions (*e.g.* when thermal and visco-inertial scattering are not significant). In these systems, it is simple to use ultrasonic measurements to determine Φ once the ultrasonic properties of the component phases are known. Alternatively, if the ultrasonic properties of the continuous phase, Φ and ρ_2 are known, the adiabatic compressibility of the dispersed phase can be determined by measuring the ultrasonic velocity. This is particularly useful for materials where it is difficult to measure κ directly in the bulk form (*e.g.* powders, granular materials, blood cells).

Ultrasonic propagation in scattering systems

Ultrasound scattering in emulsions and suspensions. Scattering of ultrasound is important in many emulsions and suspensions and can have a significant effect on their ultrasonic properties, making the velocity and attenuation dependent on particle size as well as on concentration. Scattering theory is an attempt to relate the ultrasonic properties of an emulsion or suspension to its physical properties, composition and microstructure; this has been the subject of much research over the last 40 years, using bodies of various shapes — particularly spherical [44]. There are two stages in formulating scattering

theory. First, the scattering characteristics of a single particle are calculated and then the scattering characteristics of an ensemble of particles such as an emulsion or suspension are determined by calculating how the scattering from the individual particles combines.

Scattering from a single particle.   The interactions between an ultrasonic wave and an emulsion or suspension droplet are complex. Under specific physical conditions, however, interactions are small in number and the mathematical description of ultrasonic propagation can be simplified significantly by dividing propagation into three categories according to the relationship between droplet radius and ultrasonic wavelength. (Fig. 9.7), namely: (1) the long wavelength regime (LWR), where $r \ll \lambda$; (2) the intermediate wavelength regime (IWR), where $r \approx \lambda$; and (3) the short wavelength regime (SWR), where $r \gg \lambda$.

Calculations of the extent of each regime for typical emulsion droplet sizes (0.01–100 μm) and ultrasonic frequencies (0.1–100 MHz) indicate that almost all emulsions of practical importance fall into either the LW or the IW regime (Fig. 9.8). Ultrasound can be used to determine the size of large droplets (< 1 mm); however, this is usually done with ultrasonic imaging rather than ultrasonic spectrometry [45]. Note that if one examines a system containing droplets of unknown size, it is impossible to ascertain which region one is in before testing. In this situation, one must either use the entire ultrasonic theory or know the approximate size of the droplets beforehand.

Long wavelength regime.   The two most important forms of scattering in the LWR are caused by *visco-inertial* and *thermal* transport mechanisms which occur at the interface between a particle and the surrounding fluid. The LWR is that where particle size is much smaller than the ultrasonic wavelength λ ($r < 0.05\,\lambda$), which is the case with most emulsions and suspensions (*e.g.* $\lambda \approx 150$ μm at 10 MHz in water). *Visco-inertial scattering* occurs when a suspended particle and the surrounding liquid differ in density. In the presence of an ultrasonic wave, a net inertial force acts on the particle and causes it to
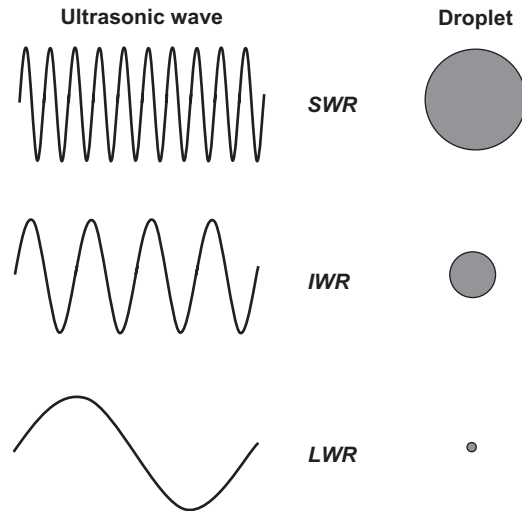
FIGURE 9.7. *Relationship between droplet radius (r) and ultrasonic wavelength. The regions shown are a function of the relative value of the variable: long wavelength regime (LWR) ($r \ll \lambda$), intermediate wavelength regime (IWR) ($r \approx \lambda$) and short wavelength regime (SWR) ($r \gg \lambda$).*
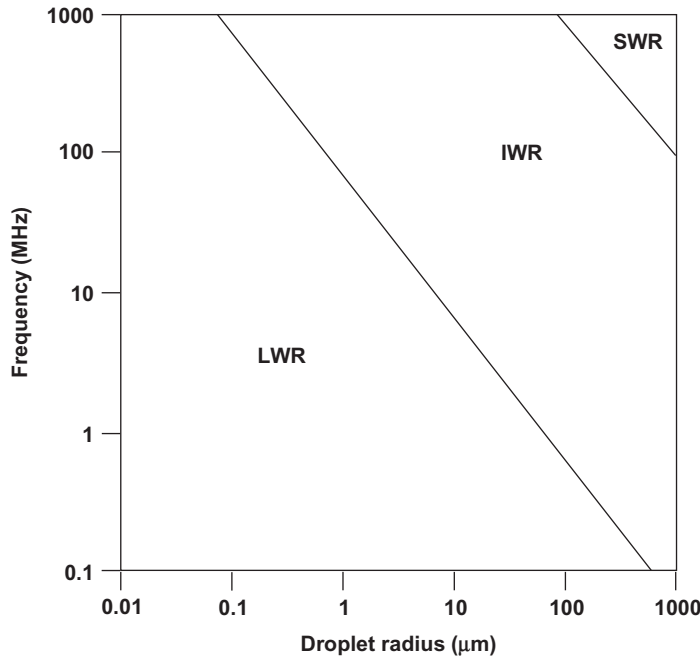
FIGURE 9.8. *Dependence of the long, intermediate and short wavelength regimes on droplet radius and ultrasonic frequency on the assumption of r < 0.05λ for long wavelength regime (LWR); 0.05λ < r < 50λ for intermediate wavelength regime (IWR) and r > λ for short wavelength regime (SWR).*

oscillate relative to the surrounding liquid, the oscillation being damped by the viscosity of the liquid. The magnitude of this effect depends on the density difference between the component phases. *Thermal scattering* occurs by the effect of an ultrasonic wave passing through a material causing temperature fluctuations around the equilibrium value as a result of pressure–temperature coupling. In a two-phase system, where some thermal properties of the component phases are different, temperature fluctuations in the particle and surrounding fluid are different, so heat energy flows across the interface and as a result the particle pulsates. The magnitude of this effect depends on the difference in thermal properties between the component phases. Pulsation and oscillation of the particles constitute the source of scattered waves. Both visco-inertial and thermal scattering can have a significant effect on the velocity and attenuation of ultrasound in emulsions and suspensions.

Figure 9.9 shows the scattering profile of a single particle in the presence of an ultrasonic wave in the LWR. The overall profile consists of a monopole component due to the particle pulsation caused by thermal scattering and a dipole component due to the particle oscillation caused by visco-inertial scattering. By measuring the amplitude of the scattered signal as a function of the scattering angle one can obtain information about the physical properties of the particle. Most ultrasonic experiments, however, use measurements of the velocity and attenuation of the wave which travels directly through
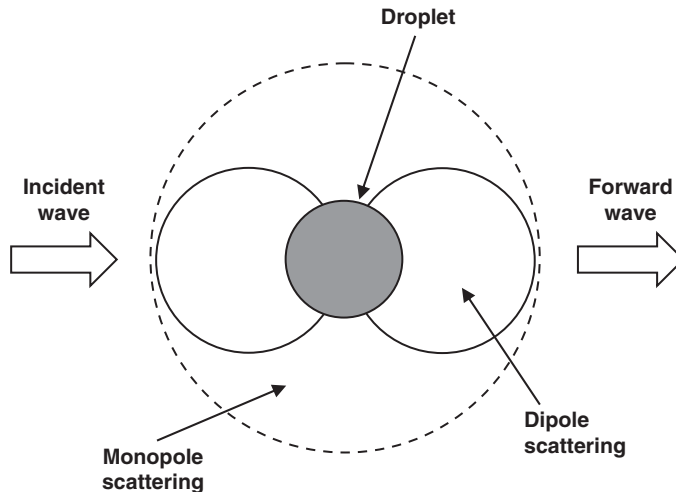
FIGURE 9.9. *The two most important types of interaction between an ultrasonic wave and an emulsion droplet in the long wavelength regime: droplet oscillation and pulsation. Pulsation leads to the generation of a monopole wave, whilst oscillation produces a dipole wave. Ultrasonic energy is also lost through thermal and visco-inertial absorption associated with droplets pulsation and oscillation.*

the material (*viz.* the forward wave in Fig. 9.9). The amplitude of this wave is reduced when a particle is present because some of the incident wave is scattered and some absorbed by damping mechanisms associated with visco-inertial and thermal scattering. The phase — and hence the velocity — of the forward wave is different from that of the incident wave because the latter interacts with a part of the scattered wave which travels in the forward direction.

The monopole and dipole fields of a single particle are characterized by their scattering coefficients (A_o and A_1). These relate the amplitude of the various scattered waves to that of the incident wave. The mathematical procedure for calculating the scattering coefficients is described elsewhere [46]. Briefly, wave equations for the propagation of compressional, shear and thermal waves in both the particle and the surrounding fluid are derived that are then solved in terms of series expansions containing the scattering coefficients. The appropriate wave equations for each phase are then related to one another by considering the boundary conditions at the surface of the particle (*i.e.* the velocity and stress components, the temperature and continuous heat flow). A set of simultaneous equations are thus obtained which can be solved for the various scattering coefficients. The scattering coefficients of a liquid droplet suspended in a liquid continuous phase have been derived [47], as have those for a solid particle [46]. The magnitude of the scattering coefficients depends on the thermophysical properties of the component phases (*viz.* density, compressibility, specific heat capacity, coefficient of volume expansion and thermal conductivity), the particle radius (r) and the frequency.

Intermediate wavelength regime.   Emulsions which contain fairly large emulsion droplets (typically >10 μm) tend to fall in IWR, especially when relatively high ultrasonic frequencies (>10 MHz) are used. Interactions between ultrasonic waves and emulsion droplets are most complicated in this regime, and a wide variety of scattered waves are generated.

This requires using many more scattering coefficients (A_n) to calculate the ultrasonic properties of an emulsion or suspension than the two (A_o and A_1) used in LWR. Scattering of ultrasonic waves prevails over other types of interaction in IWR, so ultrasonic properties can be calculated from simplified expressions for the A_o terms. The number of A_n terms needed to calculate properties in this case varies with the frequency and is determined at each frequency by incrementally increasing the value of n and calculating the complex propagation constant until it no longer changes.

The ultrasonic properties of emulsions and suspensions are especially sensitive to droplet size in the region $0.1 < r/\lambda < 50$ in IWR [48]. By using an instrument capable of measuring the ultrasonic velocity and attenuation coefficient over the frequency range 0.1–100 MHz, one can analyse droplets in sizes from about 1 µm to a few metres. Thus, by utilizing measurements in both LWR and IWR, one can cover the whole range of significant droplet sizes for emulsions and suspensions.

Scattering from an ensemble of particles. The ultrasonic properties of an ensemble of particles can be described in terms of a complex propagation constant $\beta(= \omega / c + j \cdot \alpha)$. Parameter β is calculated by working out the total scattering from all particles in a system; based on their spatial distribution, a complex propagation constant for an ensemble of point scatters randomly distributed in space is derived on the assumption that the proportion of energy scattered from a particle on to a neighbouring particle is insignificant. This theory is therefore a *single scattering* theory and applicable to dilute systems only.

Equation 9.13, where $k_1(= \omega / c_1 + j \cdot \alpha_1)$ is the wave number of the continuous phase, illustrates how the scattering coefficients of a single particle are related to the ultrasonic properties of an ensemble of particles.

$$\left(\frac{\beta}{k_1} \right)^2 = \left(\frac{1 - 3 \cdot j \cdot \Phi(A_o + 3A_1)}{(\kappa_1 r)^3} \right) \tag{9.13}$$

In concentrated systems, *multiple scattering* is important (*i.e.* a significant proportion of the energy scattered from one particle is incident upon neighbouring particles). If one considers multiple scattering in the derivation of the complex propagation constant [49], then Eq. 9.13 becomes:

$$\left(\frac{\beta}{k_1} \right)^2 = \left(1 - 3 \cdot j \cdot \Phi \cdot \frac{A_o}{\kappa_1 r} \right)^3 \cdot \left[1 - 9 \cdot j \cdot \Phi \cdot \frac{A_1}{(\kappa_1 r)^3} \right] \tag{9.14}$$

Provided $\alpha_1 \ll \omega / c_1$, which is usually the case, this equation can be resolved into two expressions for the effective complex density and effective adiabatic compressibility [50]:

$$\kappa = \kappa_1 \left(1 - 3 \cdot j \cdot \Phi \cdot \frac{A_o}{(\kappa_1 r)^3} \right) \tag{9.15}$$

$$\rho = \rho_1 \left(1 - 9 \cdot j \cdot \Phi \cdot \frac{A_1}{(\kappa_1 r)^3} \right) \tag{9.16}$$

This allows the velocity and attenuation to be calculated as: $1/c = \mathrm{Re}(\sqrt{\kappa \rho})$ and $\alpha = \omega \cdot \mathrm{Im}(\sqrt{\kappa \rho})$. As can be seen, visco-inertial scattering modifies

the effective density (through A_1), and thermal scattering modifies the effective adiabatic compressibility (through A_o). In order to use these equations to relate the ultrasonic properties of a scattering material to its physical properties, one must know the thermophysical properties of the component phases of the system under study. These can either be measured or taken from the literature [51].

Ultrasound scattering in solids. Solids also exhibit various scattering regions depending on the wavelength *(λ)* to mean grain size (*D*) ratio. Thus, in the Rayleigh scattering region $\lambda \gg 2\pi D$, in the stochastic scattering region $\lambda \approx 2\pi D$ and in the diffuse scattering region $\lambda < 2\pi D$.

Potential and restrictions of attenuation measurements. The huge information provided by attenuation measurements under appropriate working conditions includes data that allow stirred and ultrasonicated slurries to be distinguished [52] as discussed in Chapter 8. However, attenuation is also markedly influenced by variables other than scattering, as recently demonstrated by Goodenough *et al*. [53]. As can be seen in Fig. 9.10, the attenuation caused by an industrial, particulate sample increases with increasing concentration and decreases with increasing temperature, especially at higher frequencies. A comparison of Figs. 9.10A and B reveals that, below 6 MHz, attenuation is independent of temperature but responsive to the particulate concentration for a given type of sample. The effect can vary widely depending on the particular type of sample (see the industrial sample and samples B and C in Fig. 9.11, which were prepared from silica and sucrose in order to test the independence of the experimental variables of the concentration of insoluble and soluble solids, respectively, at a fixed US frequency of 5 MHz). Attenuation measurements can be an excellent tool for determining the concentration of solids in sample A, but not in B or C; this entails optimizing the working conditions for each type of sample with provision for both the matrix and suspended or dissolved solids.

Use of primary data: velocity or attenuation

Attenuation is the best variable for characterizing dispersed phase composition and particle size; by contrast, the speed of sound is better for characterizing chemical composition at a molecular level [54]. The ability to use single primary data to determine insoluble, dissolved and total solids is one of the strengths of diagnostic US by virtue of the different behaviour of these variables depending on the sample nature (*e.g.* samples A, B and C in the previous section [53]). Unlike attenuation in the spectra of Figure 9.10, the phase velocity was found to be roughly frequency independent, whereas the speed of US changed markedly with temperature [55]. Therefore, attenuation is to be preferred as the primary datum of choice for directly measuring the concentration of particles. Figure 9.12 illustrates the rather disparate behaviour of attenuation and speed of US at variable temperatures for samples A and B as compared with distilled water. All tests were conducted at 5 MHz. As can be seen from the figure, attenuation from the silica sample increased slightly with increasing temperature, which can be ascribed to changes in the attenuative properties of the silica with temperature. However, the industrial particles exhibited a marked decrease in attenuation above 70°C as a result of more marked dissolution of particles at increased temperatures so much to that, at 150°C, the industrial particles were almost completely soluble, with an attenuation value close to that of water. On the other hand, the speed of sound for the samples and distilled water exhibited the typical maximum at approximately 70°C and decreased at higher temperatures. All these factors should be considered in dealing with unknown samples.
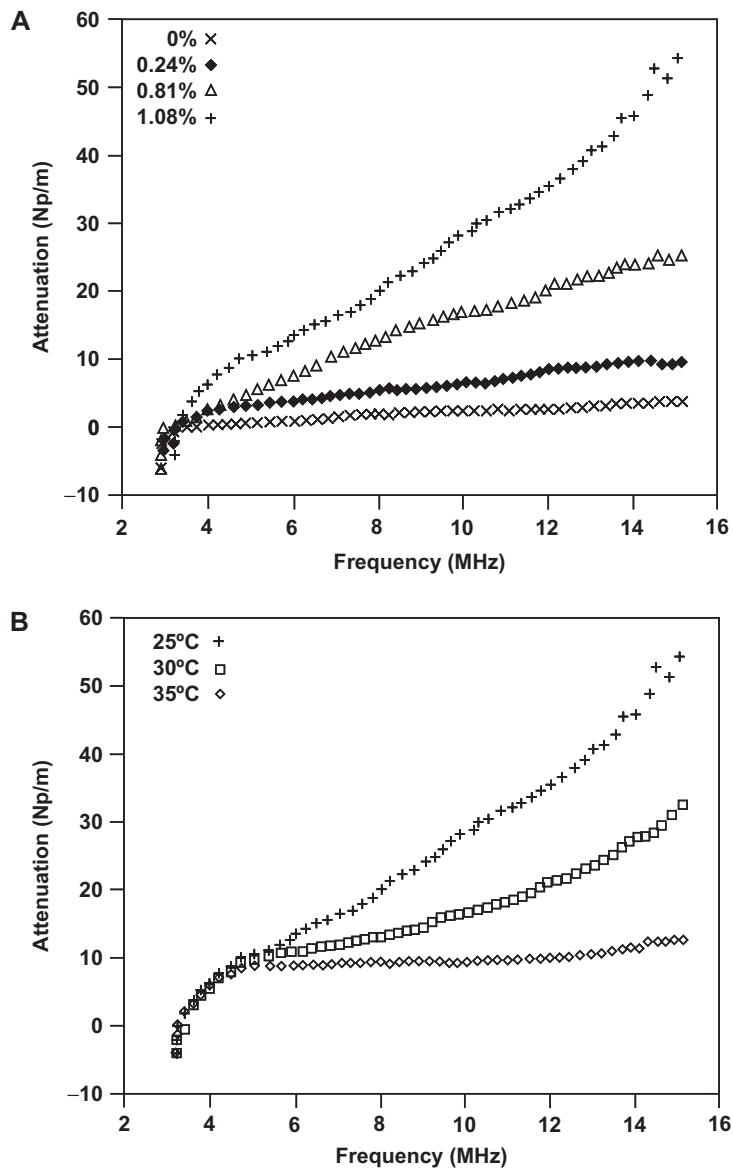
FIGURE 9.10. *Attenuation spectra for sample solutions made from industrial particles. (A) Variable concentrations of particles from 0 to 1.08% measured at 25°C. Note the increase in attenuation with increasing concentration, especially at the highest frequencies. (B) Variation with temperature of the 1.08% particle solution. Increased temperatures reduce attenuation, especially at the highest temperatures. (Reproduced with permission of Elsevier, Ref. [53].)*
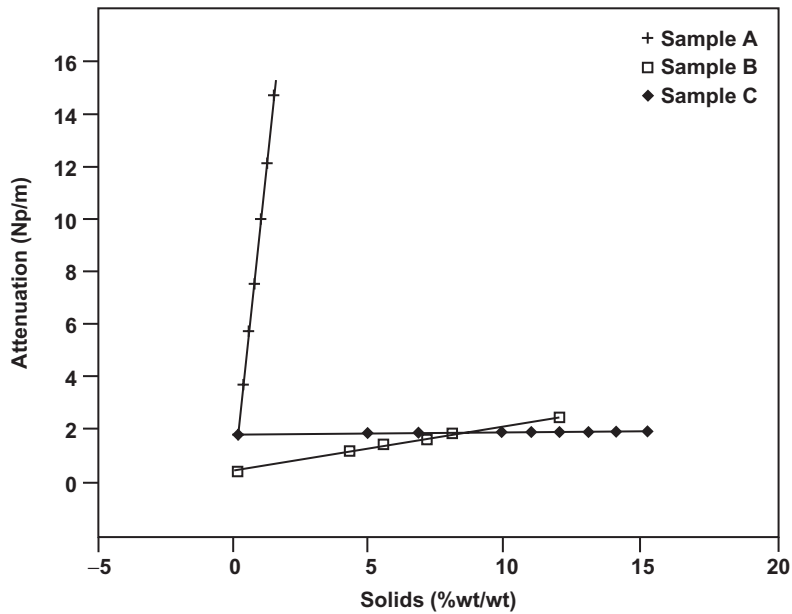
FIGURE 9.11. *5-MHz attenuation of US measurements at variable concentrations of samples A, B and C, corresponding to industrial particles, silica and sucrose, respectively. (Reproduced with permission of Elsevier, Ref. [53].)*

Factors influencing propagation

There are a series of factors which affect ultrasonic propagation and should therefore be considered in determining variables related to the interaction of the wave with a given sample. Some of the most influential factors are commented below.

Presence of gas bubbles.   Ultrasonic propagation in liquids containing gas bubbles can be examined with a view to (1) characterize the system concerned or (2) establish the influence of the gas on the target properties.

The presence of gas bubbles in a system can have a dramatic influence on its ultrasonic properties by the effect of the phenomenon known as *resonant scattering* [56], which arises from the large difference in compressibility between the gas and the liquid. The frequency at which resonance occurs (ω_r) depends on the physical properties of the component phases and bubble size:

$$\omega_r^2 = \frac{3\rho_b c_b^2}{\rho r^2},$$ (9.17)

where ρ is the density of the liquid, ρ_b and c_b are the density and ultrasonic velocity of the gas bubble, respectively, and r is the radius of the bubble. This equation is applicable to fairly large bubbles ($r > 3$ μm); for smaller bubbles, however, the effects of viscosity, heat conduction and surface tension should be included [57].
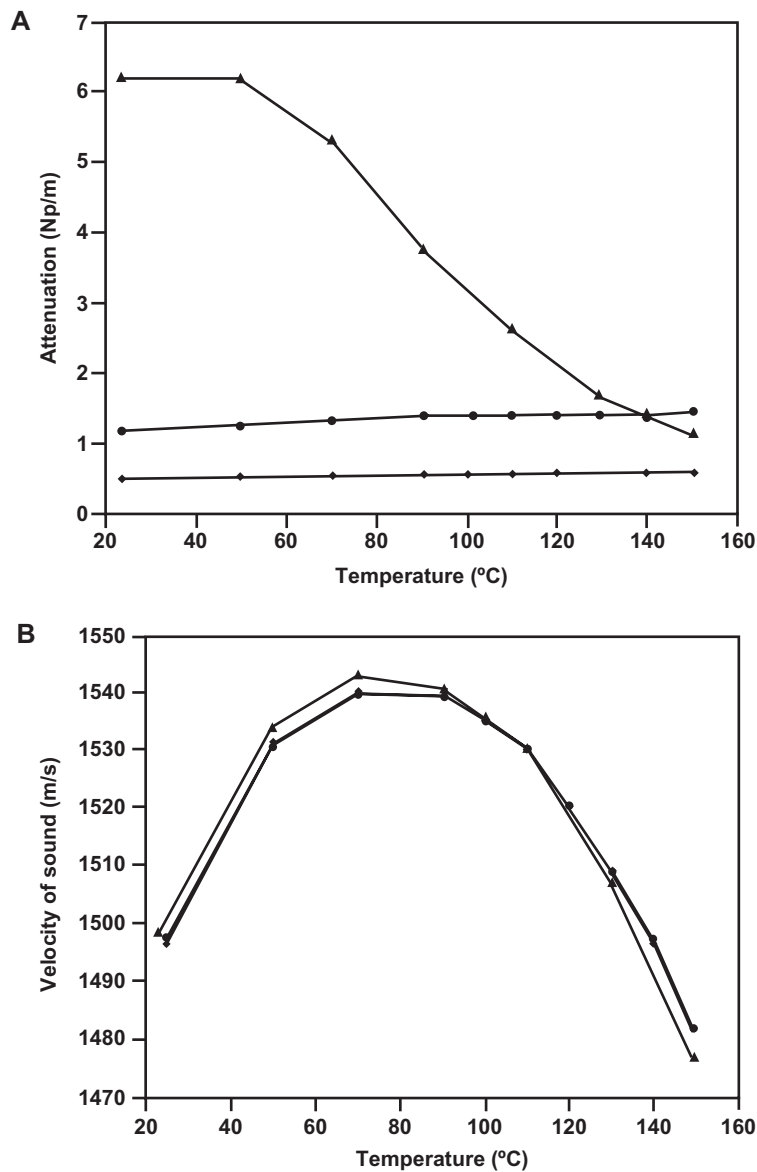
FIGURE 9.12. *Ultrasonic attenuation (A) and velocity (B) spectra for samples measured at temperatures up to 150°C. (▲) 0.81% insoluble particles suspension; (●) 4.4% silica particles; and (♦) distilled water. The decreased attenuation of the industrial particles above 70°C is due to a change in solubility. (Reproduced with permission of Elsevier, Ref. [53].)*

The effect of resonance on the ultrasonic velocity and attenuation of bubbly water is that, at frequencies below resonance, the ultrasonic velocity is much lower than that of the continuous phase and may even be lower than that of the gas phase. In the vicinity of resonance, the velocity is very sensitive to frequency, whilst at frequencies well above resonance it tends to the velocity of the continuous phase. Attenuation is greatest at near-resonance frequencies. It is often so large that US cannot be transmitted through systems containing even a low concentration of bubbles ($\Phi < 10^{-4}$). This problem is exacerbated in real systems containing a range of bubble sizes, where the attenuation peak spans a wide range of frequencies. Ultrasonics may therefore have limited use with systems containing entrained gas bubbles unless these can be removed or measurements made at frequencies away from resonance. However, there are often some practical difficulties associated with making measurements at very low and high frequencies. The dependence of ultrasonic properties on the size and concentration of gas bubbles allows ultrasonics to be used to measure these quantities.

Particle size. The scattering theory described above assumes that the particles are spherical in shape. Although emulsion droplets can usually be assumed to be spherical because of the effects of surface tension, they may become deformed under shear flow or in concentrated systems where they are closely packed. Many solid particles are non-spherical (granular, crystalline, fibrous). Non-sphericity can have a substantial effect on ultrasonic measurements and a number of theories have been derived to consider such an effect [58–60].

Multiple scattering. The multiple scattering theory described above assumes that the exciting field incident upon a particle is the same as the field that would occur if the particles were not present. This assumption is only valid when the following condition is met [46]:

$$\frac{n\sigma}{k_1} \ll 1, \tag{9.18}$$

where n is the number of particles per unit volume ($= 3\Phi/4\pi r^3$) and σ the scattering cross section ($= 4\pi|A_o + 3A_1|^2/k^2_1$). Most emulsions and suspensions are weakly scattering systems in which the fraction of energy scattered from a particle is much smaller than the energy of the incident wave, so this condition applies up to fairly high volume fractions ($\Phi > 0.4$). In strongly scattering systems (*e.g.* bubbly liquids), this condition may break down at gas contents as low as a fraction of 1%. Multiple scattering theory has also been formulated to take into account this limitation [61,62].

Multiple scattering theory also assumes that the particles are randomly distributed in the continuous phase (*i.e.* that they are uncorrelated). In some systems, this is not true and ultrasonic properties can depend on the radial distribution function of the particles.

Attempts have also been made to include the effects of droplet flocculation in ultrasonic scattering theory [63].

Particle interaction. Scattering theory does not take account of physical interactions between particles. In concentrated systems such as pastes or sediments, the particles are in contact with each other and different theories have to be used to describe their ultrasonic behaviour [64,65]. The ultrasonic properties can be affected, even in dilute systems, if flocculation occurs. The dependence of the ultrasonic properties of a material on the degree of particle interaction allows ultrasonics to be used to investigate this phenomenon.

Miscellaneous factors. It is often assumed that the continuous phase which surrounds the particles has the same physical properties as the bulk continuous phase, but this is not

always the case (*e.g.* it has been shown that the viscosity of the continuous phase is modified by the presence of suspended particles [66]). The viscosity of the continuous phase may also be frequency dependent (*e.g.* in visco-elastic materials, the viscosity measured at low frequencies with a viscometer is different from that measured at ultrasonic frequencies [67]). In addition, the magnitude of visco-inertial scattering in an emulsion or suspension containing charged particles can be affected by electroviscous effects [68].

9.5.2. *Basic principles of ultrasonic secondary responses in ultrasound-based detection techniques*

As stated above, US secondary responses are obtained under specific conditions such as resonance, are derived from primary responses such as impedance or are a fraction of the overall primary response (*e.g.* absorption, reflection). Measurements made under resonance conditions are the basis for resonance ultrasonic spectroscopy (RUS), also known as "high-resolution ultrasonic spectroscopy" — the latter name was given by the leading manufacturer of RUS instruments. The importance of this technique warrants discussion of its basic principles below.

Ultrasonic resonance

The US resonance phenomenon for the case of a plane parallel-type resonator consists of excitation by one of the piezotransducers of the ultrasonic wave travelling in the direction of the second piezotransducer. Upon reflection by the second piezotransducer, the wave comes back and is reflected again. At the frequencies corresponding to a whole number of half wavelength between the piezotransducers, resonance occurs and increases the amplitude of the signal at the second piezotransducer.

For the resonance phenomenon to occur, the ultrasonic cell forms an acoustic resonator, the ultrasonic velocity is determined from measurements of ultrasound frequency at resonance and ultrasonic attenuation is estimated from the energy losses at resonance. Decreasing the volume of the resonator cell increases the number of reflections of the ultrasonic wave at the resonator walls, the total length of the path of the ultrasonic wave in the sample remaining nearly constant. Taking full advantage of contactless EMAT entails obtaining the amplitude spectrum, which allows the phase velocity or thickness, and the relaxation time to be derived from the received ringdown signal at resonance [69].

Resonant ultrasound: principles and measurements

The principles behind resonance US measurements differ depending on the liquid or solid nature of the sample.

Resonant US in liquids.   Measurements of ultrasonic resonance in liquids involve using a resonator cell comprising two major elements, namely: a resonator chamber, where acoustic resonance forms and two transducers (usually piezoelectric), which excite and detect ultrasonic vibrations.

In an ideal resonator, where the effects of diffraction, non-ideal reflection and other perturbations can be negligible, the resonance condition can be expressed by the following relationship:

$$\frac{n\lambda_n}{2} = d, \tag{9.19}$$

where n is any whole number, λ_n the ultrasonic wavelength in the sample at the nth resonance and d the distance between the piezotransducers. The wavelength λ is determined by the ultrasonic velocity, c, and frequency, f:

$$\lambda_n = \frac{c}{f_n}, \tag{9.20}$$

where f_n is the frequency at the maximum of the nth resonance. A combination of Eqs. 9.21 and 9.22 provides the relationship between the change of the ultrasonic velocity δc and the corresponding shift of the frequency of the nth resonance, δf_n:

$$\frac{\delta c}{c} = \frac{\delta f_n}{f_n} \tag{9.21}$$

The absolute value of the ultrasonic velocity can be obtained from the frequencies of any two nth and (n–1)th resonances:

$$c = 2d(f_n - f_{n-1}) \tag{9.22}$$

This equation is also a consequence of Eqs. 9.19 and 9.20. The distance between the piezotransducers, d, can be determined from measurements of $(f_n - f_{n-1})$ for the resonator filled with a liquid of known ultrasonic velocity, c. Based on the simple model for an ideal resonator, Eqs. 9.21 and 9.22 work surprisingly well in real resonators at frequencies that are close to the resonance frequency of the piezotransducer. These equations have been widely used with high-resolution measurements of ultrasonic velocity in liquids. The scope of these equations has been expanded by including empirical correction factors [70].

Ultrasonic resonance in solids. The mechanical resonances of a freely suspended solid object are special solutions to the equations of motion that depend only on the density, elastic moduli and shape. These solutions determine all the possible frequencies at which such an object would "ring" if struck. Because a solid with N_o atoms in it has $6N_o$ degrees of freedom, there are $6N_o$ — 6 possible resonances (*viz.* six frequencies corresponding to three rigid rotations and three rigid translations are removed). Most such resonances cannot be detected as individual modes because dissipation in the solid broadens the higher frequency resonances to an extent that they overlap to form a continuum response.

The calculation of the resonant frequencies in solids starts with the Lagrangian of the elastic body. A free-standing body can sustain non-attenuated vibrations at a series of resonant frequencies ω_m. At such frequencies, the time-independent part of the Lagrangian,

$$L^1 = \int C_{ijkl} \varepsilon_{ij}(u) \varepsilon_{kl}(u) dV \tag{9.23}$$

is an extremum under the normalization conditions:

$$\int u_i u_j \delta_{ij} \mathrm{d}V \tag{9.24}$$

and the extrema give $\rho\omega_m^2$. Here, C_{ijkl} is the elastic constant tensor and $\varepsilon_{ij}(u)$ the position-dependent strain tensor. The solutions are found by expanding the displacement u in basis functions appropriate to the geometry of the body. By truncating the basis at a convenient limit, N, the problem is reduced to that of diagonalizing an $N \times N$ matrix (the eigenvalue problem due to instantaneous peak displacement). Demarest [71] and Ohno [72] used normalized Legendre polynomials as basis functions and found them to lead to rapid convergence on the numerical solution for a cube-shaped specimen. On the other hand, Visscher *et al.* [73] used power series expansion and found that, although convergence was slower, the numerical problem was quite readily solved, especially with current fast desk-top computers. Power series expansion is simpler to implement for samples of arbitrary shape. The numerical code developed by Visscher is at present available in commercial software applicable to samples of cylindrical or parallelepiped geometry.

The derivation of the elastic constant tensor to be used in RUS is an indirect iterative procedure. Provided the sample dimensions, density and elastic constants are known, the spectrum of resonant frequencies can be easily calculated. The inverse problem (*viz.* calculating the elastic constants from a measured spectrum of mechanical resonances) has no known solution, however. For the indirect method, a starting resonant frequency spectrum, $f_n^{cal}(n=1,2,\ )$, can be calculated by elastic constants estimated from theory or from literature data for similar materials in addition to the known sample dimension and density. The difference between the calculated and measured resonance frequency spectrum, $f_n^{mea}(n=1,2,\ )$, is identified by a figure-of-merit function,

$$F = \sum_n w_n (f_n^{cal} f_n^{mea})^2 \tag{9.25}$$

where $f_n^{mea}(n=1,2,\ )$, are weight coefficients reflecting the confidence on individual resonance measurements. Then, F is minimized by regressing the values of all the elastic constants with the aid of dedicated software. The software searches for a global minimum of the function F in a multidimensional space of dimensions equal to the number of unknown elastic constants. The curvature of F differs between elastic constants; as a result, some elastic constants can be determined with higher precision than others. The accuracy of RUS depends on the quality of the sample and the number of resonances measured. Experience has shown that such a number should be at least 5–10 times the number of independent elastic constants to be determined. Typically, pure shear elastic constants are the easiest to determine, with errors less than 0.1%, and off-diagonal elastic constants are those determined with the least accuracy (typically about 2%).

Acoustic impedance

The *specific acoustic impedance* (*Z*) of a material is defined as the ratio of the instantaneous acoustic excess pressure (*P*) to the particle velocity (*c*), and can be expressed as:

$$Z = \frac{P}{c} = \omega \cdot \frac{\rho}{k} \tag{9.26}$$

In general, Z is complex and can be split into a real part and an imaginary part:

$$Z = R_z + j \cdot X_z, \tag{9.27}$$

where R_z is called the *resistive* component and X_z the *reactive* component. For many materials, $\alpha \ll \omega/c$, so $Z = R_z = \rho c$, which is called the *characteristic impedance*.

In dealing with US reflectance measurements, the magnitude M and phase φ of the pulse can be measured as a function of the frequency by using Fourier transform analysis and the reflectance value provided by the formula [74]:

$$R_S = \frac{R_C M_S}{M_C \exp i(\varphi_S - \varphi_C)}, \tag{9.28}$$

where R is the reflectance and the subscripts S and C refer to the sample and calibration material, respectively. The acoustic impedance is related to the spectral reflectance by the equation [74]:

$$Z_S = Z_{DL}\left(\frac{1 - R_S}{1 + R_S}\right), \tag{9.29}$$

where Z_{DL} is the acoustic impedance of the delay-line, which is known, and Z_S is that of the sample, which is to be determined.

Ultrasonic relaxation

This parameter derives from a special treatment of the data from ultrasonic absorption measurements. Thus, after calculation of the ultrasonic absorption coefficient, α (Np/cm), using a frequency in the 10–100 MHz range, the frequency dependency of this parameter is analysed in terms of the equation:

$$\frac{\alpha}{f^2} = \frac{A}{1 + (f/f_r)^2} + B, \tag{9.30}$$

where f is the measured frequency, f_r the relaxation frequency, A the relaxation amplitude and B the contribution to the sound absorption of any other processes potentially occurring at higher frequencies beyond the experimental range.

The relaxation time of the dissociation for the micelle–monomer exchange process (fast relaxation process) [75] is given by

$$\frac{1}{\tau} = 2\pi f_r = \frac{k_{-1}}{\sigma^2} + \frac{k_{-1}}{m}\left(\frac{C}{C_1} - 1\right), \tag{9.31}$$

where τ is the relaxation time, and C and C_1 are the total and monomer concentration of surfactants, respectively. Parameters m, σ and k_{-1} are the mean aggregation number, the variance of the size distribution function and the mean dissociation rate constant, respectively. The isentropic volume change ΔV_s due to the micelle–monomer exchange process

can be estimated from the ultrasonic absorption maxima for each wavelength, μ_{max}, using the expression [76]

$$\mu_{max} = \frac{\pi \rho c^2 (\Delta V_s)^2 C_1 \left(\dfrac{\sigma^2}{m} \right) \left(\dfrac{C}{C_1 - 1} \right)}{2RT \left\{ 1 + \left(\dfrac{\sigma^2}{m} \right) \left(\dfrac{C}{C_1 - 1} \right) \right\}}, \tag{9.32}$$

where the symbols have their usual meaning.

These equations allow the volume change during the micelle–monomer exchange process, the dissociation rate constant for a salt-free system, the effect of added salts on the micelle distribution width σ and the dissociation rate constant for the system upon addition of a salt to be calculated [77].

Photon responses from sample–ultrasonic (or hypersonic) interaction

The phase shift in laser light upon interaction with ultrasound waves moving in a material is the origin of the phenomenon known as Brillouin scattering. From a strictly classical point of view, the compression of the medium alters the index of refraction, thereby causing some reflection or scattering at any point where the index changes. From a quantum point of view, the process can be considered as one of interaction of light photons with acoustic or vibration quanta (phonons).

Thermal fluctuations in the density of gases, liquids and solids can be studied directly by examining the interaction of a coherent beam of photons with thermally driven phonons. Based on Debye's theory of specific heat, the thermal fluctuations of molecules in a macroscopic sample can be considered a superposition of acoustic modes including all directions of wave propagation and a broad distribution of wavelengths. If a beam of monochromatic light with a small aperture is scattered from the thermal spectrum of acoustic modes, then conservation of momentum leads to a selection of particular acoustic waves from the thermal spectrum. Such waves propagate in both directions of the bisector of the scattering angle. Also, their wavelength obeys Bragg's law of reflection. The smallest acoustic wavelength λ that can thus be selected amounts to half the wavelength of the electromagnetic wave. Hence, if visible light is used, $\lambda = \lambda_{light}/(2\sin(\varphi/2))$ can be as small as 0.2 µm. Here, λ_{light} is the wavelength of the incident light and φ denotes the scattering angle. In water at room temperature ($c_s = 1500$ m/s) the smallest wavelength λ_{min} corresponds to the highest frequency υ_{max} ($= c_s/\lambda_{min}$) = 7.5 GHz. While this is quite a high frequency, high ultrasonic frequencies can easily reach it.

By the effect of energy preservation, the scattering of photons by thermally driven US waves produces Doppler-shifted lines in the light spectrum. In correspondence with the two possible directions of wave propagation along the bisector of scattering angle, a down-shifted Stokes line and an up-shifted anti-Stokes line appear in addition to the central (unshifted) Rayleigh line. The magnitude of the Doppler shift, $(\delta\upsilon)_{light}$, equals the frequency υ of the acoustic wave concerned; therefore, the sound velocity of a liquid or solid can be determined by measuring the scattering angle and the shift in the light spectrum. By using light as a carrier-frequency wave, which is modulated by the selected acoustic modes, relative frequency shifts $(\delta\upsilon)_{light}/\upsilon_{light}$ in the region of 10^{-6} can be accurately measured. The requirements for the optical instrument are, obviously even more stringent if

measurements are made with a view to determine the half-width $\Delta \upsilon_B$ of the Brillouin (Stokes and anti-Stokes) lines in terms of the attenuation coefficient α of the selected acoustic modes, which are mutually related by:

$$\alpha = \frac{\pi \Delta \upsilon_B}{c_S} \qquad (9.33)$$

The finite half-widths of both the (non-Lorentzian) Brillouin lines and the central Rayleigh line constitute the lower frequency limit of thermal ultrasonic waves that can be studied from Brillouin scattering. The integrated intensity of the Brillouin peaks ($2I_B$) and of the central Rayleigh line (I_R) is given by the Landau–Placzek ratio [78]:

$$\frac{2I_B}{I_R} = \frac{c_p - c_v}{c_v}, \qquad (9.34)$$

where c_p and c_v denote the specific heat capacities at a constant pressure and volume, respectively. Such a ratio is small ($\approx 10^{-6}$ for liquids); this calls for highly accurate measurements in order to facilitate separation of the Brillouin peaks from the branches of the central line.

It should be noted that Brillouin scattering refers only to the two peaks it produces; in the simplified theory of Mountain [79,80], experimentally measured Brillouin spectra are described by three Lorentzians, one corresponding to the Rayleigh component — which is unshifted relative to the incident light frequency — and the other two corresponding to the Brillouin doublet. At present, the Brillouin spectrum is referred to as consisting of one elastic Rayleigh component and two Brillouin components [81].

9.5.3. Types of measurements

The frequency dependence of the ultrasonic properties of materials can be divided in a number of ways based on pulse-echo, transmission or interferometric measurements. The principal differences between them are the way ultrasonic energy is applied to the sample (Fig. 9.4) and the experimental set-up used to make the measurements.

Transmission measurements

For transmission measurements, the target is held in a measurement cell between two ultrasonic transducers one of which acts as a generator and the other as a receiver. The generating transducer produces a pulse of US which travels across the sample and is detected by the receiving transducer. The ultrasonic velocity and attenuation coefficient of the sample are determined by measuring the time-of-flight (t) and amplitude (A) of the ultrasonic pulse which has travelled through the sample. The ultrasonic velocity is equal to the length of the sample (d) divided by the time taken to travel such a distance: $c = d/t$. The attenuation coefficient, α, is calculated by comparing the reduction in amplitude of a pulse which has travelled through the material being analysed with that of a pulse which has travelled through a material the attenuation coefficient of which is known: $\alpha_2 = \alpha_1 - \ln (A_2/A_1)/2d$, where the subscripts 1 and 2 refer to the properties of the reference material and the material being tested, respectively. Obtaining accurate attenuation measurements entails measuring the amplitude of echoes at a single frequency, or a narrow range of

frequencies, by either using a narrow-band ultrasonic transducer or Fourier transform analysis of broad-band echoes. In principle, ultrasonic measurements are simple to perform; in practice, however, obtaining accurate, reliable measurements depends on a number of factors. Thus, the measurement cell must be carefully designed in order to minimize temperature fluctuations, reverberation of ultrasonic pulses in cell walls and transducers, diffraction effects and phase cancellation at non-parallel walls.

There are two approaches using different pulse types to measure the frequency-dependent ultrasonic properties of samples with this technique. One involves application of a *broad single pulse* containing a wide range of frequencies and analysing the pulse after it has travelled through the sample by using a Fourier transform algorithm to determine t and A (and hence c and α) as a function of frequency. Covering the whole frequency range (0.1–100 MHz) requires using a number of transducers (typically three or four) with different frequencies. The other approach involves applying a *tone-burst pulse* containing a number of cycles of US at a particular frequency. In this case, the transducer is tuned to a particular frequency and the velocity and attenuation are measured. The transducer is then tuned to another frequency and the process repeated. Because measurements are made separately at a number of different frequencies, this approach is more labour intensive and time consuming than that based on broad-band pulses.

Pulse-echo measurements

The simplest and widely used approach in performing ultrasonic measurements is based on the *pulse-echo* principle. A typical experimental set-up consists of a measurement cell accommodating the sample, a pulse generator and ultrasonic transducer, and an oscilloscope or a computer interface. The pulse from the generator is converted into an ultrasonic pulse by the transducer and propagates through the sample until it reaches the far wall of the measurement cell, where it is reflected back to the transducer. The transducer now acts as a receiver and converts the ultrasonic pulse into an electrical pulse, which is then either displayed on the oscilloscope or acquired by the computer. Because each pulse is partially transmitted and partially reflected at the cell walls, a series of echoes are obtained from which the velocity, attenuation coefficient and acoustic impedance are determined. Because each echo travels a distance twice the cell length (d) further than the previous one, the velocity can be calculated by measuring the time interval t between successive echoes: $c = 2\ d/t$. The attenuation coefficient is determined by measuring the amplitude of successive echoes: $A = A_i \exp 2\alpha d$. Finally, the acoustic impedance can be determined by measuring the fraction of an ultrasonic wave that is reflected from the surface of the material.

Pulse-echo measurements have for a long time been the most popular in ultrasonic analysis, particularly of liquids, by virtue of the simple construction of ultrasonic cells and electronics, and the lower cost of the instrumentation. The greatest disadvantage of these measurements has traditionally been the relatively high measuring cell volumes required for precise measurements. The pathway of the ultrasonic pulse should be long enough to allow the propagation time and the amplitude decay to be detected with adequate resolution. This has restricted the use of the pulse technique in some fields of research — particularly in biomolecular studies, where liquids or their components are extremely expensive.

The frequency-dependent ultrasonic properties of a material can be measured in almost exactly the same manner by using this approach and the transmission-based one, except that a single transducer is used to both generate and receive the ultrasonic pulses.

Also, the velocity and attenuation coefficient are calculated in exactly the same manner as described for the transmission technique, except that the pulse now travels a distance 2d rather than d.

Interferometric measurements

In an interferometer, the sample is held in a measurement cell located between an ultrasonic transducer and a movable reflector plate. Usually, a sinusoidal electrical or light signal of a specific frequency is applied to the transducer for conversion into a sinusoidal ultrasonic wave that propagates into the sample and is reflected back-and-forth between the reflector plate and the transducer; this produces standing waves in the sample. As the reflector plate is moved vertically through the sample, the amplitude of the signal received by the transducer goes through a series of maxima and minima as destructive and constructive interference occurs. The distance between successive maxima is equal to half the ultrasonic wavelength of the material, so the velocity can be calculated as $c = f\lambda$. The amplitude of the maxima decreases as the distance between the reflector plate and the transducer is increased through attenuation by the sample, reflection at the boundaries and diffraction. The attenuation coefficient is determined by measuring the amplitude of the maxima and minima as a function of distance for the sample and for a calibration material. The measurement accuracy can be improved by measuring the amplitude of, and distance between, a large number of successive maxima. The frequency of measurements is dictated by the resonant frequency of the crystal in the transducer. Crystals can be operated at odd-harmonics of their resonant frequency (f_R, $3f_R$, $5f_R$, etc.), so measurements can be made over a wide range of frequencies by using a single transducer. However, measurements must be carried out separately at each individual frequency, which is more labour intensive and time consuming than with the above-described broad-band pulsed techniques. Some interferometers use tone-burst signals rather than continuous sinusoidal waves, so the ultrasonic energy is not applied continuously to the sample.

Laser interferometry employs the principle of optical interference to recover the sought acoustic information from the light reflected from, or scattered by, a surface under ultrasonic vibration. Its non-contact nature makes laser probing a preferred alternative to contact methods in studying surface waves, their diffraction and damping by intrinsically rough surfaces.

Resonance measurements

Ultrasound resonance spectroscopic measurements are commonly obtained by applying a broad-pulse and selecting the frequency at which the sample enters into resonance at the frequency concerned. Under these conditions, the velocity, attenuation, impedance and other characteristics of US can be measured and subsequently processed as required.

Back-scattered Rayleigh surface wave measurements

A back-scattered Rayleigh surface wave is the leaky ultrasonic energy returning to a transmitting transducer — along the opposite direction to the incident beam — from the

backward propagating leaky surface wave, which is converted from the forward surface wave generated in the incident region. When US impinges at a certain angle near the Rayleigh critical angle onto a specimen immersed in water, a Rayleigh surface wave is generated by mode conversion that propagates along the plate and is reflected at the edge of the specimen. A portion of its energy leaks into water and can be detected with a transducer. In performing pulse-echo measurements of ultrasonic back-scattering, one can acquire three types of responses, namely: (1) direct scatter at the incident position; (2) leak of the Rayleigh surface wave propagating backward upon impingement on a microstructure; and (3) leak of the Rayleigh surface wave reflected at the edge of the specimen. The last, which is often called the "averaging method", provides the highest amplitude that can be detected and processed without spatial averaging, so it is the most frequently used.

Diffraction measurements

Diffraction as a secondary parameter for deriving information about liquids and slurries is measured by placing a grating surface in contact with the sample. The ultrasonic beam from the transducer strikes the back of the grating and produces a transmitted $m = 1$ beam in the liquid the angle of which increases with decreasing frequency, the critical frequency (F_{CR}) occurring at an angle of 90°. At frequencies below F_{CR}, the $m = 1$ beam does not exist and its energy is shared with the other types of waves. Under these conditions, the signal of the reflected $m = 0$ wave is observed and an increase in the signal results at F_{CR}. This information is used to calculate the velocity of sound in the liquid and the particle size [82].

9.5.4. Signal processing

A number of modern processing routines and software are used to analyse the data obtained by US interrogation in order to improve their quality. Thus, averaging a large number of signals reduces the inherent noise which can often obscure the information of interest. High-frequency noise is also reduced by digital smoothing, which works by replacing each point of the received signal with an average of itself and its nearest neighbours. In many applications, the desired information is contained in the frequency spectrum of a signal and can be obtained from a digitized signal in the time domain using Fourier Transform (in the direct, fast or short-time versions) by calculating the magnitude and phase of a series of sine waves of different frequency which makes up the signal in the time domain. This is particularly useful for analysing the frequency content of broadband ultrasonic pulses as it means that measurements can be made over a wide range of frequencies by using a single pulse rather than the more labour-intensive and time-consuming method of making measurements at each individual frequency under toneburst or continuous-wave excitation.

9.6. ULTRASOUND-BASED DETECTION TECHNIQUES

Ultrasound-based detection techniques constitute a broad group of techniques that use ultrasound energy to interrogate and measure the response of a given specimen or only as interrogating force. These techniques have been named according to the way US is

applied, detected and processed. No conceptual distinction has been made, however, between techniques and methods, which has raised confusion in this field.

In order to facilitate the designation of similar techniques differing only slightly, the word "mode" is used here to distinguish them according to their essential characteristics. Such characteristics are included in their names.

9.6.1. Ultrasonic spectrometry

General ultrasonic spectrometry relies on direct measurements of the physical changes caused by the US–sample interaction, namely: velocity changes and attenuation of the radiation. The different modes of this technique arise from factors such as (1) the way US is applied (*e.g.* as a single frequency, broad-band pulses, scanning frequency), after which modes are named; (2) the way US impinges on the sample (normal, parallel, oblique), after which the waves produced in the material (longitudinal, shear, oblique) are named; (3) the way the experimental data provided are used (*viz.* amplitude or phase spectra) or processed (*viz.* frequency or time domain).

9.6.2. Ultrasound resonance spectrometry

The underlying principles of this technique are discussed in Section 9.5, where the differences between its application to liquids and solids are established.

Notwithstanding its significant potential for high-resolution ultrasonic measurements in the analysis of liquids, this technique has for a long time been used mainly by professional ultrasonic laboratories. More widespread use of US for liquid monitoring and analysis has been limited by hindrances such as the following:

(a) the inability to perform measurements involving simple cell filling, short measuring times, automatic operation, effective stirring, and the use of unstable organic solvents, acids and bases, among others;

(b) the large volume of measuring cells and high cost of analyses, especially with expensive liquids;

(c) the poor resolution of measurements, which is limited to 10^{-3}% for ultrasonic velocity and about 1% for attenuation even with specialized sophisticated scientific devices in most cases;

(d) the difficulty of interpreting ultrasonic characteristics, which hinders use in routine analyses.

Recent advances in ultrasonic resonators have facilitated the development of inexpensive, convenient devices for fast measurement of ultrasonic velocity and attenuation in small volumes (down to 0.1 ml) with resolution better than 10^{-4}% for velocity and 0.1% for attenuation. In addition, comprehensive studies on ultrasonic parameters of liquids in a number of laboratories over the last decade have provided a solid background for the interpretation of ultrasonic data.

One variant of RUS, the resonant sphere technique (RST), is of special interest in this context as a spherical specimen can be readily made accurately and its natural frequencies solved theoretically as shown by Fraser and LeCraw [83], whose methodology was subsequently refined by Soga and Anderson [84]. Recently, Yaoita *et al.* showed that, because RUS is based on the principle that the mechanical resonant response of solids

depends on their elastic moduli, shape and density, these properties can be identified from resonant frequencies as the inverse problem. In this way, a method for determining the elastic moduli of spherical specimens in the absence of information about resonant mode was developed [85] and the following facts have been confirmed: (a) resonant frequencies have to be measured under free-surface conditions; (b) the number of resonant frequencies used in calculations must be high enough to include the sensitive mode to Poisson's ratio.

One of the advantages of RUS for the analysis of solids is that it can use small samples — as small as a single crystal — for measurement. Recently, this technique has proved useful for determining the dependence of the modulus and attenuation of single-crystal $La_{2-x}Sr_xCuO_4$ in the low doping region ($x = 0.01$) on the temperature and magnetic field up to 7 T working in the 0.1–2 MHz frequency region [86].

One recent example of the flexibility of RUS is its use to determine the elastic stiffness coefficient of thin films through free-vibration resonance frequencies of a film-substrate-layered solid and to measure deformation distributions on the vibrating specimen by laser–Doppler interferometry [87].

9.6.3. *Laser-based ultrasound detection techniques*

Laser-based ultrasonic techniques possess many attractive features including the ability to make non-contact, non-destructive and remote measurements. These optical detection modes have a relatively low sensitivity relative to their contact transducer counterparts wherever available. In fact, their sensitivity is typically one or two orders of magnitude lower than that of contact transducer modes.

This lack of sensitivity is the source of a major problem with all-optical acoustic microscopes, where measuring expeditiousness is usually essential. It should be noted that the SNR of an all-optical system in the thermoelastic regime is proportional to $P_{gen}\sqrt{P_{det}}$, where P_{gen} is the optical power used to generate the acoustic wave and P_{det} that used to detect it. This relationship indicates that much more can be gained, in terms of SNR, by increasing the total generation power rather than the detection power. Usually, the maximum amount of generation power that can be used is restricted by the risk of surface damage, whereas that of detection power is usually limited by financial cost. Using tailored generation–distributions helps overcome the limitation associated with the risk of damage and allows the SNR to be increased by using more generation power.

Acoustic microscopy (AM)

Acoustic microscopy (AM), also known as "scanning acoustic microscopy" (SAM), uses transmitted ultra high-frequency US in the range from 10 MHz to 2 GHz to produce images, mainly of biological structures, with a resolution approaching that of light microscopy. This technique, which is usually sensitive to the mechanical properties of the materials under inspection and contrast, provides useful information about the physical structure of the sample. There are two major AM modes that differ in whether or not a couplant (usually water) is used in order to allow acoustic waves to be coupled into the sample. In the former case, the couplant can pose problems such as contamination of the material surface, perturbation of measurements and restriction of access to samples with complex geometries. The first problem may be the main reason why SAM has not been widely adopted in some areas (*e.g.* the semiconductor industry); the second is a major bar

to the use of SAM for quantitative measurements (of velocity and attenuation) and for revealing some types of contrast; the third may restrict examination of real industrial components such as turbine blades. Despite these problems, there are obvious advantages in being able to make remote measurements in many circumstances where direct contact with the sample may be difficult.

The so-called "scanning acoustic microscope" has a transmitting and a receiving US transducer between which the target specimen is placed. Specimen areas of approximately 250 μm^2 can be scanned within about 2 s with highly focused US. The pixel size in the final image is approximately 1 μm, and the image contrast (*i.e.* the pixel intensity or grey level) is determined by the US attenuation, which, at GHz frequencies, is determined mainly by the elasticity of the specimen components.

In addition to the conventional focus of the US beam on small sample surfaces, the laser transmitting transducer can drive to the sample a line-focus-beam by using a cylindrical lens to obtain leaky SAWs [42]; alternatively, a computer-generated hologram can be used to produce Rayleigh surface waves with a circular wavefront [88]. In this way, a wide range of parameters including bulk acoustic wave velocities, dielectric constants and densities in both isotropic and anisotropic materials can be determined. Strict control of the instrument and room temperature increases measurement reproducibility at a single point to ±0.002% [42].

Brillouin scattering spectroscopy (BSS)

This ultrasonic–optical technique (or half-optical technique [89]) was also a hyphenated technique in terms of energy sources (*viz.* thermal and optical for phonon and photon production, respectively). Thermal surface phonons restrict practical application of the technique owing to their low scattering efficiency, which results in overly long data collection times (typically several hours for a single spectrum, even with advanced multipass interferometers). Similar to active Raman spectroscopy, coherent acoustic phonons are assumed to be excited by two narrow-line frequency tunable laser beams at different frequencies or by laser pulses of short duration compared to the acoustic period.

Brillouin scattering spectroscopy is a hypersound technique as Brillouin peaks corresponding to acoustic modes with frequencies below a few hundred kilohertz can hardly be discriminated from the central Rayleigh line; this makes measurements of photon–phonon interactions at low frequencies impracticable, even if Brillouin scattering is stimulated [90] and (or) acoustic diffraction applied [91]. Unfortunately, the amplitude of the spontaneous density fluctuations is too small to be directly detectable by acoustic methods and to be clearly resolved from the noise that is produced in the measuring devices themselves. Increasing the SNR therefore entails feeding a small disturbing signal to the sample and detecting the response. Based on the time dependence of the excited signal, BSS can be implemented in the time-domain or frequency-domain mode.

Time-domain BSS. Because counter-propagating acoustic waves produce a standing wave, the diffracted intensity oscillates in time and the oscillation can be recorded by using a fast photodetector and a digitizing oscilloscope; a surface phonon spectrum can thus be obtained from a Fourier-transform of the data.

Frequency-domain BSS. In this mode, the spectrum of the diffracted probe light is obtained by using a Fabry–Perot interferometer. Light is diffracted by incoherent thermal phonons and the scattering wavevector is determined by the detection angle, which can be accurately fixed by limiting the collection aperture.

9.6.4 Ultrasonic relaxation spectroscopy (URS)

Ultrasonic relaxation spectroscopy (URS) is nothing but a special treatment of data from ultrasonic absorption measurements. Micelle dynamics involves characteristic relaxation processes, namely: micelle–monomer exchange and micelle formation–breakdown. Ultrasonics can provide information about the kinetics of the latter, the fast relaxation process; also, theoretical expressions for the relaxation time and relaxation strength such as those derived by Teubner [76] provide self-consistent estimates of both.

9.6.5. Ultrasonic diffraction grating spectroscopy (UDGS)

This is a new technique also involving measurements of parameters of the secondary type that was recently developed and required much research to confirm the initial findings and broaden its scope. As established by its developers, the purpose of this technique is to measure the speed of sound in liquids [92] and slurries, and the particle size of slurries [82]. To this end, ultrasonic diffraction grating is used; the grating is obtained by machining parallel triangle-shaped grooves spaced 300 μm apart with 120° included angle on the flat surface of a half-cylinder of 5.08 cm diameter and 3.8 cm height. The grating is placed in an immersion chamber and the send and receive transducers are mounted on brackets at an angle of 30° with respect to the normal. A tone-burst signal of the desired frequency is delivered to the send transducer, the longitudinal wave formed striking the back of the grating at an incident angle of 30°. The receive transducer measures the reflected diffracted $m = 0$ longitudinal wave. As the frequency decreases, the $m = 1$ transmitted longitudinal wave in the liquid moves to a larger angle. For water, the angle becomes 90° at a frequency of 5.67 MHz. At such a frequency, called the "critical frequency", the wave becomes evanescent, and, at a slightly lower one, the evanescent wave disappears. In order to conserve the energy, this is redistributed to all other waves, so an increase in amplitude of the reflected $m = 0$ signal is observed. The utility of UDGS for measuring particle size arises from the fact that the evanescent wave penetrates into the slurry: as the wave interacts with the particles, some signal attenuation occurs and as a result the signal measured by the receive transducer decreases in amplitude. An appropriate algorithm can be used to determine the particle size.

Higher sensitivity and more comprehensive information can be obtained by modifying the experimental design as follows: mounting the immersion chamber on a turntable that is motorized and computer-controlled to an angular placement with an accuracy of 0.1°. The receive transducer is mounted on the non-rotating base of the turntable so it cannot move. The desired angle between the send and receive transducers is obtained by rotating the turntable with the immersion chamber with the attached send transducer. The data acquisition system consists of a commercially available pulser-receiver card and a digitizer card mounted on a PC. The pulser emits a sinusoidal tone-burst signal having an amplitude of about 330 V peak-to-peak of the desired frequency. A grating equation and one for the critical angle have been established, and the peak width has been found to decrease and peak height to increase with increasing number of illuminated grooves. Two types of measurements are thus possible in UDGS, namely: (a) *scan over frequency range* using a fixed angle between transducers, and (b) *scan over angular range* using a fixed frequency tone-burst signal. The information about transmitted longitudinal (both $m = 0$ and $m = 1$) waves provided by the instrument can be expanded by including a 5-MHz shear wave transducer. No $m = 1$ transmitted longitudinal wave exists below the critical frequency, so the grating and the blank (*i.e.* a unit with the same dimensions as the grating, but a smooth face) behave similarly. Above the critical frequency, the energy is shared

by the $m = 0$ and $m = 1$ transmitted longitudinal waves. At the critical frequency (that is, during the transition), the energy is shared primarily by the reflected $m = 0$ shear wave and the $m = 0$ transmitted longitudinal wave.

Further research is needed with a view to obtain comprehensive information about scans over angle and over frequency. In the former, positioning the send transducer at a 30° angle, using the receiver to observe the $m = 1$ transmitted wave in the liquid and rotating the immersion chamber over selected angle ranges produces peaks of decreased amplitude for water and increased amplitude for 30% sugar solutions. This effect occurs even before the $m = 1$ wave becomes evanescent. In the case of scan over frequency, the differences between water and 30% sugar in water depart from the predictions. Further research is therefore needed for effective exploitation of this new technique.

9.6.6. Other ultrasound-based detection techniques

Pulsed Fourier-transform ultrasonic spectroscopy

This US-based technique, devised for operation at room temperature [93], has so far been scarcely used but was recently employed in studies at ultra-low temperatures in a manner similar to pulsed FT–NMR. It provides several advantages over conventional time-of-flight acoustic techniques [94] the most significant of which is the ability to observe the frequency spectrum while independently tuning the temperature, pressure and magnetic field. Using longitudinal $LiNbO_3$ transducers operating both on- and off-resonance allows several broad-band frequency windows (namely, 16–25, 60–70 and 105–111 MHz) to be studied. Interferences from echoes are avoided by analysing direct transmitted signals only, which involves zero-blanking long time-periods.

9.7. GENERAL SCHEMES OF ULTRASOUND-BASED SPECTROSCOPIC INSTRUMENTS

9.7.1. Laboratory-made instruments for ultrasound-based measurements

Laser-based ultrasound approaches

The most recent US-based measurement methodologies are based on laser sources and are of two general types, namely: (a) all-laser approaches, where both US generation and detection are laser based; and (b) half-laser approaches, where laser light is used either for generation or detection of US, but not both.

Laser–ultrasound resonance (LUR) for solid analysis. A prototype of an instrument that can be used on-line as shown by its installation at an inspection line in Cleveland [95] is described as an example of LUR for solid analysis.

The instrument. Figure 9.13 shows a typical set-up for implementing LUR measurements in solids. It consists of (1) a pulsed excimer laser to generate an ultrasonic pulse in the solid (a metal sheet) and (2) a laser interferometer to detect the ultrasonic signal that reverberates in the sheet thickness. The signal detected by the laser interferometer is analysed using Fourier Transform to locate resonance frequencies associated with longitudinal and shear propagating modes. The ultrasonic parameters are associated with sheet thickness, texture coefficients and mechanical properties with provision for the facts that one polarization exists for longitudinal waves (L), with vibrations parallel to the
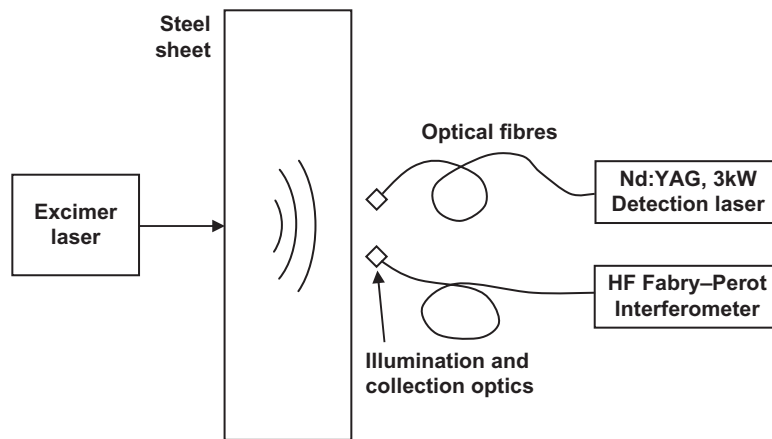
FIGURE 9.13. *Basic components and configuration of LUR spectroscopy. The pulsed source of radiation for ultrasound generation can be placed either on the same side as the detection laser and interferometer or on the opposite side. (Reproduced with permission of Elsevier, Ref. [95].)*

thickness direction, and two for shear waves [95]. A UV light pulse from the excimer laser is shone on the metal surface to generate the US because US light is better absorbed by metals and oils (used to lubricate or to protect the surface against oxidation) than other radiation. Typically 100–200 mJ of UV radiation in pulses lasting 3–6 ns can be focused on an area a few millimetres in diameter. If the pulse energy density (the fluence) is large enough, the UV light pulse causes slight ablation of the surface — or of the dirt and oil present on the surface — and the recoil energy generates an ultrasonic pulse in the direction normal to the sheet surface. This ultrasonic pulse is broad-band in its frequency content (typically between 1 and 40 MHz or higher). A laser interferometer is used on either side to sense the surface displacement caused by each successive echo. The interferometer's main components are a long pulse, 3 kW peak power, Nd:YAG laser and a confocal Fabry–Perot interferometer which has a large light gathering capability and is insensitive to speckles. The instrument is not in contact with the sample: the stand-off distance which may be as large as required, but is usually set to about 30 cm. Vertical motion of the moving sheet has no effect as long as the sheet remains within the depth of focus of the focusing optics (a few centimetres). Line speeds of up to tens of metres per second, depending on the optical properties of the Fabry–Perot cavity and the sheet surface, are possible.

Measurements and information. A single broad-band longitudinal pulse is used to excite the entire frequency range of interest and self-conducted mode conversion allows shear and longitudinal resonances to build up. The identification of all through-thickness resonances occurs simultaneously and allows nearly instantaneous measurement at a single location of the moving sheet. The order of the harmonics is determined from *a priori* knowledge of the approximate sheet thickness and sound velocity. Alternatively, the approximate sheet thickness may be obtained from the time delay between the first two longitudinal echoes and an approximate value of the longitudinal sound velocity. The fundamental frequency of each propagating mode is obtained by measuring the frequency at the maximum of the selected resonance and dividing it into the order of the

harmonic. Interpolation methods may be used to evaluate the resonance frequencies with increased precision.

Brillouin scattering spectroscopy. The present interest in this acoustic–optical technique and the use of laser sources to generate both types of energy warrant detailed description of the measuring instrument.

The instrument. Figure 9.14 is a block diagram of the instrument for BSS designed by Kaatze *et al*. [96], the central part of which is a pair of thermally coupled laser light
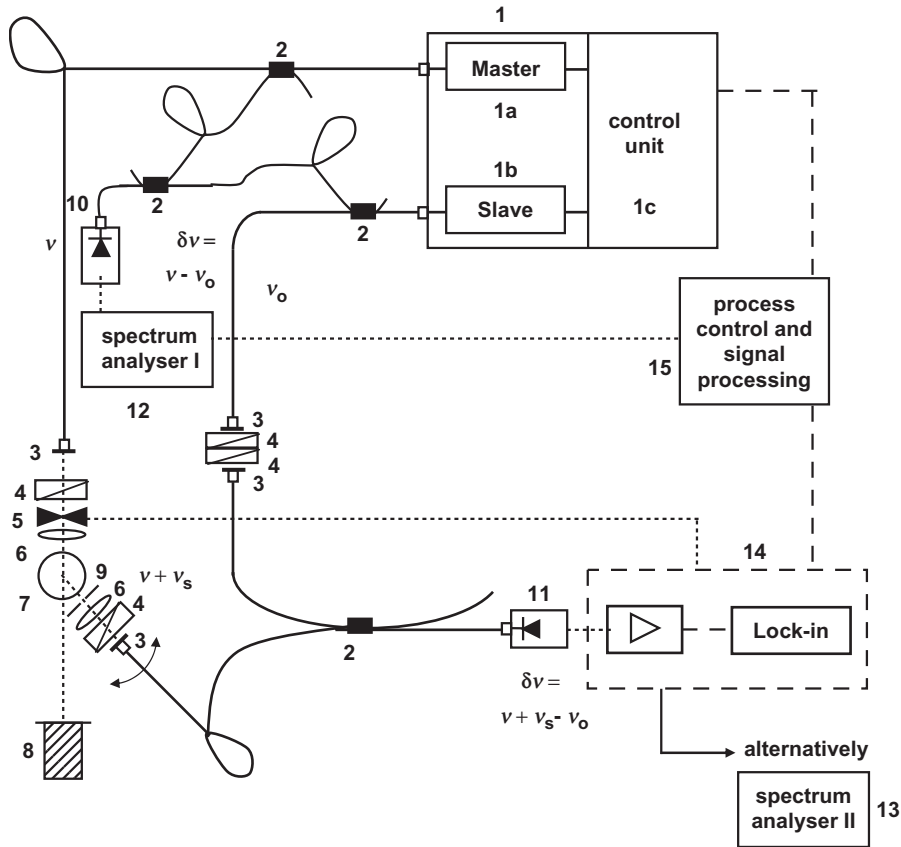
FIGURE 9.14. *Brillouin spectrometer using fibre optics to increase the signal-to-noise ratio. (1) Light source consisting of a master laser: (1a) a slave with matched frequency (1b) and control unit (1c) for sensitive stabilization of the difference frequency δv. (2) Signal splitter. (3) Fibre coupler. (4) Polarizer. (5) Chopper. (6) Lens. (7) Cuvette placed on a goniometer. (8) Termination. (9) Slit. (10) Broad-band (10 GHz) APD. (11) Photodiode with a smaller bandwidth (1 GHz). (12) Spectrum analyser (10 GHz) for controlling the intermediate frequency, δv. (13) Spectrum analyser (1 GHz) for the measurement of the half-power bandwidth, Δv, of the Brillouin peak. (14) Amplifier system. (15) Process control computer. (Reproduced with permission of Elsevier, Ref. [96].)*

sources — preferably two single-axial mode, continuous-wave (cw) output, frequency-doubled Nd:YAG lasers equipped with monolithic ring resonators. Such lasers ensure stable signals at λ_{light} = 532 nm (corresponding to υ_{light} = 5.6 × 10^{-14} s^{-1}) with frequency jitter smaller than 150 kHz/s. They provide a tuning range of 10 GHz in their output frequency; hence, if the lasers are carefully selected in order to ensure appropriate frequency overlap, then the frequency of their difference signal will span the whole frequency range from the unshifted Rayleigh line to a Doppler-shifted Brillouin peak. Since the difference frequency can be measured very accurately with electronic counters, the frequency resolution in this type of measurement is much higher than in the optical filter methods. A sensitive avalanche photodiode (APD) with a small bandwidth of about 1 GHz is used for signal detection after scattering. In order to cover the whole frequency range from about 10 MHz to 10 GHz, which, in principle, is usable in Brillouin spectroscopy, the frequency υ of the master laser (the signal source) or that of the slave laser (the local oscillator) has to be tuned by about 10 GHz. For this purpose, part of the light from both lasers is mixed in a broad-band APD and recorded by a spectrum analyser, the output signal of which is used for frequency control of the laser system. In order to obtain stable difference signals of such small intermediate frequency, the master and the slave laser must be thermally coupled. Also, in order to reduce unwanted disturbances from outside light sources, the instrument is based on fibre-optic technology.

Measurements and information. Signal processing allows both time- and frequency-domain information to be obtained depending on the type of specimen studied. In addition, the use of frequency-tunable laser to generate density variations within the sample results in thermal expansion by absorption of light. Compared to spontaneous Brillouin scattering, the SNR in this "forced" Brillouin spectrometry is substantially enhanced by the generation of coherent phonons within the sample.

Acoustic microscopy. Although this technique is mainly used in the medical field, various interesting analytical applications have been developed and analytical chemists are encouraged to contribute new ones by exploiting advances in instrumentation in this field. An acoustic microscope, which also constitutes an example of a half-laser instrument, is described below.

The instrument. Figure 9.15 is a schematic diagram of an all-optical SAM operating at 82 and 164 MHz [97]. The generating laser is a 2 W (average power), Q-switched, mode-locked lamp pumped Nd:YAG laser with a Q-switch frequency of 0.1–5 kHz and a fundamental mode-locking frequency of 82 MHz. It produces a tone-burst of 30 short pulses separated by 12.1 ns every 500 μs. A computer-generated hologram is used to produce 16 arcs with a mean focal length of 2 mm on the sample, the separation of the arcs depends on the material velocity. The detector is a knife-edge design using a split photodiode and a differential rf amplifier instead of a simple knife edge. Signals are captured by a simple phase and amplitude measuring system. The phase is measured with respect to a reference signal from the generating laser's mode-lock driver, which is coherent with the laser pulses. The sample and detector are mounted on scanning stages, thus allowing the scanning of the sample in order to build up an acoustic image and of the detector to examine the resulting distribution of ultrasound.

Measurements and information. The above-described instrument can form images at 82 and 164 MHz with a signal bandwidth around 5 MHz. In order not to narrow such a bandwidth, the maximum number of lines or arcs used must not exceed 16. The microscope currently uses various computer-generated holograms to tailor the optical distribution on the sample surface and is being converted to use an SLM. The stand-off distance from the optics to the sample is around 50 mm, which is determined by the need to resolve the SAWs at 164 MHz.
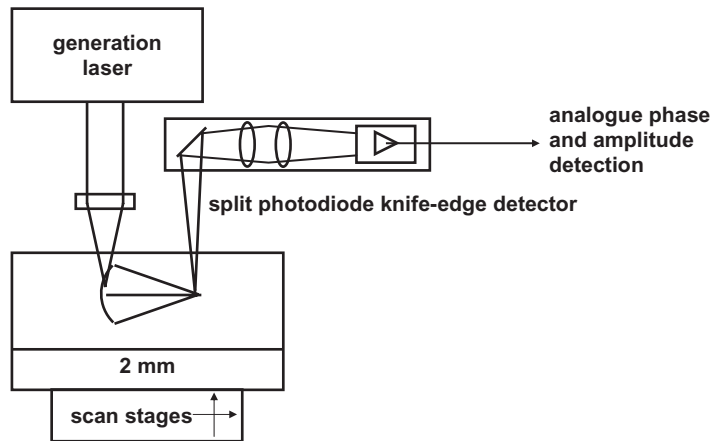
FIGURE 9.15. *Schematic diagram of an all-optical SAM. For details, see text. (Reproduced with permission of Elsevier, Ref. [97]).*

9.7.2. Commercial instruments for ultrasound-based measurements

Present commercially available US-based instruments can be crudely grouped into those involving discrete frequency scanning and those using broad-band pulses. The former use relatively sophisticated electronics to maintain a steady continuous wave (cw) and often require multiple transducers to provide the required frequency range; the latter are significantly less complex. This reflects in their price and extent of use. One example of a cw device, the Ultrasizer, from Malvern, UK, out of the market at present, utilizes the attenuation spectrum for complete particle size characterization of colloidal systems with accuracy comparable to that of optical detectors. By contrast, the pulse-based instrument UVM1 (Cygnus Instruments, UK) only provides speed of sound values, albeit at a fraction of the cost. The two instruments also differ in operational time, with the former taking up to 5 min for a single reading as opposed to 30 readings per second in the latter — expeditiousness is mandatory for commercial and on-line systems. The possibility of producing more complex ultrasonic data from a pulse-based system was first envisaged by McClements and Fairley [98], who developed the FSUPER (frequency scanning pulse echo reflectometer) to obtain attenuation spectra from simple broad-band pulses. The instrument was subsequently modified [99] to obtain phase velocity spectra.

However, pulsed US devices are subject to several shortcomings, namely: (1) the need for reference fluid calibration, success of which relies on reference fluid integrity, reference value and temperature measurement accuracy and the absence of thermal expansion of the cell after calibration; (2) probe delay, diffraction and impedance mismatches between the reference and test fluid; (3) low accuracy and repeatability; (4) a limited range of ultrasonic parameters, with systems often specializing in either time-domain or frequency-domain data, but not both. These shortcomings can be circumvented by making measurements over a range of distances; this avoids the reliance on absolute distance measurements, allows same-fluid normalization of amplitude data and intrinsically averages measurements for improved accuracy and repeatability.

A number of firms in various countries (*e.g.* RITEC, Inc. in USA, Ultrasonic Sciences, Ltd. and Cygnus Instruments, Ltd. in UK, Mittal Enterprises in India) commercialize instruments for laboratory analysis in addition to small equipment for ultrasonic inspection, usually based on multiple echo measurements, and portable equipment of very small dimensions for applications such as the following:

(1) Metal thickness monitoring on cranes, marine structures and conveying systems;
(2) Corrosion checks on ship shell plates, bulkheads and structures;
(3) Metal thickness safety checks on steam and pressurized water systems, transportable gas containers and compressed air systems;
(4) Systematic wall thickness and corrosion monitoring of storage tanks and process vessels;
(5) Quality assurance of metal thickness checks;
(6) Maintenance and safety checks on bridges and street lighting columns;
(7) Pipeline wall thickness monitoring.

Also, small animal scanners that operate at frequencies beyond 40 MHz, thereby making US biomicroscopy (UBM) practical, have recently become available and tested in biomedical US research. These scanners have also been used together with optical coherence tomography, which measures low-coherence optical interferometry to obtain micron-scale resolution tomographic images of subsurface tissue.

Note that US-based detector manufacturers are usually reluctant to provide technical information and schemes of their instruments (*e.g.* types of components, assembly, performance). By exception, Dr. Dukhin has kindly allowed part of the description of the DT100 acoustic spectrometer [100] to be included in this section.

Dispersion Technology DT100 acoustic spectrometer. This instrument is a modern example of commercial equipment which, in its basic design, follows the transmission tone-burst variable gap technique pioneered by Andreae [101–103]. Figure 9.16A shows a photograph of a typical unit.

The instrument. Figures 9.16 and 9.17 show the two parts that make up the instrument (*viz*. the measuring unit and the associated electronics, respectively).

Figure 9.16A shows the whole instrument and Fig. 9.16B the two different views of the acoustic sensor, the portion of the measuring unit that contains the sample being measured and positions the piezoelectric transducers appropriately for attenuation measurements. The sensor utilizes two identical piezoelectric transducers separated by an adjustable gap that is controlled *via* a stepping motor. Each transducer has a quartz delay rod providing a delay of 2.5 μs. The transmitting transducer (on the right side of the photographs) is fixed, but has an accurately set adjustment that keeps the two transducers parallel. The receiving transducer (on the left side) is mounted on a piston assembly the position of which can be adjusted. The gap between the face of the transmitting and receiving transducers can be set from close to zero up to 20 mm. The moving piston is sealed against the sample by a wiper seal and supplemental O-rings. The space between the seals is filled with fluid to keep the withdrawn portion of the piston wetted in order to prevent build-up of any dried deposit. Ports associated with this space between the seals can be used to periodically inspect the intra-seal fluid for contamination. The presence of any contamination serves as advance warning of potential seal degradation when making continuous measurements of highly aggressive samples (*e.g.* concentrated Portland cement). The position of the receiving transducer piston is controlled by a stepping motor linear actuator that is in turn controlled with a precision of a few microns *via* the associated electronics and software. The sample is held in the space between the transducers. Depending on the particular implementation,
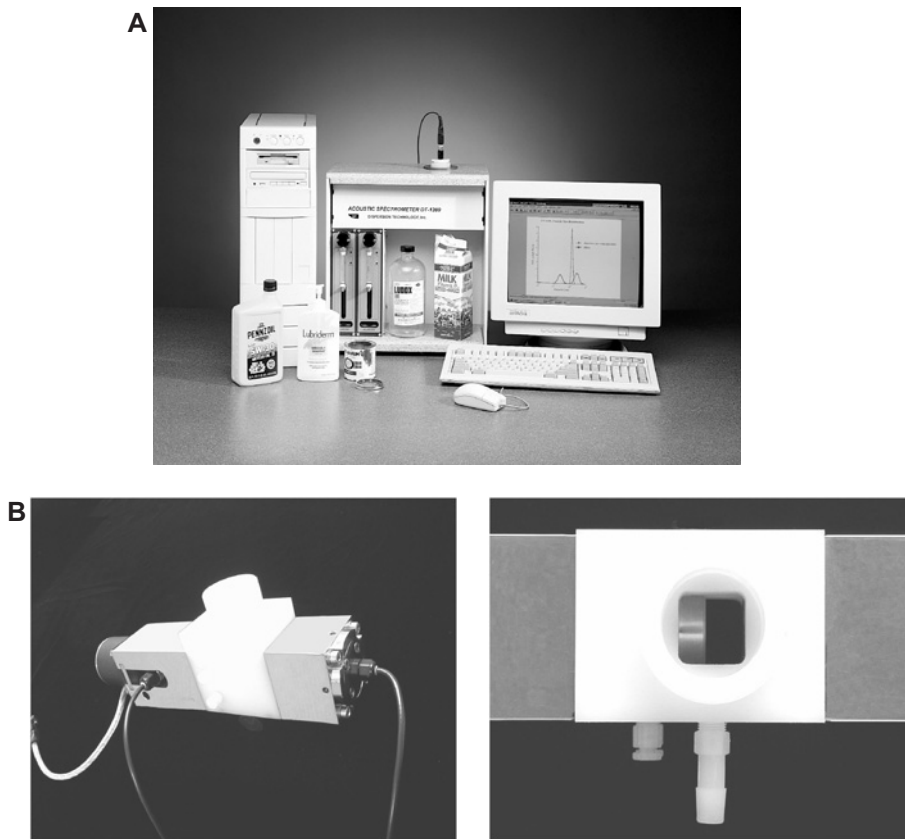
FIGURE 9.16. *(A) The Dispersion Technology DT100 acoustic spectrometer. (B) Perspective and top views of the acoustic sensor. (Reproduced with permission of Elsevier, Ref. [100].)*

the sample can be stirred with a magnetic stir bar, pumped through the sensor by a peristaltic pump or not stirred at all. When the piston is fully withdrawn, the transducers are essentially flush with the walls of the sample compartment to facilitate cleaning. During operation, tone-bursts at selected frequencies are applied to the transmitting transducer. The amplitude of the received pulses, which are subject to some delay, is then measured.

As can be seen in the block diagram of Fig. 9.17, the electronics unit comprises a frequency synthesizer **30** that generates a continuous wave (cw) rf signal **31**, a field programmable gate array **32** (FPGA) controlled by the host computer *via* a digital interface **60** that generates transmit gate **33**, an attenuator control **34**, a receive gate **35**, a switch control **36**, and an A/D strobe command **37**. The transmit gate **33** is used by the gated amplifier **38** to form a pulsed rf signal from the synthesizer cw signal **31**. A power amplifier **39** increases the peak power of this rf pulse to approximately 1 W. A directional coupler **40** provides a low-loss path for the forward signal from the power amplifier to the transmit switch **41**, which then routes the 1 W rf pulse **61** to any of the three channels, labelled A, B and C
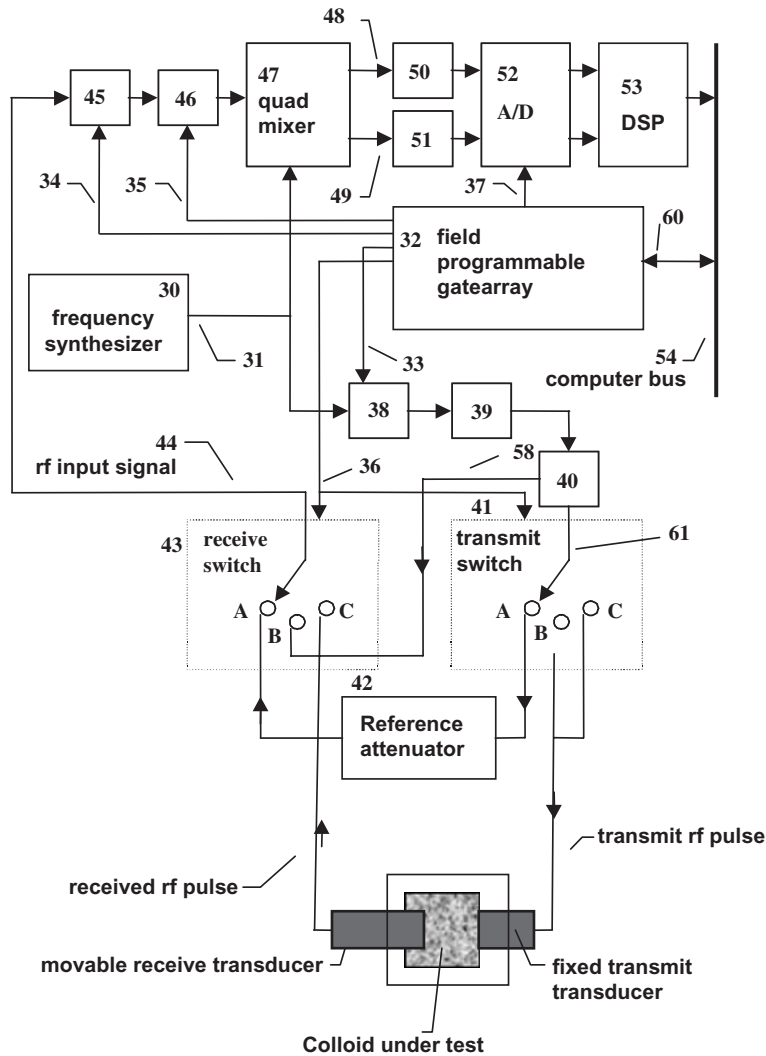
FIGURE 9.17. *Block diagram of the electronics of the DT100 acoustic spectrometer. (Reproduced with permission of Elsevier, Ref. [100].)*

according to the FPGA switch control **36**. Channel A is called the reference channel; in this case, the output pulse is routed to a precision fixed 40 dB reference attenuator **42** the output of which is connected to channel A of the receive switch **43**, where it is then routed to the rf input signal **44**. The rf input signal is connected to a wide band rf amplifier **45** having a programmable gain set by FPGA attenuator control **34**, and thence to a gated amplifier **46** controlled by the FPGA receiver gate **35**, which allows only pulses arriving within a preset

time interval to pass, and hence to a quadrature mixer **47** keyed by the synthesizer output **31**, which demodulates the received signal and provides analogue pulses **48** and **49** proportional to the in-phase and quadrature components of the received rf pulse, respectively thence to separate matched filters **50**, **51** for the in-phase and quadrature components, thence to a dual A/D converter **52** which digitizes the peak amplitude of these quadrature signals upon an A/D strobe command **37**, thence to a digital signal processor (DSP) **53** chip that accumulates data from a large number of such pulses and generates statistical data on a given pulse set. Finally, this statistical data is routed to the computer bus **54** so that the data can be analysed to determine the amplitude and phase of the input signal level **44** for this reference condition. This reference signal level is computed in the following way: the statistical data from the two-channel A/D provides an accurate measure of the in-phase and quadrature components of the received signal at the A/D input, the magnitude being computed by calculating the square root of the sum of the squares of these two signals. The phase is computed from the inverse tangent of the ratio of the in-phase and quadrature components, and the magnitude of the rf input signal **44** is then computed by taking into account the overall gain of the rf signal processor as modified by the gain control signal **34**.

The use of this reference channel with a known attenuation allows the attenuation to be measured precisely when using the remaining channels B and C. Since the input signal level for the 40-dB reference attenuator is known, any increase or decrease in this signal when using either of the other channels will be proportional to any increase or decrease with respect to this 40 dB reference value. When the transmit switch and receive switch are set to position C, the pulsed rf signal is routed to the transmit transducer in the acoustic sensor, where it is converted to an acoustic pulse and launched down the quartz delay rod. A portion of the pulse is then transmitted into the sample, traverses it, is partially transmitted into the quartz delay rod of the receiving transducer and, after passing through this delay rod, is converted back into an electrical pulse. The received pulse is then routed to port C of the receive switch for processing by the receiver.

Measurements and information. The above-described instrument can perform measurements for just one frequency or for a chosen set of frequencies from 1 to 100 MHz. Typically, the system averages at 800 pulses, but may accumulate as many as several million pulses if necessary in order to ensure an acceptable SNR. The number of pulses measured will depend on the properties of the particular sample. For example, concentrated slurries at high frequency and large gaps may require a large number of pulses. Since the attenuation is determined by measuring the relative change in signal *versus* the relative change in gap, one need not know the absolute value of the gap precisely. The precision with which the relative gap can be measured is determined by the accuracy of the lead screw used in the linear displacement stepping motor. However, the absolute position is calibrated to an accuracy of just a few microns the first time a measurement is made after the program is started. Calibration is carried out simply by moving the receiving transducer towards the transmitting transducer long enough to ensure that the two have contacted one another and the motor has stalled in that position. The gap position is then reset, so additional measurements are made relative to this known initial position.

Measurements are made by using a defined grid consisting of a certain number of frequencies and gaps. By default, the system selects 18 frequencies between 1 and 100 MHz in logarithmic steps, and 21 gaps between 0.15 and 20 mm, also in logarithmic steps. These grid values may be modified automatically by the program, depending on the available knowledge about the sample, or manually by an experienced user.

9.8. CONCLUSIONS

Because the principal aim of this chapter is to arouse the interest — or at least curiosity — of analytical chemists in this type of detection, readers are encouraged to delve deeper into the subject in specific monographies on the particular US-detection technique they suspect can either fit their research guidelines or be used as the basis for a new research line after reading the selected applications described in Chapter 10.

Including further information about US-based detection techniques or dealing more extensively with them was therefore unwarranted, particularly on the grounds of their scant use in analytical chemistry relative to US for sample preparation or for the uses discussed in Chapter 8. In any case, the authors encourage interested analytical chemists to explore these detection techniques.

As the readers may see, quartz crystal resonator (QCR) sensors are out of the content of this chapter because their fundamentals are far from spectrometric aspects. These acoustic devices, especially applied in direct contact to an aqueous liquid, are commonly known as quartz crystal microbalance (QCM) [104] and used to convert a mass or a mass accumulation on the surface of the quartz crystal or, almost equivalent, the thickness or a thickness increase of a foreign layer on the crystal surface, into a frequency shift — a decrease in the ultrasonic frequency — then converted into an electrical signal. This unspecific response can be made selective, even specific, in the case of QCM immunosensors [105]. Despite non-gravimetric contributions have been attributed to the QCR response, such as the effect of single-film viscoelasticity [106], these contributions are also showed by a shift of the fixed US frequency applied to the resonator; so, the spectrum of the system under study is never obtained and the methods developed with the help of these devices cannot be considered spectrometric. Recent studies on acoustic properties of living cells on the sub-second timescale have involved both a QCM and an impedance analyser; thus susceptance and conductance spectra are obtained by the latter [107].

References

1. S.E. Barnes, E.C. Brown, M.G. Sibley, H.G.M. Edwards and P.D. Coates, *Analyst*, 130 (2005) 286.
2. C.M. Lagier, I. Efimov and A.R. Hillman, *Anal. Chem.*, 77 (2005) 335.
3. A. Pal Singh, D.J. McClements and A.D. Marangoni, *Food Res. Int.*, 37 (2004) 545.
4. X.L. Su, B.S. Yu, H.W. Tan, X.R. Yang, L.H. Nie and S.Z. Yao, *J. Pharm. Biomed. Anal.*, 16 (1998) 759.
5. X.L. Su, W. Wei, L.H. Nie and S.Z. Yao, *Analyst*, 123 (1998) 221.
6. X.L. Su, L.H. Nei and S.Z. Yao, *Fresenius J. Anal. Chem.*, 360 (1998) 272.
7. M.F. Insana and W.F. Walter, Ed., *Ultrasonic Imaging and Signal Processing*, Proceedings of SPIE, 2002.
8. A. Yaoita, T. Adachi and A. Yamaji, *NDT & E Intern.*, XX (2005) 1.
9. J. Maynard, *Phys. Today*, 49 (1996) 26.
10. A. Migliori, J.L. Sarrao, *Resonant Ultrasound Spectroscopy*, Wiley, New York, 1997.
11. H. Ledbetter, C. Fortunko and P. Heyliger, *J. Appl. Phys.*, 78 (1995) 1542.
12. Valpey Fischer, Hopkinton, MA 01748, USA.
13. Y. He, R.B. Schwartz, T. Darling, M. Hundley, S.H. Whang and Z.M. Wang, *Mater. Sci. Eng.*, A239–A240 (1997) 157.
14. T. Goto and O.L. Anderson, *Rev. Sci. Instrum.*, 59 (1988) 1405.
15. C.P. Hsieh and B.Y. Khuri-Yakub, *Appl. Phys. Lett.*, 62 (1993) 3091.
16. R.B. Schwarz and J.F. Vuorinen, *J. Alloys Comp.*, 310 (2000) 243.

17. W.L. Johnson, G.A. Alers and B.A. Auld, U.S. Patent No. 5 813 280. 1998 and U.S. Patent No. 5 895 856.
18. E.P. Papadakis, Ultrasonic Measurement Methods, in R.N. Thurston and A.D. Pierce (Eds.), *Physical Acoustics*, vol. XIX, 1990, p. 107.
19. H. Jeong and D.K. Hsu, *Ultrasonics*, 33 (1995) 195.
20. H. Ogi, M. Hirao and T. Honda, *J. Acoust. Soc. Am.*, 98 (1995) 458.
21. M. Blodgett and P.B. Nagy, *Appl. Phys. Lett.*, 72 (1998) 1045.
22. C.B. Scruby and L.E. Drain, *Laser-Ultrasonics: Techniques and Applications*, IOP Publishing, Ltd. Bristol, UK, 1990.
23. J.P. Monchalin, Progress Towards the Application of Laser–Ultrasonics in Industry, in: D.O. Thompson and D.E. Chimenti (Eds.), *Review of Progress in Quantitative Nondestructive Evaluation*, Plenum Press, New York, 1993, pp. 495–506.
24. J.P. Monchalin, *IEEE Trans. Ultrason. Ferroelectr. Freq. Control*, 33 (1986) 485.
25. V.N. In'kov, E.B. Cherepetskaya, V.L. Shkuratnik, A.A. Karabutov and V.A. Makarov, *J. Appl. Mech. Tech. Phys.*, 46 (2005) 452.
26. M. Dubois, P.W. Lorraine, R.J. Filkins, T.D. Drake, K.R. Yawn and S.Y. Chuang, *Ultrasonics*, 40 (2002) 809.
27. S.I. Stepanov, *Appl. Opt.*, 33 (1994) 915.
28. M. Clark, S.D. Sharples and M. Somekh, *IEEE Trans. Ultrason. Ferroelectr. Freq. Control*, 47 (1999) 65.
29. V.V. Aleksandrov and Ju.B. Potapova, *Solid State Commun.*, 84 (1992) 401.
30. M.H. Kuok, S.C. Ng, Z.L. Rang and T. Liu, *Solid State Commun.*, 110 (1999) 185.
31. M. Redwood, *J. Acoust. Soc. Am.*, 33 (1961) 527.
32. M.R. Layton, E.F. Carome, H.D. Hardy and J.A. Bucaro, *J. Acoust. Soc. Am.*, 64 (1978) 250.
33. A. Ilan and J.P. Weight, *J. Acoust. Soc. Am.*, 88 (1990) 1142.
34. T.J. Kim and W. Grill, *Ultrasonics*, 36 (1998) 233.
35. G.L. Gooberman, *Ultrasonics: Theory and Practice*, English University Press, London, 1968.
36. A. Neubrand and P. Hess, *J. Appl. Phys.*, 71 (1992) 227.
37. H. Coufal, K. Meyer, R.K. Grygier and P. Hess, *J. Acoust. Soc. Am.*, 95 (1994) 1158.
38. Y. Hong, S.D. Sharples, M. Clark and M.G. Somekh, *Ultrasonics*, 42 (2004) 515.
39. R.M. White, *J. Appl. Phys.*, 34 (1963) 3559.
40. J. Jarzynski and I.H. Berthelot, *J. Acoust. Soc. Am.*, 85 (1989) 158.
41. J. Blitz, *Fundamentals of Ultrasonics*, Butterworths, London, 1963.
42. J. Kushibiki and Y. Ono and I. Takanaga, *Electron. Commun. Jpn.*, 83 (2000) 8.
43. A.B. Bhatia, *Ultrasonic Absorption*, Dover, New York, 1967.
44. P. Grabielli and M. Mercier-Finidori, *J. Sound Vib.*, 241 (2001) 423.
45. P. Gregus, *Ultrasonic Imaging: Seeing by Sound*, Focal Press, New York, 1980.
46. J.R. Allegra and S.A. Hawley, *J. Acoust. Soc. Am.*, 51 (1972) 1545.
47. P.S. Epstein and R.R. Carhart, *J. Acoust. Soc. Am.*, 25 (1953) 553.
48. D.J. McClements, *Langmuir*, 12 (1996) 3454.
49. P.C. Waterman and R. Truell, *J. Math. Phys.*, 2 (1961) 512.
50. D.J. McClements, P. Fairley and M.J.W. Povey, *J. Acoust. Soc. Am.*, 87 (1990) 2244.
51. L.W. Anson and R.C. Chivers, *Ultrasonics*, 28 (1990) 16.
52. S. Takeda and P.J. Goetz, *Colloid Surface A*, 143 (1998) 35.
53. T.I.J. Goodenough, V.S. Rajendram, S. Meyer and D. Prêtre, *Ultrasonics*, 43 (2005) 231.
54. A.S. Dukhin and P.J. Goetz, *Ultrasound for Characterising Liquid Based Food Products*. Dispersion Technology Inc. Publication, 1999.
55. V.A. Del Grosso and C.W. Mader, *J. Acoust. Soc. Am.*, 52 (1972) 442.
56. G.C. Gaunaurd and H. Uberall, *J. Acoust. Soc. Am.*, 69 (1981) 362.
57. R.Y. Nishi, *Acustica*, 33 (1975) 65.
58. C.C. Habeger, *J. Acoust. Soc. Am.*, 72 (1982) 870.
59. A.S. Ahuja and W.R. Hendee, *J. Acoust. Soc. Am.*, 63 (1978) 1074.
60. W.H. Lin and A.C. Raptis, *J. Acoust. Soc. Am.*, 74 (1983) 1542.
61. V. Twersky, *J. Math. Phys.*, 18 (1977) 2468.
62. Y. Ma, V.K. Varadan and V.V. Varadan, *J. Acoust. Soc. Am.*, 87 (1990) 2779.

63. M.A. Al-Nimr and V.S. Arpaci, *J. Acoust. Soc. Am*., 93 (1993) 813.
64. L.D. Hampton, *J. Acoust. Soc. Am*., 42 (1967) 882.
65. A.L. Anderson and L.D. Hampton, *J. Acoust. Soc. Am*., 67 (1980) 1865.
66. A.H. Harker and J.A.G. Temple, *J. Phys. D. Appl. Phys*., 21 (1988) 1576.
67. D.J. Hiberd, A.M. Howe, A.R. Mackie, P.W. Purdy and M.M. Robins, *Food Emulsions and Foams*, Royal Society of Chemistry, London, 1987, p. 219.
68. A.J. Babchin, R.S. Chow and R.P. Sanatzky, *Adv. Colloids. Int. Sci*., 30 (1990) 111.
69. M. Hirao and H. Ogi, *Ultrasonics*, 35 (1997) 413.
70. A.P. Sarvazyan and T.V. Chalikian, *Ultrasonics*, 29 (1991) 119.
71. H.H. Demarest Jr., *J. Acoust. Soc. Amer*., 49 (1971) 768.
72. I. Ohno, *J. Phys. Earth*, 24 (1976) 355.
73. W.M. Visscher, A. Migliory, T.M. Bell and R.A. Reinert, *J. Acoust. Soc. Amer*., 90 (1991) 2154.
74. D.J. McClements and P. Farley, *Ultrasonics*, 30 (1992) 403.
75. E.A.G. Aniansson and S.N. Wall, *J. Phys. Chem*., 78 (1974) 1042.
76. M. Teubner, *J. Phys. Chem*., 83 (1979) 2917.
77. H. Nomura, S. Koda, T.Matsuoka, T. Hiyama, R. Shibata and S. Kato, *J. Colloid Interf. Sci*., 230 (2000) 22.
78. L. Landau and G. Placzek, *Phys. Z. Sow*., 5 (1934) 172.
79. J.P. Boon and S. Yip, *Molecular Hydrodynamics*, McGraw-Hill, New York, 1980.
80. B.J. Berne and R. Pecora, *Dynamic Light Scattering*, Wiley Interscience, New York, 1976.
81. Y. Ike and S. Kojima, *J. Mol. Struct*., 744–747 (2005) 521.
82. M.S. Greenwood, A. Brodsky, L. Burgess, L.J. Bond and M. Hamad, *Ultrasonics*, 42 (2004) 531.
83. D.B. Fraser and R.C. LeCraw, *Rev. Sci. Instrum*., 35 (1964)1113.
84. N. Soga and O.L. Anderson, *J. Geophys. Res*., 72 (1967) 1733.
85. A. Yaoita, T. Adachi and A. Yamaji, *NDT & E Intern*., 38 (2005) 554.
86. T. Geiges, G. D'Anna, S. Komiya and Y. Ando, *Physica C*, 408–410 (2004) 455.
87. N. Nakamura, H. Ogi and M. Hirao, *Ultrasonics*, 42 (2004) 491.
88. M. Clark, S.D. Sharples and M.G. Somekh, *IEEE Trans. Ultrason. Freq. Control*, 47 (2000) 65.
89. D. Schneider, B. Brenner and T. Schwarz, *J. Nondestr. Eval*., 14 (1995) 735.
90. C. Montes, D. Bahloul and I. Bongrand, *J. Op. Soc. Am*., B16 (1999) 932.
91. V. Grimalsky, E. Gutiérrez, S. Koshevaya and S. Mansurova, *Optik*, 3 (2003) 134.
92. M.S. Greenwood, A. Brodsky, L. Burges and L.J. Bond, *Review of Progress in Quantitative Nondestructive Evaluation*, 22B (2002) 1637.
93. C. Barnes, J.A. Evans and T.J. Lewis, *Ultrasonics*, 24 (1986) 267.
94. N. Masuhara, B.C. Watson and M.W. Meisel, *J. Low Temp. Phys*., 121 (2000) 815.
95. A. Moreau, D. Lévesque, M. Lord, M. Dubois, J.P. Monchalin, C. Padioleau and J.F. Bussière, *Ultrasonics*, 40 (2002) 1047.
96. U. Kaatze, R. Behrends and K. Lautscham, *Ultrasonics*, 39 (2001) 393.
97. M. Clark, S. Sharples and M. Somekh, *Meas. Sci. Technol*., 11 (2000) 1792.
98. D.J. McClements and P. Fairley, *Ultrasonics*, 30 (1992) 403.
99. T. Tong and J.W. Povey, *Ultrasonics*, 40 (2002) 37.
100. A.S. Dukhin and P.J. Goetz, *Ultrasound for Characterizing Colloids. Particle Sizing, Zeta potential, Rheology,* Elsevier, Amsterdam, 2002.
101. J. Andreae, R. Bass, E. Heasell and J. Lamb, *Acustica,* 8 (1958) 131.
102. J. Andreae and P. Joyce, *Brit. J. Appl. Phys.,* 13 (1962) 462.
103. P.D. Edmonds, V.F. Pearce and J. Andreae, *Brit. J. Appl. Phys.,* 13 (1962) 551.
104. C. Lu and A.W. Czanderna, Ed., *Piezoelectric Quartz Crystal Microbalances,* Elsevier, Amsterdam, 1984.
105. S. Kurosawa, H. Aizawa and J.W. Park, *Analyst,* 130 (2005) 1495.
106. R. Lucklum, *Analyst,* 130 (2005) 1465.
107. M. Pax, J.Rieger, R.H. Eibl, C. Thielemann and D. Johannasmann, *Analyst,* 130 (2005) 1474.

This page intentionally left blank

CHAPTER 10

Applications of Ultrasound-Based Detection Techniques

10.1. INTRODUCTION

Because ultrasound (US) can penetrate optically opaque materials, provides high-quality information about bulk properties at low cost in a rapid, non-invasive manner, and enables on-line measurements, detection techniques based on this form of energy have something to offer scientists and engineers at large and warrants consideration by anyone concerned with automated analyses and measurements.

Ultrasound-based detection techniques and their ensuing methods are being increasingly developed outside the traditional physical and electronic engineering environments of the earliest implementation. A wide range of disciplines currently use these techniques and have helped develop them further. Because each discipline has developed US-detection techniques as tools to an end rather than as ends in themselves, developments often have not been communicated beyond a small circle.

Clarifying some concepts of US-based detection techniques may help increase the appeal of the applications discussed below. Thus, these techniques require no cavitation as the power levels of US-based instruments are up to millions of times lower than those of US baths and probes. For example, US velocity measurements are usually made at very low power levels, so the analysed material is normally left intact. In addition, the use of low US power levels (*e.g.* below *ca*. 10 kW/m^2 in water at room temperature) results in elastic displacements (*i.e.* strain and stress are linearly related).

For some reason, there is the widespread belief that US velocity, on which many measurements are based, depends mainly on the density of the material through which US propagates. One connected misconception is that US velocity in a mixture of materials will be some average of the velocities of the mixture components.

Some types of measurements are given different names (*e.g.* "pulse-echo" measurements are also known as "pitch and catch", "pulse-echo time of flight" or "acoustic time of flight" measurements).

The wide acceptance of US-based detection techniques is a result of its non-invasive character and the variety of direct and indirect measurements it affords. Most measurements in ultrasonic spectrometry are based on two independent parameters namely ultrasonic attenuation and ultrasonic velocity. The former is determined by the energy losses in ultrasonic waves and can be expressed in terms of the high-frequency viscosity of the medium or its longitudinal modulus. This allows elucidation of the kinetics of fast chemical reactions, texture and microstructure, density and porosity in terms of particle size, aggregation, gelation, crystallization and other process characteristics, and also elastic constants, mechanical properties, corrosion and residual stress of materials. Ultrasonic velocity is determined by the density and elastic response of the sample to the oscillating pressure in the ultrasonic wave and can thus be expressed in terms of compressibility or the storage modulus. It is extremely sensitive to the molecular organization, composition and intermolecular interactions in the analysed medium, and is the basis for most applications of ultrasonic spectrometry to the analysis of chemical properties of materials.

However, measuring ultrasonic velocity requires the use of extremely sensitive instruments that were unavailable until fairly recently.

As with any analytical technique, it is important for US spectrometry users to have a thorough understanding of its underlying physical principles and of potential sources of errors adversely affecting measurements. The basis of ultrasonic analyses in a number of fields (particularly in food analysis) is the relationship between the measurable ultrasonic properties (velocity, attenuation and impedance, mainly) and the physicochemical properties of the sample (*e.g.* composition, structure, physical state). Such a relationship can be established empirically from a calibration curve that relates the property of interest to the measured ultrasonic property, or theoretically from equations describing the propagation of ultrasound through materials.

Before we discuss the applications of US-based detection techniques, we should emphasize the difference between the measured data and the desired output parameters. In ultrasound spectrometry, the measured data can be the attenuation coefficient, the sound speed and the acoustic impedance. However, the researcher is rarely interested in these measured properties, but rather on elastic moduli of solid samples; particle size distributions or rheological properties of heterogeneous samples; and concentrations, rheology, stability and chemical reactivity of liquids (particularly emulsions).

Obtaining these desired output parameters involves two steps. In the first step, tests are conducted on the target system in order to obtain a set of measured values for macroscopic properties such as temperature, pH, ultrasonic attenuation, etc. In the second, the previously measured data are analysed in order to compute the desired microscopic properties. Such analysis requires three tools: a model dispersion, a prediction theory and an analysis engine.

A "model dispersion" is used to describe the actual behaviour of the system under study in terms of a set of model parameters obviously including the desired microscopic characteristics. In fact, the model makes a set of assumptions about the real world in order to simplify the complexity of the phenomena involved and thereby also simplify the task of developing a suitable prediction theory. For example, most instruments measuring particle size assume that the particles are spherical, which allows a complete geometrical description of the particle to be given in terms of a single parameter (its diameter). Obviously, such a model could never accurately describe a dispersion of high-aspect ratio carpet fibres, so any theory based on such an over-simplified model might well give incorrect results. The model dispersion may also attempt to limit the complexity of a particle size distribution by assuming that it can be described by certain conventional distribution functions (*e.g.* a log-normal distribution).

A "prediction theory" consists of a set of equations that describes some of the measurable macroscopic properties in terms of the microscopic properties of the model system.

Finally, an "analysis engine" is essentially a set of algorithms implemented in a computer program which calculates the desired microscopic properties from the measured macroscopic data, using the knowledge contained in the prediction theory. The analysis can be thought of as the opposite, or inverse, of prediction. Prediction describes some of the measurable macroscopic properties in terms of the model dispersion. Analysis, on the other hand, given perhaps only few values for the model parameters, attempts to calculate the remaining microscopic properties by evaluating the measured data. A number of well-documented approaches to this analysis task have been reported.

The scheme followed to discuss the applications of US-based detection techniques is supported on the physical state of the measured system. Thus, a general distinction is made between applications to solid or liquid samples, and those involving two different states (*viz.* solid–liquid, solid–gas and liquid–gas systems).

10.2. ULTRASONIC ANALYSIS OF SOLID SAMPLES

Ultrasound detection as applied to solid samples can provide a variety of information depending on the particular technique and measured parameter(s). In addition to traditional US-based detection techniques for the analysis of solids (*e.g.* RUS [1]), a number of new techniques, modes and methods have been reported over the last five years which have opened up new avenues for the examination of solids.

The lack of sensitivity of laser-ultrasonics has been overcome by changing the generation wavelength from 10.6 μm of the CO_2 laser to the 3–4 μm range of an optical parametric oscillator based on a potassium titanyl arsenate crystal and an Nd:YAG laser, thereby significantly improving the generation efficiency [2]. Laser-ultrasonic surface wave dispersion spectrometry was long regarded as one of the leading candidates for non-destructive characterization of surface-treated metals on the grounds of its ability to probe material properties at different penetration depths depending on the inspection frequency. Recently, the dispersion of the surface wave has been found to be a superposition of different effects of surface treatment in the target material, including surface roughness, compressive residual stress and cold work. Although the surface roughness induced component is often the dominating part of the overall dispersion, experimental results also indicate that it is feasible to observe a perceivable change in the dispersion of the SAW when the specimen is heat-treated at different temperatures, which has no perceivable effect on the surface roughness [3]. Adaptive laser-US modes afford measurements of the phase velocity of laser generated and detected acoustic waves by means of an optical grating produced by an electronically addressable spatial light modulator (SLM); the SLM was imaged onto the sample surface in order to generate surface acoustic waves, the frequency and wavefront of which were controlled by the SLM. When the grating period matched the surface acoustic wavelength, the surface wave was strongly excited, which allowed the wavelength and hence the phase velocity, angular dispersion of the generalized surface wave and *pseudo*-surface wave of the specimen to be determined [4].

It is worthy of special note here that the advances in Brillouin scattering spectroscopy (BSS), have significantly broadened its scope of application, particularly as regards the characterization of mechanical properties of solids and thin solid films. The restriction imposed by the very low scattering efficiency of thermal surface phonons, which resulted in rather long data collection times (typically several hours for a single spectrum even if advanced multipass filters were used) was overcome by using light not only to detect, but also to excite surface phonons [5]. The joint use of generalized surface acoustic waves and *pseudo*-surface acoustic waves [6], and studies of the influence of temperature on the results of BSS at temperatures of 40–300 K [7] or up to 2500 K [8], among others, have fostered the use of this technique.

10.2.1. Ultrasonic parameters

The changes undergone by US on interacting with a solid, and the information that can thus be obtained from the solid, have been measured mainly through the US velocity and attenuation under resonant conditions. The ultrasonic parameters to be used and their processing are dictated by the final information required. Thus, the resistance to deformation is obtained by calculating the elastic moduli, the number and nature of which are a function of the nature of the solid (*e.g.* isotropic, anisotropic). However, equations relating the acoustic measurement to sample density, dimensions, material microstructure and thickness can usually be derived from simple parameters such as US velocity

and (or) attenuation. This allows more abundant and complex information to be obtained with present sophisticated US-based detection techniques or more flexible variants of conventional ones, as discussed below.

10.2.2. Determination of elastic constants

The constants that provide information about resistance to deformation in solids (*elastic moduli*) are of great importance in areas such as engineering, mechanical design, fracture analysis and life-time estimation. Ultrasound methods allow the determination of dynamic moduli, which are slightly higher than the static values generated by standard mechanical testing. The number of elastic moduli required to describe the response to stress (*i.e.* the force applied per unit area) depends on the nature of the solid; thus, an isotropic solid such as ordinary glass needs only two elastic moduli to describe its resistance to stress, the number increasing with increasing anisotropy. One of the moduli typically used to describe solids is the shear modulus; the others vary widely and include Young's modulus, Poisson's ratio, the compression modulus (K), the bulk modulus and the modulus that determines the longitudinal sound velocity. Young's modulus is a measure of stiffness when a long thin bar is stretched and stress is only applied at the ends; Poisson's ratio is the negative of the ratio of the strain — strain being the displacement caused by a stress — in the 2nd direction to the strain in the 1st direction.

One common feature of all moduli is that any strain generated in a solid is linearly proportional to the stress. This obviously requires that whatever stress is applied should not break or permanently bend the sample and that no significant energy be dissipated when the sample is strained. To revert to a careful dynamic description of the displacements, forces and energy is mandatory for high dissipation materials.

The most salient feature of the shear modulus is that it describes the stiffness of a solid to forces that do not change its volume. The complication is that there is no unique arrangement of forces producing a given shear distortion, as depicted in Fig. 10.1. The forces in boxes *a* and *c* are called "simple shear", presumably because they are the forces that most readily come to mind; however, the forces that generate simple shear also produce a rotation. The forces on *b* produce what is called "pure shear", presumably because they cause no rotation. However, the energy required to generate each of these distortions must be independent of the arrangement of forces.

Low-symmetry crystals posses some interesting, difficult to assimilate properties relating to stress waves and elasticity. Such properties relate to what is called "internal strain", by which an external stress produces strains in the unit cell of the crystal different from the macroscopic strain. This can occur if, for example, a lattice has at each lattice point a group of atoms (the basis) with symmetry different from that of the lattice.

In high-symmetry crystals, however, there are certain special directions and types of waves in which the polarization (motion of atoms) is either parallel (longitudinal) or perpendicular (shear) to the direction of propagation, just like in an isotropic solid. These include cubic, hexagonal, tetragonal and orthorhombic crystal symmetries, all characterized by having three mutually perpendicular planes of mirror symmetry; as a result, any compressive stress applied normal to a mirror symmetry can produce no lateral or shear strain because the crystal does not know which way to go.

Most methods for calculating elastic moduli are based on resonance ultrasound spectroscopy (RUS), which is applicable to specimens lesser than 1 mm^3. The equations relating the resonance frequencies of a solid with its density, dimensions and elastic moduli allow
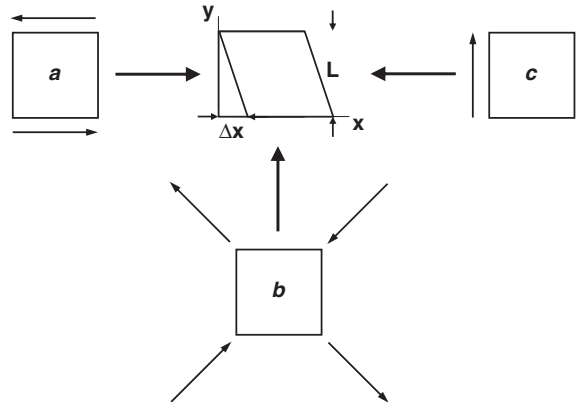
FIGURE 10.1. *Combinations of forces that lead to the same distortion without changing the volume. (Reproduced with permission of Wiley Interscience, Ref. [1].)*

efficient calculation of the resonance frequencies of the solid provided its density, dimensions and elastic moduli are known; also it allows one to work backward and determine these parameters from a measurement of the body's resonance frequencies [1]. A very fast, accurate solution to the direct problem (*i.e.* elastic moduli → resonance frequencies) is the key tool or the solution of the inverse problem (resonance frequencies → elastic moduli). However, the inverse problem is not as straightforward as there is no unique solution in this case; therefore, a non-linear optimization procedure must be used to determine a set of parameters producing resonance frequencies that are in the best possible agreement with the measured spectrum of the sample.

Theoretically, a maximum of 21 tensor elements of elastic stiffness for the triclinic crystal (the lowest-symmetry crystal) can be determined with one specimen. However, it is difficult to assimilate properties relating to stress waves and elasticity for such a low-symmetry crystal. In practice, RUS can determine nine tensor elements for orthotropic symmetry as well as for higher symmetry (isotropic, cubic, hexagonal or tetragonal).

One of the key uses of RUS is to determine the symmetry and obtain a rough estimate of the elastic stiffness in advance. The initial estimate should be close to the true value and can be obtained from the literature, experience, other measurements, etc. The test sample should be machined accurately. The calculated resonance frequencies and modes should be matched to the RUS measured values and the elastic stiffness can be converged by comparison and iteration.

The uses of RUS until 1997 (*e.g.* structural phase transitions, superconducting transitions, magnetic transitions) are widely discussed in Migliori's book [1]; therefore, interested readers are referred to it for such applications. More recent, key applications are discussed below.

High-temperature RUS has been used to determine dynamic anisotropic elastic constants of Zr–2.5Nb alloy for the pressure tubes in deuterium uranium reactors. The resonance frequencies were measured using a couple of alumina waveguides and wide-band ultrasonic transducers in a small furnace; rectangular parallelepiped specimens were fabricated along the longitudinal, radial and transverse direction of the pressure tubes. A nine elastic stiffness tensor for orthotropic symmetry was determined in the

range of room temperature up to 500°C. The elastic tensor, C_{ij}, decreased gradually with increasing temperature. Higher elastic constants along the transverse direction compared to those along the longitudinal or radial direction were found to be similar to Young's modulus or the shear modulus. Crossing of elastic constants along the longitudinal and radial directions — which correlated with the crossing characteristics of c_{44} and c_{66} in a zirconium crystal — was observed near 120–150°C [9]. Recently, the elastic moduli of polycrystalline $TiCr_{1.8}$ over the temperature range of 3–410 K were reported [10].

The effective elastic properties of a porous material may be quite different from those corresponding to a fully dense material and difficult to predict from microstructural parameters, especially if the volume fraction of the pores is high or the pores are highly non-spherical. Obviously, both the effective moduli and the effective density are reduced by the presence of pores. While the density decreases linearly with increasing volume fraction of pores, the dependence of elastic moduli on porosity is much more complex as it is not just governed by the volume fraction of the pores, but also by their shape, spatial and orientation distribution. For certain simple shapes and arrangements, there exist theories that can be used to predict the effective elastic moduli for spherical and disk-like pores; in practice, however, reliable modulus data must very often be determined experimentally because the available theories do not apply or because the effort to obtain the input parameters required for a reliable theory-based prediction would be enormous. Owing to strong attenuation caused by scattering, standard high-frequency ultrasonic propagation methods very often cannot be used on small-sized specimens of porous materials. In this situation, ultrasonic phase spectroscopy involving relatively low-frequency continuous waves transmitted through the specimen provides viable methods to measure wave velocities — and also acoustic impedances and elastic constants as a result — along relatively short pathlengths in extremely porous, strongly attenuating materials [11].

Preliminary studies of the effect of high magnetic fields (up to 7 T) and low temperatures on the elastic constants and US attenuation in single-crystal $La_{2-x}Sr_{-x}CuO_4$ in the low doping region ($x = 0.01$) by using RUS in the frequency range 0.1–2 MHz have demonstrated that, below 10 K, an increased modulus and a large increase in attenuation occur; below 5 K, the attenuation decreases further [12]. The behaviour of both parameters was studied at all resonance frequencies observable at such low temperatures. Concerning the effect of the magnetic field, no change in the modulus was observed within the accuracy range of the measurements. It should be noted that similar tests involving a magnetic field of around 5 T along the x-axis and undoped La_2CuO_4 exposed a weak ferromagnetic transition [13,14].

The name of resonant sphere technique (RST) is given to the methods using a spherical specimen. This name is inappropriate inasmuch as it is contradictory; thus, the correct designation would be "resonant sphere methods" (RSMs). Such methods are of special interest because they allow a spherical specimen to be made accurately and its natural frequencies to be solved theoretically. This type of methods, developed by Fraser and LeCraw [15] and improved by Soga and Anderson [16], are widely applied in material science, geophysics and non-destructive inspections, among other areas. Methods for measuring the elastic moduli of both isotropic and anisotropic materials [17], the pressure dependence on elasticity [18,19] and surface defect inspection [20] of spherical samples have been reported, all of which determine elastic moduli in the resonant modes. Recently, Yaoita *et al*. reported two methods for determining the elastic moduli of spherical specimens that require no information about the resonant modes. One is a full-search method that compares the measured frequencies with the theoretical ones computed from assumed transverse wave velocity and Poisson's ratio; the other is a simplified method for determining only Poisson's ratio after evaluating the transverse wave velocity from the lowest resonant frequency. These methods require adequate numbers of

resonant frequencies including the sensitive mode to Poisson's ratio without any identification of the vibration mode. Both methods were validated by determining the elastic moduli of ball lenses made of glass; the frequencies calculated from the elastic mode thus determined were in good agreement with the measured values; thus, the absolute inaccuracy in Δf was less than 0.4% (see Table 10.1) [21].

A recent method for studying the elastic properties of thin films uses RUS in combination with measurements of deformation distributions on the vibrating specimen surface obtained by laser-Doppler interferometry [22]. The two main difficulties faced in the determination of a reliable set of film C_{ij} values were accurately measuring the resonance frequencies and correctly matching calculations and measurements. Because the contributions of the film's C_{ij} values to the resonance frequencies are usually small, they must be measured with a high accuracy; this requirement was met by developing the piezoelectric tripod of Fig. 10.2, on which the specimen (a silicon substrate with a 1.9 μm copper film) was placed. The tripod consists of two pinducers and a support stick: one pinducer supplies a sinusoidal continuous wave (cw) signal to vibrate the specimen and the other detects the oscillation amplitude. By sweeping the frequency of the cw signal and measuring the oscillation amplitude as a function of the frequency, the multipeak resonance spectrum of Fig. 10.3, was obtained; fitting the Lorentzian function to the peaks allowed the free-vibration resonance frequencies to be determined. Ideal free vibration occurred because the piezoelectric tripod required no coupling agent between the transducers and the specimen, and no force was applied to the specimen except for its own weight. The resonance peak heights varied depending on the positions of the contacting pinducers on the specimen face; however, the resonance frequencies did not change, so they were measured at a constant temperature of 30°C, with deviations better than 10^{-4} — which was much smaller than the contributions of the film C_{ij} to the resonance frequencies. In order to carry out the inverse calculation, and taking into account that the modes of the calculated resonance frequencies were known, the identical modes from the measured spectrum must be found. The large number of resonance frequencies and peak overlap

TABLE 10.1 *Comparison of measured resonant frequencies (f^{exp}) and frequencies (f^{cal}) calculated with the two methods proposed by Yaoita et al.*

K	1Mode	2Measured (f^{exp})	Full-search f^{cal}	Full-search $\triangle f$(%)	Simplified method f^{cal}	Simplified method $\triangle f$(%)
1	$_1T_2$	1.437	1.434	0.248	1.437	0.000
2	$_1S_2$	1.512	1.510	0.108	1.514	− 0.134
3	$_2S_1$	1.913	1.914	− 0.042	1.917	− 0.215
4	$_1T_3$	2.213	2.216	− 0.129	2.221	− 0.377
5	$_1S_3$	2.234	2.235	− 0.062	2.240	− 0.296
6	$_1S_0$	2.355	2.355	0.025	2.355	0.012
7	$_2S_2$	2.724	2.724	− 0.015	2.728	− 0.193
8	$_1S_4$	2.854	2.854	− 0.006	2.860	− 0.236
9	$_1T_4$	2.921	2.921	0.015	2.927	− 0.233
10	$_2T_1$	3.306	3.304	0.068	3.311	− 0.180
Transverse wave velocity			3602 m/s		3610 m/s	
Poisson's ratio (v)			0.212		0.210	

Units are in MHz. $\Delta f = (f^{exp} — f^{cal})/f^{exp}$
(Reproduced with permission of Elsevier, Ref. [21].)
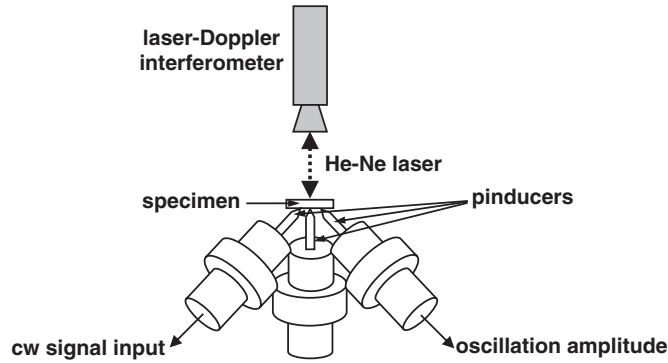
FIGURE 10.2. *Experimental set-up used to study the elastic properties of thin films by RUS. The resonance frequencies are measured with the piezoelectric tripod. The scanning laser-Doppler interferometer draws the oscillation displacement of specimen surface. (Reproduced with permission of Elsevier, Ref. [22].)*

made mode identification difficult; unmistakable mode identification was provided by laser-Doppler interferometry, which allowed the out-of-plane displacement of the vibrating specimen at each resonance mode to be determined. The frequency of the reflected laser beam changed depending on the vibration frequency because of the Doppler effect. Measurement errors in the resonance frequencies caused deviations in the resulting film C_{ij}; the error bands (ΔC_{ij}) from the contributions of C_{ij} to the resonance frequencies ($f/(C_{ij})$ and the measurement errors of the resonance frequencies Δf were estimated as

$$\Delta C_{ij} = \frac{1}{\partial f / \partial C_{ij}} \Delta f \qquad (10.1)$$

where f/C_{ij} can be obtained from the inverse calculation [23].
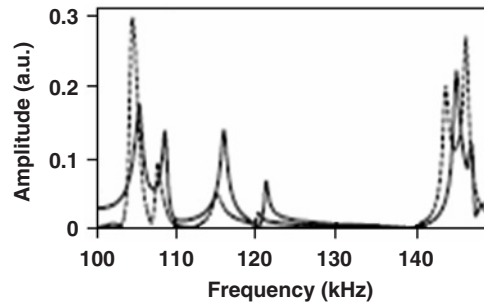
FIGURE 10.3. *Resonance spectra obtained with the piezoelectric tripod in Fig. 10.2. Solid and dashed lines represent the resonance spectra for the substrate alone (made of silicon) and for copper (1.9 µm thick)/silicon specimen, respectively. After deposition, the resonance peaks shifted to lower frequencies. (Reproduced with permission of Elsevier, Ref. [22].)*

The information provided by RUS and reflected leaky Lamb waves (LLWs) for the determination of ultrasonic wave velocities and phase velocity dispersion curves of an Inconel 600 plate — a material employed to produce steam generator tubes for nuclear power plants — were compared [24] and the longitudinal and the transverse wave velocities of the specimen determined by RUS, pulse-echo and cut-off frequencies of LLWs. The wave velocities obtained by RUS under the assumption of isotropic symmetry differed from those provided by other methods. However, the wave velocities in the direction of thickness obtained by RUS under the assumption of orthotropic symmetry were quite similar to those obtained with other methods as they measured wave velocities in the direction of thickness.

The diffusion bond strength between two identical materials can be determined from a single normal incidence ultrasonic measurement based on the fact that imperfections in diffusion bonds result in reflection of some ultrasonic energy from the interface separating the two substrates. The imperfect diffusion bond is characterized by the interfacial spring stiffness, which is determined from the reflected signal spectrum [25].

Comparison of the use of infrared absorption and US techniques based on pulse-echo measurements confirmed and supplemented the results provided by each other, thus helping clarify the anomalous behaviour of manganese–phosphate glasses doped with Nd_2O_3 in three composition regions as observed by IR [26]. Also, complementary studies of elastic properties by continuous-wave phase ultrasound spectroscopy and microstructural changes of plasma-sprayed alumina during consolidation of metastable phases exposed to high temperatures by electron microscopy, X-ray diffraction and porosimetry provided interesting information about the evolution and relationship of microstructural changes and elastic properties; this further testifies that ultrasonic spectroscopy is especially suited to porous, highly attenuating materials [27].

10.2.3. Microstructure and thickness studies using ultrasound-based detection techniques

The microstructural characterization of materials and investigation of elastic properties have been two topics of interest for a long time. Attenuation and velocity are the two main ultrasonic parameters used to extract information from materials. It is generally believed that, in polycrystalline materials, ultrasonic waves are attenuated predominantly by scattering, so theoretical expressions describing ultrasonic attenuation through grain scattering [28] and relating the effective grain size to the average size over the grain distribution [29] have been reported. Many of the earliest ultrasonic studies involved piezoelectric transducers in contact with the sample [30,31] and were later followed by electromagnetic, non-contact transducers [32] and eddy current testing [33].

The need for an uncoated area in the substrate in order to obtain a reference signal from the substrate surface was overcome by Hänel using a lens that focused acoustic waves first on the front of the sample and then on its back (see Fig. 10.4A) and collecting the sound echoes from both zones. In this way, he obtained the response of Fig. 10.4B, from which the thickness of the samples was calculated from known relations following the determination of the longitudinal sound velocity using an equation derived by Hänel [34].

A unique set of interfacial stiffness constants suffices to characterize the macroscopic elastic response of an interface between two rough contact surfaces regardless of the direction of incidence of the ultrasonic wave [35]. In addition, the stiffness constants of a double interface can be successfully recovered by combining ultrasonic spectroscopy and pulse-echo measurements with the theoretical procedures available for a single imperfect interface.
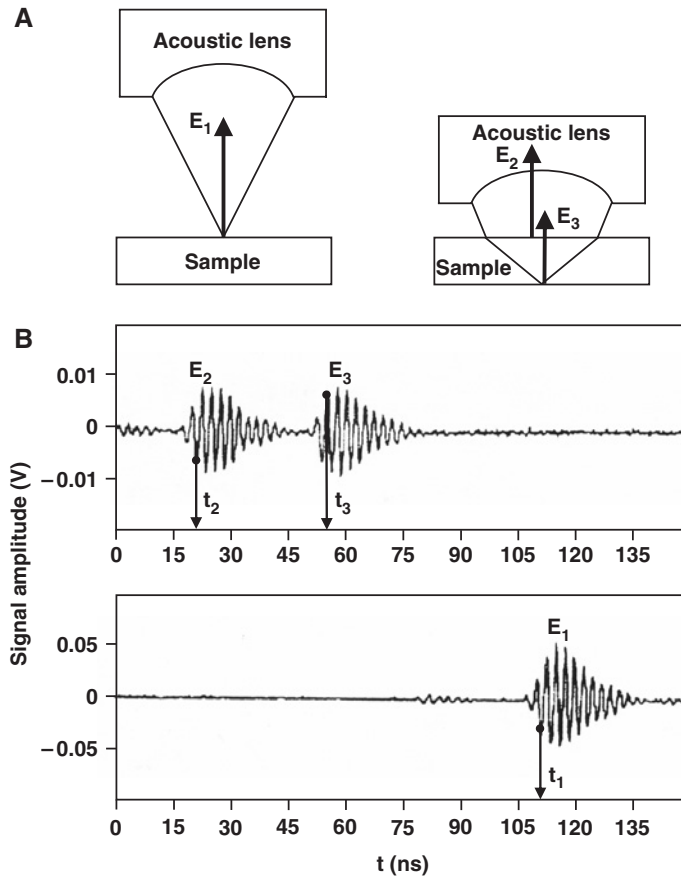
FIGURE 10.4. *(A) Acoustic lens focused on the front (left) and back (right) the acoustic waves. (B) Measured sound echoes from both zones. Above: front and back echo with the lens focused on the sample's back. Below: front echo with the lens focused on the sample front. (Reproduced with permission of the American Institute of Physics, Ref. [34].)*

At present, laser ultrasonic equipment is used in non-contact ultrasonic studies involving the excitation and detection of bulk elastic waves in point sources of planar geometry [36], the determination of material properties by use of laser-excited and detected surface acoustic (Rayleigh) waves [37], that of surface roughness by using a dual-probe laser interferometer and attenuation of Rayleigh waves [38] or elucidating the effect of hardening treatments of steel on the velocity of laser-induced Rayleigh waves [39]. The ensuing methods were all laser surface acoustic wave methods — which differ from half-optical methods in which the latter only use optical means for generation or detection — this avoids the acoustic coupling problems of piezoelectric transducer-based methods (*e.g.* damping in the transducer and the couplant, reflection and transmission losses). Contrary to the bulk wave regime, only one sample side is needed for excitation and

detection. This not only facilitates measurements but also avoids the need for an accurate knowledge and uniformity of the sample thickness.

Figure 9.14 depicts the instrumentation required to implement these methods, which was used to study the microstructure of cast iron (*i.e.* precipitated graphite particles of variable morphology embedded in an iron matrix) and its influence of some properties of the material. Thus, cast iron samples of diverse graphic morphology were subjected to non-contact, non-destructive evaluation by using Rayleigh waves from a focused laser line source and detecting the resulting displacements with a laser interferometer. The influence of microstructure sensitivity on ultrasonic attenuation and velocity was clearly apparent from the substantial differences in ultrasonic parameters between samples. The frequency dependence of the ultrasonic attenuation was determined in a band-width including the three characteristic regions of scattering. The results were used to evaluate the average scattered size of the samples using scattering theory, which correlated well with the particle size obtained from a quantitative micrographic analysis [40]. This study encouraged further research on the elucidation of the effects of scattered size distribution on the attenuation spectrum and on the inverse problem (*i.e.* the ultrasonic determination of the grain size distribution). Thus, a structural analysis of ferrous quartz was carried out in the three characteristic regions given by the theoretical model of longitudinal wave scattering as a function of the wavelength and average size of inhomogeneities (*e.g.* pores, grain, microcrystals) [41]. The method involved producing short acoustic pulses during the absorption of laser emission in optophone, irradiation of the geomaterial surface, data collection of US disturbances passed through the sample at high temporal resolution and comparison with complex spectra of the probing acoustic pulse and the signal transmitted through the sample in order to determine the attenuation spectrum. This was analysed by a software package including fast Fourier transform, consideration of amplitude coefficients of ultrasonic wave reflection on the medium boundary and diffraction of acoustic beams in a *quasi*-optical approximation.

Art characterization and conservation have also exploited the advantages of ultrasonic laser spectroscopy. The shortcomings of use of typical US-based instruments (*e.g.* the need to bring the transducer in close contact with a flat surface and the inability of commonly used ultrasound frequencies (1–20 MHz) to resolve sub-millimeter details within a paint layer) have been circumvented by using laser-induced stress waves generated by illuminating one surface of the artwork with a Q-switched laser beam. The light explosively ablates a minute portion of the surface, thereby launching an ultrasonic pulse into the material. When the wave reaches the opposite surface, it is detected with a laser vibrometer. This provides a non-contact way of ultrasonically mapping artwork interiors and detecting flaws, interfaces and detachments [42].

Scanning ultrasound microscopy (SAM) provides one other way of investigating microstructures by using US waves to measure the mechanical properties of the sample constituents. The resulting image shows the impedance contrast among the constituents, which is determined by variations in their densities and elastic properties (velocity and attenuation). Thus, SAM can provide images of the material that are complementary to optical and scanning electron microscopy images.

Thin films and coatings are widely used for manufacturing purposes in the microelectronics, automotive and aerospace industries, among others. Their applications range from ordinary paint to produce coatings in optical systems, wear-resistant layers in gear boxes and thermal barriers in combustion chambers. Significant efforts have been devoted to the development and characterization of new coatings, the mechanical properties and adhesion to substrates of which are difficult to measure with traditional methods; a pressing need for non-destructive quantitative methods for surface layer characterization therefore exists.

One of such methods is based on spectra obtained from normal and oblique incidence reflection and transmission US, which are plotted as a function of six non-dimensional parameters of the coating determined from two types of spectra. The six non-dimensional parameters allow the reconstruction process to be transformed from one search in a six-dimensional space to two searches in three-dimensional spaces (one search for normal incidence and one for oblique incidences). Thickness density and longitudinal and shear elastic moduli of the coating and attenuations can be determined for thicknesses less than the ultrasonic wavelength from the non-dimensional parameters [43]. It should be noted that US-based examination of coatings is particularly useful for polymer-coated systems as the impedance of metals is about tenfold more than that of common polymers.

10.2.4. Evolution monitoring

The productivity and quality objectives of today's industry require tighter control and the development of new process technologies. These new demands have led to the development of more sophisticated sensors for all process stages.

The evolution of viscoelastic properties during the formation of polymer films has been determined by using an ultrasound-reflection method [44]. First, the complex share modulus G^* and the complex longitudinal modulus $L^* = K^* + 4/3 \, G^*$ of the samples were derived from the measured complex reflection coefficients of an ultrasonic shear and longitudinal wave, respectively; from them, Young's modulus (E), the compression modulus (K) and the Poisson ratio (ν) for isotropic materials can be calculated, as in the study of the time-dependence of the moduli during film formation from an aqueous polymer dispersion or that of isothermal curing of an epoxy resin. The simultaneous excitation of longitudinal and transversal ultrasonic waves in a cell with normal incidence of both types of waves enabled the determination of various elastic constants in a single measurement. Figure 10.5 shows the time evolution of the moduli G and K (A), and the Poisson ratio (B), during the reaction of an epoxy resin.

Acoustic attenuation spectra have proved a powerful tool for studying relaxation processes in glassy electrolytes as they exhibit distinct peaks corresponding to transport mechanisms originating from the different types of sites responsible for ionic hopping. Spectra were analysed in connection with the frequency response, activation energy at spectral peaks and peak intensities, using theoretical double-power-law-function models and a suitable mathematical treatment for the simulations in order to fit the experimental data. The influence of chemical composition on ion transport mechanisms, frequency response, peak intensity and activation energy was established [45].

The evolution of the capillary network of reactive powder concrete during hydration processes was monitored by pulse-echo US in combination with shrinkage measurements. Two characteristic porous classes were thus identified, namely: one of 10–20 nm, and the other of 1 or 2 nm, associated with the porous space between C–S–H hydrate clusters and the internal porosity of the hydrate, respectively. The evolution of the active capillary radius as a function of the degree of hydration is consistent with the strong interaction between the capillary network size and the chemical activity given by the dissipated calorimetric power curve [46]. The mechanical aspect of ageing of blown extruded polyethylene films exposed to severe weathering conditions outdoors was monitored by measuring velocities and attenuations of ultrasonic waves propagating in several directions in the film plane. Calculation of stiffness constants and energy dissipation terms showed that stiffening of the material led to an increase in velocity and a decrease in wave attenuation [47].
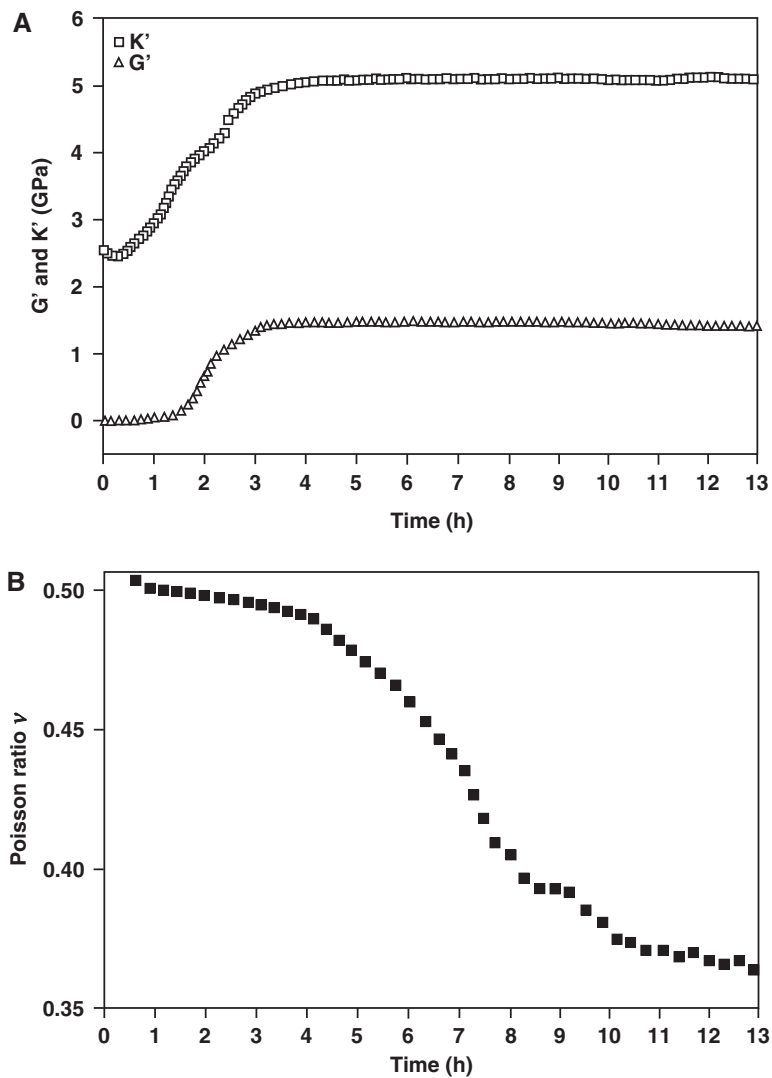
FIGURE 10.5. *(A) Temporal changes in the moduli G′ and K′ during curing of an epoxy resin. (B) Variation of the Poisson ratio during the curing of an epoxy resin. (Reproduced with permission of Wiley, Ref. [44].)*

The evolution of US-induced crystallization around the glass transition temperature for metallic glass was monitored by electromagnetic acoustic resonance, which allowed resonance frequencies and internal frictions to be measured. In an as-cast glassy sample, such frequencies jumped up just above the glass temperature transition at the beginning of the process under ultrasonic vibration; this was ascribed to nano-crystallization as confirmed by an X-ray diffraction profile, which was absent in the absence of US. Irregular Λ-shaped internal-friction peaks were also observed prior to abrupt crystallization [48].

Resonant US spectroscopy is also the technique of choice for studying the vibration behaviour of the metastable β phase near the martensic transformation of a single crystal Cu–27.96 at.% Al–3.62 at.% Ni shape memory alloy. The elastic constants C_{ij} of the anysotropic material and the internal friction Q^{-1} (C_{ij}) were determined, and the elastic constants C' and C_{44} found to be the quantitities controlling the vibrational response of the β phase near the martensic transformation; on the other hand, the evolution of the internal friction was found to be correlated with the elastic behaviour of the alloy [49].

Moreau *et al*. developed on-line measurements of texture, thickness and plastic strain ratio of sheet metal on the production line by laser-US resonance spectroscopy [50]. A short laser pulse was used to generate a broad-band US pulse that was detected with a laser interferometer. A large number of echoes were collected and analysed using Fourier approaches to determine the natural resonance frequencies in the thickness of the sheet. One longitudinal and two shear frequencies, and their harmonics, were measured and two crystallographic orientation distribution coefficients and highly accurate measurements of the sheet thickness corrected for changes in ultrasonic velocity caused by texture variations were obtained. The calculated coefficients enabled evaluation of the average and in-plane twofold and fourfold variations of the plastic strain ratio, with sensitivities sufficient to detect systematic variations in texture along the length of production coils with on-line repeatability of the order of *ca*. ± 0.02.

Ultrasound-based sensors for metal-coated fiber optic measurements based on interferometric determination of the displacement using a Michelson interferometer have also been designed. The input acoustic field can be detected by using two reference methods, namely: (a) time-delay spectroscopy with a calibrated hydrophone (a hydrophone with known frequency response determining the sound pressure, the input displacement being obtained by simple algebra); and (b) the interferometric foil technique (the displacement of a metallized foil situated at the surface of the fluid measured by the interferometer used for fibre tip measurements). The frequency dependence of the transfer function compared well with the theoretical models [51].

10.2.5. Ultrasound-based determination of fatigue, damage and degradation

Measurements of fatigue, damage and degradation of materials under typical or extreme conditions are essential in a number of industries (*e.g.* aircrafts, marine, off-shore oil platforms, automotive) for safety reasons. Such is the case with thermo-mechanically produced low-carbon steels, which have a high strength and excellent weldability compared to conventional carbon steels; this has promoted their use as structural material for construction, ship building and offshore application. However, they are relatively prone to corrosion, damage being generally accelerated by external fatigue loads, stress concentration and welding residual stress. This required evaluating microstructure evolution during tension–compression fatigue tests in order to elucidate the environmental fracture characteristics of steels for safety design and integrity evaluation, preferably using non-destructive methods. Electromagnetic resonance studies have shown that US attenuation is highly sensitive to the accumulative fatigue damage and exhibits a minimum at around 20% of the lifetime; this has been ascribed to a dramatic change in dislocation mobility and rearrangement, which is supported by TEM images of the dislocation structure [52]. Not only US attenuation, but also US velocity has proved to be useful for obtaining information on corrosion-fatigue tests of these materials. The back-scattering profile of Rayleigh surface waves (*i.e.* the amplitude variation of back-scattered US with the incident angle) was measured after a corrosion-fatigue test and revealed that the velocity

of Rayleigh surface waves as determined from the incident angle at which the profile of back-scattered US peaked, decreased for the specimen exhibiting the largest number of cycles to failure in the corrosion-fatigue test [53].

Also, a number of RUS methods have been used for microdamage diagnostic. Thus, non-linear elastic waves have proved as class of powerful tools for exploring the dynamic non-linear stress–strain features in the compliant bond system of a micro-inhomogeneous material and linked them to micro-scale damage. Hysteresis and non-linearity in the constitutive relation resulted in ultrasonic wave distortion, which caused changes in the resonance frequencies as a function of the drive amplitude, generation of accompanying harmonics, non-linear attenuation and multiplication of waves of different frequencies. The sensitivity of non-linear methods to the detection of damage features seems to be far greater than that of linear acoustic methods (*viz.* methods based on measurement of wave speed and dissipation) [54]. Recently, a method incorporating high frequency pulsed angle beam ultrasonic measurements modulated by low frequency vibrations of a bonded structure was reported. The use of parametric non-linear mixing between high and low frequencies to characterize adhesive degradation showed that good quality — undamaged — bonds exhibit little dependence of ultrasonic signature on the overlay of low frequency vibration loads; however, environmentally degraded or imperfect bonds exhibit strong modulation of the resonance frequency of the ultrasonic signal reflected from the bond [55]. The elastic properties and anisotropy of intermetallic laminate composites, and the effect of internal stresses due to differences in the thermal expansion coefficient on fracture toughness have also been examined by RUS [56].

Laser-induced US spectroscopy has been used to study the effect of microcracks in rock specimens on non-linear distortion of the elastic pulse shape [57].

Comparison of several techniques (namely Fourier transform infrared spectroscopy (FTIR), simultaneous thermogravimetric analysis–differential scanning calorimetry (TGA–DSC) and ultrasonic spectroscopy) for assessing the residual physical and mechanical characteristics of polymer matrix composites (PMCs) exposed to excessive thermal loads showed the measured power spectra of ultrasonic energy to correlate with performance of graphite fibre epoxy matrix composites exposed to thermal degradation, and also that analyses with the three techniques all pointed to the same critical temperature at which thermally induced damage increased sharply [58].

Complementary studies based on measurements of US-velocity changes and Raman spectroscopy were performed on bulk single-crystalline silicon irradiated with high doses of fast neutrons and compared with the non-irradiated material; this revealed the presence of tunnelling states in highly coordinated bulk silicon [59].

10.2.6. *Membrane compaction and fouling–cleaning studies by ultrasonic time-domain reflectometry*

The examination of synthetic membrane processes involves considering phenomena in three different regions: (a) the membrane; (b) the fluid boundary layer including the membrane–fluid interface and the potential presence of a cake or fouling layer; and (c) the bulk fluid in the membrane module. The performance of the membrane process is determined by the nature of the three regions and the way they interact. Thus, the intrinsic transport properties of the membrane are influenced by concentration polarization and fouling, which are in turn affected by the hydrodynamics of the membrane module or housing. A number of techniques including refractometry and interferometry, photo-interrupt sensoring, video, fluorimetry, particle image velocimetry, impedance spectrometry, ultrasonic

reflectometry, constant temperature anemometry, NMR, computer-aided tomography and electrochemical and radio isotope techniques have been used for the non-invasive observation of membrane processes [60]. Few techniques such as ultrasonic reflectometry have made the transition from difficult to use research equipment to the robust equipment required for in-field use, however.

Much has been written over the last 30 years about the relationship between permeate flux decline and changes in membrane structure upon application of a transmembrane pressure. This phenomenon has been termed "*compaction*" and documented in reverse osmosis, ultrafiltration, gas separation and, more recently, in membrane distillation. Although there has been considerable disagreement on the exact nature of these morphological changes, the decrease in membrane thickness observed has been recognized as a predominantly viscoelastic response (*i.e.* creep, in which strain changes as a function of time in response to the application of a constant compressive stress). Creep is generally represented in terms of an instantaneous elastic component, a time-dependent, recoverable component and a time-dependent but non-recoverable viscous component. Additional aspects which make the mechanical behaviour of membranes difficult to assess include the effects of localized stress concentrations at the pore wall/sub-structure interface and the response to pressure cycling.

One major limitation in compaction studies has been the inability to obtain direct simultaneous measurements of permeate flux and membrane thickness changes in real time; thus, compressive strains have been obtained indirectly *via* flux-decline experiments, or independently using a variety of mechanical testing arrangements. Whereas the accuracy of the former depends on the nature of the assumptions that underlie the flux-decline model utilized, compressive strains measured *via* the latter typically overestimate the actual mechanical response because the influence of fluid under pressure moving through the membrane pores is not included in these "static" tests.

Ultrasonic time-domain reflectometry (TDR) has proved to be an excellent tool for obtaining compaction measurements in real time under realistic operating conditions, thus enabling quantification of membrane compressive strain. The experimental set-up used for this purpose is depicted in Fig. 10.6A. One requirement of the ultrasonic transducer size (for generating and receiving the ultrasonic signals) was an area (a 0.5-cm diameter circular contact area) much larger than the size scale of any inhomogeneities due to features such as the membrane pores. The membrane sample was placed on a rigid, metallic porous support with an average pore size of *ca*. 5 μm and sealed between two aluminium cell plates. The vertical distance between the membrane and the top plate was *ca*. 2 mm. Figure 10.6B shows the measurements needed to apply the theory underlying the use of ultrasonic TDR for membrane application, which can be found elsewhere [61,62]. In summary, partial reflection of a longitudinal ultrasonic wave can occur from any planar interface across which a difference in acoustic impedance exists. Reflections can be obtained from the top plate–feed solution interface (a), the feed solution–top membrane surface interface (b) and the bottom membrane surface–support plate interface (c). Since each of these waves will travel a different distance to and from the transducer, they can be distinguished on the basis of their different arrival times if sufficient signal resolution is available. During compaction, the top membrane surface will move farther from the transducer, causing a change in the arrival time of signal b, as shown in Fig. 10.6C. The difference in signal arrival time between reflections b and b′ can be quantified and converted into a change in membrane thickness by using a simple relationship [63].

Membrane fouling is a very complex phenomenon owing to the wide variety of foulants that can be encountered in practice. Even for a specific application, fouling depends on

A

B

C
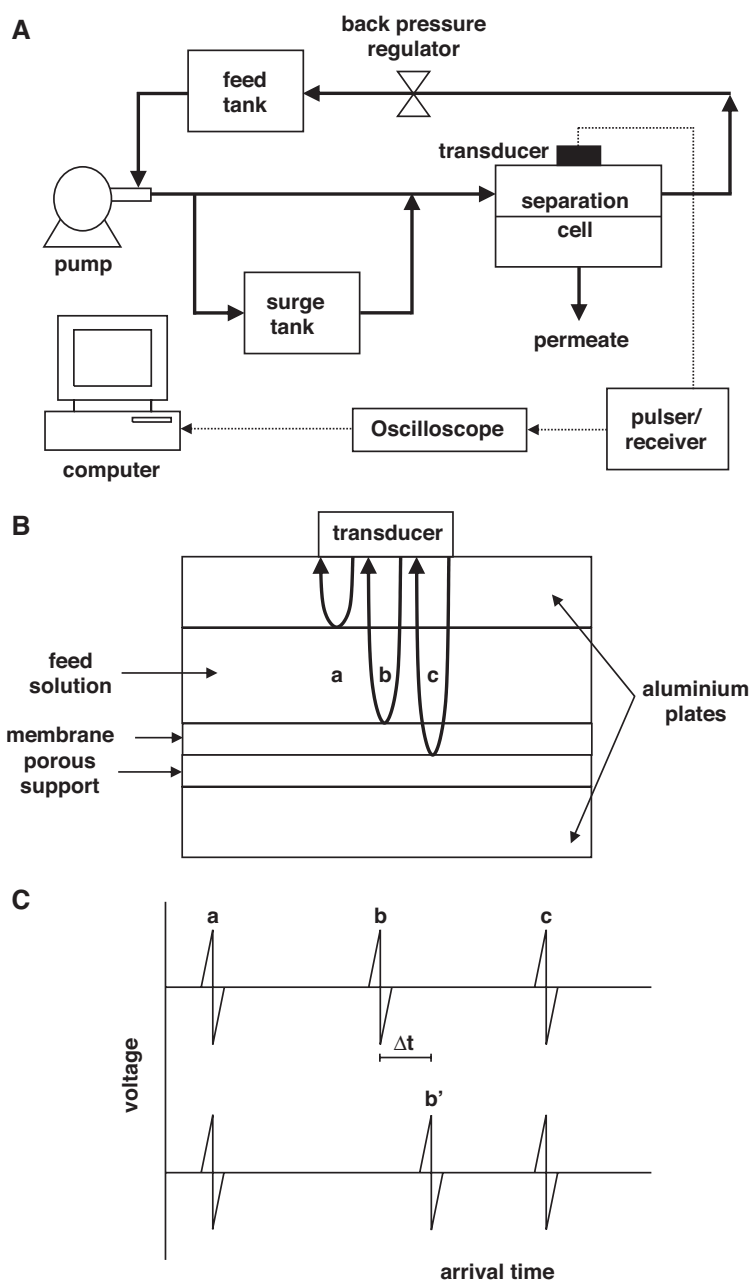
FIGURE 10.6. *(A) Experimental set-up used for membrane compaction studies of a high-pressure separation system by ultrasonic time-domain reflectometry. (B) Scheme of the separation cell showing the externally mounted transducer and the primary reflections identified as a, b and c, which correspond to the top plate–feed solution interface, feed solution–top membrane surface interface and bottom membrane surface–support plate interface, respectively. (C) Change of the arrival time which translates into changes in membrane thickness during compaction. (Reproduced with permission of Elsevier, Ref. [63].)*

physical and chemical parameters such as concentration, temperature, pH, ionic strength, contacting hydrodynamics and specific interactions in the separation system. The occurrence of fouling is traditionally inferred from a decline over time in flux or product quality in terms of the concentration of the rejected component in the permeate. However, such an inference is complicated by the fact that membrane compaction and degradation may occur simultaneously with fouling. Since each of these processes can contribute to a flux decrease or product quality change, it is often impossible to identify the particular combination of phenomena associated with an observed performance decline. Predictive measures of fouling tendencies for a given feed solution can also be obtained *via* "fouling tests" that provide parameters such as the silt-density index, modified fouling index or Langelier saturation index; these parameters, however, have proved unreliable as a result of significant differences between actual operating conditions and laboratory testing environments. Membrane autopsy has been employed for after-the-fact characterization of fouled membranes in order to identify major foulants and optimize pretreatment and cleaning procedures. Clearly, such destructive analyses come at the cost of productivity and efficiency. Preventive measures that minimize fouling and reduce the need for cleaning are the key solution; this is also provided by TDR, which is ideally suited to real time monitoring of membrane fouling. Mairal *et al*. found changes in the ultrasonic TDR signal amplitude to be well correlated with development of the fouling layer and with surface coverage as the permeate flux declines [64].

Concerning cleaning tests, the US amplitude of TDR responds to fouling layer removal at least as rapidly as the permeation rate, not only at high pressure, but also at atmospheric pressure, confirmed by after-the-fact permeability tests and morphological analyses. Since most industrial cleaning strategies involve ambient pressure operation, the ability to detect fouling removal at atmospheric pressure in real time is quite useful for optimizing fouling remediation strategies. Moreover, the ability of this technique to detect subtle changes (*e.g.* partial disengagement) in the fouling layer may aid in understanding the mechanisms of membrane cleaning. In any case, the suitability of this technique for monitoring commercial membrane separation processes depends on the sensitivity of ultrasonic TDR to a wide range of foulants [65].

10.2.7. Medical applications of ultrasound-based detection techniques

Diagnostic US, used in almost all medical fields and becoming the preferred imaging mode in a variety of clinical situations, is obviously a topic outside the scope of this book. However, interested readers can find an excellent picture of the near past, present and foreseeable near future in a review by Lewin [66], and also in the proceedings of SPIE, Vol. 4687, devoted to "Medical Imaging and Signal Processing 2002", which encompasses signal processing and detection, beam forming, array transducers, rf analysis, tissue elasticity, Doppler effect, vascular imaging, and segmentation classification, among other salient topics [67].

10.2.8. Analytical applications of ultrasound-based detection techniques to solids

Most analytical applications of US-based detection to solids are concerned with food analysis. Thus, the sugar content of melons [68], and the composition of fish [69,70], pork meat mixtures [71] and other meat-based products [72] are but a few salient applications

in this field. In some, the US velocity at one or several temperatures was measured for composition estimation using Eq. 10.2 under the assumption that the samples consisted of a mixture of different components of known proportions and ultrasonic velocities:

$$\frac{100}{c^2} = \frac{\sum \varphi_j}{c_j^2}$$

(10.2)

where φ_j and c_j are the mass percentage and ultrasonic velocity of component j. This equation proved a good estimator of the ultrasonic velocity in food materials, where scattering is insubstantial because their air content is probably low [70].

10.3. ULTRASONIC ANALYSIS OF LIQUID SAMPLES

In spite of the significant potential of ultrasonic measurements for the analysis of liquids, the use of US-based spectrometric techniques has so far been concentrated mainly in professional ultrasonic laboratories. A wider application of US for liquid monitoring and analysis has been restricted by several limitations. One is the convenience of measurements which involve sample cell filling, short measuring times, automatic operation, efficient stirring, stability to organic solvents, acids, bases and others. Another reason is the large volume of measuring cells and the high cost of analyses (especially with expensive liquids). In addition, resolution is limited to 10^{-3}% in most cases, even with specialized, sophisticated scientific devices. Modern instrument avenue has facilitated the construction of relatively inexpensive, convenient devices for fast measurements (mainly of velocity and attenuation) in volumes as small as 0.1 ml with resolution better than 10^{-4}% for velocity and 0.1% for attenuation. Other reason that previously limited the application of ultrasonic detection to routine analyses of liquids was the difficulty of interpreting ultrasonic characteristics. This problem has been overcome by extensive studies conducted over the last decade [73] which have made ultrasonic measurements competitive with other, well-established types of measurement and, in many cases, a unique analytical tool for the characterization of the quality of liquids and their components, measurement of concentrations and detection of chemical reactions, among others.

Ultrasound propagation is adiabatic in homogeneous media at the frequencies typically used in US-based detection techniques. Therefore, although temperature fluctuations inevitably accompany pressure fluctuations in US, thermal dissipation is small and it is adiabatic compressibility which matters. As a second derivative of thermodynamic potentials, compressibility is extremely sensitive to structure and intermolecular interactions in liquids (*e.g.* the compressibility of water near charged ions or atomic groups of macromolecules differs from that of bulk water by 50–100%).

Measuring US velocity is the only direct way of determining adiabatic compressibility. This type of measurement has opened the door to a new world of materials characterization, a world that hitherto has remained the province of specialists. Thus, US allows biochemists to determine protein hydration, food scientists to monitor changes in solid fat content, physical chemists to measure solute–solute and solute–solvent interactions, and physicians to measure cell aggregation, just to name a single use in some key areas.

Most applications of US-detection in liquids use compressive, longitudinal waves; shear waves propagate over macroscopic distances in solids, but not in liquids, and other modes of US propagation are of little use with liquid samples.

10.3.1. Variables influencing ultrasound measurements in liquid systems

The most influential variables on US measurements in liquids are temperature, dissolved air concentration and pressure. Also, moisture is a key variable with non-aqueous media.

Temperature

The influence of temperature is especially significant for aqueous systems. Thus, US velocity in water varies by approximately 3 m/s per °C at 20°C; therefore, an error of 0.1°C in temperature will result in an error of 0.3 m/s in velocity. It should be noted that the temperature coefficient of the US velocity in pure water at temperatures up to 74°C is positive, unlike most other liquids.

Air in liquid samples

Although dissolved air — as opposed to air bubbles — has a very small effect on US properties such as velocity, small changes in pressure can release dissolved air from the solution and produce bubbles. Moreover, natural waters often contain tiny bubbles called "microbubbles" as small as 1 μm or less. It is essential therefore to take great care in de-aerating aqueous systems prior to US measurement. This can be done by sonicating the sample or by bubbling nitrogen through it; however, centrifugation may be needed for highly viscous materials or in the presence of surfactants. Fortunately, US is itself an excellent detector of gas bubbles (see Section 9.5.1.), the presence should be suspected whenever anomalous US measurements are obtained. This allows the efficiency of degassing to be estimated by monitoring US velocity during the process.

Pressure

Pressure exerted on a liquid system influences the measurements of US parameters. Equations for quantifying such influence and that of temperature on US velocity have been derived by Pierce [74] for distilled water over the ranges 0–20°C and 1–100 atm.

Ultrasound velocity and concentration: the Urick equation

The magnitude of the fluctuations in volume (dilatation) and density (condensation) associated with US wave is controlled by the properties of the medium and the applied forces. The velocity of sound in mixtures and suspensions will therefore be controlled by the mean density and mean compressibility as expressed by the Urick equation (see Eq.9.7–9.10). The equation can be formulated in terms of partial molar volumes by forming an identity between the volume fraction of the solute, its partial volume (V_{M2}), the mean molar volume of the solution (V_M) and the mole fraction (c_M) as follows:

$$\Phi = V_{M2} c_M / V_M \tag{10.3}$$

which establishes a quadratic dependence of US velocity on concentration.

10.3.2. Ultrasound-assisted detection and liquid systems

Ultrasound measurements in liquids have been conducted in a variety of systems to extract a variety of information. More than fifteen years ago, Sarvazyan reviewed the topic and noted that US-based detection techniques could be used to study the hydration of biological substances and establish the status of water in the hydration shell, molecular transitions and interactions, thermodynamics and P–V–T state of biological substances in solution, and the conformational dynamics of proteins [75]. The expectations raised by this review have been fulfilled to a great extent judging by the increasing number of publications that have ensued, which are briefly discussed in this section on various aspects of liquid systems. Thus, if the liquid consists of several immiscible liquids, the characteristics of the emulsions formed can be used as the targets of US measurements. If miscible, changes in the solution properties with changes in the relative proportion of its components can be the target. Finally, determining a given analyte can be another target of US measurements.

Emulsions studies

Many natural and processed materials (*e.g.* blood, milk, agrochemicals, explosives, foods, petrochemical and pharmaceuticals) consist either partially or wholly of emulsions, or have been in an emulsified state some time during their existence. Also, many important physico-chemical properties of emulsions including rheology, appearance, stability and chemical reactivity depend on the size of the droplets they contain. The importance of emulsions in nature and industry has given considerable impetus to the development of analytical techniques intended to provide information about droplet size (*e.g.* light microscopy, electron microscopy, dynamic and static light scattering and electrical conductivity), each having its own advantages and limitations, and a specific niche of materials or applications is especially well suited to. Microscopic techniques provide the most direct information about the overall microstructure of emulsions (*viz.* the size and spatial distribution of droplets); however, sample preparation for analysis is often time consuming and laborious, and can alter the structures being examined. Particle-sizing instruments based on light scattering are simple to operate and give rapid measurements over a wide range of droplet size distribution (typically 0.1–1000 µm); however, concentrated samples must be diluted prior to analysis. Because of the need to dilute or physically disrupt emulsions prior to analysis, most existing techniques have limited use for analysing concentrated emulsions or for on-line measurements. Nuclear magnetic resonance (NMR) affords measurements of droplet size distribution of concentrated and optically opaque emulsions; however, the equipment needed is relatively expensive, requires highly skilled operators and is not easily adapted to on-line measurements. Ultrasound spectrometry provides a useful way for particle sizing in emulsions by using two-step methods (namely, measurement of the ultrasonic velocity or attenuation, most often in the emulsion, over a wide range of frequencies and conversion of the data obtained into a droplet size distribution by using a suitable mathematical theory — as described in Chapter 9).

The greatest advantages of ultrasonic spectrometry over other particle sizing methods are its non-destructive, non-invasive nature; its applicability to concentrated and optically opaque emulsions; its relatively low cost and its measurement expeditiousness. In addition, ultrasonic spectrometry can be easily adapted for on-line measurements, which is particularly useful for monitoring manufacturing operations involving emulsions. On the other hand, its greatest restrictions in this field are that it cannot be used to study

emulsions containing gas bubbles because these scatter US with high efficiency (even at low concentrations); and that it has limited application to highly dilute emulsions, where changes in ultrasonic properties with droplet size are of the same order of magnitude as the experimental error — the upper concentration limit, however, is only restricted by the ability to develop appropriate equations [76].

The ultrasonic properties of emulsions are usually frequency dependent, as are the effects of diffraction and transmission–reflection at multilayer boundaries. Thus, the frequency content of a US pulse used in an experiment is important. If a pulse contains a wide range of frequencies, then each frequency component will travel through a material at a different velocity and will be attenuated to a different extent, so only average values will be measured. This problem can be overcome by conducting experiments at a particular frequency or by using Fourier analysis to examine the frequency content of broad-band pulses.

Determining the droplet size distribution of an emulsion by ultrasonic spectrometry involves two steps. First, the ultrasonic velocity and (or) attenuation coefficient of the emulsion is measured as a function of the frequency — preferably over as wide a range as possible. Second, the experimental measurements are compared with theoretical predictions of the ultrasonic properties of the emulsion, and the droplet size distribution providing the best fit between theory and experiment is determined.

Progress in theoretical and applied aspects of emulsions is reflected in the literature. One case in point is the comparison of velocity dispersion measurements of a broad-band pulse-echo method with those from a frequency scanning pulse-echo reflectometer, evaluation of the equation parameters by applying discrete Fourier transform to the echo signals and using the full-size information instead of mono-size information. Figure 10.7 shows the measured velocity dispersion in *n*-tetradecane in water emulsions at different concentrations, as well as the measured particle size information used to obtain the velocity reference by applying Lloys and Berry's multiple scattering theory [77].

On the other hand, the fact that ultrasonic velocity is independent of droplet size in the low and high frequency limits allows droplet concentrations to be determined without prior knowledge of the droplet size distribution from ultrasonic velocity measurements. Whether measurements are to be made in the low- or high-frequency regime depends on the size of the droplets and the range of frequencies which can be measured using available ultrasonic equipment (typically 0.1–100 MHz).

Ultrasonic techniques have also been used to study typical oil-in-water emulsions as such and those undergoing either depletion flocculation or floc disruption. These studies are of industrial interest as flocculation of the droplets within an emulsion may often be the first stage in the deterioration of a product; however, it can also be beneficial by increasing the apparent viscosity of the product *via* the formation of a continuous network of droplets.

In an early three-part experiment involving three emulsions representing unflocculated, partially flocculated and fully flocculated systems, short acoustic pulses (10 ns) were transmitted through the test liquid and the signals at the receiver transducer amplified and digitized at 400 MHz. Signal processing involved correcting for radiation coupling and transducer effects, and obtaining the frequency response of propagation through the liquid from the fast Fourier transform of the corrected signal. The flocculating emulsions exhibited large changes during flocculation that could not be readily modelled using single-particle scattering theory; on the other hand, the ultrasonic properties of the unflocculated emulsion did not change during the measurement time, which confirmed that ultrasonic techniques are capable of detecting flocculation [78].

Depletion flocculation has also been induced in oil-in-water emulsions by adding different concentrations of a non-adsorbing biopolymer (xanthan) to the aqueous phase. At low frequencies, the attenuation coefficient of the emulsions decreased with increasing
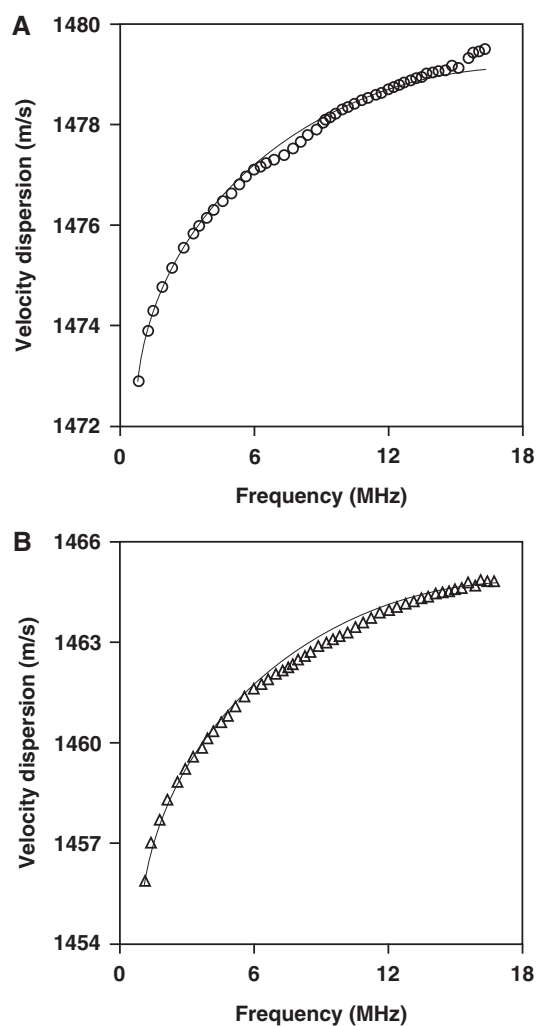
FIGURE. 10.7. *Velocity dispersion in n-tetradecane in water emulsions at different concentrations. (A) 5%. (B) 10%.*

flocculation through overlap of the thermal waves generated by the droplets; observations, which were in good agreement with the theory, accounted for the influence of droplet flocculation on the ultrasonic properties of the emulsions. The ultrasonic technique was also used to monitor the breakdown of flocs under shear flow and revealed that ultrasonic attenuation is an appropriate tool for studying droplet interactions in concentrated emulsions [79].

One topic of special interest in Spain is that involving two immiscible phases that form no emulsion such as that in the waste from the three starting phases in the extraction of
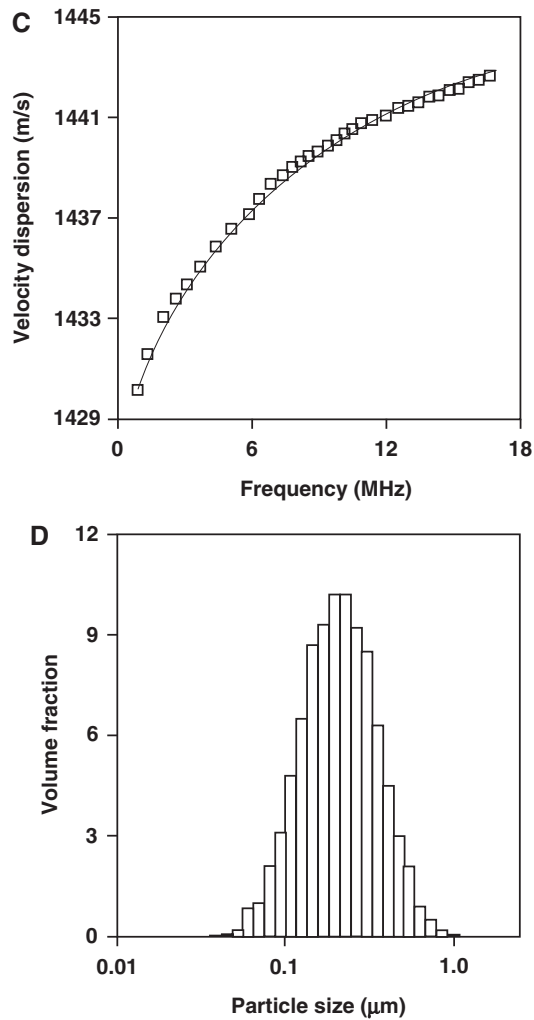
FIGURE. 10.7. *Cont'd. (C) 15%. Marks are the measured results while full lines are the reference values. (D) Particle size information measured to obtain a reference velocity by applying Lloys' and Berry's multiple scattering theory. (Reproduced with permission of Elsevier, Ref. [77].)*

olive oil (namely: the solid peel and bone phase, the aqueous phase and the oil phase); [80]. The aqueous phase known as "alpechín" contains small amounts of oil and — mainly — phenols, proteins and other organic polar compounds that are more soluble in the aqueous phase than in the oil phase; its monitoring during olive oil production provides information of use for process control. The study involved measuring the ultrasonic velocity of water, oil and alpechín over the range 6 to 50°C at 1 MHz. Two semi-empirical

equations were used to assess the composition of oil and water which provided the determination of coefficients higher than 0.97 for both media with no appreciable differences between vacuum or agitation conditions (see Fig. 10.8A). Figures 10.8B and C illustrate the behaviour of water, oil and alpechín with temperature — which was similar for water and alpechín and disparate for oil; and that of alpechín with variable oil contents are shown. The experiment demonstrated the feasibility of measuring the composition of alpechín by ultrasonically monitoring the extraction process in-line in order to calculate oil losses and adjust or stop the process if required. The temperature coefficient for the ultrasonic velocity of olive oil (– 3.45 m/s per °C) is very similar to that found by Ghaedian *et al*. [70] for sunflower oil (– 3.40 m/s per °C); therefore, this coefficient is not an effective choice for discriminating oil types and absolute values of velocity at specific temperatures may provide a more sound approach.
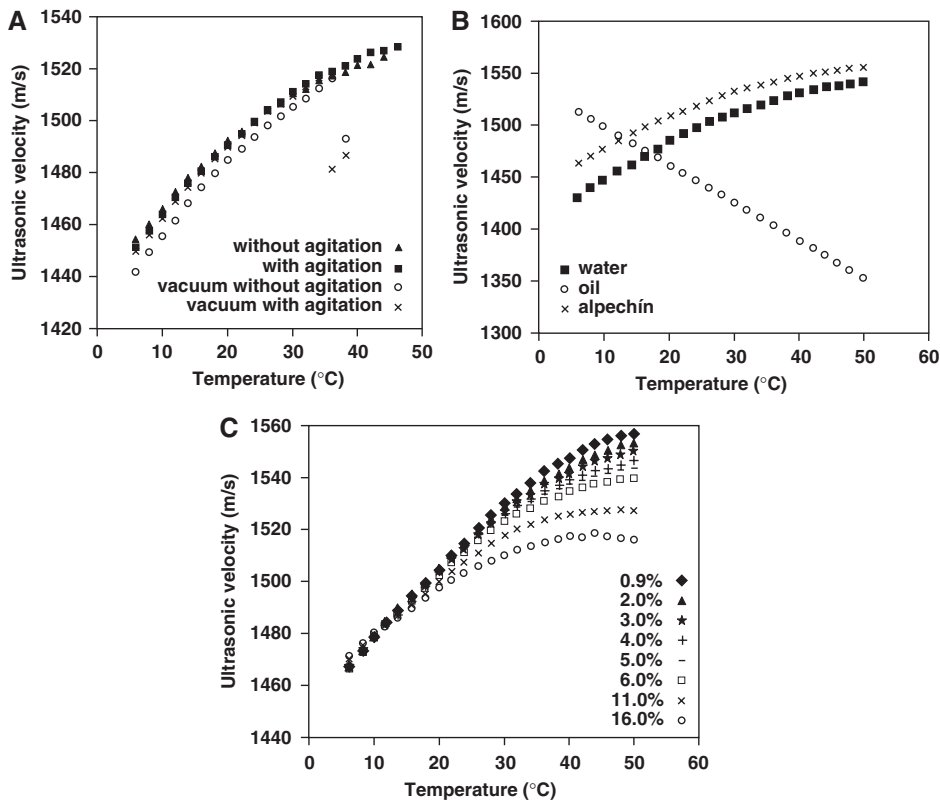
FIGURE. 10.8. *Dependence of ultrasonic velocity on temperature in: (A) Alpechín under various experimental vacuum conditions and agitation. (B) Water, oil and alpechín. (C) Alpechín with variable oil contents as determined from in-line measurements. (Reproduced with permission of Elsevier, Ref. [80]).*

Studies of miscible liquids

The study of molecular interactions in liquid mixtures is of considerable importance in the elucidation of the structural properties of molecules. Interactions between molecules influence the structural arrangement and shape of molecules. Dielectric relaxation of polar molecules in non-polar solvents using microwave absorption has been widely employed to study molecular structures and molecular interactions in liquid mixtures [81]. Ever since Lagemann and Dunbar developed a US velocity approach for the qualitative determination of the degree of association in liquids [82], a number of scientists have used ultrasonic waves of low amplitude to investigate the nature of molecular interactions and the physico-chemical behaviour of pure liquids and binary, ternary and quaternary liquid mixtures, and found complex formation to occur if the observed values of excess parameters (*e.g.* excess adiabatic compressibility, intermolecular free length or volume) are negative. These parameters can be calculated from those for ultrasonic velocity (*c*) and density (*ρ*). Thus,

$$\text{Adiabatic compressibility } (\beta) = 1/c^2\rho \tag{10.4}$$

$$\text{Intermolecular free length } (L_f) \ K\beta^{1/2} \tag{10.5}$$

where *K* adopts different values depending on the temperature.

$$\text{Molar sound velocity } (R) = c^{1/3}V \tag{10.6}$$

$$\text{Molar compressibility } (B) = (M/\rho)\beta^{-1/7} \tag{10.7}$$

where *V* and *M* are the molar volume and molecular weight, respectively.

$$\text{Specific acoustic impedance } (Z) = \rho c \tag{10.8}$$

The excess adiabatic compressibility (β^E) and excess intermolecular free length (L^E_f) can be evaluated from:

$$\beta^E = \beta_{\text{exp}} - \beta_{\text{ideal}} \tag{10.9}$$

and

$$L^L_f = L_{f \ \text{exp}} - L_{f \ \text{ideal}} \tag{10.10}$$

where β_{ideal} and $L_{f \ \text{ideal}}$, and their excess in mixture can be defined under the volume additive rule [83].

Other equations for calculating excess or apparent values, and tabulated values of selected US measurements of apparent molar adiabatic compressibility in a variety of solutions, can be found elsewhere [84].

Resonance US spectrometry has been widely used in studies involving miscible liquids. One examined the compressibility of alkyltrimethylammonium bromide micelles spanning a wide range of concentrations above and below their critical micelle concentrations. Measurements were made at 25°C and the resolution achieved, 10^{-4} %, was more than 20 times better than in previous studies. The apparent molar adiabatic compressibilities

of the monomer forms were found to decrease with increasing chain lengths — by a given amount per CH_2 group, — and the opposite trend was observed for the micelle forms. The coefficient of adiabatic compressibility of the internal cores of micelles was estimated to be very close to, but slightly lower than, that of pure hydrocarbon liquids having the same number of CH_2 groups [85]. The same research group recently investigated demixing and remixing in poly(*N*-isopropyl acrylamide)–water solutions by RUS and compared the results to those provided by modulated temperature differential scanning calorimetry. The former technique was found to be capable of distinguishing between regions created as a function of temperature, namely a homogeneous region and a heterogeneous region, the latter consisting of two zones with and without interference of partial vitrification of the phase rich in the amide. The ultrasonic velocity decreased during phase separation by effect of a change in the hydration structure around the polymer chains; on the other hand, ultrasonic attenuation increased as aggregation set in. Isothermal measurements exhibited clearly a time-dependence of both velocity and attenuation [86]. Resonant US spectrometry has also been used in studies of polymers, as for the examination of segmental motion and ion binding in polyelectrolyte polyacrylate, polyphosphate and polystyrene-sulphonate solutions by relaxation [87] and poly(vinyl alcohol)–dextran–water mixtures. Comparative results of US velocity, density, adiabatic compressibility, acoustic impedance and viscosity relaxation time as a function of temperature and concentration at 3 MHz proved the mode of interaction and the compatibility and miscibility between the two biologically active macromolecules at all concentrations and temperatures by cross-linking *via* hydrogen bonding of both biomacromolecules [88]. Assays with aqueous–dextran solutions of six molecular weights involving measurements of acoustic attenuation, velocity, impedance and density in the ultra-high frequency (UHF) and very high frequency (VHF) regions showed all four parameters to increase with increasing concentration and also that increasing the molecular weight increased the attenuation coefficient and decreased the velocity [89].

Ultrasonic interferometry has been used to study ternary mixtures of dimethylsulphoxide, phenol and *o*-cresol in carbon tetrachloride. The variation of adiabatic compressibility and intermolecular free length with the concentration suggested the occurrence of complex formation by intermolecular hydrogen bonding, which was confirmed from IR spectra [90].

Recently, Brillouin scattering has proved useful in this area for studying the frequency dependence of hypersonic (GHz zone) absorption and dispersion velocity in liquid sulphur dioxide [91]; the effect of isotopes on hydrodynamic fluctuations in self-associated fluids [92]; and the elastic properties of polyethylene glycol solutions in water, benzene and toluene [93].

Analytical uses of ultrasound spectrometry in homogeneous solutions

Ultrasound-based detection is an excellent choice for food industries, where its use is in continuous expansion. Most studies in this area have used ultrasonic velocity to extract information about products, probably because it is the simplest, most reliable type of ultrasonic measurement. Thus, it has been used to determine the chemical structure (including chain length and degree of unsaturation) of various oils [94], oil composition and adulteration [95]; the correlation of the proportion of polar compounds to ultrasonic velocity and attenuation in fried olive oil [96].

Ultrasound-based detection is of great interest for the pharmaceutical industry as, in addition to its ability for fast non-destructive analysis and easy adaptation to real process time monitoring in both batch and continuous systems, it has the potential to simultaneously monitor concentrations of both the drug and the excipient in a solution. These possibilities have recently been demonstrated by using a high-resolution ultrasonic spectrometer

for the simultaneous monitoring of a model excipient (hypromellose acetate succinate polymer) and a model drug (Fenofibrate) in an acetone solution with adequate accuracy and precision from velocity or attenuation measurements. The latter parameter was found to be directly proportional to the concentrations of both polymer and drug, and attenuation to be directly proportional to the polymer concentration in solution; this allowed both concentrations to be simultaneously determined in a test solution. However, both temperature and moisture had a significant influence on measurements; thus, the change in velocity was inversely proportional to the change in temperature, and directly proportional to the change in moisture content in the solutions [97].

In 1998, Su *et al.* reported several continuous methods based on the combination of a flow injection manifold, a gas-diffusion unit and a bulk acoustic impedance sensor. The sensor was constructed by connecting an AT-cut piezoelectric quartz crystal and a conductivity electrode in series and provided some advantages over classical conductimeters. Figure 10.9 shows the overall system. Samples (namely blood for the determination of total ammonia or total carbon dioxide [98], fermentation products for the determination of volatile acidity [99], wines for the determination of sulphite [100] and water or human saliva for the determination of nitrite or nitrate [101]) were injected into a carrier stream and merged with the reagent to form volatile species which were passed through the diffusion membrane to an acceptor stream for transfer to the detector (with or without their previous derivatization). The lack of selectivity of the sensor was overcome by previously separating the target analytes.

More recently, the previous group used the same impedance sensor batchwise for *in situ* monitoring of the whole process behind DNA oxidative damage induced by the vitamin C–Fe(III) system through its real-time response to density–viscosity changes in the tested solution due to the damage in the DNA molecules. The end-point frequency change of the sensor was found to be linearly related to the initial concentration of DNA over the range 40–1000 μg/ml; also, the exponential relationship between the frequency change and the damaging time suggested a first-order kinetics for the reaction [102].
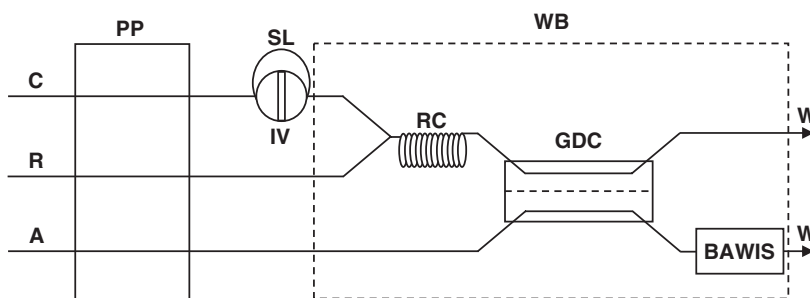
FIGURE 10.9. *Continuous system used by Su et al. to implement various analytical methods including a flow-injection manifold, a gas-diffusion unit and a bulk acoustic impedance sensor. A acceptor, BAWIS bulk acoustic wave impedance sensor, C — carrier, GDC — gas diffusion cell, IV — injection valve, PP — peristaltic pump, R — reagent, RC — reaction coil, SL — sample loop, W — waste, WB — water bath. (Reproduced with permission of Elsevier, Ref. [98].)*

10.4. ULTRASONIC ANALYSIS OF HETEROGENEOUS SAMPLES

This section deals with measurements in systems involving two different physical states. Although immiscible liquids are also heterogeneous from a chemical point of view, they have been included in Section 10.3 as they are ultimately liquid systems, therefore, only solid–liquid, solid–gas and liquid–gas systems are dealt with in.

10.4.1. Solid–liquid samples

Advances in the understanding of US propagation through liquid and viscoelastic materials have allowed scientists to successfully use US for the characterization of suspensions in addition to emulsions and solutions. Of the two major primary US spectrometry variables, velocity (phase) is used mainly to study inter- and intra-molecular processes and attenuation (amplitude) for particle sizing. Both types of measurement are provided by commercial instruments and used in combination to ensure more accurate particle size and particle size distribution determinations than can either by itself.

Ultrasound attenuation spectrometry (UAS), also known as "ultrasonic extinction spectrometry", has proved to be applicable over a wide range of particle sizes (between 10 nm to 1 mm) and at very high concentrations (volume fractions from 0.1 to 50%), thus dispensing with the need for sample dilution and preparation, and enabling the study of particle systems in their original state of dispersion and facilitating the determination of, for example, agglomeration or flocculation parameters. These features make UAS attractive for monitoring particle formation processes as it allows the rapid characterization of particulate suspensions by using models such as that of Epstein–Carhart–Allegra–Hawley (ECAH) [103] to transform US attenuation measurements into particle size and concentration information, provided a set of physical properties is known for the suspending and the suspended media. This model can be implemented in terms of the velocity or attenuation of the ultrasonic wave; the density of the target system; or its thermal expansion coefficient, heat capacity, thermal conductivity, viscosity (for the continuous phase and dispersed liquids) or shear rigidity (for a solid dispersed phase). Reliable data for all these properties are not always available and inaccuracies in them influence particle size and concentration calculated values. Errors in these properties should be less than 1% if errors in calculated mean size and concentration are to be kept below 3 and 6%, respectively [103].

Moreover, particle sizing by UAS involves not only the accurate description of the functional dependence of US attenuation on particle size and frequency, but the inversion from measured attenuation spectra to particle size distribution as well. Since the spectroscopic measurements are conducted at a certain number of frequencies, the calculated size distribution can be described ideally by the same number of parameters. In practice, however, this number is considerably reduced, because measurement errors cause loss of information. This effect results from the physical nature of UAS and applies to any measurement problem involving integral equations with smooth kernel functions (*e.g.* light scattering and electroacoustics) [104]. The development of new ultrasonic transducer technology, together with advances in digital signal processing is paving the way for more powerful uses of UAS. One case in point is the multi-frequency pulse instrument for on-line measurements reported by Goodenough *et al.*, a variable path length pulse device which produces both time- and frequency-domain data and was designed to solve problems identified with pulse ultrasonic devices such as: (1) reference fluid calibration, which is susceptible to reference fluid integrity, reference value and temperature measurement

accuracy, and thermal expansion of the cell after calibration; (2) probe delay, diffraction and impedance mismatches between the reference and test fluid; (3) poor accuracy and repeatability; (4) limited range of ultrasonic parameters, with systems often specializing in either time-domain or frequency-domain data, but not both. These problems can be solved by making amplitude and time-of-flight measurements at multiple distances and using rates of their change to calculate US attenuation and velocity over a range of distances; this avoids the need to rely on absolute distance measurements, allows fluid normalization of amplitude data, and intrinsically averages measurements for greater accuracy and repeatability [105]. This instrument was found to provide accurate measurements of the concentration of particulate matter in a fluctuating high temperature liquid system, where the two main problems (*viz.* thermal expansion and thermal variation in ultrasonic outputs) were solved by using multi-distance measurements and low-frequency spectrometry (2–16 MHz), respectively [106].

Most areas of interest for determinations of particle size have been covered by ultrasonic spectrometry, and are discussed briefly below.

Food analysis

Some foods that are liquid over long time periods can behave like solids when stressed over short time periods (shear thickening) and *vice versa* (shear thinning). Shear thinning foods include yogurt and gravy and shear thickening foods custard powder mixed with little sugar and milk which behaves like a liquid when stirred slowly, but thickens into a solid when stirred more quickly. There is experimental evidence of the utility of US-based detection with these types of samples. Thus, measurements of ultrasonic attenuation can be used to extract information on aggregation and molecular relaxation from whey protein molecules — which are used as functional ingredients in food products on account of their ability to enhance the texture and stability of emulsions, foams and gels — in aqueous solutions. This information can be employed to probe changes in both molecular relaxation and aggregation with variables such as temperature, pH, ionic strength and mechanical forces with a view to improving available knowledge about the relationship between the molecular and functional properties of proteins [107]. Ultrasonic velocity has been used in addition to attenuation to study the gelation of milk components, which is related to the action of milk proteins [108,109].

Ultrasonic velocity spectroscopy has been used for the determination of the solid fat content in anhydrous milk fat, cocoa butter and mixtures thereof with canola oil. For this purpose, *in situ* measurements of ultrasonic velocity during cooling (50–5°C) and heating (5–50°C) of the fat at 1°C/min were performed. One shortcoming encountered was that ultrasonic velocity was highly dependent on the microstructure and polymorphism of the solid fat, being higher for fats in more stable polymorphic forms. Also, high signal attenuation was observed in milk fat and cocoa butter at low temperatures, particularly after a 24-h storage [110].

Other industrial areas

Inhomogeneities in particle-packed structures arising during shape forming of ceramic powders should be carefully controlled because they can cause fracture in sintered materials or lead to shape distorsion and cracking during drying, pyrolysis and sintering. Such inhomogeneities are closely related to the particle size distribution in highly concentrated slurries prepared without dilution. Ultrasonic attenuation spectroscopy is an

effective alternative to light scattering spectroscopy for the determination of particle size distributions in these materials as it allows one to discriminate between well-dispersed and flocculated states in highly concentrated slurries [111]. This type of analysis can easily avoid problems arising prior other operations such as casting or firing.

As noted in Section 10.2.4, solid formation from a liquid medium has been efficiently monitored with US-based detection techniques of widespread industrial use. Thus, pulse-echo ultrasonic spectroscopy has proved to be an effective choice for the on-line monitoring of the solidification rate of metallic alloys and allowed the development of a method for controlling the growth velocity during directional solidification *via* the furnace velocity and accomplishing steady-state solidification [112]. Pulse-echo ultrasonic spectroscopy has also been employed to monitor the polymerization of dicyclopentadiene, which gives a commercially important thermoset polymer with high modulus, impact strength and chemical resistance. The monitored parameters were the density, wave speed, acoustic modulus and attenuation. The rate constants for the metathesis of cyclopentyl unsaturation provided by ultrasonic spectroscopy were similar to those obtained with FTIR; however, consistency was not so good for other steps of this polymerization reaction (particularly norbornyl unsaturation) [113].

Measurements of ultrasonic attenuation and velocity have been used to study the rheological properties of concentrated dispersions, which are of great importance in many technological applications. One example is the use of carbon black for manufacturing inks, where it is often used in combination with waterborne acrylic resins acting as cross-linking polymer networks. Although the printing process involves many high-shear interactions, understanding the low-shear behaviour of the ink is the key to determine its properties (*viz.* tack, transference, cohesion and drying) [114].

Less common ultrasound-based detection techniques for
solid–liquid measurements

Brillouin scattering spectrometry (BSS) is also highly suitable for measurements of solid–liquid systems since the viscoelastic properties of materials determine the dynamics of thermal density fluctuations in liquids and reflect in the Brillouin spectrum. As a result, BSS has become a powerful tool for examining the dynamic properties of glass-forming materials. The use of tandem multi-pass Fabry–Perot interferometers (FPI) has facilitated strong progress in contrast and resolution, and allowed the obtainment of overlap-free Brillouin spectra over wide frequency ranges (*e.g.* from 0.5 to 1000 GHz). The relatively long acquisition time of conventional scanning-type FPI has been a problem for measuring acoustic properties in transient changes such as those arising during liquid–glass transitions in low molecular weight compounds. Small-sized molecular liquids need a fast cooling rate to change into a glassy state and avoid crystallization; therefore, they require a short acquisition time. The evolution of non-scanning angular dispersion FPI (ADFPI) instruments, which are combinations of a solid etalon and a multichannel detector such as a CCD or a photodiode array detector, has recently solved the problem by enabling the Brillouin spectra from normal and supercooled liquids to the glassy state to be monitored. The glass-forming or crystallization tendency, and the behaviour of aminopropanols with different chemical structures, were thus determined and the different vitrification tendency between racemic liquids and their pure enantiomers over the cooling rate range 2–4 K/min was established [115].

Ultrasonic diffraction grating spectrometry (UDGS) has proved to be a useful technique for measuring US velocity in liquids and slurries, and particle size in a slurry by using

a special type of attenuation. As explained in Chapter 9, the back of a grating surface in contact with the liquid or slurry is struck by a longitudinal wave from the send transducer at an incident angle of 30° and the receive transducer is used to measure the reflected diffracted $m = 0$ longitudinal wave. As the frequency decreases, the $m = 1$ transmitted longitudinal wave in the liquid moves to a larger angle (*e.g.* for water, the angle becomes 90° at 5.67 MHz); at such a frequency, called the "critical frequency", the wave becomes evanescent and, at a slightly smaller frequency, the evanescent wave disappears. In order to conserve the energy, this is distributed to all other waves, and an increase in amplitude of the reflected $m = 0$ signal is observed. The ability of UDGS to measure particle size arises from penetration of the evanescent wave into the slurry, where some attenuation of the signal occurs as the wave interacts with the particles, so the signal measured by the receive transducer decreases in amplitude as a result. Since the attenuation is dependent upon particle size, an algorithm can be developed to determine particle size or a calibration curve constructed from appropriate standards [116].

A special type of hybrid measurements involving a quartz crystal microbalance (QCM) and an impedance analyser was used to study the variability of acoustic properties of living cells on the sub-second time scale. Changes in susceptance and conductance caused by changing the ultrasonic frequency were monitored in a fast mode in order to detect periodic, synchronous contractions of the cell layer in the quartz crystal; the contractions were clearly reflected in periodic variations of the resonance frequency and bandwidth [117].

10.4.2. Solid–gas samples

Applications of ultrasonic techniques to solid–gas systems rely on the fact that velocity and attenuation of US-waves in porous materials is closely related to pore size, porosity, tortuosity, permeability and flux resistivity. Thus, the flux resistivity of acoustic absorbents can be related to US attenuation [118,119], while the velocity of slow longitudinal US is related to pore tortuosity and diffusion, and transport properties, of other porous materials [120]. Ultrasound attenuation is very sensitive to the presence of an external agent such as moisture in the pore space [121] and has been used to monitor wetting and drying processes [122]; on the other hand, US velocity has been used to measure the elastic coefficients of different types of paper and correlate them with properties such as tensile breaking strength, compressive strength, etc. [123].

The so-called "gas-coupled ultrasonic spectroscopy" is the most useful US-based detection choice for extracting valuable information from gas–solid systems. This technique is based on the spectral analysis of broad-band ultrasonic pulses transmitted through samples and on the solution of the so-called "inverse problem" [124]. The situation is schematically depicted in Fig. 10.10. The transmitter transducer launches US signal which travels through a gas gap and impinges normally on the sample surface; part of the energy is reflected back while the rest is transmitted into the sample. The transmitted wave propagates through the sample and reaches the back surface; there, part of the energy is reflected back and the rest is transmitted through the interface and received at the receive transducer after travelling through a gas phase. This process is repeated for each of the multiple internal reflections in the sample. When the delay time between consecutive internal reflections at the sample surface equals $1/f$ (f being the wave frequency) a constructive interference between multiple reflections within the sample is built up. When this constructive interference takes place at the rear surface of the sample, the maximum value of the transmitted energy is observed: this is a thickness resonance of the sample.
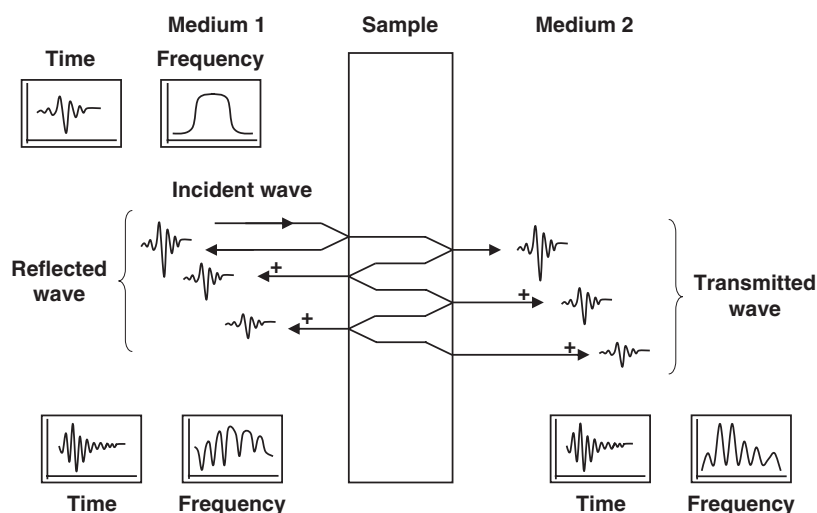
FIGURE 10.10. *Scheme of the process occurring in the gas-coupled ultrasonic spectroscopy of gas–solid systems. (Reproduced with permission of Elsevier, Ref. [125].)*

Theoretical modelling of the problem of transmission of US waves through a sample separating two media has been carried out in terms of plane longitudinal waves, normal incidence and one-dimensional model and a membrane as sample; also, the US velocity and attenuation, and the density of the membrane have been determined [125]. Comparison of the results with properties of the membranes showed US attenuation to be independent of pore size, water flow and bubble point; on the other hand, US velocity was found to be clearly correlated with all these factors. Applicability of the theoretical analysis required that the sample be homogeneous and plate-shaped (with its surfaces flat and parallel); plane wave is assumed in such a way that diffraction effects of the US beam must be negligible and the pore size much smaller than the wavelength, so that the two-phase porous media can be replaced by an effective homogeneous medium. A more refined approach to examine wave propagation in porous media is provided by Biot's theory [126], which predicts the appearance of two different longitudinal modes.

Typical applications of gas-coupled ultrasonic spectroscopy include the characterization of other porous materials such as rocks [120], paper [127], wood [128] and silica aerogels [129].

One other wide field of application of solid–gas US-based detection is food analysis of heterogeneous, solid-gas samples as many foods consist of air bubbles or cells distributed in a visco-elastic solid matrix (*e.g.* confectionary). The shelf life, texture and appearance of these foods are strongly influenced by the size and concentration of the bubbles they contain. It is therefore important to prevent changes in the characteristics of the bubbles over time. There is currently a lack of analytical techniques capable of providing information on bubble characteristics in aerated foods for fundamental studies aimed at improving our understanding of the relationship between bubble characteristics and bulk properties of aerated foods, many of which are optically opaque or have delicate structures that are easily damaged by physical manipulation. Research in progress aimed

at establishing theoretical equations fitting most real-life situations should be supplemented with further work aimed at quantifying bubble size and concentration in aerated foods.

10.4.3. Liquid–gas samples

It has been known for many years that US can be used to determine the size and concentration of air bubbles in highly dilute systems [130] by recording the ultrasonic velocity and (or) attenuation spectra for an ultrasonic wave transmitted through a bubbly liquid. Information about bubble properties can thus be obtained by interpreting the spectra in the light of an appropriate theory. This approach is unsuitable for the analysis of aerated materials containing relatively high concentrations of bubbles (>0.1%) because the ultrasonic signal is so highly attenuated that it cannot be propagated far enough through the sample to be detected. Preliminary studies conducted in the early 2000s showed that information about bubble characteristics in concentrated systems can be obtained if the ultrasonic wave is reflected from the surface of the sample rather than transmitted through it [131]. These achievements were later confirmed by the development of an ultrasonic spectrometer generating a broad-band pulse (1 to 7 MHz) that travelled along a perspex delay line and was reflected from the delay line–sample interface, the reflected pulse being detected by the same transducer. The received signal was averaged 200 times in order to improve the signal-to-noise ratio, and the magnitude M and phase of the pulse ψ handled as a function of the frequency, using FT analysis. The reflectance of foams cannot be calculated from Eq.9.27 — neither can the impedance thus be obtained from it, — as characterizing aerated systems requires relating the measured acoustic impedance to the bubble characteristics, which, in the case of a bubbly liquid, are related to its physical and acoustic properties by the equation:

$$Z = \omega\rho/K \qquad (10.11)$$

where ω is the angular frequency (= $2\pi f$), ρ the density and K the propagation constant. For a dilute suspension of non-interacting spherical bubbles having radii appreciably smaller than the acoustic wavelength, the following expression can be used for the propagation constant:

$$K = k_1 \sqrt{\left(1 - \frac{3i\Phi A_o}{\left(k_1 r\right)^3}\right)\left(1 - \frac{9i\Phi A_1}{\left(k_1 r\right)^3}\right)} \qquad (10.12)$$

where k_1 is the propagation constant of the continuous phase (= $\omega/c_1 + ia\alpha_1$), c the ultrasonic velocity, α the attenuation coefficient, $i = -1$, Φ the volume fraction of the bubbles, r their radius, and A_o and A_1 are the monopole and dipole scattering coefficients of the bubbles. Expressions for these scattering coefficients available in the literature [132,133] have been employed by their proponents as no general expressions for the propagation constant of concentrated bubbly liquids have been derived owing to the difficulties involved in theoretically modelling the propagation of ultrasonic waves through such a complex system. Despite these limitations, ultrasonic impedance spectra were shown to vary with bubble size and concentration in a manner that can be qualitatively predicted by the theory [134].

Ultrasonic detection has proved to be an excellent tool for characterizing blowing processes, as shown by monitoring blowing in sponge rubber *via* measurements

of the amplitude of echo signals and the travel time of ultrasonic waves into the rubber samples under heating to decompose the chemical blowing agent at atmospheric pressure at a constant sample thickness between the ultrasonic probes [135]. Also, ultrasonic *quasi*-static characterization can effectively mimic the pressure, temperature and time conditions prevailing during the injection molding of cross-linked low density foams; this allows the blowing process to be monitored *via* ultrasonic velocity, attenuation and specific volume measurements [136].

As with solid–gas systems, food analysis is one of the widest fields of application of US-based detection since typical foods such as ice cream or whipped cream consist of air bubbles distributed in a visco–elastic liquid [137].

10.5. CONCLUSION

This Chapter aims to provide an overview of the underexploited, poorly known potential of US-based detection techniques in the analytical field.

Readers interested in delving deeper into this subject should take into account that the performance of available instrumentation and the continuous emergence of new systems from which information is required, need the development of new, more ambitious applications.

References

1. A. Migliori and J.L. Sarrao, *Resonant Ultrasound Spectroscopy. Applications to Physics, Material Measurements, and Nondestructive Evaluation*, John Wiley & Sons Inc., New York, 1997.
2. M. Dubois, P.W. Lorraine, R.J. Filkins, T.E. Drake, K.R. Yawn and S.Y. Chuang, *Ultrasonics*, 40 (2002) 809.
3. A. Ruiz and P.B. Nagy, *Ultrasonics*, 42 (2004) 665.
4. Y. Hong, S.D. Sharples, M. Clark and M.G. Somekh, *Ultrasonics*, 42 (2004) 515.
5. A.A. Maznev, K.A. Nelson and T. Yagi, *Solid State Comm.*, 100 (1996) 807.
6. M.H. Kuok, S.C. Ng, Z.L. Rang and T. Liu, *Solid State Comm.*, 110 (1999) 185.
7. M.M. Seikh, C. Narayana, S. Parashar and A.K. Sood, *Solid State Comm.*, 127 (2003) 209.
8. S.V. Sinogeikin, D.L. Lakshtanov, J.D. Nicholas and J.D. Bass, *Phys. Earth Planet. Inter.*, 143–144 (2004) 575.
9. Y.M. Cheong, S.S. Kim and Y.S. Kim, *J. Nuclear Mat.*, 303 (2002) 83.
10. J.E. Atteberry, D.S. Agosta, R.G. Leisure, O. Beeri and M.H. Mintz, *J. Alloys Comp.*, 365 (2004) 68.
11. A. Wanner, *Mat. Sci. Eng. A*, 248 (1998) 35.
12. T. Geiges, G. D'Anna, S. Komiya and Y. Ando, *Physica C.*, 408 (2004) 455.
13. T. Thio, T.R. Thurston, N.W. Preyer, P.J. Picone, M.A. Kastner, H.P. Jenssen, D.R. Gabbe, C.Y. Chen, R.J. Birgeneau and A. Aharony, *Phys. Rev. B*, 38 (1988) 905.
14. M.A. Kastner, R.J. Birgeneau, T.R. Thurston, P.J. Picone, H.P. Jenssen, D.R. Gabbe, M. Sato, K. Fukuda, S. Shamoto, Y. Endoh, K. Yamada and G. Shirane, *Phys. Rev. B*, 38 (1988) 6636.
15. D.B. Fraser and R.C. LeCraw, *Rev. Sci. Instrum.*, 35(9) (1964) 1113.
16. N. Soga and O.L. Anderson, *J. Geophys. Res.*, 72 (1967) 1733.
17. I. Suzuki, I. Ohno and O.L. Anderson, *Am. Mineral.*, 85 (2000) 304.
18. I. Ohno, M. Abe, M. Kimura, Y. Hanayama, H. Oda and I. Suzuki, *Am. Mineral.*, 85 (2000) 288.
19. I. Ohno, M. Kimura, Y. Hanayama, H. Oda and I. Suzuki, *J. Acoust. Soc. Am.*, 110 (2001) 830.
20. K. Yamanaka, A. Saito, S. Ishikawa and H. Cho, *Jpn. J. Appl. Phys.*, 41 (2002) 3498.
21. A. Yaoita, T. Adachi and A. Yamaji, *NDT&E International*, 38 (2005) 554.
22. N. Nakamura, H. Ogi and M. Hirao, *Ultrasonics*, 42 (2004) 491.

23. A. Migliori, F. Sarrao, W.M. Visscher, T.M. Bell, M. Lei, Z. Fisk and R.G. Leisure, *Physica B*, 183 (1993) 1.
24. Y.H. Kim, S.J. Song, S.D. Kwon, Y.M. Cheong and H.K. Jung, *Ultrasonics*, 42 (2004) 551.
25. A.I. Lavrentyev and J.T. Beals, *Ultrasonics*, 38 (2000) 513.
26. A.H. Khafagy, *Phys. State Sol.*, 186(1) (2001) 105.
27. R.J. Damani and A. Wanner, *J. Mat. Sci.*, 35 (2000) 4307.
28. R. Truell, C. Elbaum and B.B. Chick, *Ultrasonic Methods in Solid State Physics*, Academic Press, New York, 1969.
29. E.P. Papadakis, *J. Acoust. Soc. Am.*, 37 (1965) 703.
30. E.P. Papadakis, Ultrasonics Measurement Methods, *Physical Acoustics*, Vol. XIX, Academic Press, New York, 1990, p. 107.
31. H. Jeong and D.K. Hsu, *Ultrasonics*, 33 (1995) 195.
32. H. Ogi, M. Hirao and T. Honda, *J. Acoust. Soc. Am.*, 98 (1995) 458.
33. M. Blodgett and P.B. Nagy, *Appl. Phys. Lett.*, 72 (1998) 1045.
34. V. Hänel, *J. Appl. Phys.*, 84 (1998) 668.
35. A. Baltazar, S.I. Rokhlin and C. Pecorari, *J. Mechanics Phys. Sol.*, 50 (2002) 1397.
36. B.F. Pouet and N.J.P. Rasolofosaon, *J. Acoust. Soc. Am.*, 93 (1993) 1286.
37. K. Dransfeld and E. Salzmann, Excitation, Detection and Attenuation of High-Frequency Elastic Surface Waves, *Physical Acoustic Principles and Methods*, Vol. VII, Academic Press, New York, 1970, p. 219.
38. J. Huang and J.D. Achenbach, *J. Acoust. Soc. Am.*, 90 (1991) 1269.
39. W. Gao, C. Glorieux, K. Van de Rostyne, M. Wevers, W. Lauriks and J. Thorn, in *Photoacoustic and Photothermal Phenomena*, *10th International Conference*, American Institute of Physics, New York, 1999, p. 454.
40. W. Gao, C. Glorieux S.E. Kruger, K. Van de Rostyne, V. Gusev, W. Lauriks and J.Thoen, *Mat. Sci. Eng. A*, 313 (2001) 170.
41. M.A. Belov, E.B. Cherepetskaya, V.L. Shkuratnik, A.A. Karabutov, V.A. Makarov and N.B. Podymova, *J. Mining Sci.*, 39(5) (2003) 419.
42. J.F. Asmus, *J. Cult. Herit.*, 4 (2003) 289s.
43. A.I. Lavrentyev and S.I. Rokhlin, *Ultrasonics*, 39 (2001) 211.
44. D. Lellinger, S. Tadjbach and I. Alig, *Macromol. Symp.*, 184 (2002) 203.
45. P. Bury, P. Hockicko, S. Jurecka and M. Jamnicky, *Phys. State Sol.* 1 (2004) 2888.
46. V. Morin, F. Cohen-Tenoudji, A. Feylessoufi and P. Richard, *Cement Concrete Res.*, 32 (2002) 1907.
47. S.F. Chabira, R. Huchon and M. Sebaa, *J. Appl. Polym.*, 90 (2003) 559.
48. T. Ichitsubo, E. Matsubara, S. Kai and M. Hirao, *Acta Materialia*, 52 (2004) 423.
49. J.I. Pérez-Landazábal, V. Recarte, J.M. Ezpeleta, P.P. Rodríguez, J. San Juan and M.L. Nó, *Mat. Sci. Eng. A*, 378 (2004) 243.
50. A. Moreau, D. Lévesque, M. Lord, M. Dubois, J.P. Monchalin, C. Padioleau and J.F. Bussière, *Ultrasonics*, 40 (2002) 1047.
51. C. Koch, G. Ludwig and W. Molkenstruck, *Ultrasonics*, 35 (1997) 297.
52. T. Ohtani, H. Ogi, Y. Minami and M. Hiraro, *J. Alloys Comp.*, 310 (2000) 440.
53. Y.H. Kim, S.J. Song, D.H. Bae and S.D. Kwon, *Ultrasonics*, 42 (2004) 545.
54. K.E.A. Van den Abeele, A. Sutin, J. Carmeliet and P.A. Johnson, *NDT&E Intern.*, 34 (2001) 239.
55. S.I. Rokhlin, L.Wang, B. Xie, V.A. Yakovlev and L. Adler, *Ultrasonics*, 42 (2004) 1037.
56. T. Li, F. Grignon, D.J. Benson, K.S. Vecchio, E.A. Olexsky, F. Jiang, A. Rohatgi, R.B. Schwarz and M.A. Meyers, *Mat. Sci. Engineer. A*, 374 (2004) 10.
57. V.N. In'kov, E.B. Cherepetskaya, V.L. Shkuratnik, A.A. Karabutov and V.A. Makarov, *J. App. Mech. Techn. Physics*, 46(3) (2005) 452.
58. G.T. Schueneman, A.J. Lesser, T.R. Hobbs and B.M. Novak, *J. Polym. Sci. B*, 37 (1999) 2601.
59. M. Coeck, C. Laermans and E. Peeters, *Physica B*, 263 (1999) 152.
60. V. Chen, H. Li and A.G. Fane, *J. Memb. Sci.*, 2421 (2004) 23.
61. W.F.C. Kools, S. Konagurthu, A.R. Greenberg, L.J. Bond, W.B. Krantz, Th. van den Boomgaard and H. Strathmann, *J. Appl. Polym. Sci.*, 69 (1998) 2013.
62. A.P. Mairal, A.R. Greenberg, W.B. Krantz and L.J. Bond, *J. Membrane Sci.*, 159 (1999) 185.

63. R.A. Peterson, A.R. Greenberg, L.J. Bond and W.B. Krantz, *Desalination*, 116 (1998) 115.
64. A.P. Mairal, A.R. Greenberg and W.B. Krantz, *Desalination*, 116 (1998) 115.
65. A.P. Mairal, A.R. Greenberg and W.B. Krantz, *Desalination*, 130 (2000) 45.
66. P.A. Lewin, *Ultrasonics*, 42 (2004) 1.
67. M.F. Insana and W.F. Walker, *Ultrasonic Imaging and Signal Processing*, Proc. SPIE, Vol. 4687, The International Society for Optical Engineering, Washington.
68. A. Mizrach, N. Galili, S. Gan-mor, U. Flitsanov and I. Prigozin, *J. Agr. Eng. Res.*, 65 (1996) 261.
69. R. Ghaedian, E.A. Decker and D.J. McClements, *J. Food Sci.*, 62 (1997) 500.
70. R. Ghaedian, J. Couplant, J.N. Decker and D.J. McClements, *Food Eng.*, 35 (1998) 323.
71. J. Benedito, J.A. Cárcel, C. Roselló and A. Milet, *Meat Sci.*, 57 (2001) 365.
72. S. Simal, J. Benedito, G. Clemente, A. Fenmenia and C. Roselló, *J. Food Eng.*, 58 (2003) 253.
73. V. Buckin and C. Smyth, *Sem. Food Anal.*, 4(2) (1999) 113.
74. A.D. Pierce, *Acoustics: An Introduction to its Physical Principles and Applications*, Acoustical Soc. Amer., New York, 1989.
75. A.P. Sarvazyan, *Ann. Rev. Biophysics Biophysical Chem.*, 20 (1991) 321.
76. D.J. McClements and J.N. Coupland, *Colloids Surf.*, 117 (1996) 161.
77. J. Tong and M.J.W. Povey, *Ultrasonics*, 40 (2002) 37.
78. D. Hibberd, A. Holmes, M. Garrood, A. Fillery-Travis, M.Robins and R. Challis, *J. Colloid Interface Sci.*, 193 (1997) 77.
79. R. Chanamai, N. Herrmann and D.J. McClements, *J. Colloid Interface Sci.*, 204 (1998) 268.
80. J. Benedito, A. Mulet, G. Clemente and J.V. García-Pérez, *Food Res. Intern.*, 37 (2004) 595.
81. M. Jorg, A. Ghoneim, G. Turky and M. Stockhausen, *Phys. Chem. Liq.*, 29 (1995) 263.
82. R.J. Lagemann and W.S. Dunbar, *J. Phys. Chem.*, 49 (1945) 420.
83. S.B. Kashare and B.A. Patki, *Indian Pure Appl. Phys.*, 25 (1987) 180.
84. M.J.M. Povey, *Ultrasonic Techniques for Fluids Characterization*, Academic Press, San Diego, 1997.
85. E. Kudryashov, T. Capustina,S. Morrissey, V. Buckin and K. Dawson, *J. Colloids Interface Sci.*, 203 (1998) 59.
86. K. van Durme, L. Delellio, E. Kudryashov, V. Buckin and B. van Mele, *J. Polym. Sci.*, 43 (2005) 1283.
87. S. Koda, Y. Sugi, T. Masuoka and H. Nomura, *J. Sol. Chem.*, 33 (2004) 747.
88. P.K. Sahoo, R. Mohapatra, A. Sahoo and S.K. Swain, *J. Appl. Polym. Sci.*, 88 (2003) 3196.
89. N. Akashi, J.I. Kushibiki and F. Dunn, *Ultrasonics*, 38 (2000) 915.
90. A. Awasthi and J.P. Shukla, *Ultrasonics*, 41 (2003) 477.
91. M. Musso, F. Aliotta, C. Vasi, R. Aschauer, A. Asenbaum and E. Wilhelm, *J. Mol. Liq.*, 110 (2004) 33.
92. P. Sassi, A. Raudino and R.S. Cataliotti, *Chem. Physics*, 314 (2005) 199.
93. Z. Blaszczak, M. Pochylski, I. Iwaszkiewicz-Kostka, P. Ziobrowski, M. Drozdowski and M. Farhoud, *J. Mol. Liq.*, 121 (2005) 75.
94. C. Javanaud and R.R. Rahalkah, *Fat Sci. Technol.*, 90, (1988) 73.
95. R.C. Raghupathi, R.C. Siva and C.A.R. Prabhu, *Current Sci.*, 49 (1980) 185.
96. J. Benedito, A. Mulet, J. Velasco and M.C. Dobarganes, *J. Agr. Food Chem.*, 50 (2002) 4531.
97. R.R. Chen, T. Zelesky, N. Ilasi and S.S. Sekulic, *J. Pharm. Biomed. Anal.*, 37 (2005) 239.
98. X.L. Su, B.S. Yu, H.W. Tan, X.R. Yang, L.H. Nie and S.Z. Yao, *J. Pharm. Biomed. Anal.*, 16 (1998) 759.
99. X.L. Su, L.H. Nie and S.Z. Yao, *Fresenius, J. Anal.Chem.*, 360 (1998) 272.
100. X.L. Su, W.Z. Wei, L.H. Nie and S.Z. Yao, *Analyst*, 123 (1998) 221.
101. X.L. Su, P. Chen, X.G. Qu, W.Z. Wei and S.Z. Yao, *Microchem. J.*, 59 (1998) 341.
102. B. Guo, Y.Yuan, Y. Wu, Q. Xie and S. Yao, *Anal. Biochem.*, 305 (2002) 139.
103. P. Mougin, D. Wilkinson, K.J. Roberts, R. Jack and P. Kippax, *Power Technol.*, 134 (2003) 243.
104. F. Babick and S. Ripperger, *Part. Part. Syst. Char.* 19 (2002) 176.
105. T.I.J. Goodenough, V.S. Rajendram, S. Meyer and D. Prêtre, *Ultrasonics*, 43 (2005) 165.
106. T.I.J. Goodenough, V.S. Rajendram, S. Meyer and D. Prêtre, *Ultrasonics*, 43 (2005) 231.
107. C.M. Bryant and D.J. McClements, *J. Sci. Food Agric.*, 79 (1999) 1754.

108. M. Corredig, M. Alexander and D.G. Dalgleish, *Food Res. Int.*, 37 (2004) 557.
109. D.G. Dalgleish, M. Alexander and M. Corredig, *Food Hydrocolloid*, 18 (2004) 747.
110. A. Pal Singh, D.J. McClements and A.G. Marangoni, *Food Res. Int.*, 37 (2004) 545.
111. S. Takeda and P.J. Goetz, *Colloid Surface A*, 143 (1998) 35.
112. A. Drevermann, C. Pickmann, R. Tiefers and G. Zimmermann, *Ultrasonics*, 42 (2004) 105.
113. G.S. Constable, A.J. Lesser and B. Coughlin, *J. Polymer Sci. B*, 41 (2003) 1323.
114. C.L. Barrie, P.C. Griffiths, R.J. Abbott, I. Grillo, E. Kudryashov and C. Smyth, *J. Colloid Interface Sci.*, 272 (2004) 210.
115. Y. Ike and S. Kojima, *J. Mol. Struct.*, 744 (2005) 521.
116. M.S. Greenwood, A. Brodsky, L. Burgess, L.J. Bond and M. Hamad, *Ultrasonics*, 42 (2004) 531.
117. M. Pax, J. Rieger, R.H. Eibl, C. Thielemann and D. Johannasmann, *Analyst*, 130 (2005) 1474.
118. M.E. Delay and E.N. Bazley, *Appl. Acoust.*, 3 (1970) 105.
119. W. Qunli, *Appl. Acoust.*, 25 (1988) 141.
120. P. Nagy and L. Adler, *Appl. Phys. Lett.*, 56 (1990) 2504.
121. T. Schief, J. Gross and J. Frick, *J. Non-Cryst. Solids*, 145 (1992) 223.
122. J. Stor-Pellinen, E. Haeggström and M. Luukkala, *Meas. Sci. Technol.*, 1 (2000) 406.
123. P.L. Ridgway, A.J. Hunt, M. Quinby-Hunt and R.E. Russo, *Ultrasonics*, 37 (1999) 395.
124. L. Flax, G.C. Gaunarud and H. Überall, Theory of resonance scattering, W.P. Mason and R.N. Thurston, Eds., *Physical Acoustics*, Vol. 15, Academic Press, New York, 1981.
125. T.E. Gómez Álvarez-Arenas, *J. Memb. Sci.*, 213 (2003) 195.
126. M.A. Biot, *J. Acoust. Soc. Am.*, 28 (1956) 179.
127. M. Khoury, G.E. Tourtolletand and A. Schröder, *Ultrasonics*, 37 (1999) 133.
128. C.M. Fortunko, M.D. Renken and A. Murray, *IEEE Ultrasonics, IEEE*, New York (1990) 1099.
129. T.E. Gómez Álvarez-Arenas, F. Montero, M. Moner-Girona, E. Rodríguez, A. Roig and E. Molins, *Appl. Phys. Lett.*, 81 (2002) 1198.
130. E. Silberman, *J. Acoustic Soc. Am.*, 29 (1957) 92.
131. P. Fairley, D.J. McClements and M.J.W. Povey, *Ultrasonics Intern. Conf. Proc.*, (1991) 79.
132. J.R. Allegra and S.A. Hawley, *J. Acoust. Soc. Am.*, 51 (1972), 1545.
133. C.G. Guanaurd and H. Uberall, *J. Acoust. Soc. Am.*, 71 (1982) 282.
134. A. Kulmyrzaev, C. Cancelliere and D.J. McClements, *J. Food Eng.*, 46 (2000) 235.
135. D. Datta, J. Kirchhoff, D. Mewes, W. Herrmann and G. Galinsky, *Polym. Testing*, 21 (2002) 209.
136. J. Tatibouët, R. Gendron and L. Haïder, *Polym. Testing*, 23 (2004) 125.
137. D.J. McClements, *Trends Food Sci. Technol.*, 6 (1995) 293.

LIST OF ABBREVIATIONS

A	–	ultrasound amplitude
α	–	ultrasound attenuation
AAS	–	atomic absorption spectrometry
ADFPI	–	angular dispersion Fabry–Perot interferometer
AES	–	atomic emission spectrometry
AFM	–	atomic force microscopy
AFS	–	atomic fluorescence spectrometry
AM	–	acoustic microscopy
AOM	–	active oxygen method
APD	–	avalanche photodiode
ASE	–	accelerated solvent extraction
atm	–	atmosphere
ATP	–	adenosine triphosphate
a.u.	–	arbitrary unit
β	–	complex propagation constant
BSS	–	Brillouin scattering spectroscopy
C	–	concentration
c	–	ultrasound velocity
c_{ij}	–	elastic constant
$ca.$	–	circa (approximately)
CCD	–	coupled-charge detector
CE	–	capillary electrophoresis
COD	–	chemical oxygen demand
CRM	–	certified reference material
CUSAL	–	continuous ultrasound-assisted leaching
dB	–	decibel
DFT	–	Discrete Fourier Transform
DMF	–	dimethyl formamide
DMG	–	dimethylglyoxime
DNA	–	deoxyribonucleic acid
DPD	–	diamond particle density
DPhT	–	diphenyltin
DUSAL	–	discrete ultrasound-assisted leaching
ED	–	electrodynamic
EDTA	–	ethylenediaminetetraacetic acid
$e.g.$	–	exempli gratia (for example)
EM	–	electromagnetic
EMAT	–	electromagnetic-acoustic transducer
ESWL	–	extracorporeal shock wave lithotripsy
$et\ al.$	–	et alii (and others)
ETAAS	–	electrothermal atomic absorption spectrometry
f	–	frequency
FAAS	–	flame atomic absorption spectrometry
FI	–	flow injection
FID	–	flame ionization detector
Fig.	–	figure

FPI	–	Fabry–Perot interferometer
FTIR	–	Fourier transform infrared
GC	–	gas chromatography
GHz	–	gigahertz
GPa	–	gigapascal
GSAW	–	generalized surface acoustic wave
GUV	–	giant unilamellar vesicle
HAp	–	hydroxyapatite
HG	–	hydride generation
HIFU	–	high-intensity focused ultrasound
HLB	–	hydrophile-lipophile balance
Hz	–	hertz
ICP	–	inductively coupled plasma
i.e.	–	id est (that is)
IUPAC	–	International Union of Pure and Applied Chemistry
IWR	–	intermediate wavelength regime
kDa	–	kilo dalton
KHP	–	potassium hydrogen phthalate
kHz	–	kilohertz
l	–	litre
LC	–	liquid chromatography
LED	–	light-emitting diode
LIF	–	laser-induced fluorescence
LIP	–	laser-induced phosphorescence
LLE	–	liquid–liquid extraction
LLW	–	leaky Lamb wave
LMP	–	liquid membrane process
LUR	–	laser–ultrasound resonance
LUV	–	large unilamellar vesicle
LVI	–	large-volume injection
LWR	–	long wavelength regime
MAE	–	microwave-assisted extraction
MALDI	–	matrix-assisted laser desorption-ionization
MART	–	magnetostrictive transducer
MF	–	microfiltration
MHz	–	megahertz
min	–	minute
MIP	–	microwave-induced plasma
MIRS	–	mid-infrared spectrometry
MLV	–	multilamellar vesicle
MPa	–	megapascal
MPhT	–	monophenyltin
MS	–	mass spectrometry
MVV	–	multi-vesicular vesicle
NAP	–	near-field acoustic processor
Nd:YAG	–	neodymium:yttrium aluminium garnet
NMR	–	nuclear magnetic resonance
Np	–	neper
NUSA	–	non-ultrasound-assisted
Oe	–	oersted

OED	–	Oxford English Dictionary
P	–	instantaneous acoustic excess pressure
PAH	–	polycyclic aromatic hydrocarbon
PAN	–	polyacrylonitrile
PCB	–	polychlorinated biphenyl
PCR	–	polymerase chain reaction
PLE	–	pressurized liquid extraction
PMC	–	polymer matrix composite
PSAW	–	*pseudo*-surface acoustic wave
PTFE	–	polytetrafluoroethylene
PTV	–	programmed-temperature vaporizer
PVDF	–	polyvinylidene fluoride
QCM	–	quartz crystal microbalance
R	–	reflection coefficient
rf	–	radio frequency
RM	–	reference material
RSD	–	relative standard deviation
RST	–	resonant sphere technique
RUS	–	resonance ultrasound spectroscopy
s	–	second
SAM	–	scanning acoustic microscopy
SAW	–	surface acoustic wave
SCE	–	saturated-calomel electrode
SDME	–	single-drop microextraction
SEM	–	scanning electron microscopy
SERS	–	surface-enhanced Raman scattering
SFE	–	supercritical fluid extraction
SLM	–	spatial light modulator
SLS	–	sodium lauryl sulphate
SM&T	–	Standards, Measurement and Testing Programme
SNR	–	signal-to-noise ratio
SONAR	–	SOund Navigation And Ranging
SP	–	sample preparation
SPE	–	solid-phase extraction
SPME	–	solid-phase microextraction
SUV	–	small unilamellar vesicle
SWR	–	short wavelength regime
T	–	transmission coefficient
TDR	–	time-domain reflectometry
TGA–DSC	–	thermogravimetric analysis–differential scanning calorimetry
ThOD	–	theoretical oxygen demand
TPhT	–	triphenyltin
TT	–	time threshold
UAS	–	ultrasound attenuation spectrometry
UBM	–	ultrasound biomicroscopy
UDGS	–	ultrasonic diffraction grating spectroscopy
UF	–	ultrafiltration
UHF	–	ultra-high frequency
URS	–	ultrasonic relaxation spectroscopy
US	–	ultrasound

USAL   – ultrasound-assisted leaching
USASD   – ultrasound-assisted soft digestion
USASTD   – ultrasound-assisted strong digestion
USLLE   – ultrasound-assisted liquid–liquid extraction
USN   – ultrasonic nebulizer
USNn   – ultrasonic nebulization
VHF   – very-high frequency
viz.   – videlicet (namely)
vs   – versus (against)
W   – watt
ω – angular frequency
WTNID   – Webster's Third New International Dictionary
Z – acoustic impedance

INDEX